

University of Southampton Research Repository

Copyright © and Moral Rights for this thesis and, where applicable, any accompanying data are retained by the author and/or other copyright owners. A copy can be downloaded for personal non-commercial research or study, without prior permission or charge. This thesis and the accompanying data cannot be reproduced or quoted extensively from without first obtaining permission in writing from the copyright holder/s. The content of the thesis and accompanying research data (where applicable) must not be changed in any way or sold commercially in any format or medium without the formal permission of the copyright holder/s.

When referring to this thesis and any accompanying data, full bibliographic details must be given, e.g.

Thesis: Author (Year of Submission) "Full thesis title", University of Southampton, name of the University Faculty or School or Department, PhD Thesis, pagination.

Data: Author (Year) Title. URI [dataset]

University of Southampton

FACULTY OF ENVIRONMENTAL AND LIFE SCIENCES

School of Biological Sciences



Light-induced plasticity of *Drosophila* central and peripheral circadian clock function

by

Charles Mark Hurdle, BSc (Hons)

Thesis for the degree of Doctor of Philosophy

February 2020

University of Southampton

Abstract

Faculty of Environmental and Life Sciences
School of Biological Sciences

Thesis for the degree of Doctor of Philosophy

Light-induced plasticity of *Drosophila* central and peripheral circadian clock function

Charles Mark Hurdle, BSc (Hons)

Daily fluctuations in light and temperature act as environmental cues for synchronising circadian clocks, with light being the dominant synchronising factor. Properly entraining behaviour and physiology in-line with environmental Light:Dark (LD) cycles will contribute to the fitness and well-being of an organism. The circadian clocks of *Drosophila melanogaster* have been extensively studied with light-induced plasticity assayed with either brief light-pulses, varied photocycles or re-entrainment to a shifted LD regime. In this thesis, extreme equinox photocycles were used to stretch central and peripheral molecular oscillators to the limits of light-induced entrainment. At these limits, the clockwork has to constantly re-set its phase away from its inherent 24 h periodicity and therefore provides a more sensitive measure of plasticity. In doing so we reveal how the molecular oscillators in the brain and peripheral tissues adapt to maintain entrainment to extremely long and short photocycles. We also show that both the CRY/JET pathway and the visual system are required to facilitate central clock entrainment to extreme LD cycles, with CRY/JET expression in the PDF-expressing M-cells playing a significant role. The visual system plays no role in peripheral light entrainment, but both CRY and JET are essential. Our work thus furthers our understanding of; how the underlying circadian oscillator adapts to facilitate light-dependent plasticity at the behavioural and molecular level; the relative contributions of each light input pathway to central and peripheral clock entrainment; and in the case of central clocks, where in the circadian circuitry CRY/JET are required to allow behavioural entrainment to extreme equinox photocycles. Furthermore, we have shown that entrainment to extreme photocycles has a direct impact on fly physiology. As such, it may be possible to utilise such photocycles to induce internal desynchrony in *Drosophila* and model other physiological aspects of jet-lag and circadian disruption to further investigate the impact of circadian dysfunction on physiology and well-being of other invertebrate species as well as mammals.

Table of Contents

| | |
|---|--------------|
| Table of Contents | i |
| Table of Tables | ix |
| Table of Figures | xi |
| Table of Supplementary Data | xiv |
| Research Thesis: Declaration of Authorship | xix |
| Acknowledgements | xxi |
| Definitions and Abbreviations | xxiii |
| Chapter 1: Review of the Literature | 1 |
| 1.1 Overview of Circadian Rhythms | 1 |
| 1.1.1 Key principles in circadian biology | 2 |
| 1.1.2 Historical research and evolutionary relevance of circadian rhythms | 3 |
| 1.1.3 Circadian rhythms in mammals..... | 4 |
| 1.1.4 Impact of circadian desynchrony on human physiology and well-being..... | 5 |
| 1.2 Circadian Rhythms in <i>Drosophila melanogaster</i> | 7 |
| 1.2.1 <i>Drosophila</i> as a model organism | 7 |
| 1.2.1.1 Practical applications of invertebrate circadian research..... | 8 |
| 1.2.1.2 Use of <i>Drosophila</i> in circadian research..... | 8 |
| 1.2.2 Central and Peripheral Oscillators in <i>Drosophila</i> | 9 |
| 1.2.3 The <i>Drosophila</i> Molecular Oscillator..... | 9 |
| 1.2.3.1 Key components of the molecular clockwork..... | 9 |
| 1.2.3.2 The core circadian feedback loop | 11 |
| 1.2.3.3 Interlocked feedback loops | 14 |
| 1.2.4 <i>Drosophila</i> Central Clock Circuitry | 16 |
| 1.2.4.1 Clock cell clusters and network organisation..... | 16 |
| 1.2.4.2 Classical dual oscillator model for <i>Drosophila</i> locomotor behaviour ... | 19 |
| 1.2.5 Light entrainment of Central Circadian Clocks..... | 21 |
| 1.2.5.1 The CRY/JET pathway | 22 |
| 1.2.5.2 Visual photoreception in <i>Drosophila</i> | 29 |

Table of Supplementary Data

| | | |
|---|--|-----------|
| 1.2.5.3 | Red light | 36 |
| 1.2.5.4 | Temperature entrainment and other zeitgebers | 37 |
| 1.2.6 | Communication, Co-ordination and Synchronisation of Neuronal Clocks | 39 |
| 1.2.6.1 | Neuropeptides and neurotransmitters required for communication across the circuitry | 39 |
| 1.2.6.2 | Circadian network for light entrainment | 42 |
| 1.2.7 | Transducing Clock Function to Locomotor Output..... | 45 |
| 1.2.8 | <i>Drosophila</i> Peripheral Oscillators | 46 |
| 1.2.8.1 | The role of CRY in peripheral clock function..... | 47 |
| 1.2.8.2 | Peripheral light entrainment | 48 |
| 1.2.8.3 | Communication between central and peripheral oscillators | 49 |
| 1.3 | Summary and Project Aims..... | 51 |
| Chapter 2: Light-dependent plasticity of wild-type <i>Drosophila</i> behavioural and molecular rhythms | | 53 |
| 2.1 | Introduction | 53 |
| 2.1.1 | Aims | 55 |
| 2.2 | Methods..... | 56 |
| 2.2.1 | Analysis of <i>Drosophila</i> Locomotor Behaviour..... | 56 |
| 2.2.1.1 | DAM Behavioural Assay | 56 |
| 2.2.1.2 | Quantitative Analyses | 57 |
| 2.2.2 | Analysis of the <i>Drosophila</i> central molecular clockwork..... | 60 |
| 2.2.2.1 | Confocal Immunofluorescence Microscopy | 60 |
| 2.2.2.2 | Image analysis | 61 |
| 2.2.3 | Analysis of <i>Drosophila</i> Longevity | 62 |
| 2.3 | Results..... | 64 |
| 2.3.1 | Light-dependent plasticity of wild-type <i>Drosophila</i> behavioural rhythms..... | 64 |
| 2.3.1.1 | Wild-type locomotor rhythms are entrainable to a wide-range of equinox photocycles | 64 |

| | | |
|---|--|-----------|
| 2.3.2 | Light-dependent plasticity of the molecular rhythms in the clock neurons of wild-type <i>Drosophila</i> | 71 |
| 2.3.2.1 | Robust molecular oscillations in PER protein were observed across the neural clock circuit during 7 and 5c/wk LD cycles..... | 71 |
| 2.3.2.2 | Clock neurons in 10c/wk photocycles exhibited entrained circadian rhythms rather than purely light-driven molecular responses..... | 78 |
| 2.3.3 | Defining the limits of light-induced behavioural entrainment | 80 |
| 2.3.4 | Free-running period lengths revert back to ~24 h following extreme LD entrainment | 83 |
| 2.3.5 | Entrainment to extreme LD cycles reduces longevity in wild-type females.... | 85 |
| 2.4 | Discussion | 87 |
| Chapter 3: CRYPTOCHROME, JETLAG and the visual system are required for effective light-induced plasticity of the central clock | | 93 |
| 3.1 | Introduction..... | 93 |
| 3.1.1 | Aims..... | 95 |
| 3.2 | Methods | 96 |
| 3.2.1 | Analysis of <i>Drosophila</i> Locomotor behaviour | 96 |
| 3.2.1.1 | DAM Behavioural Assay and Quantitative Analyses | 96 |
| 3.2.2 | Spatial Control of Gene Expression..... | 97 |
| 3.2.2.1 | Gene Knockdown – Inhibition of Gene Expression | 97 |
| 3.3 | Results | 99 |
| 3.3.1 | The CRY/JET pathway and the visual system are both required for behavioural entrainment to extreme photocycles | 99 |
| 3.3.2 | Spatial characterisation of CRY and JET requirement for photocycle entrainment | 105 |
| 3.3.2.1 | Pan-circadian knockdown of <i>cry</i> and <i>jet</i> limited behavioural photocycle entrainment..... | 105 |
| 3.3.2.2 | CRY/JET expression in both the M- and E- cells was required for behavioural entrainment | 112 |

Table of Supplementary Data

| | | |
|-------------------|---|------------|
| 3.3.2.3 | CRY expression in just the PDF cells was sufficient to rescue rhythmicity in long photocycles | 117 |
| 3.3.3 | The visual system facilitates red-light entrainment via histamine signalling | 120 |
| 3.4 | Discussion..... | 125 |
| Chapter 4: | Light-dependent plasticity of <i>Drosophila</i> peripheral clocks..... | 133 |
| 4.1 | Introduction | 133 |
| 4.1.1 | Aims | 135 |
| 4.2 | Methods..... | 136 |
| 4.2.1 | Analysis of peripheral clock rhythms <i>in vivo</i> | 136 |
| 4.2.1.1 | TopCount <i>in vivo</i> Luciferase Assay | 136 |
| 4.2.1.2 | Qualitative, Quantitative and Statistical Analysis..... | 136 |
| 4.2.2 | Analysis of the <i>Drosophila</i> peripheral molecular clockwork | 137 |
| 4.2.2.1 | Quantitative Reverse Transcriptase-PCR (qRT-PCR)..... | 137 |
| 4.2.2.2 | Western Blot | 139 |
| 4.3 | Results..... | 141 |
| 4.3.1 | Light-dependent plasticity of <i>Drosophila</i> peripheral rhythms <i>in vivo</i> | 141 |
| 4.3.1.1 | Defining the limits of wild-type peripheral clock entrainment | 141 |
| 4.3.1.2 | CRY/JET-mediated light entrainment is required for light-induced plasticity of <i>Drosophila</i> peripheral oscillators | 144 |
| 4.3.2 | Molecular analysis of peripheral clock entrainment | 147 |
| 4.3.2.1 | Light-induced plasticity of the molecular oscillator is associated with selective reorganisation of clock gene mRNA rhythms | 147 |
| 4.3.2.2 | Robust oscillations in PER protein are locked to the Light:Dark cycle | 151 |
| 4.4 | Discussion..... | 154 |
| Chapter 5: | General Discussion and Conclusions | 159 |
| 5.1 | General Discussion..... | 159 |
| 5.1.1 | Light-dependent plasticity of <i>Drosophila</i> central and peripheral clocks..... | 159 |

| | | |
|---|--|------------|
| 5.1.1.1 | How does the underlying circadian molecular oscillator adapt to facilitate light entrainment?..... | 159 |
| 5.1.1.2 | What light input pathways are required?..... | 160 |
| 5.1.1.3 | Why are the limits of entrainment different between central and peripheral clocks?..... | 161 |
| 5.1.2 | Can <i>Drosophila</i> be used to model effects of circadian dysfunction and desynchrony? | 162 |
| 5.1.3 | Wide-reaching impact of CRY on <i>Drosophila</i> physiology..... | 163 |
| 5.2 | Conclusions..... | 165 |
| 5.3 | Future Directions..... | 169 |
| Appendix A:Supplementary Data | | 171 |
| A.1 | Genotyping..... | 171 |
| A.2 | Supplementary Tables: Chapter 2..... | 175 |
| A.3 | Supplementary Figures: Chapter 2..... | 194 |
| A.4 | Supplementary Tables: Chapter 3..... | 201 |
| A.5 | Supplementary Figures: Chapter 3..... | 228 |
| A.6 | Supplementary Tables: Chapter 4..... | 239 |
| A.7 | Supplementary Figures: Chapter 4..... | 251 |
| Appendix B:Supplementary Materials and Methods | | 257 |
| B.1 | <i>Drosophila</i> Husbandry..... | 257 |
| B.1.1 | Media..... | 257 |
| B.1.2 | Stocks and Genetic Crosses..... | 257 |
| B.2 | Light:Dark Cycle Schedule for all photocycles assayed | 261 |
| B.3 | Analysis of <i>Drosophila</i> Locomotor Behaviour | 263 |
| B.3.1 | DAM Behavioural Assay | 263 |
| B.3.2 | DAM Behavioural Assay with a Combined LD and Temperature Cycle | 263 |
| B.3.3 | Analysis of Activity Counts | 264 |
| B.4 | Analysis of the <i>Drosophila</i> central molecular clockwork..... | 266 |
| B.4.1 | <i>D.melanogaster</i> Adult Brain Dissection and Immunostaining..... | 267 |
| B.4.2 | PERIOD antibody preparation | 268 |

Table of Supplementary Data

| | | |
|-------|--|-----|
| B.4.3 | PERIOD antibody purification | 269 |
| B.5 | Analysis of peripheral clock rhythms <i>in vivo</i> – TopCount..... | 270 |
| B.6 | Analysis of the <i>Drosophila</i> peripheral molecular clockwork - qRT-PCR | 271 |
| B.6.1 | Quantitative Reverse Transcriptase-PCR (qRT-PCR)..... | 271 |
| B.6.2 | Standard Curves and Primer efficiencies..... | 272 |
| B.6.3 | RNA extraction protocol | 273 |
| B.6.4 | qRT-PCR and Cycling Protocol..... | 274 |
| B.7 | Analysis of the <i>Drosophila</i> peripheral molecular clockwork - Western Blot..... | 275 |
| B.7.1 | Reagents..... | 275 |
| B.7.2 | Buffers..... | 275 |
| B.7.3 | Antibodies | 276 |
| B.7.4 | Protein extraction protocol | 277 |
| B.7.5 | Western Blot protocol | 278 |
| B.8 | Genotyping..... | 281 |
| B.8.1 | DNA Extraction Protocol | 282 |
| B.8.2 | PCR protocol | 283 |
| B.8.3 | Gel Electrophoresis Protocol | 284 |
| B.8.4 | PCR Product Purification Protocol | 285 |

Appendix C: Magnetoreception and other physiological functions of *Drosophila*

| | | |
|---------|---|------------|
| | CRYPTOCHROME | 287 |
| C.1 | Introduction | 287 |
| C.1.1 | Magnetoreception: A New Function of CRYPTOCHROME | 287 |
| C.1.1.1 | Geomagnetic fields | 287 |
| C.1.1.2 | Mechanisms for Biological Magnetoreception..... | 287 |
| C.1.1.3 | Magnetic Field Effects on Circadian Rhythms..... | 288 |
| C.1.1.4 | Possible mechanisms for CRY-mediated Magnetoreception | 289 |
| C.1.2 | Wide-reaching Influences of CRY..... | 290 |
| C.1.3 | Aims | 292 |
| C.2 | Methods..... | 293 |
| C.2.1 | Negative Geotaxis | 293 |

| | | |
|-------|--|------------|
| C.2.2 | DAM Behavioural Assay | 294 |
| C.3 | Results | 296 |
| C.3.1 | Effect of an electromagnetic field on negative geotaxis..... | 296 |
| C.3.2 | Mutations effecting possible CRY mediated membrane excitability have no effect on behavioural entrainment..... | 300 |
| C.3.3 | An electromagnetic field increases nocturnality in <i>cyc⁰¹</i> flies | 302 |
| C.4 | Conclusions..... | 304 |
| | Bibliography | 305 |

Table of Tables

| | | |
|------------------|--|------------|
| Table 2.1 | Antibodies and their concentration used in immunofluorescence assays. . | 61 |
| Table 4.1 | Primer pairs used for mRNA amplification via qRT-PCR | 138 |
| Table 4.2 | Antibodies used for protein labelling during western blot | 140 |

Table of Figures

| | | |
|------------|--|----|
| Figure 1.1 | Key principles in circadian biology. | 3 |
| Figure 1.2 | The core molecular TTFL that drives circadian rhythms in <i>Drosophila</i> | 12 |
| Figure 1.3 | <i>Clk</i> -dependent feedback loops which interlock with the core molecular oscillator. | 16 |
| Figure 1.4 | Network organisation of the central circadian circuitry of the <i>Drosophila</i> brain. | 19 |
| Figure 1.5 | Dual oscillator model for <i>Drosophila</i> locomotor behaviour in an LD cycle. . | 21 |
| Figure 1.6 | The CRY/JET pathway for light-dependent re-setting of the core molecular oscillator. | 25 |
| Figure 1.7 | Organisation of the <i>Drosophila</i> visual system. | 32 |
| Figure 1.8 | Multi-oscillator model for <i>Drosophila</i> locomotor behaviour in an LD cycle. | 44 |
| Figure 2.1 | Schematic of TriKinetics DAM system and example Actogram. | 56 |
| Figure 2.2 | Quantitative analysis of <i>Drosophila</i> Locomotor Behaviour..... | 60 |
| Figure 2.3 | Robust entrainment of wild-type locomotor activity rhythms to a wide range of photocycles. | 66 |
| Figure 2.4 | Wild-type behaviour in extreme LD cycles reflects true entrainment and not just masking..... | 70 |
| Figure 2.5 | Rhythms in PER cycling and nuclear localisation were robust in 7 and 5c/wk LD cycles, but selectively weakened in 10c/wk. | 76 |
| Figure 2.6 | PER localisation and cycling rhythms were comparable across most cell types with some differences during short 10c/wk photocycles..... | 77 |
| Figure 2.7 | VRI cycling rhythms persisted in 10c/wk photocycles..... | 79 |
| Figure 2.8 | Behavioural entrainment breaks down beyond a 10c/wk LD cycle. | 81 |
| Figure 2.9 | In a 56 h photocycle clock neuron molecular oscillations exhibit features of 28 h cycling. | 82 |

Table of Figures

| | | |
|-------------|---|-----|
| Figure 2.10 | DD period lengths revert to close to the intrinsic period length, irrespective of prior LD entrainment. | 84 |
| Figure 2.11 | Extreme equinox photoperiods impact on wild-type life-span, especially in females..... | 86 |
| Figure 3.1 | Schematic for the system used for spatial regulation of gene expression. ... | 98 |
| Figure 3.2 | Both the CRY/JET pathway and the visual system are required for behavioural plasticity in extreme photocycles..... | 100 |
| Figure 3.3 | Mutants to the CRY/JET pathway resulted in circadian (~24 h) period lengths in extreme LD cycles. | 103 |
| Figure 3.4 | Pan-circadian knockdown of <i>cry</i> or <i>jet</i> reduced behavioural entrainment to extreme photocycles. | 109 |
| Figure 3.5 | Significant reductions in entrainment are evident when <i>cry</i> or <i>jet</i> are knocked-down in all clock cells in both 10 and 5c/wk LD but not 7c/wk. | 111 |
| Figure 3.6 | Selective knockdown of <i>cry</i> indicates where CRY is required to allow behavioural entrainment to extreme photocycles. | 113 |
| Figure 3.7 | Selective knockdown of <i>jet</i> indicates where JET is required to allow behavioural entrainment to extreme photocycles. | 115 |
| Figure 3.8 | Rescue of CRY expression, in a <i>cry</i> ⁰¹ background, indicates where CRY is needed to allow light-induced behavioural plasticity..... | 119 |
| Figure 3.9 | The visual system and histamine signalling are required to allow behavioural entrainment to extreme RED light photocycles. | 124 |
| Figure 4.1 | Peripheral oscillators of wild-type flies show a high level of light-induced plasticity..... | 143 |
| Figure 4.2 | CRY and JET are required for light-induced plasticity of peripheral clocks. | 146 |
| Figure 4.3 | <i>per</i> and <i>Clk</i> mRNA cycling indicate the state of the molecular oscillator under extreme photocycles – Male. | 149 |
| Figure 4.4 | <i>per</i> and <i>Clk</i> mRNA cycling indicate the state of the molecular oscillator under extreme photocycles – Female..... | 150 |

| | |
|-------------------|---|
| Figure 4.5 | PER protein oscillations are locked to LD cycles as PER is light-degradable. 152 |
| Figure 5.1 | Graphical summary: Light-induced plasticity of <i>Drosophila</i> central and peripheral circadian clock function.167 |

Table of Supplementary Data

| | | |
|------------|--|-----|
| S.Table 1 | Summary of genotyping results testing for <i>tim</i> and <i>jet</i> isoforms..... | 172 |
| S.Figure 1 | Comparison of wild-type locomotor behaviour with differing <i>tim</i> isoforms. | 173 |
| S.Table 2 | Male and Female locomotor activity of wild-type and per mutant flies in 11 – 3c/wk equinox LD cycles. | 179 |
| S.Table 3 | Results of Dunn’s Multiple comparison test between RRP for all LD cycles. | 181 |
| S.Table 4 | Results of Dunn’s Multiple comparison test between RRP(ExT)/RRP(x1.5 or x0.5) for all LD cycles..... | 183 |
| S.Table 5 | Male and female locomotor activity of wild-type and period mutants in DD following 10, 7 and 5c/wk LD entrainment (30min bins)..... | 185 |
| S.Table 6 | Quantification of anti-PER immunofluorescence rhythms during 10, 7, 5 and 3c/wk LD in different clock cell subsets in the male <i>Drosophila</i> brain. | 188 |
| S.Table 7 | Quantification of anti-VRI immunofluorescence rhythms during 10c/wk LD in different clock cell subsets in the male <i>Drosophila</i> brain. | 189 |
| S.Table 8 | PER and VRI molecular analysis statistical summary..... | 192 |
| S.Table 9 | Number of cells analysed for all clock cell subset at each time-point for each LD cycle tested | 193 |
| S.Figure 2 | Heterozygote controls for <i>jet^{set}</i> mutant also show robust behavioural entrainment | 194 |
| S.Figure 3 | PER localisation and cycling rhythms are comparable across most cell types, some differences arise during short cycles..... | 196 |
| S.Figure 4 | Molecular cycling of nuclear PER in all clock cell subsets analysed in 10, 7 and 5c/wk LD. | 197 |
| S.Figure 5 | PER cycling across different clock cell types during a 3c/wk LD cycle. | 198 |
| S.Figure 6 | VRI cycling across different clock cell types during a 10c/wk LD cycle. | 200 |
| S.Table 10 | Male and Female locomotor activity of mutant genotypes in 10, 7 and 5c/wk equinox LD cycles..... | 203 |

| | | |
|-------------|---|-----|
| S.Table 11 | Locomotor activity of male and female flies with <i>ds-cry</i> RNA (3772R2) in different clock cell subsets in 10, 7 and 5c/wk LD cycles. | 209 |
| S.Table 12 | Locomotor activity of male and female flies with <i>ds-jet</i> RNA (JF01506) in different clock cell subsets in 10, 7 and 5c/wk LD cycles. | 215 |
| S.Table 13 | Locomotor activity of male and female flies with <i>ds-cry</i> RNA (3772R2) in all clock cell subset with added spatial regulation using Gal80 constructs in 10, 7 and 5c/wk LD cycles. | 219 |
| S.Table 14 | Locomotor activity of male and female flies with <i>ds-jet</i> RNA (JF01506) in all clock cell subset with added spatial regulation using Gal80 constructs in 10, 7 and 5c/wk LD cycles. | 222 |
| S.Table 15 | Locomotor activity of male and female flies with rescue of CRY expression in different clock cell subsets, in a <i>cry⁰¹</i> background, in 10, 7 and 5c/wk LD cycles. | 224 |
| S.Table 16 | Male and Female locomotor activity of mutant genotypes in 10, 7 and 5c/wk equinox red light LD cycles. | 227 |
| S.Figure 7 | Other mutations to circadian genes affect aspects of locomotor behaviour but show no impact on entrainment to extreme photocycles | 228 |
| S.Figure 8 | A functional visual system is required for behavioural plasticity in extreme photocycles..... | 230 |
| S.Figure 9 | Histamine signalling mutants do not greatly reduce behavioural entrainment in white LD cycles..... | 231 |
| S.Figure 10 | <i>cry⁰¹</i> mutants show a preference for temperature cycling compared to light. | 232 |
| S.Figure 11 | Social interaction effects locomotion of group housed flies irrespective of light and temperature cycles. | 233 |
| S.Figure 12 | Approximate location of neuronal clock cell subsets and specific cells targeted via different Gal4 driver lines..... | 234 |
| S.Figure 13 | WT flies show advanced evening activity in RD, similar to that of <i>Pdf⁰¹</i> flies in white LD. | 235 |

Table of Supplementary Data

| | | |
|--------------|--|-----|
| S.Figure 14 | RR rescues DD arrhythmicity in PDF signalling mutants. | 236 |
| S.Figure 15 | Knockdown of the HISCL1 receptor reduces the rhythmicity of PDFR mutants in RR. | 237 |
| S.Table 17 | Male and Female <i>in vivo</i> luciferase activity of wild-type ($y^1w^*;;tim-luc:10$) and mutant genotypes in a wide range (4-10c/wk) equinox LD cycles. | 243 |
| S.Table 18 | Quantification of fold change in <i>per</i> , <i>Clk</i> and <i>luc</i> transcript in 9, 7 and 5c/wk LD from wild-type adult heads. | 246 |
| S.Table 19 | Quantification of fold change in <i>per</i> , <i>Clk</i> and <i>luc</i> transcript in 10c/wk LD from wild-type adult heads. | 247 |
| S.Table 20 | Effect size calculation for short cycle qPCR of <i>per</i> , <i>Clk</i> and <i>luc</i> transcripts. | 248 |
| S.Table 21 | Quantification of PER protein in 10, 9, 7 and 5c/wk LD from wild-type adult heads. | 249 |
| S.Table 22 | PER protein cycling statistics summary. | 250 |
| S.Figure 16 | Strength of peripheral rhythms in 10-4c/wk LD cycles, quantification indicates strongest rhythms in 5 and 4c/wk. | 251 |
| S.Figure 17 | Phase of peripheral luciferase activity W.R.T photoperiod for $y^1w^*;;tim-luc:10$ males. | 252 |
| S.Figure 18 | Luciferase activity traces for $y^1w^*tim-luc;tim^{01}$ (tim^{01}) males. | 253 |
| S.Figure 19 | CRY and JET are not components of the peripheral oscillator. | 254 |
| S.Figure 20 | Female flies show better peripheral rhythms than males in a temperature cycle for both controls and <i>cry/jet</i> mutants..... | 255 |
| S.Figure 21 | mRNA expression cycling of <i>per</i> , <i>Clk</i> and <i>luc</i> in 10c/wk LD. | 256 |
| S.Table B. 1 | Standard Cornmeal Medium | 257 |
| S.Table B. 2 | Mutants and Strains..... | 258 |
| S.Table B. 3 | Gal4, Gal80 and UAS Constructs | 259 |
| S.Table B. 4 | Sugar-agar Medium (5% sucrose, 1% agar and 0.07% Tegosept) | 263 |
| S.Table B. 5 | Analysis parameters used for Light:Dark DAM behavioural analysis. | 265 |

| | | |
|---------------|--|-----|
| S.Figure B. 1 | Dissection schedule for confocal immunofluorescence | 266 |
| S.Table B. 6 | Sugar-agar Medium with D-Luciferin..... | 270 |
| S.Figure B. 2 | Sample collection schedule for qRT-PCR..... | 271 |
| S.Table B. 7 | Equations of standard curves for primers used for qRT-PCR..... | 272 |
| S.Table B. 8 | Primers pairs used for PCR..... | 281 |
| S.Table B. 9 | Primer pairs used for sequencing..... | 281 |
| S.Figure C. 1 | Apparatus for Negative Geotaxis Assay..... | 293 |
| S.Figure C. 2 | Negative Geotaxis Assay Set-up..... | 294 |
| S.Figure C. 3 | Negative geotaxis behaviour is affected both by genotype and magnetic fields. | 299 |
| S.Figure C. 4 | Membrane Excitability mutants do not greatly reduce behavioural entrainment in white LD cycles..... | 301 |
| S.Figure C. 5 | An EMF drives <i>cyc</i> ⁰¹ flies to become 'more nocturnal'..... | 303 |

Research Thesis: Declaration of Authorship

| | |
|-------------|---------------------|
| Print name: | Charles Mark Hurdle |
|-------------|---------------------|

| | |
|------------------|---|
| Title of thesis: | Light-induced plasticity of <i>Drosophila</i> central and peripheral circadian clock function |
|------------------|---|

I declare that this thesis and the work presented in it are my own and has been generated by me as the result of my own original research.

I confirm that:

1. This work was done wholly or mainly while in candidature for a research degree at this University;
2. Where any part of this thesis has previously been submitted for a degree or any other qualification at this University or any other institution, this has been clearly stated;
3. Where I have consulted the published work of others, this is always clearly attributed;
4. Where I have quoted from the work of others, the source is always given. With the exception of such quotations, this thesis is entirely my own work;
5. I have acknowledged all main sources of help;
6. Where the thesis is based on work done by myself jointly with others, I have made clear exactly what was done by others and what I have contributed myself;
7. None of this work has been published before submission

| | | | |
|------------|--|-------|--|
| Signature: | | Date: | |
|------------|--|-------|--|

Acknowledgements

Over the past four years I have been lucky enough to receive a ridiculous amount of help and support from a number incredible people which has enabled me to get to where I am now and I am extremely grateful to you all. Firstly I would like to say a MASSIVE thank you to Dr Herman Wijnen, who has been an incredible supervisor and mentor for the past four years (5 if you include undergrad!); your help, support, encouragement and guidance has been invaluable. It has been an honour to work alongside you and I count myself lucky to have been part of the Wijnen lab. You always had time to discuss my work, your endless interest and enthusiasm was infectious and you promoted a fantastic working environment which was great to be a part of. I would also like to thank Dr Chris Jackson, and although the EMF work didn't really take off, your advice and support was very much appreciated. I must also say a huge thank you to the Gerald Kerkut Charitable trust for your continued support throughout my PhD, for funding trips to overseas conferences and providing excellent opportunities to present my work at the annual symposiums.

Secondly, I would like to thank the rest of the Wijnen lab, past and present. I have to say a particular thank you to Dr Karolina Mirowska, Dr Akanksha Bafna and Dr Miguel Ramirez-Moreno for all your help and teaching me all the techniques I needed, especially when I had no idea what I was doing. In addition, I am very grateful for Dr Bethan Shaw and Miguel for listening to my moans and answering any silly questions I had, you have been great colleagues and friends. I would also like to thank Dr Amrit Mudher and the entire Mudher lab, our discussions in lab meetings and your help (particularly from Dr Meghan Sealy) setting up my Western Blots was invaluable. I need to also extend an enormous thank you to all the students who have worked with me over the last four years, and in some cases contributed to this thesis; Mike Price, Dom Barker, Nanthilde Malandain, Chloe Ellison, Racheal Anderson and George Pateman. All of your hard work and dedication was greatly appreciated and I wish you all the best in the future! Thank you to all the technical staff in Building 85, in particular Rachel Fitzearle and Maddie Brown for their incredible work in the Invertebrate facility; and also Dr Mark Willet for his help and expertise in the Imaging Facility

I have been lucky enough to meet some incredible people whilst living in Southampton. The PhD gang; George Devitt, Emelia Assar, Rachel Owen and Chris Winnard (we're all almost there!); as well as all the members of BSPS and the guys at Stoneham RFC have all made the tough times far easier and helped me maintain some degree of sanity.

My family have been an unmovable pillar of support who without I don't think any of this will be possible. Your constant positivity, belief and encouragement have taught me to always strive to do my best and it has no doubt made me into the person I am today. I can't thank you enough.

Last but certainly not least, Dr K. E. Askew. You believed in me when I doubted myself. You put up with my constant moaning about writing up and how much 'I hate words'. You have been an incredible driving force pushing me to carry on when I wanted to sit and do nothing. You have just been there when I needed you and I appreciate it an unbelievable amount. Cheers bud.

It has been an incredible four years and I can't believe it's all over...time really does fly.

Definitions and Abbreviations

| | |
|------------------|---|
| aMe: | accessory Medulla |
| AOT: | Anterior optic tract |
| AR: | Arrhythmic |
| ASQ: | Anionic semiquinone (reduced FAD) |
| bHLH: | basic-Helix-Loop-Helix |
| BMAL1: | Brain And Muscle Arnt-Like protein 1 |
| BRWD3: | Bromodomain and WD repeat domain containing 3 |
| bZip: | basic-leucine Zipper |
| c/wk: | Cycles per week |
| cAMP: | Cyclic adenosine monophosphate |
| <i>ChAT</i> : | Choline acetyltransferase |
| CK2: | Casein Kinase 2 |
| <i>Clk/CLK</i> : | Clock |
| CLOCK: | Clock Locomotor Output Kaput |
| cps: | Counts per second |
| <i>cry/CRY</i> : | Cryptochrome |
| CRL4: | Cullin-RING E3 Ligase |
| CTCF: | Corrected total cell fluorescence |
| CTL: | Carboxyl-terminal tail like |
| CTT: | Carboxyl-terminal tail |
| CUL-3: | Cullin-3 |
| <i>cwo/CWO</i> : | Clockwork Orange |
| <i>cyc/CYC</i> : | Cycle |
| DBT: | Doubletime |
| DCR: | Dicer-2 endonuclease |
| DD: | Constant darkness (Dark:Dark) |
| DFC: | Dorsal-Fusion-Commissure |
| DNs: | Dorsal Neurons |
| DN1s: | type 1 Dorsal Neurons |

Definitions and Abbreviations

| | |
|------------------------|---|
| DN1 _a s: | anterior type 1 Dorsal Neurons |
| DN1 _p s: | posterior type 1 Dorsal Neurons |
| DN2s: | type 2 Dorsal Neurons |
| DN3: | type 3 Dorsal Neurons |
| dsRNA: | double-stranded RNA |
| E: | Evening (peak, oscillator or neurons) |
| EAG: | Ether-a-go-go |
| EB: | Ellipsoid body |
| EB-RNs: | Ellipsoid body rind neurones |
| EMF: | Electromagnetic field |
| EMS: | Ethyl methanesulfonate |
| ERG: | EAG-related gene |
| ExT: | Entrained |
| FAD: | Flavin Adenine Dinucleotide |
| FAD _{ox} : | Oxidised FAD |
| FFT-NLLS: | Fast Fourier Transform – Non-Linear Last Squares |
| GABA: | γ-aminobutyric acid |
| GPCR: | G-protein coupled receptor |
| H-B eyelet: | Hofbauer-Buchner eyelet |
| hD: | Hours of dark, in an LD cycle |
| <i>Hdc</i> /HDC: | Histidine decarboxylase |
| Hid: | Head involution defective |
| <i>HisCl1</i> /HISCL1: | Histamine-gated chloride channel 1 |
| Hk: | Hyperkinetic |
| hL: | Hours of light, in an LD cycle |
| h: | hour |
| HSP-70: | Heat-Shock Protein 70 |
| ipRGCs: | intrinsically photosensitive Retinal Ganglion Cells |
| ITP: | Ion Transport Peptide |
| <i>jet</i> /JET: | Jetlag |
| LD: | Light:Dark |

| | |
|-------------------------------|---------------------------------------|
| LED: | Light-Emitting Diode |
| LL: | Constant light (Light:Light) |
| l-LN _v s: | large ventrolateral neurons |
| LN _d s: | dorsolateral neurons |
| LN _s : | Lateral Neurons |
| LPN: | Lateral Posterior Neurons |
| LRR: | Leucine-rich repeat |
| <i>luc</i> /LUC: | Luciferase |
| M: | Morning (peak, oscillator or neurons) |
| MB: | Mushroom body |
| mCRY: | Mammalian cryptochrome |
| mPER: | Mammalian period |
| mRNA: | messenger RNA |
| MSG: | Mixed Sex Group |
| MT: | Malpighian tubules |
| NLS: | Nuclear localisation sequence |
| NMO: | Nemo |
| NOCTE: | no circadian temperature entrainment |
| <i>norpA</i> / <i>norpA</i> : | no receptor potential A |
| NPF: | Neuropeptide F |
| OL: | Optic lobe |
| <i>ort</i> /ORT: | Ora transientless |
| PAR: | Proline and Amino acid Rich Domain |
| PAS: | Per-Arnt-Sim domain |
| <i>Pdf</i> /PDF: | Pigment Dispersing Factor |
| <i>Pdfr</i> /PDFR: | Pigment Dispersing Factor Receptor |
| <i>Pdp1ε</i> /PDP1ε: | PAR-domain protein 1ε |
| <i>per</i> /PER: | Period |
| PG: | Prothoracic gland |
| PHD: | Photolyase homology domain |
| PI: | Pars Intercerebralis |

Definitions and Abbreviations

| | |
|----------------------|--|
| PIP ₂ : | Phosphatidylinositol 4, 5 bisphosphate |
| POT: | Posterior optic tract |
| PP1: | Protein phosphatase 1 |
| PP2a: | Protein phosphatase 2a |
| R: | Rhythmic |
| R1-8: | Photoreceptors cells of the Compound eye |
| RAE: | Relative amplitude error |
| RAM: | Ramshackle |
| Rh: | Rhodopsin |
| RHT: | Retinohypthalamic tract |
| RISC: | RNA-Induced Silencing Complex |
| RLD: | Red Light:Dark |
| RNAi: | RNA interference |
| ROI: | Region of interest |
| RPM: | Radical pair mechanism |
| RR: | Constant red-light (Red:Red) |
| RRP: | Relative rhythmic power |
| SCF: | Skp1/Cullin/F-box protein |
| SCN: | Suprachiasmatic nucleus |
| SCRIP: | Spin correlated radical pair |
| SFF: | Spontaneous firing frequency |
| SGG: | Shaggy |
| SLIMB: | Supernumerary limb |
| s-LN _v s: | small ventrolateral neurons |
| sNPF: | small Neuropeptide F |
| SSF: | Single Sex group of Females |
| SSM: | Single Sex group of Males |
| τ : | tau, period length |
| TH: | Tyrosine hydroxylase |
| <i>tim</i> /TIM: | Timeless |
| TTFL: | Transcription-translation feedback loop |

| | |
|-----------------|---------------------------------|
| <i>TUG:</i> | <i>tim(UAS)-Gal4</i> |
| UAS: | Upstream Activation Sequence |
| UPS: | Ubiquitin-Proteasome System |
| UV: | Ultraviolet |
| WR: | Weakly rhythmic |
| WT: | Wild-type |
| V/P box: | VRI/PDP1 box |
| VGLUT: | Vesicular glutamate transporter |
| VIP : | Vasoactive intestinal peptide |
| <i>vri/VRI:</i> | Vrille |
| ZT: | Zeitgeber Time |

Chapter 1: Review of the Literature

The purpose of this project has been to further our understanding of how light impacts the underlying molecular oscillatory mechanism that governs circadian rhythmicity in the fruit fly, *Drosophila melanogaster*. This chapter therefore aims to review the existing literature regarding circadian rhythms in *Drosophila* with a particular focus on light-dependent plasticity of molecular and behavioural rhythmicity.

1.1 Overview of Circadian Rhythms

The rotation of the Earth around its axis with respect to the Sun generates rhythmic fluctuations of light and temperature that cycle with ~24 h periodicity. Continued exposure to predictable environmental cycles favoured the formation of endogenous time-keeping mechanisms, or 'clocks' that drive daily rhythms in physiology and behaviour (Panda, Hogenesch and Kay, 2002). These clocks and their rhythmic outputs were termed circadian, derived from the Latin for about (*circa*) a day (*diem*) (Halberg *et al.*, 2003). As well as circadian rhythms, ultradian (< 24 h), infradian (> 24 h) and circannual/seasonal (~1 year) rhythms make up the broader field of Chronobiology (Wollnik, 1989); however the circadian clockwork mechanism is the focal point of this project.

Circadian clocks are abundant in nature and highly diverse; however all possess three canonical properties that define circadian rhythmicity (Pittendrigh, 1954; Dunlap, Loros and DeCoursey, 2004):

1. **Display self-sustained ~24 h rhythms in the absence of external stimuli.** As the clock is cycling on its own this is termed 'free-run' which in *Drosophila* is traditionally assayed in constant darkness (DD) at constant temperature. Lack of rhythmicity in DD is indicative of a dysfunctional clockwork.
2. **Can receive and respond to external stimuli in order to synchronise, or entrain, physiology to the environment.** Light and temperature provide reliable time-of-day information to the clock and act as potent entrainment cues, termed zeitgebers (*German: time givers*) (Aschoff, 1960). Light is the strongest and most reliable zeitgeber, with predictable daily cycles of light and dark resulting from the diurnal cycle of night and day (Hardin, 2011). The impact of light on circadian clock function and entrainment is discussed in detail in 1.2.5; with the effects of

Chapter 1:

temperature and other zeitgebers capable of synchronising clocks discussed in 1.2.5.4.

Zeitgeber time (ZT) is commonly used to indicate the presence of an external stimuli where ZT0 denotes the onset of the stimuli i.e. in a equinox 24 h Light:Dark (LD) cycle with 12 h of light and 12 h of dark, ZT0 represents 'lights-on' and ZT12 is 'lights-off'.

3. **Possess a mechanism capable of compensating for changes in temperature.** The rate/speed of the molecular oscillations that underlie circadian rhythmicity, and therefore the resultant period lengths, do not vary greatly with changing temperature (Pittendrigh, Bruce and Kaus, 1958; Pittendrigh, 1954; Huang, Curtin and Rosbash, 1995). Paradoxically circadian clocks can both compensate for and entrain to changes in temperature (1.2.5.4).

Circadian clocks provide a cell-autonomous and self-sustaining mechanism of keeping biological time which in *Drosophila*, and many other organisms, is driven by a core circadian transcription-translation feedback loop (TTFL), resulting in rhythmic oscillations of gene expression (Hardin, Hall and Rosbash, 1992; Zeng, Hardin and Rosbash, 1994), explained in detail in 1.2.3.

1.1.1 Key principles in circadian biology

As circadian clocks generate daily oscillations, circadian rhythms can be represented by a simple sine wave. Using this representation, some key principles of circadian biology which are used to assess clock function and entrainment can be identified i.e. period, phase and amplitude (**Figure 1.1**).

- **Period Length** – Peak-to-peak interval i.e. the time between peaks in protein/gene expression or behaviour. By definition circadian period lengths are ~24 h in DD but can vary in the presence of environmental cycles e.g. an LD cycle, indicating entrainment.
- **Phase** – The relationship between a given rhythm and a stable entrainment condition i.e. timing of a rhythmic peak/trough relative to an LD cycle. Phase relationships may be altered with varying entrainment conditions.
- **Amplitude** – Magnitude of a given peak or trough i.e. level of relative expression at any given time-point. Amplitude can also be indicative of the strength of an oscillation i.e. a robust rhythm will likely have a high amplitude.

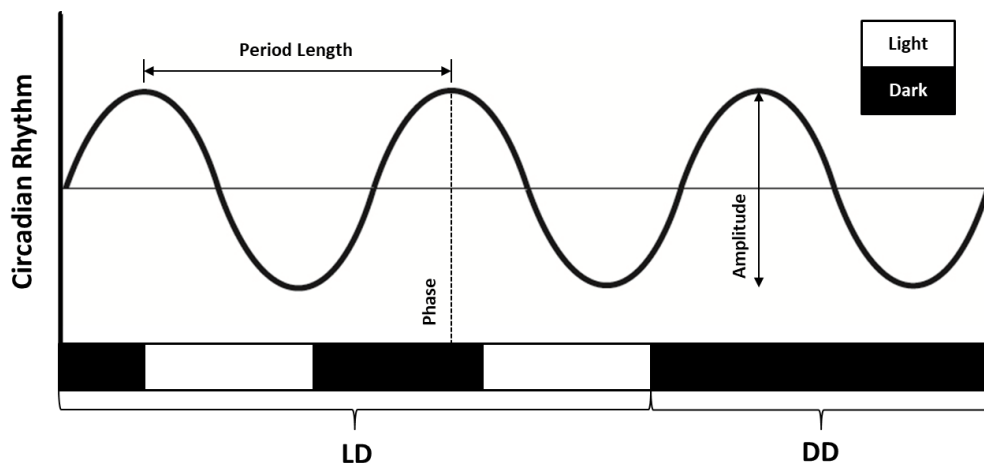


Figure 1.1 Key principles in circadian biology.

Adapted from Bell-Pedersen *et al.* (2005). Representation of a circadian rhythm modelled by a sine wave to highlight key aspects of circadian biology; period length, phase and amplitude (discussed in 1.1.1). LD – Light:Dark, indicates an entrainment condition with a cycle of light (white boxes) and dark (black boxes). DD – Constant Darkness, indicates a free running condition used to assay fundamental clock function.

1.1.2 Historical research and evolutionary relevance of circadian rhythms

The first documentation of circadian rhythms in scientific literature followed the observations by the French astronomer de Mairan, who noted that daily leaf movement of the heliotrope plant (likely *Mimosa pudica*) persisted in constant darkness (de Mairan, 1729); however, initial observations of daily leaf movement date back to ~400 BC (McClung, 2006). Two hundred years later, Edwin Bünning determined the intrinsic period length of bean plants and showed that periodicity was hereditary (Bünning, 1935). Colin Pittendrigh's analysis of *Drosophila* eclosion rhythms and investigations into how these rhythms were affected by environmental changes, helped to define the fundamental characteristics of circadian rhythmicity (1.1.1) (Pittendrigh, 1954; Pittendrigh, Bruce and Kaus, 1958). In the 1960's, Jürgen Aschoff's investigation into human rhythmicity in the absence of external stimuli showed that endogenous rhythms in humans exhibit a periodicity slightly longer than 24 h (Aschoff, 1960). The aforementioned work led to Pittendrigh, Aschoff and Bünning being considered as the co-founders of the field of Chronobiology. The 1960's also saw the discovery of circadian rhythms in many microscopic organisms, both prokaryotic and eukaryotic, including *Neurospora crassa* (fungus), *Chlamydomonas* (green algae) and cyanobacteria (Baker, Loros and Dunlap, 2012; Matsuo and Ishiura, 2010; Golden *et al.*, 1997).

Chapter 1:

Observations of circadian rhythmicity in a diverse range of organisms, of varying complexity, suggests a high level of conservation between the underlying circadian clock mechanisms (Bhadra *et al.*, 2017). The first mechanistic insights were gained by the pioneering experiments of Ron Konopka and Seymour Benzer who, following on from the work of Pittendrigh, began to unpick the genetic basis of circadian rhythmicity in *Drosophila* (Konopka and Benzer, 1971), detailed in 1.2.3.1. The work of Konopka and Benzer instigated a surge of research into the *Drosophila* molecular oscillator which eventually earned Hall, Rosbash and Young the 2017 Nobel Prize in Physiology or Medicine (Young, 2018; Huang, 2018).

The importance of circadian timekeeping is evident as circadian clockwork mechanisms are well conserved across a wide range of taxa, from bacteria to humans (Bhadra *et al.*, 2017). Life has evolved in the presence of daily cycles of light and dark and an ability to anticipate daily environmental changes and entrain physiology greatly contributes to the fitness and survival of an organism, and therefore provides an evolutionary advantage (Helfrich-Förster, 2005; Allada and Chung, 2010). Advantages conferred by the synchrony of endogenous clocks and the environment are well documented with examples including improved Darwinian fitness in flies and cyanobacteria; and increased photosynthesis and growth in plants (Beaver *et al.*, 2002; Dodd *et al.*, 2005; Bhadra *et al.*, 2017). Many behavioural and physiological processes such as sleep-wake behaviour, body temperature, heart rate, blood pressure and hormone secretion exhibit a ~24 h rhythm in humans and other higher order organisms. Disruption of circadian rhythmicity and entrainment has been shown to have severe effects of human physiology and wellbeing (1.1.4).

1.1.3 Circadian rhythms in mammals

The suprachiasmatic nucleus (SCN), located above the optic chiasm in the anterior hypothalamus, is composed of around ~20,000 clock containing neurons and is the master oscillator that governs circadian rhythmicity in mammals (Mohawk, Green and Takahashi, 2012; Hastings, Brancaccio and Maywood, 2014; Evans, 2016). The mammalian molecular oscillator is also a TTFL which exhibits striking similarity to that of *Drosophila*, detailed in (1.2.3.2). The SCN receives direct light input via specialised non-visual photoreceptors in the retina, called intrinsically photoreceptive retinal ganglion cells (ipRGCs), which express the novel photopigment melanopsin. ipRGCs signal photic stimuli to the SCN via the retinohypthalamic tract (RHT) to mediate light entrainment (Hastings, Brancaccio and Maywood, 2014; Mohawk, Green and Takahashi, 2012; Ruby *et al.*, 2002; Do and Yau, 2010). In the absence of light the SCN cycles autonomously, visual light input therefore acts to synchronise the SCN clock with the solar cycle (Hastings, Brancaccio and Maywood, 2014).

A synchronous circuit is able to generate more robust and precise rhythms than isolated neurons. Synchrony across the SCN circuit is achieved via paracrine signalling between clock neurons using vasoactive intestinal peptide (VIP) (Evans, 2016; Hastings, Brancaccio and Maywood, 2014). Temporal information from the SCN is relayed to numerous clocks residing in peripheral tissues such as the liver, adipose tissue, skeletal muscle and the heart (Hastings, Brancaccio and Maywood, 2014; Mohawk, Green and Takahashi, 2012) using a plethora of mechanisms including autonomic innervation, humeral signalling, and regulation of body temperature (Mohawk, Green and Takahashi, 2012). In many cases, the absence of the SCN results in desynchrony of peripheral oscillators (Yoo *et al.*, 2004), indicating that some peripheral clocks are ‘slave’ to the ‘master’ clock as they rely on SCN input to entrain to the environment.

As well as innervation from the master oscillator in the brain, mammalian peripheral clocks receive ‘local’ input that can modulate function and, in some cases, even result in the uncoupling of peripheral oscillators from SCN control (Mohawk, Green and Takahashi, 2012; Albrecht, 2012). Behavioural processes such as locomotion or feeding, which are co-ordinated by the SCN, impact on local endocrine signalling and body temperature. It has been shown that altered feeding patterns can affect the phase relationship between the clocks residing in the liver and the brain i.e. the clocks in the two tissues are no longer synchronous (Damiola *et al.*, 2000; Albrecht, 2012). This suggests that changes in metabolism can influence rhythmicity without input from the SCN, showing not all peripheral clocks are ‘slave’ to the SCN.

Although this project focuses on *Drosophila*, there is remarkable homology between the molecular oscillators in flies and mammals. Parallels and differences in both oscillator function and light-dependent entrainment will be presented throughout this thesis.

1.1.4 Impact of circadian desynchrony on human physiology and well-being

Humans are a diurnal species; however chronotype is highly variable across the population. Chronotype is governed by the circadian clock and is a measure of an individual's preferred timing of sleep/wake activity, often leading to categorisation into either a “morning” or “evening” person (Horne and Östberg, 1977; Wittmann *et al.*, 2006). Circadian rhythmicity and entrainment often goes unnoticed, but when disrupted can have detrimental impacts on human physiology and well-being. Modern society provides many opportunities to oppose one's internal rhythm e.g. the use of artificial lighting and light-emitting devices late at night or trans-meridian travel (Foster and Wulff, 2005; Tähkämö, Partonen and Pesonen, 2019), with the latter resulting the archetypal example of circadian disruption, jet-lag. Travelling across time-zones results in the misalignment

Chapter 1:

of endogenous clocks with each other and the environment which manifests as symptoms including tiredness, mental confusion and dysphoria (Hastings, Brancaccio and Maywood, 2014), until a time when synchrony is regained.

Epidemiological studies have revealed a significant link between clock disruption as a consequence of shift-work and increased risk of pathophysiologies including cancer, cardiovascular disease and neurodegenerative disease (Hastings, Reddy and Maywood, 2003; Stevens *et al.*, 2007; Musiek, 2015). Furthermore, the incidence of cardiovascular events i.e. myocardial infarction, ventricular tachycardia and sudden death, have been shown to exhibit daily fluctuations in a time-of-day-dependent manner (Dominguez-Rodriguez *et al.*, 2010). Circadian timekeeping also plays a key role in metabolic processes i.e. glycogen storage and glycogenesis, as well as detoxification in mammalian systems. As a result, circadian dysfunction has been linked with metabolic conditions such as obesity and diabetes (Levi and Schibler, 2007; Bass and Takahashi, 2010; Albrecht, 2012).

Lack of biological entrainment either with the physical environment or with society i.e. 'Social Jet-lag' due to work patterns or chronotype (Wittmann *et al.*, 2006), have been shown to be a key contributing factor to certain psychiatric conditions including Seasonal Affective Disorder, Bipolar Disorder and Major Depressive Disorder (McClung, 2007; Mansour, Monk and Nimgaonkar, 2005). Genetics studies have highlighted that underlying abnormalities in circadian genes correlate with the increased prevalence of these disorders (Johansson *et al.*, 2003; Benedetti *et al.*, 2003; DeBruyne, Weaver and Reppert, 2007). In addition, some of the conventional treatments for mood disorders include total sleep deprivation and bright light therapy, which act to shift or re-set the patient's circadian clock (McClung, 2007). Work in animal models has shown that light can directly regulate mood-related behaviours and cognitive function; however the mechanism by which light facilitates such affects remains elusive (LeGates *et al.*, 2012).

Clinical researchers are now beginning to utilise circadian rhythmicity in order to either selectively modify peripheral oscillators where aberrant cycling is contributing to a particular disease/condition or as therapeutic tool (Hastings, Reddy and Maywood, 2003). For example, xenobiotic detoxification is circadian regulated, therefore matching drug administration optimally with the circadian cycle could maximise therapeutic effect, thus introducing the concept of chronopharmacology (Levi and Schibler, 2007; Levi *et al.*, 2010). Circadian disruption is associated with many possible deleterious effects on physiology; therefore gaining further understanding of the molecular oscillations that underlie rhythmicity and how these oscillators shift to facilitate entrainment could be of significant benefit.

1.2 Circadian Rhythms in *Drosophila melanogaster*

1.2.1 *Drosophila* as a model organism

Drosophila melanogaster (the fruit fly) has been used as a model organism across biological sciences for over 100 years, contributing key findings in fields ranging from ecology to neuroscience. Fruit flies are still a popular, and appropriate, model organism for circadian research and fulfil the following requirements set out by Ashburner (1989) and Bolker (1995);

- **Cultivation** – Large numbers of flies can be stored easily in a relatively small space. Equipment/reagents needed for fly husbandry are inexpensive and readily available.
- **Development and life-cycle** – New adult offspring can be obtained in ~10 days post egg laying (at 25°C) as a result of fast development and a short life cycle. *Drosophila* are holometabolous insects i.e. they undergo complete metamorphosis, with four distinct life stages; embryo, larva (three instars, L1-3, separated by cuticle moulting with increased size), pupa and adult.
- **Generation size** – A single female can produce hundreds of offspring (allowing large numbers of flies for each assay).
- **Size of organism** – Flies small size aids the ease of storage, however they are large enough to be used in a range of behavioural and molecular assays.
- **Genetics** – The *Drosophila* genome has been sequenced and is relatively simple. Many tools have been developed to manipulate fly genetics i.e. allowing spatial and temporal control over expression with the Gal4/UAS system (3.2) (Brand and Perrimon, 1993).
- **Stock Availability** – In addition to commercial stock centres that allow the purchase/deposition of many stocks, *Drosophila* scientists often generously share stocks. In the eventuality that a stock does not yet exist, new transgenic lines can be generated or existing mutations combined (See Appendix B.).

Parallels can be drawn between the molecular oscillators that drive circadian rhythms in *Drosophila* and many other species. More simplistic clocks, like those of cyanobacteria, regulate rhythmic oscillations in a post-translational manner (Kondo, 2007), whereas higher order organisms keep time via regulation of gene expression. This regulation involves the action of activator and inhibitor proteins and it is these constituent parts that vary in a well-conserved TTFL mechanism (Bell-Pedersen *et al.*, 2005). This high-level of homology identifies *Drosophila* as a powerful model to study circadian biology and should continue to provide insight into the molecular underpinning of rhythmicity in flies, other invertebrates and even mammals.

Chapter 1:

1.2.1.1 Practical applications of invertebrate circadian research

Horticultural pest species such as *Drosophila suzukii* (spotted wing *Drosophila*) and *Putella xylostella* (diamondback moth) decimate soft- and stone-fruit crops and brassicaceous crops, respectively, causing both yield and economic losses (Shaw, Fountain and Wijnen, 2018; Shaw *et al.*, 2018; Sarfraz, Keddie and Dossall, 2005). Research into the behavioural and molecular rhythms of such species may provide more targeted means of pest management (Shaw, Fountain and Wijnen, 2018). Furthermore, studies in *Drosophila melanogaster* have identified daily fluctuations in xenobiotic detoxification enzymes (Hooven *et al.*, 2009), which confer a time-of-day dependent toxicity, termed chronotoxicity. It is therefore possible that pesticide dosage can be timed to coincide with low levels of detoxification enzymes and increase pesticide efficacy (Hooven *et al.*, 2009); therefore findings regarding chronotoxicity in flies may be translatable to other invertebrate pests.

In addition to horticultural pests, there is an increased drive to understand rhythmic behaviours of haematophagous insects i.e. those that feed on blood, which can act as vectors for disease e.g. the *Anopheles* Mosquito in the spread of malaria (Rund *et al.*, 2016). Blood feeding, locomotion and oviposition (egg laying) are all circadian phenotypes; therefore further study and development of new techniques could unveil new therapeutic targets to intervene with such diseases (Meireles-Filho and Kyriacou, 2013).

Finally, a synergistic relationship exists between pollinators and flowering plants e.g. bumble-bees and snap-dragons, where the circadian driven foraging activity of the bee is matched by a rhythmic production and emission of the attractant methyl benzoate, a volatile scent compound (Kolossova *et al.*, 2001). The diurnal rhythms of both organisms peak during the day as to maximise the benefits for both constituents, a relationship that could potentially be utilised to increase crop pollination.

1.2.1.2 Use of *Drosophila* in circadian research

Drosophila display strong behavioural rhythms and protocols, equipment, automated recording systems and analysis programs exist to assay these rhythmic behaviours. This project utilised locomotor behaviour which, as flies are crepuscular organisms, manifests in peaks of activity at dawn and dusk separated by a midday siesta, discussed in more detail in 1.2.4.2 (Konopka and Benzer, 1971; Hamblen-Coyle *et al.*, 1992). Patterns in behavioural output are co-ordinated centrally by clocks residing in the fly brain; the anatomy and network organisation of the circadian circuitry is well characterised and can therefore be utilised to assess the molecular clock-work in

distinct clock-cell clusters, which are defined in 1.2.4.1. Furthermore, molecular rhythmicity in peripheral tissues was also assayed via *in vivo* luciferase assays (Plautz *et al.*, 1997b; Stanewsky *et al.*, 1997), a technique used across circadian research which has elucidated key characteristics of circadian rhythmicity, most notably the identification of the blue-light photoreceptor CRYPTOCHROME (CRY), discussed in 1.2.5.1. In addition, more standard biochemical techniques can be used to assay the molecular clock in flies with qRT-PCR and Western Blotting used to analyse transcript and protein cycling respectively, both of which show rhythmic oscillations (1.2.3). *Drosophila* also show rhythms in many other processes that are not explored in this project, including olfaction (Krishnan, Dryer and Hardin, 1999), feeding (Xu, Zheng and Sehgal, 2008), courtship (Roche, Talyn and Dowse, 1998) and mating (Sakai and Ishida, 2001); confirming that *Drosophila* is a powerful, useful and appropriate model organism for circadian research.

1.2.2 Central and Peripheral Oscillators in *Drosophila*

Clock containing cells are found in both the *Drosophila* brain (central) as well as in many peripheral tissues including the antenna, compound eye and internal reproductive and digestive organs (reviewed by Ito and Tomioka, 2016). *Drosophila* peripheral clocks are heterogeneous in nature and partake in a wide range of physiological processes, and unlike mammalian peripheral clocks (1.1.3), they largely function autonomously i.e. without central clock input (Ito and Tomioka, 2016). The majority of this chapter will focus on the central clocks of the fly brain (1.2.3-1.2.7); however any similarities and differences between molecular oscillations and light-dependent entrainment of peripheral clocks, as well as the communication between central and peripheral oscillators, are detailed in 1.2.8.

1.2.3 The *Drosophila* Molecular Oscillator

1.2.3.1 Key components of the molecular clockwork

Konopka and Benzer's ground-breaking work, using *Drosophila*, led to the identification of the first clock gene (Konopka and Benzer, 1971). Using ethyl methanesulfonate to introduce random genetic mutations, Konopka generated hundreds of mutant fly lines. A genetic screen of these mutants was conducted by assaying clock-dependent eclosion, the emergence of an adult fly from the pupa case, which occurs rhythmically in the first few hours following dawn and persists in DD (Pittendrigh, 1954). Most mutant lines still exhibited a ~24 h free-running periodicity in eclosion, however there were three exceptions. One mutant had a short ~19 h period, one a longer ~28 h period and a third displayed arrhythmic eclosion i.e. no rhythm at all. These three mutations

Chapter 1:

mapped to the same locus on the X-chromosome and affected the same gene, which was consequently named *period* (*per*) (Konopka and Benzer, 1971). The mutants were named *per^s* (short), *per^l* (long) and *per⁰* (null) respectively, with the first two the result of independent missense point mutations and the last a nonsense point mutation. The landmark discovery of *Drosophila period* gene and its role in circadian time-keeping paved the way for the unravelling of the molecular oscillator responsible for circadian rhythmicity.

Technical advances in the early 1980's allowed *per* gene to be isolated, cloned and used to rescue rhythmicity in arrhythmic *per⁰¹* mutants (Bargiello and Young, 1984; Bargiello, Jackson and Young, 1984; Reddy *et al.*, 1984; Zehring *et al.*, 1984). As a result of this pioneering work, circadian cycling in *per* mRNA and PERIOD (PER) protein was demonstrated in the in the fly brain (Hardin, Hall and Rosbash, 1990; Siwicki *et al.*, 1988). It was also observed that PER protein is required for *per* mRNA cycling (Hardin, Hall and Rosbash, 1990; Zeng, Hardin and Rosbash, 1994), with this regulation a result of PER being a transcriptional repressor (Hardin, Hall and Rosbash, 1992). Furthermore, PER localisation is predominantly nuclear showing that it must be shuttled between the cytoplasm and nucleus (Liu *et al.*, 1992). Together these findings suggested that *period* contributed to circadian rhythmicity via a feedback loop in which PER protein regulates rhythmic *per* transcription. This led to the development of the transcription-translation feedback loop (TTFL) model of molecular clock function.

Further genetic screens identified many clock genes including those now known to be involved in the TTFL; *timeless* (*tim*) (Sehgal *et al.*, 1994), *Clock* (*Clk*) (Allada *et al.*, 1998) and *cycle* (*cyc*) (Rutila *et al.*, 1998); discussed in 1.2.3.2. A direct interaction between TIMELESS (TIM) and PER proteins was revealed via a screen for PER binding partners, with TIM binding to a Per-Arnt-Sim (PAS) domain in PER, which often have a role in dimerisation (Gekakis *et al.*, 1995). Analysis of the *per* promoter identified a canonical E-box element (5'-CACGTG-3') required for transcription of *per* (Hao, Allen and Hardin, 1997). This E-box sequence is highly conserved in circadian regulated genes in many species, however the E-box element alone cannot generate rhythmic transcription (Hardin, 2004; Hardin, 2011; Hao, Allen and Hardin, 1997). CLOCK (CLK) and CYCLE (CYC) are both basic-Helix-Loop-Helix-PAS (bHLH-PAS) transcription factors, which bind to E-box elements and drive transcription (Gekakis *et al.*, 1995; Rutila *et al.*, 1998). The precise interplay between these four key components, with some additional regulation, forms a cell autonomous core TTFL which is fundamental to circadian rhythmicity (1.2.3.2) (**Figure 1.2**).

1.2.3.2 The core circadian feedback loop

Circadian rhythms are generated via a delayed negative TTFL driven by molecular oscillations in core clock mRNA transcripts and their subsequent proteins products, as alluded to in 1.2.3.1 (Hardin *et al.*, 2003; Allada and Chung, 2010; Hardin, 2011).

CLK and CYC bind to form a heterodimeric transcription factor (CLK/CYC) which then binds the conserved 'circadian' enhancer element (E-box) found in the promotor region of many clock controlled genes; including two key circadian clock genes *per* and *tim*, as previously mentioned (1.2.3.1) (**Figure 1.2**) (Hardin, Hall and Rosbash, 1990; Hao, Allen and Hardin, 1997; Allada *et al.*, 1998; Rutila *et al.*, 1998; Bell-Pedersen *et al.*, 2005; Konopka and Benzer, 1971; Sehgal *et al.*, 1994). CLK/CYC binding drives transcription of *per* and *tim* from ~ZT4 to ~ZT18 with peak transcription at ~ZT16, where ZT0/12 represents 'lights-on/lights-off' respectively in the context of a 24 h LD cycle with 12hL:12hD (1.1) (Allada *et al.*, 1998; Rutila *et al.*, 1998; Darlington *et al.*, 1998; Hardin, 2004; Zheng and Sehgal, 2008). Cytoplasmic accumulation of PER and TIM proteins is seen at the start of the dark phase (~ZT12), 6-8 h post initial transcription of their respective mRNAs (see reviews by Hardin (2005); Zheng and Sehgal (2008); Allada and Chung (2010) and Hardin (2011)). PER and TIM begin to dimerise in the early night, with TIM binding to the PAS domain of PER (Gekakis *et al.*, 1995; Saez and Young, 1996), and when protein levels peak around midnight (~ZT18), the PER/TIM heterodimer translocates to the nucleus (**Figure 1.2**) (Shafer, Rosbash and Truman, 2002; Sathyanarayanan *et al.*, 2004; Yu and Hardin, 2006; Fang, Sathyanarayanan and Sehgal, 2007).

TIM performs two major functions: firstly it stabilises PER, which is inherently prone to degradation (Price *et al.*, 1995); and secondly targets and facilitates nuclear uptake of the PER/TIM heterodimer via a nuclear localisation sequence (NLS) residing in the TIM protein (Saez *et al.*, 2011). TIM NLS mutagenesis studies indicated that the NLS is a key determinant in nuclear accumulation of TIM and PER (Saez *et al.*, 2011), with mutations within the NLS decreasing nuclear localisation and resulting in increased cytoplasmic accumulation of PER/TIM and an extension of the circadian period length to ~30hrs (Saez *et al.*, 2011). Stabilisation of PER by TIM, along with action of kinases and phosphatases (discussed in 1.2.3.2.1), act to delay the clockwork in order to generate a molecular oscillator with a near 24 h periodicity, far longer than would be expected for a standard TTFL.

Once nuclear, PER inhibits CLK/CYC DNA binding and transcriptional activity in the late night (~ZT18 to ~ZT4) (**Figure 1.2**), resulting in a reduction in *per* and *tim* transcription (Lee, Bae and

Chapter 1:

Edery, 1999; Bae *et al.*, 2000; Yu and Hardin, 2006; Menet *et al.*, 2010). TIM is rapidly degraded at ZT0 following lights-on (see 1.2.5 for mechanism of light-dependent TIM degradation) (Hunter-Ensor, Ousley and Sehgal, 1996; Myers *et al.*, 1996; Zeng *et al.*, 1996), reducing PER stability and allowing progressive phosphorylation and subsequent proteasomal degradation of PER ~ZT4 (1.2.3.2.1) (Naidoo *et al.*, 1999; Kloss *et al.*, 2001; Grima *et al.*, 2002; Ko, Jiang and Edery, 2002). As TIM degradation is light-dependent and PER degradation is indirectly coupled to light, minimum levels are seen at the end of the light phase; however, rhythmic PER and TIM expression is maintained in DD (Zerr *et al.*, 1990; Curtin, Huang and Rosbash, 1995; Shafer, Rosbash and Truman, 2002). Degradation of PER and TIM alleviates CLK/CYC inhibition thus allowing a new cycle of *per* and *tim* transcription and translation.

CLK/CYC drives transcription of *per/tim* which, following translation and additional regulation, inhibit their own transcription; CLK/CYC and PER/TIM are therefore considered the positive and negative arms of the clockwork respectively. The core circadian clockwork mechanism of *Drosophila* is very well characterised and shares a high degree of similarity to mammalian clocks. Where variation does exist, it is between the constituent components of the TTFL (Meyer-Bernstein and Sehgal, 2001; Yu and Hardin, 2006). The positive arm of the mammalian molecular circadian clockwork consists of CLOCK and BMAL1 (a mammalian orthologue of *Drosophila* CYCLE); and the negative arm contains PERIOD, of which there are three homologues (PER1, 2 and 3) (Shearman *et al.*, 1997; Archer *et al.*, 2003), and mammalian CRYPTOCHROME (mCRY), instead of TIM (Ko and Takahashi, 2006).

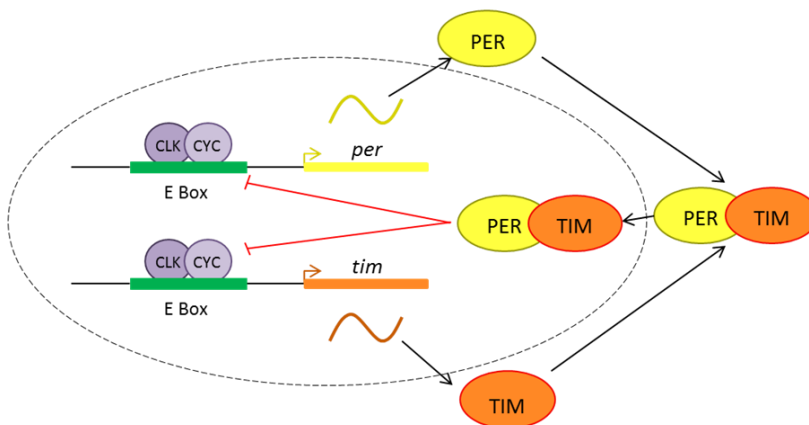


Figure 1.2 The core molecular TTFL that drives circadian rhythms in *Drosophila*.

PER/TIM modulate their own expression by inhibiting the heterodimeric transcription factor CLK/CYC. Indicated elements; CLOCK (CLK), CYCLE (CYC), PERIOD (*per*/PER) and TIMELESS (*tim*/TIM). Italics indicate a gene and all capitals denote a protein. Dashed line denotes the nuclear envelope. Black arrows indicate movement. Red lines indicate repression/inhibition.

1.2.3.2.1 Post-translational regulation of PER, TIM and CLK

To generate a 24 h circadian oscillator, as described in 1.2.3.2, additional regulation is required to delay molecular cycling and stretch the TTFL out over the course of one day. Kinases and phosphatases act to regulate the balance of cytoplasmic and nuclear PER and TIM (Hardin, 2011). DOUBLETIME (DBT), a homolog of CASEIN KINASE 1 ϵ (Kloss *et al.*, 1998; Price *et al.*, 1998), phosphorylates PER promoting phosphorylation-dependent degradation, thus destabilising PER and contributing to the lag in PER accumulation following expression (Zeng *et al.*, 1996; Curtin, Huang and Rosbash, 1995; Gekakis *et al.*, 1995). TIM binds and stabilises PER, resulting in the build-up of DBT-PER-TIM complexes, whereby TIM and DBT are working antagonistically to regulate PER levels (Price *et al.*, 1995). Nuclear localisation is promoted via the phosphorylation of PER-DBT by CASEIN KINASE 2 (CK2) (Akten *et al.*, 2003) and TIM by SHAGGY (SGG), a homologue of mammalian glycogen synthase kinase 3 β (Martinek *et al.*, 2001). Two phosphatases act to oppose the action of the aforementioned kinases, PROTEIN PHOSPHATASE 2a (PP2a) and PROTEIN PHOSPHATASE 1 (PP1) cleave phosphates from PER and TIM respectively, increasing stability and regulating nuclear localisation (Fang, Sathyanarayanan and Sehgal, 2007; Sathyanarayanan *et al.*, 2004).

PER carries DBT into the nucleus where PER-DBT binds to and promotes the phosphorylation of CLK, reducing CLK/CYC binding affinity for the E-box, downregulating *per* and *tim* transcription (Menet *et al.*, 2010; Kloss *et al.*, 2001). DBT is required for CLK phosphorylation (Yu *et al.*, 2006; Kim and Edery, 2006; Yu *et al.*, 2009), however DBT does not phosphorylate CLK directly and is therefore thought to have a non-catalytic role (Yu *et al.*, 2009). CLK phosphorylation is thought to be mediated by multiple, mostly unidentified, kinases. NEMO (NMO) is one such kinase which has been implicated in CLK phosphorylation and increased NMO function results in decreased CLK levels, and *vice versa*, which affects periodicity as increased and decreased CLK levels shorten and lengthen circadian period respectively (Kadener *et al.*, 2008; Chiu, Ko and Edery, 2011; Yu, Houl and Hardin, 2011). It has been postulated that NMO promotes CLK degradation to slow the circadian cycle; however whether NMO phosphorylates CLK directly or acts in-directly remains unknown (Yu, Houl and Hardin, 2011).

Following light-dependent TIM degradation (1.2.3.2 and 1.2.5.1), the protection of PER conferred by TIM is removed and allows progressive phosphorylation of PER by DBT. Site-specific phosphorylation ultimately leads to PER being bound and ubiquitinated by an F-box E3 ubiquitin ligase, called SUPERNUMERARY LIMB (SLIMB), which targets PER for degradation via the proteasome ~4 h after lights-on (Grima *et al.*, 2002; Ko, Jiang and Edery, 2002; Naidoo *et al.*, 1999;

Chapter 1:

Kloss *et al.*, 2001). After PER degradation, hyper-phosphorylated CLK accumulates and is degraded, or possibly dephosphorylated (Yu *et al.*, 2006; Hardin, 2011); then newly synthesised CLK and CYC, which themselves are circadian regulated (1.2.3.3), hetero-dimerise and initiate a new circadian cycle.

1.2.3.3 Interlocked feedback loops

Unlike *per* and *tim* mRNA cycling, which peaks in the early evening, peak *Clk* mRNA abundance occurs in the early morning (Darlington *et al.*, 1998; Bae *et al.*, 1998). Null mutations in both *period* (*per⁰¹*) and *timeless* (*tim⁰¹*) suppressed *Clk* mRNA rhythms resulting in constant low *Clk* mRNA levels showing that rhythmic *Clk* transcription is dependent on the core circadian TTFL, with PER and TIM acting as possible transcriptional activators (Bae *et al.*, 1998). Another interesting observation came from studies of *Clk^{Jrk}* and *cyc⁰¹* flies, a severe loss-of-function and a null mutant respectively, which have abolished *per* and *tim* cycling (Allada *et al.*, 1998; Rutila *et al.*, 1998). Due to the lack of PER and TIM, it was assumed the *Clk* levels would be low (Bae *et al.*, 1998), this was not the case as peak levels of *Clk* expression were seen in *Clk^{Jrk}* and *cyc⁰¹* flies (Glossop, Lyons and Hardin, 1999), suggesting that CLK/CYC represses *Clk* transcription. A second feedback loop was postulated that interlocked with the core feedback loop and regulates *Clk* mRNA cycling via CLK/CYC binding to E-box elements in genes which modulate rhythmic *Clk* transcription (Glossop, Lyons and Hardin, 1999).

Par-domain protein 1ε (*Pdp1ε*) and *vriille* (*vri*) have E-box elements in their promotor regions and therefore their transcription is activated by CLK/CYC (Blau and Young, 1999; Cyran *et al.*, 2003; Glossop *et al.*, 2003; Zheng *et al.*, 2009). *vri* and *Pdp1ε* transcripts cycle in-phase with *per* and *tim*, which is to be expected due to CLK/CYC activity (1.2.3.2); however peak VRI is seen ~4 h earlier than peak PDP1ε (~ZT14 and 18 respectively) (Blau and Young, 1999; Cyran *et al.*, 2003; Glossop *et al.*, 2003). VRI is a basic-leucine zipper (bZip) repressor which binds to upstream promotor sequences in the *Clk* gene called VRI/PDP1 (V/P) boxes and inhibits *Clk* transcription (Glossop *et al.*, 2003; Cyran *et al.*, 2003). Alongside CLK/CYC inhibition by PER-DBT-TIM complexes (1.2.3.2.1), declining VRI levels permit a new round of *Clk* transcription which is, to some extent, driven by binding of bZip activator PDP1ε to V/P-boxes (Cyran *et al.*, 2003; Zheng *et al.*, 2009). Therefore, PDP1ε and VRI act antagonistically to modulate CLK expression. Consequently CLK expression is in antiphase to PER/TIM expression (Kadener *et al.*, 2008; Kadener *et al.*, 2007) (**Figure 1.3**).

High levels of *Clk* transcription in *Clk^{Jrk}* and *cyc⁰¹* mutants indicates *Clk* expression is constitutively active and independent of clock function (Glossop, Lyons and Hardin, 1999), this calls into

question the impact of PDP1 ϵ in activating *Clk* transcription. However, homozygous *Pdp1 ϵ* mutants show arrhythmic behaviour in LD cycles and DD, as well as much reduced expression of CLK and PER (Zheng *et al.*, 2009). Expression of PDP1 ϵ restores rhythmicity in *Pdp1 ϵ* mutants, however driving CLK expression in the same mutant rescues PER expression but not rhythmicity; together suggesting that PDP1 ϵ functions both in the core molecular oscillator and in output gene expression (Benito, Zheng and Hardin, 2007; Zheng *et al.*, 2009). It isn't know whether or not VRI is required for oscillator function as null mutants are not viable, however this could suggest a role for VRI in regulating rhythmic expression of output genes, similar to PDP1 ϵ (Cyran *et al.*, 2003).

CLK/CYC also drives expression of the bHLH-orange transcriptional repressor CLOCKWORK ORANGE (CWO) via E-box binding (Kadener *et al.*, 2007; Lim *et al.*, 2007; Matsumoto *et al.*, 2007), introducing a second interlocked feedback loop. CWO is a competitive inhibitor for CLK/CYC, binding at the same site in the E-box, thus reinforcing and potentiating existing inhibition of CLK/CYC by PER-DBT (1.2.3.2.1) (Kadener *et al.*, 2007) (**Figure 1.3**). Furthermore, CWO impacts *Clk* transcription via modulating CLK/CYC-dependent *vri* and *Pdp1* expression. It has been proposed that CWO imposes an adjustable threshold on E-box transcriptional activity as *cwo* mutants have lower levels of *per*, *tim*, *vri* and *Pdp1 ϵ* implying that CWO is necessary for high-level of CLK/CYC controlled gene transcription (Lim *et al.*, 2007; Matsumoto *et al.*, 2007).

Clk and *per/tim* mRNA cycle in antiphase to each other and as such you could assume they are of equal importance to circadian rhythms, but this is not the case (Hardin, 2006). PER-DBT represses transcription of VRI via CLK/CYC inhibition, therefore the *per/tim* loop can regulate *Clk* expression. Also, if you were to reverse *Clk* mRNA cycling i.e. now in-phase with *per/tim* mRNA cycling, little effect is seen on behavioural and molecular rhythms of *Drosophila* (Yu and Hardin, 2006; Kim *et al.*, 2002).

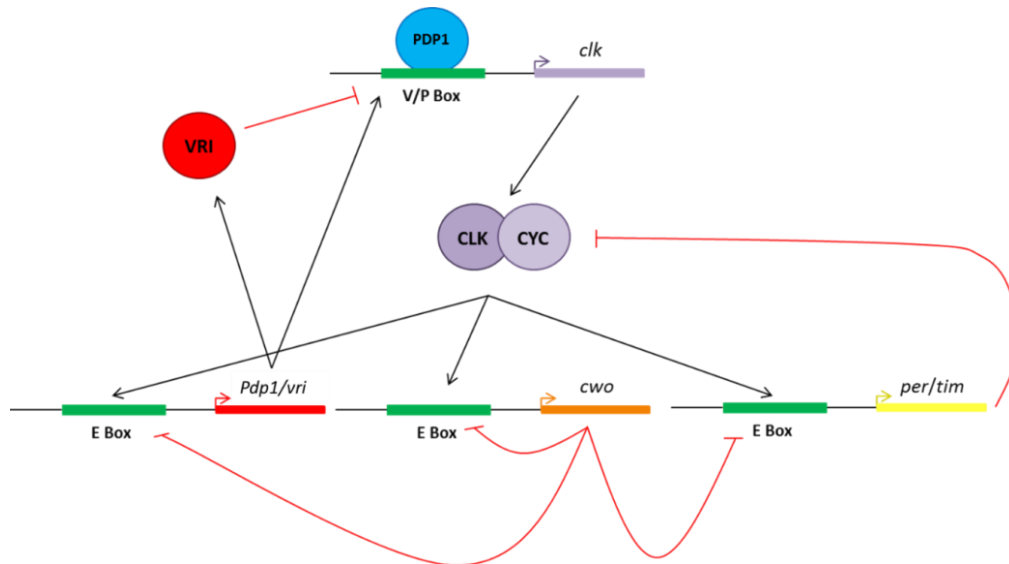


Figure 1.3 *Clk*-dependent feedback loops which interlock with the core molecular oscillator. CLK/CYC binds to E-box elements in the promotor region of many genes including *per*, *tim*, *vri*, *Pdp1* and *cwo*, and activates transcription. *per* and *tim* partake in the core molecular TTFL where PER/TIM inhibits CLK/CYC transcriptional activity (**Figure 1.2**). *vri* and *Pdp1* act antagonistically to regulate *Clk* transcription. *cwo* is a competitive inhibitor of CLK/CYC and binds to E-boxes repressing CLK/CYC mediated transcription. Indicated elements: CLOCK (*Clk*/CLK), CYCLE (CYC), PERIOD (*per*), TIMELESS (*tim*/TIM), VRILLE (*vri*/VRI), PAR-DOMAIN PROTEIN 1 (*Pdp1*/PDP1) and CLOCKWORK ORANGE (*cwo*/CWO). Italics indicate a gene and all capitals denote a protein. Red lines indicate repression/inhibition.

1.2.4 *Drosophila* Central Clock Circuitry

The key anatomical characteristics of the cells which constitute the central circadian circuitry are detailed in 1.2.4.1 with the first insights into how these clock cells generate a behavioural output presented in 1.2.4.2. An appreciation of circadian network organisation and the resultant behavioural output is required for section 1.2.5; however further insights regarding communication and integration across the circuitry are discussed in 1.2.6.

1.2.4.1 Clock cell clusters and network organisation

Approximately 150 neurons in the *Drosophila* brain (75 per hemisphere) express the core clock genes *per*, *tim*, *cyc* and *Clk*, generating a functional cell autonomous core molecular oscillator and identifying these cells as clock neurons (Helfrich-Förster, 2004; Lear, Zhang and Allada, 2009; Förster, 2010). Besides these 150 neurons, PER and TIM cycling is seen in some *Drosophila* glial cells, and although not categorised as ‘clock cells’ it is thought that such glia help modulate circadian rhythms (Jackson, 2011).

Clock neurons are classified into distinct subsets based on anatomical location and function (**Figure 1.4**). Brain hemispheres are separated in the sagittal plane and the location of cell subsets are defined by their position in the coronal (anterior-posterior) and horizontal (ventral-dorsal) planes. These subsets are broadly divided into lateral neurons (LNs) and dorsal neurons (DNs), which are further classified into: ventrolateral neurons (LN_vs); dorsolateral neurons (LN_ds); lateral posterior neurons (LPNs); and three distinct groups of dorsal neurons (DN1s, DN2s and DN3s) (Förster, 2010). The key features of each clock cell cluster are as follows;

- **LN_vs** – There are approximately 10 LN_vs per hemisphere which are further subdivided into the 5 small- and 3-5 large-LN_vs (s- and l-LN_v respectively), named due to the size of the soma. s- and l-LN_v cell bodies are located in the central brain, close to the optic lobe, and can be distinguished not only by soma size but also by their characteristic axonal and dendritic projection patterns (Kaneko, 1998; Kaneko and Hall, 2000). All LN_vs, except the 5th s-LN_v, express the neuropeptide Pigment Dispersing Factor (PDF) which plays a key role in synchronisation across the clock circuit (detailed in 1.2.6.1.1) (Renn *et al.*, 1999; Stoleru *et al.*, 2005).
 - **s-LN_vs** - The 4 PDF-positive s-LN_vs send projections to dorsal and ipsilateral brain regions as well as to the accessory medulla (aMe), a neuropil in the optic lobe with proposed circadian function in insects (Helfrich-Förster, Stengl and Homberg, 1998; Loesel and Homberg, 2001; Helfrich-Förster *et al.*, 2007). Dorsal projections arborize and contact the DN1s, specifically the DN1_ps, and the LN_ds (Gorostiza *et al.*, 2014); and are subject to circadian remodelling displaying a daily pattern in arborisation complexity i.e. axonal termini expand in the morning and contract in evening (Fernández, Berni and Ceriani, 2008).
 - **l-LN_vs** – Project to ipsilateral and contralateral brain regions, with the contralateral fibres traversing the brain via the posterior optic tract (POT). l-LN_vs also project to the aMe and have extensive arborisations in the optic lobe (Helfrich-Förster *et al.*, 2007).
 - **5th s-LN_v** – Is genetically distinct from other LN_vs and does not express PDF. The 5th s-LN_v cell body is often located amongst those of the l-LN_vs and 5th s-LN_v dorsal projections extend to the opposite brain hemisphere (Schubert *et al.*, 2018).
- **LN_ds** - Each hemisphere has 6 LN_ds located close to the optic lobe, like the LN_vs, but towards the dorsal brain (Helfrich-Förster, 2005; Helfrich-Förster *et al.*, 2007). LN_ds project to the dorsal part of the brain, with some projections looping around the anterior optic tract (AOT) and extending to the opposite hemisphere through the dorsal-fusion-commissure (DFC). LN_ds also project to the aMe via both ipsi- and contralateral projections (Helfrich-Förster *et al.*,

Chapter 1:

2007). The LN_s are a diverse cluster of neurons with varying expression profiles of clock-related genes which further define distinct LN_s subgroups (see 1.2.5.1 and 1.2.6.1) (Beckwith and Ceriani, 2015).

- **LPNs** – The LPNs are the least well characterised of all the clock neurons. There are 3-4 LPN cell bodies per hemisphere located in the posterior brain which have been shown to be receptive to temperature cues (Kaneko and Hall, 2000; Shafer *et al.*, 2006; Busza, Murad and Emery, 2007).
- **DNs** - The DNs are a heterogeneous group of neurons located in the dorsal brain and divided into three subgroups based on anatomical and genetic differences.
 - **DN1s** – There are approximately 16-20 DN1 cells per hemisphere which are further divided into anterior and posterior, DN1_as and DN1_ps respectively, based on their anatomical location (Shafer *et al.*, 2006; Lear, Zhang and Allada, 2009; Zhang *et al.*, 2010a). DN1_ps make up the majority of the DN1s and have been shown to contact and modulate s-LN_v activity (Zhang *et al.*, 2010a; Zhang *et al.*, 2010b). It is also thought that the DN1s play a key role in transducing clock circuit function to rhythmic output, discussed in detail in 1.2.7 (Cavanaugh *et al.*, 2014; Lamaze *et al.*, 2018; Guo *et al.*, 2018; King and Sehgal, 2018).
 - **DN2s** – Relatively little is known about the expression profile of the DN2s, of which there are only 2 per hemisphere (Shafer *et al.*, 2006; Helfrich-Förster *et al.*, 2007). DN2 projections are seen in the DFC and, like the DN1s, are thought to contribute to rhythmic output.
 - **DN3s** – Like the DN2s, the DN3s have not been studied in depth; however they are the most numerous cluster with ~40 cells per hemisphere which project towards the midline of the brain with 2 neurons projecting towards the aMe (Shafer *et al.*, 2006; Helfrich-Förster *et al.*, 2007).

As is evident, clock cell subsets are not equal and as such not all contribute equally to circadian rhythmicity, as discussed in 1.2.4.2 and 1.2.6.2. Furthermore, environmental inputs are not perceived uniformly across the circuit and it is therefore thought that certain clock cells are more important than others for entrainment to external synchronisation cues, see 1.2.5.

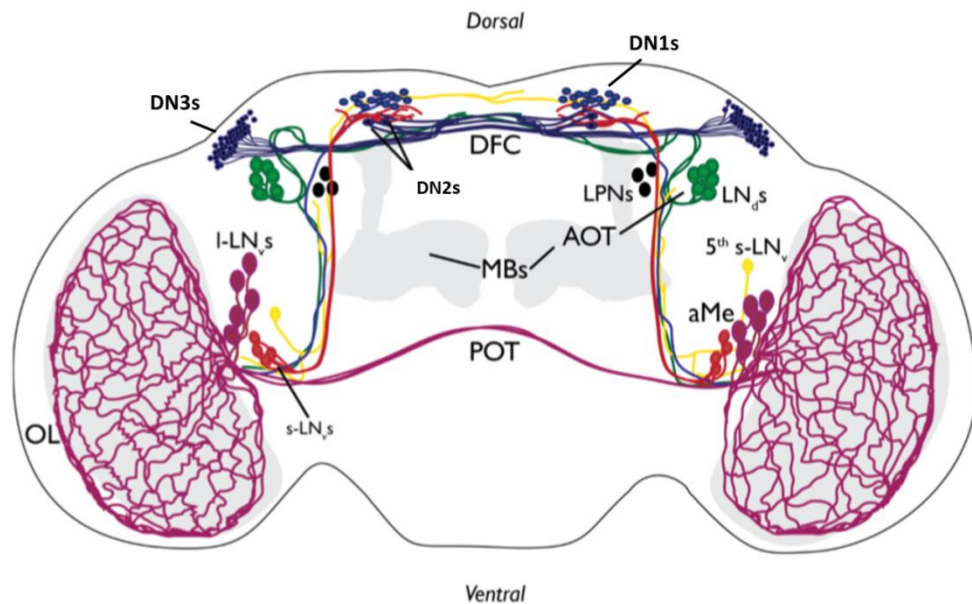


Figure 1.4 Network organisation of the central circadian circuitry of the *Drosophila* brain.

Figure generated by Miguel Ramirez-Moreno and included with his permission (Ramirez-Moreno, 2017). Horizontal (dorsoventral) plane of adult *Drosophila* brain with circadian circuitry divided into clock cell clusters: large ventrolateral neurons (l-LN_{v,s}), small ventrolateral neurons (s-LN_{v,s}), the 5th small ventrolateral neurons (5th s-LN_v), dorsolateral neurons (LN_{d,s}), lateral posterior neurons (LPNs) and three classes of dorsal neurons (DN1s, DN2s and DN3s). Cell bodies and projections are colour coded (except LPNs where no projections are shown). Key anatomical regions are also identified: accessory medulla (aMe), anterior optic tract (AOT), posterior optic tract (POT), optic lobe (OL), dorsal-fusion-commissure (DFC) and the mushroom bodies (MBs).

1.2.4.2 Classical dual oscillator model for *Drosophila* locomotor behaviour

Clock neurons co-ordinate and drive daily rhythms in many physiological processes of the fly including the widely studied rhythm in locomotor behaviour. *Drosophila* are crepuscular organisms and, in a standard 12hL:12hD condition at constant temperature, display archetypal bimodal locomotor activity patterns with peaks of activity in the morning (i.e. dawn or 'lights-on') and the evening (i.e. dusk or 'lights-off'), denoted the M- and E-peaks respectively (**Figure 1.5**) (Hamblen-Coyle *et al.*, 1992; Wheeler *et al.*, 1993). Prior to M- and E-peaks, activity ramps up in anticipation of dawn and dusk, a feature absent in *per*⁰¹ flies (i.e. flies without a functional clock) indicating that behavioural rhythms are dependent on clock function (Grima *et al.*, 2004). M- and E-peaks are separated by a period of relatively low activity referred to as the siesta period (Hamblen-Coyle *et al.*, 1992), which is often more pronounced in male flies (Ho and Sehgal, 2005; Khericha, Kolenchery and Tauber, 2016). Bimodality in *Drosophila* locomotor behaviour can be

Chapter 1:

explained by a dual oscillator model where a distinct subset of cells is responsible for morning activity (M-cells) and another for evening activity (E-cells); a concept originally proposed by Pittendrigh and Daan (1975).

Two experimental approaches were utilised to identify the M- and E-cells; genetic ablation of specific clock cells and selectively rescuing clock function in *per⁰¹* flies with targeted transgenic *per* expression (Stoleru *et al.*, 2004; Grima *et al.*, 2004; Rieger *et al.*, 2006). The results of which revealed the LN_vs as the M-cells and the LN_ds, 5th s-LN_v and some DN1s as the E-cells i.e. a functional clock in the M- or E-cells is required for correct timing of the morning and evening activity peaks respectively (**Figure 1.5**) (Stoleru *et al.*, 2004; Grima *et al.*, 2004; Rieger *et al.*, 2006).

The neuropeptide PDF is expressed in 18 of the 20 LN_v neurons (1.2.4.1) (Helfrich-Förster, 1995; Kaneko, Helfrich-Förster and Hall, 1997; Renn *et al.*, 1999; Stoleru *et al.*, 2005), and it was shown that flies lacking PDF (*Pdf⁰¹*) lack morning anticipatory behaviour, compounding the evidence for the LN_vs being the morning oscillator (Renn *et al.*, 1999). Interestingly the evening peak of activity of *Pdf⁰¹* flies was advanced relative to the LD cycle, which suggests that PDF signalling does not only regulate morning anticipation but also delays evening anticipatory activity governed by the E-cells (discussed further in 1.2.6.1.1) (Renn *et al.*, 1999; Lear, Zhang and Allada, 2009; Zhang *et al.*, 2010a; Schlichting *et al.*, 2016). This suggests a hierarchy between the two oscillators whereby the PDF-positive M-cells exert a level of dominance over the circuit. However this is only the case in the dark and dominance switches to the E-cells in the light (1.2.6.2) (Picot *et al.*, 2007; Stoleru *et al.*, 2007). Furthermore, it has been shown that the LN_vs, in particular the s-LN_vs are required to maintain rhythmicity in DD indicating the s-LN_vs as the master 'pacemaker' neurons in the *Drosophila* brain (Helfrich-Förster, 1998; Renn *et al.*, 1999), although recent research has shown the maintenance of DD rhythmicity requires communication from other clock cells to the s-LN_vs, with a significant contribution for the LN_ds (Bulthuis *et al.*, 2019).

As alluded to in 1.2.4.1, clock cells differ greatly between clusters as well as within clusters.

Alongside PDF, many other neuropeptides are expressed across the circuitry which contribute to circadian rhythmicity (discussed in 1.2.6.1) and environmental input differs between clock cells (1.2.5). Therefore, a dual oscillator model is a somewhat simplistic representation of the true network organisation that facilitates rhythmic output and instead a multi-oscillator network is likely more realistic (discussed in 1.2.6.2).

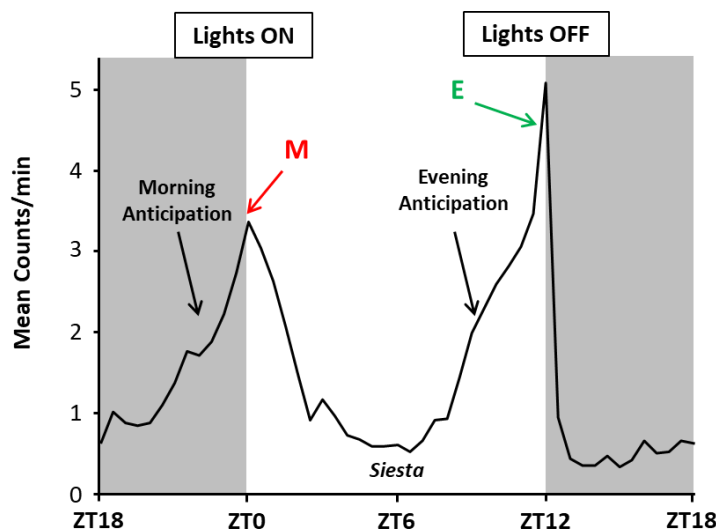


Figure 1.5 Dual oscillator model for *Drosophila* locomotor behaviour in an LD cycle.

Average activity profile of male flies over 10 days in a 12hL:12hD Light:Dark (LD) cycle at a constant temperature. ZT0 and ZT12 indicate lights-on and lights-off respectively. ZT6 is midday and ZT18 is midnight. Morning (M, red) and evening (E, green) activity peaks and siesta period are annotated. Morning and evening anticipatory activity, governed by the M-cells (LN_vs) and E-cells (5th s-LN_v, LN_ds and some DN1s) respectively, are indicated in figure.

1.2.5 Light entrainment of Central Circadian Clocks

As introduced in 1.1, entrainment refers to the alignment of endogenous rhythms in behaviour and physiology with the external environment (Yoshii *et al.*, 2015; Hardin, 2011). Environmental synchronising factors, zeitgebers (Aschoff, 1960), entrain circadian clocks and light is the most reliable and potent zeitgeber (Yoshii *et al.*, 2015), although other cues such as temperature, social interaction and electromagnetic fields can also facilitate circadian entrainment (1.2.5.4) (Yoshii, Ahmad and Helfrich-Förster, 2009).

Drosophila central clocks receive light input via canonical opsin-based visual photoreception, like in mammals (1.1.3), mediated by the visual organs; the compound eyes, ocelli and the extra-retinal Hofbauer-Buchner (H-B) eyelets (discussed in 1.2.5.2) (Helfrich-Förster *et al.*, 2001; Rieger, Stanewsky and Helfrich-Förster, 2003). In addition to the visual system, *Drosophila* also possesses a cell-autonomous circadian photoreceptor, called CRYPTCHROME (CRY), which is present in a subset of clock cells and provides light input direct to the molecular oscillator (discussed in 1.2.5.1) (Stanewsky *et al.*, 1998; Emery *et al.*, 1998). Light can penetrate the *Drosophila* cuticle, and as such, flies can detect light via CRY independently from the visual light input (Rieger, Stanewsky and Helfrich-Förster, 2003). CRY-dependent light input is mechanistically well

Chapter 1:

understood (1.2.5.1 and 1.2.5.1.1); however our understanding of the pathway for visual light input to the clock is still developing (1.2.5.2.3).

Wild-type (WT) flies adapt their characteristic behavioural profile (1.2.4.2) in response to equinox photoperiods shorter than 24 h i.e. 8hL:8hD, demonstrating an ability to entrain their behaviour to a 16 h LD cycle (Wheeler *et al.*, 1993); however the converse experiments in photoperiods longer than 24 h were not carried out. Flies without a functional clock i.e. *per⁰¹*, still display a diurnal rhythm in an LD cycle with activity peaks that align with 'lights-on' and 'lights-off' like WT flies (1.2.4.2) (Wheeler *et al.*, 1993), however they cannot be entrained as they do not have a clock. This artefact is attributed to the promotion of activity during the light phase and inhibition of activity in the dark without the need of an endogenous oscillator, termed 'masking' (Rieger, Stanewsky and Helfrich-Förster, 2003; Mrosovsky, 1999). It is therefore important to make a distinction between rhythms that are simply driven by a change in environmental condition and those which impact on the cycling of the molecular oscillator and entrain circadian clocks.

1.2.5.1 The CRY/JET pathway

Significant reductions in TIM levels can be seen within 30 mins of white-light exposure resulting in a phase shift of the core molecular oscillator via PER destabilisation and alleviation of CLK/CYC inhibition (1.2.3) (Hunter-Ensor, Ousley and Sehgal, 1996; Myers *et al.*, 1996; Zeng *et al.*, 1996). Light-pulses applied at different stages of the circadian cycle result in differential effects on the circadian phase: an early evening light pulse generates a phase delay – TIM protein levels are high, therefore the depleted TIM is replenished within a few hours; a late night light pulse induces a phase advance – low TIM protein levels are further depleted, re-setting the molecular clock around dawn (Hunter-Ensor, Ousley and Sehgal, 1996; Myers *et al.*, 1996; Zeng *et al.*, 1996).

A genetic screen for mutations that affect bioluminescence rhythms of transgenic flies carrying *per-luc* reporter constructs, which rhythmically express luciferase enzyme (Brandes *et al.*, 1996; Plautz *et al.*, 1997b), revealed a role for the blue-light photoreceptor CRYPTOCHROME (CRY) in light entrainment (Stanewsky *et al.*, 1998; Emery *et al.*, 1998). Bioluminescence rhythms in a 12hL:12hD LD cycle were abolished in flies with the severely hypomorphic *cry^b* mutation, however rhythmicity was maintained in a temperature cycle (Stanewsky *et al.*, 1998). *cry^b* flies show rhythmic locomotor behaviour in the same 12hL:12hD LD cycle, due to light input from the visual system; however were not able to respond to brief light pulses (Stanewsky *et al.*, 1998; Emery *et al.*, 2000a). These behavioural entrainment deficits were rescued by the expression of CRY in central clock neurons demonstrating that CRY acts cell-autonomously to re-set circadian rhythms

in response to light (Emery *et al.*, 2000b). *Drosophila* CRY shares a high level of homology with blue-light sensitive plant CRYs, involved in light-driven growth responses, as well as the non-photoreceptive mCRY, which acts as a transcriptional repressor in the mammalian core TTFL (1.2.3.2) (Ahmad and Cashmore, 1993; Ko and Takahashi, 2006). Interestingly, monarch butterflies express two cryptochromes; one partaking in *Drosophila*-like light-induced TIM degradation and the second is the major transcriptional repressor of CLK/CYC, like in mammals (Zhu *et al.*, 2008).

CRY's spectrum of activity lies in the blue-light range ($450 \text{ nm} < \lambda < 500 \text{ nm}$) (VanVickle-Chavez and Van Gelder, 2007), as such, blue-light triggers a conformation change in CRY, driven by its flavin adenine dinucleotide (FAD) cofactor, which enables CRY to bind TIM in a light-dependent manner (mechanistic details regarding blue-light excitation are presented in 1.2.5.1.1) (Ceriani *et al.*, 1999; Busza *et al.*, 2004; Dissel *et al.*, 2004; Peschel *et al.*, 2009; Vaidya *et al.*, 2013).

Immunohistochemical analysis revealed that to degrade TIM to almost undetectable levels requires a light-pulse of 120 mins (Busza *et al.*, 2004; Yoshii *et al.*, 2008; Yoshii *et al.*, 2015); however in the absence of CRY, TIM levels remain unchanged following the same light pulse, clearly indicating light-dependent TIM degradation is CRY-mediated (Yoshii *et al.*, 2015). Light-dependent degradation of TIM, and subsequent degradation of PER, is carried out by the ubiquitin-proteasome system (UPS), as mentioned in 1.2.3.2.1 (Ceriani *et al.*, 1999; Lin *et al.*, 2001; Naidoo *et al.*, 1999; Peschel, Veleri and Stanewsky, 2006). UPS substrates are targeted for degradation via SCF (Skp1/Cullin/F-box protein) ubiquitin E3 ligase complexes (Cardozo and Pagano, 2004). The *Drosophila* genome encodes 25 F-box proteins, two such proteins are SLIMB, involved in the degradation of PER (1.2.3.2.1) (Grima *et al.*, 2002) and JETLAG (JET), which was shown to facilitate light-dependent TIM degradation (Koh, Zheng and Sehgal, 2006; Peschel *et al.*, 2009).

Light-activated CRY binds TIM, promoting the phosphorylation of TIM by a currently unidentified tyrosine kinase (Y kinase) (Naidoo *et al.*, 1999). JET then binds phosphorylated TIM, targeting it for ubiquitination by a SCF ubiquitin E3 ligase complex and degradation via the UPS (Koh, Zheng and Sehgal, 2006; Ceriani *et al.*, 1999; Peschel *et al.*, 2009). Downstream of JET, the COP9 signalosome, which is a general regulator of protein degradation, acts to enhance proteasomal degradation of TIM (Knowles *et al.*, 2009) (**Figure 1.6**). In constant light (LL), CRY is constitutively active and therefore is constantly trying to re-set the clock which results in arrhythmicity in WT flies (Konopka, Pittendrigh and Orr, 1989). Mutants with dysfunctional CRY, JET or COP9 are all rhythmic in LL, suggesting a common pathway for these proteins in the mediation of light-dependent TIM degradation and re-setting of circadian clocks (**Figure 1.6**) (Emery *et al.*, 2000a;

Chapter 1:

Koh, Zheng and Sehgal, 2006; Peschel, Veleri and Stanewsky, 2006; Dolezelova, Dolezel and Hall, 2007; Knowles *et al.*, 2009).

CRY is also photodegradable and once TIM is degraded, CRY itself is degraded via the UPS (Lin *et al.*, 2001; Koh, Zheng and Sehgal, 2006; Peschel, Veleri and Stanewsky, 2006; Peschel *et al.*, 2009). As well as binding to TIM, light-activated CRY has also been shown to bind to JET (Ozturk *et al.*, 2011); however there is no evidence suggesting JET facilitates CRY ubiquitination and degradation (Ozturk *et al.*, 2013). A yeast two-hybrid assay using mCRY identified RAMSHACKLE (RAM), a homologue of mammalian BRWD3, as a potential candidate for promoting ubiquitination of *Drosophila* CRY (Ozturk *et al.*, 2013). BRWD3 contains WD40 motifs, commonly present in substrate receptors for CRL4 ubiquitin E3 ligases (Jackson and Xiong, 2009). Attenuation of light-induced CRY degradation was evident in BRWD3 knockdown experiments (D'Costa *et al.*, 2006), therefore providing a possible mechanism for CRY degradation, whereby RAM binds light-activated CRY and facilitates ubiquitination by a CRL4 ubiquitin E3 ligase (Ozturk *et al.*, 2013) (**Figure 1.6**).

Light-dependent degradation of TIM by the CRY/JET pathway, and subsequent degradation of PER, alleviates CLK/CYC inhibition, initiating a new cycle of PER/TIM expression and accumulation (1.2.3.2), explaining CRY and JETs role in light-dependent re-setting of the core molecular oscillator.

CRY expression is clock controlled with VRI inhibiting and PDP1 activating *cry* transcription (Glossop *et al.*, 2003; Zheng *et al.*, 2009), analogous to the regulation of *Clk* transcription (1.2.3.3). CRY therefore accumulates in the dark, with levels falling throughout the light phase as CRY is photodegradable, therefore CRY abundance is governed by LD cycles (Hardin, 2005). About half of all clock cells in the fly brain express CRY; the s- and l-LN_vs, the 5th s-LN_v, 3 of the 6 LN_ds, the DN1_as and some DN1_ps are all CRY-positive (**Figure 1.4**) (Klarsfeld *et al.*, 2004; Benito *et al.*, 2008; Yoshii *et al.*, 2008). As such CRY-mediated light input is not uniform across the clock circuitry meaning different clock cell subsets are more sensitive to light than others, discussed in 1.2.5.1.3 and 1.2.6.2.

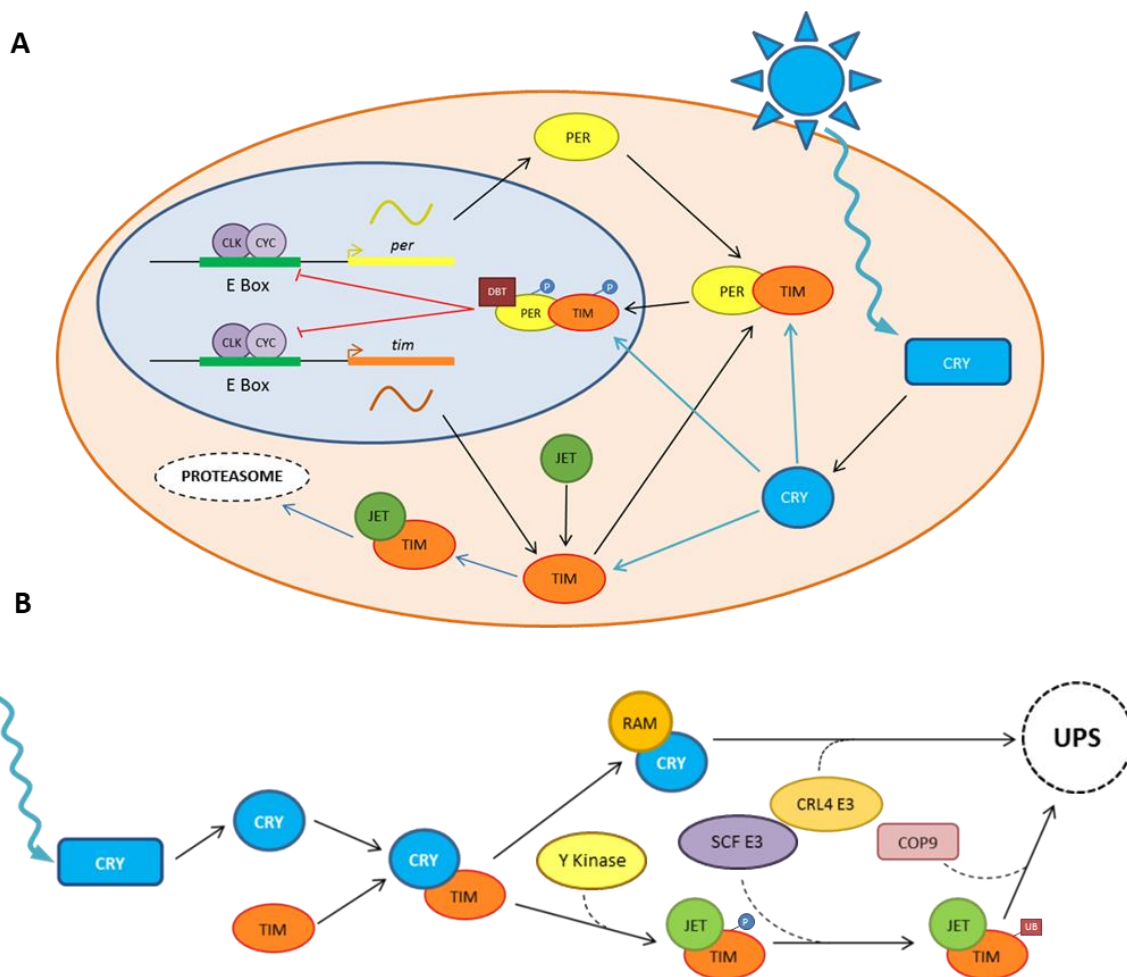


Figure 1.6

The CRY/JET pathway for light-dependent re-setting of the core molecular oscillator.

A) Blue-light excitation of CRY induces a conformational change allowing binding and targeting of TIM for proteasomal degradation facilitated by JET. TIM depletion impacts the core TTFL (**Figure 1.2**) by destabilising PER, alleviating CLK/CYC repression and allowing for a new round of gene transcription. **B)** The sequence of events following CRY activation. TIM undergoes phosphorylation and ubiquitination resulting in proteasomal degradation. CRY is also photo-degradable, and is target for ubiquitination and degradation by RAM. Indicated elements; CLOCK (CLK), CYCLE (CYC), PERIOD (*per*/PER), TIMELESS (*tim*/TIM), DOUBLETIME (DBT), CRYPTOCHROME (CRY), JETLAG (JET), RAMSHACKLE (RAM), Tyrosine kinase (Y kinase), SCF ubiquitin E3 ligase (SCF E3), CRL4 ubiquitin E3 ligase (CRL4 E3), COP9 Signalosome (COP9), ubiquitin-proteasome system (UPS), phosphate (P) and ubiquitin (UB). Italics indicate a gene and all capitals denote a protein.

1.2.5.1.1 Mechanistic insights into CRY function

Cryptochromes, of which there are four distinct classes (Mei and Dvornyk, 2015), share a high level of homology with photolyase proteins involved in DNA repair and contain a conserved

Chapter 1:

photolyase homology domain (PHD) (Brettel and Byrdin, 2010; Muller and Carell, 2009; Sancar, 2003).

Molecular and behavioural studies have highlighted a key role for the 21-residue C-terminal tail (CTT) of *Drosophila* CRY in mediating light-dependent CRY activity as when the CTT is removed, CRY is rendered constitutively active, resulting in similar phenotypes seen with WT flies in LL (Dissel *et al.*, 2004; Busza *et al.*, 2004; Rosato *et al.*, 2001; Hemsley *et al.*, 2007). Crystallisation of full length *Drosophila* cryptochrome has enabled the 3D structure of CRY to be determined therefore providing key insight into the structure-function relationship of *Drosophila* CRY (Zoltowski *et al.*, 2013; Czarna *et al.*, 2013). Structural studies indicated the presence of a binding pocket within the PHD capable of binding the CTT (Vaidya *et al.*, 2013). The precise three-dimensional arrangement of the CTT within the PHD allows for its close juxtaposition to CRY's associated light sensitive redox cofactor, FAD. Thus, revealing the CTT as a prime candidate for the light-induced conformational change of CRY, underpinned by the photochemistry of FAD (Vaidya *et al.*, 2013; Zoltowski, 2015).

FAD is comprised of adenosine diphosphate linked via an alkyl chain to an isoalloxazine ring, which can adopt several distinct oxidation states, providing FAD with its biological relevance (Hoang *et al.*, 2008; Iwata *et al.*, 2010). *Drosophila* CRY typically exists either in its oxidised ground state (FAD_{ox}), or upon blue-light excitation, is reduced to form an anionic semiquinone (ASQ), which is thought to be the key oxidation state involved in CRY light sensitivity (Zoltowski *et al.*, 2013; Vaidya *et al.*, 2013; Zoltowski, 2015). Conflicting models exist regarding the light-induced conformational change of CRY, centred on the identity of true ground state of FAD i.e. oxidised or reduced (Ozturk *et al.*, 2008; Hoang *et al.*, 2008; Ozturk *et al.*, 2011; Vaidya *et al.*, 2013; Ozturk *et al.*, 2014). However, there is currently more evidence suggesting a simple "flip-flop" conformational switch between in-active and activated states driven by the light-dependent reduction of FAD_{ox} to an ASQ (Vaidya *et al.*, 2013).

Light-induced rearrangement of the CTT with respect to the PHD implicates the CTT in gating CRY activity (Vaidya *et al.*, 2013). CRY's circadian target TIM possesses a region sharing high sequence homology with CRY's CTT, termed TIM-CTL (Vaidya *et al.*, 2013; Zoltowski *et al.*, 2013). Therefore, in the dark the CTT is bound in the flavin pocket and blocks TIM binding (Busza *et al.*, 2004; Peschel *et al.*, 2009); however, following light-excitation and FAD reduction to an ASQ, the CTT is expelled and TIM is free to bind within the flavin pocket (Vaidya *et al.*, 2013). In some instances, *Drosophila* CRY has also been shown to interact with PER, much like mCRY (Rosato *et al.*, 2001); however no such interaction is found in the absence of TIM, therefore the reported co-

immunoprecipitation of PER in such studies is likely a result of the strong PER-TIM interaction (Busza *et al.*, 2004).

Most investigations into CRY function use high-intensity light, however CRY has been shown to respond to low-intensity light stimuli via a process of photic-integration (Vinayak *et al.*, 2013). This temporal integration of photons, over long timescales up to 6 h, allows CRY to compensate for limited light stimuli, thus allowing a mechanism for enhanced photosensitivity (Vinayak *et al.*, 2013). In addition to blue-light, CRY can also detect ultraviolet (UV) wavelengths (<400 nm) (VanVickle-Chavez and Van Gelder, 2007) and has been shown to mediate physiological and behavioural responses to UV light stimuli (Baik *et al.*, 2017; Baik *et al.*, 2019).

Besides circadian entrainment, CRY has been shown to act at the membrane, via specific potassium channels, to modulate the spontaneous firing frequency of neurons in response to blue-light (Fogle *et al.*, 2015; Fogle *et al.*, 2011). In addition, CRY has been identified as a prime candidate for a biological magnetoreceptor and is required for the sensing of electromagnetic fields in *Drosophila* (Gegear *et al.*, 2008; Yoshii, Ahmad and Helfrich-Förster, 2009; Fedele *et al.*, 2014b). Both of these additional functions of CRY are discussed in Appendix C.

1.2.5.1.2 The impact of CRY/JET mutations on light entrainment

The aforementioned *cry^b* mutant which revealed a role for CRY in circadian light entrainment (1.2.5.1), possess an amino-acid substitution within the FAD binding site of CRY, thus rendering CRY less responsive to light (Stanewsky *et al.*, 1998; Emery *et al.*, 1998). As well as having a profound effect on LD entrainment of bioluminescence rhythms, which in the most part comes from *Drosophila* peripheral tissues (1.2.8), brief light pulses administered in DD elicited no behavioural phase shifts in *cry^b* flies, which also exhibited rhythmic behaviour in LL, indicating a role for CRY photoreception in the fly brain (Stanewsky *et al.*, 1998; Emery *et al.*, 2000a). However, *cry^b* flies were able to re-synchronise their behaviour to a shifted LD cycle, although it did require more time compared to WT individuals (Stanewsky *et al.*, 1998; Emery *et al.*, 2000a; Emery *et al.*, 2000b), indicating *cry^b* flies retain some residual circadian photoreceptive capability (Dolezelova, Dolezel and Hall, 2007). To investigate the full circadian impact of CRY, true *cry* null mutants were engineered (Dolezelova, Dolezel and Hall, 2007). *cry* null (*cry⁰¹* and *cry⁰²*) flies maintain normal axonal projections from clock neurons and exhibit rhythmicity in DD, as the core circadian oscillator still functions in the absence of CRY, producing a free-running period length of ~24 h (Dolezelova, Dolezel and Hall, 2007). *cry* null mutants exhibit characteristic LL rhythmicity, indicative of the absence of CRY (1.2.5.1), which displayed two free-running components i.e. a

Chapter 1:

split rhythm, likely as a result of light input from the visual system (1.2.5.2) (Hardin, 2011; Dolezelova, Dolezel and Hall, 2007). Although lacking CRY, individual *cry* null flies were seen to effectively re-entrain to an 8 h shifted LD cycle, like *cry^b* flies, as well as entrain locomotor behaviour to a 28 h (14hL:14hD) LD cycle (Dolezelova, Dolezel and Hall, 2007). Entrainment seen in *cry* null flies suggest that light input from the visual organs, which also signals light input to the circadian circuitry, is capable of entraining behaviour (1.2.5.2) (Helfrich-Förster *et al.*, 2001).

The role of JET in CRY-mediated light entrainment was proposed following the initial discovery of two *jetlag* mutants called *jet^f* and *jet^c* which possess a rare or common mutation, respectively, within a conserved leucine-rich repeat (LRR) region (Koh, Zheng and Sehgal, 2006; Peschel, Veleri and Stanewsky, 2006), a domain involved in protein-protein interaction and target recognition (Cardozo and Pagano, 2004). Both *jet^f* and *jet^c* mutants were rhythmic in LL and showed some aberrant circadian photoresponses; however these phenotypes were only observed when flies also carried the *long-short-tim* (*ls-tim/tim^{ls}*) allele (Koh, Zheng and Sehgal, 2006; Peschel, Veleri and Stanewsky, 2006). There are two naturally occurring *tim* alleles, *tim^{ls}* and *short-tim* (*s-tim/tim^s*) which encode a long and short TIM isoforms respectively. The long TIM isoform has a reduced affinity for CRY compared to the short isoform, and as such flies carrying *tim^{ls}* are less sensitive to light (Rosato *et al.*, 1997; Sandrelli *et al.*, 2007), explaining why *jet^f* and *jet^c* phenotypes are only seen in *tim^{ls}* flies. A loss-of-function mutation in the *jetlag* gene, named *jet^{set}*, generates a profound effect on circadian entrainment similar to that seen in *cry* null flies, with a common impact on circadian photoresponses (Lamba *et al.*, 2014). In *jet^{set}* mutants TIM was not degraded and no behavioural responses were observed following a 5 min light pulse administered in the early or late night (Lamba *et al.*, 2014). However, TIM cycling in LD was not completely abolished, due to light-independent TIM cycling by CULLIN-3 (CUL-3), which is required for circadian control of PER and TIM oscillations (Grima *et al.*, 2012). CUL-3 has also been implicated in CRY-independent phase-shifting of the circadian oscillator via TIM degradation (Guo *et al.*, 2014). PDF-positive morning cells secrete PDF when stimulated by light, the visual system or other clock cells, which when detected by its cognate receptor on the evening cells (see 1.2.6.1.1), induces intercellular TIM degradation via CUL-3 (Guo *et al.*, 2014).

1.2.5.1.3 Spatial characterisation of CRY/JET requirement

CRY expression is reported in the LN_vs, 3 LN_ds and some DN1s (1.2.5.1), which encompasses both the M- and E-cells (1.2.4.2). Ectopic expression of CRY in the DN2s was sufficient to allow entrainment of these cells to LD cycles, indicating that CRY acts cell-autonomously to entrain the molecular oscillator to light (Klarsfeld *et al.*, 2004). In order to assess where in the clock circuitry

CRY is required to allow behavioural entrainment, CRY expression was 'rescued' by targeting transgenic *cry* expression in specific clock neuronal subsets of *cry⁰¹* flies and assaying re-entrainment to a 8 h delayed LD cycle (Yoshii *et al.*, 2015). Unsurprisingly, rescuing CRY expression in all clock cells resulted in WT levels of re-entrainment (Kaneko *et al.*, 2000; Yoshii *et al.*, 2015). CRY expression in both the s- and l-LN_vs generated significantly better re-entrainment compared to *cry* null (Yoshii *et al.*, 2015); however entrainment still required several days (Yoshii *et al.*, 2015). More rapid re-entrainment was seen when CRY expression was driven in the three CRY-positive LN_d and the 5th s-LN_v (Stoleru *et al.*, 2004; Yoshii *et al.*, 2015), implicating this subset of E-cells as key mediators of light entrainment (Yoshii *et al.*, 2015).

Similar experiments were conducted in order to map JET function across the circuitry, with JET expression rescued in distinct subsets and assaying behavioural responses to a 5 min light pulse (Lamba *et al.*, 2014). The expected light-pulse induced phase shifts were fully rescued by driving JET expression in all clock cells (Kaneko *et al.*, 2000; Lamba *et al.*, 2014). JET expression in both the M and E-oscillators (1.2.4.2), completely rescues behaviour in *jet^{set}* mutants to WT levels (Grima *et al.*, 2004; Lamba *et al.*, 2014). Targeted JET expression in the M- and E-cells independently yielded no rescue of phase shifts (Renn *et al.*, 1999; Stoleru *et al.*, 2004; Lamba *et al.*, 2014). Therefore, JET is required in both the M and E-oscillators for circadian entrainment to light (Lamba *et al.*, 2014). Another interesting observation from this study was that JET expression in the M-cells could promote non-cell-autonomous TIM degradation in the E-cells, further indicating cooperation between the M and E-oscillators is required for light entrainment (Lamba *et al.*, 2014).

Together these results indicate that both the M and E cells are important for light entrainment of the circadian clock. However, it appears that CRY expression in the E-cells alone is sufficient to facilitate light entrainment to shifted LD cycles. This discrepancy may be as a result of the differing experimental paradigms used posing different entrainment challenges on the circuitry, thus further mapping of CRY/JET function is needed. How CRY/JET mediated light input is integrated and communicated across the circadian circuitry in order to establish an entrained behavioural response is discussed in 1.2.6.2.

1.2.5.2 Visual photoreception in *Drosophila*

CRY acts directly in the clock cells to entrain the molecular oscillator to light (1.2.5.1). However, in the absence of CRY, molecular oscillations in PER and TIM in the s-LN_vs, LN_ds and DN1s are still able to synchronise to light (Stanewsky *et al.*, 1998; Helfrich-Förster *et al.*, 2001; Cusumano *et al.*,

Chapter 1:

2009; Zhang *et al.*, 2009; Yoshii *et al.*, 2015). This CRY-independent entrainment is attributed to visual photoreception.

The *Drosophila* visual system is comprised of 2 compound eyes, 2 extra-retinal Hofbauer-Buchner (H-B) eyelets and 3 ocelli (1.2.5) (Hofbauer and Buchner, 1989; Helfrich-Förster *et al.*, 2001; Rieger, Stanewsky and Helfrich-Förster, 2003; Behnia and Desplan, 2015). The compound eyes are the largest photoreceptive organ and play a key role in circadian entrainment (1.2.5.2.2), as well as measuring day length and moonlight detection (Rieger, Stanewsky and Helfrich-Förster, 2003; Schlichting *et al.*, 2014; Yoshii, Hermann-Luibl and Helfrich-Förster, 2016). The H-B eyelets, which sit between the retina and the lamina of the optic lobe, are the remnants of the Bolwig's organs, the larval photoreceptors (Hofbauer and Buchner, 1989; Yasuyama and Meinertzhagen, 1999); and the ocelli, found on the top of the fly head between the antennae, are a collection of non-visual photoreceptors involved in flight stabilisation (Pollock and Benzer, 1988; Taylor, Krapp and Simpson, 2007). Both the H-B eyelets and the ocelli are thought to contribute to light entrainment (1.2.5.2.2); however their contributions are modest compared to that of compound eye (Rieger, Stanewsky and Helfrich-Förster, 2003). Visual photoreceptor cells relay light stimuli to the brain via the optic lobe through distinct circuits involved in visual processing, motion detection and phototaxis (Behnia and Desplan, 2015), as well as through newly uncovered pathways for visual light entrainment of the central circadian clock in *Drosophila* (1.2.5.2.3) (Li *et al.*, 2018; Schlichting *et al.*, 2019; Alejevski *et al.*, 2019).

Flies that lack functional CRY can still entrain to external light stimuli (1.2.5.1.2), the same is true for flies with a compromised visual system, however flies lacking both light input pathways can no longer entrain to light cues (discussed in 1.2.5.2.2) (Helfrich-Förster *et al.*, 2001; Wheeler *et al.*, 1993). The *Drosophila* visual system is highly sensitive and can detect a wide range of wavelengths (1.2.5.2.1), including blue-light, suggesting a degree of a redundancy in maintaining both light input pathways (Stanewsky *et al.*, 1998; Helfrich-Förster *et al.*, 2001; Veleri *et al.*, 2003; Rieger, Stanewsky and Helfrich-Förster, 2003). This however is not the case as the CRY/JET and visual light input pathways have different effects on the circadian clock. The CRY/JET pathway mediates rapid light entrainment whereas entrainment via the visual system is slower (Yoshii, Hermann-Luibl and Helfrich-Förster, 2016; Helfrich-Förster *et al.*, 2001; Kistenpfennig *et al.*, 2017b). The visual system is better at delaying the evening activity peak, acting against rapid CRY/JET activity, and facilitating more precise entrainment to longer day lengths (Kistenpfennig *et al.*, 2017b). The spectral range and sensitivity of the visual system, in addition to CRY acting directly within the clock neurons, enables *Drosophila* to perceive environmental light stimuli which varies greatly in both spectral composition and intensity over the course of a day (Senthilan *et al.*, 2019).

Therefore possessing two light input pathways to detect and entrain the clock to light must provide a physiological benefit.

1.2.5.2.1 Organisation of the *Drosophila* visual system

Visual photoreception is mediated by six different light sensitive Rhodopsins (Rh1-6) which are differentially expressed in the photoreceptor cells of the *Drosophila* visual system (Behnia and Desplan, 2015; Senthilan *et al.*, 2019). These rhodopsins confer the aforementioned spectral sensitivity to a wide-ranging wavelengths of light in both the visible spectrum and UV (1.2.5.2); Rh1 absorbs both blue and UV wavelengths and is therefore termed a 'broadband' photoreceptor; Rh2 is sensitive to violet-light; Rh3 and Rh4 are UV sensitive; Rh5 absorbs blue-light and Rh6 absorbs green and yellow wavelengths (Salcedo *et al.*, 2000; Behnia and Desplan, 2015; Senthilan *et al.*, 2019). In addition, Rh1 and Rh6 have also been shown to be required for detecting red-light stimuli (1.2.5.3) (Hanai, Hamasaka and Ishida, 2008).

Each compound eye is made up of approximately 800 independent units called ommatidia, with each ommatidium composed of 6 outer photoreceptor cells, R1-6, and 2 inner photoreceptor cells R7-8 (**Figure 1.7**) (Behnia and Desplan, 2015). The outer R1-6 cells of all ommatidia express Rh1, span the entire depth of the retina and project to the lamina neuropil of the optic lobe. R1-6 photoreceptors are considered comparable to vertebrate rod cells, with roles including dim-light vision and motion detection (**Figure 1.7**) (O'Tousa *et al.*, 1985; Zuker, Cowman and Rubin, 1985; Schnaitmann *et al.*, 2013). Rh3-6 are expressed in the two inner photoreceptors R7 (Rh3/4) and R8 (Rh5/6). R7 and R8 are arranged on top of each other and project toward the medulla of the optic lobe (**Figure 1.7**) (Senthilan *et al.*, 2019). There are two distinct combinations of R7 and R8 cells which define two subtypes of ommatidia, depending on the rhodopsins they express. 'Pale' ommatidia are composed of an Rh3-expressing R7 cell and an Rh5-expressing R8 cell, whereas 'yellow' ommatidia combine an Rh4-expressing R7 cell and an Rh6-expressing R8 cell (**Figure 1.7**); the 'yellow' ommatidia are more common than the 'pale', and constitute around 70% of the compound eye (Fryxell and Meyerowitz, 1987; Montell *et al.*, 1987; Zuker *et al.*, 1987; Chou *et al.*, 1999; Chou *et al.*, 1996; Huber *et al.*, 1997; Papatsenko, Sheng and Desplan, 1997; Salcedo *et al.*, 2000). The H-B eyelets contain 4 photoreceptor cells which exclusively express Rh6 and send projections to the aMe of the optic lobe into close proximity of the dendritic processes of the LN_vs (**Figure 1.7**) (1.2.4.1) (Hofbauer and Buchner, 1989; Yasuyama and Meinertzhagen, 1999; Malpel, Klarsfeld and Rouyer, 2002; Helfrich-Förster *et al.*, 2002). Rh2 is only expressed in the 80 photoreceptors of the ocelli (Pollock and Benzer, 1988). Furthermore, Rh1, Rh3, Rh4 and Rh6 can all mediate circadian entrainment to extremely low light levels, indicating the versatility in

Chapter 1:

rhodopsin-mediated light input as it can not only detect a variety of wavelengths but is also sensitive to different light intensities (Saint-Charles *et al.*, 2016).

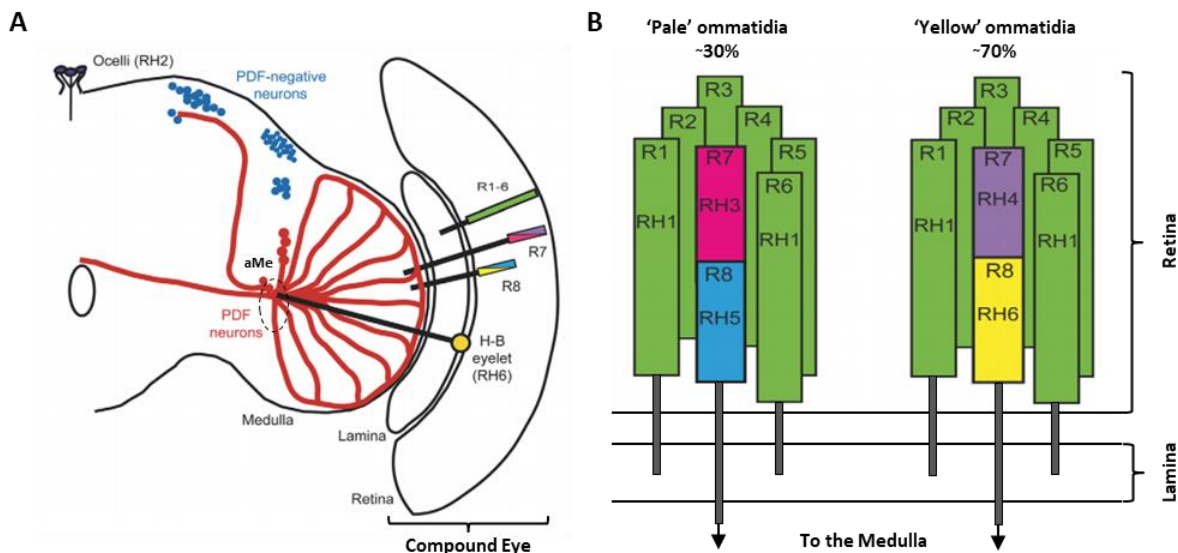


Figure 1.7 Organisation of the *Drosophila* visual system.

Adapted from Saint-Charles *et al.* (2016). **A**) Schematic of one hemisphere of the adult *Drosophila* brain with PDF-positive and negative clock cells, shown in red and blue respectively, with the projections for PDF-positive cells also indicated. Key structures indicated include the medulla, accessory medulla (aMe) and lamina of the optic lobe, the retina of the compound eye, the Hofbauer-Buchner (H-B) eyelet, complete with projection, and the ocelli. Representative location and rhodopsin expression patterns of the photoreceptors in the compound eye are indicated; R1-6 express Rh1, R7 express either Rh3 or Rh4 and R8 express either Rh5 or Rh6. The extra-retinal H-B eyelets express Rh6 and projects to the aMe. The ocelli express Rh2. **B**) Simple representation of the structure of the two main types of retinal ommatidia 'pale' and 'yellow' composed of Rh1 expressing R1-6 outer photoreceptors which span the depth of the retina and project to the lamina; and the inner R7 (Rh3/4) and R8 (Rh5/6) cells which are organised one above the other and project to the medulla. (Saint-Charles *et al.*, 2016; Senthilan *et al.*, 2019).

A seventh less well characterised UV-sensitive rhodopsin (Rh7) was recently uncovered which appears to participate in light entrainment; however, the exact localisation and contribution of Rh7 remains unclear (Grebler *et al.*, 2017; Kistenpfennig *et al.*, 2017a; Ni *et al.*, 2017; Sakai *et al.*, 2017). Rh7 expression has been reported in both the compound eye and the brain, albeit at very low levels (Senthilan *et al.*, 2019). Within the brain, Rh7 expression is detected in some clock neurons, which may explain the reported contributions to light entrainment and siesta behaviour (Ni *et al.*, 2017; Kistenpfennig *et al.*, 2017a; Senthilan *et al.*, 2019). Expression of Rh7 in the

compound eye appears to reduce their light sensitivity, particularly when present in the R8 cells (Senthilan *et al.*, 2019; Grebler *et al.*, 2017). It has therefore been proposed that alongside a role in light entrainment, the main function of Rh7 is to fine-tune light sensitivity in the compound eye, possibly protecting against bright-light flashes (Senthilan *et al.*, 2019).

Light-excitation of rhodopsins, which are G-protein coupled receptors (GPCR), triggers a signalling cascade where Gq α activates the *no receptor potential A (norpA)*-encoded phospholipase C. Phospholipase C hydrolyses phosphatidylinositol 4, 5 bisphosphate (PIP₂) which in turn triggers the opening of cation channels, depolarising the photoreceptors and triggering the release of histamine (Bloomquist *et al.*, 1988; Hardie and Juusola, 2015), the main neurotransmitter in the *Drosophila* visual system (1.2.5.2.3). Photoreceptors in the retina, H-B eyelet and the ocelli all express NORPA and this NORPA-dependent mechanism is considered the canonical phototransduction pathway in *Drosophila*, however, some rhodopsins can signal via alternative NORPA-independent phototransduction pathways (Zhu, McKay and Shortridge, 1993; Malpel, Klarsfeld and Rouyer, 2002; Ogueta, Hardie and Stanewsky, 2018). In the absence of NORPA; Rh1, Rh5 and Rh6 can activate a second phospholipase encoded by *Plc21C*, triggering a Gq-dependent signalling cascade which targets light stimuli directly to the s-LN_{v,s} (Ogueta, Hardie and Stanewsky, 2018).

1.2.5.2.2 The impact of mutations affecting the visual system on light entrainment

Flies that are devoid of all photoreceptor cells (*gl*), lacking Rh1 (*ninaE*) or carrying a *norpA* mutation all displayed reduced entrainment to LD cycles (Wheeler *et al.*, 1993; Helfrich-Förster *et al.*, 2001; Stanewsky *et al.*, 1998). As alluded to in 1.2.5, entrainment is only lost completely when mutations are present which remove both visual light input and CRY-mediated light input i.e. *gl*^{60j} *cry*^b double mutants (Helfrich-Förster *et al.*, 2001), indicating that in some conditions one light input pathway can compensate for the other. The relative contribution of each facet of the visual system was assessed with developmental mutants which possessed different combinations of the visual organs; *eyes absent (cli*^{ey^a}) lack the compound eyes but retain the H-B eyelets and ocelli; *sin oculus (so*¹) only retain the ocelli; and *GMR-hid* flies lack the entire visual system (Rieger, Stanewsky and Helfrich-Förster, 2003; Klarsfeld *et al.*, 2004). Locomotor behaviour of these mutants in 24 h LD cycles with differing photoperiods (i.e. 16hL:8hD or 8hL:16hD), revealed that the compound eyes contribute significantly to light entrainment, whereas the ocelli and H-B eyelet only make modest contributions, as previously mentioned in 1.2.5.2 (Helfrich-Förster *et al.*, 2001; Rieger, Stanewsky and Helfrich-Förster, 2003). Furthermore, no differences were observed between the behaviour of flies who are unable to synthesise histamine (*Hdc*^{JK910}) compared to

Chapter 1:

flies lacking the compound eye, indicating histamine signalling is paramount to visual light entrainment (1.2.5.2.3) (Rieger, Stanewsky and Helfrich-Förster, 2003).

When visual phototransduction is blocked i.e. in *norpA* mutants, flies are often called ‘visually blind’ and when this is coupled to a *cry* mutation, flies are effectively ‘circadian blind’ meaning the clock receives little to no light stimuli (Dolezelova, Dolezel and Hall, 2007). *norpA^{P21}cry^b* and *norpA^{P24}cry⁰* double mutants cannot entrain to low intensity light stimuli but can entrain slowly to higher light intensities (Stanewsky *et al.*, 1998; Emery *et al.*, 2000b; Szular *et al.*, 2012; Saint-Charles *et al.*, 2016). This slow entrainment is abolished if the Rh5 expressing cells are ablated or silenced as well as if Rh5 or Rh6 are mutated in combination with the *norpA* and *cry* mutations; indicating this slow entrainment was mediated by the R8 photoreceptors via a NORPA-independent pathway (Mealey-Ferrara, Montalvo and Hall, 2003; Veleri *et al.*, 2007; Szular *et al.*, 2012; Saint-Charles *et al.*, 2016). In the absence of CRY, the visual system can entrain the molecular oscillator (1.2.5.1.2). In *norpA^{P21}cry^b* double mutants, the s-LN_vs are still light entrainable suggesting that they can be entrained by a NORPA-independent pathway, whereas the LN_ds and DN1s rely on canonical visual transduction (Helfrich-Förster *et al.*, 2001; Yoshii *et al.*, 2015).

1.2.5.2.3 Signalling visual light input to the clock

The extensive arborisation of LN_v projections, particularly the l-LN_vs (1.2.4.1), into the optic lobe identified the PDF-expressing cells as prime candidates for signalling visual light stimuli to the clock (Helfrich-Förster *et al.*, 2007). A direct connection has been reported between the H-B eyelet and the LN_vs which proved to be important for circadian entrainment (Veleri *et al.*, 2007), with the eyelets either aiding or antagonising CRY-dependent light entrainment in s- and l-LN_vs respectively (Schlichting *et al.*, 2016). Additionally, PDF signalling of visual light input was shown to be important for phase shifting E-cell activity, highlighting the E-cells as a site for CRY-independent light input (Yoshii *et al.*, 2015), as well as CRY-dependent light input (1.2.5.1.3). This represents a hierarchical model whereby visual light input is received by the PDF cells which then synchronise the rest of the clock circuit.

A more recent study mapped the electrophysiological responses of each clock cell subset following light input from the visual system (Li *et al.*, 2018). Patch-clamp recordings indicated that all LN_vs, one LN_d (which expresses the Ion Transport Peptide, ITP, see 1.2.6.1.2), the DN1_as and some DN3s increased action potential firing in response to light. These light-evoked responses required NORPA-dependent canonical phototransduction in either the compound eyes, H-B

eyelets, or both; however the ocelli had no impact (Li *et al.*, 2018). In the absence of PDF signalling, the E-cells i.e. the ITP-LN_d and the 5th s-LN_v, still showed robust responses to light. Furthermore, the DN1_ss showed light responses when the LN_vs and LN_ss were genetically silenced. Together these results suggest that all clock cells receive visual light input independently of each other, arguing against a hierarchical model (Li *et al.*, 2018). Light responsive clock neurons, which send dendritic process to the aMe (1.2.4.1), showed no responses to light following laser ablation of the aMe, suggesting that the aMe acts as a hub which facilitates visual light input to the clock circuit (Li *et al.*, 2018). Consistent with previous work, direct connections were reported between the H-B eyelet and clock neurons; however, communication between the compound eye and the clock required the involvement of interneurons to pass the signal from the photoreceptors to the aMe (Li *et al.*, 2018).

As mentioned in 1.2.5.2.1, histamine is the main neurotransmitter used in *Drosophila* visual photoreception and as such the retinal photoreceptors and projections from the H-B eyelet are histaminergic (Burg *et al.*, 1993; Hong *et al.*, 2006; Hamasaka and Nassel, 2006; Pantazis *et al.*, 2008; Yusein *et al.*, 2008; Oh *et al.*, 2013). *Drosophila* express two histamine receptors; *ora transientless* (*ort*) and *Histamine-gated chloride channel 1* (*HisCl1*), both of which are histamine gated chloride channels (Zheng *et al.*, 2002). *ORT* is expressed in the lamina and medulla of the optic lobe, whereas *HISCL1* is expressed by the glial cells of the lamina and Rh6-expressing R8 photoreceptor cells (Hong *et al.*, 2006; Pantazis *et al.*, 2008; Gao *et al.*, 2008; Alejevski *et al.*, 2019). Behavioural re-entrainment assays showed that histamine signalling was required for light entrainment. However it was shown that *ORT* expression in *HISCL1* expressing cells can compensate for the loss of *HISCL1*, but not the other way round, suggesting the two receptors act via different pathways (Alejevski *et al.*, 2019). It was proposed that the interneurons of the optic lobes express *ORT* which binds histamine released by the photoreceptors and signals to the clock cells to mediate light entrainment (Alejevski *et al.*, 2019). Furthermore, the Rh6-expressing R8 cells were shown to play a key role in circadian entrainment, both as photoreceptors and interneurons. Alongside direct light innervation, expression of the *HISCL1* receptor on the Rh6-expressing R8 cells means these cells can also receive light input in-directly from nearby light-excited photoreceptors (Alejevski *et al.*, 2019). The Rh6-expressing R8 cells then signal to other optic lobe interneurons, or directly to the clock cells, to mediate light entrainment, possibly via the release of acetylcholine (Alejevski *et al.*, 2019). It has been shown that acetylcholine released directly from the H-B eyelet, as well as from neurons in the optic lobe, signals to the LN_vs to increase action potential firing (Schlichting *et al.*, 2019). Integration of light stimuli by the Rh6-

Chapter 1:

expressing R8 is reminiscent of the role of ipRGCs in mammalian light entrainment (1.1.3) (Hastings, Brancaccio and Maywood, 2014).

This relay of histaminergic and cholinergic signalling provides a possible pathway for entraining the circadian circuitry to visual light input, with communication between the visual system and the clock centred in the aMe neuropil of the optic lobe (Alejevski *et al.*, 2019; Li *et al.*, 2018; Schlichting *et al.*, 2019). However, the exact mechanism which couples rhodopsin-mediated light input and molecular entrainment is still unclear (Alejevski *et al.*, 2019). It has been shown that visual light input is not coupled to rapid TIM degradation like CRY-mediated light input (Stanewsky *et al.*, 1998; Yang *et al.*, 1998; Emery *et al.*, 2000b); although action potential firing in central clock pacemaker neurons has been shown to result in slow TIM degradation mediated by the E3-ligase CUL-3 (previously mentioned in 1.2.5.1.2) (Guo *et al.*, 2014). This provides a possible mechanism for light entrainment of the molecular oscillator following visual photoreception.

1.2.5.3 Red light

As mentioned in 1.2.5.1, CRY's spectrum of activity lies in the blue-light range (VanVickle-Chavez and Van Gelder, 2007), therefore detecting red-light is solely the responsibility of the visual system. Mutants lacking the compound eye or visual phototransduction cannot entrain behaviour to red-light dark (RLD) cycles and it was shown that it is Rh1 and Rh6, expressed in the R1-6 and R8 photoreceptors respectively (1.2.5.2.1), which detect red-light wavelengths and mediate entrainment (Hanai, Hamasaka and Ishida, 2008). Rh6 is also expressed in the H-B eyelet which signals light input directly to the clock (1.2.5.2.1 and 1.2.5.2.3), and although the eyelets play a modest role in white-light entrainment, it is possible that with limited input the eyelets play a larger role in red-light entrainment (Rieger, Stanewsky and Helfrich-Förster, 2003; Veleri *et al.*, 2007; Schlichting *et al.*, 2019). Interestingly, Rh1, Rh5 and Rh6 have also been shown to help entrain the circadian clock, along with CRY, to both yellow and green wavelengths of light (Hanai and Ishida, 2009).

Entrainment to shifted red-light cycles occurs more slowly than to white-light dark cycles, mirroring the observations of *cry* mutant behaviour (1.2.5.1.2), indicative of indirect light input via the visual system (1.2.5.2) (Hanai, Hamasaka and Ishida, 2008). Daily activity patterns of WT flies in RLD cycles are very similar to WT flies in white-light (1.2.4.2) (Cusumano *et al.*, 2009); however a constant red-light stimuli (RR) generates a new free-running condition (somewhat similar *cry* mutants to LL) and appears to change the hierarchical structure of the WT clock circuitry (Unpublished data from Wijnen Lab) (Cusumano *et al.*, 2009). In DD, the PDF cells drive

rhythmicity across the circuit (1.2.4.2) (Helfrich-Förster, 1998; Renn *et al.*, 1999); however, RR appears to marginalise the contribution of the PDF cells suggesting a switch in dominance to a currently unidentified 'RR pacemaker' (*Unpublished data from Wijnen Lab*) (Cusumano *et al.*, 2009).

1.2.5.4 Temperature entrainment and other zeitgebers

Drosophila and other insects are poikilotherms and are therefore sensitive to changes in environmental temperature. Light and temperature cycles *in-phase* with each other act synergistically to synchronise the circadian clock, however, a misalignment of the two environmental inputs severely alters molecular and behavioural rhythms (Currie, Goda and Wijnen, 2009; Harper *et al.*, 2016). Temperature cycles alone are sufficient to drive circadian entrainment and a cycling amplitude of only 2-3°C is required for stable synchronisation of behavioural rhythms (Wheeler *et al.*, 1993; Glaser and Stanewsky, 2007; Currie, Goda and Wijnen, 2009). When flies are moved from an LD cycle to a temperature cycle with a 6 h phase shift, entrainment to the new phase takes several days (Currie, Goda and Wijnen, 2009). This is longer than seen in similar experiments with shifted LD cycles demonstrating that temperature is indeed a weaker zeitgeber. Furthermore, isolated fly tissues are entrainable to temperature cycles (Glaser and Stanewsky, 2007), showing temperature entrainment is cell-autonomous, however the exact mechanism for temperature entrainment is yet to be conclusively determined.

Amongst the circadian circuitry, the LN_vs, LPNs and some dorsal neurons are known to be temperature sensitive, with changes in temperature capable of entraining the molecular oscillator in these cells (Busza, Murad and Emery, 2007; Tomioka, Miyasako and Umezaki, 2008; Zhang *et al.*, 2010b; Yoshii *et al.*, 2005). It has also been shown that *per* transcript levels are directly affected by temperature via temperature-driven transcription and splicing (Kornmann *et al.*, 2007; Goda, Sharp and Wijnen, 2014). Cold-induced *per* expression is involved in resetting the molecular oscillator in *Drosophila*, interestingly mammalian *per2* expression has also been reported to be temperature-regulated; however, in this instance by increased temperature (Goda, Sharp and Wijnen, 2014; Majercak *et al.*, 1999). No circadian temperature entrainment (NOCTE) is a possible candidate for imposing temperature entrainment to the circadian clock and is expressed in the *Drosophila* chordotonal organs (proprioceptive organs found the joints) (Glaser and Stanewsky, 2007). Temperature cycles can be used to drive rhythmicity in LL, when WT flies are normally arrhythmic (1.2.5.1) (Yoshii *et al.*, 2005). NOCTE mutants showed impaired behavioural and molecular rhythms under a temperature cycle in LL indicating a role for NOCTE in temperature entrainment (Glaser and Stanewsky, 2007; Sehadova *et al.*, 2009). Somewhat surprisingly, *norpA*

Chapter 1:

mutants were indistinguishable from *nocte* mutants, indicating that *norpA* also plays a role in temperature entrainment (Glaser and Stanewsky, 2007). A more recent study has demonstrated that NOCTE temperature input is targeted to the DN1s and is capable of synchronising behavioural and molecular rhythms to temperature cycles (Chen *et al.*, 2018). Interestingly, NOCTE is also important for entrainment to combined LD and temperature cycles and therefore plays a role in the integration of sensory stimuli (Chen *et al.*, 2018).

CRY has been implicated in modulating circadian synchronisation to temperature cycles as differential temperature entrainment has been noted in CRY-positive and CRY-negative neurons (Yoshii, Hermann and Helfrich-Förster, 2010). Logically, CRY-positive neurons are directly light entrainable, and CRY-negative are not, however CRY-negative cells can be entrained to temperature and communicate that entrainment to the circadian neuronal network (Yoshii, Hermann and Helfrich-Förster, 2010). Furthermore, CRY-positive cells have been shown to contribute to temperature cycle entrainment, as flies with a functional clock in just the CRY expressing cells are temperature sensitive (Busza, Murad and Emery, 2007). To further these observations, Gentile *et al.* (2013) spatially restricted *per* expression to demonstrate preferential entrainment of neuronal clock subsets to different temperature ranges; dorsal neurons synchronise to high temperature cycles (20-29°C); and ventral neurons to cooler temperatures (16-25°C). CRY was shown to dampen temperature-induced *per-luc* oscillations at the molecular level, and the removal of CRY, coupled with restricted expression of *per* in a few dorsal neurons, allowed behavioural entrainment to high and low temperature cycles, independent of light (Gentile *et al.*, 2013). Taken together, these findings indicate that CRY dampens temperature input to the circadian oscillator and suggests another mechanism of the integration of two zeitgebers, this time mediated by CRY.

Light and temperature are the most studied and best understood external synchronising cues, however other zeitgebers are capable of synchronising circadian clocks. Social interactions have been shown to affect circadian phase, whether that be a fly entrained to one condition altering the phase of another or the shift from day-time to night-time activity as a result of courtship behaviour (Levine *et al.*, 2002b; Fujii *et al.*, 2007); both of which are governed by olfactory cues (Levine *et al.*, 2002b; Fujii *et al.*, 2007; Krupp *et al.*, 2008; Krupp *et al.*, 2013). In addition, the male DN1 neurons can be entrained by sexual activity, however entrainment of these cells alone does not influence locomotor behaviour (Levine *et al.*, 2002b; Hanafusa *et al.*, 2013). Since the 1960's, it has been postulated that electromagnetic fields (EMF) could be potential zeitgebers (Yoshii, Ahmad and Helfrich-Förster, 2009). Several studies have indicated that an EMF can be detected by *Drosophila* and entrain locomotor behaviour via a blue-light and CRY-dependent

mechanism (see Appendix C) (Gegebar *et al.*, 2008; Yoshii, Ahmad and Helfrich-Förster, 2009; Fedele *et al.*, 2014b).

1.2.6 Communication, Co-ordination and Synchronisation of Neuronal Clocks

To generate rhythmic and entrained circadian output, light input needs to be communicated across the clock circuitry. Communication between clock neurons is essential in order to generate a reliable, robust and coherent circadian rhythm (Yao *et al.*, 2016). The classical dual oscillator model states that PDF-positive M-cells, which are the DD pacemakers, govern activity in the dark and drive morning anticipation (1.2.4.2); whereas E-cells, in particular the CRY-positive LN_s and 5th s-LN_v (1.2.5.1.3), are responsible for day-time activity and evening anticipatory behaviour (1.2.4.2) (Hardin, 2011). Many neuropeptides and neurotransmitters are involved in communication across the circuit (1.2.6.1); how this complex network comes together to coordinate entrainment to light is discussed in 1.2.6.2.

1.2.6.1 Neuropeptides and neurotransmitters required for communication across the circuitry

Clock cells are neurons and as such make use of a multitude of signals to communicate external inputs to other clock cells and output centres (1.2.7) which facilitate rhythms in behaviour and physiology. Interestingly, membrane potential and firing frequency are another circadian regulated output (Sheeba *et al.*, 2008; Cao and Nitabach, 2008; Flourakis *et al.*, 2015), indicating that clocks can modulate arousal and communication between other neuronal circuits.

1.2.6.1.1 Pigment Dispersing Factor signalling

As discussed in 1.2.4.2, the neuropeptide Pigment Dispersing Factor (PDF) expressed in all LN_s, with the exception of the 5th s-LN_v, is paramount for rhythmicity in DD and controlling the phase of M-cell and E-cell activity in an LD cycle (Helfrich-Förster, 1995; Kaneko, Helfrich-Förster and Hall, 1997; Renn *et al.*, 1999; Stoleru *et al.*, 2005; Lear, Zhang and Allada, 2009; Zhang *et al.*, 2010a; Schlichting *et al.*, 2016). PDF accumulation in the axonal terminals of the PDF-positive s-LN_s is rhythmic, with levels peaking after lights-on and falling to its lowest levels after lights-off (Park *et al.*, 2000). This rhythmicity appears to be clock-controlled as rhythms in PDF release are lost in *per* null mutants and PDF expression falls dramatically in both *cyc* null and *Clk^{irk}* mutants (Park *et al.*, 2000; Blau and Young, 1999); however little is known about how the clock itself regulates PDF expression (Mezan *et al.*, 2016; Gunawardhana and Hardin, 2017).

Chapter 1:

The PDF receptor (PDFR) is a Class II GPCR, which when mutated generates a remarkably similar phenotype to *Pdf⁰¹* (1.2.4.2) (Mertens *et al.*, 2005; Hyun *et al.*, 2005; Lear *et al.*, 2005). PDFR expression is reported in the s-LN_vs (including the 5th s-LN_v), 2 l-LN_vs, 3 LN_ds, some DN1s (both DN1_as and several DN1_ps), both DN2s and some DN3s; indicating the M-cells can signal directly to the E-cells using PDF as well as receive autocrine feedback signals, which acts to consolidate synchronisation of the 'pacemaker' cells (Shafer *et al.*, 2008; Shafer and Yao, 2014; Im and Taghert, 2010; Im, Li and Taghert, 2011). PDF signalling synchronises cells across the circuit (Renn *et al.*, 1999), analogous to VIP in mammals (1.1.3), and the wide-reaching expression of the PDFR indicates that PDF signalling plays a key role in circadian function. PDF has also been implicated in arousal as a promotor of wakefulness i.e. drives flies to be active (Sheeba *et al.*, 2008; Parisky *et al.*, 2008). Furthermore, outside of the clock circuitry, PDFR expression has been reported in the Ellipsoid body (EB), a key *Drosophila* locomotor centre thus linking PDF signalling to possible output pathways (1.2.7) (Parisky *et al.*, 2008); and on the lamina-retina boundary of the compound eye, where it is thought that PDF may modulate visual light input (Im and Taghert, 2010).

The exact downstream mechanism following PDF binding to the PDFR is unknown. It has been shown that PDF binding is coupled to an increase in cyclic adenosine monophosphate (cAMP) levels, alluding to a signalling mechanism involving adenylate cyclase (Mertens *et al.*, 2005; Shafer *et al.*, 2008). cAMP is key intracellular second messenger involved in cell-signalling (Nassel and Winther, 2010) and altered cAMP levels have been implicated in clock function (Li *et al.*, 2014; Tomioka, Miyasako and Umezaki, 2008). However, more recent research has shown that PDF signalling alters the phase of PDF-responsive cells by slowing down their Ca²⁺ oscillations (Liang, Holy and Taghert, 2016; Liang, Holy and Taghert, 2017).

1.2.6.1.2 Other neuropeptides and neurotransmitters

Alongside PDF, three other neuropeptides are expressed by clock cells which likely act as intra-network communication signals, aiding the generation of robust and synchronous circadian rhythms (Johard *et al.*, 2009; He *et al.*, 2013; Beckwith and Ceriani, 2015).

- **Neuropeptide F (NPF)** - Expressed in 3 LN_ds (1 CRY-positive and 2 CRY-negative), the 5th s-LN_v and some l-LN_vs; with its cognate GPCR expressed in some DN1s and some LN_ds (Johard *et al.*, 2009; Hermann *et al.*, 2012; He *et al.*, 2013). Downregulation of NPF or its receptor results in the lack of evening anticipatory behaviour in LD cycles (Dubruille and Emery, 2008).

- **Small Neuropeptide F (sNPF)** – Within the clock circuit, sNPF is expressed in the s-LN_vs and 2 CRY-positive LN_ds, which are strongly coupled to the s-LN_vs (Johard *et al.*, 2009; Yao and Shafer, 2014); however broad expression is seen across the nervous system (Vecsey, Pérez and Griffith, 2013). sNPF promotes sleep in *Drosophila* likely via its hyperpolarising effects on neurons in the Pars Intercerebralis (PI), an output centre in the fly (1.2.7) (Shang *et al.*, 2013; Chen *et al.*, 2013; Vecsey, Pérez and Griffith, 2013).
- **Ion Transport Peptide (ITP)** - Expression is restricted to just one LN_d (which co-expresses CRY, NPF and PDFR) and the 5th s-LN_v (also CRY and PDFR-positive), as well as some non-clock cells in the *Drosophila* brain (Johard *et al.*, 2009; Hermann-Luibl *et al.*, 2014). ITP is rhythmically released in LD and DD, and flies with reduced ITP levels have mistimed and reduced evening activity as well as a subtly shorter period (Hermann-Luibl *et al.*, 2014), indicating that ITP may complement PDF signalling and aid the regulation of evening activity peaks (Johard *et al.*, 2009; Hermann-Luibl *et al.*, 2014). The pathway for ITP signalling is still to be fully described (Beckwith and Ceriani, 2015).

Some neuropeptides that are expressed outside of the clock circuitry have been shown to impact on circadian rhythms, such as diuretic hormones 31 and 44 (DH31 and DH44), leucokinin neuropeptide and allatostatin (reviewed in He *et al.*, 2017).

Clock cells also communicate using several classical neurotransmitters which have been shown to impact on circadian activity (Muraro, Pérez and Ceriani, 2013). Acetylcholine is synthesised and released by the NPF-positive LN_ds and the 5th s-LN_v, interestingly the s-LN_vs are sensitive to acetylcholine suggesting that cholinergic clock cells can signal back to the s-LN_vs (Johard *et al.*, 2009; Lelito and Shafer, 2012). Furthermore, as discussed in 1.2.5.2.3, acetylcholine is utilised by the visual system to relay light input to the clock (Schlichting *et al.*, 2019; Alejevski *et al.*, 2019). Some DN1 and DN3 neurons release glutamate which signals to LN_vs and has been shown to be required for robust rhythms, likely by reinforcing circuit synchrony i.e. feeding information back to the ‘pacemakers’ (Hamasaka *et al.*, 2007; Collins *et al.*, 2014; Guo *et al.*, 2016). γ -aminobutyric acid (GABA) A receptor expression has been documented in the s-LN_vs. GABA-signalling is thought to contribute to s-LN_v pacemaker function by helping set 24 h periodicity; however the identity of the GABA-secreting neurons which signal to the s-LN_vs is still unclear (Hamasaka, Wegener and Nassel, 2005; Dahdal *et al.*, 2010; Lelito and Shafer, 2012).

Chapter 1:

1.2.6.2 Circadian network for light entrainment

Drosophila central circadian clocks receive light input via two distinct pathways; CRY/JET (1.2.5.1) and the visual system (1.2.5.2). Visual light input is received by each clock cell cluster independently from each other via a relay of histaminergic and cholinergic signalling centred in the aMe neuropil of the optic lobe (1.2.5.2.3). CRY signals light stimuli direct to the molecular oscillator by the light-dependent degradation of TIM (1.2.5.1); however CRY is only present in about half of the clock cells in the fly brain (the s- and l-LN_vs, the 5th s-LN_v, 3 of the 6 LN_ds, the DN1_as and some DN1_ps) and as such light input across the circuitry is not uniform (1.2.5.1).

According to the longstanding dual oscillator model for circadian rhythmicity, the PDF-expressing M-cells (s-LN_vs) are dominant in the dark and dominance switches to the E-cells following dawn (1.2.4.2) (Helfrich-Förster, 1998; Renn *et al.*, 1999; Picot *et al.*, 2007; Stoleru *et al.*, 2007). As discussed in 1.2.5.1.3, it has been shown that CRY expression in a subset of E-cells (3 CRY-positive LN_ds and the 5th s-LN_v) alone is sufficient to allow behavioural entrainment to shifted LD cycles (Yoshii *et al.*, 2015). However, the M-cells and PDF signalling have been shown to play a key role in circadian light responses. The l-LN_vs, although less important than the s-LN_vs in generating activity rhythms (1.2.4.2), are essential for light-mediated phase advances at dawn (Grima *et al.*, 2004; Shang, Griffith and Rosbash, 2008), and PDF signalling specifically from the l-LN_vs to the E-cells is required to set the correct phase of evening activity in an LD cycle (Schlichting *et al.*, 2016). Furthermore, flies that lack both CRY and PDF signalling lack the evening activity peak in LD, have damped molecular PER rhythms in the E-cells and are not able to entrain to a delayed 8 h LD cycle (Cusumano *et al.*, 2009; Zhang *et al.*, 2009; Im, Li and Taghert, 2011); showing that CRY acts alongside PDF to help govern E-peak phase and amplitude.

It has also been shown that a subset of posterior DNs, the DN1_ps (1.2.4.1), can promote both M- and E-behavioural activity peaks (Zhang *et al.*, 2010b). PDF signalling specifically to the DN1_ps is required for a normal M-peak of activity (Lear, Zhang and Allada, 2009; Zhang *et al.*, 2010a), with the same subset of cells also responsible for damping E-activity in response to high light levels (Zhang *et al.*, 2010b; Zhang *et al.*, 2010a). The DN1_ps are a heterogeneous cluster of cells, with variable expression of CRY, PDF and the Vesicular glutamate transporter (VGLUT) seen across the subset (Zhang *et al.*, 2010b; Im and Taghert, 2010; Collins *et al.*, 2014; Hamasaka *et al.*, 2007; Guo *et al.*, 2016). Glutamatergic DN1s have been shown to negatively feedback on the M- and E-cells to promote sleep, especially around midday i.e. the siesta period (Guo *et al.*, 2016). Most CRY-positive DN1_ps co-express VGLUT, conversely VGLUT-negative DN1_ps appear to lack CRY (Chatterjee *et al.*, 2018). Oscillator function in the CRY/VGLUT-positive DN1_ps alone was only

sufficient to drive morning anticipation, whereas an oscillator only in the DN1_ps lacking both CRY and VGLUT could generate evening, but not morning, anticipatory behaviour (Chatterjee *et al.*, 2018). This therefore indicates a second pair of oscillators, residing in the dorsal neurons, which couples with the previously defined lateral oscillator pair to generate the archetypal fly behaviour in a 12hL:12hD LD cycle (1.2.4.2) (**Figure 1.8**) (Chatterjee *et al.*, 2018).

In the dark, there is a strong association between the s-LN_vs and the CRY/VGLUT-positive DN1_ps. Changes in the periodicity of former is mirrored in the latter, indicating that the CRY/VGLUT-positive DN1_ps are enslaved by the s-LN_vs (Chatterjee *et al.*, 2018). However, in the light the s-LN_vs switch their enslaved oscillator and instead drive rhythmicity in the 3 CRY-positive LN_ds and the 5th s-LN_v (Chatterjee *et al.*, 2018). Interactions between the s-LN_vs and their enslaved oscillators requires PDF signalling and it was shown that signalling to the PDFR receptors present on either the CRY/VGLUT-positive DN1_ps or the 3 CRY-positive LN_ds and the 5th s-LN_v was increased in the dark and light respectively (Chatterjee *et al.*, 2018). Therefore, light changed the strength of coupling between the PDF-positive morning cells and PDF-negative slave oscillators (Chatterjee *et al.*, 2018), reconfiguring the network hierarchy (**Figure 1.8**).

As previously stated, PDF signalling from the s-LN_vs to the CRY/VGLUT-positive DN1_ps is required for correct phasing of morning activity (Lear, Zhang and Allada, 2009; Zhang *et al.*, 2010a; Chatterjee *et al.*, 2018). It has now been shown that electrical activity in the DN1_ps is also required for correct M-activity; however not via the aforementioned feedback signalling to the LN_vs (1.2.6.1.2), but instead the DN1_ps partake in feedforward signalling to govern M-activity (Chatterjee *et al.*, 2018). This suggests a single signalling axis is responsible for morning activity i.e. both M-oscillators act in series (**Figure 1.8**) (Chatterjee *et al.*, 2018). In contrast, the CRY/VGLUT-negative DN1_ps influence E-activity independently of the 3 CRY-positive LN_ds and the 5th s-LN_v (**Figure 1.8**) (Chatterjee *et al.*, 2018). A properly aligned evening peak is indicative of proper entrainment to an LD cycle (Stoleru *et al.*, 2004; Grima *et al.*, 2004; Rieger *et al.*, 2006), therefore having two separate means of controlling E-activity may reflect the importance evening activity entrainment (Chatterjee *et al.*, 2018). Under high-light intensities, the CRY/VGLUT-negative DN1_ps inhibit evening activity (Zhang *et al.*, 2010b; Zhang *et al.*, 2010a; Chatterjee *et al.*, 2018). This inhibition is due to increased PDF signalling from the s-LN_vs in response to increased light input from the visual system (1.2.5.2), indicating PDF signalling can gate evening activity promoted by the CRY/VGLUT-negative DN1_ps (**Figure 1.8**) (Chatterjee *et al.*, 2018).

These results, as well as multiple other studies (Rieger *et al.*, 2006; Yao and Shafer, 2014; Dissel *et al.*, 2014; Yao *et al.*, 2016), expose the simplicity of a dual oscillator model (1.2.4.2) and instead

Chapter 1:

suggest that the circadian network is made up by multiple functional subunits defined by their light sensitivity (1.2.5), expression profile (1.2.6.1) and connectivity.

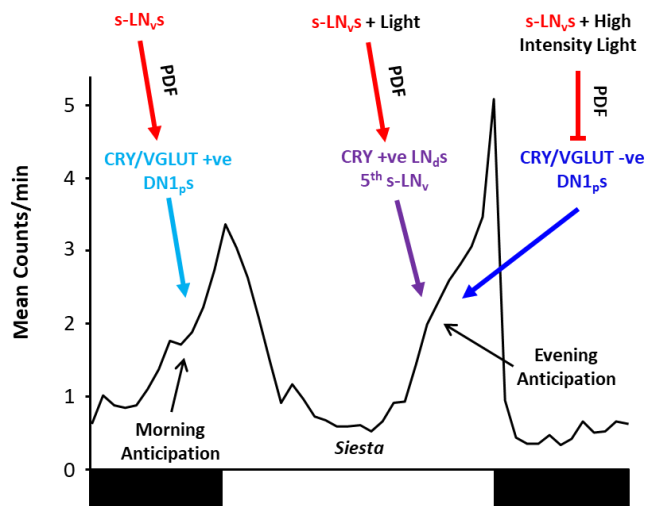


Figure 1.8 Multi-oscillator model for *Drosophila* locomotor behaviour in an LD cycle.

Adapted from Chatterjee *et al.* (2018). Average activity profile of male flies over 10 days in a 12hL:12hD Light:Dark (LD) cycle at a constant temperature (Light = white box, Dark = black boxes). Morning and evening anticipatory behaviour and the siesta period are annotated in the figure. The s-LN_vs and CRY/VGLUT-positive DN1_ps work in series to govern morning activity whereas the CRY-positive LN_ds and 5th s-LN_v and CRY/VGLUT-negative DN1_ps work in parallel to generate evening activity. PDF signalling from s-LN_vs to the CRY/VGLUT-positive DN1_ps is required for morning activity and in the light, the s-LN_vs switches enslaved oscillator to the CRY-positive LN_ds and 5th s-LN_v where PDF signalling influences the phase of evening activity. In high light intensities, PDF signalling inhibits CRY/VGLUT-negative DN1_ps and suppresses evening activity output.

The above model explains circuit organisation in a standard 12hL:12hD cycle but does not explore how the circuit adapts in response to changing light stimuli. It has been proposed that defined clock cell clusters may be required to phase advance or phase delay the clock in response to light stimuli (l-LN_vs and DN1s respectively) (Shang, Griffith and Rosbash, 2008; Tang *et al.*, 2010). However, it was shown more recently that JET expression is required in both the M- and E-cells to mediate behavioural phase shifts to light-pulses (1.2.5.1.3) (Lamba *et al.*, 2014), suggesting that the circuitry works together to reset the circadian phase in response to light.

If activity is induced in the PDF neurons, phase shifts are seen in PDF-receptive cells comparable to phase shifts evoked by light-pulses, indicating the PDF cells as key mediators in light entrainment (Guo *et al.*, 2014). Conversely, recording the light-responses of clock neurons in a *Drosophila* whole-brain explant suggested that the LN_ds are the driving force behind synchronising

the network to phase-advancing light pulses (Roberts *et al.*, 2015). More recent research suggests that clock function in either the classically defined M- or E- oscillators is sufficient to allow behavioural phase delays and advances to light-pulses; however, robust entrainment requires co-ordinated entrainment across the entire circuit which is mediated largely by PDF signalling (Lamba, Foley and Emery, 2018). The ability to phase shift the circadian network in the absence of either a designated M- or E-oscillator suggests that these phase shifts are a consequence of the cell-autonomous activity of CRY (Lamba, Foley and Emery, 2018).

In summary, precise neuronal communication keeps the clock entrained in standard an LD cycle with light driving an opportunistic swap between enslaved oscillator partners of the s-LN_{v,s} (Chatterjee *et al.*, 2018). When challenged to reset the clock in response to light, communication across the circuitry is paramount in order to generate a robust entrained response (Lamba, Foley and Emery, 2018). CRY and the visual system signal light input widely across the circuitry (1.2.5) and both trigger light entrainment in individual clock cells independently i.e. CRY acts cell-autonomously (1.2.5.1) and visual light input is signalled to the circuit in parallel via the aMe (1.2.5.2.3). In both cases, it is therefore likely that light synchronisation of individual cells is communicated across the circuit in order to generate an entrained network.

1.2.7 Transducing Clock Function to Locomotor Output

Despite our current understanding of the cellular and molecular basis of circadian rhythmicity, the exact mechanism that couples neuronal clock function and a rhythmic behavioural output is still unclear. Functional connections exist between clock cells and regions of the *Drosophila* brain which have proposed roles in co-ordinating output rhythms. The DN1_{p,s} have been shown to directly contact and signal to the Pars Intercerebralis (PI), the fly equivalent of the mammalian hypothalamus, which in turn signals to the dorsal tritocerebrum which sends projections to locomotor centres in the fly thorax that mediate movement (Rajashekhar and Singh, 1994; Cavanaugh *et al.*, 2014; King and Sehgal, 2018).

A screen for neuronal groups that could initiate locomotor activity when innervated revealed the ring neurons of the Ellipsoid body (EB-RNs) as prime candidates for transducing clock activity to locomotor output (Robie *et al.*, 2017). The EB is a pre-motor centre that forms part of the central complex, the primary locomotor control centre in insects involved in higher coordination and motor behaviour (Strauss and Heisenberg, 1993). Over recent years, several studies have linked the EB-RNs to the regulation of sleep-wake cycles in *Drosophila*. Independently, two groups have demonstrated that a subset of anterior projecting DN1_{p,s} signal to neurons in the anterior optic

Chapter 1:

tubercle, a visual processing centre, which relays clock function to subgroups of EB-RNs to regulate sleep and arousal (Lamaze *et al.*, 2018; Guo *et al.*, 2018).

Using a multiplicity of innovative techniques, it has been shown that the EB-RNs exhibit spontaneous peaks of activity that correlate to morning and evening bouts of activity (Liang *et al.*, 2019) and that these timed activity peaks are driven independently by the M- and E-oscillators of the circadian clockwork (Liang *et al.*, 2019). No direct links between any clock neuron and the EB have been reported (Helfrich-Förster, 2005); however, both the M- and E-cells signal to a pair of dopaminergic neurons, called PPM3 (Liang *et al.*, 2019). The PPM3 neurons innervate the EB-RNs, thus indicating a pathway for how M- and E-cells regulate EB-RN activity, and the subsequent downstream locomotor effects, via a specific relay of dopamine signalling (Liang *et al.*, 2019). These results provide the best insight to date into the mechanism which transduces clock function into rhythmic locomotor output.

1.2.8 *Drosophila* Peripheral Oscillators

As introduced in 1.2.2, endogenous time-keeping mechanisms reside in many peripheral tissues of *Drosophila* which regulate physiological rhythms in an organ/tissue specific manner (Ito and Tomioka, 2016). These tissues include, but are not limited to, the chemosensory hairs of the antenna, proboscis, legs and wing margins (Plautz *et al.*, 1997a); some excretory, digestive and reproductive organs (Giebultowicz and Hege, 1997; Giebultowicz, Ivanchenko and Vollintine, 2001); the visual system (Chen *et al.*, 1992); the secretory oenocytes (Krupp *et al.*, 2008; Krupp *et al.*, 2013); and the endocrine prothoracic gland (Myers, Yu and Sehgal, 2003; Morioka, Matsumoto and Ikeda, 2012). Many studies into peripheral oscillator function utilise a luciferase reporter assay where the *firefly luciferase (luc)* gene is conjugated to a clock-gene promoter i.e. the *per* or *tim* promoter. Luciferase enzyme is therefore expressed rhythmically, under the control of CLK/CYC (1.2.3.2), and in the presence of its luciferin substrate, will generate rhythms in bioluminescence (Brandes *et al.*, 1996; Plautz *et al.*, 1997b). Bioluminescence is therefore a proxy for clock driven transcriptional activity and can be used to assess peripheral clock function in whole flies or dissected tissues (Plautz *et al.*, 1997a; Plautz *et al.*, 1997b; Stanewsky *et al.*, 1997).

Molecular analysis of peripheral clocks indicated that the same molecular oscillator that governs central clock rhythmicity (as detailed in 1.2.3), also governs rhythmicity of peripheral clocks (Plautz *et al.*, 1997a; Hardin *et al.*, 2003). There is however some discrepancy regarding the role of CRY in the periphery (1.2.8.1) with conflicting reports arguing that CRY either acts solely as a photoreceptor, like in central clocks (1.2.5.1) (Ito *et al.*, 2008; Agrawal *et al.*, 2017), or functions as

both a photoreceptor as well as part of the core molecular TTFL (1.2.3.2) (Stanewsky *et al.*, 1998; Ivanchenko, Stanewsky and Giebultowicz, 2001; Collins *et al.*, 2006).

1.2.8.1 The role of CRY in peripheral clock function

A genetic screen for mutants that impacted peripheral rhythmicity initially revealed CRY as an integral component in light entrainment (1.2.5.1). The hypomorphic *cry^b* mutation rendered whole fly bioluminescence rhythms arrhythmic under a standard 12hL:12hD LD cycle (1.2.5.1) (Stanewsky *et al.*, 1998). The vast majority of bioluminescence signal in a whole fly is generated by peripheral oscillators, in particular those present in the head and the compound eye (Brandes *et al.*, 1996). Therefore, arrhythmic bioluminescence rhythms suggests arrhythmicity of peripheral clocks, indicating that CRY is required for core clock function (Stanewsky *et al.*, 1998). Multiple studies in isolated peripheral tissues also suggest that alongside a role in circadian photoreception, CRY is required for peripheral core clock function. For example, a light-pulse results in TIM degradation in the Malpighian tubules (MT), an effect not observed in *cry^b* flies (Ivanchenko, Stanewsky and Giebultowicz, 2001). Without functional CRY, the MT no longer exhibit PER and TIM oscillations, suggesting CRY is required for light entrainment and clock function in the MT (Ivanchenko, Stanewsky and Giebultowicz, 2001). It was shown that an overexpression of CRY and PER in the compound eye, as well as in cell culture, inhibited CLK/CYC transcriptional activity (Collins *et al.*, 2006). CRY acting as a transcriptional repressor in the periphery, analogous to mCRY (1.2.3.2 and 1.2.5.1.1), explains why peripheral rhythmicity was lost in *cry^b* flies (Levine *et al.*, 2002a; Collins *et al.*, 2006; Ko and Takahashi, 2006).

It has however been proposed that desynchrony between peripheral oscillators i.e. clocks across the organism are oscillating with different phases to each other, can result in a loss of bioluminescence rhythms (Koh, Zheng and Sehgal, 2006). CRY is a circadian photoreceptor acting to synchronise the molecular oscillator to light (1.2.5.1) (Stanewsky *et al.*, 1998; Emery *et al.*, 2000b; Emery *et al.*, 2000a), therefore a lack of functional CRY decreases light entrainability, thus providing an alternative explanation for the arrhythmicity seen in *cry^b* flies (Ito and Tomioka, 2016).

In some peripheral tissues CRY functions only as a photoreceptor and is not required for clock function, two examples of which are the epidermis and the prothoracic gland (PG). Cuticle deposition rhythms are regulated by clocks residing in *Drosophila* epidermal cells and are entrained by LD cycles (Ito *et al.*, 2008). In *cry^b* and *cry⁰* mutants, cuticle deposition rhythms were no longer able to synchronise to light but were rhythmic in free-running conditions, indicating CRY

Chapter 1:

isn't needed for clock function in the epidermis (Ito *et al.*, 2008). Studies into rhythmic eclosion lead to the identification of *per* (1.2.3.1) (Konopka and Benzer, 1971). Eclosion is a once-in-a-life-time event that occurs rhythmically in a given fly population (Pittendrigh, 1954; Pittendrigh, Bruce and Kaus, 1958). Timing of eclosion is under the control of two oscillators in the pupa, one residing in the LN_vs of the pupal brain and the other in the PG (Myers, Yu and Sehgal, 2003). In *cry* mutants, rhythmic eclosion persists in both LD cycles and DD, and molecular oscillations of PER and TIM are still rhythmic in the PG (Mealey-Ferrara, Montalvo and Hall, 2003; Dolezelova, Dolezel and Hall, 2007; Morioka, Matsumoto and Ikeda, 2012). CRY in the PG was shown to regulate light-dependent TIM degradation (Morioka, Matsumoto and Ikeda, 2012), showing that, like in cuticle deposition, CRY is involved in light entrainment but isn't required for clock function. This conclusion is supported by a recent study which demonstrated that there is no interaction between CRY and either PER or CLK in the periphery (Agrawal *et al.*, 2017), arguing against a role for CRY as a transcriptional repression in the core molecular TTFL.

The exact role of CRY in the periphery is therefore still to be determined. However, despite the obvious discrepancies a common theme exists between both lines of experimentation; CRY acts as a circadian photoreceptor in the periphery (1.2.8.2).

1.2.8.2 Peripheral light entrainment

Most isolated peripheral tissues, maintained in culture, respond directly to a light stimulus (Plautz *et al.*, 1997a), and rhythmic bioluminescence, in-line with imposed LD conditions, was observed in the wings, antenna and proboscis (Plautz *et al.*, 1997a; Levine *et al.*, 2002a). Light can penetrate the *Drosophila* cuticle (Rieger, Stanewsky and Helfrich-Förster, 2003), and therefore peripheral oscillators can receive light stimuli independently from each other and the brain. As discussed previously, CRY confers light sensitivity to peripheral tissues (1.2.8.1) (Stanewsky *et al.*, 1998; Ivanchenko, Stanewsky and Giebultowicz, 2001). However, other than reported expression in the compound eye, the peripheral expression pattern of CRY remained relatively uncharacterised (Yoshii *et al.*, 2008; Agrawal *et al.*, 2017). Using transgenic GFP-CRY, which mimics endogenous CRY expression in the brain, peripheral CRY expression was mapped in the MT, intestine and fat body (Agrawal *et al.*, 2017).

Studies from whole fly heads showed CRY binds to TIM outside of the brain (Busza *et al.*, 2004), highlighting the possibility that CRY-mediated peripheral light entrainment occurs via the canonical circadian mechanism of light-induced TIM degradation (1.2.5.1). Indeed, the kinetics of light-evoked TIM degradation in the MT, fly heads and cell culture models matched that of

neuronal clock cells and is CRY-dependent (Ivanchenko, Stanewsky and Giebultowicz, 2001; Koh, Zheng and Sehgal, 2006; Peschel *et al.*, 2009; Agrawal *et al.*, 2017), further suggesting that peripheral CRY photoreception is mechanistically the same as in central clocks (1.2.5.1). However, unlike *cry* mutants, *jet^f* had no impact on peripheral rhythmicity (Koh, Zheng and Sehgal, 2006) but as discussed in 1.2.5.1.2, this mutation also has very little effect on behavioural light entrainment (Koh, Zheng and Sehgal, 2006; Peschel, Veleri and Stanewsky, 2006). Further investigation into the role of JET peripheral light entrainment is therefore required.

Unlike mammalian peripheral clocks (1.1.3), communication between central and peripheral oscillators is not common in flies (discussed in 1.2.8.3) (Ito and Tomioka, 2016; Mohawk, Green and Takahashi, 2012). Central clocks residing in the fly brain receive light input via two distinct pathways (1.2.5), however at present there are no documented means of signalling visual light input to the periphery. Therefore light entrainment of *Drosophila* peripheral oscillators appears to rely exclusively on CRY-mediated light synchronisation.

1.2.8.3 Communication between central and peripheral oscillators

Drosophila peripheral clocks are heterogeneous in nature and are present in many tissues where they partake in a variety of physiological functions (1.2.8). The molecular oscillator itself is cell-autonomous (1.2.3), however the resident clock cells of the brain form complex networks to maintain synchrony and generate rhythmic output (1.2.6 and 1.2.7). This is not the case in the periphery.

The majority of peripheral oscillators, including those in the MT, antenna, proboscis, epidermis and fat body, function independently of central clock function (Plautz *et al.*, 1997a; Giebultowicz and Hege, 1997; Giebultowicz, Ivanchenko and Vollintine, 2001; Ito *et al.*, 2008; Xu, Zheng and Sehgal, 2008). There are however two examples of central clock activity governing peripheral clock function, although the relationship between the central and peripheral oscillators differs between the two. Oenocytes, which are involved in sex pheromone production, possess a self-sustaining molecular oscillator (Krupp *et al.*, 2008). As mentioned in 1.2.5.4, pheromones and other olfactory cues produced by one individual can act as zeitgebers capable of entraining the behaviour of others (Levine *et al.*, 2002b; Fujii *et al.*, 2007). The phase of the oenocyte oscillator can be modulated by PDF signalling from the central clock (Krupp *et al.*, 2013), which as discussed previously plays a pivotal role in synchronisation across the central clock network (1.2.6) (Renn *et al.*, 1999), suggesting the oenocyte oscillator is enslaved by the central clock.

Chapter 1:

Rhythmic eclosion is controlled by the action of two oscillators, as mentioned in 1.2.8.1 (Myers, Yu and Sehgal, 2003). Oscillator function in both the LN_vs and PG is required for rhythmic eclosion. The PG clock was shown to be governed by the LN_v oscillator as when the LN_vs are ablated, eclosion rhythms and molecular TIM oscillations in the PG are lost (Myers, Yu and Sehgal, 2003). It was shown more recently that light input from the central clock is required to maintain PER oscillations in the PG and that in DD, PER oscillations are lost (Morioka, Matsumoto and Ikeda, 2012). Interestingly, the same was not true for TIM. Communication from the central clock appears to contribute significantly to the molecular oscillators in the PG, suggesting the PG oscillator is driven by the central clock.

The autonomy amongst peripheral oscillators highlights the importance of CRY-mediated light entrainment in maintaining synchrony across the peripheral clocks of *Drosophila*.

1.3 Summary and Project Aims

Daily fluctuations in light and temperature act as environmental cues for synchronising endogenous circadian clocks. Properly entraining behaviour and physiology in-line with environmental cycles contributes to the fitness, well-being and overall success of an organism. Light is the most potent and reliable zeitgeber, however environmental light is also spectrally complex and highly variable. In order to detect and entrain effectively to this complex input, *Drosophila* central clocks receive light input via two independent pathways; CRY/JET and the visual system, conferring immense light sensitivity. Furthermore the network organisation of the central circadian circuitry generates a co-ordinated response to light stimuli, resulting in robust rhythmic output. In contrast, peripheral clocks function independently of each other, and the central clock, and receive synchronising light input exclusively from the circadian photoreceptor CRY.

Light entrainment of *Drosophila* circadian clocks has been extensively studied by assaying behavioural and molecular responses to brief light-pulses, varied photocycles or re-entrainment to a shifted Light:Dark regime; all of which do not require the clockwork to deviate greatly from its inherent 24 h periodicity. In this thesis, extreme equinox photocycles are used to stretch the oscillator to the limits of light-induced entrainment. At these limits the clockwork has to constantly shift or re-set the molecular oscillator, away from free-running 24 h periodicity, to keep time with the environmental condition, providing a highly sensitive measure of plasticity. If we can stretch central and peripheral molecular clocks to the limits of light-induced entrainment we may reveal more about how the underlying circadian circuitry adapts to facilitate plasticity at the behavioural and molecular level in the clocks of the *Drosophila* brain and periphery.

Such research into invertebrate circadian rhythms using *Drosophila melanogaster* as a model has many potential practical applications e.g. informing targeted means of invertebrate pest management (1.2.1.1). Furthermore, a greater understanding of circadian plasticity in *Drosophila* may inform our understanding of circadian regulation in humans and other higher order organisms, where circadian dysfunction has a detrimental impact on health and well-being (1.1.4).

Therefore, the main aim of this project is:

- **To investigate the light-induced plasticity of *Drosophila* central and peripheral clocks in the presence of extreme equinox photocycles.**

Chapter 1:

This main aim can be broken down into more specific aims which are addressed throughout following chapters:

Chapter 2;

- Investigate the inherent plasticity of circadian clock mechanisms by defining the limits of wild-type *Drosophila* behavioural entrainment to equinox Light:Dark cycles.
- Investigate how the molecular oscillator adapts at these extremes of light-induced entrainment in order to generate rhythmic behavioural output.
- Determine whether or not entrainment to extreme photocycles impacts *Drosophila* life-span.

Chapter 3;

- Investigate what components of the *Drosophila* circadian clockwork are required to allow behavioural entrainment to long and short equinox photocycles. In particular, assess the relative contributions of the CRY/JET pathway and the visual system.
- Determine where in the clock circuitry CRY/JET are needed to facilitate entrainment to extreme LD cycles.
- In the absence of CRY, is the visual system sufficient to entrain behaviour to red-light dark cycles?

Chapter 4;

- Investigate the inherent plasticity of peripheral circadian clock mechanisms by defining the limits of wild-type *Drosophila* peripheral entrainment to equinox Light:Dark cycles.
- Determine the light input pathways in peripheral entrainment to equinox photocycles.
- Investigate how the peripheral molecular oscillator adapts at the extremes of light-induced entrainment.

Chapter 2: Light-dependent plasticity of wild-type *Drosophila* behavioural and molecular rhythms

2.1 Introduction

Endogenous clocks have evolved as a result of the predictable changes which occur over the course of our 24 h day. These circadian clocks possess the ability to receive and respond to environmental cues, thus allowing organisms to anticipate these changes and entrain their physiology optimally with the world around them, contributing significantly to the overall fitness and survival of an organism (Helfrich-Förster, 2005; Allada and Chung, 2010). Cycles in temperature and humidity can impact on the circadian clockwork; however the dominant synchronising factor is light, which entrains rhythms to the 24 h solar cycle (Hardin, 2011).

In relation to external photoperiods, flies with an intact clockwork can adapt their characteristic behavioural profile in response to both 24 h and 16 h photoperiods, when compared to the 'driven rhythmicity' elicited in *per⁰* flies (Wheeler *et al.*, 1993). *per⁰* flies carry a point mutation in *per* which renders rhythms in activity and eclosion arrhythmic (Konopka and Benzer, 1971). As a result, behavioural rhythms seen in *per⁰* flies are 'startle responses' driven by changes in environmental light exposure and do not require an endogenous oscillator (Rieger, Stanewsky and Helfrich-Förster, 2003; Mrosovsky, 1999). The ability to extend the clockwork and entrain to cycles in excess of 24 h was not investigated nor was the state of the molecular oscillator when challenged to entrain to these different photoperiods. Entrainment of *cry* and visual system mutants has been assayed in varying equinox LD cycles, including photocycles in excess of 24 h (9hL:9hD, 13hL:13hD and 14hL:14hD); however wild-type entrainment in these conditions was not investigated (Dolezelova, Dolezel and Hall, 2007). Administering a brief light pulse at different times of day demonstrated the impact that light can have by either delaying or advancing the phase of the core circadian molecular oscillator (Myers *et al.*, 1996; Saunders, Gillanders and Lewis, 1994). These effects are explained by the induction of CRY-dependent TIM degradation where; a pulse in the early night elicits a phase delay as PER and TIM accumulation is interrupted; and a pulse in the late night results in a phase advance due to de-repression of CLK/CYC. Further experiments where flies are challenged to entrain to 24 h cycles with varying amounts of light and dark (Shafer *et al.*, 2004), as well as re-entrainment to shifted 24 h LD regimes (Suri *et al.*, 1998), have indicated how molecular rhythms in PER and TIM adjust to allow entrainment.

Chapter 2:

Interestingly, following LD entrainment, mammalian circadian clocks show a persistence of entrained rhythms when left to free-run in constant darkness (Pittendrigh and Daan, 1975). This maintenance of entrained rhythmicity is known as an 'after effect' and is the result of DNA-methylation triggered by light entrainment (Beaule and Cheng, 2011). The *Drosophila* genome does not encode a CpG DNA methylase (Pegoraro *et al.*, 2016) and as such, 'after-effects' are not thought to occur in flies; however varying LD cycles given during development were shown to impact on the free-running rhythms of *per* mutants (Tomioka, Uwozumi and Matsumoto, 1997).

A vast amount has been uncovered by light pulse, varied 24 h photocycle and re-entrainment experiments, however these represent a single challenge to a system which must constantly adapt to an ever changing environment or entrainment to cycles which are similar to their intrinsic periodicity. We hypothesise that, if we can use light to stretch the oscillator to the limits of entrainment by utilising equinox photocycles, extending the work by Wheeler *et al.* (1993), we may reveal more about how the underlying circadian circuitry adapts to facilitate plasticity at the behavioural and molecular level in the clocks of the *Drosophila* brain. Such research into invertebrate circadian rhythms using *Drosophila melanogaster* as a model has many potential practical applications, for example, informing the control of both horticultural pest species e.g. *Drosophila suzukii* and disease vectors e.g. *Anopheles* Mosquito (Meireles-Filho and Kyriacou, 2013; Shaw, Fountain and Wijnen, 2018). Furthermore, a greater understanding of circadian plasticity in *Drosophila* may inform our understanding of circadian regulation in higher order organisms, including humans, where circadian dysfunction and desynchrony impacts greatly on physiology and well-being (Hastings, Reddy and Maywood, 2003). It has been shown that aged mice that experience chronic jet-lag (i.e. their internal clocks are 'out of sync' with the external photoperiod) have decreased life-span (Davidson *et al.*, 2006). It may therefore be possible to learn more about the impact of circadian desynchrony on physiology by investigating the effect of extreme photocycle entrainment on *Drosophila*.

2.1.1 Aims

- Investigate the inherent plasticity of circadian clock mechanisms by defining the limits of wild-type *Drosophila* behavioural entrainment to equinox Light:Dark cycles.
- Investigate how the molecular oscillator adapts at these extremes of light-induced entrainment in order to generate rhythmic behavioural output.
- Determine whether or not entrainment to extreme photocycles impacts *Drosophila* life-span.

2.2 Methods

2.2.1 Analysis of *Drosophila* Locomotor Behaviour

2.2.1.1 DAM Behavioural Assay

Behavioural locomotor rhythms were assayed using the *Drosophila* Activity Monitoring System (DAM System; TriKinetics, Waltham, MA). Post eclosion, adult flies were anaesthetised using CO₂ and individually loaded into small glass cuvettes (5mm diameter/ 50-60mm length). Each cuvette was capped at one end containing ~10 mm of solid sugar-agar medium (**S.Table B.4**) (5% sucrose, 1% agar and 0.07% Tegosept) and the opposite end was plugged with cotton to prevent the fly escaping but still allowing gas exchange. Tegosept (see Appendix B.1.1) is added as an anti-fungal agent. Each DAM monitor housed 32 cuvettes with locomotion monitored via breaks in an infrared beam, beam breaks were recorded on DAM System software, provided by the manufacturer, and pooled in 5 minute bins (Currie, Goda and Wijnen, 2009)(**Figure 2.1, A**).

Individual monitors were loaded into light-tight black boxes (SolentPlastic) inside environmentally controlled rooms. Flies were subjected to equinox Light:Dark (LD) cycles ranging from 3-11c/wk (11c/wk = 7.64hL:7.64hD; 10c/wk = 8.4hL:8.4hD; 9c/wk = 9.33hL:9.33hD; 8c/wk = 10.5hL:10.5hD; 7c/wk = 12hL:12hD; 6c/wk = 14hL:14hD; 5c/wk = 16.8hL:16.8hD; 4c/wk = 21hL:21hD and 3c/wk = 28hL:28hD) at 23°C and ~70% relative humidity. White light LEDs provided illumination during the light phase of assays; sharp spectra peak at 441 nm and a smaller broader peak at 547 nm with an intensity of ~20 μW/cm² and were controlled by timers (see Appendix B.2 for LD regimes). Following 10 days in LD, monitors were moved to free-running conditions (constant darkness – DD) for a further 10 days.

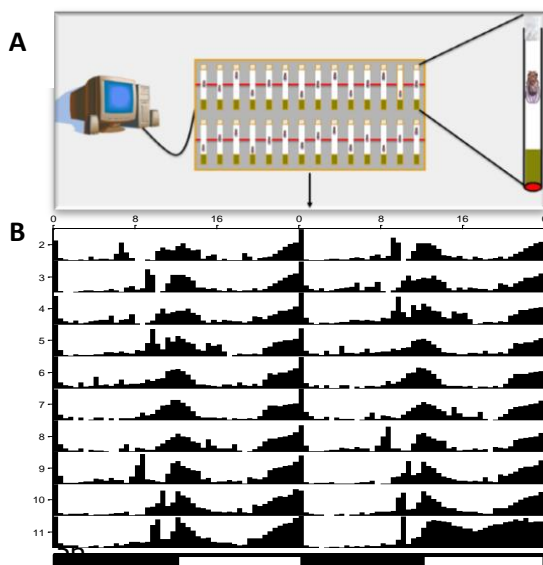


Figure 2.1 Schematic of TriKinetics DAM system and example Actogram.

A) Cartoon of a *Drosophila* activity monitor with an enlarged detail of a fly loaded into a locomotor cuvette. Interruptions of the infrared beam were recorded as fly activity events. Data was recorded on a computer using TriKinetics DAM System software. **B)** Average actogram of normalized activity for *cry*⁰¹ heterozygote (*w*¹¹¹⁸;;*cry*⁰¹/+) control flies during 10 days in a 7c/wk entrainment incubator.

Locomotor data was analysed and interpreted using ClockLab software (ActiMetrics; Wilmette, IL, USA). Data from all surviving flies was then collated and averaged according to gender, genotype and experimental condition in order to generate qualitative graphs. Average activity was pooled into either 5 or 30 minute bins (stated in figure).

Actograms displayed activity over time, plotted on a 24 h scale (unless stated otherwise). All actograms were double-plotted, i.e. each day was displayed twice with day 1 and 2 on the first line of the graph, day 2 and 3 on the second, and so on. Average activity for each bin was represented by a black bar, with the height of the bar corresponding to the amount of activity (**Figure 2.1, B**).

Periodicity and rhythmic strength were presented using a χ^2 -periodogram plot for the averaged cohorts. Amplitude, a measure of rhythmic strength, was plotted as a function of period length (h) in χ^2 -periodograms. Significant rhythmicity in these diagrams is evident where the amplitude values exceed that of the set confidence level ($p < 0.01$ - green line on plots), at a given period length. Periodograms were plotted from 12 - 48 h (unless stated otherwise) in order to capture the wide range of period lengths displayed.

To investigate phase of activity, relative to the LD condition, activity profiles were generated to display average activity over 10 days in the context of a single LD cycle. Activity profiles were centred around mid-day, as denoted by the LD bar above the plot (Black = dark phase and White = light phase). Activity profiles were plotted on a scale corresponding to the period length of experimental LD cycle, so that phase of activity was aligned to the imposed environmental condition.

2.2.1.2 Quantitative Analyses

χ^2 periodogram analysis was used to calculate a period length, as well as the corresponding power and significance of that rhythm, for each individual fly. Unless otherwise stated in figures, data was pooled into 30 minute intervals for analysis. Period length analysis windows were defined for each LD cycle tested to include both the period length of the LD cycle (entrained - ExT) as well as the intrinsic circadian (~24 h) period length: 13-26 h for 10c/wk; 15 – 30 h for 7c/wk and 18-36 h for 5c/wk (see 'Standard Parameters' in **S.Table B.5** for all cycles). It is important to note that for 11 and 10c/wk LD conditions, the period length range used for analysis also included a possible 'harmonic' component at 1.5x the entrained period length (11c/wk; ExT = 15.27 h and 1.5x Harmonic = 22.9 h; 10c/wk; ExT = 16.8 h and 1.5x Harmonic = 25.2 h), a result of *Drosophila's* bimodal circadian activity pattern. In addition, ClockLab did not allow analysis of period lengths in

Chapter 2:

excess of 50 h. Therefore, in order to analyse data collected for 3c/wk (56 h cycle), the collection interval in the raw data file was adjusted to read 4 min instead of 5 min. This enables analysis of the data in ClockLab across an interval including the period representing the photocycle length (44.8 h = $\frac{4}{5}$ of 56 h). Prior to quantitative analysis, individual period length values were multiplied by 5/4 to reflect the true period length in a 3c/wk condition. DD behavioural analysis was conducted over the first 7 days in DD following 10 days of prior LD entrainment and analysed for rhythms spanning a 12-48 h range.

Entrainment to an imposed LD cycle was defined as the alignment of behavioural rhythmicity to that of the external condition. Therefore, flies were initially designated as entrained to the external LD cycle according to whether or not their period length fell within a defined entrained or harmonic range (see **S.Table B.5**). Rhythmic flies with a period length outside these entrained or harmonic ranges were categorised as 'other' and flies with no detectable rhythm were deemed to be arrhythmic.

Alongside period length, the strength of a rhythm was assessed by Relative Rhythmic Power (RRP), calculated by dividing the 'power' by the 'significance'. Flies were determined to be rhythmic (R), weakly rhythmic (WR) or arrhythmic (AR) dependent on the relative rhythmic power. (R – $RRP > 1.5$, WR – $RRP < 1.5$, AR – no definable period length, therefore RRP cannot be calculated). AR flies were assigned an RRP of 1 (upper limit of arrhythmicity) so that they could be included in subsequent analysis.

In cases where it was possible to detect a 1.5x photocycle length 'harmonic' peak (11 and 10c/wk) close to the circadian range, χ^2 periodogram analysis was extended to detect both primary and secondary periodicities for each individual to determine to what extent flies with a primary periodicity in the circadian or 1.5x photocycle range were entrained. RRP values for the primary and secondary peaks were compared and the peak and associated period length with the higher RRP was considered dominant. This dominant period length was then used to categorise the flies as 'entrained' or 'other' using only the entrained range, not the harmonic range (see **S.Table B.5**); as such, flies with a dominant peak in the harmonic range were now classified as 'other'.

In order to better assess the quality of entrainment, further χ^2 periodogram analysis with more refined parameters (narrower period length range) was conducted to compare to strength of entrainment at the entrained period length to that at either 0.5x or 1.5x the entrained period length (and both for 7c/wk) (see **S.Table B.5**). A comparison of RRP across genotypes/conditions using this refined entrained window indicated a direct unambiguous measure of entrainment as it did not consider 'harmonic' period lengths. A ratio of $RRP(EXT)$ and either $RRP(0.5x)$ or $RRP(1.5x)$

was used to indicate in which conditions entrainment favoured the entrained or 'harmonic' rhythm ($RRP(ExT)/RRP(0.5x \text{ or } 1.5x \text{ harmonic}) > 1$ indicated a preferences for the entrained rhythm).

Composite bar charts were used to display the percentage of flies that were either entrained (green), displayed an 'other' (blue) rhythm or were arrhythmic (red). The significance of the differential distribution of flies into these defined categories was analysed using the *Fisher's exact test*.

GraphPad Prism 7.05 was used to generate all graphs and conduct statistical analysis. Analysis of variance (ANOVA) between genotypes or conditions were made with the non-parametric *Kruskal-Wallis test* with pairwise comparisons made using post hoc tests i.e. *Dunn's multiple comparison test* and *Mann-Whitney test* (test used is noted in figures). $p^{****} < 0.0001$; $0.0001 < p^{***} < 0.001$; $0.001 < p^{**} < 0.01$ and $0.01 < p^* < 0.05$.

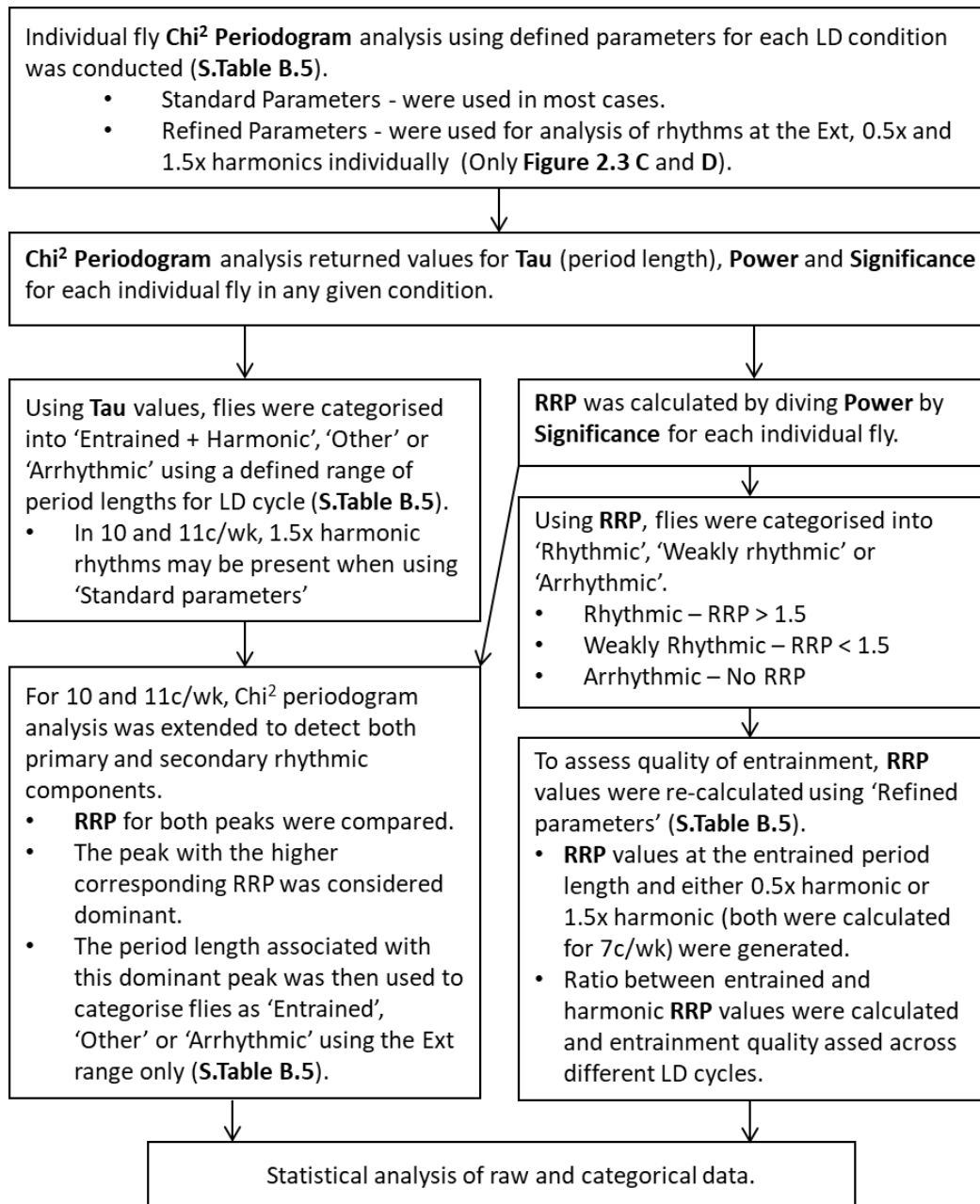


Figure 2.2 Quantitative analysis of *Drosophila* Locomotor Behaviour

2.2.2 Analysis of the *Drosophila* central molecular clockwork

2.2.2.1 Confocal Immunofluorescence Microscopy

The state of the molecular clocks of the *Drosophila* brain during long and short photocycles was assessed using confocal immunofluorescence microscopy. Wild-type flies of the genotype *w;tim(UAS)-Gal4;UAS-CD8::GFP* (double homozygotes), which expressed membrane-bound GFP in all clock-bearing cells of the *Drosophila* brain, were entrained to either a 10, 7, 5 or 3c/wk LD cycle (using the same light-tight boxes detailed in 2.2.1.1) for 3 days prior to brain dissection at three

distinct time-points during the LD regime. Brain dissections were conducted as previously described by (Wu and Luo, 2006), and detailed in Appendix B.4.1. Dissection time-points for all conditions are shown in **S.Figure B.1** and were selected with the intention of capturing the peak of PER expression for each condition.

Following dissection, brains were fixed in 4% paraformaldehyde, washed and stained for either PER or VRI, as well as GFP. Full staining protocol is detailed in Appendix B.4.1, and all antibody concentrations can be found in **Table 2.1**. Following staining, brains were mounted onto a microscope slide (Menzel Gläser, 76x26mm, B57011/2) within a dried square of nail polish, in VECTASHIELD hardset mounting medium (Vectorlabs, H-1400). The nail polish provided a barrier to the brains and prevented the samples being squashed by the glass coverslip (22x22mm). The coverslip edge was then sealed with nail polish to prevent the samples from drying out.

Images were acquired on a Leica SP8 confocal microscope, controlled with LAS X software (Leica Microsystems), using a 40X objective in Leica type F immersion oil. Imaging settings remained constant throughout all imaging experiments and were as follows; General: scan speed = 400 ns/pixel, pinhole = 1 AU, format = 1024x1024 and frame average = 3; GFP: 488 laser (5% power) and gain = 500-600; PER/VRI: 568 laser (1.5% power) and gain = 555. Z-stacks were generated using a step size of 1.04 μm (optical section for settings used) scanning each channel in sequence to prevent cross-excitation.

Table 2.1 Antibodies and their concentration used in immunofluorescence assays.

| Class | Antibody | Concentration | Source |
|-----------|----------------------------|---------------|--|
| Primary | Chicken anti-GFP | 1:200 | Abcam, Ab13970 |
| | Rabbit anti-PER | 1:4000 | J.C. Hall (Liu <i>et al.</i> , 1992) |
| | Guinea pig anti-VRI | 1:15000 | P.E. Hardin (Glossop <i>et al.</i> , 2003) |
| Secondary | Goat anti-Chicken (488) | 1:200 | Thermo-fisher, A-11039 |
| | Goat anti-Rabbit (568) | 1:300 | Thermo-fisher, A-11036 |
| | Goat anti-Guinea pig (568) | 1:200 | Thermo-fisher, A-11075 |

2.2.2.2 Image analysis

Quantification of PER/VRI levels in the cell bodies of clock cells was conducted using ImageJ. GFP staining was used to identify different clock cell clusters based on morphology, number and anatomical location, allowing regions of interest (ROI) to be generated for the cell body (soma) and nucleus of each cell. Using these ROIs, values for area, integrated density (total intensity in the area i.e. the sum of all the pixels) and mean grey value were obtained for PER/VRI fluorescence, as well as background measurements for each image (one background

Chapter 2:

measurement was taken for each cell body ROI per image, with a minimum of three measurements per image). All images were blinded prior to quantification to avoid analysis bias.

Corrected total cell fluorescence (CTCF) for each ROI was calculated using the following formula;

$$CTCF_{ROI} = Integrated\ Density_{ROI} - (Area_{ROI} \times Mean\ fluorescence\ of\ background)$$

Total and nuclear PER/VRI CTCF values, relative to background, were calculated for each cell identified, as well as a ratio between nuclear and cytoplasmic staining using the formula;

$$Nuclear/Cytoplasmic\ Ratio = Nuclear\ CTCF / (Total\ CTCF - Nuclear\ CTCF)$$

Subcellular localisation of PER/VRI was determined using this ratio where a *Nuclear/Cytoplasmic Ratio* > 1 indicates nuclear localisation.

GraphPad Prism 7.05 was used to generate all graphs and conduct statistical analysis. Total CTCF and Nuclear/Cytoplasmic Ratio were plotted both in real-time and scaled to a 24 h LD cycle (annotated in figure) to allow analysis of protein turnover kinetics as well as relative phase of accumulation across different LD cycles and clock cell groups. Analysis of variance (ANOVA) was conducted across all time-points within each condition using the non-parametric *Kruskal-Wallis test*. Pairwise comparisons between consecutive time-points, within each condition, were made using *Tukey's multiple comparisons test*. $p^{****} < 0.0001$; $0.0001 < p^{***} < 0.001$; $0.001 < p^{**} < 0.01$ and $0.01 < p^* < 0.05$.

Representative images for each cell type in each condition tested were generated using ImageJ. Cell-type specific ROIs were used to select the same representative area per cell-type across all experiments and in all cases the scale bar = 5 μ m.

2.2.3 Analysis of *Drosophila* Longevity

The impact of extreme photocycles on *Drosophila* life-span was assessed using a longevity assay, detailed by (Linford *et al.*, 2013). Flies were exposed to equinox LD cycles of 10c/wk = 8.4hL:8.4hD; 7c/wk = 12hL:12hD and 5c/wk = 16.8hL:16.8hD at 23°C and ~70% relative humidity (using the same light-tight boxes detailed in 2.2.1.1). All longevity assays conducted were on wild-type flies of genotype $w^{1118};cry^{01}/+$, which were the result of a genetic cross set in synchrony to allow for the easy collection of age-matched flies. Ten cohorts of ten individual newly eclosed adult flies (1-3 days old), segregated by gender, were housed on fresh cornmeal media (**S. Table B. 1**), totalling 100 flies per gender, per condition.

Initially, male flies were transferred to new media every 7 days, females every 3-4 days, and number of dead flies noted. Females were transferred more regularly as the appearance of larvae in the food made the food more liquid and increased the likelihood of flies getting stuck. Flies that got stuck in food or escaped over the course of the assay were not included in the analysis as their absence is not a reflection on life-span. When flies began to die, male flies were also flipped every 3-4 days to increase resolution of data.

GraphPad prism 7.05 was used to generate survival plots, conduct statistical analysis and calculate median survival for each condition. Survival plots show percentage survival over time (days). The *Log-rank (Mantel-Cox) test* was used to compare life-span across conditions for each gender.

$p^{****} < 0.0001$; $0.0001 < p^{***} < 0.001$; $0.001 < p^{**} < 0.01$ and $0.01 < p^* < 0.05$.

2.3 Results

2.3.1 Light-dependent plasticity of wild-type *Drosophila* behavioural rhythms

Locomotor behaviour was assayed as an *in-vivo* readout of central clock activity for 'wild-type control' flies of genotype $w^{1118};;cry^{01}/+$ using the DAM locomotor assay (2.2.1) to investigate light-induced plasticity of the *Drosophila* central circadian clock. Flies heterozygous for the cry^{01} mutation were used as the control strain as they showed equivalent behavioural entrainment (**S.Figure 1**), but improved longevity in comparison with the w^{1118} control strain (BDSC stock 5905).

2.3.1.1 Wild-type locomotor rhythms are entrainable to a wide-range of equinox photocycles

Wild-type flies displayed archetypal bimodal locomotor behaviour during a 7c/wk LD cycle with peaks of activity at dawn (lights-on) and at dusk (lights-off), representing the well documented M and E peaks of activity respectively (2.1), separated by a midday siesta. Activity ramped up prior to these LD transitions indicating the presence of an internal time-keeping mechanism which allowed anticipation of dawn and dusk (**Figure 2.3, A**). This anticipatory behaviour is modulated by PDF signalling (Lear, Zhang and Allada, 2009), as previously discussed. Bimodal rhythmic activity was still seen in flies lacking a functional clockwork. per^{01} flies, with a null mutation for the *period* gene, were behaviourally arrhythmic in DD (Konopka and Benzer, 1971) but exhibited sharp peaks of activity at dawn and dusk during a 7c/wk LD cycle (**Figure 2.3, B**). These peaks lacked prior anticipation and represented acute increases in locomotor activity following an abrupt change in light conditions, also referred to as 'startle responses'. Thus, comparison of the daily activity profiles of wild-type control versus arrhythmic per^{01} flies provided a means of distinguishing entrained versus driven rhythms.

As the photocycle was shortened below 24 h in 9, 10 and 11c/wk, wild-type behaviour was advanced day on day, shown in the actograms in **Figure 2.3, A**. Anticipation of both dawn and dusk was lost. Instead, a rapid increase of activity was observed at LD transitions, similar to that seen in per^{01} flies. However clear differences between the waveforms of the activity profiles for wild-type and per^{01} could still be seen at 9, 10 and 11c/wk. Following peak activity, wild-type flies showed a slow decrease in activity (i.e. a broader peak), whereas per^{01} flies still exhibited sharp peaks of activity followed by arrhythmic behaviour (**Figure 2.3, A, B**); however, per^{01} peaks did appear to get progressively broad as the photocycle shortens.

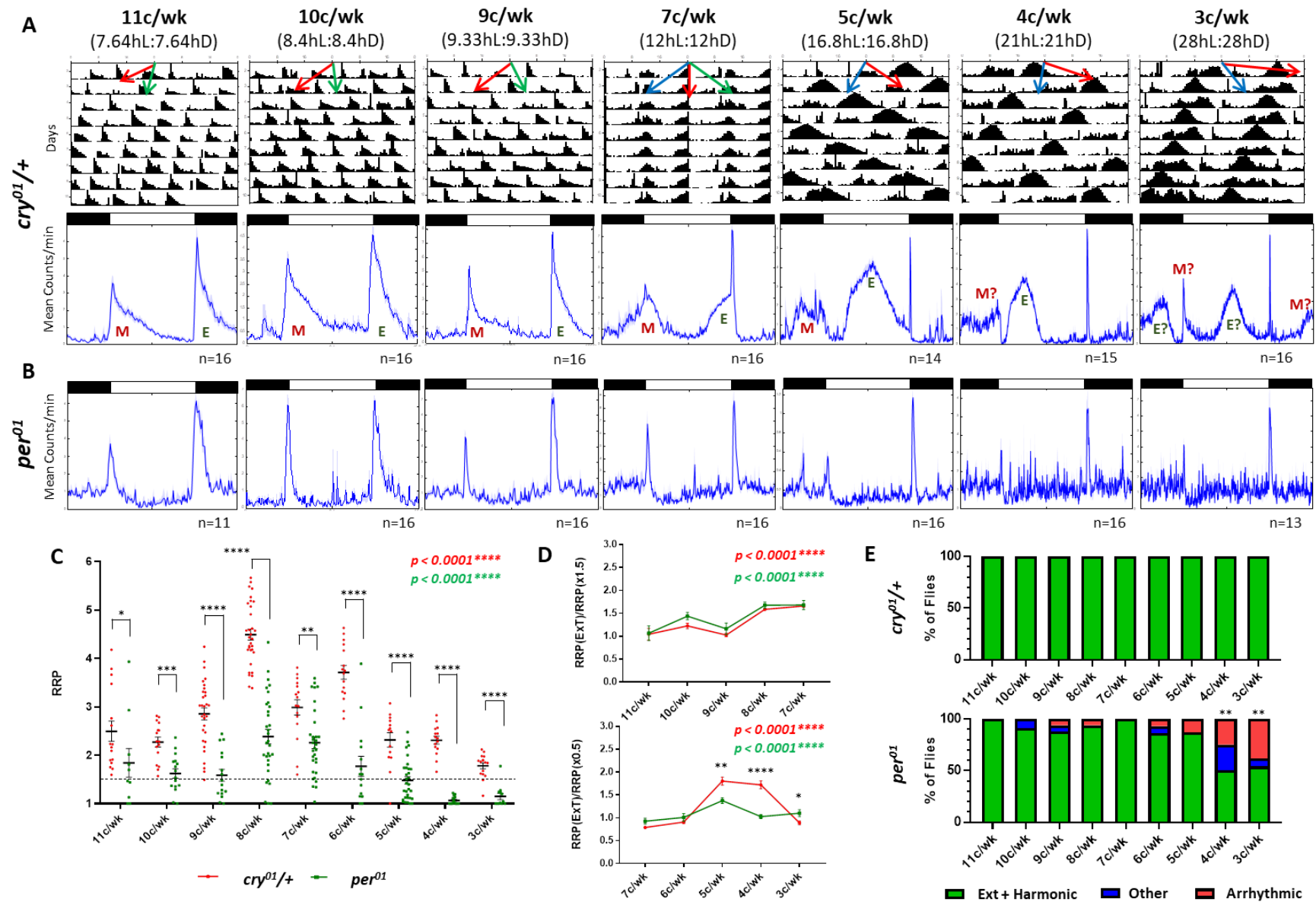


Figure 2.3 Robust entrainment of wild-type locomotor activity rhythms to a wide range of photocycles.

A) Average locomotor activity of adult male flies of genotype $w^{1118};cry^{01}/+$ in 11, 10, 9, 7, 5, 4 and 3c/wk (from left to right) equinox LD cycles shown by double plotted actograms (9 days - 24 hr scale) summed into 30 min bins (top) and activity profiles summed into 5 min bins (bottom), complete with LD bar (black=dark; white=light). Activity profiles show the average of 10 days of activity plotted over entrained period length for each condition (11c/wk=15.25 h; 10c/wk=16.8 h; 9c/wk=18.7 h; 7c/wk=24 h; 5c/wk=33.6 h; 4c/wk=42 h and 3c/wk=56 h). 'n' denotes number of flies. Red, blue and green arrows on actograms indicate entrained, 0.5x photocycle length 'harmonic' and 1.5x photocycle length 'harmonic' components of rhythmic behaviour respectively. 'M' and 'E' on activity profiles denote the morning and evening peak of activity, respectively, and blue shading is \pm SEM. **B)** Activity profiles (plotted as in **A**) for male flies of genotype $y^1 per^{01} w^*$ in 11, 10, 9, 7, 5, 4 and 3c/wk (from left to right) equinox LD cycles where 'n' denotes number of flies. per^{01} flies do not have a functional clockwork and therefore just responded to LD transitions. **C)** Individual male RRP at expected entrained period length for each LD cycle using refined analysis parameters, plotted for $cry^{01}/+$ (red) and per^{01} (green) in 11, 10, 9, 8, 7, 6, 5, 4 and 3c/wk (left to right). Error bars show mean RRP \pm SEM. Dashed line indicates a RRP of 1.5. Arrhythmic flies are assigned an RRP of 1. *p* values (top right) indicate results of *Kruskal-Wallis test* across all conditions for $cry^{01}/+$ (red) and per^{01} (green). Comparison between genotypes at each condition with *Mann-Whitney test* (11c/wk: $p=0.0226$; 10c/wk: $p=0.0002$; 7c/wk: $p=0.0016$; 9, 8, 6, 5, 4 and 3c/wk: $p<0.0001$). **D)** Ratio of entrained RRP and RRP at 1.5x entrained period length (top - short cycles) and RRP at 0.5x entrained period length (bottom - long cycles) for $cry^{01}/+$ (red) and per^{01} (green) – see methods. *p* values (top right) indicate results of *Kruskal-Wallis test* across all conditions for $cry^{01}/+$ (red) and per^{01} (green). *Mann-Whitney* for comparison between genotypes (5c/wk: $p=0.001$; 4c/wk: $p<0.0001$ and 3c/wk: $p=0.0146$). Error bars show mean \pm SEM. **E)** Composite bar charts showing percentage of flies with entrained + harmonic (green), other (blue) or arrhythmic (red) locomotor behaviour (see methods) for $cry^{01}/+$ (top) and per^{01} (bottom). *Fisher's exact test* to compare distribution of entrained, other and arrhythmic individuals for each condition vs. 7c/wk.

Wild-type behaviour showed a delay over consecutive days as the photoperiod was lengthened beyond 24 h in 5, 4 and 3c/wk, shown in the actograms in **Figure 2.3, A**. The evening peak of activity during these long cycles was advanced relative to the LD cycle where the peak fell during the light phase, shown in activity profiles in **Figure 2.3, A**. The extent of the relative advance was dependent on the length of LD cycle due to the evening peak of activity occurring ~12 h after lights-on in all conditions i.e. 4c/wk was relatively more advanced compared to 5c/wk. This advance indicated an inability to delay the evening peak of activity to coincide with lights-off, as is achieved in 7c/wk via PDF signalling (Lear, Zhang and Allada, 2009), however behavioural rhythms were entrained. When flies were subjected to a 3c/wk (56 h) LD cycle, two major peaks of activity were seen for each photocycle with a unimodal peak occurring in the middle of light phase and a second, bimodal, peak marking the middle of the dark phase (**Figure 2.3, A**). This contrasts with the single major active period observed during each photocycle for 4c/wk conditions. As with all cycles, *per⁰¹* flies simply responded to the LD transitions in long photocycles (**Figure 2.3, B**).

Comparing RRP at the entrained period length using refined analysis parameters (2.2.1.2 and **S.Table B.5**), across all photocycles tested for both wild-type and *per⁰¹* highlighted that behavioural rhythms were strongest when the photocycle was close to the intrinsic period length i.e. 8 (21 h), 7 (24 h) and 6c/wk (28 h) (**Figure 2.3, C**). RRP values steadily declined towards the more extreme cycles, indicating weaker rhythms (see **S.Table 2** and **S.Table 3** for more detail). In all photocycles, wild-type flies showed significantly stronger rhythms than *per⁰¹* (**Figure 2.3, C**), however this was least significant at 11c/wk.

To further explore possible differences between entrained wild-type rhythms and driven arrhythmic mutant rhythms, the ratio of rhythmic power at the entrained period length over that at the 0.5x or 1.5x photocycle length 'harmonic' was determined for wild-type and *per⁰¹* flies exposed to the range of photocycles. Due to the bimodal nature of the behavioural rhythms this ratio was often close to 1. A clear departure from this bimodality was observed for wild-type flies that successfully entrained to the longer periods of 5c/wk and 4c/wk photocycles in significant contrast to the behaviour of the arrhythmic *per⁰¹* flies under these conditions. Notably, bimodality returned for wild-type flies exposed to 3c/wk photocycles, suggesting the possibility that those flies completed two internal circadian cycles per photocycle (**Figure 2.3, D**). This interpretation was also consistent with the frequency of major activity intervals observed in the 5, 4 and 3c/wk actograms in **Figure 2.3, A**. For further detail see **S.Table 2** and **S.Table 4**.

Chapter 2:

Flies were categorised as either exhibiting entrained rhythmicity (including ‘harmonic’ rhythms), ‘other’ rhythmicity or arrhythmicity (2.2.1.2) based on χ^2 periodogram analyses that took into account the bimodal nature of the daily activity patterns (**S.Table B.5**). Based on these criteria 100% of wild-type flies entrained to each LD cycle assayed (**Figure 2.3, E**). Entrainment of *per*⁰¹ flies, however, was significantly reduced in 4 and 3c/wk photocycles when compared to 7c/wk (**Figure 2.3, E**). However, upon differentiating between the relative strength of the entrained rhythm at the photocycle length versus the 1.5x photocycle length ‘harmonic’ period length (2.2.1.2) a significant increase in ‘harmonic’ rhythmicity was observed for both wild-type and *per*⁰¹ in 11c/wk photocycles (63% of wild-type and 73% of *per*⁰¹ flies displayed a period length outside of the entrained range), whereas data for 10c/wk remained unchanged for wild-type and shows a slight increase in ‘harmonic’ for *per*⁰¹ (**S.Table 2**).

Combined, this data suggested that wild-type flies effectively entrained their behavioural rhythms to equinox LD cycles ranging from 10-4c/wk. Entrainment appeared to break down to some degree beyond either extreme. However further analysis was required to confirm the limits of behavioural plasticity (2.3.3). Wild-type females overall exhibited similar behavioural entrainment to their male counterparts, however specific defects in rhythmicity were apparent at 11c/wk and 3c/wk. In both cases, there was a significant increase in arrhythmia compared to 7c/wk where 40% of individuals in 11c/wk and 62% in 3c/wk displayed arrhythmic locomotion (**S.Table 2**). This corroborates the observations made from the male data which suggested that rhythmicity breaks down at photocycles beyond 16.8 – 42 h. See **S.Table 2**, **S.Table 3** and **S.Table 4** for more detail and data for female wild-type and *per*⁰¹ flies.

2.3.1.1.1 The *tim*^{ls} isoform may reduce rhythmicity in short photocycles

There are two naturally occurring *timeless* isoforms which confer different light-sensitivity to the circadian clockwork (2.1). To assess the impact of *tim* isoform on entrainment; behavioural locomotion of three wild-type strains, which vary in their *tim* isoform, was assayed in 10, 7 and 5c/wk LD (**S.Figure 1**). Minimal differences were seen between *tim*^{s/l^s} transheterozygotes (*w*¹¹¹⁸; *cry*⁰¹/+) versus *tim*^s homozygotes (*w*^{*}; *tim*(*UAS-Gal4*); *UAS-CD8::GFP*) except for a slight increased RRP in 7c/wk and a couple of individuals showed 1.5x photocycle length ‘harmonic’ in 10c/wk (~13%) for *tim*^s wild-types compared to the transheterozygotes. Significant differences in both period length and rhythmic power were apparent for *tim*^{ls} homozygotes (*w*¹¹¹⁸) versus the *tim*^{s/l^s} and *tim*^s lines in 10c/wk (**S.Figure 1, B, C**). Flies with the *tim*^{ls} isoform struggled to effectively entrain to this short photocycle and showed significantly weaker rhythms with reduced RRP values compared to *tim*^{s/l^s} (Mean RRP \pm SEM in 10c/wk; *tim*^{ls} - 2.164 \pm 0.134; *tim*^{s/l^s} = 3.427

± 0.164). This could be explained due to the reduction in light-sensitivity of the *tim^{LS}* isoform resulting in less efficient light-dependent TIM degradation (Rosato *et al.*, 1997; Sandrelli *et al.*, 2007) and therefore poorer entrainment. In 10c/wk, average period length of *tim^{LS}* wild-type flies was significantly different to both *tim^S* and *tim^{S/LS}* wild-type flies, and ~35% of *tim^{LS}* wild-type individuals showed 1.5x photocycle length ‘harmonic’ rhythmicity (**S.Figure 1**).

2.3.1.1.2 Wild-type locomotion in these extreme LD cycles is true behavioural entrainment and not masking

The terms ‘masking’ and ‘startle response’ have been used to refer to changes in behavioural activity driven by changes in environmental light exposure without the need of an endogenous oscillator (Rieger, Stanewsky and Helfrich-Förster, 2003; Mrosovsky, 1999). The driven hyperactive responses of *per⁰¹* at the transitions between light and dark in LD cycles shown previously (2.3.1.1) represents a good example. To confirm that the behavioural entrainment seen with wild-type flies was in fact true entrainment mediated via circadian clock function, mutants with either an intrinsically fast (*per^S*) or slow (*per^L*) period length (Konopka and Benzer, 1971; Hamblen-Coyle *et al.*, 1992; Wheeler *et al.*, 1993) were assayed at 10, 7 and 5c/wk LD, to assess if entrainment to extreme photocycles was influenced by an intrinsic circadian period length.

As described previously (2.3.1.1), the evening peak of the wild-type behavioural profile advanced as the photocycle was lengthened and in short LD cycles anticipation was lost with behaviour now following the LD transitions (**Figure 2.4, A**). *per^S* flies, which had an intrinsically short period length, showed an advanced evening peak during 7c/wk, which was further advanced in 5c/wk (**Figure 2.4, A**), to a similar extent to what was seen for wild-type in 5 and 4c/wk respectively. During 10c/wk LD, *per^S* flies now displayed anticipatory behaviour (a ramping up of activity prior to lights-on and lights-off), like seen in wild-type flies in 7c/wk, suggesting effective behavioural entrainment in short photocycles, likely as a result of an accelerated intrinsic period length. In contrast, the evening activity peak of *per^L* flies, which have a slow intrinsic circadian periodicity, now fell within the dark phase for both 7 and 10c/wk LD. However, when photocycle length exceeded intrinsic periodicity (during 5c/wk LD) the evening peak did anticipate lights-off (**Figure 2.4, A**). In comparison, *per⁰¹* simply respond to the LD transitions irrespective of photocycle length (**Figure 2.4, A**).

per^S and *per^L* flies exhibited significant entrainment to each of the photocycles tested (**Figure 2.4, B**). However, in 10c/wk about half of the *per^S* flies showed stronger oscillations at the 1.5x photocycle length ‘harmonic’ component indicating strong bimodality in their rhythms, while

Chapter 2:

some arrhythmicity was seen for *per^L* flies in 10c/wk and 7c/wk photocycles. Female *per^S* and *per^L* flies showed a similar ability to entrain; however overall rhythms are weaker compared to males i.e. RRP values were lower and more arrhythmicity was seen (See **S.Table 2** and **S.Table 3**).

The manner in which flies exhibited anticipatory behaviour in the different photocycle lengths was clearly associated with their intrinsic period lengths, confirming that this behavioural feature requires circadian clock function.

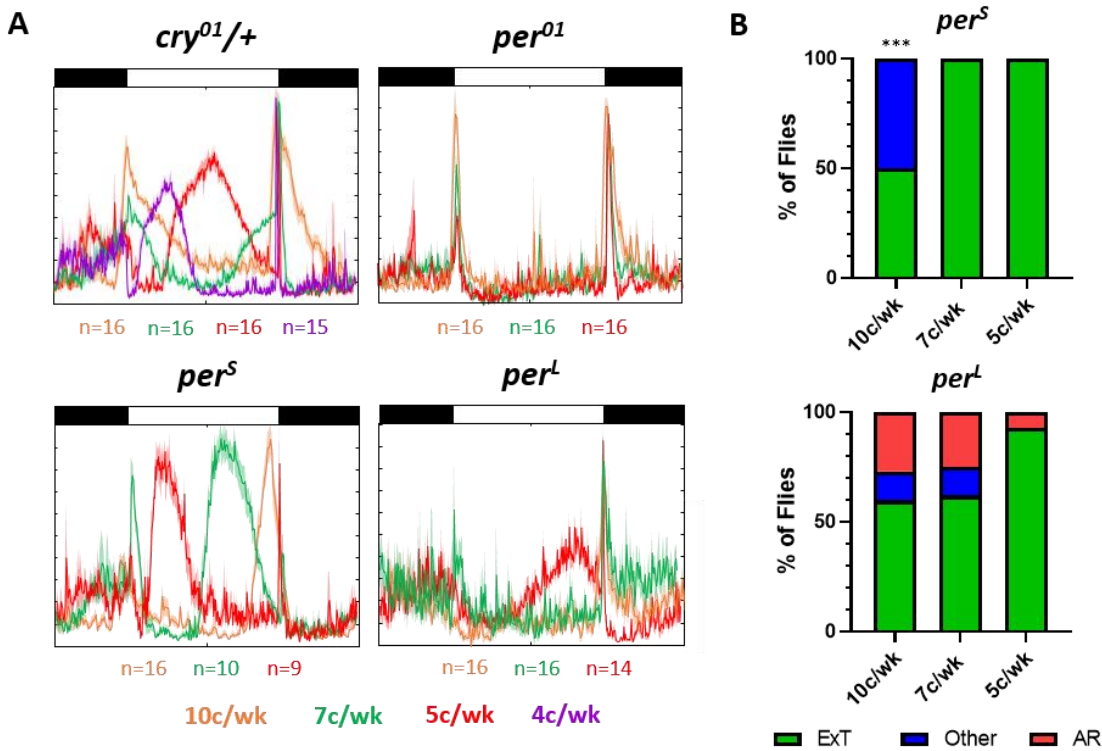


Figure 2.4 Wild-type behaviour in extreme LD cycles reflects true entrainment and not just masking.
A) Average locomotor activity (10 days) shown by activity profiles (5 min bins), for adult male flies of genotype $w^{1118};cry^{01}/+, y^1 per^{01} w^*$, *per^S* and *per^L* in 10 (orange), 7 (green) and 5c/wk (Red) equinox LD cycles. 4c/wk (purple) is also included for *cry⁰¹/+*. Activity profiles are plotted over entrained period length for each condition (10c/wk = 16.8 h, 7c/wk = 24 h, 5c/wk = 33.6 h and 4c/wk = 42 h) and overlaid for each genotype. LD bar: black=dark; white=light. ‘n’ denotes number of flies and shading is \pm SEM – colour coded for each condition. **B)** Composite bar charts showing percentage of flies showing entrained (green), ‘other’ (blue) or arrhythmic (red) locomotor behaviour (see methods) for *per^S* (top) and *per^L* (bottom). For 10c/wk, primary and secondary periodicities were compared for each individual and the dominant period length was used to categorise flies using only the ‘Ext’ range (See methods). *Fisher’s exact test* to compare distribution of entrained, other and arrhythmic individuals for each condition vs. 7c/wk.

2.3.2 Light-dependent plasticity of the molecular rhythms in the clock neurons of wild-type *Drosophila*

The molecular clockwork is a delayed negative feedback loop of transcription and translation, as previously discussed, which is fundamental in generating rhythmic output and therefore underpins behavioural rhythmicity. Wild-type behavioural rhythms are incredibly plastic and are able to entrain to a wide range of LD cycles (2.3.1). Confocal immunofluorescence microscopy was used to investigate how the molecular oscillator, in distinct subsets of clock cells in the *Drosophila* brain, adapted under extreme LD cycles in order to facilitate light-induced entrainment. All molecular analysis were conducted on wild-type flies of the genotype *w^{*};tim(UAS)-Gal4;UAS-CD8::GFP*, enabling the identification of distinct clock cell subsets (2.2.2.2). Dissection time-points are detailed in **S.Figure B.1**.

2.3.2.1 Robust molecular oscillations in PER protein were observed across the neural clock circuit during 7 and 5c/wk LD cycles

All clock cell subsets analysed exhibited rhythms in total PER protein with peak PER immunofluorescence occurring at a similar time with respect to 'dusk' across all photocycles, when plotted in real-time (**Figure 2.5** and **Figure 2.6**). Thus, photocycle entrainment did not fundamentally alter the kinetics of PER accumulation following lights-off. However, when the same data was scaled to the LD cycle, relative changes in the PER protein rhythm became apparent. During 7c/wk LD, PER protein peaked at the end of the dark phase and decreased during the light phase, as previously reported (Zerr *et al.*, 1990; Curtin, Huang and Rosbash, 1995; Shafer, Rosbash and Truman, 2002), in all clock cells (**Figure 2.5** and **Figure 2.6**). This clear increase in PER immunofluorescence was seen at ZT23.2 in the s-LN_vs and LN_ds, **Figure 2.5, A** and **D** respectively (as well as all other clock cells analysed in **S.Figure 3**). The decrease in PER staining during the light phase evident in **Figure 2.5** and **S.Figure 3** was expected as PER turnover is known to be indirectly stimulated by light (Hunter-Ensor, Ousley and Sehgal, 1996; Myers *et al.*, 1996; Zeng *et al.*, 1996).

A phase advance in peak PER protein expression relative to the LD cycle, was seen in all clock cells during 5c/wk LD, mirroring the relative advance in evening activity seen in wild-type behaviour in the same condition (**Figure 2.3** and **Figure 2.4**). The relatively advanced accumulation of PER in longer photocycles was simply accounted for by a more or less constant absolute rate of accumulation throughout an extended night. Following peak PER accumulation at 11.2 h post-lights-off, detected PER levels began to decrease. Photocycle-dependent modulation of PER

Chapter 2:

turnover was then observed such that PER levels at the next time-point (16.8 h following lights-off) were higher when this sample was taken at the light/dark transition (ZT0; 5c/wk) than when it was taken following 4.8 h into the light phase (ZT4.8; 7c/wk); i.e. PER levels remained elevated in the elongated dark phase (**Figure 2.5** and **Figure 2.6**). This holds true for all clock cell subsets assayed with significantly higher PER abundance 16.8 h following lights-off in 5c/wk when compared to the same time-point in a pairwise manner to both 7 and 10c/wk LD (**S.Table 6**).

Conversely, in 10c/wk a phase delay of PER expression rhythms relative to the photocycle was evident across all clock neuron subsets. However, a reduced PER cycling amplitude compared to 7c/wk was seen in all cells except DNs (**Figure 2.5** and **Figure 2.6**). Significant reductions in peak PER abundance were seen in 10c/wk when compared to both 7 and 5c/wk in the s-LN_vs, l-LN_v and LN_ds at 11.2 h post lights-off (**S.Table 6**). While s-LN_vs and DN1s (**Figure 2.5, A** and **S.Figure 3, B**) showed a strong increase in PER levels between the last time-point in the dark (ZT20) and the first in the light (ZT4), LN_ds exhibited a more modest increase (**Figure 2.5, D**) and this was even further reduced for the other clock neuron subsets (**Figure 2.6, C, D**). This widespread reduction in PER protein amplitude may be due to the incomplete separation of the phases of PER accumulation and PER turnover in short photocycles.

Similarly to PER accumulation, rhythms were also seen in PER subcellular localisation. PER only exerts its negative repression of CLK/CYC in the nucleus (Hardin, 2005), therefore examining the ratio between nuclear and cytoplasmic PER is analogous to quantifying functional PER. Peak nuclear PER localisation, indicated by the highest ratio, coincided with a time close to dawn for all clock cell subsets in 5c/wk (ZT0) and 7c/wk (ZT23.2) respectively (**Figure 2.5** and **Figure 2.6** – ‘24 h scale’ plots). In a standard 7c/wk LD cycle, PER nuclear entry occurs around midnight when PER protein levels are at their highest (Shafer, Rosbash and Truman, 2002; Harms *et al.*, 2004). This was, indeed, corroborated by the data presented here. However in 5c/wk, nuclear PER localisation appeared relatively delayed in terms of time since dusk compared to 7c/wk, in all cell types except DN1s and DN2s (**Figure 2.5** and **Figure 2.6** – ‘real-time’ plots), suggesting that the duration of the prior light phase may impact this parameter.

Regardless of cell subset, the rhythm in subcellular PER localisation was damped in 10c/wk LD, indicated by the reduced significance between consecutive time-points in this condition compared to 7 and 5c/wk (**Figure 2.5** and **Figure 2.6**). Furthermore, nuclear/cytoplasmic ratios in 10c/wk are significantly reduced at both 11.2 h and 16.8 h following lights when compared to the same time-points in 7 and 5c/wk in most cell types (**S.Table 6**). This may reflect a failure to

complete nuclear translocation of PER prior to the onset of its turnover when entraining to abnormally short photocycles.

Chapter 2:

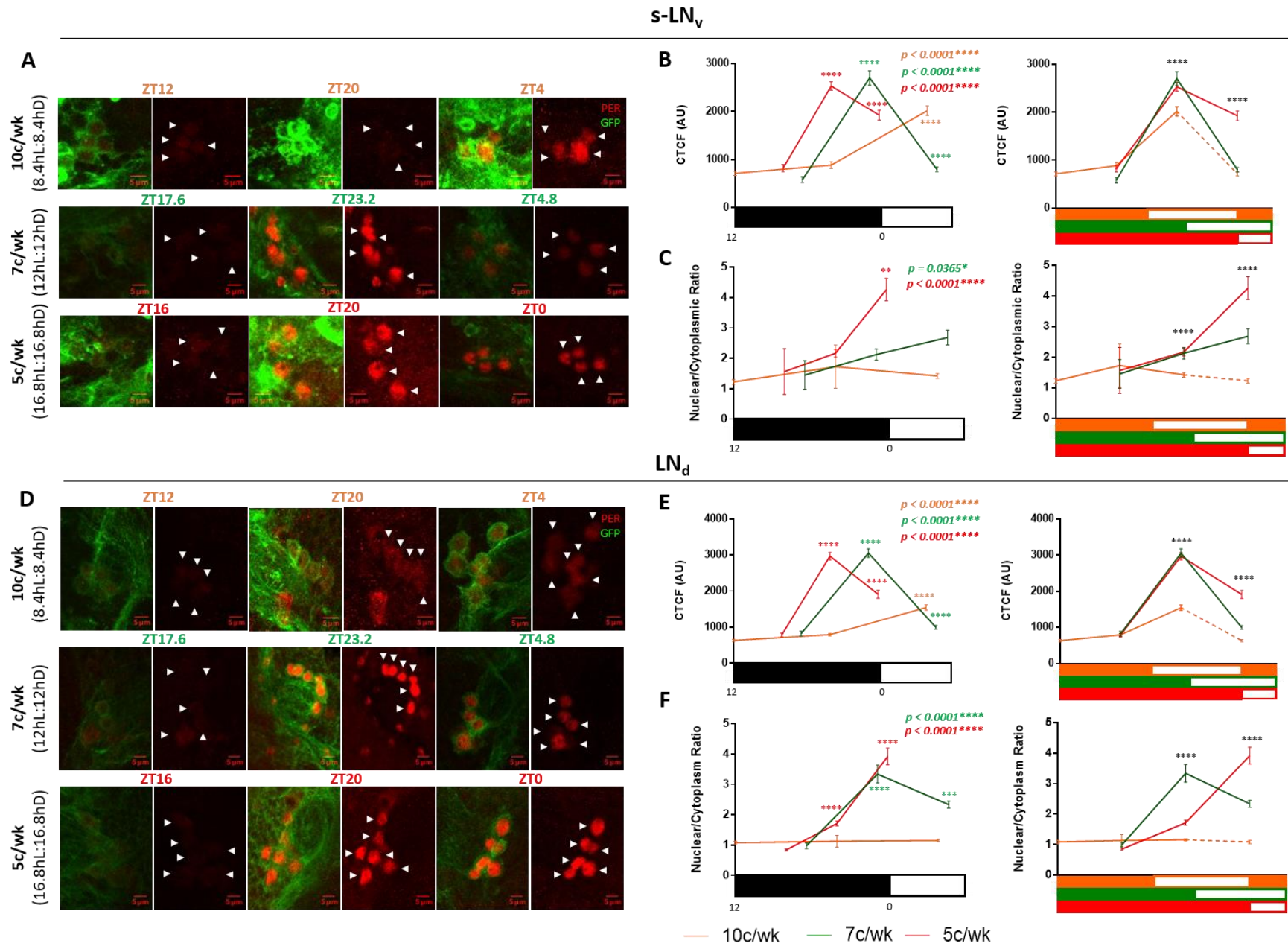


Figure 2.5 Rhythms in PER cycling and nuclear localisation were robust in 7 and 5c/wk LD cycles, but selectively weakened in 10c/wk.

Molecular analysis of PER protein cycling in wild-type adult male fly brains (*w^{*};tim(UAS)-Gal4;UAS-CD8::GFP*) at three time-points during 10, 7 and 5c/wk equinox LD cycles. **A, D**) Representative images of s-LN_vs (**A**) and LN_ds (**D**) for 10 (top), 7 (middle) and 5c/wk (bottom) stained for PER (red) and GFP (green). Time-points annotated were scaled to a 24 h LD cycle to allow comparison. Merge and PER alone images are presented for each time-point. Scale bar=5 μm. Arrows indicate cells quantified. **B, E**) Quantification of total PER staining - CTCF (see methods), in s-LN_vs (**B**) and LN_ds (**E**) for 10 (orange), 7 (green) and 5c/wk (red) plotted W.R.T a 24 hr LD cycle (left - black=dark; white=light) and in real-time (right - LD bar for each cycle where orange, green and red represent the dark phase for 10, 7 and 5c/wk respectively; white=light). *p* values (top right - reported on 24 h scale plots) indicate results of *Kruskal-Wallis test* across all time-points within each condition (10c/wk = orange, 7c/wk = green and 5c/wk = red). Comparison between consecutive time-points, within each condition, with *Tukey's multiple comparisons test* (shown on 24 h scale plots - see **S.Table 8** for *p* values). Comparison between matching time-points across all three conditions using *Kruskal-Wallis test* (reported on real-time plots - pairwise comparisons between conditions at each time-point are reported in **S.Table 6**). Error bars show mean ± SEM. **C, F**) Ratio of nuclear and cytoplasmic PER staining in s-LN_vs (**C**) and LN_ds (**F**) - plotted as described for **B** and **E**. NB: Dashed orange lines indicate an extrapolation of the 10c/wk data (repeat of data at 10c/wk ZT12).

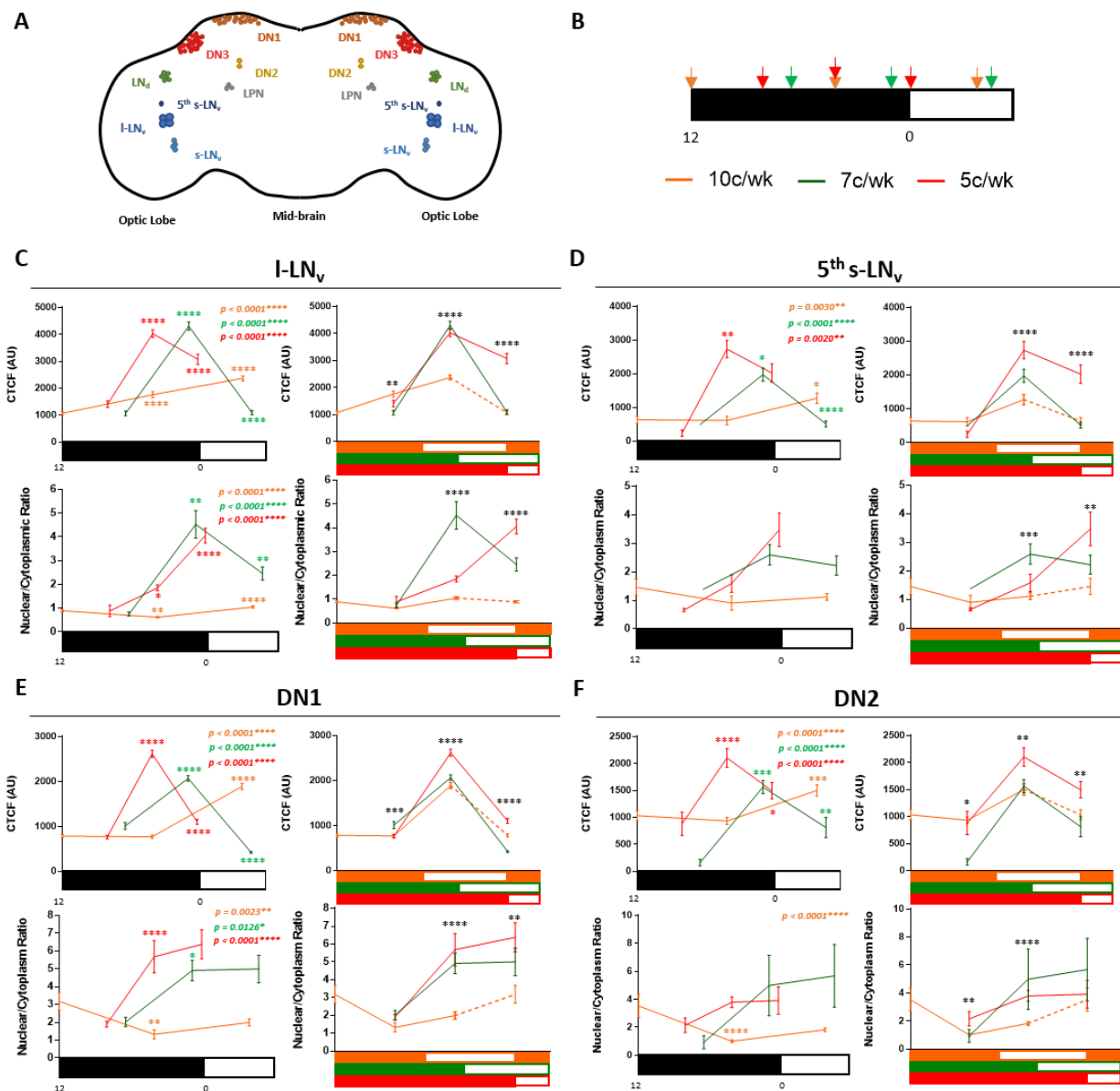


Figure 2.6 PER localisation and cycling rhythms were comparable across most cell types with some differences during short 10c/wk photoperiods.

Molecular analysis of PER protein cycling in wild-type adult male fly brains (w^* ; $tim(UAS)-Gal4; UAS-CD8::GFP$) at three time-points during 10, 7 and 5c/wk equinox LD cycles. **A)**

Location of clock cell subsets in the fly brain. **B)** Sampling scheme relative to the experimental photoperiod (on a '24 h cycle' scale). **C-F)** Quantification of total PER staining (top – CTCF), and nuclear localisation (bottom – nuclear/cytoplasmic ratio) in I-LN_vs (**C**), 5th s-LN_v (**D**), DN1s (**E**) and DN2s (**F**) for 10 (orange), 7 (green) and 5c/wk (red) plotted relative to the photoperiod h (left - black=dark; white=light) and in real-time (right – LD bar for each cycle where orange, green and red represent the dark phase for 10, 7 and 5c/wk respectively; white=light). *p* values (top right – reported on 24 h scale plots) indicate results of *Kruskal-Wallis* test across all time-points within each condition (10c/wk = orange, 7c/wk = green and 5c/wk = red).

Chapter 2:

Fig 2.6 (cont): Comparison between consecutive time-points, within each condition, with *Tukey's multiple comparisons test* (shown on 24 h scale plots – see **S.Table 8** for *p* values). Comparison between matching time-points across all three conditions using *Kruskal-Wallis test* (reported on real-time plots – pairwise comparisons between conditions at each time-point are reported in **S.Table 6**). Error bars show mean \pm SEM. NB: Dashed orange lines indicate an extrapolation of the 10c/wk data (repeat of data at 10c/wk ZT12).

2.3.2.2 Clock neurons in 10c/wk photocycles exhibited entrained circadian rhythms rather than purely light-driven molecular responses.

In 10c/wk LD wild-type flies no longer showed behavioural anticipation of dawn or dusk (2.3.1.1, **Figure 2.3**) and molecular PER cycling appeared to be damped across the majority of the clock circuitry (2.3.2.1, **Figure 2.5** and **Figure 2.6**). Therefore it was important to investigate whether rhythmic clock function was present in 10c/wk beyond rhythms in the light-sensitive PER/TIM complex. This was accomplished by repeating the immunofluorescence experiment in 2.3.2.1, but now staining for VRI, a core clock component with no known direct light sensitivity, in a 10c/wk LD cycle. VRI is expressed under CLK/CYC control and provides negative feedback via its impact on *Clk* transcription (**Figure 2.7, A**) (Blau and Young, 1999; Glossop *et al.*, 2003). Based on prior studies, VRI is expected to cycle as a result of rhythmic CLK/CYC activity with a peak in protein levels that is significantly advanced relative to PER (Glossop *et al.*, 2003; Cyran *et al.*, 2003).

Robust cycling was seen in anti-VRI immunofluorescence in all clock cells analysed (**Figure 2.7** and **S.Figure 6**). Peak VRI occurred around dawn (ZT20-ZT4), with significantly higher VRI levels compared to PER at 5.6 h following lights-off in all clock cell subsets (**S.Table 7**), confirming the anticipated phase advance relative to PER. VRI cycling was significant in all clock neuron subsets (**Figure 2.7, D, S.Table 7** and **S.Figure 6, D**), but higher peak VRI values were exhibited in the lateral neurons compared to the dorsal neurons (**S.Table 7** and **S.Figure 6, D**). As VRI oscillations are reflective of rhythmic CLK/CYC activity, these results indicate that a functioning clock with rhythmic output persists in clock neurons under 10c/wk LD conditions.

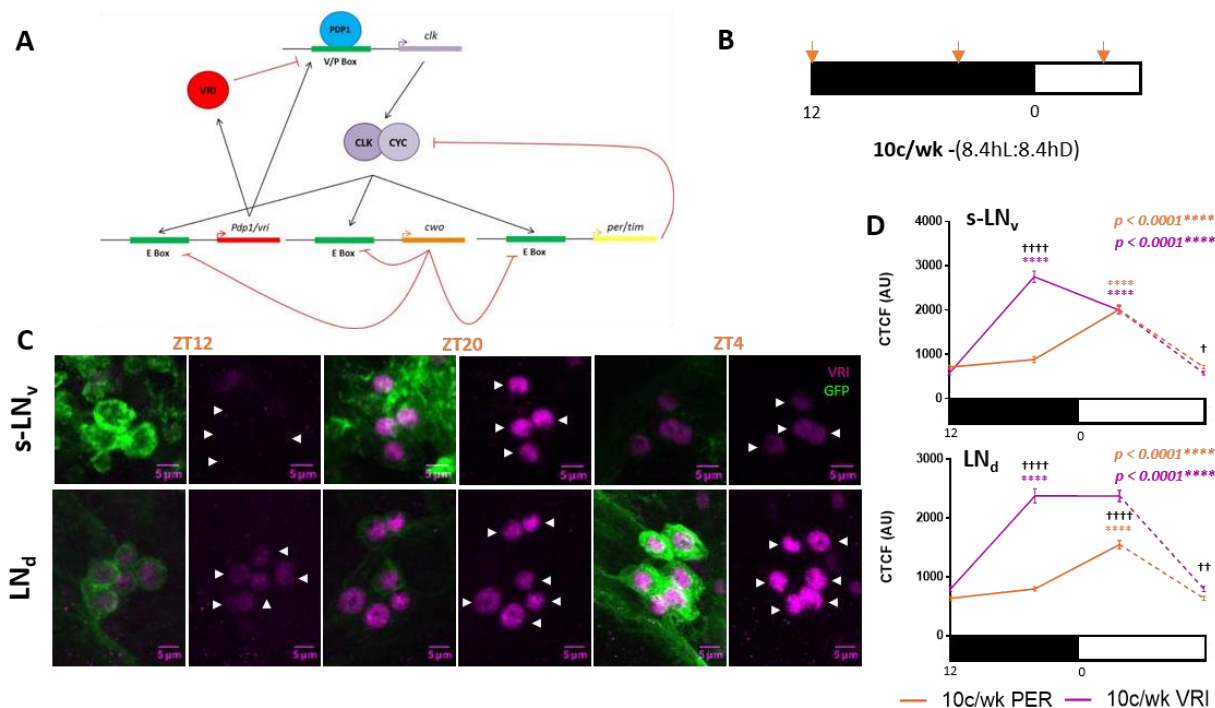


Figure 2.7 VRI cycling rhythms persisted in 10c/wk photocycles.

Molecular analysis of VRI protein cycling in wild-type adult male fly brains (*w*⁺;tim(UAS)-Gal4;UAS-CD8::GFP*) at three time-points during a 10c/wk equinox LD cycle. **A**) VRI's role in circadian interlocked feedback loops that modulate the expression of the core clock protein CLK. **B**) Sampling scheme relative to the experimental photocycle (on a '24 h cycle' scale). **C**) Representative images of s-LN_vs (top) and LN_ds (bottom) during 10c/wk LD stained for VRI (magenta) and GFP (green). Time-points annotated were scaled to a 24 h LD cycle. Merge and VRI alone images presented for each time-point. Scale bar=5 μ m. Arrows indicate cells quantified. **D**) Quantification of total PER (orange) and VRI (magenta) staining (CTCF), in s-LN_vs (top) and LN_ds (bottom) during a 10c/wk LD cycle, plotted relative to the photocycle (black=dark; white=light). *p* values (top right) indicate results of *Kruskal-Wallis test* across all time-points for each protein (PER = orange and VRI = magenta). Comparison between consecutive time-points, within each condition, with *Tukey's multiple comparisons test* (see **S.Table 8** for *p* values). Comparison between VRI and PER staining at matching time-points using *Kruskal-Wallis test* (†). Error bars show mean \pm SEM.

2.3.3 Defining the limits of light-induced behavioural entrainment

Behavioural entrainment appeared to increasingly break down at 11c/wk at one extreme and 3c/wk at the other (2.3.1). Therefore, further analysis was required to ascertain if entrainment was occurring at these extremes. In the χ^2 periodograms presented in **Figure 2.8, A**, it is clear that the amplitude at the period length matching the entrained photocycle of wild-type flies in 11c/wk is clearly smaller than that for flies in 10c/wk, whereas the opposite is true for the 1.5x photocycle length 'harmonic' (22.9 h vs. 25.2 h) (**Figure 2.8, A**).

This preference for the 1.5x photocycle length 'harmonic' rhythm was also evident from the individual fly analyses depicted in **Figure 2.8, B**, where the majority display a 22.9 h period length in 11c/wk, instead of the entrained 15.27 h, however all show the entrained 16.8 h period length in 10c/wk. Of note, *per⁰¹* flies mirror these behavioural features of wild-type flies in 11 versus 10c/wk (**Figure 2.8, A, B**), suggesting that clock-independent behavioural features may contribute to these differences. Moreover, 40% of the wild-type female flies exhibited arrhythmia at 11c/wk versus 19% at 9c/wk and 0% for all other photocycle lengths shorter than 48 h (**S.Table 2**). This observation contrasted with the analogous comparison of LD-driven *per⁰¹* female rhythms across these photocycles, which featured 0% arrhythmia at 11c/wk. Thus, 11c/wk photocycle length interfered specifically with efficient entrainment of clock-bearing wild-type females while leaving the LD-driven rhythms of *per⁰¹* females unaffected.

At the other end of the scale, 3c/wk photocycles elicited two major peaks of activity per cycle suggesting a 28 h rhythm instead of an entrained 56 h rhythm (**Figure 2.9, A**), as reported in 2.3.1.1. Both the 28 h and 56 h components were highly prominent in 3c/wk χ^2 periodograms, whereas in 4c/wk a dominant peak was seen at the entrained 42 h component but the 0.5x photocycle length 'harmonic' rhythm (21 h) barely reached significance (**Figure 2.9, B**), suggesting the hypothesis that the upper limit of entrainable photocycle length, between 42 h and 56 h, was explained by the tendency of the *Drosophila* circadian clock to complete two internal oscillations per external LD cycle in this range. To address this hypothesis molecular analysis of PER protein oscillations during 3c/wk LD was carried out (2.2.2.1) to determine if there was evidence for a second molecular oscillation at the level of PER protein. Across the time-points analysed (see **S.Figure B.1**), total PER immunofluorescence signal peaked around mid-night and decreased significantly approaching dawn in all clock cell subsets analysed, except DN1s (**Figure 2.9, C, D**, see **S.Figure 5** for representative images of other subsets). This contrasted with established PER protein profiles in clock neurons in a standard 24 h LD cycle where PER protein accumulates throughout the night peaking at dawn (Zerr *et al.*, 1990; Curtin, Huang and Rosbash, 1995; Shafer,

Rosbash and Truman, 2002). Furthermore, the significant increase in total PER at ZT1.7 seen in the s-LN_vs, LN_ds and DN1s was indicative of the initiation of a second cycle of PER transcription and translation (**Figure 2.9, D**). A rhythm in PER localisation was present whereby PER was nuclear around midnight and more cytoplasmic around dawn (**Figure 2.9, F**), which corresponds to the increase in PER translation seen at ZT1.7 (**Figure 2.9, D**), for all cell types apart from DN1s where PER appeared more nuclear following dawn.

As discussed in 2.3.2.1, PER exerts its function in the nucleus, therefore examining the ratio between nuclear and cytoplasmic PER further probes the state of the molecular clockwork. Despite the trend of increased cytoplasmic PER localisation at dawn, the amount of nuclear PER, which represented the measure with the most direct relevance to PER's function as a negative regulator of transcription, clearly exhibited an increase in both s-LN_vs and DN1s (**Figure 2.9, E** and **S.Table 6**). This increase of functional PER around dawn, especially in the pacemaker s-LN_vs, is consistent with the hypothesis of 28 h molecular cycling in the 3c/wk photocycle condition; indicating a second period of PER-mediated transcriptional repression.

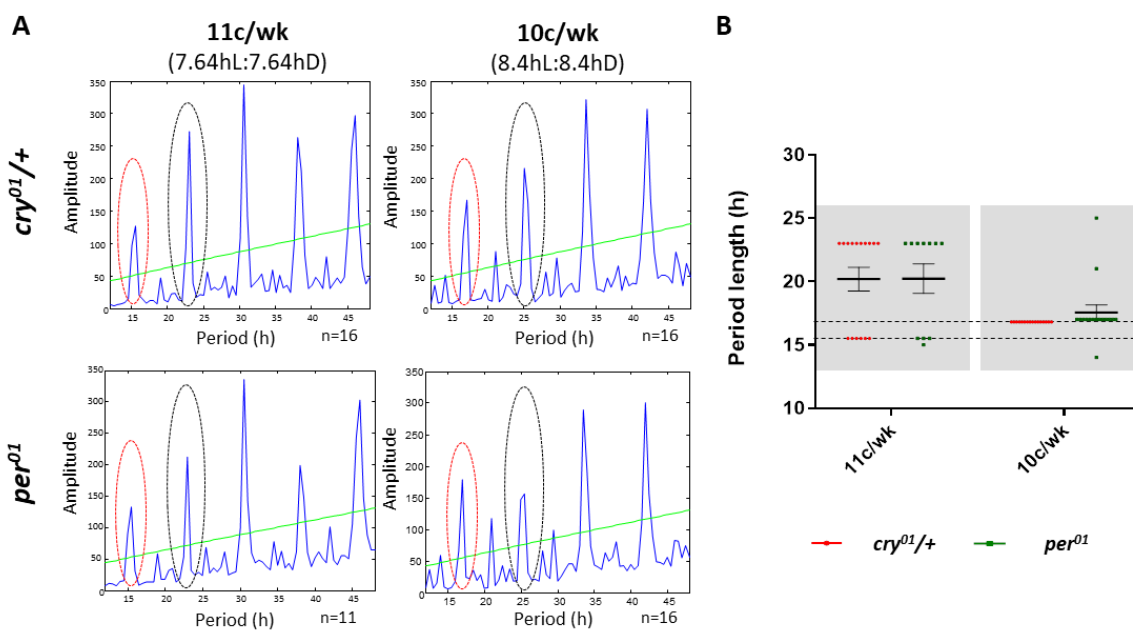


Figure 2.8 Behavioural entrainment breaks down beyond a 10c/wk LD cycle.

A) χ^2 periodograms for $w^{1118}; cry^{01/+}$ (top) and $y^1 per^{01} w^*$ (bottom) males in 11 (left) and 10c/wk (right), plotted from 12-48 h. 'n' denotes number of flies. Dashed red and black ovals indicate peaks at the entrained and 1.5x photocycle length 'harmonic' period lengths respectively for each photocycle. **B**) Individual male period lengths at 11 and 10c/wk LD cycles, plotted for *cry^{01/+}* (red) and *per⁰¹* (green). Error bars show mean period length \pm SEM, dashed lines show entrained period length for 10 (top) and 11c/wk (bottom). Grey shading indicates analysis interval used for individual fly analysis.

Chapter 2:

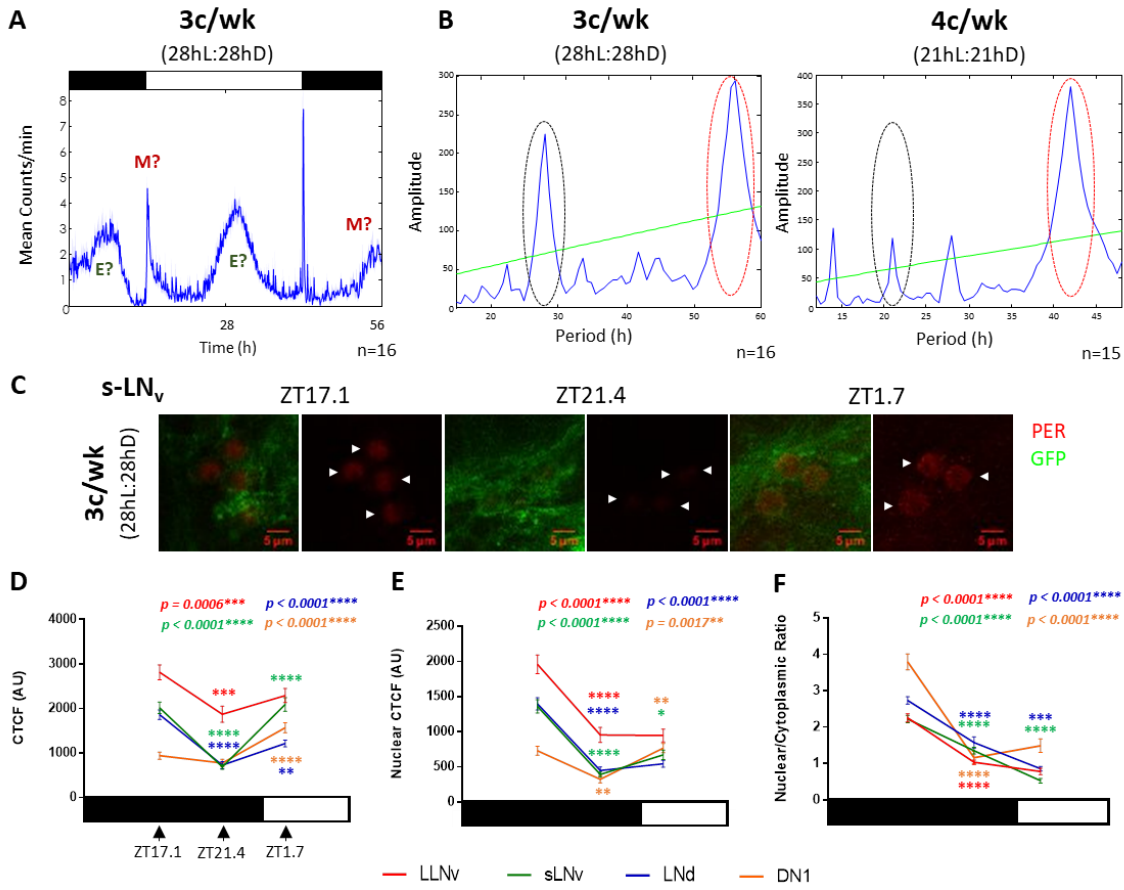


Figure 2.9 In a 56 h photocycle clock neuron molecular oscillations exhibit features of 28 h cycling.
A, B) Adult male flies of genotype $w^{1118};cry^01/+$ in 3 (A and B) and 4c/wk (B) equinox LD cycles, where ‘n’ denotes number of flies. **A)** Average locomotor activity (10 days) shown as an activity profile, summed into 5 min bins complete with LD bar (black=dark; white=light), plotted over entrained period length (56 h). ‘M’ and ‘E’ denote possible morning and evening peaks of activity respectively and blue shading is \pm SEM. **B)** χ^2 periodogram plotted from 15-60 h (3c/wk) or 12-48h (4c/wk). Dashed black and red ovals indicate peaks at the 0.5x photocycle length ‘harmonic’ and entrained period lengths respectively for each photocycle.
C, D, E, F) Molecular analysis of PER protein cycling in wild-type adult male fly brains ($w^*;tim(UAS)-Gal4;UAS-CDB::GFP$) at three time-points during a 3c/wk equinox LD cycle. **C)** Representative images of s-LN_vs stained for PER (red) and GFP (green), merge and PER alone images presented for each time-point (expressed on a ‘24 h’ scale). Scale bar=5 μ m. Arrowheads indicate cells quantified. **D, E, F)** Quantification; l-LN_v (red), s-LN_v (green), LN_d (blue) and DN1 (orange) plotted W.R.T a 24 h LD cycle (black=dark; white=light). *p* values (top right) indicate results of *Kruskal-Wallis test* across all time-points for each cell type (l-LN_v = red, s-LN_v = green, LN_d = blue and DN1 = orange). Comparison between consecutive time-points, within each condition, with *Tukey’s multiple comparisons test* (see **S.Table 8** for *p* values). Error bars show mean \pm SEM. **D)** Quantification of total PER CTCF. **E)** Quantification of nuclear PER CTCF. **F)** Ratio of nuclear and cytoplasmic PER staining.

2.3.4 Free-running period lengths revert back to ~24 h following extreme LD entrainment

Mammalian circadian clocks exhibit 'after-effects' following LD entrainment as a result of LD cycle induced DNA methylation (2.1). The *Drosophila* genomes does not encode a CpG DNA methylase (Pegoraro *et al.*, 2016); however due to the extreme LD conditions used, free-running periodicity was assayed following entrainment to 10, 7 and 5c/wk LD to assess the presence or absence of any 'after-effects'.

When left to free-run in DD, wild-type fly behaviour reverted back to a near circadian period length irrespective of the prior LD cycle, within 1 day of DD (**Figure 2.10, A**), using the last lights-off transition as the main phase determinant of the subsequent activity pattern. DD behaviour following 10, 7 and 5c/wk LD exhibited bimodality for the first 1-3 days, as seen in the LD portion of the actograms in **Figure 2.10, A**. However, over subsequent days this activity began to manifest as one longer bout of activity, occurring during the subjective day/evening following 7c/wk entrainment (**Figure 2.10, A**) (Wheeler *et al.*, 1993; Tomioka, Uwozumi and Matsumoto, 1997). Periodogram analysis over 7 days in DD indicated significant period lengths of 23-24 h following each LD condition (**Figure 2.10, B**), which was a drastic change from the entrained period lengths seen at 10 and 5c/wk LD. Although indirect effects of photocycle length on subsequent free-running period length in DD were relatively modest, a significantly shorter free-running period length was seen with prior 10c/wk LD entrainment compared to both 7 and 5c/wk when individual period lengths were compared (**Figure 2.10, C** and **S.Table 5**). This significantly shorter free-running period length was also observed for wild-type females following prior 10c/wk when compared to 7 and 5c/wk (**S.Table 5**).

per^s and *per^l*, like wild-type, revert back to their free-running period lengths, ~19.5 and ~28 h respectively, following prior LD entrainment to 10, 7 and 5c/wk (**Figure 2.10, D**), although the majority of *per^l* male flies are arrhythmic in DD. Unlike wild-type, a significantly shorter free-running period length was only seen for male *per^s* following prior 10c/wk LD entrainment when compared to prior 7c/wk LD (**Figure 2.10, D** and **S.Table 5**). Female *per^s* and *per^l* exhibited no apparent 'after-effects' following any prior LD entrainment, however both genotypes displayed a high proportion of arrhythmicity in DD (**S.Table 5**). Unsurprisingly, *per⁰¹* flies of either gender were mostly arrhythmic in DD irrespective of prior LD condition due to the lack of a functional oscillator (**S.Table 5**).

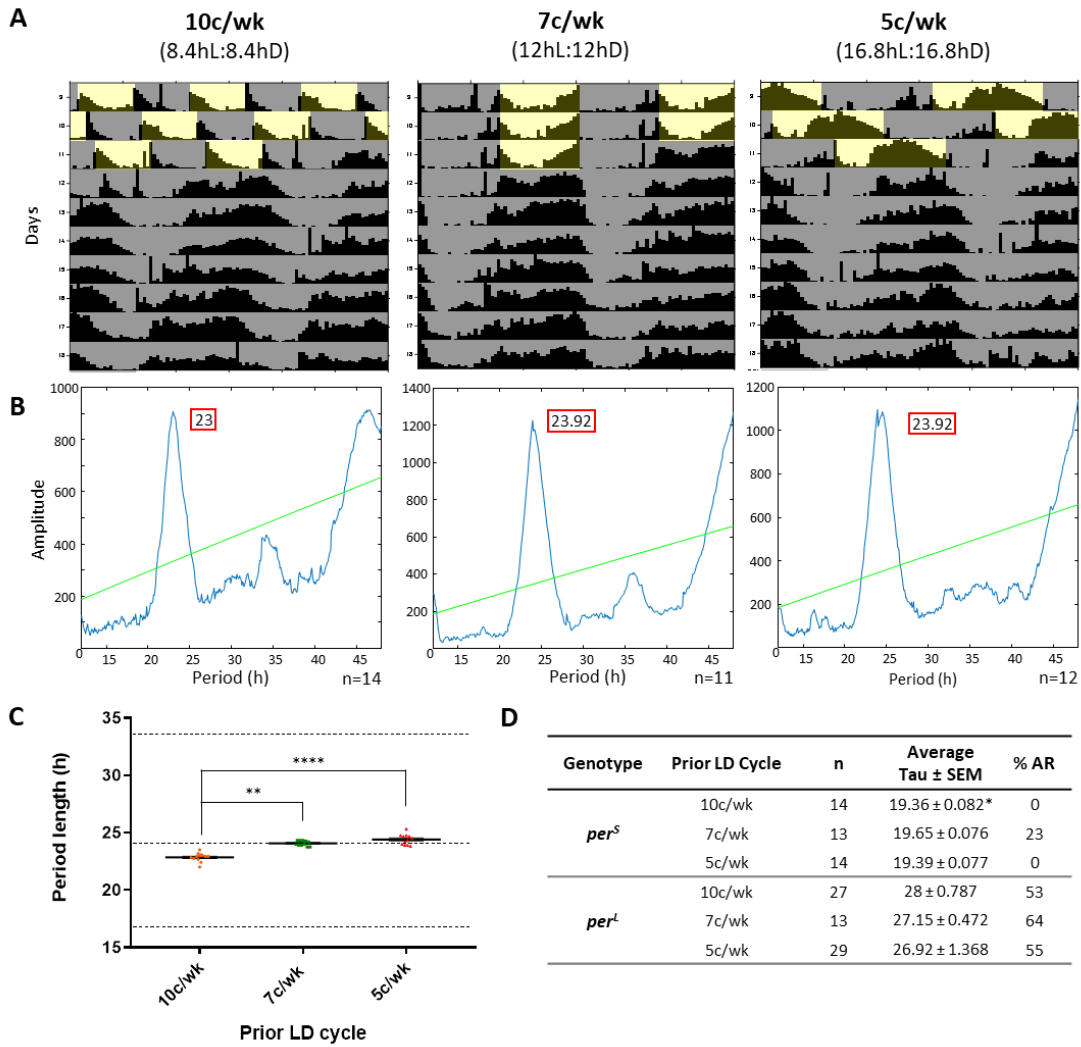


Figure 2.10 DD period lengths revert to close to the intrinsic period length, irrespective of prior LD entrainment.

A) Double plotted actograms (30 min bins) showing average locomotor activity for adult male flies of genotype $w^{1118};cry^{01}/+$ in 3 days of 10, 7 and 5c/wk (left to right) equinox LD cycles (yellow = lights-on; black = lights-off), each followed by 7 days of DD. **B)** Chi² periodograms (5 min bins) for $cry^{01}/+$ males in 7 days of DD following prior 10, 7 and 5c/wk (left to right) LD entrainment, plotted from 12-48 h with the dominant period peak annotated. ‘n’ denotes number for flies. **C)** Individual DD period lengths following prior LD entrainment. Error bars show mean period length ± SEM. Dashed lines represent entrained LD period length for 10 (bottom – 16.8 h), 7 (middle – 24 h) and 5c/wk (top – 33.6 h). Comparison between LD cycles using *Dunn’s multiple comparison test* (10 vs. 7c/wk; $p=0.0061$ and 10 vs. 5c/wk; $p<0.0001$). **D)** Table of average period length (tau) during 7 days of DD (± SEM) for *per^S* and *per^L* males following prior LD entrainment. Comparison between LD cycles using *Dunn’s multiple comparison test* (*per^S* - 10 vs. 7c/wk; $p=0.0246$). *per^S* and *per^L* DD experiments were carried out and analysed by Miss Nanthilde Malandain.

2.3.5 Entrainment to extreme LD cycles reduces longevity in wild-type females

Chronic jet-lag was shown to decrease the life-span of aged mice (2.1), demonstrating the potential impact that prolonged circadian disruption can have on physiology and well-being. In our assay, entrainment to extreme photocycles may be thought to impact on the well-being of the flies due to the constant need to re-set the oscillator and create abnormal phase alignments, such as 'evening activity' in the middle of the day during long cycles (**Figure 2.3**). To address this issue, comparative longevity experiments were performed for male and female wild-type flies in 5, 7, and 10c/wk photocycles (2.2.3). A minor reduction in the life-span of male flies was only seen during a long photocycle (**Figure 2.11**). In contrast, female flies exhibited highly significant reductions in life-span in both 5 and 10c/wk compared to 7c/wk (**Figure 2.11, A**). Median survival was only 40 and 52 days for females in 5 and 10c/wk respectively (**Figure 2.11, A**); suggesting that, like in males, 5c/wk has a greater detrimental impact on longevity. This indicated that extreme photoperiods impact on *Drosophila* life-span, especially in females, showing that constantly re-setting the clock away from the inherent circadian 24 h periodicity can have deleterious effects on physiology.

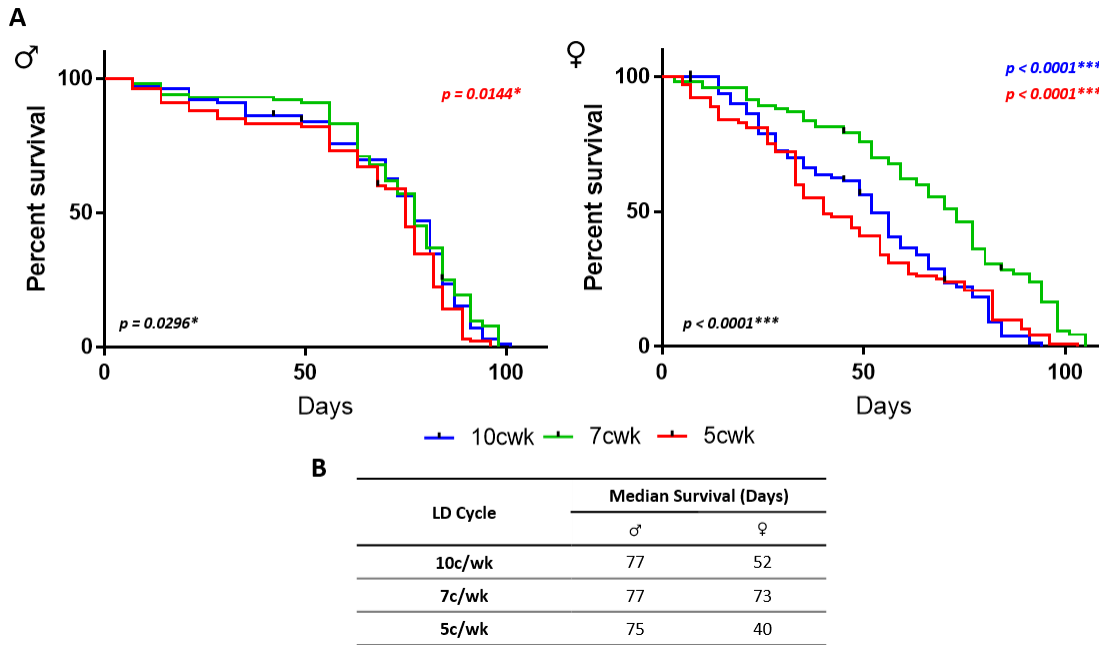


Figure 2.11 Extreme equinox photoperiods impact on wild-type life-span, especially in females.

A) Longevity plots showing percentage survival of male (left) and female (right) wild-type ($w^{1118};cry^{01}/+$) flies at 23°C in 10 (blue), 7 (green) and 5c/wk (red) equinox LD cycles. $n=100$ for both genders in each condition. *Log rank (Mantel-cox) test* across all three conditions (bottom left – black), and pairwise between 7 and either 10 or 5c/wk (top right – 7 vs. 5c/wk = red; 7 vs. 10c/wk = blue). **B)** Table of median survival of male and females in each condition. Longevity assay were set up by Miss Nanthilde Malandain and completed with the help of Miss Chloe Ellison and Miss Racheal Anderson. Data was analysed by Miss Chloe Ellison.

2.4 Discussion

Light-dependent resetting of the *Drosophila* molecular oscillator is achieved via cell-autonomous CRY photoreception driving TIM degradation (Ashmore and Sehgal, 2003), supplemented by light input through photoreception in the visual organs i.e. compound eyes, ocelli and HB-eyelet (Helfrich-Förster *et al.*, 2001; Rieger, Stanewsky and Helfrich-Förster, 2003) (2.1).

Circadian entrainment in response to light has been studied in *Drosophila* using either brief light pulses (Myers *et al.*, 1996; Saunders, Gillanders and Lewis, 1994), re-entrainment to a shifted LD regime (Suri *et al.*, 1998), or varied photocycles (Wheeler *et al.*, 1993). To further explore the impact of light on the molecular and neural clock circuits as well as clock-controlled behaviour, equinox photocycles were used in order to stretch the oscillator to the limits of light-induced entrainment. These extreme LD cycles provided a sensitive measure of light-dependent plasticity as the clockwork had to constantly shift/re-set the molecular oscillator to keep time with the environmental condition.

In a standard 24 h (7c/wk) photocycle wild-type flies displayed a characteristic bimodal activity pattern complete with anticipation of dawn and dusk (**Figure 2.3, A**) (Hamblen-Coyle *et al.*, 1992; Grima *et al.*, 2004; Stoleru *et al.*, 2004). PER cycling is paramount to circadian function (Konopka and Benzer, 1971; Yang and Sehgal, 2001; Hardin *et al.*, 2003), so unveiling the molecular oscillations of PER in different photocycles should reveal molecular light-induced entrainment. Molecular analysis of PER protein cycling in 7c/wk agreed with published data documenting PER protein accumulation throughout the night with nuclear entry around mid-night as well as peak and trough levels at dawn and dusk, respectively (**Figure 2.5** and **Figure 2.6**) (Zerr *et al.*, 1990; Curtin, Huang and Rosbash, 1995; Shafer, Rosbash and Truman, 2002; Harms *et al.*, 2004). The light-dependent nature of TIM and, therefore PER degradation, explains why the lowest PER levels are seen at the end of the light phase (Emery *et al.*, 1998) and why the lights-off transition plays a crucial role in determining the phase of behavioural and molecular rhythms (Qiu and Hardin, 1996).

We have demonstrated robust molecular and behavioural entrainment in the presence of extremely long photocycles, of up to 42 h (4c/wk) behaviourally and 33.6 h (5c/wk) molecularly. When entrained in 5c/wk, PER protein accumulation appeared phase-advanced relative to the LD cycle. This is explained by the fact that PER accumulation is synchronised to the lights-off transition and that negative feedback will start upon nuclear entry approximately 6 h later. This was mirrored by the behavioural advance seen in the evening peak of activity under the same

Chapter 2:

condition. Indeed, PER accumulation followed similar kinetics in 5 and 10c/wk as it does in 7c/wk, peaking at the 11.2 h post-lights-off time-point in all conditions. However, the PER profiles for 5, 7 and 10c/wk also reflect the impact of the lights-on transitions as PER levels were comparatively lower at post-lights-off time-points that fell in the next light phase. Thus, PER levels at the time-point corresponding to 11.2 h post-lights-off were lower in 10c/wk when lights had already been on for 2.8 h. Analogously, PER levels at the 16.8 h post-lights-off time-point remained considerably higher in the 5c/wk condition, where this time-point coincided with the lights-on transition whereas in 7 or 10c/wk, it fell 4.8 h into the morning or at the next lights-off transition, respectively. Thus the differences in the daily PER protein profiles between the 10, 7 and 5c/wk conditions are accounted for by the differences in night length, with light-driven degradation of TIM and subsequently PER responsible for both the synchronous onset of PER accumulation after lights-off, as well as the differential timing of PER turnover. As discussed previously, not all clock cell subsets are equal (2.1). However, significant PER cycling was detected across all subsets analysed in 5 and 7c/wk LD. Neuronal interactions between clock cell subsets are required for effective light-resetting of molecular and behavioural rhythms (Tang *et al.*, 2010; Lamba *et al.*, 2014; Roberts *et al.*, 2015; Yoshii *et al.*, 2015) and although behavioural phase shifts are possible with just the M cells or just the E cells, entrainment is at this most effective when the entire circuit is synchronous (Lamba, Foley and Emery, 2018). The uniformity in PER cycling across the clock circuitry reported here may explain why such robust behavioural rhythmicity is seen in 24–42 h photocycles.

When photocycles were extended considerably further, to 56 h, a breakdown in behavioural entrainment was clearly visible. 3c/wk behavioural and molecular analyses indicated a prominent 28 h rhythm. At the behavioural level two rather than one major activity peak was detected each cycle, while at the molecular level PER protein was observed to exhibit two phases of increased expression separated by a dip in expression in the late night. Given the light-induced turnover of TIM and, subsequently also PER, during extended periods of light exposure this pattern, observed across various clock neuron subsets (s-LN_vs, LN_ds and DN1s), can be interpreted as a bimodal pattern with two PER protein peaks per cycle. Importantly, this bimodal pattern of PER expression extended also to the level of nuclear PER, at least for s-LN_vs and DN1s. Thus, two phases of PER-mediated negative feedback on CLK/CYC (Hardin, 2005) are predicted to occur per 56 h photocycle, which would help explain the 28 h behavioural rhythm. As the s-LN_vs express PDF and act as the pacemaker cells responsible for DD rhythmicity and anticipation of LD transitions (Renn *et al.*, 1999; Stoleru *et al.*, 2005) their bimodal rhythms in PER are of particular relevance. The DN1s, on the other hand may also be important in linking bimodal molecular rhythms to bimodal

behavioural rhythms as they have been found to connect to peptidergic output pathways (Cavanaugh *et al.*, 2014; King and Sehgal, 2018).

It has been shown that dorsal neurons can influence the activity of the s-LN_vs, as well as the other M-cells; dorsal projections from the M-cells have been shown anatomically in close proximity to the ventral projections of some of the DN1s (Zhang *et al.*, 2010). Additionally, when a functional clock is only present in a subset of the DN1s, the DN1_ps, morning anticipation is rescued, as well as an observable modulation of morning activity in response to low temperatures, suggesting a regulation of M-cell output via the DN1_ps (Zhang *et al.*, 2010). Furthermore, inhibition of s-LN_v activity by the larval DN1s, progenitors to adult DN1_as, has been reported (Collins *et al.*, 2012). These observations coupled with the data presented in this report suggest rhythmic PER in the DN1s may feedback to the s-LN_vs and help drive behavioural rhythmicity.

Short photocycles pose a different challenge as the photoperiod is shorter than the intrinsic free-running period length of wild-type flies (~24 h). Dawn and dusk occur sooner than anticipated triggering a hyperactive startle response at the LD transitions. However, for all photocycles of 16.8 h or longer the daily activity profile was distinguishable from that of arrhythmic *per*⁰¹ flies due to the presence of more gradual subsequent decreases in locomotor activity (**Figure 2.3**). Moreover, all wild-type flies exhibited significant entrainment to the environmental photocycle with a relative rhythmic power exceeding that of arrhythmic mutant flies. For the 11c/wk photocycle (15.27 h) the difference in the daily activity profiles of wild-type versus arrhythmic mutant flies became less clear and a substantial fraction of wild-type females exhibited arrhythmia. Moreover, a majority of both wild-type and *per*⁰¹ flies showed increased rhythmic strength at the 1.5x photocycle length 'harmonic' of the photocycle period length (22.9 h) indicating a strong bimodal component of the rhythm (Hamblen-Coyle *et al.*, 1992). Wheeler *et al.* (1993) reported that wild-type flies could entrain to a 8hL:8hD, but not a 6hL:6hD cycle, while *per*⁰¹ flies showed driven rhythms matching both photocycles. Indeed, our results are consistent with the notion that entrainment of circadian behaviour deteriorates as photocycles shorten to ~16 h and beyond. We observed that molecular rhythms in PER accumulation and subcellular localisation were damped across most of the circadian circuitry in 10c/wk LD, with more robust oscillations persisting in s-LN_vs and DN1s. While there was no clear distinction between CRY-positive and CRY-negative clock neuron subsets, the stronger rhythms in the s-LN_vs might be representative of the synergism of light inputs via CRY as well as the H-B eyelet in these cells (Schlichting *et al.*, 2016). Moreover, consistent with our results implicating both PDF-expressing s-LN_vs and DN1s in light-mediated plasticity of behavioural entrainment, prior studies have identified PDF as well as signals from a

Chapter 2:

subset of DN1s as important modifiers of cell-autonomous CRY-mediated phase responses (Tang *et al.*, 2010; Lamba, Foley and Emery, 2018).

In 10c/wk photocycles, rhythms in VRI expression persisted with the expected phase relationship to PER protein rhythms (**Figure 2.7**), showing more widespread molecular rhythmicity under these conditions. The fact that VRI appeared to cycle with a stronger amplitude than PER in lateral neuron subsets under 10c/wk conditions may reflect a conflict between circadian and light-mediated regulation of PER rhythms in this context. That is, there may be insufficient time for significant PER accumulation before lights-on. Thus, the limit of short photocycle entrainment may be imposed by the minimum time interval required to separate the nuclear accumulation and degradation phases of PER.

Light-driven masking responses to short photocycles could be confused with successful behavioural entrainment (Mrosovsky, 1999). However, we took advantage of differences between the daily activity profiles of wild-type and clock-less flies to help identify the presence of true behavioural entrainment (Wheeler *et al.*, 1993). Furthermore, the documented relationship between intrinsic period length and photocycle entrainability was exploited to identify features in the daily activity profile representative of clock-mediated anticipatory activity (Srivastava *et al.*, 2019). Evening activity in 7c/wk conditions was advanced in short period *per^S* mutants and delayed in long period *per^L* mutants (Hamblen-Coyle *et al.*, 1992), similar to what was seen for wildtype flies in 5 and 10c/wk respectively (**Figure 2.4**).

Free-running periodicity remained largely unaffected irrespective of prior LD entrainment except for a slight period shortening following 10c/wk LD. We hypothesise that 10c/wk is close the limit of entrainment and as such this difference may be the result of a breakdown in molecular rhythms during short photocycles, leading to molecular de-synchrony, which in-turn impacts on the free-running period length. Mammalian circadian clocks show a persistence of entrained rhythms when moved into free-run (Pittendrigh and Daan, 1975), termed 'after-effects', as a result of DNA methylation triggered by light entrainment (Beaule and Cheng, 2011). *Drosophila* do not possess a CpG DNA methylase (Pegoraro *et al.*, 2016), which could explain why after-effects are either absent or much more modest in *Drosophila* (Tomioka, Uwozumi and Matsumoto, 1997) i.e. molecular rhythms revert back to their inherent 24 h periodicity in DD, generating circadian free-running behaviour.

From the data presented, we conclude that the limit of entrainment to long photocycles is ~42 h and short photocycles is ~16.8 h. Beyond either extreme there is an evident breakdown in both molecular and behavioural entrainment, resulting in desynchrony between the internal circadian

oscillator and the external environment. Although the clockwork is entrained at 5 and 10c/wk, the molecular oscillator has to constantly re-set itself away from inherent circadian period length. It achieves this with either phase advances or delays, in long or short cycles respectively, to facilitate efficient behavioural entrainment, with the oscillator in the s-LN_vs being particularly good at phase shifting in all cases. However, this constant phase re-setting has a detrimental impact on physiology with the life-span of female flies severely reduced in both long and short photocycles. The evident sexual dimorphism with regards to life-span may reflect the increased mortality documented in female flies associated with mating (Fowler and Partridge, 1989). These data present a possible opportunity to utilise *Drosophila* behaviour and longevity in these extreme photocycles to further investigate the effect of circadian disruption on physiology and well-being in other invertebrates as well as mammals.

Chapter 3: CRYPTOCHROME, JETLAG and the visual system are required for effective light-induced plasticity of the central clock

3.1 Introduction

The daily rotation of the Earth generates predictable fluctuations in light and temperature which act as synchronising cues, or Zeitgebers, for endogenous circadian clocks. Such internal time-keeping mechanisms are present in a diverse range of organisms, including *Drosophila* (Hardin, 2005; Yu and Hardin, 2006). These clockworks are self-sustaining by nature (Bell-Pedersen *et al.*, 2005); however an ability to anticipate environmental changes and align, or entrain, behaviour and physiology alongside such daily oscillations contributes to the fitness and survival of an organism (Helfrich-Förster, 2005; Allada and Chung, 2010). Accurately entraining the clockwork is therefore crucial.

Light is the most potent and reliable Zeitgeber for the circadian clocks of most organisms. *Drosophila* has two pathways for relaying light information to the clockwork; the cell-autonomous blue-light photoreceptor CRYPTOCHROME (CRY) (Stanewsky *et al.*, 1998; Emery *et al.*, 1998); and rhodopsin-mediated photoreception by the visual system (Helfrich-Förster *et al.*, 2001; Rieger, Stanewsky and Helfrich-Förster, 2003). Flies carrying a severely hypomorphic point mutation in the *cry* gene (*cry^b*) are less light sensitive (Stanewsky *et al.*, 1998; Helfrich-Förster *et al.*, 2001), with even more severe null mutations resulting in light entrainment defects (Dolezelova, Dolezel and Hall, 2007). In addition, aberrant behavioural phase-shifts in response to light-pulse were also seen with mutations to the *jet* gene, most notably in *jet^{set}* loss-of-function mutants where such circadian light responses were profoundly disrupted (Koh, Zheng and Sehgal, 2006; Peschel, Veleri and Stanewsky, 2006; Lamba *et al.*, 2014); indicating that the CRY/JET pathway greatly impacts light-dependent circadian entrainment.

Around 50% of central clock cells of the fly brain are CRY positive including the all the LN_vs, 3 of the 6 LN_ds and a subset of DN1s (Klarsfeld *et al.*, 2004; Benito *et al.*, 2008; Yoshii *et al.*, 2008). Restoring CRY to just the E-cells in *cry* null mutants is sufficient to rescue entrainment deficits when challenged with a delayed 24 h LD cycle (Yoshii *et al.*, 2015). The requirement for JET appears more widespread with expression required in both the Morning (M-) and Evening (E-)

Chapter 3:

cells (1.2.4) to rescue circadian photoresponses to brief light pulses (Lamba *et al.*, 2014).

Furthermore, M- and E- oscillators do not respond equally to short light pulses (Shang, Griffith and Rosbash, 2008; Tang *et al.*, 2010; Lamba *et al.*, 2014); indicating the possibility of differential contributions of each to entrainment. However, a more recent study demonstrated that the circadian network retains the ability to phase shift in response to light pulses in the absence of either the M- or E-oscillator, suggesting that these phase shifts are a consequence of the cell-autonomous activity of CRY (Lamba, Foley and Emery, 2018). In addition, it was shown that coordination across the circuit, largely mediated by PDF signalling, is required for robust entrainment (Lamba, Foley and Emery, 2018).

The compound eyes, extra-retinal Hofbauer-Buchner (H-B) eyelets and 3 ocelli, which express at least 6 different rhodopsins (Rh1-6), make up the *Drosophila* visual system (Hofbauer and Buchner, 1989; Salcedo *et al.*, 2000; Behnia and Desplan, 2015). Manipulations affecting the visual system demonstrated the compound eyes provide a significant contribution to light entrainment; whereas inputs from the H-B eyelet and ocelli are more modest (Helfrich-Förster *et al.*, 2001; Rieger, Stanewsky and Helfrich-Förster, 2003; Yoshii, Hermann-Luibl and Helfrich-Förster, 2016). Disrupting NORPA-dependent phototransduction or histamine signalling also results in deficits in circadian light responses (Bloomquist *et al.*, 1988; Burg *et al.*, 1993; Pantazis *et al.*, 2008). It is therefore clear that the visual system impacts on light-dependent behavioural entrainment; additionally visual light input has shown to directly modulate subsets of clock cells (Zhang *et al.*, 2010; Chatterjee *et al.*, 2018; Picot *et al.*, 2007), further cementing the importance of this light input pathway.

Re-entrainment and short light pulse experiments have elucidated a wealth of information regarding the contributions of CRY/JET and the visual system in allowing circadian light entrainment. In Chapter 2 we show the wild-type circadian clockwork show a large degree of plasticity, and in extreme LD cycles, is capable of advancing and delaying the molecular and behavioural oscillators to extremely long and short photocycles. We hypothesise that stretching the clockwork to the limits of its entrainable range may reveal the relative contributions of each light input pathway, the influence of other circadian components on entrainment and where in the circadian circuitry light input is required to facilitate behavioural rhythmicity in such extreme conditions. Entrainment to environmental cycles contributes significantly to overall fitness and well-being of an organism; therefore the mechanisms facilitating such entrainment to external photocycle are of real importance.

3.1.1 Aims

- Investigate what components of the *Drosophila* circadian clockwork are required to allow behavioural entrainment to long and short equinox photocycles. In particular, assess the relative contributions of the CRY/JET pathway and the visual system.
- Determine where in the clock circuitry CRY/JET are needed to facilitate entrainment to extreme LD cycles.
- In the absence of CRY, is the visual system sufficient to entrain behaviour to red-light dark cycles?

3.2 Methods

3.2.1 Analysis of *Drosophila* Locomotor behaviour

3.2.1.1 DAM Behavioural Assay and Quantitative Analyses

Behavioural locomotor assays were conducted as described in 2.2.1. Flies were subjected to 10 days in equinox Light:Dark (LD) cycles of 10, 7 or 5c/wk (10c/wk = 8.4hL:8.4hD; 7c/wk = 12hL:12hD or 5c/wk = 16.8hL:16.8hD) at 23°C and ~70% relative humidity. Illumination was provided by white light LEDs (sharp spectra peak at 441 nm and a smaller broader peak at 547 nm with an intensity ~20 $\mu\text{W}/\text{cm}^2$) (as in 2.2.1) in most cases, and red light LEDs with a single peak around 630nm and an intensity of ~7 $\mu\text{W}/\text{cm}^2$ in **Figure 3.9**.

During re-entrainment experiments (**Figure 3.9, D and E**) flies were exposed to 3 days of a 12hL:12hD white LD (WLD) cycle and then shifted to a 6 h delayed 12hL:12hD red LD (RLD) cycle for 15 days, at 23°C and ~70% relative humidity.

Data analysis was conducted as described in 2.2.1.1 and 2.2.1.2 respectively. The parameters used for Chi² periodogram analysis of individual flies are specified in **S.Table B.5**, with the 'Standard' analysis parameters used for all analysis in this chapter. The presence of 'harmonic' entrainment components was taken into consideration to discriminate between entrained and 'other' rhythms for 10c/wk LD cycles throughout this chapter (2.2.1.2).

To quantify re-entrainment, the phase of daily activity offset was determined for each individual fly, on each day of the experiment, using actograms generated in ClockLab (ActiMetrics; Wilmette, IL, USA). Relative phase shift for consecutive days were then calculated relative to lights-off during white LD phase.

GraphPad Prism 7.05 was used to generate all graphs and conduct statistical analysis. Analysis of variance (ANOVA) between genotypes or conditions were conducted with the non-parametric *Kruskal-Wallis test* with pairwise comparisons made using post hoc tests i.e. *Dunn's multiple comparison test* and *Mann-Whitney test* (test used is noted in figures). Differences between the distributions of flies across categories of entrained, 'other' or arrhythmic was analysed using the *Fisher's exact test*, used in the analysis of contingency tables. $p^{****} < 0.0001$; $0.0001 < p^{***} < 0.001$; $0.001 < p^{**} < 0.01$ and $0.01 < p^* < 0.05$.

3.2.2 Spatial Control of Gene Expression

Gal4 and *UAS* elements were combined using genetic crosses to achieve spatial control of gene expression, i.e. cell type-specific expression of a gene of interest (Fischer *et al.*, 1988; Duffy, 2002). *Gal4* encodes an 881 residue protein found in yeast, *S. cerevisiae*, which acts a positive regulator in galactose-induced gene expression (Duffy, 2002). Studies by (Fischer *et al.*, 1988) demonstrated how Gal4 can drive the expression of reporter genes in *Drosophila* which are under the control of *UAS* (Upstream Activator Sequence). A gene of interest can be incorporated in transgenic *UAS* reporter constructs, where it is placed under the regulation of a promoter containing Gal4-responsive *UAS* elements, such that its expression will mirror that of Gal4 (Brand and Perrimon, 1993). The resulting expression pattern is, thus, determined via transgenic constructs, known as *drivers*, that place *Gal4* gene under control of specific promoter sequences of interest (**Figure 3.1, A**). For example, in *tim-Gal4/UAS-CD8::GFP*, the *timeless* promoter sequences drive expression of Gal4 and, therefore, also the membrane-tethered CD8::GFP protein in all clock-bearing cells. Despite there being no *Drosophila* homologue of Gal4, there are reports of side effects resulting from off-target Gal4 binding (Fischer *et al.*, 1988; Liu and Lehmann, 2008).

To further hone spatial regulation of gene expression *Gal80* constructs were used to block expression of a gene of interest in certain cells or tissues. Gal80 is a natural repressor of Gal4 found in the same galactose-induced gene expression pathway in yeast (Suster *et al.*, 2004)(**Figure 3.1, B**). This allows for refined spatial mapping as cells with a promoter element linked to *Gal80* are excluded from those targeted by Gal4 (Pfeiffer *et al.*, 2010).

3.2.2.1 Gene Knockdown – Inhibition of Gene Expression

Inhibition of gene expression was achieved using RNA interference (*RNAi*) lines, which express double stranded RNA (*dsRNA*), under *UAS* control, complementary to that of the gene of interest (Fire *et al.*, 1998). To enhance *RNAi* gene knockdown, *dsRNA* fly lines are supplemented with a *UAS-Dcr-2* element. The endoribonuclease Dicer-2 helps initiate *dsRNA* mediated gene knockdown, resulting in improved knockdown efficiency, by cleaving *dsRNA* molecules into shorter fragments (~20 nucleotides). These fragments then separate and the guide strand forms part of the RNA-INDUCED SILENCING COMPLEX (RISC), an existing cellular mechanism involved in the protection against foreign RNA (Dietzl *et al.*, 2007; Jana *et al.*, 2004).

Chapter 3:

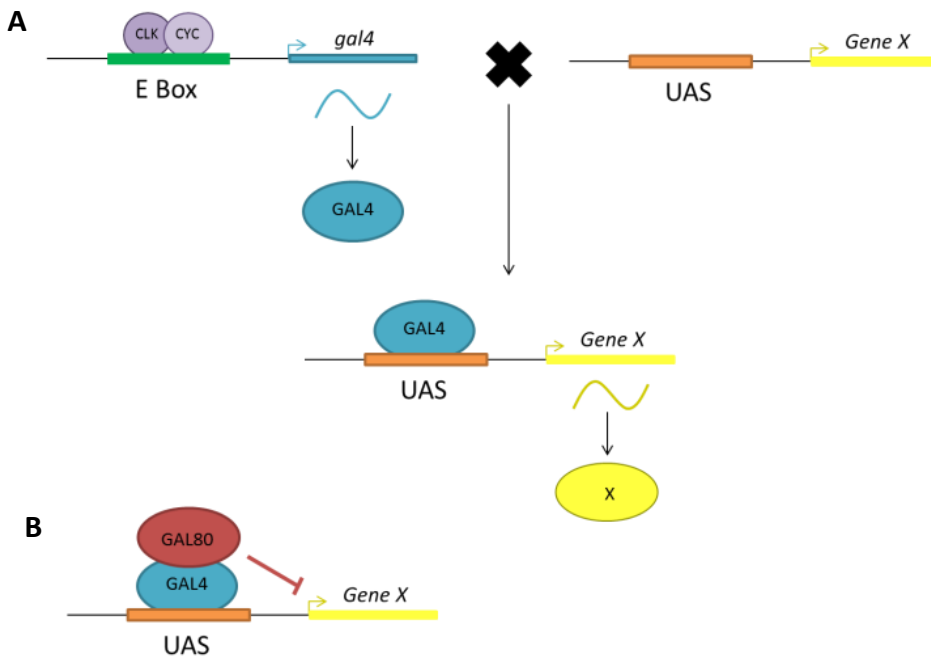


Figure 3.1 Schematic for the system used for spatial regulation of gene expression.

A) Gal4/UAS system for spatial control of gene expression whereby *Gal4* is under the control of a cell-type specific promoter, drives expression of a gene of interested under the control of *UAS*. **B)** Gal80 inhibits Gal4 to further restrict spatial regulation.

3.3 Results

3.3.1 The CRY/JET pathway and the visual system are both required for behavioural entrainment to extreme photocycles

As discussed in Chapter 2, wild-type flies can entrain their behavioural and molecular rhythms to a wide range of equinox photocycles. In order to investigate the components of the clockwork necessary to allow this entrainment, multiple mutant genotypes (details of which are located in **S.Table B.2**), were challenged with LD cycles of various periods. 10, 7 and 5c/wk LD were selected corresponding to 16.8 h, 24 h and 33.6 h photocycles respectively.

Wild-type (*cry⁰¹/+*) fly behaviour was characteristically bimodal in 7c/wk, with peaks of activity at dawn and dusk, and either showed a progressive advance or delay, in 10 and 5c/wk respectively, over consecutive days when plotted over a 24 h scale (**Figure 3.2, A**). Flies homozygous for either a *cry* null mutation (*cry⁰¹*) or a *jet* loss-of function mutation (*jet^{set}*) displayed wild-type-like behaviour in 7c/wk LD (**Figure 3.2, A**). Similarly, flies with a compromised visual system due to either failed development of compound eyes (*eya²- eyes absent*) or apoptosis of visual organs (*GMR-hid*); or having a mutation in phospholipase C which removes the visual transduction pathway (*norpA⁷- no receptor potential A*), also showed bimodality in behavioural rhythms in 7c/wk (**Figure 3.2, A**). In all cases, anticipation was seen before activity peaks in the morning (M) and evening (E), as well as a defined siesta. M-activity was less apparent in *eya²* and behavioural peaks for *GMR-hid* and *norpA⁷* flies appeared broader and less concise than the other genotypes (**Figure 3.2, A**). For all these mutant genotypes in both 10c/wk short and 5c/wk long photocycles, behavioural rhythms weakened, and for *cry⁰¹*, *jet^{set}* and *eya²* a near-24 h rhythm was frequently exhibited (**Figure 3.2, A**).

These differences relative to wild-type controls under divergent LD cycles were confirmed quantitatively in terms of the distributions across different categories of rhythmicity in 10 and 5c/wk photocycles (**Figure 3.2, B**). Notably, non-entrained 'other' rhythms in the near-circadian range were more frequently observed for *cry⁰¹* and *jet^{set}* mutants, whereas lack of entrainment in visual mutants was more frequently characterised by increased arrhythmicity, although high levels of arrhythmicity were also seen in *jet^{set}* flies in 5c/wk LD (**Figure 3.2, B, C**). Although entrainment was clearly compromised by mutations in *cry*, *jet* or genetic manipulation of the visual system, one or more male flies of each genotype did maintain the correct entrained period length in each condition (**Figure 3.2, B, C**).

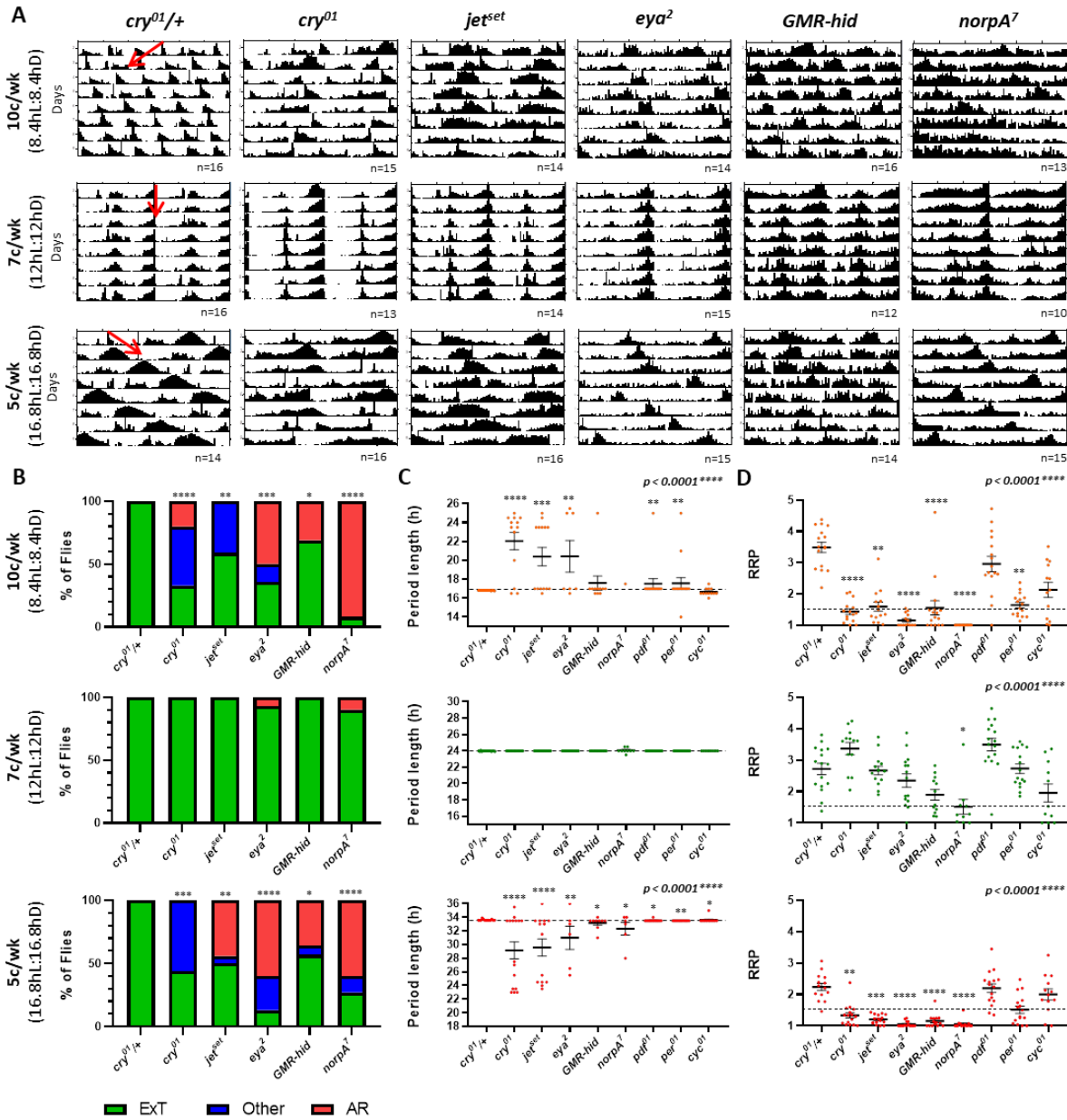


Figure 3.2 Both the CRY/JET pathway and the visual system are required for behavioural plasticity in extreme photocycles.

A) Average locomotor activity presented in double plotted actograms (30 min bins) showing 8 days of activity, plotted over a 24 h scale, for adult male flies of a control genotype ($w^{1118};cry^{01/+}$), or mutant genotypes affecting *cry* ($w^{1118};cry^{01}$), *jet* ($y^1w^*;jet^{set}$), development of compound eyes (*eya²*) or visual organs in general (*GMR-hid*) and *visual phototransduction* (*norpA⁷*) (left to right); in 10 (top), 7 (middle) and 5c/wk (bottom) equinox LD cycles. ‘n’ denotes number of flies and red arrows on *cry^{01/+}* actograms indicate the direction of rhythmic behaviour. **B**) Composite bar charts showing percentage of flies showing entrained (green), ‘other’ (blue) or arrhythmic (red) locomotor behaviour (see methods) over 10 days in 10 (top), 7 (middle) and 5c/wk (bottom). *Fisher’s exact test* to compare distribution of

Fig 3.2 (cont.): entrained, 'other' and arrhythmic individuals for each genotype vs. *cry*⁰¹/+. For 10c/wk, primary and secondary periodicities were compared for each individual and the dominant period length was used to categorise flies using only the 'Ext' range. **C, D)** Individual male period lengths (C) and RRP (D) for the same 6 genotypes, with the addition of *y*¹*w*^{*}; *Pdf*⁰¹ (*Pdf*⁰¹), *y*¹ *per*⁰¹ *w*^{*} (*per*⁰¹) and *cyc*⁰¹ *ry*⁵⁰⁶ (*cyc*⁰¹), in 10, 7 and 5c/wk (top to bottom). *p* values (top right) indicate results of *Kruskal-Wallis test* across all genotypes within each condition. Asterisks indicate pairwise comparison of each genotype vs. *cry*⁰¹/+ in each condition with *Mann-Whitney test*. **C)** Graphs plotted over the range of period lengths used for individual fly analysis in each LD cycle. Error bars show mean period length ± SEM. Dashed lines indicate entrained period length for each condition. **D)** Error bars show mean RRP ± SEM. Dashed line indicates a RRP of 1.5. Arrhythmic flies are assigned an RRP of 1.

In both 10 and 5c/wk LD relative rhythmic strength (RRP) decreased dramatically in *cry*, *jet* and visual mutants versus controls indicating weak rhythmicity (RRP < 1.5). However, rhythms remained robust in all but *norpA*⁷ flies in 7c/wk (**Figure 3.2, D**). The most severe loss of rhythmicity was seen for the *eya*² and *norpA*⁷ mutant flies (**Figure 3.2**). This may be associated with the fact that the *eya*² and *norpA*⁷ lines used here possess the less light sensitive *tim*^{ls} isoform (**S.Table 1**) which may impact on entrainment, especially in short (10c/wk) photocycles (**S.Figure 1**), as discussed in 2.3.1.1.1.

Mutations to core clock genes *per* and *cyc* as well as the circadian neuropeptide gene *Pdf* impacted fly behaviour but did not reduce the detection of male behavioural rhythms matching the imposed 5, 7 or 10c/wk photocycles (**S.Figure 7**). Flies lacking the phase setting neuropeptide PDF required for DD rhythmicity and normal daily activity patterns in LD, showed the well-documented advance in E-peak activity at 5 and 7c/wk and a widened E peak at 10c/wk (**S.Figure 7**) (Renn *et al.*, 1999). In contrast, *per*⁰¹ and *cyc*⁰¹ mutants that lacked an essential component of the core molecular oscillator exhibited photocycle-driven rhythmicity lacking anticipation of light/dark transitions in any of the environmental contexts, as discussed in Chapter 2. Of note, *cyc*⁰¹ displayed nocturnal behaviour where activity was high in the night and suppressed following lights on (**S.Figure 7**), as previously published (Rutila *et al.*, 1998). Thus, these 'other' circadian mutations, for various reasons, maintained photocycle-associated rhythms in male flies under all three conditions examined (**Figure 3.2, C, D**).

As noted above, *cry* and *jet* mutants frequently exhibited alternative period lengths under 10 and 5c/wk photocycle conditions. An in-depth look at the composition of *cry*⁰¹ and *jet*^{set} rhythmic components indicated a substantial peak around 24 h, irrespective of the LD cycle, as well as weaker entrained components at 5 and 10c/wk (**Figure 3.3**). Wild-type flies in all conditions, as

Chapter 3:

well as *cry* and *jet* mutants in 7c/wk, showed clear peaks in activity at entrained and 'harmonic' peaks of activity (**Figure 3.3, A**). 'Harmonic' rhythms at multiples of 0.5x the photocycle length are thought to occur due to the bimodal nature of fly circadian locomotor behaviour as discussed in Chapter 2. However, the near ~24 h rhythmic components in the χ^2 periodograms of *cry* and *jet* mutants in 5 and 10c/wk, did not correlate well with such 'harmonic' peaks. Thus, CRY/JET-independent light input is insufficient for efficient behavioural entrainment to 5 and 10c/wk photocycles and intrinsic free-running periodicity appears to emerge under these conditions. For further analysis and female data see **S.Table 10**. In most cases, female flies displayed the same genotype and photocycle dependent behavioural deficits as their male counterparts. However, rhythmic strength tended to be weaker in control and *cyc*⁰¹ females, respectively across all photocycles and preferentially in 5 and 10c/wk. As a result *cyc*⁰¹ females exhibited significantly reduced rhythmicity compared with controls at 5 and 10c/wk, suggesting that the photocycle-driven behaviour of *cyc*⁰¹ flies was affected in gender-specific manner. The relatively poor daily locomotor rhythmicity and sexual dimorphism in sleep/wake patterns observed previously for *cyc*⁰¹ were consistent with these results (Rutila *et al.*, 1998; C Hendricks *et al.*, 2003). Nevertheless, in relation to the mutational analysis of the CRY/JET and visual input pathways, results from both genders indicated a requirement for each of these pathways for behavioural entrainment to extreme LD cycles.

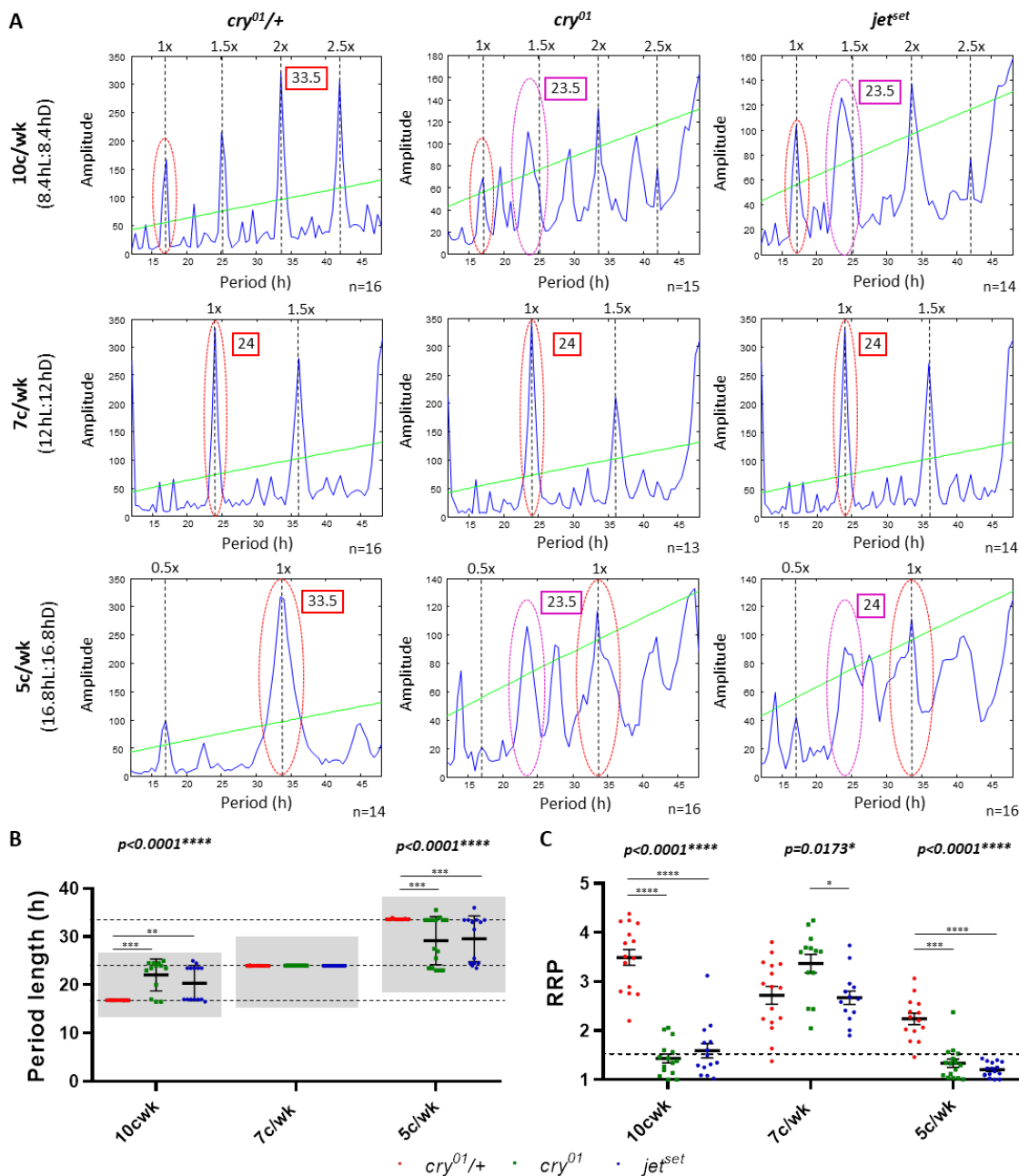


Figure 3.3 Mutants to the CRY/JET pathway resulted in circadian (~24 h) period lengths in extreme LD cycles.

A Chi² periodograms for adult male flies of genotype; $w^{1118};cry^{01}/+$, $w^{1118};cry^{01}$ and $y^1w^*;jet^{set}$ (left to right); in 10 (top), 7 (middle) and 5c/wk (bottom) equinox LD cycles, plotted from 12-48 h with the dominant period peak annotated. Dashed vertical lines indicate 'harmonic' components. Dashed red ovals indicate the entrained peaks for each LD cycle. Dashed magenta ovals indicate aberrant circadian (~24 h) peaks for cry^{01} and jet^{set} flies in 10 and 5c/wk. 'n' denotes number of flies. **B** Individual male period lengths for $cry^{01}/+$ (red), cry^{01} (green) and jet^{set} (blue) in 10, 7, and 5c/wk (left to right). Error bars show mean period length \pm SEM. Dashed lines show entrained period lengths for 5, 7 and 10c/wk (top to bottom). Grey shading indicates analysis range used for individual fly analysis in each LD cycle.

Chapter 3:

Fig 3.3 (cont.): *p* values (bottom) report results of *Kruskal-Wallis test* for the impact of genotype within each condition. Pairwise comparison of genotypes in each condition with *Dunn's multiple comparison test* (10c/wk; $cry^{01}/+$ vs. cry^{01} - $p=0.0003$ and $cry^{01}/+$ vs. jet^{set} - $p=0.0013$. 5c/wk; $cry^{01}/+$ vs. cry^{01} - $p=0.0005$ and $cry^{01}/+$ vs. jet^{set} - $p=0.0006$). **C)** Individual male RRP for $cry^{01}/+$ (red), cry^{01} (green) and jet^{set} (blue) in 10, 7, and 5c/wk (left to right). Error bars show mean RRP \pm SEM. Dashed line indicates a RRP of 1.5. Arrhythmic flies were assigned an RRP of 1. *p* values (top) report results of *Kruskal-Wallis test* for the impact of genotype within each condition. Pairwise comparison of genotypes in each condition with *Dunn's multiple comparison test* (10c/wk; $cry^{01}/+$ vs. cry^{01} - $p<0.0001$ and $cry^{01}/+$ vs. jet^{set} - $p<0.0001$. 7c/wk; cry^{01} vs. jet^{set} - $p=0.0277$. 5c/wk; $cry^{01}/+$ vs. cry^{01} - $p=0.0002$ and $cry^{01}/+$ vs. jet^{set} - $p<0.0001$).

3.3.2 Spatial characterisation of CRY and JET requirement for photocycle entrainment

The ~150 clock neurons of the fly circadian circuitry show molecular and functional differences with regard to their contribution to fly behaviour (see 3.1). CRY is not expressed in all clock cells, but it is found in at least all LN_vs, three LN_ds, and a subset of DN1s (Klarsfeld *et al.*, 2004; Yoshii *et al.*, 2008; Benito *et al.*, 2008). Due to JET's function in CRY-dependent TIM degradation, co-expression is expected. To spatially map the requirement for CRY and JET expression relative to photocycle-mediated behavioural plasticity within the circuitry, the Gal4/UAS system was used (3.2.2) to investigate behavioural entrainment to 10, 7 and 5c/wk LD.

3.3.2.1 Pan-circadian knockdown of *cry* and *jet* limited behavioural photocycle entrainment

Knockdown was achieved by driving expression of *dsRNA* constructs as described in 3.2.2.1. *UAS-ds-cry*^{3772R2} and *UAS-ds-jet*^{JF01506} (Ni *et al.*, 2007) were used to inhibit gene expression of *cry* and *jet*, respectively, in all clock bearing cells using *tim(UAS)-Gal4 (TUG)* (Blau and Young, 1999); M- and E- cells with *cry-Gal4-13 (cry)* (Emery *et al.*, 2000b; Stoleru *et al.*, 2004); exclusively the M- or E-cells with *Pdf-Gal4 (Pdf)* (Renn *et al.*, 1999) and *GMR78G02-Gal4 (GMR78G02)* (Schlichting *et al.*, 2016) respectively; and in cholinergic cells with *ChAT-Gal4.7.4 (ChAT)* (Lima and Miesenböck, 2005). See **S.Table B.3** for more detail and references as well as **S.Figure 12** for the expression pattern of each driver line. All the data presented follows the same labelling convention, whereby the driver line is represented by the abbreviations above and '>' denotes that is driving the expression *dsRNA* e.g. *TUG>ds-cry* describes expression of *UAS-ds-cry*^{3772R2} with *tim(UAS)-Gal4*.

Initially *TUG* was used to drive knockdown across the entire clock circuit. Driver-only isogenic control flies entrained their behaviour well to all conditions (**Figure 3.4, A**), similar to other control flies (*cry*^{01/+}) (**Figure 3.2**). *TUG* driven knock down of *cry* and *jet* did not reduce entrainment to a 7c/wk LD cycle (**Figure 3.4**), as was the case with *cry*⁰¹ and *jet*^{set} mutants (**Figure 3.2**). However, pan-circadian expression of *ds-cry* resulted in a clear loss of entrained locomotor rhythms in both 10 and 5c/wk where flies exhibited a 25 h periodicity (**Figure 3.4, B**). In both conditions the dominant rhythmic peak was at 25 h, shown by χ^2 periodograms, and peaks at the entrained and 'harmonic' (0.5x, 2x) period lengths failed to exceed the significance threshold (**Figure 3.4, B**). This shift to a circadian periodicity was similar to that described for *cry*⁰¹ flies above (**Figure 3.3, A**), but featured an even more dramatic shift away from 'other' rhythmic components. Similar observations were made for *TUG>ds-jet* where a breakdown in entrained rhythmicity was evident between control and experimental actograms for both 10 and 5c/wk

Chapter 3:

(**Figure 3.4, C**). χ^2 -periodograms featured a circadian ~25 h peak as well as decreased entrained and ‘harmonic’ peaks, compared to control, indicating a decrease in entrainment (**Figure 3.4, C**). Although *jet* knockdown with *TUG* yielded an entrainment deficit, it was not as drastic as seen with *cry*. Peaks at the expected entrained period lengths in 10 and 5c/wk persisted to a greater extent in *TUG>ds-jet* versus *TUG>ds-cry* (**Figure 3.4, B, C**).

Data from repeated experiments were pooled when conducting quantitative analysis. Isogenic control data was collated to generate a single ‘Control’ dataset, however comparisons between experimental genotypes and their corresponding isogenic control can be found in **S.Table 11** and **S.Table 12** for *cry* and *jet* knockdown respectively.

Significant reductions in entrainment are evident for *TUG>ds-cry* and *TUG>ds-jet* in both 10 and 5c/wk LD but not 7c/wk (**Figure 3.5**), corroborating the observations presented above. In most cases the difference arises from an increase in rhythms of ‘other’ period lengths and not increased arrhythmicity, mirroring what was observed for *cry*⁰¹ and *jet*^{set} (**Figure 3.2**). These ‘other’ rhythms represent the 25 h rhythmic component seen in 10 and 5c/wk χ^2 periodograms (**Figure 3.5, C, D**). As discussed in Chapter 2, 10c/wk LD can result in a ‘harmonic’ rhythm at 25.2 h (1.5x entrained rhythm of 16.8 h) due to the bimodality of *Drosophila* behaviour. However, the observed ~25 h component was stronger than the rhythmic component matching the 16.8 h entrained period length for the majority of *TUG>ds-cry* and *TUG>ds-jet* flies, while control flies exhibited stronger 16.8 h components. Thus, the ~25 h component observed for the knockdown genotypes indicated a reduced ability to entrain to 10c/wk photocycles.

No significant entrainment deficits were seen in 10, 7 and 5c/wk LD when *cry* was knocked-down with *cry*-, *Pdf*-, *GMR78G02*- or *ChAT-Gal4* (**Figure 3.5, A, C**), compared to collated or corresponding isogenic controls (**S.Table 11**). The same was true for *jet* knockdown in 7 and 5c/wk LD. However, reduced entrainment was seen to 10c/wk LD when *jet* knockdown was driven by *Pdf*-, *GMR78G02*- and *ChAT-Gal4* compared to control (**Figure 3.5, B**). However, no differences were apparent between any experimental genotype and its isogenic control for any driver in any condition, except *TUG>ds-jet* in 10 and 5c/wk (**Figure 3.5, D** and **S.Table 12**). The behavioural phenotype elicited by *jet* knockdown by *Pdf*- and *GMR78G02-Gal4* in 10c/wk was comparable to *cry* knockdown in the same condition, however the control flies for *jet* knockdown showed better entrainment than the *cry* controls (**Figure 3.5**), accounting for the selective observation of significant differences. *ChAT-Gal4* drives expression in cholinergic cells which within the clock circuitry is known to include the 2 NPF positive LN_ds and the 5th s-LN_v (Johard *et al.*, 2009). Restrictive expression of *ds-cry* and *ds-jet* with *ChAT-Gal4* appeared to reduce entrainment to a

similar degree to broader M- and E-cell drivers *Pdf-* and *GMR78G02-Gal4* respectively. Such inconsistencies could be explained by the differential efficiencies of driver lines, resulting in inefficient or incomplete knockdown. It should be noted that *ChAT-Gal4* is the only genotype that has the less light sensitive *tim^{LS}* isoform which could explain reduced entrainment to short photocycles. Females showed similar patterns of entrainment as presented here for males, although loss of entrainment via knockdown of *cry* and *jet* in females manifested more in increased arrhythmia than the persistence of circadian rhythms (**S.Table 11** and **S.Table 12**).

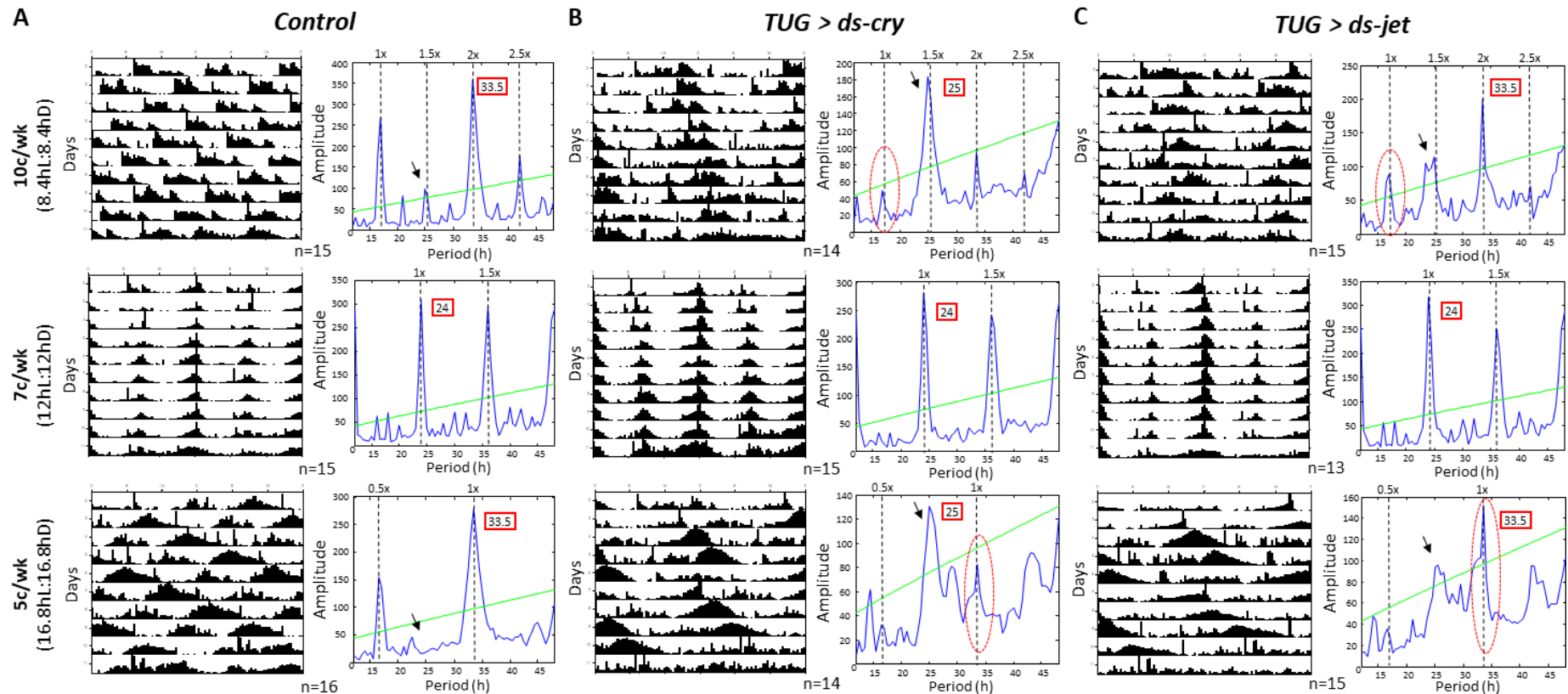


Figure 3.4 Pan-circadian knockdown of *cry* or *jet* reduced behavioural entrainment to extreme photocycles.

A, B, C Average locomotor activity presented in double plotted actograms (30 min bins) showing 10 days of activity plotted over a 24 h scale (left) and χ^2 periodograms plotted from 12-48 h (right), for adult male flies of genotype; **(A)** *UAS-Dcr-2 w**; *TUG/CyO*; +/*TM6B-Tb*¹ (**Control**), **(B)** *UAS-Dcr-2 w**; *UAS-ds-cry*^{3772R2}/*TUG*; +/*TM6B-Tb*¹ (***TUG*>*ds-cry***) and **(C)** *UAS-Dcr-2 w**; *TUG*; +/*UAS-ds-jet*^{1F01506}/+ (***TUG*>*ds-jet***); in 10 (top), 7 (middle) and 5c/wk (bottom) equinox LD cycles. ‘n’ denotes number of flies. Dominant period peaks annotated on χ^2 periodograms, with dashed lines indicating possible ‘harmonic’ components for each LD cycle. Dashed red ovals (**B** and **C**) indicate entrained peak for 10 and 5c/wk. Arrows indicate circadian (~24 h) component which was far more prominent in *TUG*>*ds-cry* and *TUG*>*ds-jet* compared to *Control* in 5 and 10c/wk. See **S.Figure 12** for Gal4 expression patterns.

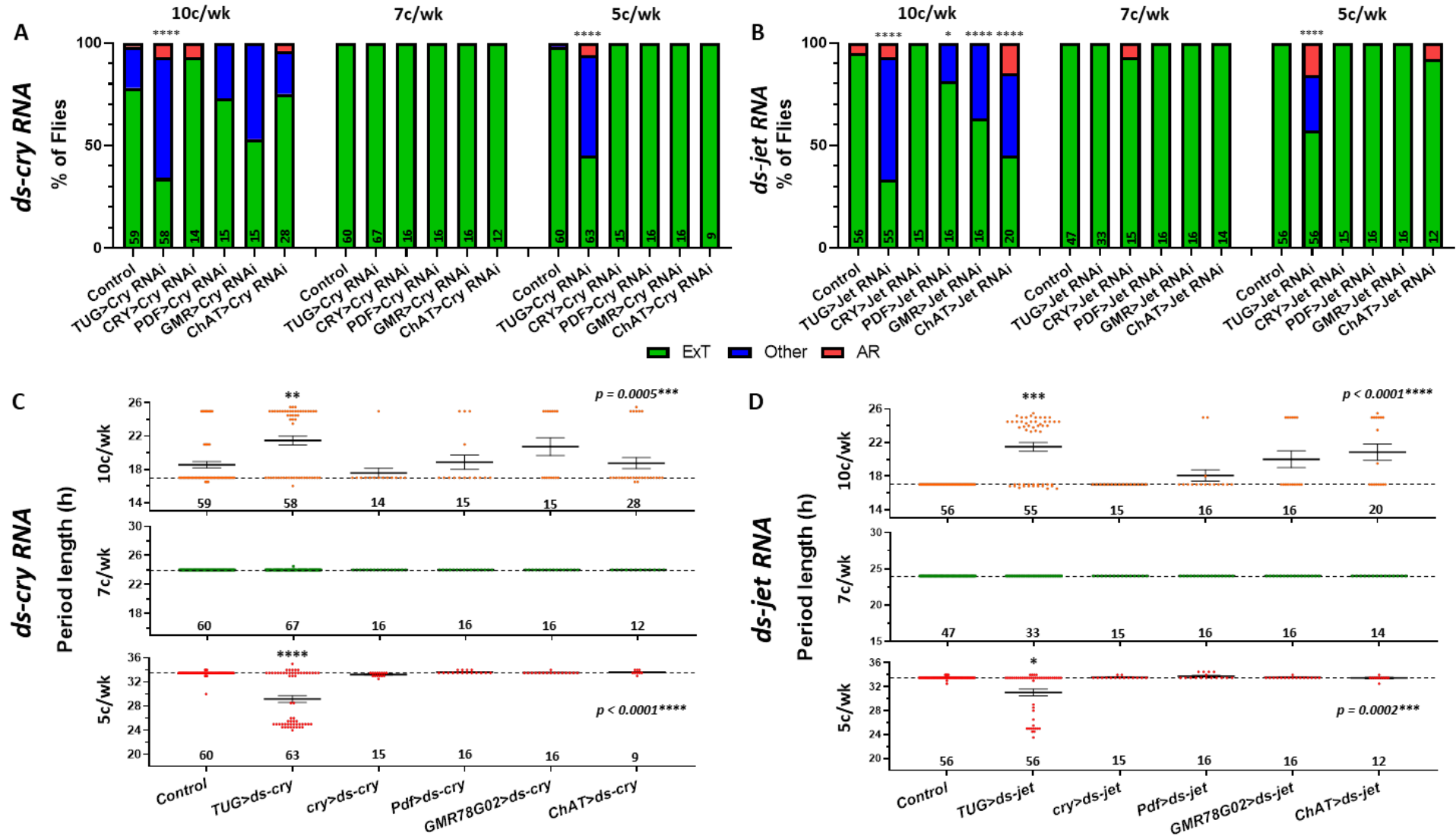


Figure 3.5 Significant reductions in entrainment are evident when *cry* or *jet* are knocked-down in all clock cells in both 10 and 5c/wk LD but not 7c/wk.

Results of *cry* (A and C) and *jet* (B and D) knockdown with a variety of Gal4 driver lines (Gal4>ds-RNA). See **S.Table 11** and **12** for full genotypes and **S.Figure 12** for Gal4 expression patterns. Data from repeat experiments are pooled and the 'n' number is displayed in the figures. *Control* represents pooled data for all isogenic controls. **A, B**) Composite bar charts showing percentage of male flies showing entrained (green), 'other' (blue) or arrhythmic (red) locomotor behaviour (see methods) over 10 days in 10, 7 and 5c/wk (left to right- annotated on figure). *Fisher's exact test* to compare distribution of entrained, 'other' and arrhythmic individuals for each genotype vs. *Control*. For 10c/wk, primary and secondary periodicities were compared for each individual and the dominant period length was used to categorise flies using only the 'Ext' range. **C, D**) Individual male period lengths in 10, 7 and 5c/wk (top to bottom). Graphs plotted over the range of period lengths used for individual fly analysis in each LD cycle. Error bars show mean period length \pm SEM. Dashed lines indicate entrained period length for each condition. *p* values indicate results of *Kruskal-Wallis test* across all genotypes within each condition. Asterisks indicate pairwise comparison of each genotype vs. *Control* in each condition with *Mann-Whitney test*.

3.3.2.2 CRY/JET expression in both the M- and E- cells was required for behavioural entrainment

A robust behavioural phenotype was seen with pan-circadian knockdown of *cry* and *jet*; however attempts to narrow down the spatial requirement of CRY and JET yielded few tangible results. In order to refine this mapping *TUG* was combined with *cry-Gal80* (Dissel *et al.*, 2014) and *Pdf-Gal80* (Stoleru *et al.*, 2004) constructs (see **S.Table B.3**) to restrict knockdown to smaller subsets of cells (**Figure 3.1**). Genotypes are presented as before i.e. *TUG>ds-cry*, with the presence of *Gal80* indicated in parenthesis e.g. *TUG(-cry)>ds-cry* denotes a knockdown of *cry* in all clock cells except those expressing *cry-Gal80*. Quantitative analysis was conducted on data pooled from repeats with isogenic control data collated, as in 3.3.2.1. Comparisons between experimental genotypes and their corresponding isogenic control, as well as further analysis, can be found in **S.Table 13** and **S.Table 14** for selective *cry* and *jet* knockdown respectively.

As was consistently the case, all genotypes displayed entrained behaviour with a 24 h periodicity in 7c/wk LD (**Figure 3.6** and **Figure 3.7**). Blocking *cry* knockdown in *cry* expressing cells with *cry-Gal80* rescued rhythmicity in both 5 and 10c/wk photocycles, compared to *TUG* knockdown alone (**Figure 3.6, A**). The same was true when *cry* expression was limited to just the *Pdf*-expressing M-cells using *Pdf-Gal80* (**Figure 3.6, A**). Behavioural patterns depicted in the actograms of *TUG(-cry)>ds-cry* and *TUG(-Pdf)>ds-cry* flies were similar to those seen for wild-type controls (**Figure 3.2, A**). These observations were supported quantitatively as *TUG(-cry)>ds-cry* and *TUG(-Pdf)>ds-cry* flies showed significant rescue of rhythmicity, back to wild-type levels, compared to *TUG>ds-cry* (**Figure 3.6, B**). The lower number of flies for *TUG(-cry)>ds-cry* may have accounted for the smaller statistical difference versus knockdown alone in 5c/wk, compared to *TUG(-Pdf)>ds-cry*. However, it was clear that expression of *cry* in the M-cells alone appeared to be sufficient to rescue behavioural entrainment.

Behavioural entrainment was also restored in *TUG(-cry)>ds-jet* and *TUG(-Pdf)>ds-jet* flies in long 5c/wk photocycles, while rescue of behavioural entrainment in these genotypes was less obvious in the 10c/wk actograms (**Figure 3.7, A**). The distribution of flies across entrained, 'other' and arrhythmic categories confirmed that behavioural entrainment was rescued with the introduction of *Pdf-Gal80* for the 5c/wk condition, while the number of *TUG(-cry)>ds-jet* flies assayed was insufficient to obtain a significant *p* value in the analogous test (**Figure 3.7, B**). The comparison across rhythmic categories did detect significant rescue of behavioural entrainment for *TUG(-cry)>ds-jet* in 10c/wk vs. *TUG>ds-jet* knockdown alone, but this was not the case for *TUG(-Pdf)>ds-jet*, which showed an intermediate percentage of entrained flies (**Figure 3.7,B**). Thus,

rescue from *jet* knockdown in just the PDF cells restored entrainment more fully in 5c/wk than 10c/wk photocycles. Females showed comparable data to males, with significant rescue of entrainment upon the introduction of *Pdf-Gal80* and comparable trends when *cry-Gal80* was introduced instead (S.Table 13 or S.Table 14).

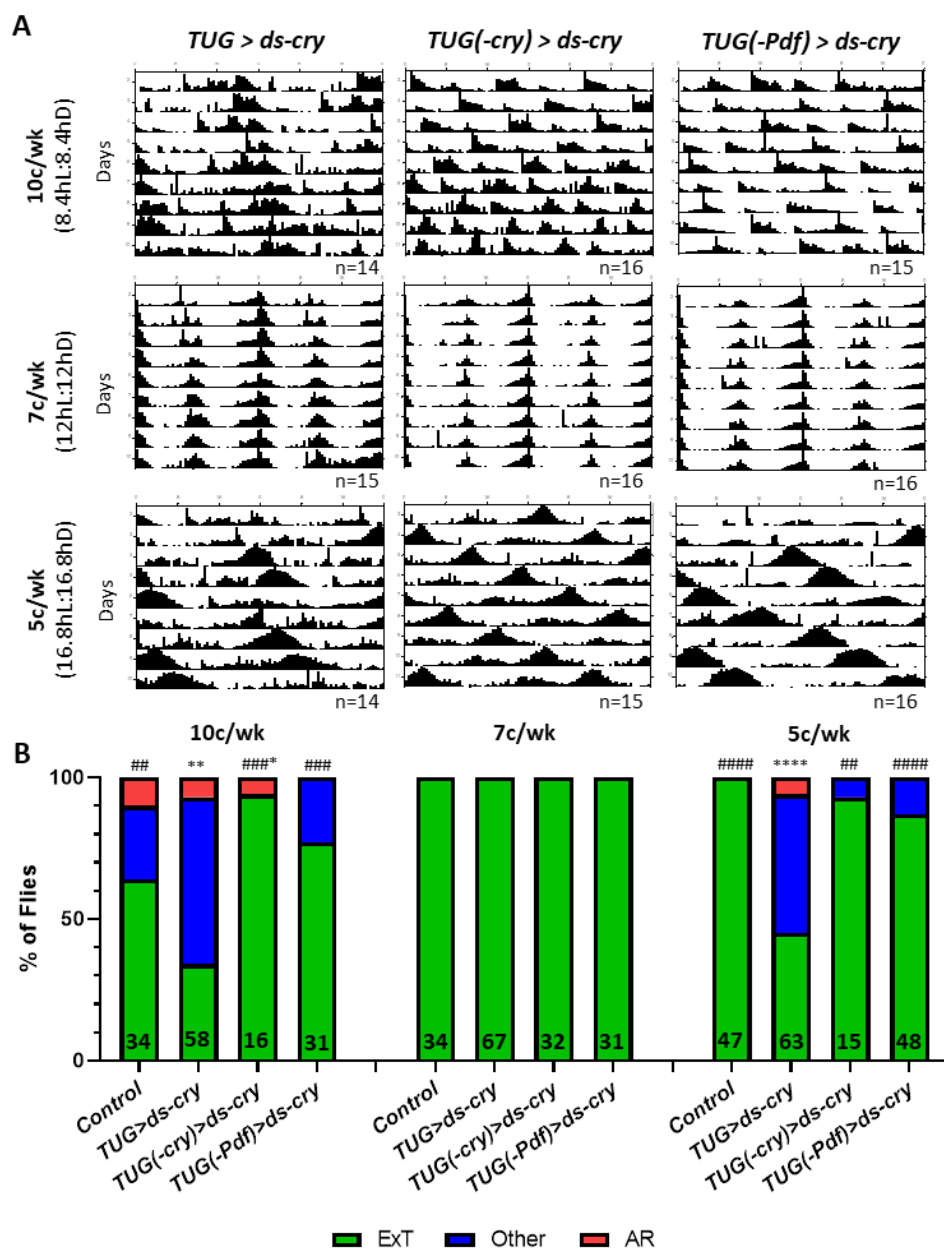


Figure 3.6 Selective knockdown of *cry* indicates where CRY is required to allow behavioural entrainment to extreme photoperiods.

A) Average locomotor activity presented in double plotted actograms (30 min bins) showing 9 days of activity plotted over a 24 h scale for adult male flies of genotype; *UAS-Dcr-2w**; *UAS-ds-cry*^{3772R2}/*tim(UAS)-Gal4*;+/TM6B-Tb¹ (**TUG>ds-cry**), *UAS-Dcr-2w**; *UAS-ds-cry*^{3772R2}/*tim(UAS)-Gal4*; *cry-Gal80*/+ (**TUG(-cry)>ds-cry**) and *UAS-Dcr-2 w**; *UAS-ds-cry*^{3772R2}/*tim(UAS)-Gal4*; *Pdf-Gal80*/+ (**TUG(-Pdf)>ds-cry**) (left to right); in 10 (top), 7 (middle) and 5c/wk (bottom) equinox

Chapter 3:

Fig 3.5 (cont.): LD cycles. 'n' denotes number of flies. **B)** Composite bar charts showing percentage of flies showing entrained (green), 'other' (blue) or arrhythmic (red) locomotor behaviour (see methods) over 10 days in 10, 7 and 5c/wk (left to right). Data from repeat experiments are pooled and the number in each bar denotes total number of flies in each genotype/condition. '**Control**' represents data pooled from isogenic flies, emerging from crosses to generate experimental offspring, which do not express *ds-cry RNA*. *Fisher's exact test* to compare distribution of entrained, 'other' and arrhythmic individuals for each genotype vs. *Control* (*) and vs. *cry* knockdown (*TUG>ds-cry*) (#). For 10c/wk, primary and secondary periodicities were compared for each individual and the dominant period length was used to categorise flies using only the 'Ext' range. This data set was generated with a significant contribution from Mr Mike Price.

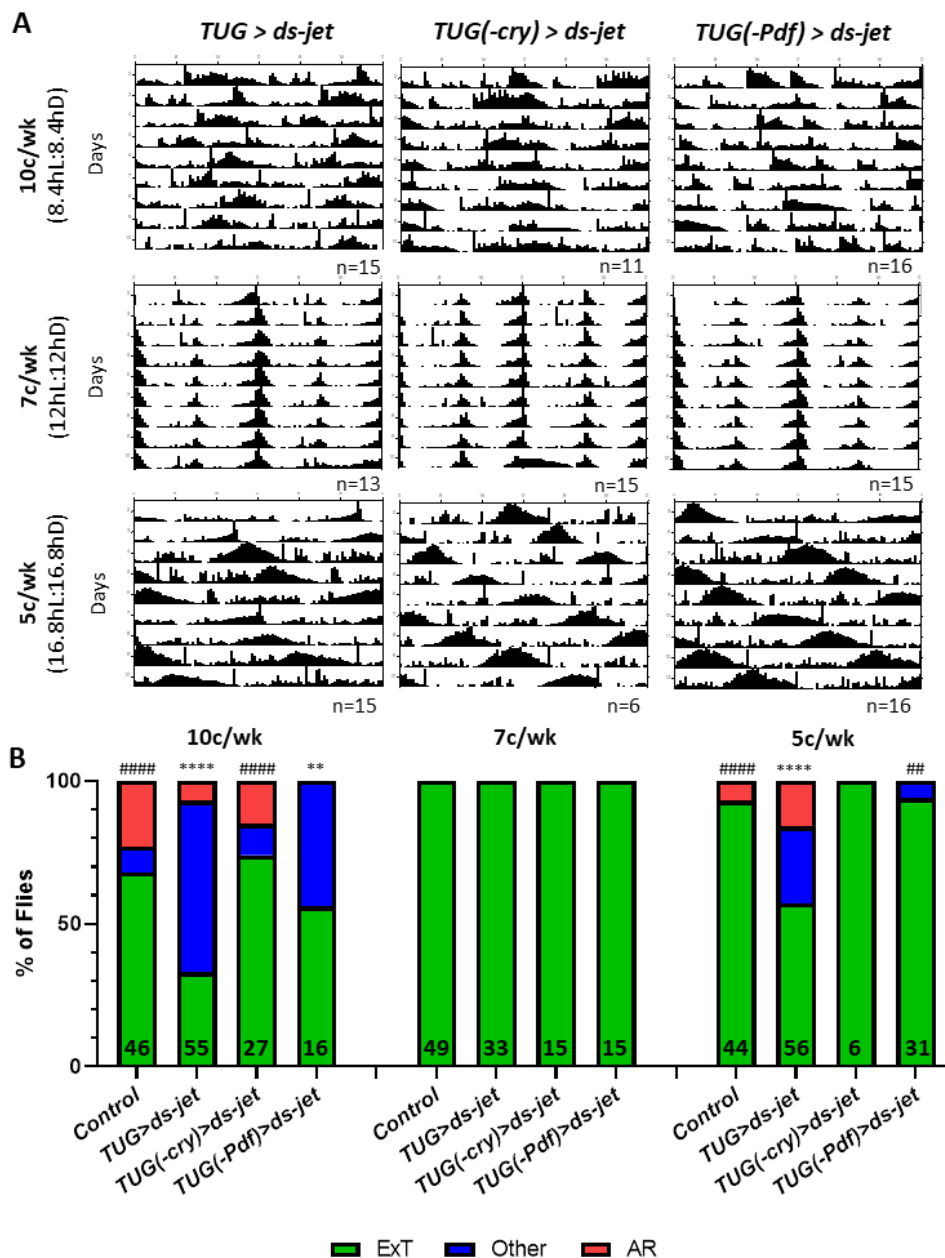


Figure 3.7 Selective knockdown of *jet* indicates where JET is required to allow behavioural entrainment to extreme photocycles.

A) Average locomotor activity presented in double plotted actograms (30 min bins) showing 9 days of activity plotted over a 24 h scale for adult male flies of genotype; *UAS-Dcr-2w**; *tim(UAS)-Gal4/+*; *UAS-ds-jet^{JF01506}/+* (**TUG > ds-jet**), *UAS-Dcr-2w**; *tim(UAS)-Gal4/+*; *UAS-ds-jet^{JF01506}/cry-Gal80* (**TUG(-cry) > ds-jet**) and *UAS-Dcr-2w**; *tim(UAS)-Gal4/+*; *UAS-ds-jet^{JF01506}/Pdf-Gal80* (**TUG(-Pdf) > ds-jet**) (left to right); in 10 (top), 7 (middle) and 5c/wk (bottom) equinox LD cycles. 'n' denotes number of flies. **B)** Composite bar charts showing percentage of flies showing entrained (green), 'other' (blue) or arrhythmic (red) locomotor behaviour (see methods) over 10 days in 10, 7 and 5c/wk (left to right). Data from repeat experiments are pooled and the number in each bar denotes total number of flies in each genotype/condition.

Chapter 3:

Fig 3.6 (Cont.): '*Control*' represents data pooled from isogenic flies, emerging from crosses to generate experimental offspring, which do not express *ds-jet RNA*. Fisher's exact test to compare distribution of entrained, 'other' and arrhythmic individuals for each genotype vs. *Control* (*) and vs. *jet* knockdown (*TUG>ds-jet*) (#). 'Control' is collated data from isogenic control flies emerging from crosses to generate experimental offspring. For 10c/wk, primary and secondary periodicities were compared for each individual and the dominant period length was used to categorise flies using only the 'Ext' range. This data set was generated with a significant contribution from Mr Mike Price.

3.3.2.3 CRY expression in just the PDF cells was sufficient to rescue rhythmicity in long photocycles

Spatial characterisation of CRY function in extreme LD cycles was also assessed by driving CRY expression in a *cry*⁰¹ background, using *UAS-cry*₂₄ (from the Emery lab), with *TUG*, *Pdf*- and *ChAT-Gal4*, as in 3.3.2.1. See **S.Table B.3** for more detail and **S.Figure 12** for driver expression patterns. Quantitative analysis was conducted on data pooled from repeats.

Control flies, which had *UAS-cry*₂₄ but no driver, exhibited locomotor behaviour comparable to *cry*⁰¹ mutants in all photocycles (**Figure 3.8** and **Figure 3.2**). Unsurprisingly, *w**; *TUG/UAS-cry*₂₄; *cry*⁰¹ flies, where *cry* was expressed in all clock cells, showed a marked rescue in rhythmicity compared to control in both 5 and 10c/wk photocycles (**Figure 3.8, A**), and behavioural patterns matched what was described for wild-type in 3.3.1 and Chapter 2. CRY expression in just the morning cells, *w**; *Pdf-Gal4/UAS-cry*₂₄; *cry*⁰¹, did not evoke the same behavioural rescue; with average actograms similar to *cry*⁰¹ featuring circadian rhythmic components in 5 and 10c/wk photocycles (**Figure 3.8, A**). In contrast, *w**; *ChAT-Gal4/UAS-cry*₂₄; *cry*⁰¹ flies, with CRY expressed in cholinergic neurons, showed a clear return to entrained rhythmic behaviour in 5 and 10c/wk (**Figure 3.8, A**).

Significant rescue of entrained period lengths, compared to control, were achieved in 5 and 10c/wk photocycles with *TUG* and *ChAT-Gal4* (**Figure 3.8, B**), as suggested by the actograms. Pan-circadian CRY expression, although restoring rhythmicity, didn't achieve wild-type levels of entrainment in 5 and 10c/wk, however cholinergic CRY expression did (**Figure 3.8, B** and **Figure 3.2, B**). Behavioural rescue in *ChAT>UAS-cry* flies above that achieved by *TUG*, suggested that there may be some targets of *ChAT-Gal4* within the clock circuitry that received better induction with this driver or, alternatively, that ectopic *cry* expression in cholinergic cells contributed to entrainment in this context. Expression of CRY in the M-cells with *Pdf-Gal4* only rescued entrainment in 5c/wk, although not to the same degree as *TUG* (**Figure 3.8, B**). *Pdf-Gal4* alone is known to exhibit a mild long period phenotype (24.8 h) (Renn *et al.*, 1999), which may have affected entrainment to long versus short photocycles differentially (see 2.3.1.1.2), however it was unlikely that this impacted greatly on entrainment to such extreme conditions. Additional analysis and female data is presented in **S.Table 15**. Rescue in long 5c/wk photocycles with *Pdf*- and *ChAT-Gal4* was emulated by females, with *Pdf>UAS-cry* exhibiting enhanced rescue over that seen in males. However, in spite of a trend for *TUG>UAS-cry* flies to exhibit stronger rhythmic power and a higher percentage of entrained flies, neither this nor any other *Gal4>UAS-cry* combination exhibited significant rescue of entrainment in 10c/wk photocycles. This gender

Chapter 3:

dimorphism may, at least in part be attributable to fact that the *cry*⁰¹ entrainment defect in 10c/wk conditions exhibited more circadian rhythmicity in males and more arrhythmicity in females (**S. Table 10**). Taken together, spatiotemporally targeted manipulation of *cry* and *jet* indicated that 10c/wk photocycle entrainment was more sensitive. Moreover, *cry* and *jet* expression in both PDF and non-PDF CRY positive clock neurons was found to contribute to plasticity in photocycle entrainment with the latter group possibly featuring important cholinergic clock neurons.

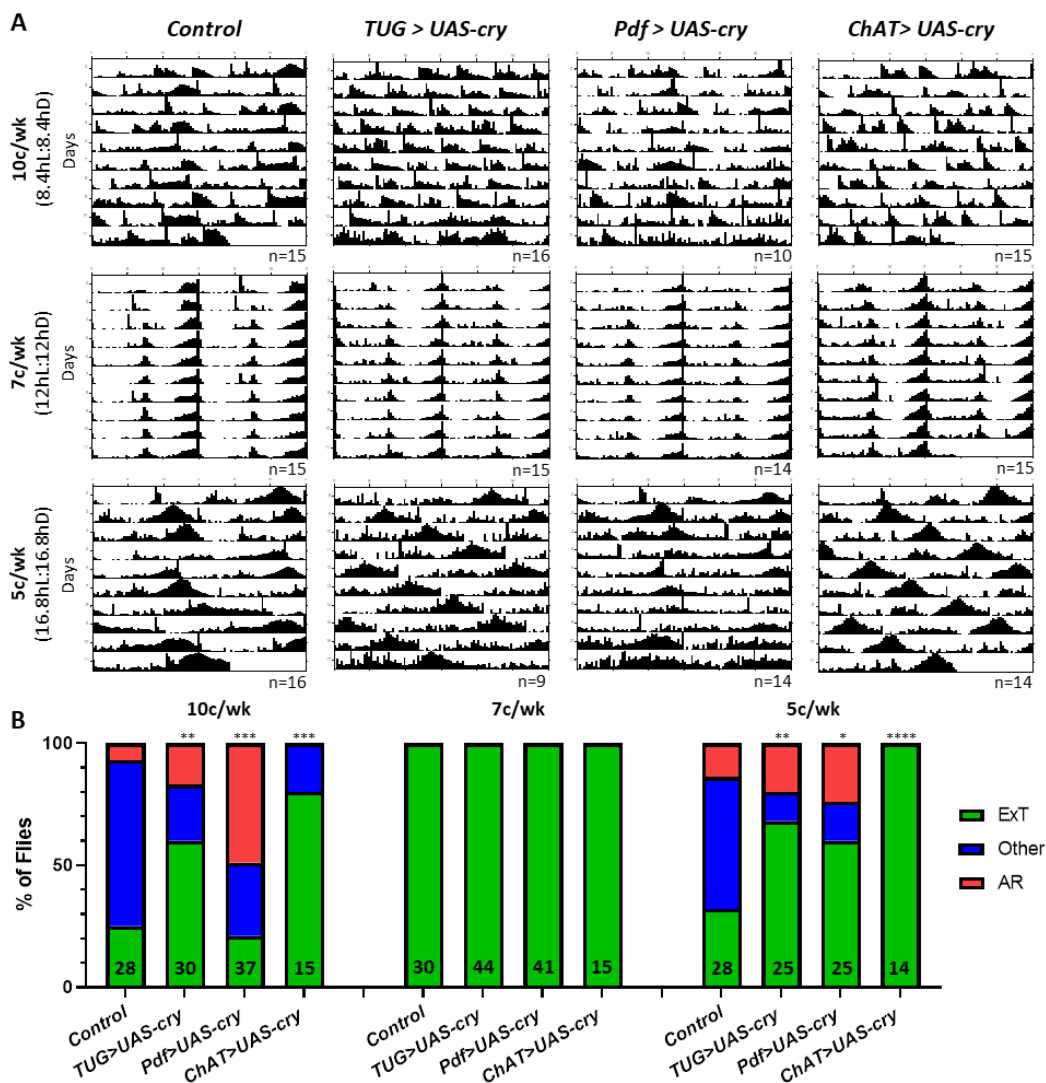


Figure 3.8 Rescue of CRY expression, in a *cry⁰¹* background, indicates where CRY is needed to allow light-induced behavioural plasticity.

A) Average locomotor activity presented in double plotted actograms (30 min bins) showing 10 days of activity plotted over a 24 h scale for adult male flies of genotype; *w;UAS-cry₂₄/CyO*; *cry⁰¹* (**Control**), *w;UAS-cry₂₄/TUG*; *cry⁰¹* (**TUG>UAS-cry**), *w;UAS-cry₂₄/Pdf-Gal4*; *cry⁰¹* (**Pdf>UAS-cry**) and *w;UAS-cry₂₄/ChAT-Gal4*; *cry⁰¹* (**ChAT>UAS-cry**); in 10 (top), 7 (middle) and 5c/wk (bottom) equinox LD cycles. ‘n’ denotes number of flies. **B)** Composite bar charts showing percentage of flies showing entrained (green), ‘other’ (blue) or arrhythmic (red) locomotor behaviour (see methods) over 10 days in 10, 7 and 5c/wk (left to right- annotated on figure). Data from repeat experiments are pooled and the number in each bar denotes total number of flies in each genotype/condition. Fisher’s exact test to compare distribution of entrained, ‘other’ and arrhythmic individuals for each genotype vs. control. For 10c/wk, primary and secondary periodicities were compared for each individual and the dominant period length was used to categorise flies using only the ‘Ext’ range. See **S.Figure 12** for Gal4 expression patterns.

3.3.3 The visual system facilitates red-light entrainment via histamine signalling

The *Drosophila* visual system is fundamental to behavioural entrainment in extreme white-light photocycles, as reported in 3.3.1. Histamine is the neurotransmitter used by *Drosophila* to propagate visual photic stimuli to other regions of the brain, via two widely expressed histamine-gated chloride channels; ORT and HISCL1 (see 3.1). In white-light photocycles, histamine biosynthesis mutants (*Hdc^{JK910}*) and HISCL1 receptor mutants (*st¹ HisCl^{T2}*) did show minor entrainment deficits to 10 and 5c/wk LD (**S.Figure 9**), however this reduced entrainment was only significant in *Hdc^{JK910}* mutants in 10c/wk where ~30% arrhythmicity was observed (**S.Figure 9**). Significant reductions in RRP were seen for both *Hdc^{JK910}* and *HisCl^{T2}* in 5 and 10c/wk, as well as 7c/wk for *Hdc^{JK910}* (**S.Figure 9**), indicating that, although entrained in most instances, rhythms were weaker. No entrainment defect was seen in any condition with ORT receptor mutants (*ort¹*).

In white-Light:Dark (WLD), both CRY and the visual system contributed to light entrainment (3.3.1). The visual system is comprised of rhodopsins (Rh1-6 and Rh7) which perceive visible-light wavelengths as well as UV (Hanai and Ishida, 2009; Ni *et al.*, 2017), whereas CRY is solely activated by blue-light wavelengths (VanVickle-Chavez and Van Gelder, 2007). Therefore red-Light:Dark (RLD) photocycles were used to further assess the contribution of the visual system, and histamine signalling, on light-dependent entrainment in the absence of CRY; red-light does not activate CRY but is detected by Rh1 and Rh6 (Hanai, Hamasaka and Ishida, 2008).

Wild-type flies showed entrained bimodal rhythmic activity in 7c/wk RLD however evening activity were advanced compared to 7c/wk WLD (**Figure 3.9, A** and **Figure 3.2, A**). This advance was reminiscent of that seen with *Pdf⁰¹* flies in WLD (**S.Figure 13**). Bimodality in behavioural rhythms was still seen in *cry⁰¹* flies in 7c/wk RLD, however the siesta period was less clear. In 5c/wk RLD wild-type and *cry⁰¹* flies showed very similar behaviour patterns, but rhythmicity in 10c/wk was more apparent for *cry⁰¹* compared to wild-type (**Figure 3.9, A and B**). A priori, plasticity in RLD photocycle entrainment in wild-type and *cry⁰¹* flies would be expected to be similar and phenocopy the phenotype of *cry⁰¹* flies exposed to WLD photocycles. However, differences in relative light intensities used for the WLD and RLD treatments (3.2.1.1) and divergence in the *tim* alleles in the two lines used (**S.Table 1**) might account for the divergence of the observed results from these predictions.

Visual system mutants; *eya²*, *GMR-hid* and *norPA⁷* (3.3.1); as well as flies lacking histamine (*Hdc^{JK910}*), showed robust behavioural rhythms with ~24 h periodicity in 7c/wk RLD (**Figure 3.9, A**). Upon closer inspection, these rhythms were different from the entrained rhythms of wild-type

and *cry*⁰¹; bimodality in behavioural rhythms was lost in *eya*² and *GMR-hid* and clearly reduced in *norpA*⁷ and *Hdc*^{JK910}. Furthermore, none of these visual system mutants showed the same immediate entrainment of activity offset to the lights-off transition that was seen for *cry*⁰¹ and control flies (**Figure 3.9, A**). When exposed to long (5c/wk) and short (10c/wk) RLD cycles, the same four mutants exhibited similar ~24 h periodicities as they did in 7c/w RLD, although *eya*² and *GMR-hid* showed slightly accelerated rhythms, indicated by the daily advance in behaviour (**Figure 3.9, A**). These observations suggested free-running behaviour, as normally observed under constant darkness (see Chapter 2), suggesting these flies did not entrain at all to the long and short RLD photocycles.

Mutations affecting either the ORT or HISCL1 histamine receptors had differential impacts on RLD entrainment. Both mutants showed bimodal rhythmic behaviour in-line with a 7c/wk RLD cycle, however it did take 3-4 days for *ort*¹ flies to align properly (**Figure 3.9, A**). In 5 and 10c/wk RLD cycles, *ort*¹ flies could effectively advance or delay behaviour accordingly, like *cry*⁰¹ and wild-type in 5 and *cry*⁰¹ in 10c/wk RLD. A breakdown in rhythmicity seemed apparent in *HisCl*^{T2} mutants in both extreme RLD conditions but unlike the phenotypes observed for visual and *Hdc*^{JK910}, there was a shift towards arrhythmia rather than non-entrained circadian rhythms (**Figure 3.9, A**).

All but *GMR-hid* showed perfect entrainment to 7c/wk when assessed quantitatively (**Figure 3.9, B**). Despite this, significant variation was seen when individual period lengths were compared. A wide range of period lengths were seen in *GMR-hid* and *norpA*⁷ mutants and average period lengths of slightly longer than 24 h were reported for these mutants as well as the *Hdc*^{JK910} and *ort*¹, presumably reflecting the relatively slow entrainment that involved phase delays over a number of days in these mutants (**Figure 3.9, C**). *eya*² flies showed a slightly shorter than 24 h period length in 7c/wk RLD not significantly different to wild-type. However, it is possible that *eya*² flies were essentially free-running through the 7c/wk RLD conditions as they showed an abnormal phase relationship with the environmental cycle throughout the experiment. The ability of these mutants to synchronise to 7c/wk RLD was investigated further by assaying re-entrainment of the offset of the main daily activity phase from a 7c/wk WLD to a 6 h delayed 7c/wk RLD (3.2.1.1). Wild-type, *ort*¹ and *HisCl*^{T2} flies all entrained to the delayed RLD cycle, however it took 5 days for *ort*¹, and *HisCl*^{T2} appeared to have a later offset of activity (**Figure 3.9, D**). In contrast, *eya*² did not display a clear response to the change in condition, whereas *GMR-hid* offset points were highly variable indicating that *GMR-hid* flies struggled to entrain correctly to even 7c/wk WLD, compared to wild-type (**Figure 3.9, D**). As *Hdc*^{JK910} and *norpA*⁷ flies showed phase delays throughout the 9 d-interval (**Figure 3.9, D**), the assay was left to run for longer for these genotypes to establish whether they would lock their activity to the offset to the RL offset.

Chapter 3:

However, their activity continued to delay (**Figure 3.9, E**), indicating the visual system and histamine signalling are required for entrainment to a 7c/wk RLD cycle.

In long 5c/wk and short 10c/wk RLD cycles, the majority of wild-type and *cry*⁰¹ flies exhibited the correct entrained period length, however ~40% of wild-type flies were arrhythmic in 10c/wk RLD. Of those that were rhythmic, most showed the correct entrained periodicity (**Figure 3.9, B, C**). The clear deficits in entrainment seen in the actograms for *eya*², *GMR-hid*, *norpA*⁷ and *Hdc*^{JK910} mutants were supported quantitatively as the majority of flies showed a rhythm outside if the entrained 5 or 10c/wk range (**Figure 3.9, B**). These 'other' period lengths were in the free-running circadian range (**Figure 3.9, C**), confirming that these mutants were unable to entrain to 5 and 10c/wk RLD cycles. All *ort*¹ flies entrained to 10c/wk and most showed the correct entrained period length in 5c/wk with a small proportion at ~24 h periodicity (**Figure 3.9, B, C**). Larger proportions of *HisCl*^{T2} mutants were arrhythmic in both 5c/wk (~75%) and 10c/wk (~45%) RLD photocycles, as was suggested by their actograms (**Figure 3.9, B**). Of the flies that were rhythmic, period lengths were spread between entrained and circadian periodicities in both conditions (**Figure 3.9, C**). This decrease in ~24 h period lengths and an increase in arrhythmicity could be attributable to conflicting rhythms within the neural clock circuits of these flies. Further analysis is presented in **S.Table 16**, along with female data which matched what the results presented here for males, with the caveat that wild-type females entrained better to 10c/wk RLD.

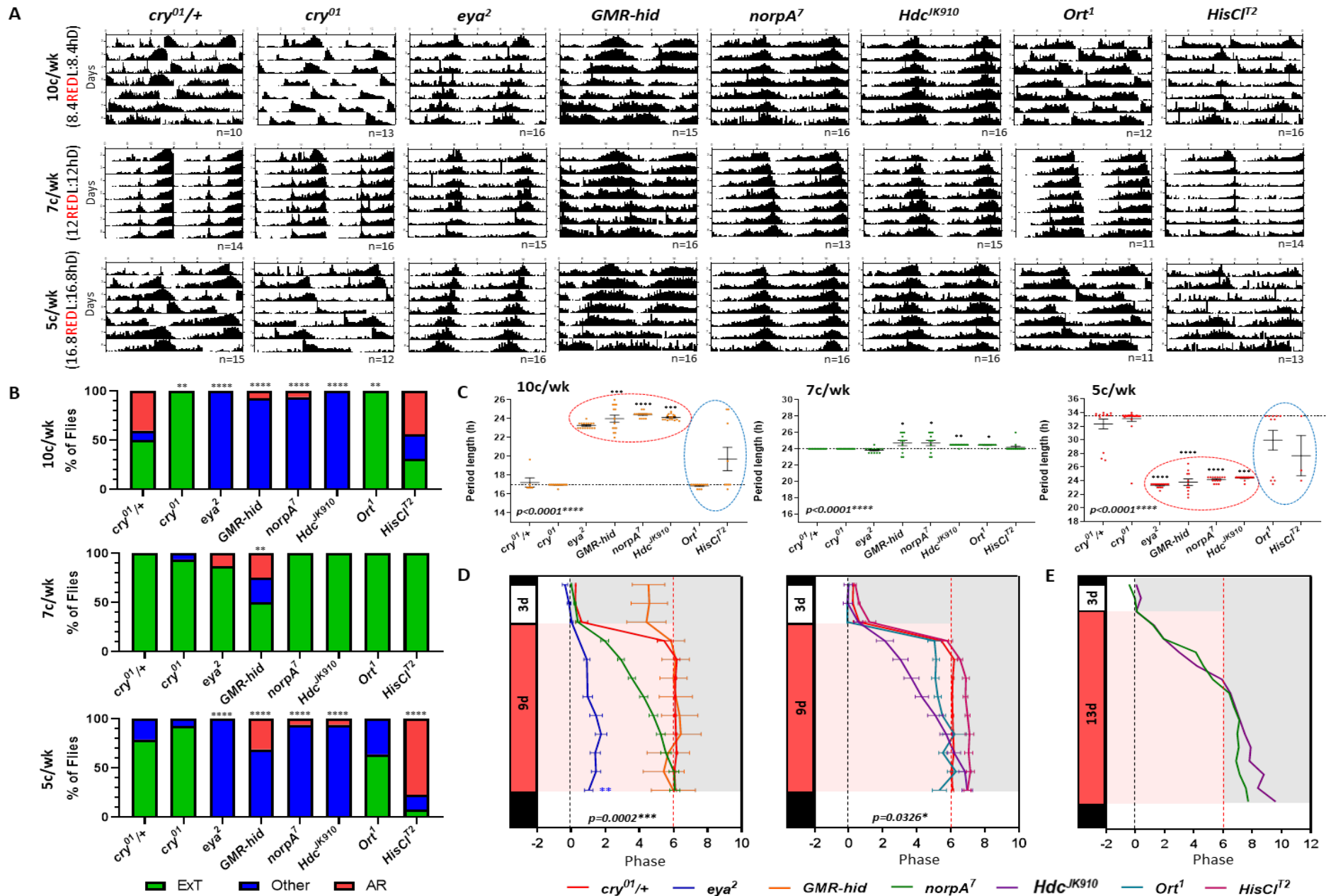


Figure 3.9 The visual system and histamine signalling are required to allow behavioural entrainment to extreme RED light photocycles.

A) Average locomotor activity presented in double plotted actograms (30 min bins) showing 7 days of activity, plotted over a 24 h scale, for adult male flies of genotype; $w^{1118};cry^{01}/+$, $w^{1118};cry^{01}$, eya^2 , *GMR-hid*, *norpA*⁷, *Hdc*^{Jk910}, *Ort*¹ and *st*¹*HisCl*^{T2} (left to right); in 10 (top), 7 (middle) and 5c/wk (bottom) equinox RED LD cycles. 'n' denotes number of flies. **B)** Composite bar charts showing percentage of flies showing entrained (green), other (blue) or arrhythmic (red) locomotor behaviour (see methods) over 10 days in 10 (top), 7 (middle) and 5c/wk (bottom) RED LD. Fisher's exact test to compare distribution of entrained, other and arrhythmic individuals for each genotype vs. $cry^{01}/+$. For 10c/wk, primary and secondary periodicities were compared for each individual and the dominant period length was used to categorise flies using only the 'Ext' range. **C)** Individual male period lengths for in 10, 7, and 5c/wk (left to right) RED LD. Error bars show mean period length \pm SEM. Dashed lines represent entrained period length for each condition. Graphs plotted over the range of period lengths used for individual fly analysis in each LD cycle. Dashed red ovals indicate genotypes with a period length \sim 24 h whilst in a 10 or 5c/wk RED LD cycle. Dashed blue ovals indicate genotypes with a mix of entrained and \sim 24 h period lengths. *p* values (bottom left) indicate results of Kruskal-Wallis test across all genotypes within each condition. Individual genotypes compared to $cry^{01}/+$ with Mann-Whitney test (10c/wk; *eya*²-*p*<0.0001, *norpA*⁷-*p*=0.0009 and *Hdc*^{Jk910}-*p*=0.0002. 7c/wk; *GMR-hid*-*p*=0.0437, *norpA*⁷-*p*=0.0437, *Hdc*^{Jk910}-*p*=0.0029 and *Ort*¹-*p*=0.0105. 5c/wk; *eya*²-*p*<0.0001, *GMR-hid*-*p*<0.0001, *norpA*⁷-*p*<0.0001 and *Hdc*^{Jk910}-*p*=0.0004). **D, E)** Plots of behavioural offsets during 3 days in a 12hL:12hD white LD cycle and the following 9 or 13 days (**D** and **E** respectively) in a 6 h delayed 12hL:12hD RED LD cycle (condition and duration indicated in figure). Relative phase shift for consecutive days were calculated W.R.T lights off during white LD phase for each genotype. Dashed lines indicate expected entrained offset point for white light phase (black) and red light phase (red) with LD indicated by shading. **D)** Left - $cry^{01}/+$ (red, n=12), *eya*² (blue, n=10), *GMR-hid* (orange, n=12) and *norpA*⁷ (green, n=12). Right - $cry^{01}/+$ (red, n=12), *Hdc*^{Jk910} (purple, n=12), *Ort*¹ (teal, n=12) and *HisCl*^{T2} (purple, n=12). Error bars show mean \pm SEM. *p* values (bottom) indicate results of Kruskal-Wallis test across all genotypes. Individual genotypes compared to $cry^{01}/+$ with Mann-Whitney test (*eya*²; *p*=0.0012). **E)** Plot of average offset over consecutive days for *norpA*⁷ (green, n=5) and *Hdc*^{Jk910} (purple, n=9). RLD experiments with visual and histamine signalling mutants were conducted and analysed by Miss Nanthilde Malandain. Re-entrainment data was collected and analysed by Miss Nanthilde Malandain, Miss Chloe Ellison and Miss Racheal Anderson.

3.4 Discussion

Light has the capacity to induce behavioural entrainment to extreme photocycles by either phase advancing or delaying the molecular oscillator, in long or short cycles respectively (Chapter 2). *Drosophila* central clocks cells perceive light through both the CRY/JET pathway and canonical visual photoreception (Rieger, Stanewsky and Helfrich-Förster, 2003), with CRY responsible for rapid light entrainment via clock neurons (Emery *et al.*, 1998; Stanewsky *et al.*, 1998) and the visual system mediating slower non-cell-autonomous photoentrainment, as in mammals (via the retinohypothalamic tract to the suprachiasmatic nuclei (SCN) of the hypothalamus) (Hattar *et al.*, 2002). Cell-autonomous light entrainment via CRY-dependent TIM degradation is well-characterised (see 3.1), with mutations to *cry* (Emery *et al.*, 1998; Stanewsky *et al.*, 1998; Dolezelova, Dolezel and Hall, 2007) and *jet* (Koh, Zheng and Sehgal, 2006; Peschel *et al.*, 2009; Lamba *et al.*, 2014) severely effecting circadian photoresponses. Similarly, mutations impacting the visual system reduce behavioural synchronisation to LD cycles (Helfrich-Förster *et al.*, 2001; Rieger, Stanewsky and Helfrich-Förster, 2003). Furthermore, flies lacking either CRY or a visual system can entrain to 24 h LD cycles, but mutations in both light input pathways render flies resistant to light entrainment (Helfrich-Förster *et al.*, 2001). Previous works have identified the contributions of CRY/JET and the visual system to re-entrainment and responses to brief light pulses; here we investigate what is required to allow behavioural entrainment to abnormally long and short equinox photocycles.

When the CRY/JET pathway is mutated flies still have a functional visual system, and *vice versa*. Either light input pathway alone is sufficient to allow behavioural entrainment to a 7c/wk LD condition, supporting previous observations (Helfrich-Förster *et al.*, 2001). Of course, the 7c/wk 24 h photocycle, matches the intrinsic circadian periodicity and, therefore, does not pose a great entrainment challenge to the oscillator. This is not the case for long 5c/wk and short 10c/wk photocycles, however, and neither the CRY/JET pathway nor the visual system alone is sufficient for efficient behavioural entrainment. This suggests that the apparent redundancy between the two light input pathways is lost under conditions requiring strong re-setting responses (Wheeler *et al.*, 1993; Helfrich-Förster *et al.*, 2001), where both entrainment pathways act synergistically to shift the oscillator. A complementary rationale for the benefits of having two input systems is provided by recent observations of Kistenpfennig *et al.* (2017), who reported that in the context of long- day photocycles, CRY hinders and the visual system assists the correct alignment of the E-peak of activity to the LD cycle. This difference centres on oscillations in PDP1 (Yoshii *et al.*, 2015;

Chapter 3:

Kistenpfennig *et al.*, 2017), which in long-day conditions are damped by CRY and amplified by the visual system (Kistenpfennig *et al.*, 2017). PDP1 is a clock protein whose expression is governed by CLK/CYC (see 1.2.3.3) and therefore cycles in phase with PER and TIM (Shafer, Rosbash and Truman, 2002; Nitabach *et al.*, 2006); and is thought to either modulate *Clk* transcription or play a role downstream of the clockwork mechanism (Benito, Zheng and Hardin, 2007; Zheng *et al.*, 2009). We did not investigate the impact of loss-of-function mutations for the circadian PDP1- ϵ isoform on extreme photocycle entrainment. However, since the isoform is required for clock function (Zheng *et al.*, 2009), corresponding such mutations would be expected to phenocopy observations for other arrhythmic mutants that were found to exhibit photocycle-driven rhythms (S.Figure 7)

As shown in **Figure 3.3**, a sizable fraction of flies with mutations disabling the CRY/JET pathway exhibit circadian periodicities in both long 5c/wk and short 10c/wk photocycles. This suggests that when light input isn't sufficient to drive entrainment in these extreme conditions, intrinsic circadian rhythms can drive behavioural output. This mixture of circadian 'free-running' and photocycle-entrained components apparently reflects a separation of the behavioural outputs for visual system-mediated entrainment signals and autonomous circadian rhythms that would normally be modulated via the CRY/JET pathway. (Kistenpfennig *et al.*, 2017) report that the visual system confers greater flexibility in the phase of M- and E-oscillators, which may explain why split rhythmicity is seen in CRY/JET mutants but arrhythmicity is more common in flies lacking visual light input. Although entrainment is clearly comprised, in most cases a proportion of both CRY/JET and visual mutants show the correct entrained period length.

Recent research into the mechanism of light input to the clock has demonstrated that visual light input appears to be received relatively independently by each clock cell subset with the aMe neuropil a key region in the fly brain for visual light signalling to the clockwork (Li *et al.*, 2018). This signal is relayed to the clock via histamine signalling which utilises Rh6-expressing R8 cells as either cholinergic interneurons, passing on light input from other outer photoreceptors cells or direct photoreceptors (Alejevski *et al.*, 2019). Mutations affecting this histamine signalling pathway have been shown to impact of *Drosophila* sleep/wake activity (Rieger, Stanewsky and Helfrich-Förster, 2003; Oh *et al.*, 2013). In our assay, reduced plasticity in entrainment to WLD cycles was seen when histamine biosynthesis was disrupted and a non-significant trend in this direction was also observed for mutation of the HISCL1 receptor, however these phenotypes were less severe than those for the visual system mutations used in **Figure 3.2**, suggesting non-histaminergic contributions to photocycle entrainment from the visual system. Notably, the pathway of light input is dependent on light intensity with high-intensity light signalled via the

inner-photoreceptors of the HB-eyelet; middle-intensity via the outer-photoreceptors of the compound eye; and low-intensity via CRY (Schlichting *et al.*, 2016). In our assay, as photoperiods are so short/long maybe all of these pathways have to contribute to facilitate light-induced plasticity.

Light is the dominant synchronising factor for circadian clocks, however in natural conditions multiple environmental cues must be integrated to maximise behavioural plasticity (Majercak *et al.*, 1999). Temperature also provides robust time-of-day information to the clockwork with temperature entrainment governed by cold-induced *per* transcription and *no circadian temperature entrainment (nocte)* (Wheeler *et al.*, 1993; Glaser and Stanewsky, 2007; Currie, Goda and Wijnen, 2009; Goda, Sharp and Wijnen, 2014; Chen *et al.*, 2018). In the presence of a temperature cycle, NOCTE targets temperature input to the DN1s to synchronise behavioural and molecular rhythms (Chen *et al.*, 2018). Mutations to *nocte* impair light entrainment in the presence of a temperature cycle alluding to the integration of environmental stimuli (Chen *et al.*, 2018). Similarly, CRY has a role in the integration of light and temperature as it is shown to damp temperature input to the circadian clock (Busza, Murad and Emery, 2007; Yoshii, Hermann and Helfrich-Förster, 2010; Gentile *et al.*, 2013). When exposed to combined light and temperature cycle, *cry* mutants showed a preference to the temperature cycle compared to the light (**S.Figure 10**), indicating a shift in dominance from light to temperature input in the absence of CRY. Interestingly, this mutant phenotype was partially alleviated when flies were assayed in groups (**S.Figure 11**); indicating that social interaction can impact on *cry*-independent circadian entrainment.

As discussed in Chapter 2, the clock circuitry can be roughly divided into two groups which are paramount to *Drosophila's* archetypal activity pattern; PDF expressing M-cells (particularly the s-LN_vs) which drive rhythmicity in the dark phase; and the non PDF-expressing E-cells (LN_ds and 5th s-LN_v) which become dominant in the light phase (Hardin, 2011; Chatterjee *et al.*, 2018).

Differential impacts of visual system input on the M- and E-oscillators have been documented, with PDF signalling of visual light stimuli capable of phase shifting E-cell activity, highlighting the E-cells as a site for CRY-independent light input via PDF (Yoshii *et al.*, 2015).

CRY is expressed in all of the M-cells, the 5th s-LN_v, 3 LN_ds and a subset of DN1s (Klarsfeld *et al.*, 2004; Yoshii *et al.*, 2008; Benito *et al.*, 2008); and it has been shown that CRY expression specifically in the E-cells (LN_ds and 5th s-LN_v) allows light entrainment to phase shifted LD cycles (Yoshii *et al.*, 2015). JET expression in M- and E-cells independently showed cell-autonomous TIM degradation in response to brief light pulses, however circadian behavioural photoresponses were

Chapter 3:

not seen unless JET was present in both the M- and E-cells (Lamba *et al.*, 2014). In order to fully understand the function of CRY and JET in light entrainment to long and short photocycles, we genetically manipulated CRY and JET expression within clock neuronal subsets to see in what clock cells CRY/JET are essential or redundant under extreme LD cycles.

Pan-circadian knockdown of *cry* and *jet* greatly reduced entrainment to long and short photocycles, however more restrictive knockdowns yielded little to no behavioural phenotypes (**Figure 3.4**). Previous results have found significant rescue of *cry*⁰¹ entrainment defects using *Pdf-Gal4* in relation to light-pulse mediated resetting as well as drivers encompassing the E-cells in relation to photocycle phase delays (Emery *et al.*, 2000b; Yoshii *et al.*, 2015). In our assay, however, knockdown in the M cells with *Pdf-Gal4*, E cells with *GMR78G02-Gal4* and *ChAT-Gal4* or both with *cry-Gal4-13*, gave much weaker phenotypes than *TUG*-driven knockdown with only a partial phenocopy of the entrainment defect in 10c/wk conditions. The lack of expected phenotypes seen may be explained by incomplete knockdown with these drivers in some of these cells.

To refine this mapping using an alternative strategy, *TUG* was combined with *Gal80* constructs to selectively block knockdown in *cry-Gal80* expressing cells, which include M- and E-cells, or in *Pdf-Gal80* expressing M-cells (**Figure 3.6** and **Figure 3.7**). The results of this analysis indicate CRY/JET expression in both the M and E-cells contributes to plasticity in photocycle entrainment. Moreover, entrainment in 10c/wk photocycles was found to be the more stringent assay for CRY/JET function. The relative importance of molecular rhythms in the M-cells is underscored by the results presented in Chapter 2, which indicate a strong association with behavioural rhythms, particularly the s-LN_vs. The molecular oscillators of CRY-expressing DN1 cells, which also exhibited strong associations with behaviour, may complement the s-LN_vs in the 10c/wk photocycle condition where CRY in only the M-cells was insufficient for full rescue of entrainment.

Rescuing CRY expression in a *cry*-null background yielded comparable results to the above mapping by *dsRNA* knockdown, where CRY expression in the M-cells alone facilitates behavioural entrainment to long photocycles but not short (**Figure 3.8**). *ChAT-Gal4* drives expression in cholinergic cells, which is known to include the 2 NPF positive LN_vs and the 5th s-LN_v within the clock circuitry (Johard *et al.*, 2009). As discussed, CRY expression in the E-cells facilitates entrainment to shifted LD cycles (Yoshii *et al.*, 2015). However the degree of rescue in both long and short photocycles, above that achieved by *TUG*, suggests that there may be some additional targets of *ChAT-Gal4* within the clock circuitry, possibly in the dorsal neurons. As discussed in Chapter 2, the DN1s maintain robust rhythms in short photocycles and can signal back to the s-

LN_vs (Zhang *et al.*, 2010). Moreover, they provide key links to rhythmic output (Cavanaugh *et al.*, 2014; King and Sehgal, 2018). It has also been shown that ectopic CRY expression can allow light-induced degradation of TIM (Rush *et al.*, 2006), so driving expression in CRY-negative clock cells as might happen with the *TUG* driver could conceivably contribute to behavioural rescue.

The differential photocycle-dependent rescue of entrainment observed for different spatiotemporal patterns of CRY/JET activity may be consistent with the notion that different subsets of clock cells have selective role in phase advancing or delaying. It has been suggested that the DN1s are important in phase delays and the I-LN_vs function in phase advances (Tang *et al.*, 2010; Shang, Griffith and Rosbash, 2008). This may be the case. However, in our assay both the M- and E-cells promoted behavioural entrainment to short (10c/wk) as well as long (5c/wk) LD cycles. Alternatively, the divergent 5 and 10c/wk entrainment phenotypes of different spatially targeted *cry* and *jet* rescue and knockdown manipulations may simply indicate that the 10c/wk photocycle length approaches the lower limit of entrainment while the 5c/wk photocycle can still be comfortably lengthened (past 4c/wk) before behavioural entrainment defects are encountered (as discussed in Chapter 2). The cell-autonomous CRY/JET pathway is thought to be paramount in governing phase advances and delays (Lamba, Foley and Emery, 2018). As discussed above, our data supports a role for CRY and JET in this context as entrainment is reduced greatly in both 5 and 10c/wk photocycles for *cry*⁰¹ and *jet*^{set} mutants. However, a role for CRY-independent light input and non-autonomous entrainment pathways has been identified as well (Yoshii *et al.*, 2015; Guo *et al.*, 2014). Interestingly, cell-autonomous light input through CRY/JET in the M-cells can entrain E-cells lacking *jet* through a non-autonomous mechanism (Lamba *et al.*, 2014), suggesting communication across the circuitry is crucial for effective entrainment. From the data presented here, as well as what is published, it is clear that there is a need for a cohesive circuitry, likely coordinated via PDF signalling by the M-cells (Cusumano *et al.*, 2009; Lamba, Foley and Emery, 2018), to allow behavioural entrainment in the face of such extreme photocycles.

Gender-specific differences were observed in both knockdown and rescue experiments with female entrainment defects exhibiting more arrhythmia and less free-running circadian rhythms than their male counterparts, while no significant rescue of *cry*⁰¹ entrainment defect was seen in females in 10c/wk photocycles. Sexual dimorphisms in circadian behaviour; affecting both clock circuitry and output, are common in many species, including *Drosophila* (Helfrich-Förster, 2000; Hendricks *et al.*, 2003; Zimmerman *et al.*, 2012; Krizo and Mintz, 2015). Stereotyped fly behaviour in a standard 24 h LD cycles differs between genders with males exhibiting a more pronounced siesta period i.e. an increase in daytime sleep (Helfrich-Förster, 2000; Isaac *et al.*, 2010;

Chapter 3:

Zimmerman *et al.*, 2012; Khericha, Kolenchery and Tauber, 2016). As the daily profiles for PER protein are associated with this phenomenon (Majercak *et al.*, 1999), it is possible that molecular mechanisms underlying this gender dimorphism may impact the limits of entrainment between the sexes. Additionally the DN1s, more specifically the DN1_ps (Lamaze *et al.*, 2018; Lamaze *et al.*, 2017), are important in sleep/wake phenotypes and contribute to daytime sleep (Guo *et al.*, 2016). DN1s neurons show gender-specific differences, with male DN1s exhibiting greater excitability and an ability to respond to sexual cues (Guo *et al.*, 2016; Hanafusa *et al.*, 2013). We report in Chapter 2 that the DN1s maintain molecular rhythmicity in 10c/wk which may enable rhythmic behavioural output at this extreme LD cycle; and as such heightened excitability in DN1s may explain better entrainment to short LD cycles observed in males.

CRY is only sensitive to wavelengths close to the blue portion of the visible spectrum. However, red-light wavelengths that go undetected by CRY are sensed via Rh1 and Rh6 found in the *Drosophila* visual system (Hanai, Hamasaka and Ishida, 2008); with Rh1 present in all outer R1-6 photoreceptor cells and Rh6 in a subset of inner R8 photoreceptor cells (see 3.1)(Salcedo *et al.*, 2000; Behnia and Desplan, 2015). The extra-retinal H-B eyelet contains 4 such Rh6-expressing R8 cells which project directly into the aMe, in close proximity to the PDF-expressing LN_vs (Hofbauer and Buchner, 1989; Renn *et al.*, 1999; Yasuyama and Meinertzhagen, 1999; Malpel, Klarsfeld and Rouyer, 2002; Helfrich-Förster *et al.*, 2007), although recent research has shown that visual input from the eyelet alone is not sufficient to facilitate entrainment (Alejevski *et al.*, 2019). RLD cycles are capable of indirectly entraining the neuronal clockwork, although it happens more slowly than comparable light regimes involving CRY-detectable wavelengths (Hanai, Hamasaka and Ishida, 2008). Genetic removal of the compound eye and disrupting visual phototransduction, as well as more specific Rh1/Rh6 double mutants all rendered flies blind to RLD cycles (Hanai, Hamasaka and Ishida, 2008); indicating the absolute requirement of the visual system in RLD entrainment.

It has been postulated that due to the extensive arborisation the LN_vs (particularly the I-LN_vs) into the optic lobe, that the PDF pacemaker cells are important in transmitting visual light information to the clockwork (Helfrich-Förster *et al.*, 2007). In particular, PDF signalling of visual input from the I-LN_vs is required to set the phase of the CRY positive LN_ds and 5th s-LN_v (E-cells)(Cusumano *et al.*, 2009; Schlichting *et al.*, 2016). In RLD conditions, and therefore the absence of CRY, PDF signalling has been shown to interact with the visual-light input pathway to set the correct phase of E-cells; and without PDF signalling, the E-activity peak is absent (Cusumano *et al.*, 2009). In our hands, wild-type flies show an advanced evening activity in 7c/wk RLD which may be explained by the absence of CRY-mediated light input to the E-cells, which as discussed, is required for effective entrainment (Yoshii *et al.*, 2015). However, this advance mirrors the behaviour of *Pdf⁰¹* flies in

7c/wk WLD (Renn *et al.*, 1999), suggesting the alternative possibility that in our RLD assay, PDF signalling maybe attenuated or bypassed to some extent resulting in the advanced E-cell activity.

Unsurprisingly, mutants affecting the visual system severely reduced entrainment to short and long RLD photocycles, as well as re-entrainment to a 6 h delayed 7c/wk RLD cycle (**Figure 3.9**) (Hanai, Hamasaka and Ishida, 2008). As previously discussed (see 3.1), histamine is a key neurotransmitter in the *Drosophila* visual system (Burg *et al.*, 1993; Hong *et al.*, 2006; Pantazis *et al.*, 2008; Yusein *et al.*, 2008; Oh *et al.*, 2013), and an absence of histamine (*Hdc*^{K910}) phenocopied the more severe visual mutants in extreme RLD photocycles. RLD behaviour of these mutants clearly differs from that in WLD, with free-running circadian behaviour more dominant in the former and loss of rhythmicity more obvious in the latter. The RLD phenotype of flies lacking compound eyes, compound eye visual transduction or histamine signalling suggested that they were effectively blind to RLD entrainment consistent with the notion that RLD input comes from RH1 and RH6 in the compound eyes and is relayed via histaminergic connections to the neural clock circuit.

Recent research has uncovered a pathway for histamine signalling input to the clockwork where both *Drosophila* histamine receptors play a vital role (Alejevski *et al.*, 2019). ORT function resides in the interneurons of the optic lobe and HISCL1 is expressed on the Rh6-expressing R8 photoreceptors which can act as both photoreceptors and interneurons in a histamine signalling pathway (Alejevski *et al.*, 2019). Although, the pathway linking depolarisation of Rh6-expressing cells following histamine signalling and the synchronisation of clock cells is still unknown. Mutating the *HisCl1* receptor resulted in a loss of rhythmicity in both short (10c/wk) and long (5c/wk) RLD photocycles, indicative of inadequate entrainment via the remaining histamine receptor, ORT. In contrast, *ort*¹ mutants showed no reduction in entrainment. These results suggest that both histamine receptors help relay RLD entrainment from the visual system with a somewhat enhanced role for HISCL1. The former, but not the latter matches the observations of (Alejevski *et al.*, 2019) who found no phenotypes for single histamine receptor mutants. In our extreme RLD photocycles, histamine signalling via ORT alone may be insufficient to allow entrainment, possibly uncovering a stronger requirement for signalling via the Rh6-expressing R8 inner photoreceptors than signalling via the Rh1-expressing outer photoreceptors (Alejevski *et al.*, 2019). Analyses with *Rh1* (*ninaE*) versus *Rh6* mutants may address this hypothesis.

Histaminergic termini from the eyelet exist in close proximity to the LN_vs dendrites allowing the possibility for direct histaminergic signalling to the clockwork (Hamasaka and Nassel, 2006). However, there is no evidence of the importance of such relatively direct histaminergic signals

Chapter 3:

onto the clock neurons in our results. Instead *HisCl1* and *ort* have been found to contribute to entrainment via the Rh6-expressing R8 cells and the optic lobe interneurons, respectively (Alejevski *et al.*, 2019).

Constant red-light (RR) generates a 'free-running' condition where wild-type flies maintain rhythmic behaviour (Cusumano *et al.*, 2009), unlike the arrhythmia seen in constant white-light (LL) as red-light does not stimulate CRY (Emery *et al.*, 2000a; Dolezelova, Dolezel and Hall, 2007). Unpublished work from the lab, as well as published data (Cusumano *et al.*, 2009), indicate a shift in pacemaker function away from the PDF expressing LN_vs in DD (**S.Figure 14**) and suggest the RR oscillator is centred in the E-cells. Preliminary data suggests histamine signalling via the HISCL1 receptor is required for RR rhythmicity in the absence of PDF signalling (**S.Figure 15**), however further experiments are needed to ascertain the exact circuitry of the RR oscillator.

From the data presented, we conclude that both the CRY/JET pathway and the visual system are required to allow light-dependent behavioural entrainment to extreme photocycles. CRY and JET must be present in both the M- and E-cells in order to align behaviour to all LD cycles, however in some instances expression in one of these subsets is sufficient to entrain the clock in extreme WLD photocycles. Finally, the visual system facilitates entrainment to extreme RLD photocycles via histamine signalling, further indicating the importance and versatility of rhodopsin-mediated photoreception to entrainment of the *Drosophila* circadian clockwork. As stated previously, entrainment to environmental cycles contributes to overall fitness and survival. In the face of extreme photocycles, the dual light input pathways of *Drosophila* work synergistically to facilitate entrainment thus conferring crucial physiological benefit.

Chapter 4: Light-dependent plasticity of *Drosophila* peripheral clocks

4.1 Introduction

In the *Drosophila* brain, endogenous circadian clocks reside in a network of ~150 neurons that integrate environmental inputs and regulate rhythmic outputs e.g. behaviour (as discussed in Chapters 2 and 3). Peripheral clocks reside and control physiology in many tissues and organs outside of the *Drosophila* brain including the antenna, proboscis, legs and compound eyes as well as internal organs involved in reproduction and digestion (Ito and Tomioka, 2016). *Drosophila* peripheral clocks are heterogeneous in nature with a diverse array of functions and can either function independently of, be slave to, or be driven by central clocks (See 1.2.8)(Ito and Tomioka, 2016). The molecular clockwork that underpins daily time-keeping is well documented, and as discussed in previous Chapters, is based on a delayed negative feedback loop of transcription and translation, a mechanism shared by both central and peripheral oscillators (Plautz *et al.*, 1997a; Hardin *et al.*, 2003).

Cloning of the firefly *luciferase* (*luc*) gene downstream of the promoter sequence of clock genes has allowed for rhythms in bioluminescence to be assayed in dissected peripheral fly tissues (such as wings and antennae), as well as in the whole flies (Brandes *et al.*, 1996). Utilisation of a transgenic *per-luc* reporter construct, whereby *luc* expression is under to control of the *per* promoter, demonstrated rhythmic bioluminescence in dissected wings, antenna and proboscis, showing that *Drosophila* peripheral rhythms are self-sustained and do not require the central clocks of the brain (Plautz *et al.*, 1997a; Brandes *et al.*, 1996). Further experiments with *per-luc* reporter constructs, demonstrated robust light entrainment of independent peripheral tissues in line with a 12hL:12hD LD cycle (Brandes *et al.*, 1996; Plautz *et al.*, 1997a; Stanewsky *et al.*, 1997; Stanewsky *et al.*, 1998; Levine *et al.*, 2002; Veleri *et al.*, 2003; Hardin, 2005; Roberts *et al.*, 2015), indicating a high degree of peripheral autonomy.

CRY is expressed in peripheral tissues of the fly as well as the brain (Agrawal *et al.*, 2017), but unlike central clocks, there is no evidence to suggest that peripheral oscillators receive light input via visual phototransduction mechanisms. Experiments conducted by Stanewsky *et al.* (1998) initially identified the *cry* gene, as a severe hypomorphic mutant (*cry^b*) rendered peripheral clocks arrhythmic when assayed via *in vivo* luminescence rhythms (1.2.5.1). How CRY partakes in peripheral entrainment is inconclusive and appears tissue dependent with two possible roles

Chapter 4:

suggested; either CRY acts as a photoreceptor and a core clock component (Stanewsky *et al.*, 1998; Ivanchenko, Stanewsky and Giebultowicz, 2001; Collins *et al.*, 2006), or CRY is only a photoreceptor (Ito *et al.*, 2008; Agrawal *et al.*, 2017). Therefore, light-activated CRY could partake solely in targeted light-dependent TIM degradation, as in the central fly clocks, or possibly act as a transcriptional repressor as well, binding PER and inhibiting CLK/CYC (1.2.8.1). Regardless of its role, CRY is paramount to *Drosophila* peripheral clock function.

Communication between the central and peripheral clocks isn't common in *Drosophila*; however some instances have been reported (Ito and Tomioka, 2016). The oenocytes, which regulate pheromone production, receive phase information from the brain (Krupp *et al.*, 2013); and functional clocks in both the LN_vs and the prothoracic gland are required for rhythmic eclosion (Myers, Yu and Sehgal, 2003; Morioka, Matsumoto and Ikeda, 2012); both of which are thought to be mediated by PDF signalling, or other neuronal or humeral signals from the central clock (Morioka, Matsumoto and Ikeda, 2012). As such connections exist, it is possible that visual light input may be signalled to the periphery from the brain, as is the case in mammals.

In Chapter 2, we report how extremely plastic the molecular oscillators that reside in the wild-type *Drosophila* brain are in response to long and short equinox Light:Dark cycles, generating entrained rhythmic behaviour to photocycles ranging from 16.8 – 42 h. Furthermore, we show that CRY/ JET and the visual system are pivotal to light entrainment of central clocks (Chapter 3). We have also demonstrated that entrainment to extreme photocycles can have a detrimental impact on physiology with the life-span of female flies severely reduced in both long and short photocycles (Chapter 2), likely a result of desynchrony between endogenous circadian oscillators and the external photoperiod. Circadian dysfunction impacts greatly on human physiology and well-being (Hastings, Reddy and Maywood, 2003), with conditions such as jet-lag arising from desynchrony between internal clocks and the external environment as well as between different endogenous internal clocks i.e. those of peripheral tissues and the brain (Roenneberg and Mellow, 2016). In this chapter we therefore look to see if peripheral clocks are equally as plastic as those residing in the *Drosophila* brain and see how the underlying circadian circuitry adapts to facilitate such plasticity; as well as investigate the light input pathways required to allow peripheral clock entrainment to such extreme photocycles.

4.1.1 Aims

- Investigate the inherent plasticity of peripheral circadian clock mechanisms by defining the limits of wild-type *Drosophila* peripheral entrainment to equinox Light:Dark cycles.
- Determine the light input pathways in peripheral entrainment to equinox photocycles.
- Investigate how the peripheral molecular oscillator adapts at the extremes of light-induced entrainment.

4.2 Methods

4.2.1 Analysis of peripheral clock rhythms *in vivo*

4.2.1.1 TopCount *in vivo* Luciferase Assay

Molecular oscillations of *Drosophila* peripheral clocks in the whole organism were assayed with an *in vivo* luciferase assay (Stanewsky *et al.*, 1997). A sugar-agar diet containing D-luciferin (100 mM; BioVision 7903-1, > 98% purity), the substrate for luciferase, was prepared (**S. Table B. 6**) and 95 μ l pipetted into every other well of a white 96-well PCR plate (OptiPlate; PerkinElmer). Adult transgenic flies, containing the gene encoding firefly luciferase fused to circadian promoters/circadian genes (Brandes *et al.*, 1996; Stanewsky *et al.*, 1997; Plautz *et al.*, 1997b), were anaesthetised with CO₂ and placed into diet-containing wells using forceps. Individual domed PCR caps were placed over each fly to secure them within the well, thus decreasing noise in bioluminescence signal (Stanewsky *et al.*, 1997), and the plate is sealed with PCR film (air holes were pierced in both the caps and film to allow gas exchange).

Bioluminescence, resulting from luciferase activity, was detected via an automated TopCount NXT Microplate scintillation and luminescence counter (PerkinElmer, Waltham, MA). Flies were subjected to 10 days in 10, 9, 7, 5 or 4c/wk (10c/wk = 8.4hL:8.4hD; 9c/wk = 9.33hL:9.33hD; 7c/wk = 12hL:12hD; 5c/wk = 16.8hL:16.8hD or 4c/wk = 21hL:21hD) equinox LD cycles at 17°C and ~70% relative humidity. Illumination was provided by florescent white light lamps with an intensity of ~2,150 μ W/cm² (white-light LEDs are ~20 μ W/cm²). Fluorescent lamps did not significantly increase the temperature of the assay room. At 17°C flies exhibit increased longevity, which facilitated long experimental runs. Due to the temperature compensation property of the clock (Huang, Curtin and Rosbash, 1995), no significant impact of on period length was expected in comparison with prior research using higher temperatures.

4.2.1.2 Qualitative, Quantitative and Statistical Analysis

Luminescence data was analysed and interpreted using BRASS software (created by Dr Paul E. Brown, University of Edinburgh). Data from all surviving flies were grouped by genotype and condition then averaged to produce line graphs of average luciferase activity measured in counts per second (cps) over time. Average traces were scaled and plotted W.R.T LD cycle, to enable easy comparison across the different LD cycles assayed.

Individual fly analysis was conducted using fast fourier transform-nonlinear least squares (FFT-NLLS) (Plautz *et al.*, 1997b), an iterative multicomponent cosine analysis. FFT-NLLS identifies the

number of rhythmic flies and their respective period length, phase, amplitude and relative amplitude error (RAE). Analysis parameters were defined for each LD cycle tested such that the period length of the LD cycle (entrained - ExT) as well as circadian (~24 h) period lengths were detectable in each case (see standard parameters – **S.Table B.5**). RAE values were used to define strength of rhythmicity of individual flies: rhythmic (R) - RAE<0.7, weakly rhythmic (WR) – RAE>0.7, no data was returned for RAE>1 and these flies should be considered arrhythmic (AR).

Entrainment to an imposed LD cycle was defined as the alignment of behavioural rhythmicity to that of the external condition. Therefore, flies were designated as being entrained to the external LD cycle according to whether or not their period length fell within a defined entrained range (see standard parameters – **S.Table B.5**). Rhythmic flies with a period length outside this entrained range were categorised as exhibiting ‘other’ rhythmicity and flies with no detectable rhythm were deemed arrhythmic.

Composite bar charts were used to display the percentage of flies that were either rhythmic (green), weakly rhythmic (blue) or arrhythmic (red), as well as either entrained (green), displaying an ‘other’ (blue) rhythm or arrhythmic (red). The significance of the differential distribution of flies into these defined categories were analysed using the *Fisher’s exact test*, used in the analysis of contingency tables.

GraphPad Prism 7.05 was used to generate all graphs and conduct statistical analysis. Analysis of variance (ANOVA) between genotypes or conditions were made with the non-parametric *Kruskal-Wallis test* with pairwise comparisons made using post hoc tests i.e. *Dunn’s multiple comparison test* and *Mann-Whitney test* (test used is noted in figures). $p^{****} < 0.0001$; $0.0001 < p^{***} < 0.001$; $0.001 < p^{**} < 0.01$ and $0.01 < p^{*} < 0.05$.

4.2.2 Analysis of the *Drosophila* peripheral molecular clockwork

4.2.2.1 Quantitative Reverse Transcriptase-PCR (qRT-PCR)

The state of the peripheral molecular oscillator was assessed using quantitative reverse transcriptase polymerase chain reaction (qRT-PCR) on whole fly heads, to assay mRNA cycling in the presence of long and short photocycles. Wild-type flies of the genotype $y^1w^{*};tim-luc:10$ were entrained to either a 10, 9, 7, or 5c/wk LD cycle at 25°C for 3 days prior to sample collection at four distinct time-points during the LD regime (see **S.Figure B.2** for sample collection schedule). At each time-point, three biological replicates, each consisting of 40 individuals (3 x n=40), were collected for each gender. Samples were collected on dry ice, and kept at -80°C until head dissection.

Chapter 4:

Collection tubes were vortexed, contents transferred onto a pre-chilled clean metal tray, and heads harvested using a brush, into RNAase free collection tubes (stored at -80°C if needed). The RNAqueous-4PCR Kit (Ambion, AM1914) was used to extract total RNA from whole head samples (see Appendix B.4.13 for full protocol) with RNA concentration and quality quantified using a NanoDrop (ND-1000) spectrophotometer (RNA quality is assessed by ratio of absorbance at 280 nm and 260 nm where “pure” RNA has a 280/260 ratio of ~2.0).

qRT-PCR was conducted using the Chromo4 system for Real-Time PCR detection (BIORAD) and the Precision OneStepPLUS qRT-PCR Mastermix (Primerdesign), which utilises SYBRgreen based detection. See **Table 4.1** for primer sequences, concentrations and efficiencies. Full cycling protocol is detailed in Appendix B.6.4.

Table 4.1 Primer pairs used for mRNA amplification via qRT-PCR

| Target Gene Source | Direction | Sequence | Conc. (μM) | Efficiency (%) |
|--------------------|-----------|--------------------------------|------------|----------------|
| <i>per</i> | f | 5'-CGCCAACAACAAGAAATACACGG-3' | 0.4 | 104 |
| Invitrogen | r | 5'-TGATGAAGGACGAGTAGAAGGAGG-3' | 0.4 | |
| <i>Clk</i> | f | 5'-GCTCCTCCGATCATTGGCTA-3' | 0.2 | 134 |
| Eurofin Genomics | r | 5'-TCACCCGTTTGCCTTAGCTC-3' | 0.2 | |
| <i>luc</i> | f | 5'-TACCGGGAAAAGGCTGGGCG-3' | 1.0 | 122 |
| Invitrogen | r | 5'-GGCGTTGGTCGCTTCCGGATT-3' | 1.0 | |
| <i>rp49</i> | f | 5'-CACTTCATCCGCCACCAGT-3' | 0.4 | 112 |
| Invitrogen | r | 5'-CGCTTGTTGATCCGTAACC-3' | 0.4 | |

4.2.2.1.1 Qualitative, Quantitative and Statistical Analysis

Opticon Monitor 3 (BIORAD) was used to inspect and quality check data post qRT-PCR, via both quantification and melting curves; to check for anomalous readings and correct test gene amplification (i.e. not primer dimers) as well as set threshold. Anomalous results were discarded and cycling threshold, C(t), data for all remaining samples was exported. C(t) is defined as the

number of amplification cycles required for fluorescent signal to cross the threshold i.e. exceed background.

Quantity of mRNA expressed was calculated using the equation of the line for the standard curve for a given primer pair (see Appendix B.6.2 for generation of Standard curve and equations). Standard curves were straight lines with equation ' $y=mx+c$ ' where ' y ' was $C(t)$ and ' x ' was $\log(\text{quantity})$ i.e. $\log q(c)$. Therefore mRNA quantity could be calculated using the following equation;

$$q(c) = 10^{((C(t)-c)/m)}$$

Ratios of test and housekeeping gene expression were then calculated i.e. test $q(c)/$ housekeeping $q(c)$, for each qRT-PCR reaction and averaged across the three biological replicates for each time-point. Fold change in mRNA expression was calculated by dividing all ratios in any given condition by the lowest average ratio of the four time-points for that given condition.

GraphPad Prism 7.05 was used to generate all graphs and conduct statistical analysis. Fold change of relative expression (/RP49) was plotted both in real-time and scaled to a 24 h LD cycle (annotated in figure) to allow analysis of mRNA cycling kinetics as well as relative phase of transcript accumulation across different LD cycles, for different genes assayed. Analysis of variance (ANOVA) was conducted across all time-points within each condition using the non-parametric *Kruskal-Wallis test*. Pairwise comparisons between consecutive time-points, within each condition, were made using *Dunn's multiple comparisons test*. $p^{****} < 0.0001$; $0.0001 < p^{***} < 0.001$; $0.001 < p^{**} < 0.01$ and $0.01 < p^* < 0.05$.

Where required, effect size was calculated with either Cohen's d where $d=0.2$ is to be considered a 'small' effect size, $d=0.5$ represents a 'medium' effect size and $d=0.8$ a 'large' effect size. Therefore if two groups' means do not differ by 0.2 standard deviations or more, the difference is trivial, even if it is statistically significant. In cases where the n number differs, Hedges' g was used instead.

4.2.2.2 Western Blot

PERIOD protein cycling was analysed via western blot. Adult flies of genotype $y^1w^{*};tim-luc:10$ were harvested in accordance to the same sample collection protocol used for qRT-PCR, across the same four LD cycles (see **S.Figure B.2**). Fly heads were collected and total protein extracted (see Appendix B.7.4 for protein extraction protocol). Colorimetric detection and quantification of total protein in each sample was conducted using the Pierce BCA Protein Assay Kit

Chapter 4:

(ThermoScientific, 23227), with samples read at 562 nm using the FLUOstar Omega spectrophotometer (BMG Labtech).

See Appendix B.7.5 for full Western blot protocol. Membranes were probed for PER and HSP70 (loading control), see **Table 4.2**, and imaged with a Li-Cor Odyssey Scanner using Image Studio 5.2 software (Li-Cor Biosciences).

Table 4.2 Antibodies used for protein labelling during western blot

| Antibody | Concentration | Source |
|--------------------------|---------------|--------------------------------------|
| Rabbit anti-PER | 1:15000 | J.C. Hall (Liu <i>et al.</i> , 1992) |
| Mouse ant-HSP70 | 1:10000 | Sigma-Aldrich, H5147 |
| Goat anti-Rabbit (800cw) | 1:20000 | Li-Cor, 827-08365 |
| Goat anti-Mouse (680cw) | 1:20000 | Li-Cor, 827-08366 |

4.2.2.2.1 Qualitative, Quantitative and Statistical Analysis

Image Studio Lite 5.2 (Li-Cor Biosciences) was used to analyse blots and quantify PER and HSP70 signal. PER/HSP70 ratio was calculated and then normalised to total amount of protein loaded (calculated using Pierce BCA Protein Assay). Normalised ratios were then averaged across the three biological replicates for each time-point.

GraphPad Prism 7.05 was used to generate all graphs and conduct statistical analysis. Normalised PER/HSP70 ratios were plotted both in real-time and scaled to a 24 h LD cycle (annotated in figure) to allow analysis of PER protein cycling kinetics as well as relative phase of protein accumulation across different LD cycles. Analysis of variance (ANOVA) was conducted across all time-points within each condition using the non-parametric *Kruskal-Wallis test*. Pairwise comparisons between consecutive time-points, within each condition, were made using *Dunn's multiple comparisons test*. $p^{****} < 0.0001$; $0.0001 < p^{***} < 0.001$; $0.001 < p^{**} < 0.01$ and $0.01 < p^* < 0.05$.

4.3 Results

4.3.1 Light-dependent plasticity of *Drosophila* peripheral rhythms *in vivo*

Peripheral clock rhythmicity was assayed in live intact flies using TopCount *in vivo* luciferase monitoring (4.2.1.1). Flies with *luciferase (luc)* gene fused to the *timeless* promoter (y^1w^* ; *tim-luc:10* or y^1w^* *tim-luc*) were effectively used as wild-type as they did not have reported behavioural or circadian abnormalities, while their *luc* expression and resultant luminescence reflected peripheral circadian transcriptional activity (Brandes *et al.*, 1996). Luciferase activity traces for all data presented were scaled to a unified LD cycle.

4.3.1.1 Defining the limits of wild-type peripheral clock entrainment

In 7c/wk (24 h) LD, peak luciferase activity occurred around midnight with the trough just after lights-on (**Figure 4.1, A**), similar to previously published data (Stanewsky *et al.*, 1998), although peak luciferase activity occurred earlier relative to the LD cycle in our data. As the photoperiod was shortened to 9c/wk (18.67 h) a phase delay in luciferase activity, relative to 7c/wk, was apparent over the first 2 cycles; however alignment of activity was achieved at cycle 3 and persisted for the rest of the assay (**Figure 4.1, A**). Activity traces during a 10c/wk (16.8 h) LD cycle were clearly out of phase relative to 7c/wk with a delay observed over the first 2 oscillations which transitioned to an advance in cycles 4 and 5; this phase relationship was even apparent when compared to 9c/wk (**Figure 4.1, A - Insert**). In a long 5c/wk (33.6 h) LD cycle, peak luciferase activity aligned with peaks in 7c/wk but were broader (**Figure 4.1, A**). Periodic oscillations in bioluminescence were hard to discern in 4c/wk (42 h) LD with average luciferase activity now flat (**Figure 4.1, A**); similar to the reported phenotype of *cry^b* mutants during 7c/wk LD (Stanewsky *et al.*, 1998). These data suggest peripheral entrainment may begin to breakdown at photocycles shorter than 18.66 h and longer than 33.6 h.

Categorisation of flies as either rhythmic, weakly rhythmic or arrhythmic based on individual RAE values following FFT-NLLS analysis (4.2.1.2) using standard analysis parameters (**S.Table B.5**) showed that robust rhythms were seen in ~75% of flies in both 7 and 5c/wk (**Figure 4.1, B** and **S.Figure 16, A**). When compared to 7c/wk; a significant increase in weakly rhythmic flies was seen in 9c/wk; whereas increased arrhythmicity drove the difference in 10 and 4c/wk (**Figure 4.1, B**). Although showing a flat average activity trace, ~60% of flies in 4c/wk showed strong rhythms at the individual level with a similar average RAE value to 5c/wk (**Figure 4.1, B** and **S.Figure 16, A**), this apparent discrepancy was due to the higher fraction of arrhythmic flies at 4c/wk. When flies were categorised into entrained, 'other' or arrhythmic based on period length, high proportions

Chapter 4:

of flies showed the correct entrained period length in 9, 7 and 5c/wk (**Figure 4.1, C**). The majority of individual period lengths were very close the expected entrained period length in each of these three conditions (**Figure 4.1, D**). The differences observed between 9 and 7c/wk with regards to rhythmic strength were not reflected to the same extent in this analysis as even flies with weak rhythms under 9c/wk conditions often exhibited entrainment at the correct period length. The opposite was true in 4c/wk, where ~45% of flies showed an 'other' rhythm despite all non-arrhythmic flies exhibiting strong rhythmic power (**Figure 4.1, B, C**). When individual period lengths were plotted, this increase in 'other' period lengths in 4c/wk was apparent and indicated that the average period length was less than 40 h instead of the expected 42 h (**Figure 4.1, D**). As mentioned previously, the majority of flies were arrhythmic in 10c/wk (54%). Of those that were rhythmic, most displayed the correct entrained period length (although slightly longer than an entrained 16.8 h) and a small cluster displayed periodicities in excess of 20 h (**Figure 4.1, D**). The significant reductions in entrainment seen in 10 and 4c/wk support the observations made from the luciferase activity traces and further indicate that limits of light-induced peripheral clock entrainment lie below 18.67 h at one extreme and above 33.6 h at the other.

Phase of luciferase activity relative to photocycle was calculated for flies with the correct entrained period length. Entrained flies in 7 and 9c/wk cycled in-phase with their respective LD cycle with the initial delay seen in 9c/wk not significantly impacting the overall phase-relationship (**S.Figure 17**). A clear phase advance was seen in 5c/wk (**S.Figure 17**). The entrainment defects at 10 and 4c/wk were evident by changes in phase relationship to the photocycle over the time course.

From the traces presented in **Figure 4.1, A**, there was a clear decrease in amplitude as the photocycle was shortened. Amplitude of luciferase activity was quantified over the first 96 h; firstly to allow for uniformity across photocycles as not every experiment was the same length; and secondly as signal decreased over time due to substrate depletion (Brandes *et al.*, 1996). Amplitude was significantly reduced in 9c/wk compared to 7c/wk, with the greatest amplitude seen in 5c/wk (**Figure 4.1, E** and **S.Figure 17, C**). The severely damped amplitude data at 4c/wk reflected disruption of photocycle entrainment (**Figure 4.1, E** and **S.Figure 17, C**).

Further analysis, as well as data for females can be found in **S.Table 17**. Female peripheral entrainment is comparable to males in the majority of photocycles. More females were arrhythmic in 9c/wk compared to males, however to a lesser extent than seen in 10c/wk for both genders.

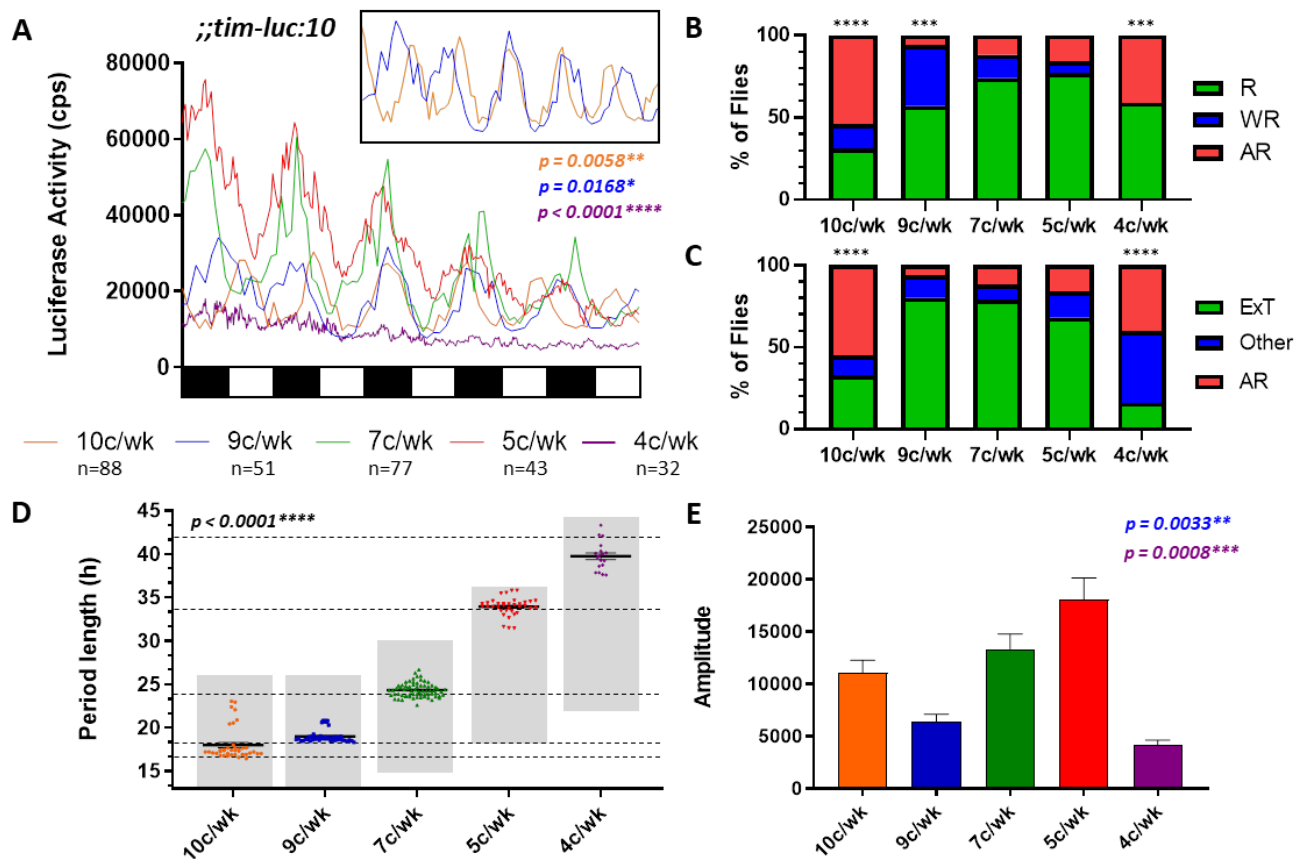


Figure 4.1 Peripheral oscillators of wild-type flies show a high level of light-induced plasticity.

Qualitative and quantitative analysis of male flies of the genotype $y^1w^{*};;tim-luc:10$ generated with the TopCount *in-vivo* luciferase assay. **A**) Luciferase activity traces for 10 (orange), 9 (blue), 7 (green), 5 (red) and 4c/wk (purple) scaled to LD cycle (5 full LD cycles). ‘n’ denotes number of flies for each condition. *Kruskal-Wallis test* comparing luciferase activity over 5 LD cycles across all conditions; $p < 0.0001$. *p* values (right) indicate results of *Mann-Whitney test* comparing luciferase activity over 5 LD cycles for each LD cycle vs. 7c/wk (10 vs. 7c/wk – orange, 9 vs. 7c/wk – blue and 4 vs. 7c/wk – purple). Inset (top right) shows luciferase activity traces for 10 (orange) and 9c/wk (blue) only, scaled to LD cycle to better highlight the phase differences in luciferase traces in short LD cycles. **B, C**) Composite bar chart showing percentage; **(B)** rhythmic (green), weakly rhythmic (blue) and arrhythmic (red); and **(C)** entrained (green), ‘other’ (blue) and arrhythmic (red) flies in each condition. *Fisher’s exact test* to compare distributions of rhythmic, weakly rhythmic and arrhythmic (**B**) and of entrained, ‘other’ and arrhythmic (**C**) individuals for each genotype vs. 7c/wk. **D**) Individual male period lengths. Error bars show mean period length \pm SEM. Dashed lines indicate entrained period lengths for 4, 5, 7, 9 and 10c/wk (top to bottom). Grey shading indicates analysis parameters used for individual fly analysis in each LD cycle. *p* value (top left) shows result of *Kruskal-Wallis test* across all conditions. **E**) Average amplitude (luciferase activity) over the first 96 h of each condition, error bars show \pm SEM. *p* values (top right) indicates results of *Mann-Whitney test* vs. 7c/wk (9c/wk– blue and 4c/wk – purple).

4.3.1.2 CRY/JET-mediated light entrainment is required for light-induced plasticity of *Drosophila* peripheral oscillators

As discussed in Chapter 3, entrainment of central clocks to extreme photocycles requires light input from both the CRY/JET pathway and the visual system. Mutations affecting these pathways were combined with a luciferase reporter (*tim-luc*) and entrainment assayed using TopCount. 9, 7 and 5c/wk LD were selected, corresponding to 18.67 h, 24 h and 33.6 h photocycles respectively, in order to assess the requirement of these photic input pathways in light-dependent peripheral plasticity at the limits of entrainment. Control data represents $y^1w^{*};tim-luc:10$ as reported in 4.3.1.1. Wherever possible, isogenic controls were assayed and comparisons between experimental genotypes and their corresponding control can be found in **S.Table 17**.

We report high-levels of plasticity in peripheral oscillators (4.3.1.1), however it has been suggested that luciferase activity can be light-driven and therefore rhythms seen may be independent of the circadian clock (Stanewsky *et al.*, 1997; Stanewsky *et al.*, 2002). Clock-less flies carrying a null mutation for the *timeless* gene (*tim⁰¹*) were mostly arrhythmic in all LD cycles tested (**Figure 4.2, A**) (See **S.Figure 18** for average *tim⁰¹* luciferase activity traces). When a rhythm was detected, the majority were categorised as weakly rhythmic (i.e. RAE is greater than 0.7) and very few showed the correct entrained period length (**Figure 4.2**). Even though there was no functioning clockwork, there was a small amount of residual rhythmicity which could be attributed to a simple light-driven response. However, the drastic reduction in rhythmicity reported showed a functional clock to be paramount to peripheral rhythmicity.

Flies with either a *cry* null mutation (*cry⁰¹*) or a *jetlag* loss-of function mutation (*jet^{set}*) showed the same drastic reduction in rhythmicity as *tim⁰¹* in 9, 7 and 5c/wk (**Figure 4.2, A**); and all were significantly different than control (except *jet^{set}* flies in 5c/wk, however this was likely due to the very low n number). The phenotype of *jet^{set}* was less severe than *cry⁰¹* as a larger proportion of *jet^{set}* flies were strongly rhythmic (**Figure 4.2, A, B**). Small proportions of both *cry⁰¹* and *jet^{set}* flies showed the expected entrained period length in 9 and 7c/wk (**Figure 4.2, C**). In 9c/wk, those that were weakly rhythmic showed a circadian rhythmicity of ~24 h, as was seen in the analysis of *cry⁰¹* and *jet^{set}* locomotor behaviour (Chapter 3) (**Figure 4.2, D**). In a long 5c/wk photocycle, all rhythmic flies were categorised as 'other' and all but one *jet^{set}* fly cycled with a ~24 h periodicity. Visual light input to the central clocks is required for effective behavioural plasticity at the limits of entrainment, however expressing a pro-apoptotic protein (*hid*) in the eye (*GMR-hid*), or having a mutation in phospholipase C which removes the visual transduction pathway (*norpA⁷- no receptor potential A*) did not reduce rhythmicity in any LD cycle (**Figure 4.2, A, B**). Visual mutants showed robust cycling of luciferase activity at the correct entrained period length demonstrating that

visual light input was not required for peripheral entrainment and suggesting that visual light input to the brain does not impact peripheral oscillators. The residual rhythmicity seen in *tim*, *cry* and *jet* mutants is, therefore, not attributed to visual light input.

Further analysis and female data is presented in **S.Table 17**. Females showed similar patterns of entrainment as reported here for males, albeit less severe. Collectively these data demonstrate a requirement for both CRY and JET in enabling peripheral entrainment to any equinox photocycle, confirming prior observations for the peripheral entrainment requirement of CRY in 7c/wk (Stanewsky *et al.*, 1998) and clarifying that the previously reported lack of peripheral entrainment phenotypes for *jet* mutants were likely due to the use of weak mutant alleles (Koh, Zheng and Sehgal, 2006). Moreover, the results presented here point to a lack of involvement of the visual system in the entrainment of peripheral luciferase rhythms across the range of entrainable photocycles.

Chapter 4:

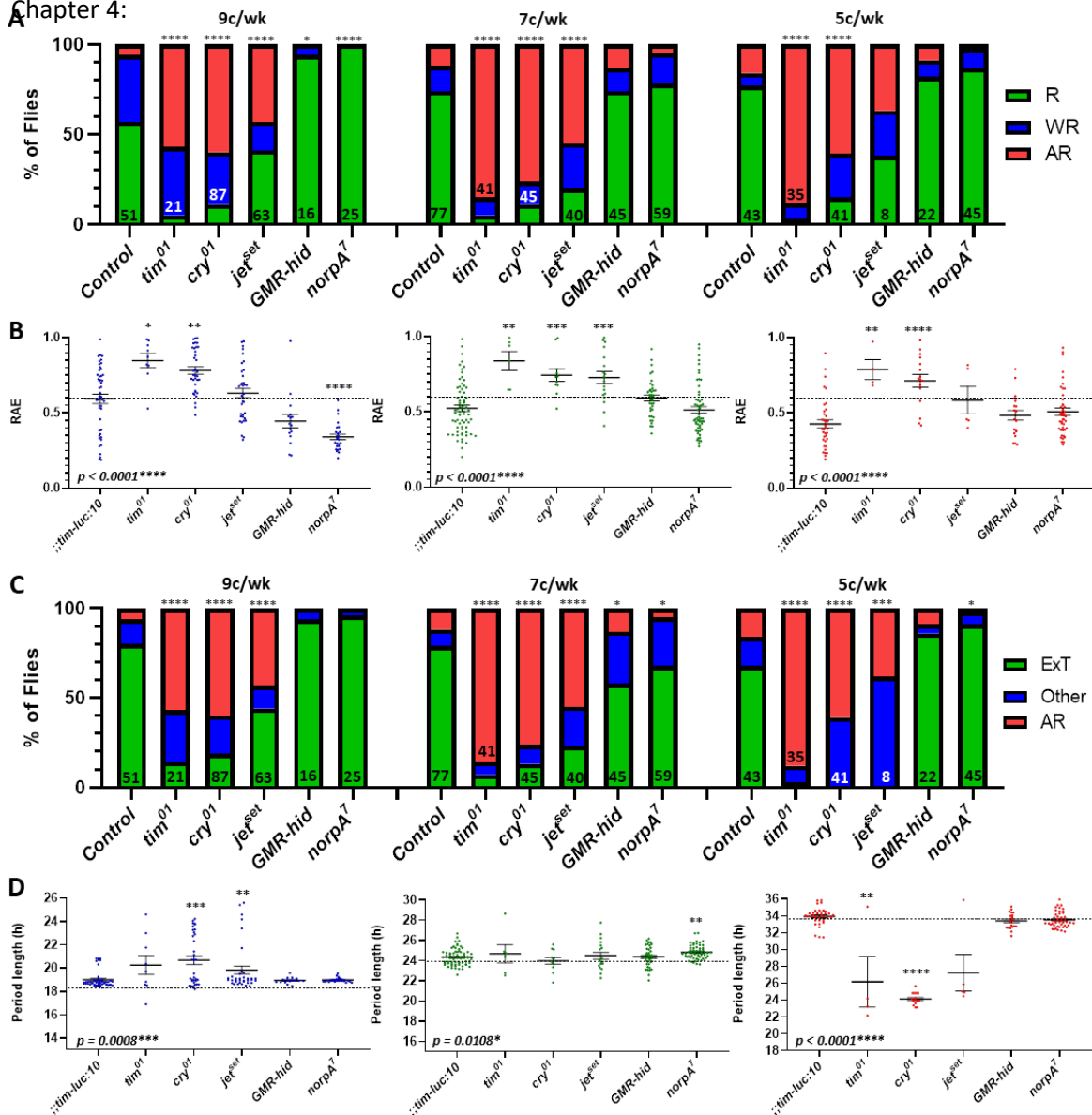


Figure 4.2 CRY and JET are required for light-induced plasticity of peripheral clocks.

A, C Composite bar charts showing percentage; (A) rhythmic (green), weakly rhythmic (blue) and arrhythmic (red) and (C) entrained (green), ‘other’ (blue) and arrhythmic (red) flies of genotypes; $y^1w^*::tim-luc:10$ (Control), $y^1w^* tim-luc:tim^{01}$, $y^1w^* tim-luc:cry^{01}$, $y^1w^* tim-luc:jet^{set}$, *GMR-hid*; *tim-luc:10* and *norPA⁷*; *tim-luc:10* in 9 (left), 7 (middle) and 5c/wk (left). n is annotated in each bar. Fisher’s exact test to compare distributions for each genotype versus control across rhythmic, weakly rhythmic and arrhythmic flies (A) and entrained, ‘other’ and arrhythmic flies (C). **B, D** Individual RAE (B) and period lengths (D) for rhythmic flies of the same genotypes in 9, 7 and 5c/wk (left to right). p values (bottom left) indicate results of Kruskal-Wallis test across all genotypes within each condition. Pairwise comparison of each genotype vs. Control in each condition with Mann-Whitney test. $p^{***}<0.0001$, $0.0001<p^{***}<0.001$, $0.001<p^{**}<0.01$ and $p^*<0.05$. **B**) Error bars show mean RAE \pm SEM. Dashed line indicated a RAE value of 0.7. **D**) Graphs plotted over the range of period lengths used for individual fly analysis in each LD cycle. Error bars show mean period length \pm SEM. Dashed lines indicate entrained period length for each condition.

4.3.2 Molecular analysis of peripheral clock entrainment

Peripheral clocks of wild-type flies show a high level of plasticity when challenged with extreme LD cycles (4.3.1.1). In order to assess how the peripheral molecular clockwork adapts to facilitate such entrainment, oscillations in the adult fly head of clock-controlled *period* (*per*) and *Clock* (*Clk*) mRNA, as well as PERIOD (PER) protein, were assayed under the same extreme photocycles using qRT-PCR and Western blot respectively (4.2.2.1 and 4.2.2.24.2.2). All molecular analysis was conducted using *y¹w^{*}::tim-luc:10* flies, matching the wild-type genotype used for *in vivo* luciferase monitoring assays (4.3.1), and time-points for tissue collection across all photocycles are shown in **S.Figure B.2**.

4.3.2.1 Light-induced plasticity of the molecular oscillator is associated with selective reorganisation of clock gene mRNA rhythms

Fold change across the day in relative mRNA expression for *per* and *Clk* transcripts, compared to the housekeeping *RP49* transcript, was plotted either scaled to a single LD cycle or in real-time for both male and female flies (see 4.2.2.1 for full detail of data acquisition and processing). A gender-specific difference in relative mRNA abundance was apparent; particularly for *Clk*, where females had a lower amplitude between peak and trough values (**Figure 4.3** and **Figure 4.4**).

In 7c/wk *Clk* and *per* transcripts both cycled rhythmically and in antiphase to each other, as expected as they represent anti-phase waves of circadian gene expression (Allada and Chung, 2010; Hardin, 2011). For both genders, *per* transcript cycled significantly across daily time with peak abundance at lights-off (ZT12) and a trough around lights-on (ZT20.4-ZT4.8) (**Figure 4.3, A** and **Figure 4.4, A**). *Clk* peaked around lights-on (ZT20.4-ZT4.8) for both males and females and exhibited a trough lights-off (ZT12), matching prior observations from male flies (Rakshit *et al.*, 2012; Hardin, 2004). However, *Clk* transcript cycling was only significant in males (**Figure 4.3, B** and **Figure 4.4, B**). Thus, oscillations in *per* and *Clk* matched the previously reported expression patterns in 7c/wk (Hardin, 2004; Rakshit *et al.*, 2012).

In a long 5c/wk LD condition both genders still exhibited a trough in *per* transcript at lights-on (ZT0) but *per* mRNA was higher than expected around midnight (ZT18) resulting in a delayed decrease in *per* transcript levels (**Figure 4.3, A** and **Figure 4.4, A**). Cycling in *per* mRNA was significant in male heads, which featured a broader peak and a similar rate of *per* accumulation in 5c/wk as seen in 7c/wk (Real-time plot **Figure 4.3, A**). When scaled to a uniform LD cycle, *Clk* transcript exhibited significant cycling with an earlier phase in 5 compared to 7c/wk in both genders (**Figure 4.3, B** and **Figure 4.4, B**). This clear advance in *Clk* phase relative to LD cycle in long cycles was consistent with uniformity in the kinetics of *Clk* transcript accumulation and

Chapter 4:

turnover in real-time (**Figure 4.3, B** and **Figure 4.4, B**). Thus, *Clk* mRNA expression appeared to be invariably locked to the lights-off transition in both 5 and 7c/wk photocycles.

In both genders *per* and *Clk* transcripts showed damped rhythms in 9c/wk LD compared to 7 and 5cwk (**Figure 4.3, Figure 4.4** and **S.Table 18**), which may indicate inefficient entrainment. Replotting the 9c/wk data using a different scale on the y-axis further clarified that there was a subtle trend for *per* transcript levels to be a little higher at lights-on than lights-off without significant oscillation. Parallel quantification of the *luciferase (luc)* from the *tim-luc* transgene present in the genotypes again produced a pattern with higher transcript levels at lights-on than lights-off in both genders (**Figure 4.3, C** and **Figure 4.4, C**). However, in spite of the higher amplitude in the *luc* pattern, cycling was, once more, not found to be significant (**Figure 4.3, C, Figure 4.4, C** and **S.Table 18**). No statistical difference was seen when comparing all time-points for each transcript in both genders. Calculating effect size between time-points in a pairwise manner suggested that there could be real difference within the 9c/wk transcript profiles that might be revealed if further replicate experiments were performed (**S.Table 20**). Increased sampling frequency might further help refine detection of these daily transcript profiles. The increased amplitude of the *tim-luc* transcript and luciferase activity at 9c/wk when compared to the *per* and *Clk* transcript profiles might, in part, be explained by additional post-transcriptional regulation for the latter two transcripts (So and Rosbash, 1997); that would not be found for the non-native *luc* transcript.

Light induces different effects on mRNA cycling depending on the transcript and the photocycle length. In long photocycles, the waveform of *per* transcript was altered with a broader peak in males and delayed turnover relative to the LD cycle in both genders. Conversely, a notable phase advance was observed in *Clk* transcript, which may indicate how peripheral oscillators adapt to allow entrainment. Transcript rhythms were damped in 9c/wk while oscillations in *luc* mRNA confirm that the clock could still generate rhythmic output in this short photocycle.

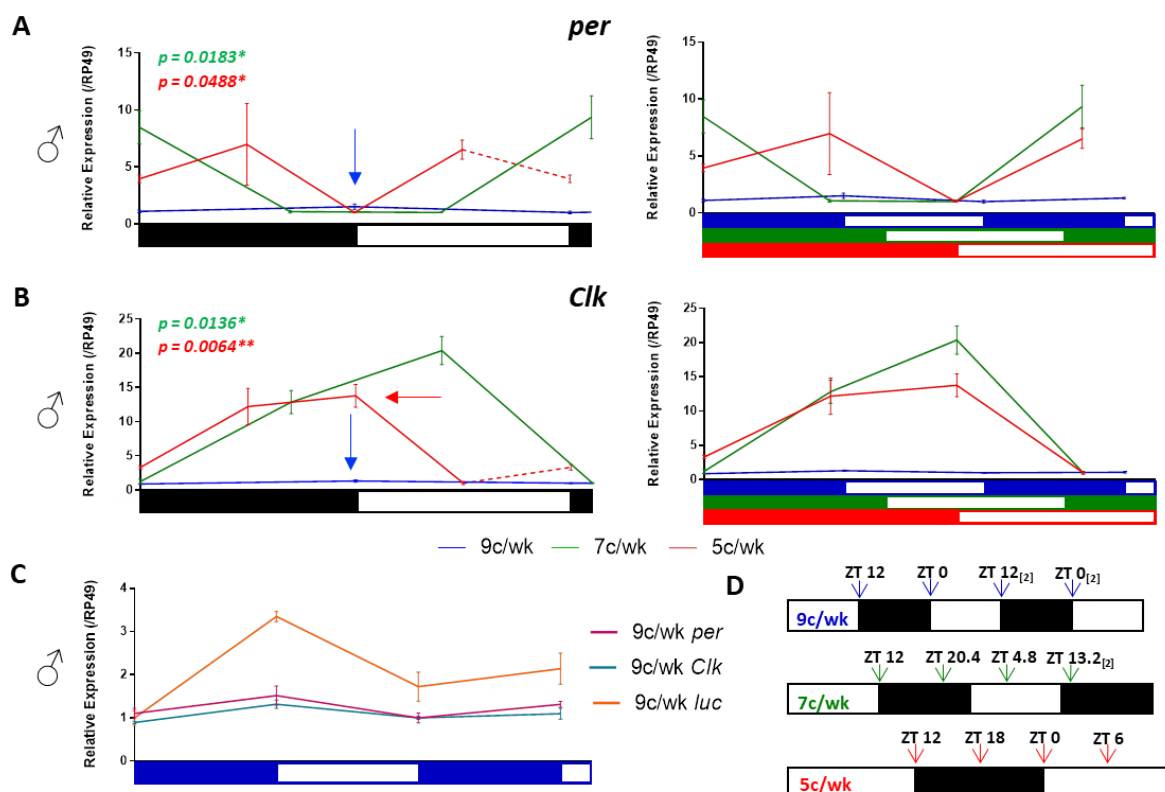


Figure 4.3 *per* and *Clk* mRNA cycling indicate the state of the molecular oscillator under extreme photocycles – Male.

A, B *per* (**A**) and *Clk* (**B**) transcript cycling from whole heads of male flies of genotype $y^1w^*;;tim-luc:10$ entrained to 9 (blue), 7 (green) and 5c/wk (red) using qRT-PCR, plotted W.R.T a 24 h LD cycle (left - black=dark; white=light) and in real-time (right – LD bar for each cycle where blue, green and red represent the dark phase for 9, 7 and 5c/wk respectively; white=light). Fold change is plotted for ratios of test transcript against *rp49* control transcript. Arrows indicate apparent wave-form differences compared to the 7c/wk profile with downward indicating damping and leftward indicating a phase advance relative to the photocycle. *p* values (top left – reported on 24 h scale plots) indicate results of *Kruskal-Wallis test* across all time-points within each condition (7c/wk = green and 5c/wk = red). Error bars show mean \pm SEM. Dashed red lines indicate an extrapolation of the 5c/wk data (repeat of data at 5c/wk ZT12). **C** *per* (magenta), *Clk* (teal) and *luc* (orange) transcript cycling in 9c/wk LD only, from whole heads of male flies of genotype $y^1w^*;;tim-luc:10$, plotted as in **A** and **B**. Error bars show mean \pm SEM. **D** Sampling scheme for 9 (blue), 7 (green) and 5c/wk (red) LD cycles. Time-points are scaled to a 24 h LD cycle and _[2] indicates time-points in the second LD cycle.

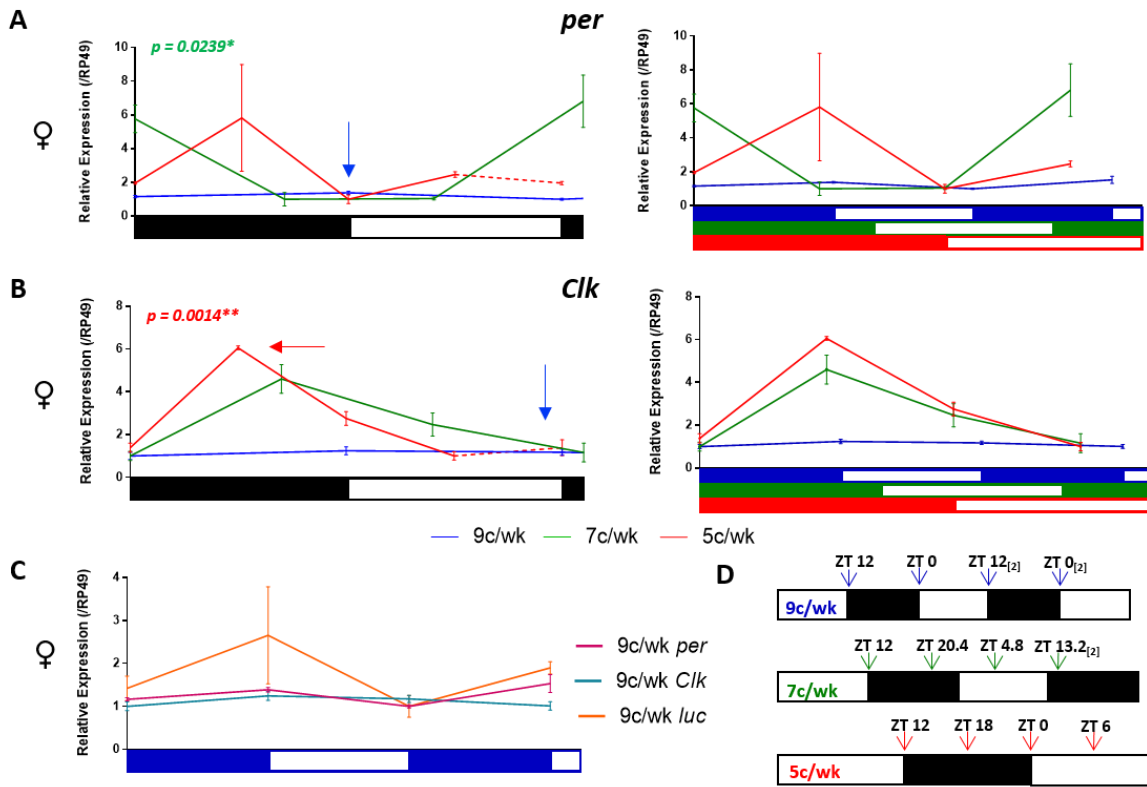


Figure 4.4 *per* and *Clk* mRNA cycling indicate the state of the molecular oscillator under extreme photocycles – Female.

A, B *per* (**A**) and *Clk* (**B**) transcript cycling from whole heads of female flies of genotype $y^1w^*;;tim-luc:10$ entrained to 9 (blue), 7 (green) and 5c/wk (red) using qRT-PCR, plotted relative to a 24 h LD cycle (left - black=dark; white=light) and in real-time (right – LD bar for each cycle where blue, green and red represent the dark phase for 9, 7 and 5c/wk respectively; white=light). Fold change is plotted for ratios of test transcript against *rp49* control transcript. Arrows indicate apparent wave-form differences compared to the 7c/wk profiles with downward indicating damping and leftward indicating a phase advance relative to the photocyple. p values (top left – reported on 24 h scale plots) indicate results of *Kruskal-Wallis test* across all time-points within each condition (7c/wk = green and 5c/wk = red). Error bars show mean \pm SEM. Dashed red lines indicate an extrapolation of the 5c/wk data (repeat of data at 5c/wk ZT12). **C** *per* (magenta), *Clk* (teal) and *luc* (orange) transcript cycling in 9c/wk LD only, from whole heads of female flies of genotype $y^1w^*;;tim-luc:10$, plotted as in **A** and **B**. Error bars show mean \pm SEM. **D** Sampling scheme for 9 (blue), 7 (green) and 5c/wk (red) LD cycles. Time-points are scaled to a 24 h LD cycle and _[2] indicates time-points in the second LD cycle.

4.3.2.2 Robust oscillations in PER protein are locked to the Light:Dark cycle

Representative blots show clear oscillations in PER protein in male flies entrained to 9, 7 and 5c/wk (**Figure 4.5, A**); PER cycling was less apparent in 10c/wk. Quantification of PER protein, relative to HSP70 and normalised to total protein, was plotted either scaled to a single LD cycle or in real-time for both male and female flies (see 4.2.2.2 for full detail of data acquisition and processing).

It is known that PER accumulates in the dark phase and decreases in the light due to the indirect light-dependent degradation of PER following light-induced TIM degradation (see 4.1). As expected, PER protein showed significant cycling across all time-points as well as pairwise differences between consecutive time-points in 9, 7 and 5c/wk for both genders (**Figure 4.5, C, D** and **S.Table 22**). In all cycles, peak PER corresponded to the time point closest to lights-on (ZT20.4 for 7c/wk and ZT0 for all others) and levels decreased during the light phase matching the expected alignment of PER cycling to the photocycle. Robust cycling was also seen in 10c/wk for females (**Figure 4.5, D**). However, the amplitude of PER rhythms in 10c/wk was damped compared to other conditions for both males and females, possibly as a consequence of incomplete entrainment as noted in the TopCount assay (**Figure 4.5, C, D** and **S.Table 21**). One peculiarity was the lack of increase in PER during the early night in 5c/wk. Among possible explanations for this phenomenon are a partial loss of synchrony across different peripheral clocks as well as the impact from the abnormally long preceding light phase. In this context, CRY would be expected to be depleted during the day as it turns over in a light-dependent manner (Koh, Zheng and Sehgal, 2006; Peschel, Veleri and Stanewsky, 2006; Peschel *et al.*, 2009) and this might lead to some accumulation of PER prior to lights-off.

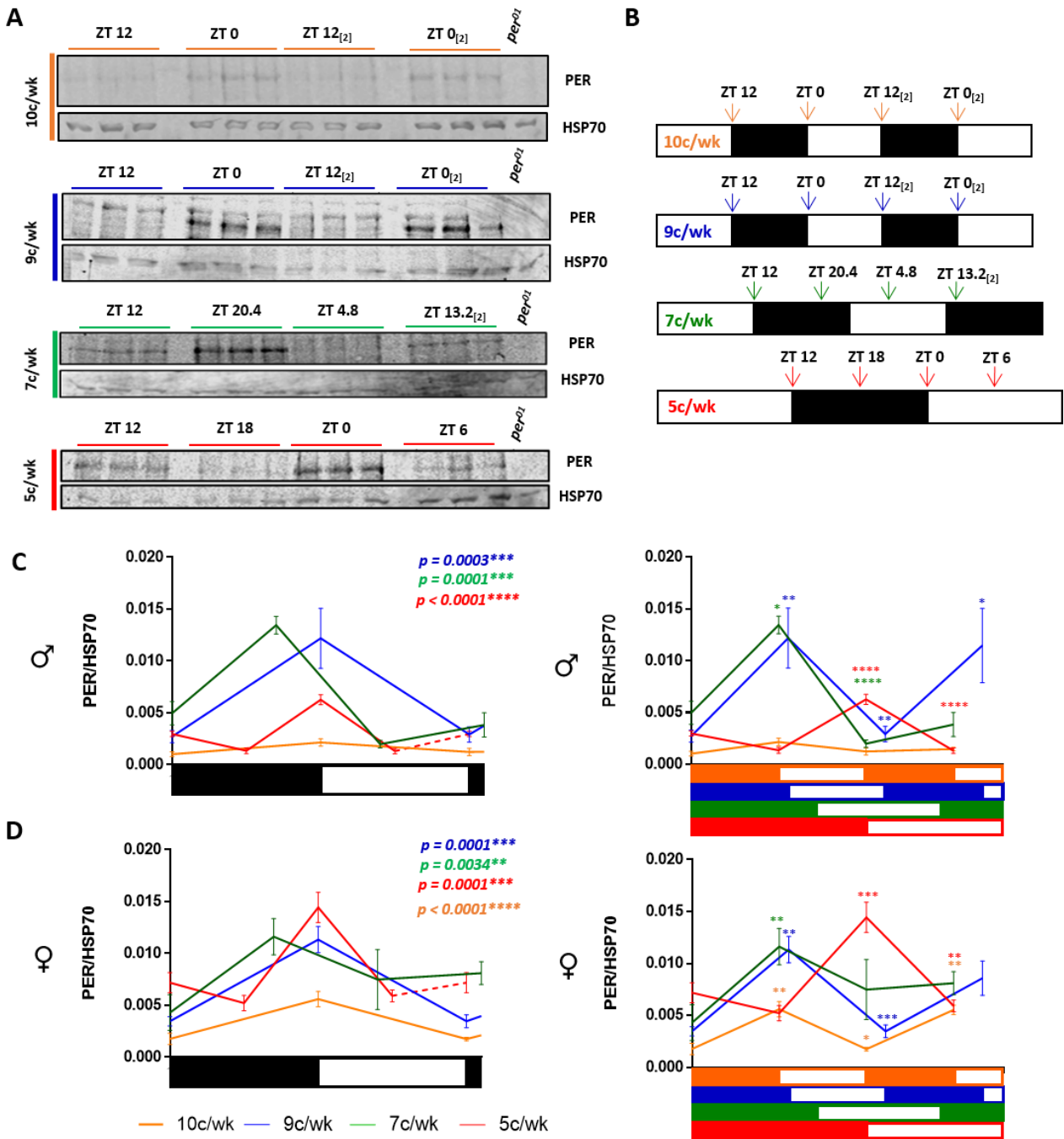


Figure 4.5 PER protein oscillations are locked to LD cycles as PER is light-degradable.

A) Representative Western blots, staining for PER and HSP70, from whole heads of male flies of genotype $y^1w^*;;tim-luc:10$ at 4 time-points during 10 (orange), 9 (blue), 7 (green) and 5c/wk (red) LD cycles (top to bottom). $y^1per^{01}w^*$ is included as a negative control. **B)** Sampling scheme for 10 (orange), 9 (blue), 7 (green) and 5c/wk (red) LD cycles. **A, B)** Time-points are scaled to a 24 h LD cycle and _[2] indicates time-points in the second LD cycle. **C, D)** PER protein oscillations (against HSP70) normalised to total protein loaded for male (**C**) and female (**D**) flies ($y^1w^*;;tim-luc:10$) plotted relative to a 24 h LD cycle (left - black=dark; white=light) and in real-time (right – LD bar for each cycle where orange, blue, green and red represent the dark phase for 10, 9, 7 and 5c/wk respectively; white=light). p values (top right

Fig 4.5 (cont.): – reported on 24 h scale plots) indicate results of *Kruskal-Wallis test* across all time-points within each condition (10c/wk = orange, 9c/k = blue, 7c/wk = green and 5c/wk = red). Comparison between consecutive time-points, within each condition, with *Dunn's multiple comparisons test* (shown on real-time plots - see **S.Table 22** for all *p* values). Error bars show mean \pm SEM. Dashed red lines indicate an extrapolation of the 5c/wk data (repeat of data at 5c/wk ZT12).

4.4 Discussion

The oscillatory mechanism that underlies circadian rhythmicity is common between *Drosophila* central and peripheral clock cells and relies on a negative feedback loop of transcription and translation (see 4.1) (Plautz *et al.*, 1997a; Hardin *et al.*, 2003). Peripheral clocks reside in many peripheral tissues and when isolated, they can maintain light entrainment and rhythmic oscillations independent of central clock input (Plautz *et al.*, 1997a; Ivanchenko, Stanewsky and Giebultowicz, 2001; Levine *et al.*, 2002); indicating autonomy in peripheral light input. Stretching the clock to the limits of entrainment using extreme equinox photocycles uncovered how the molecular oscillators, residing in the central clocks of the wild-type fly brain, adapt to facilitate behavioural entrainment to LD cycles ranging from 16.8 – 42 h (Chapter 2); and that both light input from the CRY/JET pathway and the visual system is required (Chapter 3). In order to further understand the impact of light on the peripheral molecular oscillator and the input pathways allowing light entrainment in peripheral clocks, the same rationale was implemented.

When assayed under a standard 24 h photocycle (7c/wk), peripheral oscillators displayed robust and high amplitude luciferase activity rhythms, in agreement with prior publications (Brandes *et al.*, 1996; Plautz *et al.*, 1997b; Stanewsky *et al.*, 1997). The observed high amplitudes are indicative of strong transcriptional activity and they allow us to rule out the possibility that the observed rhythms were an artefact due to changes in lighting condition as empty wells showed much lower counts (~300 cps) than wells with *luc*-expressing live flies. When challenged with 9 or 5c/wk, peripheral clocks maintained a high level of rhythmicity and the observed oscillations in luminescence were synchronized to the imposed LD cycle. Multiple peripheral clocks would have contributed to luciferase activity as bioluminescence was assayed in whole flies, therefore synchrony across these peripheral clocks would have contributed to the presented measures of period length, RAE, phase and amplitude (Koh, Zheng and Sehgal, 2006), indicating entrainment. Photocycles beyond these two extremes i.e. 10 and 4c/wk resulted in a marked reduction in rhythmicity and an inability to entrain peripheral clocks in line with the imposed LD cycle.

Circadian rhythmicity is underpinned by oscillations in clock-controlled genes and proteins. Under a standard 7c/wk LD cycle *per* transcript levels are low at lights-on (ZT0), rising to peak abundance just after lights-off (ZT12), before decreasing throughout the dark phase (Hardin, 2004). *Clk* mRNA cycles in antiphase to *per*, where lowest abundance is found at lights-off (ZT12), and peaks at lights-on (ZT0) (Hardin, 2004). Cytoplasmic PER protein accumulates 6-8 h after transcription with peak protein levels seen towards the end of the night before lights-on (Shafer, Rosbash and Truman, 2002; Harms *et al.*, 2004). Our data match these published observations with appropriately timed peaks in *per* and *Clk* transcript, as well as peak PER protein just before lights-

on, demonstrating the aforementioned lag following peak transcript mediated by post-translational modifications (Hardin, 2011). This relationship between peak *per* transcript and protein was maintained in long photocycles, but not evident in short due to the low amplitude of transcript cycling seen.

Light-induced plasticity of the peripheral molecular oscillator in response to extreme photocycles was associated with selective reorganisation of clock gene mRNA rhythms with respect to the LD cycle; most notably a phase advance in *Clk* transcript in long photocycles, which was not emulated by *per* transcript. When aligned at lights-off *Clk* mRNA expression proceeded with the same kinetics (in real-time) in both 5c/wk and 7c/wk photocycles, suggesting that it was governed by molecular clock functions phase-locked to dusk. One set of candidates for this could be VRI and PDP1, the transcriptional regulators of *Clk* (Blau and Young, 1999; Cyran *et al.*, 2003). Notably, in the 5c/wk condition an apparent phase advance relative to the photocyclus was not only evident for *Clk* transcript, but also for luciferase activity originating from the *tim-luc* transgene, which would normally be expected to be transcribed in phase with *vri*. Moreover by analogy to peripheral molecular rhythms, clock neuron molecular rhythms as well as behavioural rhythms exhibit phase advances relative to the photocyclus for the 5c/wk condition indicating this condition may allow synchrony to be preserved in clocks throughout the animal. However, lengthening of the photocyclus period beyond 5c/wk to 4c/wk led to a disruption of peripheral entrainment, but not central clock entrainment and, therefore, results in internal desynchronisation.

A reduced amplitude in both circadian mRNA and TopCount *tim-luc in vivo* luminescence rhythms was seen for 9c/wk LD. However, clearly entrained oscillations were still present in luminescence. The decreases in entrained amplitude in 9c/wk may be due to an overlap between states of transcriptional activity and negative feedback that can be separated in time in the context of longer cycles. It is also possible that lower amplitude luciferase activity seen in 9c/wk signals desynchrony between independent peripheral oscillators (Koh, Zheng and Sehgal, 2006). The absence of *per* and *Clk* transcript cycling contrasts with the robust entrainment seen in luciferase activity at this short photocyclus. This is explained at least in part by the more pronounced changes in *luc* mRNA over the photocyclus. In addition, the much higher sampling frequency in the Topcount assay may have favoured detection of these rhythms. Short photocycles may impose limits on entrainment by restricting the time required for proper circadian cycling. The time from peak transcription to CLK/CYC inhibition is ~9 h, which in a standard 24 h photocyclus all occurs in the dark phase prior to light-dependent PER degradation (see 4.1) (Hardin, 2011). The dark phase in a 9c/wk LD cycling is 9.33 h and thus may constrain proper cycling kinetics and therefore limit light entrainment. We do, however, see robust peripheral entrainment suggesting rhythmic clock

Chapter 4:

output is achieved in 9c/wk, but not when the cycle is shortened to only 16.8 h; we therefore conclude the limit of peripheral short cycle entrainment lies between these two period lengths.

Peripheral oscillations in PER protein align at lights-on irrespective of photocycle suggesting entrainment is driven by light-dependent PER degradation. This differs somewhat to what is observed in central clocks where peak PER protein occurs ~12 h following lights-off in all LD cycles (Chapter 2). The onset of light drives down PER levels, re-setting the oscillator and allowing a new circadian oscillation; confirming light-induced degradation is the driving force of molecular synchronisation in both central and peripheral clock cells. However PER accumulation kinetics in the brain appears more robust eliciting a molecular phase delay or advance in long or short cycles respectively. This further regulation may facilitate and be indicative of more refined molecular entrainment in the brain compared to the periphery.

Peripheral oscillators show high levels of light-induced plasticity, similar to that seen in the central clocks; however the entrainment range is narrowed to 18.66 – 33.6 h photocycles. Central clocks rely on light input from both the CRY/JET pathway and the visual system to entrain locomotor behaviour to extreme light dark cycles (Chapter 3). CRY is expressed in the many peripheral tissues including the compound eye (Yoshii *et al.*, 2008; Agrawal *et al.*, 2017), and can therefore provide direct cell-autonomous light input to peripheral clock cells, analogous to its role in central clock entrainment (discussed Chapter 3) (Stanewsky *et al.*, 1998; Emery *et al.*, 1998). CRY is fundamental to peripheral light entrainment (Stanewsky *et al.*, 1998), however its additional peripheral roles require further clarification. Conflicting evidence indicates CRY either functions solely as a photoreceptor required for periphery clock entrainment (Ito *et al.*, 2008; Agrawal *et al.*, 2017); or is required for clock function and partakes in the core TTFL as a transcriptional repressor (Collins *et al.*, 2006; Stanewsky *et al.*, 1998; Ivanchenko, Stanewsky and Giebultowicz, 2001), analogous to mammalian CRY (Okamura *et al.*, 1999; Horst *et al.*, 1999). There is no documented link between visual light input and peripheral clocks; however it has been shown that some peripheral clocks can receive light and temporal input from central clock cells (Myers, Yu and Sehgal, 2003; Morioka, Matsumoto and Ikeda, 2012).

Peripheral rhythmicity and entrainment in *cry⁰¹* mutants was severely reduced, to the same degree as clock-less flies, in 7c/wk and well as in long (5c/wk) and short (9c/wk) photocycles, corroborating the original observations by (Stanewsky *et al.*, 1998). *jet^{set}* mutants recapitulated the same entrainment deficits as *cry⁰¹* flies, clarifying that the phenotypes for the hypomorphs *jet^c* and *jet^f* were not informative in this respect (Koh, Zheng and Sehgal, 2006). It has been shown that both CRY and JET are involved in peripheral TIM degradation (Koh, Zheng and Sehgal, 2006; Ivanchenko, Stanewsky and Giebultowicz, 2001; Peschel *et al.*, 2009; Agrawal *et al.*, 2017),

suggesting that peripheral entrainment is achieved via light-dependent TIM degradation. Mutants affecting the visual system had no impact on peripheral entrainment, indicating CRY/JET light input alone is sufficient for entrainment and suggests that in the context of our assay any visual light input received in the brain isn't communicated to peripheral oscillators and cannot compensate for the loss of CRY or JET. Therefore, light-induced peripheral entrainment, likely via light-dependent TIM degradation, is mediated by CRY and JET; with both components vital in facilitating entrainment.

As mentioned previously, it is postulated that CRY contributes to core clock function in the periphery (Collins *et al.*, 2006; Stanewsky *et al.*, 1998; Ivanchenko, Stanewsky and Giebultowicz, 2001). To further address this, peripheral rhythms of *cry⁰¹* and *jet^{set}* mutants were assayed in constant darkness in the presence of a 24 h temperature cycle (**S.Figure 19** and **20**). Overall rhythmicity was relatively low, especially in males; however no differences were seen between controls and mutant genotypes, for either gender, suggesting that CRY and JET are not an integral part of the molecular oscillator in peripheral clocks per se. This observation agrees with the recent conclusions of (Agrawal *et al.*, 2017) who found no interaction between CRY and either PER or CLK in the periphery, arguing against a core-clock role for CRY. It is possible that the rhythms seen could just be temperature driven as seen in clock-less mutants (*per⁰¹* and *tim⁰¹*). Therefore mutants and controls should be entrained to a temperature cycle and their peripheral rhythms then assayed in DD at constant temperature. This should give a more definitive indication of the role of CRY and JET in the peripheral oscillator.

The results reported here combined with the data presented in Chapter 3 identify scenarios representing uncoupling of central and peripheral clocks. Luciferase rhythms are arrhythmic in *7c/wk* for *cry⁰¹* mutants but the behavioural rhythms of these flies are entrained. Conversely, peripheral clocks of visual mutants are entrained in long and short photocycles but behavioural entrainment is severely reduced. Luciferase reporter assays and locomotor assays were conducted at different temperatures, which should not affect light entrainment (Huang, Curtin and Rosbash, 1995); however different light sources were also used due to experimental design. LED light sources used in locomotor behaviour were lower-intensity than the fluorescent light boxes used in luciferase assays (4.2.1.1). Different light intensities have been shown to impact on entrainment (Schlichting *et al.*, 2016), and therefore could explain the differences in entrainment we report here. To address this, locomotor experiments should be conducted under the same lighting conditions used for TopCount assays to see if the uncoupling reported here is maintained.

The CRY/JET light input pathway mediates peripheral light-induced plasticity and facilitates entrainment to photocycles ranging from 18.67 – 33.6 h. The entrainment range is narrower in

Chapter 4:

the periphery compared to central clocks. This may be explained due to the dual light inputs received in the brain via both the CRY/JET pathway and the visual system, co-operating to impart greater plasticity. Furthermore, it has been reported that the visual system is better at phase shifting the oscillator than CRY/JET (Kistenpfennig *et al.*, 2017). Central clocks of the fly brain are organised into a neuronal network which allows a more complex and sophisticated approach to entrainment where two light inputs can be integrated and communicated across the circuit to generate an entrained output. This is not the case in the periphery where there appears to be a large degree of autonomy between oscillators. This more rudimentary organisation may mean desynchrony is more common, which coupled with CRY/JET being the sole light input, may explain the narrower entrainment range.

Peripheral oscillators are heterogeneous and different possible relationships between peripheral and central clocks have been reported whereby peripheral clocks are either independent of or driven by central clocks (reviewed by Ito and Tomioka, 2016). If independent of one another, mutations to one impart no effect on the other i.e. like visual system mutations on peripheral oscillations. This would allow peripheral clocks to maintain their own phase and entrain physiology optimally with the environment. However, if peripheral rhythms were set by central clocks, mutations affecting one would impact the other and disrupt crucial physiological processes reliant on peripheral clock function such as eclosion (Morioka, Matsumoto and Ikeda, 2012). This is the case in the mammalian circadian system where the master oscillator (SCN) in the brain synchronises peripheral oscillators (Glossop and Hardin, 2002). Uncoupling or desynchrony between central and peripheral oscillators in humans is likely linked with many circadian-related disorders (Hirota and Fukada, 2004; Pandi-Perumal *et al.*, 2008). Using extreme photocycles it is possible to induce a 'jet-lag-like' state in flies where central and peripheral clocks are desynchronised thus providing a possible model for investigating aspects of jet-lag and circadian disruption using *Drosophila*.

Chapter 5: General Discussion and Conclusions

5.1 General Discussion

5.1.1 Light-dependent plasticity of *Drosophila* central and peripheral clocks

This purpose of this section is to discuss the similarities and differences between light-dependent plasticity of the circadian clocks residing in the brain and peripheral tissues of *D. melanogaster*, as well as contextualise these findings in terms of the existing literature. More detailed discussions regarding individual results can be found in the chapter specific discussion sections.

5.1.1.1 How does the underlying circadian molecular oscillator adapt to facilitate light entrainment?

In utilising extreme equinox photocycles to stretch central and peripheral molecular oscillators to the limits of light-induced entrainment, we reveal how the molecular oscillator adapts to maintain entrainment when the clockwork has to constantly re-set its phase away from its inherent 24 h periodicity. This provides a more sensitive measure of plasticity compared to previous studies of light entrainment.

Entrainment of the central clocks of the *Drosophila* brain was characterised by a phase advance or delay of the molecular oscillator with respect to the Light:Dark cycle, compared to 7c/wk, as the photoperiod was lengthened or shorted respectively (2.3.2). Advances and delays observed in the central molecular oscillator correlated well with behavioural entrainment as similar advances and delays were seen in the evening peak of locomotor behaviour in long and short LD cycles respectively (2.3.1). Phase advances were also apparent in peripheral molecular oscillations. Luciferase activity rhythms and *Clk* transcript oscillations were both advanced compared to the LD cycle in 5c/wk (4.3.1 and 4.3.2.1). Analogous phase advances relative to the photocycle in 5c/wk were seen in peripheral molecular rhythms, clock neuron molecular rhythms and behavioural rhythms; indicating that this condition may allow synchrony to be maintained throughout the fly. However, photocycles longer than 5c/wk disrupted peripheral entrainment but not central entrainment, resulting in a state internal desynchronisation i.e. central and peripheral oscillators were 'out of sync'. In the central clock, the limit of long photocycle entrainment exceeds that of peripheral tissues and appears to be set by the emergence of a free-running rhythm following an extended dark phase, which was shown by the molecular analysis of flies in a 3c/wk condition with a 28 h dark phase (2.3.1.2).

Chapter 5:

In short cycles, peripheral clocks did not show a clear phase delay (4.3). Peripheral rhythms in luciferase activity and circadian transcripts were damped in short cycles (4.3.1.1 and 4.3.2.1). Similarly, PER protein oscillations in 10c/wk were reduced in most clock cells of the fly brain, where rhythms in PER nuclear localisation were also damped compared to 7 and 5c/wk (2.3.2.1). Damping of rhythms is indicative of desynchrony and a lack of entrainment and therefore the presence of reduced amplitude oscillations can be used to help define the limits of short photocycle entrainment. As such, the limit of short photocycle entrainment in central clocks may be imposed by the minimum time interval required to separate the nuclear accumulation and degradation phases of PER protein cycling; and in peripheral clocks short photocycles may impose limits on entrainment by restricting the time required for proper circadian cycling. A common theme is the insufficient time for robust molecular oscillations during such short photocycles; indicating that entrainment may require a possible trade-off between amplitude and rhythmicity.

Peripheral PER protein rhythms were governed by the Light:Dark cycle i.e. peak PER aligned with lights-on (ZT0), irrespective of the condition, and decreased in the light phase (4.3.2.2). This differed from what we observed in central PER oscillations where, as discussed above, peak PER was either advanced or delayed in long or short LD cycles respectively (2.3.2.1). In central clocks PER protein peaked ~12 h following lights-off in all conditions, indicating that PER accumulation kinetics remained the same irrespective of LD cycle (2.4). PER protein levels remained high during the elongated dark phase in a long (5c/wk) LD cycle, until lights-on, whereas PER levels peak in the light phase of a short (10c/wk) LD cycle (2.3.2.1). This highlights a difference in PER protein cycling between central and peripheral clocks whereby in the periphery light-dependent PER degradation is the driving force of entrainment; whereas in central clocks both the accumulation and light-dependent degradation of PER appear to be more tightly regulated by the clock, possibly allowing for refined entrainment.

5.1.1.2 What light input pathways are required?

Behavioural entrainment to a standard 7c/wk LD cycle can be achieved by either the CRY/JET pathway or rhodopsin-mediated photoreception by the visual system; however entrainment to short and long photocycles required light input from both pathways (3.3.1). It has been reported that CRY and the visual system act somewhat antagonistically when entraining to long-day photocycles with CRY hindering and the visual system promoting proper E-peak alignment (Kistenpennig *et al.*, 2017). In our assay, CRY/JET and the visual system worked co-operatively to facilitate entrainment to extreme photocycles (3.3.1). This may be due to the nature of the photocycles used i.e. the clock behaves differently in equinox photocycles compared to long-day/short-day photocycles, or it indicates a shift in the relative contributions of each light input

pathway, whereby in such extreme conditions, proper alignment of activity peaks is sacrificed for overall entrainment.

The same was not the case in the periphery where the visual system appeared to have no impact on light entrainment, CRY and JET however were paramount (4.3.1.2). Flies lacking CRY or JET could not entrain their peripheral clocks to a 7c/wk LD cycle, revealing the CRY/JET pathway as the sole means of light input to the periphery. The requirement of CRY in peripheral entrainment has long been known (Stanewsky *et al.*, 1998), however we reveal that JET is also required, suggesting that peripheral entrainment is mediated by light-induced TIM degradation. Therefore indicating that light entrainment of peripheral and central clocks is achieved by a common mechanism.

Another observed commonality was the severity of the light entrainment deficits evoked by *cry⁰¹* and *jet^{set}* mutations, with *cry⁰* mutants resulting in a more severe phenotype in both central and peripheral clocks (3.3.1 and 4.3.1.2). The smaller effect on entrainment elicited by *jet^{set}* could be as a result of CRY still being present to initiate targeted TIM degradation. Furthermore, *jet^{set}* is a loss-of-function mutant (Lamba *et al.*, 2014), whereas *cry⁰¹* is null mutant (Dolezelova, Dolezel and Hall, 2007), which may also contribute to the differing phenotypes. CRY is also involved in many other physiological processes, discussed in 5.1.3 and Appendix C, which may also indicate why *cry⁰¹* mutants displayed more severe entrainment deficits.

5.1.1.3 Why are the limits of entrainment different between central and peripheral clocks?

Central clock cells can entrain to a wider-range of photocycles than those residing in peripheral tissues. As discussed in Chapter 1 and Chapter 2, the ~150 central circadian clocks cells are organised into a network where distinct subsets of cells have defined roles in co-ordinating rhythmicity both across the circuit and in output i.e. behaviour in line with external LD cycles (1.2.6.2) (Chatterjee *et al.*, 2018; Lamba, Foley and Emery, 2018). In extreme LD cycles, the clocks residing in the s-LN_vs maintain robust oscillations, and with assistance from the DN1s, appear to be able to facilitate rhythmic behavioural output (2.4).

Not all clock cells, central and peripheral, express CRY. When entraining to extreme LD cycles, both CRY and JET expression was required in both the M- and E-cells to allow behavioural entrainment (3.3.2). This was previously reported for JET (Lamba *et al.*, 2014), however CRY expression is reportedly only required in the E-cells to allow light-induced plasticity (Yoshii *et al.*, 2015). An interesting observation was that when CRY/JET expression was limited to just the PDF-expressing M-cells (LN_vs), plasticity was photocycle dependent with better entrainment seen in long cycles (3.3.2.2 and 3.3.2.3). This indicates that CRY/JET input to the M-cells alone may be

Chapter 5:

sufficient to delay the clock. In such experiments, the visual system was still present and signalling light input to the clockwork, thus likely aiding entrainment (Kistenpfennig *et al.*, 2017). However, more recent research has shown that the cell-autonomous action of CRY/JET is paramount in governing phase advances and delays (Lamba, Foley and Emery, 2018). The challenge of entraining to such extremes photocycles may therefore require CRY/JET-mediated light input from more cells within the circuitry, hence the more broad mapping results we report (3.3.2).

There is a large degree of autonomy amongst peripheral clocks, as discussed in Chapter 4, and peripheral light input is solely mediated by CRY/JET. This more rudimentary organisation may result in desynchrony becoming more common as the independent oscillators are stretched towards the limits of entrainment. In central clocks however, a neuronal network can integrate light input from two distinct pathways, communicate that input across the circuitry and generate a more robust and synergistic rhythmic output in the face of extreme LD cycles (1.2.6.2 and Chapter 2). This clear difference in circadian clock organisation between central and peripheral oscillators may explain the different limits of entrainment.

5.1.2 Can *Drosophila* be used to model effects of circadian dysfunction and desynchrony?

Circadian entrainment and rhythmicity often goes unnoticed, however when disrupted there can be detrimental impacts on human health and well-being (1.1.4). Disruption of normal sleeping patterns following trans-meridian travel is known as jet-lag, with symptoms including; sleeping difficulties, poor sleep quality, tiredness and exhaustion as well as concentration and memory problems (Roenneberg and Merrow, 2016; Hastings, Brancaccio and Maywood, 2014). Jet-lag results from desynchrony between different endogenous internal clocks as well as between internal clocks and the external environment (1.1.4) (Roenneberg and Merrow, 2016). Social jet-lag is also a growing problem in modern society and is defined as the difference between the timing of sleep on work-days versus free days as a consequence of the fixed timing schedules of the working day (Roenneberg and Merrow, 2016). Being slave to the alarm clock drives misalignment of internal clocks and the external environment manifesting in similar symptoms to jet-lag, as well as being linked to increased incidence of obesity and psychiatric disorders (1.1.4) (Roenneberg and Merrow, 2016; Roenneberg *et al.*, 2012; Wittmann *et al.*, 2006).

It is possible to induce a 'jet-lag-like' state in flies, however unlike mammalian clocks, it requires extreme Light:Dark conditions. In 10 and 4c/wk LD, clocks in the *Drosophila* brain were entrained but peripheral entrainment was lost, indicating internal desynchrony between internal clocks. This was not the case in 5 and 9c/wk as entrainment was seen for both central and peripheral oscillators (Chapter 2 and 4; 5.1.1.1 and 5.1.1.3). Light input is signalled to central clocks via

multiple mechanisms which confers greater plasticity to the brain versus periphery (5.1.1.2). However, the presence of CRY in periphery allows light entrainment of peripheral oscillators independently of the brain (Chapter 4). This is not the case in mammals (1.1.3) and inability to directly entrain peripheral clocks to light may explain why mammals are more susceptible to jet-lag. Circadian disruption has a big impact on mammalian physiology (1.1.4) and it has been shown that mice with chronic jet-lag have increased mortality (Davidson *et al.*, 2006). We have demonstrated that the constant phase re-setting associated with entrainment to extreme long and short photocycles results in reduced life span, especially in female flies (2.3.5). The greater reduction in life-span observed in females might reflect the documented “cost of mating” where female flies die on average 3-8 days before their male counterparts (Fowler and Partridge, 1989). Mating and reproduction costs to females are associated with increased egg production and oviposition, both of which are very energetically demanding, as well as increased feeding and other non-mating activities (Partridge, Green and Fowler, 1987; Partridge and Fowler, 1990). Whereas, mating has a variety of benefits to males including ensuring effective sperm storage and the reduction of female receptivity (Wigby and Chapman, 2005). The sex peptide in the male ejaculate appears to be responsible for this phenotype as receipt of the sex peptide results in the aforementioned decrease in fitness in females (Chapman *et al.*, 1995; Wigby and Chapman, 2005). In addition, genetic ablation of the sex peptide eliminates this effect on life-span (Chapman *et al.*, 1995; Wigby and Chapman, 2005), and males and virgin females display similar patterns of longevity (Lee, Kim and Min, 2013), providing further evidence for the deleterious “cost of mating”.

Although flies are much more resistant to jet-lag than mammals, at extreme conditions when a ‘jet-lag-like’ state is induced, deleterious effects were observed of fly physiology and well-being. Using these conditions it may be possible to model other physiological aspects of jet-lag and circadian disruption using *Drosophila*. This could allow further investigation into the effects of circadian dysfunction and internal desynchrony on the physiology and well-being of mammals and other higher order organisms as well as other invertebrate species. For example, invasive agricultural pests such as *Drosophila suzukii* and disease vectors like the *Anopheles* Mosquito; potentially aiding the development of targeted pest management schemes (1.2.1.1) (Shaw, Fountain and Wijnen, 2018; Shaw *et al.*, 2018; Meireles-Filho and Kyriacou, 2013).

5.1.3 Wide-reaching impact of CRY on *Drosophila* physiology

Aside from the well characterised role of CRY as a circadian blue-light photoreceptor, which has been discussed at length in this thesis, many other functions of CRY have been reported in *Drosophila*. CRY has been shown to; act at the cell membrane to modulate neuronal excitability

Chapter 5:

and arousal (Fogle *et al.*, 2011; Fogle *et al.*, 2015); promote acute arousal and contribute to the nocturnal phenotype of *Clk* mutants, where there are elevated levels of CRY and Dopamine (Kumar, Chen and Sehgal, 2012); and mediate the effect of electromagnetic fields on locomotion (Fedele *et al.*, 2014), by regulating neuronal firing (Giachello *et al.*, 2016) (See Appendix C for more detail). The above effects are all blue-light dependent and impact neuronal excitability of clock-cells; however a recent study has found that CRY helps to maintain passive membrane potential in a light-independent manner in a non-clock tissue (Agrawal *et al.*, 2017). Such diverse roles for CRY allows us to postulate that CRY activity could be tissue specific or that CRY could perform multiple roles within the same cell. Irrespective of its role, CRY contributes significantly to *Drosophila* physiology.

5.2 Conclusions

The results presented in this thesis have led to the following conclusions:

- **Central clocks residing in the wild-type *Drosophila melanogaster* brain are entrainable to equinox photocycles ranging from 16.8 – 42 h.**
 - Wild-type locomotion in these extreme Light:Dark cycles is true light-dependent behavioural entrainment and not masking.
 - Behavioural entrainment is characterised by an advance or delay of the evening peak of activity, with respect to the Light:Dark cycle, as the photoperiod is lengthened or shortened respectively.
- **Light-induced plasticity of central clock cells evokes a phase advance in PER protein in 5c/wk, with a phase delay seen in 10c/wk indicating how the molecular oscillators in central clock cells facilitate entrainment.**
 - The molecular oscillator residing in the s-LN_vs is particularly good at phase-shifting in response to both long and short photocycles.
 - The DN1s and s-LN_vs maintain robust oscillations in short cycles, where other cell types show damped rhythms, suggesting that strong molecular rhythms seen here may be tightly linked to rhythmic behavioural output.
- **Both the CRY/JET pathway and the visual system are required to allow light-induced behavioural entrainment to extreme photocycles.**
 - Mutations affecting *cry*, *jet*, the compound eye or visual transduction drastically reduce behavioural entrainment in 5 and 10c/wk.
 - CRY/JET are required in both the morning and evening cells to allow behavioural entrainment in short and long photocycles. In long cycles the PDF-expressing morning cells alone can rescue entrainment suggesting that these cells contribute significantly to light-induced plasticity.
- **In red Light:Dark conditions light input from the visual system mediates behavioural entrainment via histamine signalling.**

Chapter 5:

- Removal of the compound eye, visual phototransduction and histamine biosynthesis results in flies that are un-responsive to red Light:Dark cycles indicating the importance and versatility of rhodopsin-mediated photoreception.
 - Histamine signalling via the HISCL1 receptor appears to contribute more to red Light:Dark entrainment compared to the ORT receptor.
- **Clocks residing in the peripheral tissues of *Drosophila melanogaster* are entrainable to equinox photocycles ranging from 18.6 – 33.6 h.**
 - Robust entrained luciferase activity rhythms are observed in 9, 7 and 5c/wk with an apparent phase advance, with respect to the Light:Dark cycle, seen in 5c/wk.
 - Light-induced plasticity of the peripheral molecular oscillator is associated with selective reorganisation of clock gene mRNA rhythms.
 - PER protein cycling is locked to the Light:Dark in all conditions.
- **CRY and JET are required for peripheral clock entrainment to any Light:Dark cycle, including 7c/wk.**
 - Mutations affecting *cry* or *jet* severely reduce entrainment of peripheral oscillators to all Light:Dark cycles assayed. Entrainment deficits are comparable to that of clock-less (*tim⁰¹*) flies.
 - The visual system has no impact on peripheral entrainment alluding to a lack of communication between central and peripheral clock cells, and showing peripheral light entrainment relies solely on CRY/JET mediated light input.
- **Entrainment to extreme Light:Dark cycles results in reduced *Drosophila* life-span**
 - The life-span of female flies was significantly reduced in 5 and 10c/wk Light:Dark cycles compared to 7c/wk.
 - Approaching the limits of light-induced entrainment appears to result in desynchrony between internal clocks or between an organism and the external environment leading to detrimental impacts of *Drosophila* longevity.

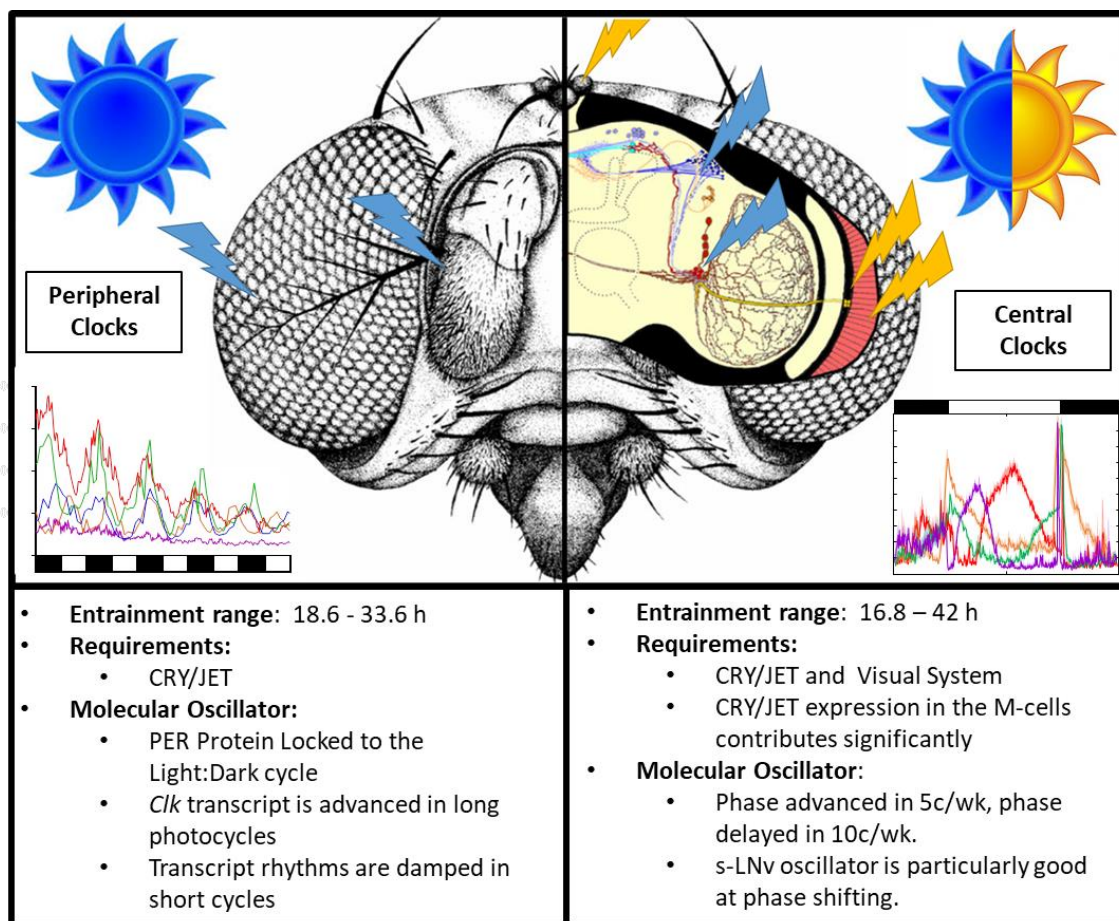


Figure 5.1 Graphical summary: Light-induced plasticity of *Drosophila* central and peripheral circadian clock function.

5.3 Future Directions

As a final consideration for this project, possible experiments are detailed here which aim to further our current understanding of the light-induced plasticity of *Drosophila* circadian clocks and possibly provide the basis for future studies.

- The limits of behavioural entrainment could be further interrogated by assaying wild-type flies in photocycles that are intermediary to our current limits and when entrainment breaks down i.e. a 16 h photocycle (8hL:8hD) and a 48 h photocycle (24hL:24hD). Data for the former has been published (Wheeler *et al.*, 1993). LD cycling in these conditions is either in factors or multiples of 24 and as such it may be assumed that robust entrainment will be seen due to the effect of 'harmonic' components resulting from the bimodality of rhythmic *Drosophila* behaviour. However it should allow further refinement to the limits of behavioural light-induced plasticity. Furthermore, it may be beneficial to re-run 11c/wk experiments with data collected more frequently i.e. every 1 minute instead of every 5 minutes. The increased resolution may improve the accuracy of data plotting and analysis, and therefore result in a more confident interpretation of the data.
- The DNs are a heterogeneous cluster of clock neurons which can receive and signal light and temperature inputs to the circadian circuitry (Beckwith and Ceriani, 2015). The DN1s are known to integrate output from both the M- and E-cells to regulate sleep/wake and locomotor activity (Zhang *et al.*, 2010; Guo *et al.*, 2016; Liang, Holy and Taghert, 2017), as well as signal to and modulate s-LN_v function (Zhang *et al.*, 2010). Furthermore, a subset of the DN1s has been shown to signal to subgroups of Ellipsoid Body Ring Neurons (EB-RN) (Lamaze *et al.*, 2018; Guo *et al.*, 2018), the primary locomotor control centre in insects as well as the Pars Intercerebralis, a neuropil which also connects to downstream locomotor centres (Cavanaugh *et al.*, 2014) (see 1.2.7). In the context of extreme LD cycles, the DN1s along with the s-LN_vs showed robust cycling even when rhythms in all other clock cell subsets were damped. It therefore may prove interesting to further explore the DNs and try to tease apart function of distinct DN clusters, particularly sub-groups of DN1s, in facilitating light-induced plasticity. This could be achieved using an imaging approach, similar to that used in Chapter 2, where specific subgroups of DN1s are identified by expressing GFP using *clk4.1M-Gal4* or *R18H11-Gal4* which is expressed in 8-10 and 7-8 DN1_p neurons respectively (Lamaze *et al.*, 2018).
- Analysis of the wild-type peripheral molecular oscillator could be furthered in two ways; firstly by assaying *tim* mRNA oscillations, as this would provide a direct comparison to *in vivo* luciferase monitoring experiments which utilised the *timeless* promoter (*tim-luc*); and secondly by increasing the sampling frequency, in both qRT-PCR and Western blot

Chapter 5:

experiments, which would increase the resolution of the peaks and troughs of transcript/protein abundance.

- The impact of CRY and JET on entrainment of central and peripheral clocks to extreme photocycles has been investigated either by locomotor activity or *in vivo* luciferase activity monitoring, respectively. Assaying the molecular clockwork in CRY and JET mutants in neuronal and peripheral clocks, as detailed in Chapter 2 and 4 respectively, could be used to evaluate whether the loss in behavioural and peripheral rhythmicity in CRY and JET mutants is recapitulated at the protein and mRNA level.
- Histamine signalling from the visual system facilitates central clock entrainment to red Light:Dark (RLD) cycles. To further investigate the role of the HISCL1 receptor in RLD entrainment, genetic mapping of HISCL1 function could be done using *ds-RNA*, as described in Chapter 3 for the mapping of CRY/JET function, to try and uncover the location of red-light input to the circadian oscillator, building on the work of (Alejevski *et al.*, 2019). Furthermore, analyses with *Rh1 (ninaE)* versus *Rh6* mutants may help address the relative contributions of the Rh1-expressing outer- and Rh6-expressing R8 inner-photoreceptors in facilitating entrainment to extreme RLD cycles. In addition, *in vivo* assessment of neuronal activity in response to red-light using techniques such as calcium imaging could help elucidate the pathway for red-light mediated entrainment (Liang, Holy and Taghert, 2016; Liang, Holy and Taghert, 2017; Liang *et al.*, 2019).
- Throughout this thesis the data for male flies has taken centre stage, as is often the case in the literature. Entrainment of wild-type flies was comparable between genders across all LD cycles assayed; however behavioural differences are apparent with respect to their pattern of daily activity where females display reduced day-time sleep (Helfrich-Förster, 2000; Isaac *et al.*, 2010; Zimmerman *et al.*, 2012; Khericha, Kolenchery and Tauber, 2016). Detailed analysis of central molecular clock function of female flies in the presence of extreme photocycles may therefore help advance our understanding of the gender contribution to circadian behaviour.
- Finally, as discussed in 5.1.2, it may be possible to utilise these extreme photocycles to induce a state of internal desynchrony between *Drosophila* central and peripheral oscillators and further investigate the impact of circadian disruption and dysfunction on physiology.

Appendix A: Supplementary Data

A.1 Genotyping

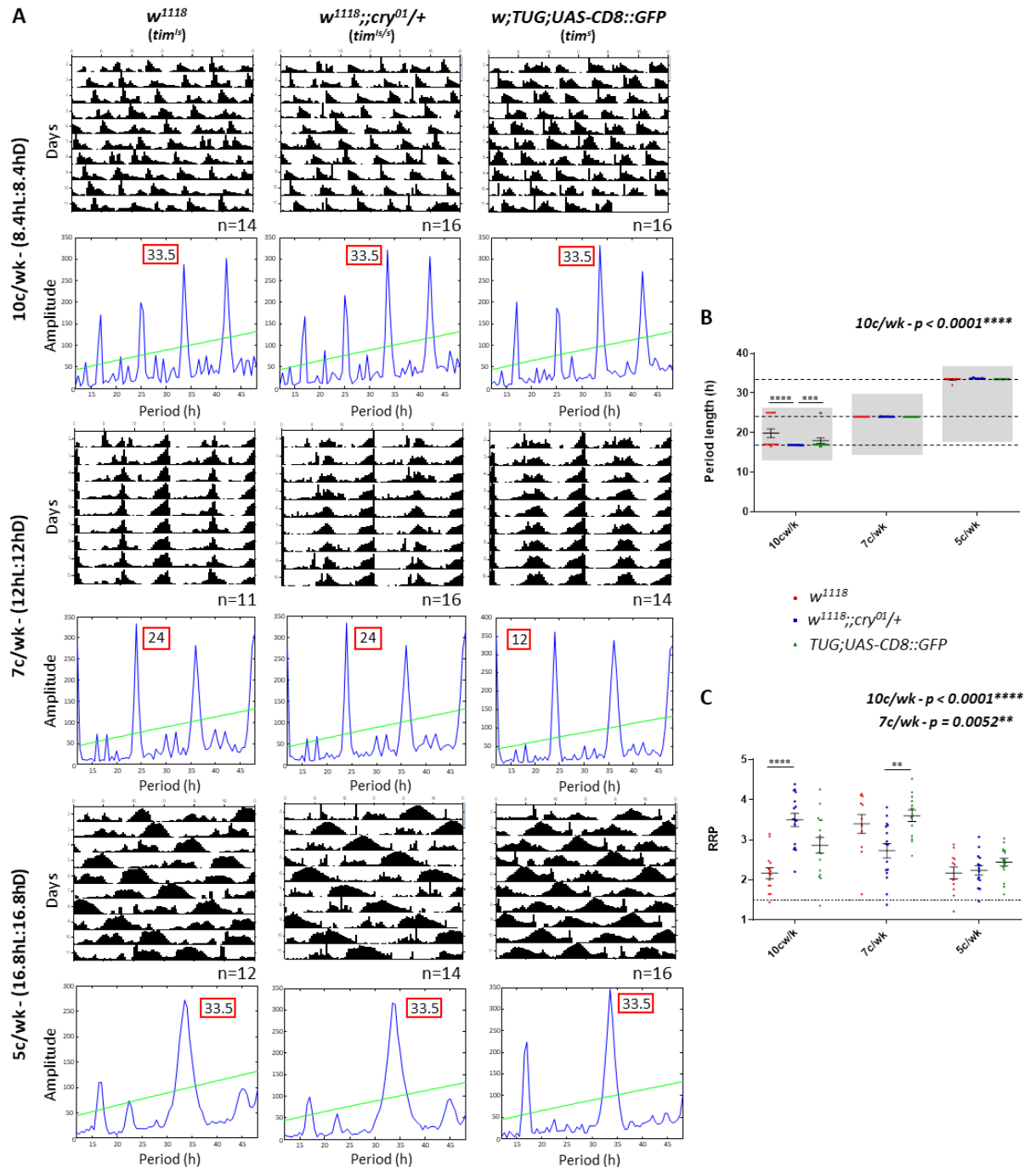
| Genotype | <i>tim</i> Isoform | <i>jet</i> Isoform |
|--|--------------------|--------------------|
| <i>w</i> ¹¹¹⁸ | ls | + |
| <i>w</i> ¹¹¹⁸ ;; <i>cry</i> ⁰¹ | s | + |
| <i>y</i> ¹ <i>w</i> *;; <i>jet</i> ^{set} | s | + |
| <i>per</i> ^s | ls | + |
| <i>per</i> ^L | s | + |
| <i>y</i> ¹ <i>w</i> *;; <i>Pdf</i> ⁰¹ | s | + |
| <i>cyc</i> ⁰¹ <i>ry</i> ⁵⁰⁶ | s | + |
| <i>eya</i> ² | ls | + |
| <i>GMR-hid</i> | s | + |
| <i>norpA</i> ⁷ | ls | + |
| <i>norpA</i> ^{P41} | s | + |
| <i>norpA</i> ⁴¹ ;; <i>cry</i> ⁰² | s | + |
| <i>st</i> ¹ <i>HisCl</i> ^{T2} | ls | + |
| <i>ort</i> ¹ | ls | + |
| <i>Hdc</i> ^{JK910} | ls | + |
| <i>y</i> ¹ <i>w</i> *;; <i>tim-luc:10</i> | s | + |
| <i>y</i> ¹ <i>w</i> * <i>tim-luc</i> ;; <i>cry</i> ⁰¹ | s | + |
| <i>y</i> ¹ <i>w</i> * <i>tim-luc</i> ;; <i>jet</i> ^{set} | s | + |
| <i>UAS-Dcr-2 w</i> *;; <i>UAS-ds-cry</i> ^{3772R2} | s | + |

Appendix A:

| | | |
|---|------|---|
| <i>UAS-Dcr-2 w*;;UAS-dsj-et^{JF01506}</i> | s | + |
| <i>w*;;tim(UAS)-Gal4;Sb¹/TM6B-Tb¹</i> | s | + |
| <i>UAS-Dcr-2 w*;;VGlut-Gal80;UAS-ds-jet^{JF01506}</i> | ls | + |
| <i>UAS-Dcr-2 w*;;UAS-ds-HisCl¹</i> | ls | + |
| <i>UAS-Dcr-2 w*;;UAS-ds-ort¹</i> | s | + |
| <i>w*;;UAS-cry²⁴;cry⁰¹</i> | s | + |
| <i>w*;;Pdf-Gal4;cry⁰¹</i> | s | + |
| <i>w*;;tim₆₂-Gal4</i> | s | + |
| <i>w*;;tim(UAS)-Gal4;UAS-CD8::GFP</i> | s | + |
| <i>w*;;Irf¹/CyO;Sb¹/TM3-Ser¹</i> | s/ls | + |
| <i>w*;;Pdf-Gal80/CyO;Sb¹/TM3-Ser¹</i> | s/ls | + |
| <i>w*;;ChAT-Gal4.7.4;cry⁰¹</i> | ls | + |
| <i>w*;;UAS-hid/CyO;Sb¹/TM3-Ser¹</i> | s | + |
| <i>w*;;UAS-Kir₁/CyO;Sb¹/TM3-Ser¹</i> | s/ls | + |

S.Table 1 Summary of genotyping results testing for *tim* and *jet* isoforms.

tim and *jet* genes were amplified and sequenced to identify possible isoform variation amongst genotypes used. *tim*; *tim^s* or *tim^{ls}*. *jet*; *jet^c* or *jet^r*. 's/ls' denotes heterozygosity. '+' indicates wild-type.



S. Figure 1 Comparison of wild-type locomotor behaviour with differing *tim* isoforms.

A) Average locomotor behaviour (10 days) for male flies of genotype *w¹¹¹⁸ (tim^{LS}* – left), *w¹¹¹⁸;cry⁰¹/+ (tim^{LS/s}* – middle) and *w;TUG;UAS-CD8::GFP (tim^S* – right) in a 10, 7 and 5c/wk LD cycles (top to bottom) shown by double plotted actograms (upper) and χ^2 periodograms (lower – 12-48 h). ‘n’ denotes number of flies and dominant period length were annotated on χ^2 periodograms. **B, C)** Individual male data, *w¹¹¹⁸* (red), *w¹¹¹⁸;cry⁰¹/+* (blue) and *w;TUG;UAS-CD8::GFP* (green). The *Kruskal-Wallis test* comparing period length and RRP across all genotypes in each cognition (reported in each panel). Pairwise comparisons between genotypes within each condition with *Dunn’s multiple comparisons test* reported on graphs. **B) S. Fig 1**

Appendix A:

(cont.): Period length data across all three LD cycles, dashed lines indicate entrained period lengths for 5, 7 and 10c/wk (top to bottom). Grey shading indicates analysis parameters used for individual fly analysis in each LD cycle. 10c/wk; w^{1118} vs. $w^{1118};cry^{01}/+$ – $p < 0.0001$ and $w^{1118};cry^{01}/+$ vs. $w;TUG;UASCD8::GFP$ – $p = 0.0008$. Error bars show mean period length \pm SEM. **C)** RRP data across all three LD cycles, dashed line denotes a RRP value 1.5. Arrhythmic flies are assigned an RRP of 1 and are not included in period length analysis. Error bars show mean RRP \pm SEM. 10c/wk; w^{1118} vs. $w^{1118};cry^{01}/+$ – $p < 0.0001$. 7c/wk; $w^{1118};cry^{01}/+$ vs. $w;TUG;UASCD8::GFP$ – $p = 0.0073$.

A.2 Supplementary Tables: Chapter 2

| Genotype (K-W test) | Condition (ExT Tau) | n | Standard Analysis Parameters | | Refined Analysis Parameters | | | |
|---|------------------------|----|------------------------------|-----------------|-----------------------------|------------------|----------------------------|----------------------------|
| | | | %R•%WR•%AR | %ExT•%Other•%AR | Tau (ExT) ±SEM (h) | RRP(ExT) ±SEM | RRP(ExT)/RRP(x1.5) ±SEM | RRP(ExT)/RRP(x0.5) ±SEM |
| <i>cry⁰¹/+</i> (****††††) | 11c/wk (15.2) | 16 | 100•0•0 | 37•63•0*** | 15.47 ±0.031 | 2.495 ±0.209 | 1.044 ±0.127*** | - |
| | 10c/wk (16.8) | 16 | 100•0•0 | 100•0•0 | 16.94 ±0.043 | 2.271 ±0.101 | 1.225 ±0.059 | - |
| | 9c/wk (18.66) | 31 | 94•6•0 | 100•0•0 | 18.53 ±0.022 | 2.854 ±0.123 | 1.027 ±0.039*** | - |
| | 8c/wk (21) | 32 | 100•0•0 | 100•0•0 | 21 ±0 | 4.492 ±0.115** | 1.586 ±0.025 | - |
| | 7c/wk (24) | 16 | 94•6•0 | 100•0•0 | 24 ±0 | 2.988 ±0.161 | 1.658 ±0.033 | 0.79 ±0.023††† |
| | 6c/wk (28) | 16 | 100•0•0 | 100•0•0 | 28 ±0 | 3.713 ±0.142 | - | 0.905 ±0.029 |
| | 5c/wk (33.6) | 14 | 93•7•0 | 100•0•0 | 33.81 ±0.07 | 2.315 ±0.147 | - | 1.803 ±0.088**** |
| | 4c/wk (42) | 15 | 87•13•0 | 100•0•0 | 42 ±0 | 2.31 ±0.08 | - | 1.721 ±0.086**** |
| | 3c/wk (56) | 16 | 87•13•0 | 100•0•0 | 56.05 ±0.075 | 1.782 ±0.062** | - | 0.889 ±0.043 |
| <i>per⁰¹</i> (****††††) | 11c/wk (15.2) | 10 | 73•27•0 | 27•73•0**** | 15.39 ±0.073 | 1.843 ±0.295† | 1.066 ±0.16** | - |
| | 10c/wk (16.8) | 16 | 54•44•0***†† | 87•13•0 | 17 ±0 | 1.624 ±0.097†† | 1.439 ±0.076 | - |
| | 9c/wk (18.66) | 16 | 44•50•6***††† | 88•6•6 | 18.53 ±0.033 | 1.586 ±0.122†††† | 1.163 ±0.126* | - |
| | 8c/wk (21) | 32 | 81•13•6 | 90•0•6 | 21.02 ±0.016 | 2.385 ±0.149†††† | 1.677 ±0.069 | - |

Appendix A:

| | | | | | | | | |
|--|---------------|----|------------------|---------------|-----------------|-----------------------|-----------------|-------------------|
| | 7c/wk (24) | 32 | 100•0•0 | 100•0•0 | 24 ±0 | 2.256 ±0.123† | 1.681 ±0.101 | 0.927 ±0.063### |
| | 6c/wk (28) | 15 | 60•33•7***†† | 86•7•7 | 28 ±0 | 1.771 ±0.207†††† | - | 1.008 ±0.085 |
| | 5c/wk (33.6) | 31 | 50•37•13***† | 87•0•13 | 33.53 ±0.055††† | 1.477 ±0.076***†††† | - | 1.375 ±0.062***†† |
| | 4c/wk (42) | 16 | 0•75•25*****†††† | 50•25•25***†† | 42.31 ±0.21 | 1.064 ±0.02*****†††† | - | 1.027 ±0.045†††† |
| | 3c/wk (44.8) | 12 | 0•62•38*****†††† | 54•8•38***†† | 55.94 ±0.118 | 1.148 ±0.065*****†††† | - | 1.102 ±0.074† |
| <i>per</i> ^s (*****††††) | 10c/wk (16.8) | 16 | 87•13•0 | 50•50•0***†† | 16.94 ±0.043 | 1.794 ±0.109**** | 1.07 ±0.062**** | - |
| | 7c/wk (24) | 10 | 100•0•0 | 100•0•0 | 24 ±0 | 3.29 ±0.198 | 2.552 ±0.133† | 1.308 ±0.06††††† |
| | 5c/wk (33.6) | 9 | 89•11•0 | 100•0•0 | 33.5 ±0† | 1.91 ±0.121** | - | 1.848 ±0.103 |
| <i>per</i> ^L | 10c/wk (16.8) | 16 | 13•56•31†††† | 56•13•31†† | 16.83 ±0.083 | 1.232 ±0.119†††† | 1.35 ±0.184 | - |
| | 7c/wk (24) | 16 | 31•44•25††† | 62•13•25† | 24 ±0 | 1.353 ±0.101†††† | 1.468 ±0.117 | 1.251 ±0.074††† |
| | 5c/wk (33.6) | 16 | 29•64•7†† | 90•0•7 | 33.77 ±0.146 | 1.369 ±0.081††† | - | 1.07 ±0.061†††† |

| Genotype (K-W test) | Condition | n | Standard Analysis Parameters | | Refined Analysis Parameters | | | | |
|-------------------------------------|--|---------------|------------------------------|-----------------|-----------------------------|-----------------|-------------------------|-------------------------|--------------|
| | | | %R•%WR•%AR | %ExT•%Other•%AR | Tau (ExT) ±SEM (h) | RRP(ExT) ±SEM | RRP(ExT)/RRP(x1.5) ±SEM | RRP(ExT)/RRP(x0.5) ±SEM | |
| ♀ | <i>cry</i> ⁰¹ / <i>+</i> (****+) | 11c/wk (15.2) | 15 | 40•20•40** | 40•20•40*** | 15.17 ±0.083 | 1.71 ±0.266 | 2.049 ±0.397 | - |
| | | 10c/wk (16.8) | 16 | 38•62•0 | 75•25•0 | 17 ±0 | 1.31 ±0.07 | 1.392 ±0.078 | - |
| | | 9c/wk (18.66) | 32 | 50•31•19* | 81•0•19 | 18.48 ±0.017 | 1.756 ±0.115 | 1.292 ±0.096 | - |
| | | 8c/wk (21) | 32 | 100•0•0**** | 100•0•0 | 21 ±0 | 3.115 ±0.118*** | 2.029 ±0.082 | - |
| | | 7c/wk (24) | 15 | 20•80•0 | 93•7•0 | 23.93 ±0.071 | 1.502 ±0.124 | 1.486 ±0.1 | 1.124 ±0.056 |
| | | 6c/wk (28) | 14 | 64•36•0* | 100•0•0 | 27.93 ±0.049 | 2.396 ±0.311 | - | 1.332 ±0.103 |
| | | 5c/wk (33.6) | 15 | 13•87•0 | 93•7•0 | 33.68 ±0.135 | 1.448 ±0.079 | - | 1.413 ±0.078 |
| | | 4c/wk (42) | 15 | 0•53•47** | 53•0•47** | 41.81 ±0.266 | 1.079 ±0.023 | - | 1.128 ±0.032 |
| | | 3c/wk (56) | 16 | 0•38•62*** | 37•0•63*** | 55.98 ±0.186 | 1.099 ±0.041 | - | 1.035 ±0.088 |
| <i>per</i> ⁰¹ (****+) | 11c/wk (15.2) | 13 | 85•15•0 | 85•15•0 | 15.15 ±0.067 | 2.153 ±0.27 | 1.714 ±0.244 | - | |
| | 10c/wk (16.8) | 15 | 100•0•0+++ | 93•7•0 | 16.9 ±0.053 | 3.118 ±0.26+++ | 2.088 ±0.199† | - | |
| | 9c/wk (18.66) | 13 | 92•8•0† | 100•0•0 | 18.5 ±0 | 2.474 ±0.242++ | 1.923 ±0.264++ | - | |
| | 8c/wk (21) | 25 | 100•0•0 | 100•0•0 | 21 ±0 | 2.387 ±0.129+++ | 2.005 ±0.125 | - | |
| | 7c/wk (24) | 29 | 87•13•0+++ | 100•0•0 | 24 ±0 | 2.387 ±0.142++ | 1.84 ±0.094 | 1.079 ±0.074+++ | |
| | 6c/wk (28) | 15 | 60•13•27 | 73•0•27* | 28 ±0 | 1.84 ±0.196 | - | 1.024 ±0.111++ | |

Appendix A:

| | | | | | | | | |
|---------------------------------|---------------|----|-----------------|-------------|-----------------|-------------------|----------------|---------------|
| | 5c/wk (33.6) | 29 | 79•14•7††† | 93•0•7 | 33.5 ±0 | 1.744 ±0.085 | - | 1.477 ±0.075 |
| | 4c/wk (42) | 16 | 6•75•19**** | 62•19•19* | 42.05 ±0.106 | 1.15 ±0.064**** | - | 1.065 ±0.098 |
| | 3c/wk (56) | 15 | 7•60•33****†††† | 67•0•33* | 56.13 ±0.09 | 1.43 ±0.077**†††† | - | 1.291 ±0.1 |
| <i>per</i> ^s (†) | 10c/wk (16.8) | 10 | 30•50•20 | 80•0•20† | 17 ±0 | 1.605 ±0.228* | 1.724 ±0.268 | - |
| | 7c/wk (24) | 12 | 75•8•17††† | 83•0•17 | 24 ±0 | 2.298 ±0.246 | 2.351 ±0.216†† | 1.652 ±0.13†† |
| | 5c/wk (33.6) | 7 | 57•53•0 | 86•14•0 | 33.14 ±0.21†† | 1.746 ±0.123 | - | 1.746 ±0.123 |
| <i>per</i> ^L (**) | 10c/wk (16.8) | 15 | 7•20•73†††† | 27•0•73†††† | 16.88 ±0.125 | 1.108 ±0.059 | 1.407 ±0.144 | - |
| | 7c/wk (24) | 14 | 0•57•43†† | 43•14•43†† | 24.17 ±0.105††† | 1.09 ±0.034 | 1.173 ±0.051 | 1.085 ±0.043 |
| | 5c/wk (33.6) | 14 | 29•64•7* | 90•0•7* | 33.62 ±0.083 | 1.422 ±0.107* | - | 1.423 ±0.116 |

S.Table 2 Male and Female locomotor activity of wild-type and per mutant flies in 11 – 3c/wk equinox LD cycles.

Male (top) and female (bottom) flies of **genotype**; $w^{1118}; cry^{01}/+, y^1 per^{01} w^*$, per^S and per^L with result of Kruskal-Wallis test comparing RRP (*) and RRP ratios (†) between all conditions within each genotype. **Condition**, LD cycle with expected entrained period length. **n**, number of flies. **%R•%WR•%AR**, percentage of flies classified and rhythmic (R), weakly rhythmic (WR) and arrhythmic (AR). **%ExT•%Other•%AR**, percentage of flies classified and entrained (ExT), other and arrhythmic (AR). Fisher's exact test for each condition vs. 7c/wk within each genotype for %R•%WR•%AR and %ExT•%Other•%AR (*). Fisher's exact test for each genotype vs. $cry^{01}/+$ in each condition for %R•%WR•%AR and %ExT•%Other•%AR (†). **Tau (ExT) ±SEM (h)**, mean period length using narrow refined analysis parameters at ExT period length. **RRP (ExT) ±SEM**, mean relative rhythmic power using narrow refined analysis parameters at ExT period length. AR flies were assigned RRP=1 and omitted from period length analysis. Pairwise Mann-Whitney test for each genotype vs. $cry^{01}/+$ in each condition for Tau (ExT) ±SEM (h) and RRP (ExT) ±SEM (†). Pairwise Mann-Whitney test in each condition vs. 7c/wk within each genotype for RRP (ExT) ±SEM (*). **RRP(ExT)/RRP(x1.5) ±SEM** and **RRP(ExT)/RRP(x0.5) ±SEM**, ratio of entrained RRP and RRP at x1.5 T cycle harmonic (short T cycles) and x0.5 T cycle harmonic (long T cycles) respectively. For crepuscular bimodal patterns these variables will be closer to 1 than for entrained patterns with stronger unimodal components. Pairwise Mann-Whitney test for RRP ratio vs. 7c/wk RRP ratio within each genotype for RRP(ExT)/RRP(x1.5) ±SEM and RRP(ExT)/RRP(x0.5) ±SEM (*). Pairwise Mann-Whitney test for each genotype vs. $cry^{01}/+$ in each condition for RRP(ExT)/RRP(x1.5) ±SEM and RRP(ExT)/RRP(x0.5) ±SEM (†). Pairwise Mann-Whitney test for RRP(ExT)/RRP(x1.5) ±SEM vs. RRP(ExT)/RRP(x0.5) ±SEM for 7c/wk within each genotype (‡). See **S.Table B.5** for standard and refined analysis parameters. In all cases (*, † and ‡): $p^{****}<0.0001$; $0.0001<p^{***}<0.001$; $0.001<p^{**}<0.01$; $0.01<p^*<0.05$.

Appendix A:

| Cycle Comparison | Male | | | | Female | | | |
|---------------------|-------------------------------------|--------------------------|-------------------------|-------------------------|-------------------------------------|--------------------------|-------------------------|-------------------------|
| | <i>cry</i> ⁰¹ / <i>+</i> | <i>per</i> ⁰¹ | <i>per</i> ^S | <i>per</i> ^L | <i>cry</i> ⁰¹ / <i>+</i> | <i>per</i> ⁰¹ | <i>per</i> ^S | <i>per</i> ^L |
| 11c/wk vs. 10c/wk | ns | ns | - | - | ns | ns | - | - |
| 11c/wk vs. 9c/wk | ns | ns | - | - | ns | ns | - | - |
| 11c/wk vs. 8c/wk | **** | ns | - | - | **** | ns | - | - |
| 11c/wk vs. 7c/wk | ns | ns | - | - | ns | ns | - | - |
| 11c/wk vs. 6c/wk | ** | ns | - | - | ns | ns | - | - |
| 11c/wk vs. 5c/wk | ns | ns | - | - | ns | ns | - | - |
| 11c/wk vs. 4c/wk | ns | ns | - | - | ns | * | - | - |
| 11c/wk vs. 3c/wk | ns | ns | - | - | ns | ns | - | - |
| 10c/wk vs. 9c/wk | ns | ns | - | - | ns | ns | - | - |
| 10c/wk vs. 8c/wk | **** | ns | - | - | **** | ns | - | - |
| 10c/wk vs. 7c/wk | ns | ns | **** | ns | ns | ns | * | ns |
| 10c/wk vs. 6c/wk | *** | ns | - | - | ns | ** | - | - |
| 10c/wk vs. 5c/wk | ns | ns | ns | ns | ns | *** | ns | ** |
| 10c/wk vs. 4c/wk | ns | * | - | - | ns | **** | - | - |
| 10c/wk vs. 3c/wk | ns | ns | - | - | ns | **** | - | - |
| 9c/wk vs. 8c/wk | **** | ns | - | - | *** | ns | - | - |
| 9c/wk vs. 7c/wk | ns | ns | - | - | ns | ns | - | - |
| 9c/wk vs. 6c/wk | ns | ns | - | - | ns | ns | - | - |
| 9c/wk vs. 5c/wk | ns | ns | - | - | ns | ns | - | - |
| 9c/wk vs. 4c/wk | ns | ns | - | - | * | *** | - | - |
| 9c/wk vs. 3c/wk | ** | ns | - | - | ** | * | - | - |
| 8c/wk vs. 7c/wk | ** | ns | - | - | *** | ns | - | - |
| 8c/wk vs. 6c/wk | ns | ns | - | - | ns | ns | - | - |
| 8c/wk vs. 5c/wk | **** | *** | - | - | *** | ns | - | - |
| 8c/wk vs. 4c/wk | **** | **** | - | - | **** | **** | - | - |
| 8c/wk vs. 3c/wk | **** | **** | - | - | **** | ** | - | - |
| 7c/wk vs. 6c/wk | ns | ns | - | - | ns | ns | - | - |
| 7c/wk vs. 5c/wk | ns | ** | ** | ns | ns | ns | ns | * |
| 7c/wk vs. 4c/wk | ns | **** | - | - | ns | **** | - | - |

| | | | | | | | | |
|-----------------|------|------|---|---|-----|----|---|---|
| 7c/wk vs. 3c/wk | ** | **** | - | - | ns | ** | - | - |
| 6c/wk vs. 5c/wk | ** | ns | - | - | ns | ns | - | - |
| 6c/wk vs. 4c/wk | ** | * | - | - | *** | ns | - | - |
| 6c/wk vs. 3c/wk | **** | ns | - | - | *** | ns | - | - |
| 5c/wk vs. 4c/wk | ns | ns | - | - | ns | ns | - | - |
| 5c/wk vs. 3c/wk | ns | ns | - | - | ns | ns | - | - |
| 4c/wk vs. 3c/wk | ns | ns | - | - | ns | ns | - | - |

S.Table 3 Results of Dunn's Multiple comparison test between RRP for all LD cycles.

Male and female flies of genotype; $w^{1118}; cry^{01}/+, y^1 per^{01} w^*, per^S$ and per^L . $p^{****} < 0.0001$; $0.0001 < p^{***} < 0.001$; $0.001 < p^{**} < 0.01$; $0.01 < p^* < 0.05$.

Appendix A:

| Cycle Comparison | Male | | Female | |
|------------------------|-------------------------------------|--------------------------|-------------------------------------|--------------------------|
| | <i>cry</i> ⁰¹ / <i>+</i> | <i>per</i> ⁰¹ | <i>cry</i> ⁰¹ / <i>+</i> | <i>per</i> ⁰¹ |
| 11c/wk vs. 10c/wk | ns | ns | ns | ns |
| 11c/wk vs. 9c/wk | ns | ns | ns | ns |
| 11c/wk vs. 8c/wk | *** | ** | ns | ns |
| 11c/wk vs. 7c/wk (1.5) | *** | ** | ns | ns |
| 11c/wk vs. 7c/wk (0.5) | ns | ns | ns | ns |
| 11c/wk vs. 6c/wk | ns | ns | ns | ns |
| 11c/wk vs. 5c/wk | *** | ns | ns | ns |
| 11c/wk vs. 4c/wk | *** | ns | ns | ns |
| 11c/wk vs. 3c/wk | ns | ns | ns | ns |
| 10c/wk vs. 9c/wk | ns | ns | ns | ns |
| 10c/wk vs. 8c/wk | ns | ns | ns | ns |
| 10c/wk vs. 7c/wk (1.5) | ns | ns | ns | ns |
| 10c/wk vs. 7c/wk (0.5) | * | *** | ns | **** |
| 10c/wk vs. 6c/wk | ns | * | ns | *** |
| 10c/wk vs. 5c/wk | ns | ns | ns | ns |
| 10c/wk vs. 4c/wk | ns | ns | ns | ** |
| 10c/wk vs. 3c/wk | ns | ns | ns | ns |
| 9c/wk vs. 8c/wk | **** | ** | **** | ns |
| 9c/wk vs. 7c/wk (1.5) | *** | * | ns | ns |
| 9c/wk vs. 7c/wk (0.5) | ns | ns | ns | ** |
| 9c/wk vs. 6c/wk | ns | ns | ns | * |
| 9c/wk vs. 5c/wk | **** | ns | ns | ns |
| 9c/wk vs. 4c/wk | *** | ns | ns | ns |
| 9c/wk vs. 3c/wk | ns | ns | ns | ns |
| 8c/wk vs. 7c/wk (1.5) | ns | ns | ns | ns |
| 8c/wk vs. 7c/wk (0.5) | **** | **** | **** | **** |
| 8c/wk vs. 6c/wk | **** | **** | *** | *** |
| 8c/wk vs. 5c/wk | ns | ns | * | ns |
| 8c/wk vs. 4c/wk | ns | ** | *** | *** |

| | | | | |
|-----------------------------|------|------|------|------|
| 8c/wk vs. 3c/wk | **** | ns | **** | * |
| 7c/wk (1.5) vs. 7c/wk (0.5) | **** | **** | ns | **** |
| 7c/wk (1.5) vs. 6c/wk | **** | *** | ns | *** |
| 7c/wk (1.5) vs. 5c/wk | ns | ns | ns | ns |
| 7c/wk (1.5) vs. 4c/wk | ns | ** | ns | ** |
| 7c/wk (1.5) vs. 3c/wk | **** | ns | ns | ns |
| 7c/wk (0.5) vs. 6c/wk | ns | ns | ns | ns |
| 7c/wk (0.5) vs. 5c/wk | **** | **** | ns | ns |
| 7c/wk (0.5) vs. 4c/wk | **** | ns | ns | ns |
| 7c/wk (0.5) vs. 3c/wk | ns | ns | ns | ns |
| 6c/wk vs. 5c/wk | **** | ns | ns | ns |
| 6c/wk vs. 4c/wk | **** | ns | ns | ns |
| 6c/wk vs. 3c/wk | ns | ns | ns | ns |
| 5c/wk vs. 4c/wk | ns | ns | ns | ns |
| 5c/wk vs. 3c/wk | **** | ns | ns | ns |
| 4c/wk vs. 3c/wk | **** | ns | ns | ns |

S.Table 4 Results of Dunn's Multiple comparison test between RRP(ExT)/RRP(x1.5 or x0.5) for all LD cycles.

Male and female flies of genotype; $w^{1118}; cry^{01}/+$ and $\gamma^1 per^{01} w^*$. $p^{****} < 0.0001$; $0.0001 < p^{***} < 0.001$; $0.001 < p^{**} < 0.01$; $0.01 < p^* < 0.05$.

Appendix A:

| | Genotype (K-W test) | Prior LD Condition | n | %R•%WR•%AR | Tau (h) ±SEM | RRP ±SEM | |
|------------------------------------|--|--|--------|--------------|------------------|-------------------|--------------|
| | | | | | | | |
| DD | <i>cry</i> ⁰¹ /+ (*****) | 10c/wk | 14 | 79•21•0 | 23 ±0.091†† | 1.692 ±0.077† | |
| | | 7c/wk | 11 | 100•0•0 | 23.95 ±0.081 | 2.206 ±0.152 | |
| | | 5c/wk | 12 | 75•25•0 | 24.54 ±0.074†††† | 1.694 ±0.097 | |
| | <i>per</i> ⁰¹ | 10c/wk | 16 | 0•31•69**** | 27.5 ±2.962 | 1.013 ±0.005**** | |
| | | 7c/wk | 13 | 0•46•54**** | 22.08 ±2.063 | 1.034 ±0.013**** | |
| | | 5c/wk | 13 | 0•8•92**** | 20 | 1.001 ±0.001****† | |
| | <i>per</i> ^s (*††††) | 10c/wk | 14 | 86•14•0†††† | 19.36 ±0.082**† | 2.547 ±0.207†† | |
| | | 7c/wk | 13 | 15•62•23**** | 19.65 ±0.076 | 1.284 ±0.109* | |
| | | 5c/wk | 14 | 93•7•0†††† | 19.39 ±0.077** | 3.204 ±0.27†††† | |
| | <i>per</i> ^L | 10c/wk | 27 | 0•47•53**** | 28 ±0.787 | 1.04 ±0.018**** | |
| | | 7c/wk | 13 | 0•36•64**** | 27.15 ±0.472 | 1.105 ±0.047**** | |
| | | 5c/wk | 29 | 4•41•55**** | 26.92 ±1.368 | 1.061 ±0.022**** | |
| | DD | <i>cry</i> ⁰¹ /+ (*****) | 10c/wk | 16 | 16•68•13 | 23.18 ±0.145† | 1.287 ±0.054 |
| | | | 7c/wk | 10 | 50•40•10 | 24.44 ±0.53 | 1.449 ±0.092 |
| | | | 5c/wk | 15 | 0•67•13 | 24.62 ±0.272††† | 1.32 ±0.071 |
| <i>per</i> ⁰¹ | | 10c/wk | 15 | 0•13•87**** | 23.75 ±5.75 | 1.008 ±0.007**** | |
| | | 7c/wk | 9 | 0•0•100**** | - | - | |
| | | 5c/wk | 11 | 0•18•82** | 25.75 ±2.75 | 1.011 ±0.009**** | |
| <i>per</i> ^s (*††††) | | 10c/wk | 16 | 50•37•13 | 19.46 ±0.533* | 1.751 ±0.2† | |
| | | 7c/wk | 6 | 17•17•66 | 19.25 ±0.25 | 1.141 ±0.121 | |
| | | 5c/wk | 15 | 20•47•33 | 19.45 ±0.05* | 1.312 ±0.126 | |
| <i>per</i> ^L | | 10c/wk | 22 | 0•45•55** | 26.7 ±1.057 | 1.082 ±0.028* | |
| | | 7c/wk | 28 | 4•25•71*** | 27.75 ±1.052 | 1.089 ±0.033**** | |
| | | 5c/wk | 24 | 0•42•58** | 29.1 ±0.446* | 1.093 ±0.032* | |

S.Table 5 Male and female locomotor activity of wild-type and period mutants in DD following 10, 7 and 5c/wk LD entrainment (30min bins).

Male (top) and female (bottom) flies of **genotype**; $w^{1118}; cry^{01}/+, y^1 per^{01} w^*$, per^S and per^L with result of *Kruskal-Wallis test* comparing Period length (*) and RRP (†) between all conditions within each genotype. **n**, number of flies. **%R•%WR•%AR**, percentage of flies classified and rhythmic (R), weakly rhythmic (WR) and arrhythmic (AR). *Fisher's exact test* vs. $cry^{01}/+$ in each condition for %R•%WR•%AR (*). *Fisher's exact test* between all conditions within each genotype for %R•%WR•%AR; vs. 7c/wk (†) and vs. 10c/wk (‡). **Tau (h) ±SEM**, mean period length. **RRP ±SEM**, mean relative rhythmic power. AR flies were assigned RRP=1 and omitted from period length analysis. *Pairwise Mann-Whitney test* vs. $cry^{01}/+$ in each condition for Tau (h) ±SEM and RRP ±SEM (*). *Dunn's Multiple Comparison test* between all conditions within each genotype for Tau (h) ±SEM and RRP ±SEM; vs. 7c/wk (†) and vs. 10c/wk (‡). In all cases (*, † and ‡): $p^{****}<0.0001$; $0.0001<p^{***}<0.001$; $0.001<p^{**}<0.01$; $0.01<p^*<0.05$. per^S and per^L DD data was collected by Miss Nanthilde Malandain.

Appendix A:

| Cell Subset | LD Cycle | ZT - [h post L _{off}] | Total CTCF ±SEM | Nuclear CTCF ±SEM | Nuclear/Cytoplasmic |
|-----------------------|-----------------|---------------------------------|------------------|-------------------|---------------------|
| | | | | | Ratio ±SEM |
| s-LN _v | 10c/wk ***** | 20 - [5.6] | 885.1 ±67.67 | 254.4 ±30.02 | 1.729 ±0.7152 |
| | | 4 - [11.2] | 2015 ±99.5*** | 1075 ±70.2**** | 1.423 ±0.07748*** |
| | | 12 - [16.8/0] | 716 ±42.14 | 397.6 ±26.63 | 1.227 ±0.07502*** |
| | 7c/wk ***** | 17.6 - [5.6] | 584.8 ±60.55 | 202.5 ±28.04 | 1.45 ±0.4721 |
| | | 23.2 - [11.2]***** | 2699 ±146.5 | 1802 ±107.3 | 2.129 ±0.186 |
| | | 4.8 - [16.8]***** | 798.5 ±46.82 | 553.1 ±39.76 | 2.684 ±0.2412 |
| | 5c/wk ***** | 16 - [5.6] | 824.7 ±74.62 | 304.4 ±42.22 | 1.564 ±0.7538 |
| | | 20 - [11.2] | 2529 ±87.23+++ | 1746 ±90.36++++ | 2.167 ±0.129++++ |
| | | 0 - [16.8] | 1923 ±100.6***** | 1502 ±84.66***** | 4.26 ±0.3722***** |
| | 3c/wk ***** | 17.1 - [12] | 2014 ±130.2 | 1362 ±94.7 | 2.223 ±0.1043 |
| | | 21.4 - [22] | 686.7 ±54.37 | 393 ±33.33 | 1.354 ±0.09456 |
| | | 1.7 - [32] | 2092 ±152.3 | 671.4 ±69.08 | 0.5269 ±0.06129 |
| I-LN _v | 10c/wk ***** | 20 - [5.6] | 1769 ±109.7** | 558.6 ±54.5 | 0.6207 ±0.03202 |
| | | 4 - [11.2] | 2378 ±90.8**** | 1132 ±50.1**** | 1.05 ±0.04754**** |
| | | 12 - [16.8/0] | 1077 ±61.89 | 498.8 ±35.15 | 0.8919 ±0.04753**** |
| | 7c/wk ***** | 17.6 - [5.6]** | 1079 ±86.06 | 356.3 ±52.52 | 0.7512 ±0.08788 |
| | | 23.2 - [11.2]***** | 4309 ±152.9 | 3281 ±150.3 | 4.533 ±0.5806 |
| | | 4.8 - [16.8]***** | 1103 ±78.5 | 674.7 ±49.35 | 2.465 ±0.2779 |
| | 5c/wk ***** | 16 - [5.6] | 1418 ±120.6 | 556.3 ±68.17 | 0.8893 ±0.2371 |
| | | 20 - [11.2] | 4035 ±144++++ | 2562 ±123.2***** | 1.855 ±0.127**++++ |
| | | 0 - [16.8] | 3082 ±188.8***** | 2470 ±167.3***** | 4.059 ±0.3081***** |
| | 3c/wk ***** | 17.1 - [12] | 2814 ±166.7 | 1959 ±132.8 | 2.256 ±0.1108 |
| | | 21.4 - [22] | 1873 ±181.8 | 954.5 ±106.5 | 1.035 ±0.05728 |
| | | 1.7 - [32] | 2290 ±163 | 946.8 ±89.4 | 0.7806 ±0.08731 |
| 5th s-LN _v | 10/wk *** | 20 - [5.6] | 617 ±125.1 | 223.6 ±60.2 | 0.9058 ±0.2457 |
| | | 4 - [11.2] | 1278 ±152.9 | 646 ±90.71* | 1.121 ±0.1173*** |
| | | 12 - [16.8/0] | 638.4 ±106.5 | 323.8 ±50.96 | 1.461 ±0.2796 |
| | 7c/wk ***** | 17.6 - [5.6] | 499.2 ±0 | 289.8 ±0 | 1.384 ±0 |
| | | 23.2 - [11.2]***** | 1978 ±192.9 | 1361 ±204.4 | 2.598 ±0.3556 |
| | | 4.8 - [16.8]***** | 518.1 ±85.11 | 314.1 ±54.09 | 2.224 ±0.335 |

| | | | | | |
|-----------------|-------------------------|----------------------------|----------------------|----------------------|-----------------------|
| | 5c/wk **†‡ | 16 - [5.6] | 245.4 ±90.67 | 82.12 ±47.53 | 0.659 ±0.05789 |
| | | 20 - [11.2] | 2739 ±258.2†††† | 1499 ±190.1†††† | 1.594 ±0.3045* |
| | | 0 - [16.8] | 2028 ±273*****††† | 1451 ±210.2*****††† | 3.476 ±0.5895†† |
| | 10c/wk *****†††† | 20 - [5.6] | 796.3 ±35.35 | 361.5 ±18.5 | 1.13 ±0.1963 |
| | | 4 - [11.2] | 1549 ±73.67**** | 802.4 ±38.05**** | 1.155 ±0.03413**** |
| | | 12 - [16.8/0] | 636.2 ±31.57**** | 331.1 ±18.44**** | 1.081 ±0.05256**** |
| LN _d | 7c/wk *****†††††††† | 17.6 - [5.6] | 820.8 ±70.01 | 275.6 ±26.51 | 0.9797 ±0.0927 |
| | | 23.2 - [11.2]*****†††††††† | 3055 ±116.7 | 2066 ±102.1 | 3.338 ±0.292 |
| | | 4.8 - [16.8]*****†††††††† | 999.5 ±50.89 | 682.9 ±40.79 | 2.337 ±0.1202 |
| | 5c/wk *****†††††††† | 16 - [5.6] | 786.9 ±52.59 | 379.4 ±31.83 | 0.8444 ±0.0343 |
| | | 20 - [11.2] | 2971 ±104.7†††† | 1959 ±131.3†††† | 1.715 ±0.08008*****†† |
| | | 0 - [16.8] | 1911 ±111.9*****†††† | 1549 ±121.7*****†††† | 3.918 ±0.2761*****††† |
| | 3c/wk *****†††††††† | 17.1 - [12] | 1863 ±107.9 | 1396 ±87.56 | 2.735 ±0.1017 |
| | | 21.4 - [22] | 729.6 ±82.14 | 449.1 ±50.93 | 1.578 ±0.1552 |
| | | 1.7 - [32] | 1215 ±77.78 | 545.2 ±48.44 | 0.8578 ±0.06395 |
| | 10c/wk *****†††† | 20 - [5.6] | 772.8 ±34.55** | 235.7 ±15.07**** | 1.332 ±0.2558 |
| | | 4 - [11.2] | 1893 ±69.47 | 1104 ±43.44**** | 1.997 ±0.2017**** |
| | | 12 - [16.8/0] | 786.6 ±36.32**** | 509.2 ±26.06**** | 3.18 ±0.5001 |
| DN1 | 7c/wk *****†††††††† | 17.6 - [5.6]*****†††† | 1014 ±76.11 | 593 ±65.75 | 2.03 ±0.2582 |
| | | 23.2 - [11.2]*****†††††††† | 2071 ±60.39 | 1504 ±64.75 | 4.918 ±0.576 |
| | | 4.8 - [16.8]*****†††††††† | 426.4 ±19.64 | 337.6 ±16.64 | 5.001 ±0.7786 |
| | 5c/wk *****†††††††† | 16 - [5.6] | 763.5 ±38.53** | 472 ±27.71†††† | 1.903 ±0.165 |
| | | 20 - [11.2] | 2622 ±77.49*****†††† | 1981 ±83.26*****†††† | 5.687 ±0.9121†††† |
| | | 0 - [16.8] | 1105 ±56.48*****†††† | 1005 ±71.46*****†††† | 6.381 ±0.8132†† |
| | 3c/wk *****†††††††† | 17.1 - [12] | 941.5 ±80.05 | 729.5 ±65.45 | 3.795 ±0.2206 |
| | | 21.4 - [22] | 774.8 ±85.45 | 323.5 ±52.47 | 1.162 ±0.1755 |
| | | 1.7 - [32] | 1567 ±115.9 | 767.6 ±67.05 | 1.489 ±0.1882 |
| DN2 | 10c/wk *****†††††††† | 20 - [5.6] | 935.6 ±64.68* | 406.7 ±28.97* | 1.01 ±0.1074 |
| | | 4 - [11.2] | 1503 ±103.5 | 932.9 ±75.62 | 1.832 ±0.1273** |
| | | 12 - [16.8/0] | 1036 ±94.11 | 650.4 ±59.66 | 3.528 ±0.8282 |
| | 7c/wk | 17.6 - [5.6]*††† | 164.2 ±58.1 | 72.2 ±29.26 | 0.9373 ±0.4578 |
| | | 23.2 - [11.2]**†††††††† | 1565 ±121 | 1143 ±150.2 | 4.99 ±2.158 |

Appendix A:

| | | | | |
|----------|------------------|----------------|---------------|-----------------|
| ****†† | 4.8 - [16.8]**** | 815.5 ±184.7 | 615.6 ±144.1 | 5.675 ±2.225 |
| 5c/wk | 16 - [5.6] | 884.4 ±213.6* | 433.8 ±111.9* | 2.151 ±0.5183†† |
| | 20 - [11.2] | 2108 ±173.6†† | 1623 ±123†††† | 3.798 ±0.3834†† |
| ****†††† | 0 - [16.8] | 1499 ±153.1**† | 1108 ±144.9*† | 3.913 ±0.984 |

S.Table 6 Quantification of anti-PER immunofluorescence rhythms during 10, 7, 5 and 3c/wk LD in different clock cell subsets in the male *Drosophila* brain.

Molecular analysis of PER protein cycling in wild-type adult male fly brains (**w***; **tim(UAS)-Gal4;UAS-CD8::GFP**) in different clock **cell Subsets**; s-LN_v, l-LN_v, 5th s-LN_v, LN_d, DN1 and DN2; at three time-points during 10, 7, 5 and 3c/wk equinox **LD cycles**. **ZT**, time-point scales to 24 h LD cycles, **h post L_{off}** in real-time in presented in []. **Total CTCF ±SEM**, mean anti-PER fluorescence of whole cells of each subset. **Nuclear CTCF ±SEM**, mean nuclear anti-PER fluorescence of cells of each subset. **Nuclear/Cytoplasmic Ratio ±SEM**, mean nuclear CTCF divided by cytoplasmic CTCF (total – nuclear CTCF). Results of *Kruskal-Wallis* test comparing Total CTCF (*), Nuclear CTCF (†) and Nuclear/Cytoplasmic Ratio (‡) across all time-points within each condition are presented in LD cycle column. Results of *Kruskal-Wallis* test comparing Total CTCF (*), Nuclear CTCF (†) and Nuclear/Cytoplasmic Ratio (‡) across all 10, 7 and 5c/wk LD cycles for matching time-points (i.e. corresponding to same h post L_{off}) are presented in ZT column. Pairwise comparisons of Total CTCF, Nuclear CTCF and Nuclear/Cytoplasmic Ratio for 10 and 5c/wk vs. 7c/wk (*) and 10c/wk vs. 5c/wk (†) LD cycles for matching time-points (i.e. corresponding to same h post L_{off}) using *Tukey's multiple comparisons test*. Pairwise comparisons between time-points within in each condition are presented in **S.Table 8**. In all cases (*, † and ‡): p ****<0.0001; 0.0001<p***<0.001; 0.001<p**<0.01; 0.01<p*<0.05.

| | Cell Subset | ZT [h post L _{off}] | Total CTCF ±SEM | Nuclear CTCF ±SEM |
|------------|---------------------|-------------------------------|-----------------|-------------------|
| 10c/wk VRI | s-lnv *****††††† | 20 [5.6] | 2754 ±127.4**** | 2548 ±111.5**** |
| | | 4 [11.2] | 2000 ±90.25 | 1748 ±82.22**** |
| | | 12 [16.8/0] | 579.4 ±42.22* | 420.8 ±32.93 |
| | l-lnv *****††††† | 20 [5.6] | 2574 ±140**** | 2144 ±118**** |
| | | 4 [11.2] | 3266 ±146.9**** | 3045 ±132.7**** |
| | | 12 [16.8/0] | 794.9 ±58.34** | 547.5 ±45.88 |
| | 5th s-lnv † | 20 [5.6] | 1872 ±339.9** | 1629 ±307.2*** |
| | | 4 [11.2] | 1913 ±255.5* | 1694 ±214.8*** |
| | | 12 [16.8/0] | 697.9 ±179.7 | 492.8 ±98.58 |
| | LNd *****††††† | 20 [5.6] | 2375 ±120**** | 2054 ±101.3**** |
| | | 4 [11.2] | 2373 ±96.06**** | 2068 ±87.34**** |
| | | 12 [16.8/0] | 792.6 ±45.95** | 599.9 ±39.66**** |
| | DN1 *****††††† | 20 [5.6] | 1710 ±45.57**** | 1378 ±35.23**** |
| | | 4 [11.2] | 1765 ±58.56 | 1529 ±46.28**** |
| | | 12 [16.8/0] | 1178 ±39.6**** | 1063 ±32.31**** |
| | DN2 *†† | 20 [5.6] | 2227 ±135.1**** | 1887 ±112.2**** |
| | | 4 [11.2] | 1798 ±139.4 | 1508 ±114.6**** |
| | | 12 [16.8/0] | 1642 ±167** | 1339 ±151.4**** |

S.Table 7 Quantification of anti-VRI immunofluorescence rhythms during 10c/wk LD in different clock cell subsets in the male *Drosophila* brain.

Molecular analysis of VRI protein cycling in wild-type adult male fly brains (*w^{*};tim(UAS)-Gal4;UAS-CD8::GFP*) in different clock cell subsets; s-LN_v, l-LN_v, 5th s-LN_v, LN_d, DN1 and DN2; at three time-points during 10c/wk LD. Results of *Kruskal-Wallis* test comparing Total CTCF (*) and Nuclear CTCF (†) across all time-points within each cell subset are reported in cell subset column. ZT, time-point scales to 24 h LD cycles, h post L_{off} in real-time in presented in []. Total CTCF ±SEM, mean anti-VRI fluorescence of whole cells of each subset. Nuclear CTCF ±SEM, mean nuclear anti-PER fluorescence of cells of each subset. Pairwise comparisons of Total CTCF and Nuclear CTCF for VRI vs. PER (S.Table 6) for matching time-points (i.e. corresponding to same h post L_{off}) in 10c/wk LD using *Welsh's t-Test*. Pairwise comparisons between time-points within in each condition are presented in S.Table 8. In all cases (* and †): p ****<0.0001; 0.0001<p***<0.001; 0.001<p**<0.01; 0.01<p*<0.05.

Appendix A:

| | | Total CTCF | | | | | | | | | | |
|-----------------------------------|---------------|---------------------------|--------------|-------------------|------------------|------------------|---------------|--------------|--------------|-------------------|------------------|------------------|
| PER | 10c/wk | | | 7c/wk | | | 5c/wk | | | 3c/wk | | |
| Cell Subset | ZT12 vs. ZT20 | ZT20 vs. ZT4 | ZT12 vs. ZT4 | ZT17.6 vs. ZT23.2 | ZT23.2 vs. ZT4.8 | ZT17.6 vs. ZT4.8 | ZT16 vs. ZT20 | ZT20 vs. ZT0 | ZT16 vs. ZT0 | ZT17.1 vs. ZT21.4 | ZT21.4 vs. ZT1.7 | ZT17.1 vs. ZT1.7 |
| s-LN _v | ns | <0.0001**** | <0.0001**** | <0.0001**** | <0.0001**** | ns | <0.0001**** | <0.0001**** | <0.0001**** | <0.0001**** | <0.0001**** | ns |
| I-LN _v | <0.0001**** | <0.0001**** | <0.0001**** | <0.0001**** | <0.0001**** | ns | <0.0001**** | <0.0001**** | <0.0001**** | 0.0003*** | ns | ns |
| 5 th s-LN _v | ns | 0.0295* | 0.0084** | 0.0185* | <0.0001**** | ns | 0.0017** | ns | 0.258* | - | - | - |
| LN _d | ns | <0.0001**** | <0.0001**** | <0.0001**** | <0.0001**** | ns | <0.0001**** | <0.0001**** | <0.0001**** | <0.0001**** | 0.0028** | <0.0001**** |
| DN1 | ns | <0.0001**** | <0.0001**** | <0.0001**** | <0.0001**** | <0.0001**** | <0.0001**** | <0.0001**** | 0.0004*** | ns | <0.0001**** | <0.0001**** |
| DN2 | ns | 0.0002*** | 0.0125* | 0.0002*** | 0.0021** | ns | <0.0001**** | 0.0421* | ns | - | - | - |
| | | Nuclear CTCF | | | | | | | | | | |
| PER | 10c/wk | | | 7c/wk | | | 5c/wk | | | 3c/wk | | |
| Cell Subset | ZT12 vs. ZT20 | ZT20 vs. ZT4 | ZT12 vs. ZT4 | ZT17.6 vs. ZT23.2 | ZT23.2 vs. ZT4.8 | ZT17.6 vs. ZT4.8 | ZT16 vs. ZT20 | ZT20 vs. ZT0 | ZT16 vs. ZT0 | ZT17.1 vs. ZT21.4 | ZT21.4 vs. ZT1.7 | ZT17.1 vs. ZT1.7 |
| s-LN _v | ns | <0.0001**** | <0.0001**** | <0.0001**** | <0.0001**** | 0.0446* | <0.0001**** | ns | <0.0001**** | <0.0001**** | 0.0329* | <0.0001**** |
| I-LN _v | ns | <0.0001**** | <0.0001**** | <0.0001**** | <0.0001**** | ns | <0.0001**** | ns | <0.0001**** | <0.0001**** | ns | <0.0001**** |
| 5 th s-LN _v | ns | 0.0322* | 0.0280* | 0.0243* | <0.0001**** | ns | 0.0375* | ns | 0.0378* | - | - | - |
| LN _d | ns | <0.0001**** | <0.0001**** | <0.0001**** | <0.0001**** | 0.0001*** | <0.0001**** | 0.006** | <0.0001**** | <0.0001**** | ns | <0.0001**** |
| DN1 | 0.0009*** | <0.0001**** | <0.0001**** | <0.0001**** | <0.0001**** | 0.0052** | <0.0001**** | <0.0001**** | <0.0001**** | 0.0028** | 0.0024** | ns |
| DN2 | ns | <0.0001**** | 0.0393* | 0.0013** | 0.0287* | ns | <0.0001**** | 0.0137* | 0.0071** | - | - | - |
| | | Nuclear/Cytoplasmic Ratio | | | | | | | | | | |
| PER | 10c/wk | | | 7c/wk | | | 5c/wk | | | 3c/wk | | |
| Cell Subset | ZT12 vs. ZT20 | ZT20 vs. ZT4 | ZT12 vs. ZT4 | ZT17.6 vs. ZT23.2 | ZT23.2 vs. ZT4.8 | ZT17.6 vs. ZT4.8 | ZT16 vs. ZT20 | ZT20 vs. ZT0 | ZT16 vs. ZT0 | ZT17.1 vs. ZT21.4 | ZT21.4 vs. ZT1.7 | ZT17.1 vs. ZT1.7 |
| s-LN _v | ns | ns | ns | ns | ns | ns | ns | 0.0011** | <0.0001**** | <0.0001**** | <0.0001**** | <0.0001**** |
| I-LN _v | 0.0045** | <0.0001**** | ns | 0.0002*** | 0.0007*** | ns | 0.0109* | <0.0001**** | <0.0001**** | <0.0001**** | ns | <0.0001**** |
| 5 th s-LN _v | ns | ns | ns | ns | ns | ns | ns | ns | ns | - | - | - |
| LN _d | ns | ns | ns | <0.0001**** | 0.0002*** | <0.0001**** | <0.0001**** | <0.0001**** | <0.0001**** | <0.0001**** | 0.0001*** | <0.0001**** |
| DN1 | 0.0036** | ns | 0.0158* | 0.0192* | ns | 0.0178* | <0.0001**** | ns | <0.0001**** | <0.0001**** | ns | <0.0001**** |
| DN2 | <0.0001**** | ns | 0.001** | ns | ns | ns | ns | ns | ns | - | - | - |

Appendix A:

| VRI | Total CTCF | | | VRI | Nuclear CTCF | | |
|-----------------------------------|---------------|--------------|--------------|-----------------------------------|---------------|--------------|--------------|
| | 10c/wk | | | | 10c/wk | | |
| Cell Subset | ZT12 vs. ZT20 | ZT20 vs. ZT4 | ZT12 vs. ZT4 | Cell Subset | ZT12 vs. ZT20 | ZT20 vs. ZT4 | ZT12 vs. ZT4 |
| s-LN _v | <0.0001**** | <0.0001**** | <0.0001**** | s-LN _v | <0.0001**** | <0.0001**** | <0.0001**** |
| l-LN _v | <0.0001**** | 0.0004**** | <0.0001**** | l-LN _v | <0.0001**** | <0.0001**** | <0.0001**** |
| 5 th s-LN _v | ns | ns | ns | 5 th s-LN _v | ns | ns | 0.0391* |
| LN _d | <0.0001**** | ns | <0.0001**** | LN _d | <0.0001**** | ns | <0.0001**** |
| DN1 | <0.0001**** | ns | <0.0001**** | DN1 | <0.0001**** | 0.0137* | <0.0001**** |
| DN2 | 0.0282* | ns | ns | DN2 | 0.0134* | 0.0495* | ns |

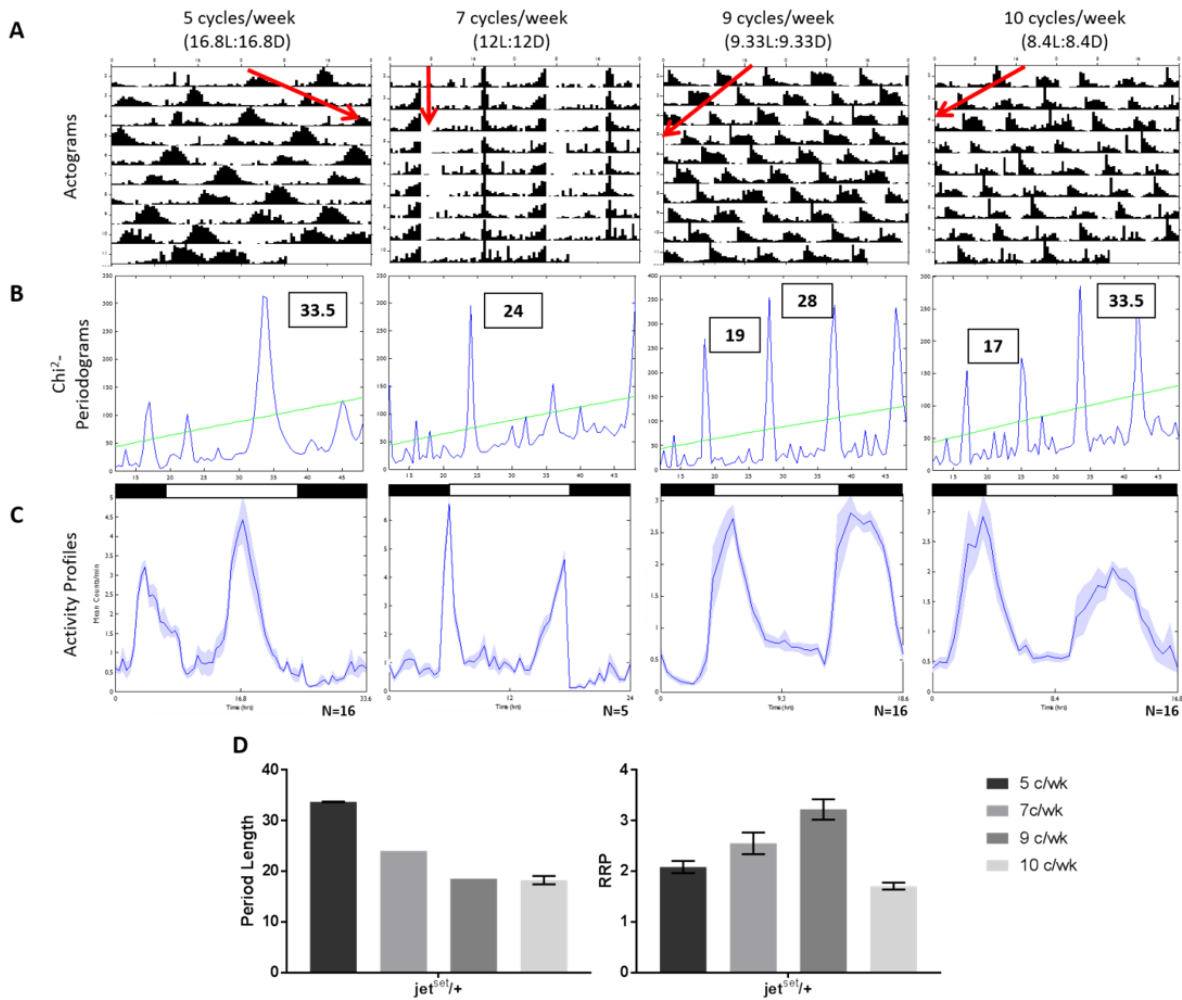
S.Table 8 PER and VRI molecular analysis statistical summary.

p values corresponding to the comparison between all time-points, within in each condition, using Tukey's multiple comparisons test for PER Total CTCF, PER Nuclear CTCF, PER Nuclear/Cytoplasmic Ratio, VRI Total CTCF and VRI Nuclear CTCF. Raw data for PER and VRI is presented in **S.Table 6** and **S.Table 7** respectively. All data shown for all cell-groups analysed – **Note:** not all cell groups were analysed in all conditions. Data for VRI was only collected during a 10c/wk LD cycle and VRI is exclusively nuclear, so no ratio can be calculated.

| Condition | ZT (h) | Number of Cells Analysed | | | | | | |
|-----------|--------|--------------------------|-------------------|-----------------------------------|-----------------|-----|-----|----|
| | | s-LN _v | I-LN _v | 5 th s-LN _v | LN _d | DN1 | DN2 | |
| PER | 10c/wk | 8.4 | 187 | 222 | 21 | 272 | 350 | 29 |
| | | 14 | 132 | 198 | 12 | 282 | 366 | 47 |
| | | 2.1 | 233 | 318 | 38 | 315 | 554 | 82 |
| | 7c/wk | 17.6 | 26 | 56 | 1 | 113 | 175 | 6 |
| | | 23.2 | 93 | 128 | 11 | 174 | 405 | 23 |
| | | 4.8 | 96 | 147 | 17 | 204 | 323 | 22 |
| | 5c/wk | 22.4 | 118 | 158 | 21 | 269 | 350 | 20 |
| | | 28 | 165 | 198 | 12 | 236 | 369 | 46 |
| | | 0 | 146 | 143 | 38 | 176 | 278 | 28 |
| | 3c/wk | 40 | 65 | 79 | - | 97 | 151 | - |
| | | 50 | 70 | 81 | - | 66 | 57 | - |
| | | 4 | 46 | 77 | - | 72 | 98 | - |
| VRI | 10c/wk | 8.4 | 104 | 115 | 4 | 177 | 284 | 30 |
| | | 14 | 136 | 181 | 19 | 184 | 487 | 56 |
| | | 2.1 | 135 | 175 | 19 | 193 | 447 | 54 |

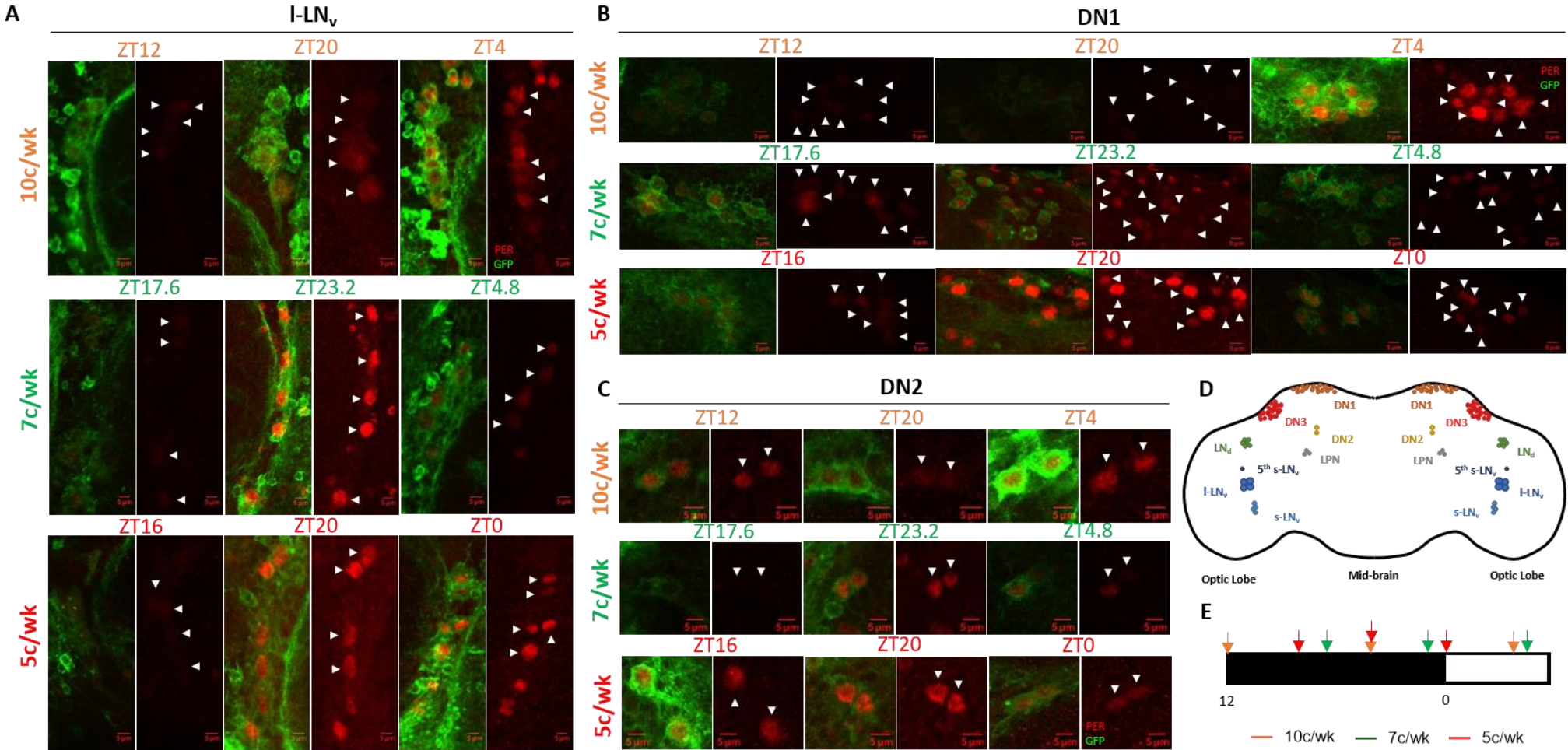
S.Table 9 Number of cells analysed for all clock cell subset at each time-point for each LD cycle tested

A.3 Supplementary Figures: Chapter 2



S.Figure 2 Heterozygote controls for *jet^{set}* mutant also show robust behavioural entrainment

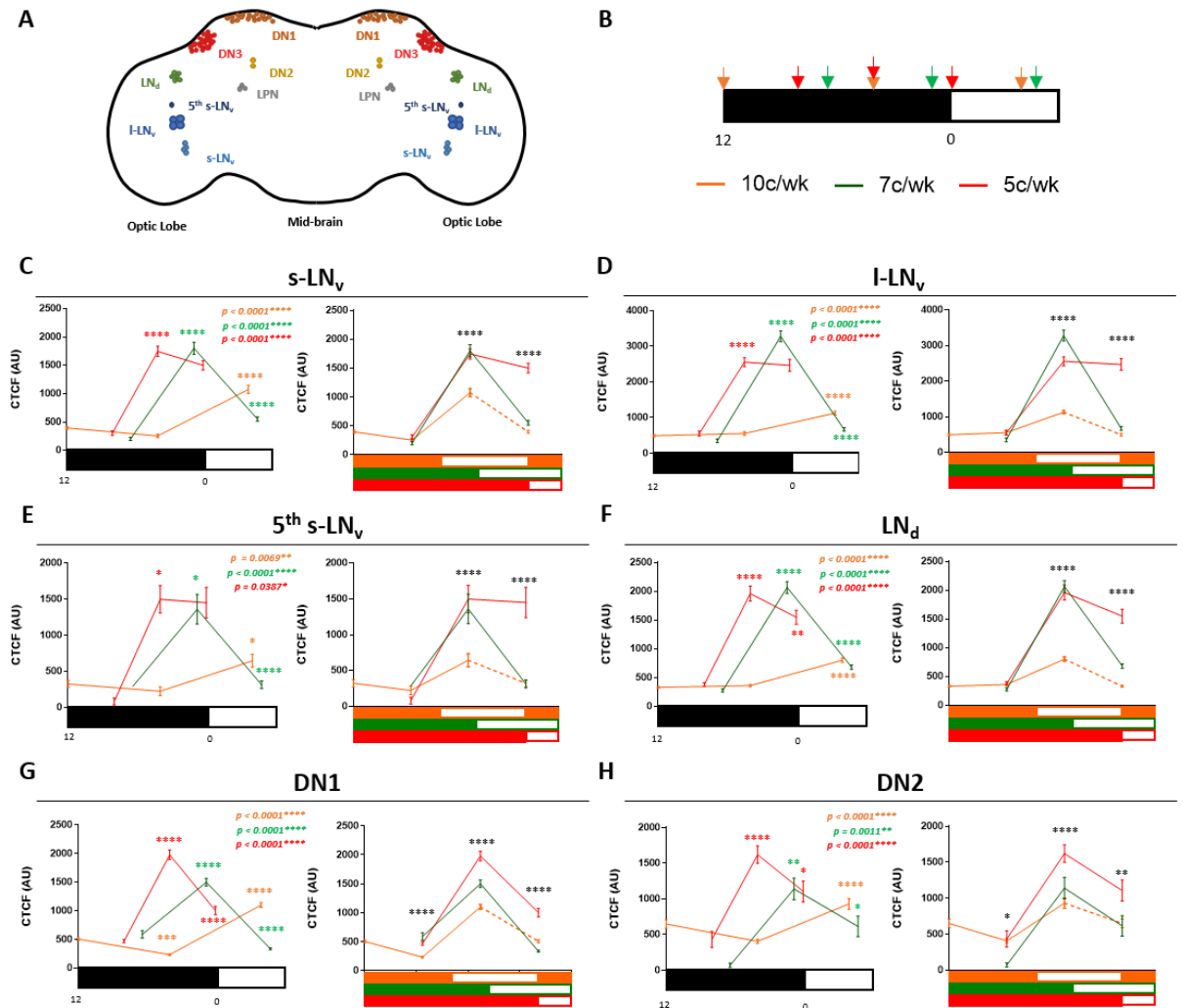
Qualitative and quantitative analysis of adult male flies of genotype γ^1w^* ; *jet^{set}/+* in 5, 7, 9 and 10c/wk (from left to right) equinox LD cycles. N denotes number of flies in each experiment. **A**) Double-plotted actograms of average locomotor activity over 10 days plotted on a 24 h timescale. Red arrows highlight the direction of rhythmic behaviour. **B**) Chi²-Periodograms annotated with dominant period-lengths (to nearest 0.5 h) plotted from 12-48 h. **C**) Activity profiles complete with LD bar (black=dark; white=light), profiles are shifted to incorporate entire light-phase flanked by half the dark phase. Each profile is plotted over a timescale dependent on the condition (5c/wk=33.6 h; 7c/wk=24 h; 9c/wk=18.8 h; and 10c/wk=16.8 h). Blue shading is \pm SEM. **D**) Bar charts showing average period length and RRP in 5, 7, 9 and 10c/wk. Error bars are SEM.



Appendix A:

S.Figure 3 PER localisation and cycling rhythms are comparable across most cell types, some differences arise during short cycles.

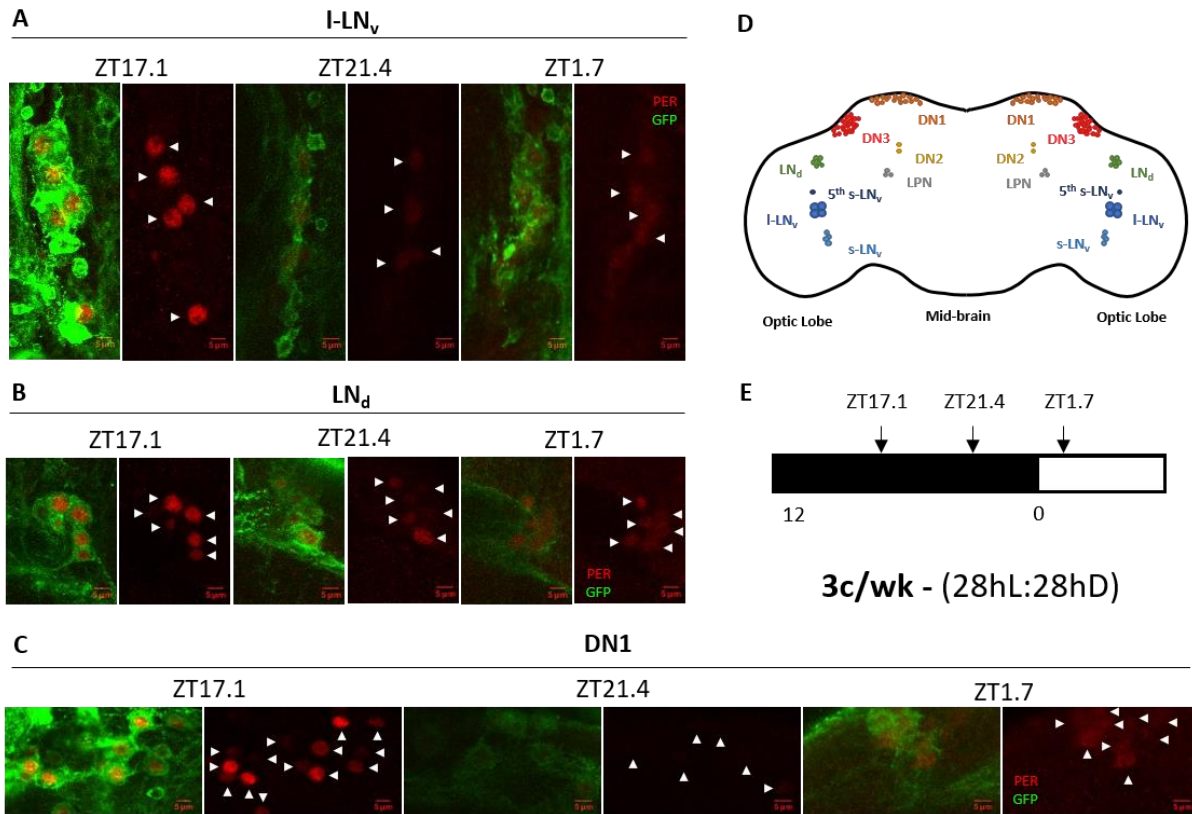
Molecular analysis of PER protein cycling in wild-type adult male fly brains (*w;TUG;UAS-CD8::GFP*) at three time-points during 10, 7 and 5c/wk equinox LD cycles. **A-C**) Representative images of l-LN_vs (**A**), DN1s (**B**) and DN2s (**C**) for 10 (top), 7 (middle) and 5c/wk (bottom) stained for PER (red) and GFP (green). Time-points annotated are scaled to a 24 h LD cycle to allow comparison. Merge and PER alone images for each time-point. Scale bar=5 μm. Arrows indicate cells quantified. **D**) Location of clock cell subsets in the fly brain. **E**) Sampling scheme W.R.T a 24 h scale.



S.Figure 4 Molecular cycling of nuclear PER in all clock cell subsets analysed in 10, 7 and 5c/wk LD.

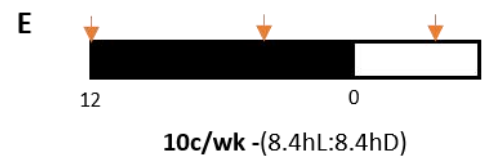
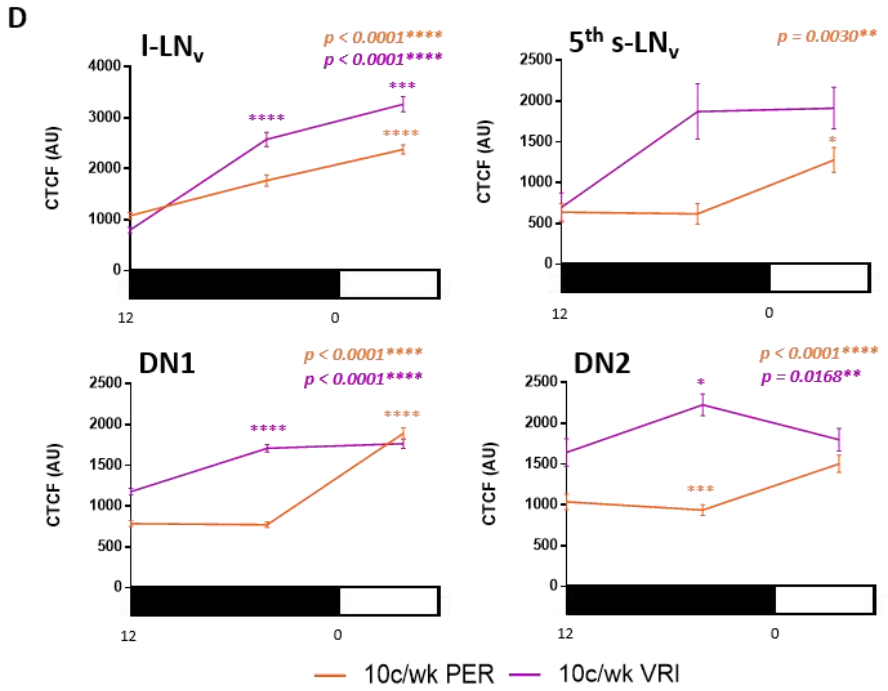
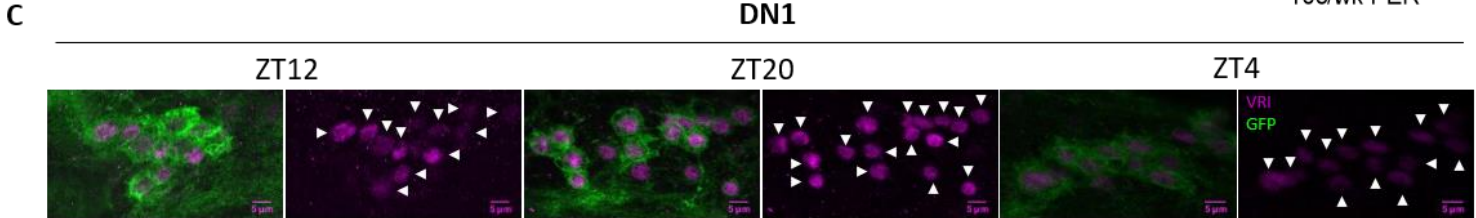
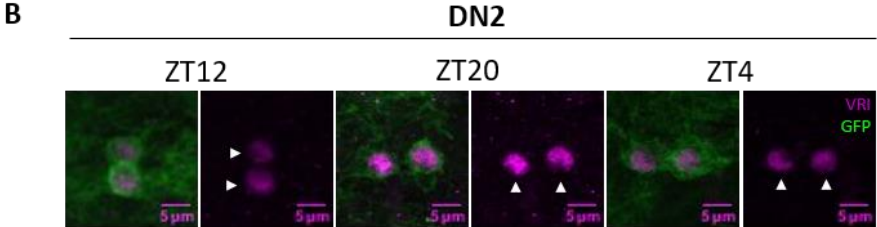
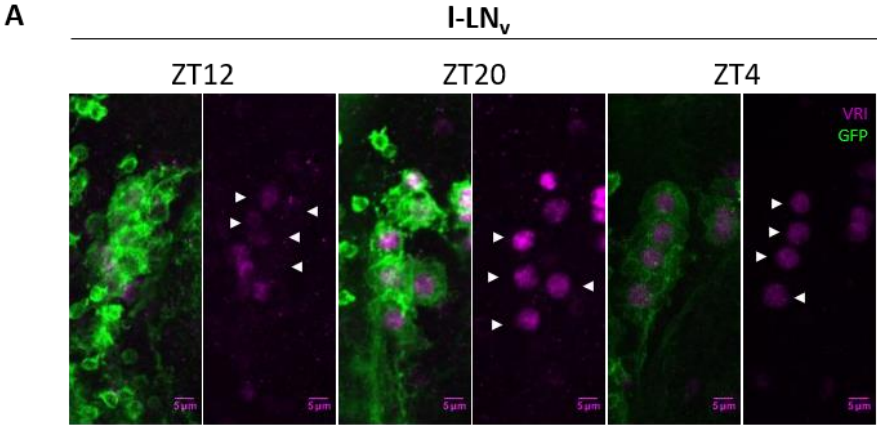
Molecular analysis of PER protein cycling in wild-type adult male fly brains (w^* ; $tim(UAS)-Gal4; UAS-CD8::GFP$) at three time-points during 10, 7 and 5c/wk equinox LD cycles. **A)** Location of clock cell subsets in the fly brain. **B)** Sampling scheme relative to the experimental photocycle (on a '24 h/cycle' scale). **C-H)** Quantification of Nuclear PER staining in s-LN_s (**C**), I-LN_v (**D**), 5th s-LN_v (**E**), LN_d (**F**), DN1s (**G**) and DN2s (**H**) for 10 (orange), 7 (green) and 5c/wk (red) plotted relative to the photocycle h (left - black=dark; white=light) and in real-time (right – LD bar for each cycle where orange, green and red represent the dark phase for 10, 7 and 5c/wk respectively; white=light). p values (top right – reported on 24 h scale plots) indicate results of Kruskal-Wallis test across all time-points within each condition (10c/wk = orange, 7c/wk = green and 5c/wk = red). Comparison between consecutive time-points, within each condition, with Tukey's multiple comparisons test (shown on 24 h scale plots – see **S.Table 8** for p values). Comparison between matching time-points across all three conditions using Kruskal-Wallis test (reported on real-time plots – pairwise comparisons between conditions at each time-point are reported in **S.Table 6**). Error bars show mean \pm SEM. NB: Dashed orange lines indicate an extrapolation of the 10c/wk data (repeat of data at 10c/wk ZT12).

Appendix A:



S.Figure 5 PER cycling across different clock cell types during a 3c/wk LD cycle.

Molecular analysis of PER protein cycling in wild-type adult male fly brains (*w;TUG;UAS-CD8::GFP*) at three time-points during a 3c/wk equinox LD cycle. **A-C**) Representative images of I-LN_vs (**A**), LN_ds (**B**) and DN1s (**C**) in 3c/wk LD stained for PER (red) and GFP (green). Time-points annotated are scaled to a 24 h LD cycle to allow comparison. Merge and PER alone images for each time-point. Scale bar=5 μm. Arrows indicate cells quantified. **D**) Location of clock cell subsets in the fly brain. **E**) Sampling scheme W.R.T a 24 h scale.



S.Figure 6 VRI cycling across different clock cell types during a 10c/wk LD cycle.

Molecular analysis of VRI protein cycling in wild-type adult male fly brains (*w;TUG;UAS-CD8::GFP*) at three time-points during a 10c/wk equinox LD cycle. **A-C**) Representative images of I-LN_vs (**A**), DN2s (**B**) and DN1s (**C**) in 10c/wk LD stained for VRI (magenta) and GFP (green). Time-points annotated are scaled to a 24 h LD cycle to allow comparison. Merge and VRI alone images for each time-point. Scale bar=5 μ m. Arrows indicate cells quantified. **D**) Quantification of total PER (orange) and VRI (magenta) staining - CTCF see methods, in I-LN_vs (top left), 5th s-LN_v (top right), DN1s (bottom left) and DN2s (bottom) during a 10c/wk LD cycle, plotted W.R.T LD cycle (black=dark; white=light). *p* values (top right) indicate results of *Kruskal-Wallis test* across all time-points for each protein (PER = orange and VRI = magenta). Comparison between consecutive time-points, within each condition, with *Tukey's multiple comparisons test* (see **S.Table 6** for *p* values). Error bars show mean \pm SEM. **E**) Sampling scheme W.R.T a 24 h scale.

A.4 Supplementary Tables: Chapter 3

| LD Condition (K-W test) | Genotype | n | %R•%WR•%AR | %ExT•%Other•%AR | Tau (h) ±SEM | RRP ±SEM |
|----------------------------|-----------------------------|-----------|------------------|-----------------|-------------------|---------------------|
| 10c/wk (*****+) | <i>cry</i> ⁰¹ /+ | 16 | 100•0•0 | 100•0•0 | 16.82 ±0.007 | 3.491 ±0.164† |
| | <i>cry</i> ⁰¹ | 15 | 33•47•20*****+† | 33•47•20*****+† | 22.04 ±0.915***** | 1.431 ±0.091*****+† |
| | <i>jet</i> ^{set} | 14 | 82•18•0† | 59•41•0**+† | 20.39 ±0.968*** | 1.591 ±0.149**+† |
| | <i>eya</i> ² | 14 | 7•43•50*****+† | 36•14•50***+† | 20.43 ±1.678** | 1.153 ±0.054*****+† |
| | <i>GMR-hid</i> | 16 | 24•44•31***** | 69•0•31*† | 17.59 ±0.744 | 1.553 ±0.227***** |
| | <i>norpA</i> ⁷ | 13 | 0•8•92*****+† | 8•0•92*****+† | 17.5 ±0 | 1 ±0*****+† |
| | <i>Pdf</i> ⁰¹ | 16 | 94•0•6 | 94•0•6 | 17.53 ±0.533** | 2.963 ±0.246 |
| | <i>per</i> ⁰¹ | 16 | 56•44•0**+† | 87•13•0 | 17.56 ±0.591** | 1.642 ±0.09**+† |
| <i>cyc</i> ⁰¹ | 13 | 69•12•8* | 92•0•8 | 16.67 ±0.112 | 2.132 ±0.244 | |
| ♂ 7c/wk (++++) | <i>cry</i> ⁰¹ /+ | 16 | 94•6•0 | 100•0•0 | 23.98 ±0.011 | 2.722 ±0.18 |
| | <i>cry</i> ⁰¹ | 13 | 100•0•0 | 100•0•0 | 24 ±0 | 3.368 ±0.189 |
| | <i>jet</i> ^{set} | 14 | 100•0•0 | 100•0•0 | 24 ±0 | 2.671 ±0.135 |
| | <i>eya</i> ² | 15 | 93•0•7 | 93•0•7 | 24 ±0 | 2.35 ±0.21 |
| | <i>GMR-hid</i> | 12 | 58•42•0 | 100•0•0 | 24 ±0 | 1.894 ±0.169 |
| | <i>norpA</i> ⁷ | 10 | 40•50•10** | 90•0•10 | 24.06 ±0.1 | 1.511 ±0.235* |
| | <i>Pdf</i> ⁰¹ | 16 | 94•6•0 | 100•0•0 | 24 ±0 | 3.492 ±0.2 |
| | <i>per</i> ⁰¹ | 16 | 100•0•0 | 100•0•0 | 24 ±0 | 2.731 ±0.15 |
| <i>cyc</i> ⁰¹ | 11 | 55•18•27* | 73•0•27 | 24 ±0 | 1.96 ±0.289 | |
| 5c/wk (*****+) | <i>cry</i> ⁰¹ /+ | 14 | 93•7•0 | 100•0•0 | 33.63 ±0.027 | 2.238 ±0.166††† |
| | <i>cry</i> ⁰¹ | 16 | 25•75•0*****+† | 44•56•0***+† | 29.16 ±1.251***** | 1.334 ±0.086**+† |
| | <i>jet</i> ^{set} | 16 | 0•56•44*****+††† | 50•6•44**+††† | 29.57 ±1.266***** | 1.204 ±0.037*****+† |
| | <i>eya</i> ² | 15 | 0•40•60*****+† | 13•27•60*****+† | 31 ±1.693** | 1.054 ±0.022*****+† |
| | <i>GMR-hid</i> | 14 | 7•57•36***** | 57•7•36*† | 33.17 ±0.301* | 1.154 ±0.056*****+† |
| | <i>norpA</i> ⁷ | 15 | 0•40•60***** | 27•13•60***** | 32.33 ±0.946* | 1.053 ±0.033***** |
| | <i>Pdf</i> ⁰¹ | 16 | 87•13•0 | 100•0•0 | 33.53 ±0.031* | 2.201 ±0.137††† |

Appendix A:

| | | | | | |
|--------------------------|----|--------------|---------|---------------|------------------|
| <i>per</i> ⁰¹ | 16 | 50•36•13*††† | 87•0•13 | 33.5 ±0** | 1.514 ±0.116†††† |
| <i>cyc</i> ⁰¹ | 13 | 84•8•8 | 92•0•8 | 33.63 ±0.125* | 2.002 ±0.174 |

| LD Condition (K-W test) | Genotype | n | %R•%WR•%AR | %ExT•%Other•%AR | Tau (h) ±SEM | RRP ±SEM |
|----------------------------|-----------------------------|-----------------------------|---------------------|---------------------|-----------------|---------------------|
| 10c/wk (**††††) | <i>cry</i> ⁰¹ /+ | 16 | 38•62•0 | 100•0•0 | 18.93 ±0.937 | 1.424 ±0.082 |
| | <i>cry</i> ⁰¹ | 16 | 27•27•46**††† | 27•27•46****†††† | 19.75 ±1.02 | 1.801 ±0.315† |
| | <i>jet</i> ^{set} | 15 | 8•44•48***††††† | 36•16•48****††††† | 19.05 ±1.045 | 1.169 ±0.05†††† |
| | <i>eya</i> ² | 16 | 13•68•49†† | 6•75•19****††††† | 23.54 ±1.139*** | 1.18 ±0.062† |
| | <i>GMR-hid</i> | 10 | 20•40•40*†† | 40•20•40****†† | 18.08 ±1.405 | 1.38 ±0.16†† |
| | <i>norpA</i> ⁷ | 15 | 0•7•93****††††† | 7•0•93****††††† | 17 | 1.005 ±0.005**†††† |
| | <i>Pdf</i> ⁰¹ | 15 | 93•0•7*** | 93•0•7 | 16.93 ±0.049 | 2.46 ±0.214 |
| | <i>per</i> ⁰¹ | 15 | 100•0•0*** | 100•0•0 | 17.47 ±0.54 | 3.089 ±0.264* |
| | <i>cyc</i> ⁰¹ | 16 | 0•11•89****††††† | 0•11•89****††††† | 17.08 ±0.083 | 1.708 ±0.202 |
| | ♀ 7c/wk (††††) | <i>cry</i> ⁰¹ /+ | 15 | 20•80•0 | 93•7•0 | 23.71 ±0.205 |
| <i>cry</i> ⁰¹ | | 15 | 86•7•7*** | 93•0•7 | 24.07 ±0.071* | 2.696 ±0.251*** |
| <i>jet</i> ^{set} | | 15 | 89•11•0**** | 100•0•0 | 24 ±0 | 2.842 ±0.118**** |
| <i>eya</i> ² | | 15 | 74•13•13** | 100•0•0 | 24 ±0 | 1.996 ±0.191 |
| <i>GMR-hid</i> | | 15 | 87•13•0*** | 100•0•0 | 23.97 ±0.033 | 2.429 ±0.212** |
| <i>norpA</i> ⁷ | | 14 | 50•21•29** | 71•0•29 | 24.05 ±0.5* | 1.754 ±0.208 |
| <i>Pdf</i> ⁰¹ | | 14 | 100•0•0**** | 100•0•0 | 24 ±0 | 2.682 ±0.133*** |
| <i>per</i> ⁰¹ | | 16 | 87•13•0*** | 100•0•0 | 24 ±0 | 2.296 ±0.144* |
| <i>cyc</i> ⁰¹ | | 14 | 79•14•7*** | 93•0•7 | 23.67 ±0.276 | 1.475 ±0.155 |
| 5c/wk (****††††) | | <i>cry</i> ⁰¹ /+ | 15 | 13•87•0 | 93•7•0 | 32.64 ±1.026 |
| | <i>cry</i> ⁰¹ | 15 | 13•80•7†††††† | 27•66•7****†††††† | 28.54 ±1.309* | 1.227 ±0.052†† |
| | <i>jet</i> ^{set} | 13 | 31•61•8††††† | 84•8•8† | 33.96 ±0.168 | 1.335 ±0.087††† |
| | <i>eya</i> ² | 16 | 0•25•75****†††††††† | 0•25•75****†††††††† | 29.88 ±1.625* | 1.046 ±0.026**††††† |
| | <i>GMR-hid</i> | 15 | 40•47•13*† | 60•27•13† | 31.38 ±1.152 | 1.48 ±0.132†† |

| | | | | | |
|---------------------------|----|----------------|-------------|--------------|-------------------|
| <i>norpA</i> ⁷ | 13 | 8•61•31†‡‡ | 46•23•31*‡‡ | 33.83 ±0.507 | 1.207 ±0.054‡ |
| <i>Pdf</i> ⁰¹ | 16 | 50•31•19***††‡ | 81•0•19 | 33.58 ±0.052 | 1.646 ±0.129†††‡ |
| <i>per</i> ⁰¹ | 14 | 79•14•7*** | 93•0•7 | 33.5 ±0 | 1.73 ±0.126††† |
| <i>cyc</i> ⁰¹ | 9 | 33•33•33** | 67•0•33*‡‡ | 33.67 ±0.105 | 1.435 ±0.244††††‡ |

S.Table 10 Male and Female locomotor activity of mutant genotypes in 10, 7 and 5c/wk equinox LD cycles.

Male (top) and female (bottom) flies of **genotype**; $w^{1118};;cry^{01}/+$, $w^{1118};;cry^{01}, y^1w^*$; $jet^{set}, eya^2, GMR-hid, norpA^7, y^1w^*; Pdf^{01}, y^1per^{01}w^*$ and $cyc^{01}ry^{506}$ with result of *Kruskal-Wallis test* comparing period length (*) and RRP (†) between all genotypes within each condition. **n**, number of flies. **%R•%WR•%AR**, percentage of flies classified and rhythmic (R), weakly rhythmic (WR) and arrhythmic (AR). **%ExT•%Other•%AR**, percentage of flies classified and entrained (ExT), other and arrhythmic (AR). *Fisher's exact test* vs. $cry^{01}/+$ in each condition for %R•%WR•%AR and %ExT•%Other•%AR (*). *Fisher's exact test* between all conditions within each genotype for %R•%WR•%AR and %ExT•%Other•%AR; 5/10 vs. 7c/wk (†) and 5 vs. 10c/wk (‡). **Tau (h) ±SEM**, mean period length – Ext period lengths; 10c/wk = 16.8 h, 7c/wk = 24 h and 5c/wk = 33.6 h. **RRP ±SEM**, mean relative rhythmic power. AR flies were assigned RRP=1 and omitted from period length analysis. *Pairwise Mann-Whitney test* vs. $cry^{01}/+$ in each condition for Tau (h) ±SEM and RRP ±SEM (*). *Dunn's Multiple Comparison test* between all conditions within each genotype for RRP ±SEM; 5/10 vs. 7c/wk (†) and 5 vs. 10c/wk (‡). In all cases (*, † and ‡): $p^{****}<0.0001$; $0.0001<p^{***}<0.001$; $0.001<p^{**}<0.01$; $0.01<p^*<0.05$.

Appendix A:

| LD Condition (K-W test) | Genotype | n | %R•%WR•%AR | %ExT•%Other•%AR | Tau (h) ±SEM | RRP ±SEM |
|----------------------------|------------------------------|----|------------------|-----------------------|-----------------|------------------------|
| ♂ | <i>Control (Pooled)</i> | 59 | 88•10•2† | 78•20•2†††† | 18.56 ±0.395 | 2.845 ±0.176††† |
| | <i>TUG Control</i> | 15 | 80•20•0 | 100•0•0 | 17.5 ±0.368 | 3.037 ±0.448 |
| | <i>TUG > ds-cry</i> | 58 | 59•34•7****††††† | 34•59•7****#####††††† | 21.47 ±0.537**# | 1.703 ±0.071****#††††† |
| | <i>cry-Gal4 Control</i> | 15 | 100•0•0 | 93•7•0 | 17.53 ±0.533 | 4.137 ±0.212 |
| | <i>cry > ds-cry</i> | 14 | 71•29•0# | 93•0•7 | 17.57 ±0.571 | 2.123 ±0.171#† |
| | <i>Pdf-Gal4 Control</i> | 15 | 73•20•7† | 27•66•7***#††††† | 21.79 ±0.938 | 1.706 ±0.103*††††† |
| | <i>Pdf > ds-cry</i> | 15 | 67•33•0† | 73•27•0† | 18.87 ±0.861 | 2.061 ±0.234††††† |
| | <i>GMR78G02-Gal4 Control</i> | 14 | 100•0•0 | 93•7•0 | 17.57 ±0.571 | 2.476 ±0.164†† |
| | <i>GMR78G02 > ds-cry</i> | 15 | 93•7•0 | 53•47•0#†† | 20.73 ±1.067 | 2.181 ±0.110 |
| | <i>ChAT > ds-cry</i> | 28 | 79•18•4 | 75•21•4 | 18.76 ±0.664 | 2.002 ±0.107††††† |
| 7c/wk (††††) | <i>Control (Pooled)</i> | 60 | 98•2•0 | 100•0•0 | 24 ±0 | 3.307 ±0.083 |
| | <i>TUG Control</i> | 15 | 93•7•0 | 100•0•0 | 24 ±0 | 3.377 ±0.208 |
| | <i>TUG > ds-cry</i> | 67 | 94•6•0 | 100•0•0 | 24.01 ±0.007 | 2.98 ±0.091 |
| | <i>cry-Gal4 Control</i> | 16 | 100•0•0 | 100•0•0 | 24 ±0 | 3.156 ±0.153 |
| | <i>cry > ds-cry</i> | 16 | 94•6•0 | 100•0•0 | 24 ±0 | 3.038 ±0.226 |
| | <i>Pdf-Gal4 Control</i> | 16 | 100•0•0 | 100•0•0 | 24 ±0 | 3.611 ±0.133 |
| | <i>Pdf > ds-cry</i> | 16 | 100•0•0 | 100•0•0 | 24 ±0 | 3.803 ±0.108 |

Appendix A:

| | | | | | | |
|-------------------|------------------------------|----|------------------|----------------------|-------------------|---------------------|
| | <i>GMR78G02-Gal4 Control</i> | 13 | 100•0•0 | 100•0•0 | 24 ±0 | 3.037 ±0.130 |
| | <i>GMR78G02 > ds-cry</i> | 16 | 100•0•0 | 100•0•0 | 24 ±0 | 2.431 ±0.093** |
| | <i>ChAT > ds-cry</i> | 12 | 100•0•0 | 100•0•0 | 24 ±0 | 3.736 ±0.183 |
| | <i>Control (Pooled)</i> | 60 | 83•17•0†† | 98•2•0‡‡‡ | 33.44 ±0.062 | 2.08 ±0.067†††††‡‡ |
| | <i>TUG Control</i> | 16 | 81•19•0 | 100•0•0 | 33.47 ±0.031 | 2.02 ±0.111††† |
| | <i>TUG > ds-cry</i> | 63 | 40•54•6****#†††† | 45 49 6****#####†††† | 29.18 ±0.559****# | 1.67 ±0.086**†††† |
| | <i>cry-Gal4 Control</i> | 16 | 100•0•0 | 100•0•0 | 33.5 ±0.046 | 2.229 ±0.111†††††‡‡ |
| 5c/wk | <i>cry > ds-cry</i> | 15 | 100•0•0‡ | 100•0•0 | 33.23 ±0.083 | 2.082 ±0.091†† |
| (****††††) | <i>Pdf-Gal4 Control</i> | 14 | 50•50•0*###†† | 93•7•0‡‡‡ | 33.25 ±0.255 | 1.506 ±0.062†††† |
| | <i>Pdf > ds-cry</i> | 16 | 100•0•0‡ | 100•0•0‡ | 33.63 ±0.056 | 2.113 ±0.094†††† |
| | <i>GMR78G02-Gal4 Control</i> | 14 | 100•0•0 | 100•0•0 | 33.54 ±0.036 | 2.551 ±0.077† |
| | <i>GMR78G02 > ds-cry</i> | 16 | 100•0•0 | 100•0•0‡‡ | 33.53 ±0.031 | 2.272 ±0.113 |
| | <i>ChAT > ds-cry</i> | 9 | 100•0•0 | 100•0•0 | 33.61 ±0.111 | 2.29 ±0.168†† |

| LD Condition (K-W test) | Genotype | n | %R•%WR•%AR | %ExT•%Other•%AR | Tau (h) ±SEM | RRP ±SEM |
|----------------------------|------------------------------|----|--------------------|-------------------|--------------|--------------------|
| ♀ | <i>Control (Pooled)</i> | 62 | 71•29•0†† | 90•10•0† | 17.72 ±0.288 | 2.089 ±0.104†††† |
| | <i>TUG Control</i> | 16 | 94•6•0 | 100•0•0 | 17 ±0.046 | 2.288 ±0.21† |
| | <i>TUG > ds-cry</i> | 63 | 40•29•32***###†††† | 59•9•32***###†††† | 17.56 ±0.313 | 1.626 ±0.098**##†† |
| | <i>cry-Gal4 Control</i> | 16 | 75•25•0 | 81•19•0 | 18.53 ±0.823 | 2.446 ±0.236 |
| | <i>cry > ds-cry</i> | 16 | 38•44•19**# | 81•0•19** | 16.88 ±0.061 | 1.626 ±0.166† |
| | <i>Pdf-Gal4 Control</i> | 14 | 21•79•0**†††† | 86•14•0 | 17.86 ±0.619 | 1.368 ±0.057†††† |
| | <i>Pdf > ds-cry</i> | 16 | 50•50•0†† | 81•19•0 | 18.41 ±0.819 | 1.777 ±0.192††† |
| | <i>GMR78G02-Gal4 Control</i> | 16 | 88•13•0 | 94•6•0 | 17.5 ±0.5 | 2.164 ±0.167†† |
| | <i>GMR78G02 > ds-cry</i> | 15 | 53•40•7 | 93•0•7 | 16.89 ±0.057 | 1.933 ±0.278 |
| | <i>ChAT > ds-cry</i> | 14 | 93•0•7*** | 93•0•7 | 16.96 ±0.038 | 2.898 ±0.255† |
| ♂ | <i>Control (Pooled)</i> | 62 | 92•6•2 | 98•0•2 | 24.01 ±0.008 | 3.088 ±0.105 |
| | <i>TUG Control</i> | 14 | 93•7•0 | 100•0•0 | 24 ±0 | 3.058 ±0.177 |
| | <i>TUG > ds-cry</i> | 52 | 63•35•2*** | 98•0•2 | 24 ±0.024 | 1.998 ±0.107***### |
| | <i>cry-Gal4 Control</i> | 16 | 81•13•6 | 94•0•6 | 24.03 ±0.033 | 2.564 ±0.217 |
| | <i>cry > ds-cry</i> | 15 | 80•13•7 | 93•0•7 | 24 ±0 | 2.119 ±0.152* |
| | <i>Pdf-Gal4 Control</i> | 16 | 100•0•0 | 100•0•0 | 24 ±0 | 3.756 ±0.176 |
| | <i>Pdf > ds-cry</i> | 16 | 100•0•0 | 100•0•0 | 24 ±0 | 2.747 ±0.161 |

Appendix A:

| | | | | | | |
|---------------|------------------------------|----|---------------------|---------------------|--------------|---------------------|
| | <i>GMR78G02-Gal4 Control</i> | 16 | 94•6•0 | 100•0•0 | 24 ±0 | 2.971 ±0.149 |
| | <i>GMR78G02 > ds-cry</i> | 16 | 69•19•13* | 88•0•12 | 24.14 ±0.143 | 1.829 ±0.167***# |
| | <i>ChAT > ds-cry</i> | 8 | 100•0•0 | 100•0•0 | 24 ±0 | 4.011 ±0.237 |
| | <i>Control (Pooled)</i> | 59 | 83•15•2 | 98•0•2 | 33.62 ±0.043 | 2.143 ±0.094++++ |
| | <i>TUG Control</i> | 14 | 79•21•0 | 100•0•0 | 33.68 ±0.1 | 1.665 ±0.103++++ |
| | <i>TUG > ds-cry</i> | 57 | 25•35•40****###++++ | 49•11•40****###++++ | 33.44 ±0.247 | 1.353 ±0.07****++++ |
| | <i>cry-Gal4 Control</i> | 16 | 69•25•6 | 94•0•6 | 33.57 ±0.108 | 2.244 ±0.194 |
| 5c/wk | <i>cry > ds-cry</i> | 12 | 25•75•0***##+ | 92•8•0 | 32.88 ±0.726 | 1.445 ±0.102+ |
| (++++) | <i>Pdf-Gal4 Control</i> | 13 | 92•8•0### | 100•0•0 | 33.69 ±0.07 | 1.838 ±0.072++ |
| | <i>Pdf > ds-cry</i> | 14 | 93•7•0‡ | 100•0•0 | 33.68± 0.085 | 1.996 ±0.082+ |
| | <i>GMR78G02-Gal4 Control</i> | 16 | 94•6•0 | 100•0•0 | 33.56 ±0.063 | 2.707 ±0.19 |
| | <i>GMR78G02 > ds-cry</i> | 14 | 93•7•0 | 100•0•0 | 33.82 ±0.135 | 2.144 ±0.138 |
| | <i>ChAT > ds-cry</i> | 12 | 100•0•0 | 100•0•0 | 33.54 ±0.074 | 2.931 ±0.177+ |

S.Table 11 Locomotor activity of male and female flies with *ds-cry* RNA (3772R2) in different clock cell subsets in 10, 7 and 5c/wk LD cycles.

Male (top) and female (bottom) flies of **genotype; Control (Pooled)** (Data for all isogenic controls combined), *UAS-Dcr-2 w*;tim(UAS)-Gal4/CyO;(Sb¹ or TM6B-Tb¹)/+* (**TUG Control**), *UAS-Dcr-2 w*; UAS-ds-cry^{3772R2}/tim(UAS)-Gal4;+/TM6B-Tb¹* (**TUG > ds-cry**), *UAS-Dcr-2 w*;+/CyO;cry-Gal4-13/+* (**cry-Gal4 Control**), *UAS-Dcr-2 w*; UAS-ds-cry^{3772R2}/+;cry-Gal4-13/+* (**cry >ds-cry**), *UAS-Dcr-2 w*;Pdf-Gal4/CyO* (**Pdf-Gal4 Control**), *UAS-Dcr-2 w*; UAS-ds-cry^{3772R2}/Pdf-Gal4* (**Pdf >ds-cry**), *UAS-Dcr-2 w*;+/CyO;GMR78G02-Gal4/+* (**GMR78G02-Gal4 Control**), *UAS-Dcr-2 w*; UAS-ds-cry^{3772R2}/+;GMR78G02-Gal4/+* (**GMR 78G02 > ds-cry**) and *UAS-Dcr-2 w*; UAS-ds-cry^{3772R2}/ChAT-Gal4* (**ChAT > ds-cry**) with result of *Kruskal-Wallis test* comparing Period length (*) and RRP (†) between genotypes within each condition. **n**, number of flies. **%R•%WR•%AR**, percentage of flies classified and rhythmic (R), weakly rhythmic (WR) and arrhythmic (AR). **%ExT•%Other•%AR**, percentage of flies classified and entrained (ExT), “other” and arrhythmic (AR). *Fisher’s exact test* for each genotype vs. *Control (All)* (*) and for knockdown (Gal4 > dsRNA) vs. isogenic control (Gal4 Control) (#) in each condition for **%R•%WR•%AR** and **%ExT•%Other•%AR**. *Fisher’s exact test* between all conditions within each genotype for **%R•%WR•%AR**; 5/10 vs. 7c/wk (†) and 5 vs. 10c/wk (‡). **Tau (h) ±SEM**, mean period length. **RRP ±SEM**, mean relative rhythmic power. AR flies were assigned RRP=1 and omitted from period length analysis. *Pairwise Mann-Whitney test* for all genotype vs. *Control (All)* (*) and for knockdown (Gal4 > dsRNA) vs. isogenic control (Gal4 Control) (#) for **Tau (h) ±SEM** and **RRP ±SEM**. *Dunn’s Multiple Comparison test* between all conditions within each genotype for **RRP ±SEM**; 5/10 vs. 7c/wk (†) and 5 vs. 10c/wk (‡). In all cases (*, #, † and ‡): $p^{****}<0.0001$; $0.0001<p^{***}<0.001$; $0.001<p^{**}<0.01$; $0.01<p^*<0.05$.

Appendix A:

| LD Condition (K-W test) | Genotype | n | %R•%WR•%AR | %ExT•%Other•%AR | Tau (h) ±SEM | RRP ±SEM |
|----------------------------|------------------------------|----|---------------------|---------------------|-----------------|--------------------------|
| ♂ | <i>Control (Pooled)</i> | 56 | 78•17•5+++ | 95•0•5 | 17 ±0 | 3.785 ±0.106+++ |
| | <i>TUG Control</i> | 16 | 94•0•6 | 94•0•4 | 17 ±0 | 3.862 ±0.287 |
| | <i>TUG > ds-jet</i> | 55 | 38•55•7***#####++++ | 33•60•7***#####++++ | 21.49 ±0.518*** | 1.576 ±0.071***#####++++ |
| | <i>cry-Gal4 Control</i> | 15 | 100•0•0 | 100•0•0 | 17 ±0 | 3.862 ±0.164++ |
| | <i>cry > ds-jet</i> | 15 | 100•0•0 | 100•0•0 | 17 ±0 | 3.136 ±0.201 |
| | <i>Pdf-Gal4 Control</i> | 15 | 100•0•0 | 100•0•0 | 17 ±0 | 3.726 ±0.122 |
| | <i>Pdf > ds-jet</i> | 16 | 75•25•0 | 81•19•0* | 18.06 ±0.68 | 1.758 ±0.148****++++ |
| | <i>GMR78G02-Gal4 Control</i> | 10 | 100•0•0 | 100•0•0 | 17 ±0 | 3.632 ±0.255 |
| | <i>GMR78G02 > ds-jet</i> | 16 | 94•6•0 | 63•37•0****+ | 20 ±1 | 2.053 ±0.121**++++ |
| | <i>ChAT > ds-jet</i> | 20 | 25•60•15****++++ | 45•40•15****+ | 20.85 ±0.963 | 1.325 ±0.057****++++ |
| 7c/wk (++) | <i>Control (Pooled)</i> | 47 | 100•0•0 | 100•0•0 | 24 ±0 | 3.069 ±0.101 |
| | <i>TUG Control</i> | 13 | 100•0•0 | 100•0•0 | 24 ±0 | 3.313 ±0.191 |
| | <i>TUG > ds-jet</i> | 33 | 100•0•0 | 100•0•0 | 24 ±0 | 3.427 ±0.078 |
| | <i>cry-Gal4 Control</i> | 13 | 100•0•0 | 100•0•0 | 24 ±0 | 2.83 ±0.193 |
| | <i>cry > ds-jet</i> | 15 | 80•13•7* | 93•0•7 | 24 ±0 | 2.848 ±0.272 |
| | <i>Pdf-Gal4 Control</i> | 12 | 100•0•0 | 100•0•0 | 24 ±0 | 3.308 ±0.192 |
| | <i>Pdf > ds-jet</i> | 16 | 100•0•0 | 100•0•0 | 24 ±0 | 3.693 ±0.099 |

Appendix A:

| | | | | | | |
|-------------------|------------------------------|----|--------------------|------------------------|---------------|-----------------------|
| | <i>GMR78G02-Gal4 Control</i> | 9 | 100•0•0 | 100•0•0 | 24 ±0 | 2.742 ±0.179 |
| | <i>GMR78G02 > ds-jet</i> | 16 | 100•0•0 | 100•0•0 | 24 ±0 | 3.103 ±0.167 |
| | <i>ChAT > ds-jet</i> | 14 | 100•0•0 | 100•0•0 | 24 ±0 | 3.086 ±0.207 |
| | <i>Control (Pooled)</i> | 56 | 82•18•0†† | 100•0•0 | 33.51 ±0.027 | 2.111 ±0.075†††††††† |
| | <i>TUG Control</i> | 16 | 56•4•0*†††† | 100•0•0 | 33.44 ±0.077 | 1.598 ±0.083†††††††† |
| | <i>TUG > ds-jet</i> | 56 | 27•57•16****#††††† | 57•27•16****##†††††††† | 31.03 ±0.557* | 1.501 ±0.081****††††† |
| | <i>cry-Gal4 Control</i> | 16 | 100•0•0 | 100•0•0 | 33.53 ±0.031 | 2.553 ±0.1†††† |
| 5c/wk | <i>cry > ds-jet</i> | 15 | 87•13•0 | 100•0•0 | 33.57 ±0.045 | 2.139 ±0.106††† |
| (****††††) | <i>Pdf-Gal4 Control</i> | 14 | 86•14•0 | 100•0•0 | 33.57 ±0.049 | 2.228 ±0.135†††††† |
| | <i>Pdf > ds-jet</i> | 16 | 94•6•0 | 100•0•0 | 33.78 ±0.115 | 2.207 ±0.116††† |
| | <i>GMR78G02-Gal4 Control</i> | 10 | 90•10•0 | 100•0•0 | 33.5 ±0 | 2.06 ±0.163††† |
| | <i>GMR78G02 > ds-jet</i> | 16 | 87•13•0 | 100•0•0‡ | 33.53 ±0.031 | 2.433 ±0.135† |
| | <i>ChAT > ds-jet</i> | 12 | 58•33•9*† | 92•0•8‡ | 33.45 ±0.106 | 1.772 ±0.194†† |

♀

| LD Condition (K-W test) | Genotype | n | %R•%WR•%AR | %ExT•%Other•%AR | Tau (h) ±SEM | RRP ±SEM |
|----------------------------|------------------------------|----|--------------|------------------|---------------|----------------------|
| 10c/wk (**††††) | <i>Control (Pooled)</i> | 56 | 32•42•26† | 74•0•26†† | 17.11 ±0.112 | 1.73 ±0.085 |
| | <i>TUG Control</i> | 14 | 28•36•36 | 64•0•36 | 17 ±0 | 1.422 ±0.132 |
| | <i>TUG > ds-jet</i> | 62 | 19•37•44†††† | 43•13•44****†††† | 18.47 ±0.563 | 1.273 ±0.051****†††† |
| | <i>cry-Gal4 Control</i> | 15 | 53•40•7 | 93•0•7 | 17 ±0 | 1.713 ±0.162 |
| | <i>cry > ds-jet</i> | 16 | 69•31•0* | 75•25•0*** | 17.31 ±0.254 | 1.741 ±0.119 |
| | <i>Pdf-Gal4 Control</i> | 15 | 67•33•0* | 93•7•0** | 17.37 ±0.367 | 1.975 ±0.197 |
| | <i>Pdf > ds-jet</i> | 16 | 56•44•0* | 100•0•0* | 17 ±0 | 1.746 ±0.133† |
| | <i>GMR78G02-Gal4 Control</i> | 12 | 67•25•8 | 92•0•8 | 17 ±0 | 1.807 ±0.157 |
| | <i>GMR78G02 > ds-jet</i> | 15 | 33•60•7 | 86•7•7 | 17.29 ±0.599* | 1.402 ±0.088† |
| | <i>ChAT > ds-jet</i> | 12 | 17•50•33† | 67•0•33 | 16.75 ±0.094 | 1.311 ±0.117†† |
| 7c/wk (††††) | <i>Control (Pooled)</i> | 54 | 46•46•8 | 89•4•7 | 23.75 ±0.23 | 1.533 ±0.072 |
| | <i>TUG Control</i> | 14 | 50•36•14 | 86•0•14 | 24 ±0 | 1.492 ±0.115 |
| | <i>TUG > ds-jet</i> | 38 | 90•5•5****## | 95•0•5 | 23.99 ±0.014 | 2.257 ±0.110****## |
| | <i>cry-Gal4 Control</i> | 14 | 21•64•12 | 79•7•14 | 23.63 ±0.707 | 1.263 ±0.073 |
| | <i>cry > ds-jet</i> | 15 | 67•33•0# | 100•0•0 | 23.97 ±0.033 | 2.223 ±0.212# |
| | <i>Pdf-Gal4 Control</i> | 16 | 63•38•0 | 100•0•0 | 24 ±0 | 1.711 ±0.16 |
| | <i>Pdf > ds-jet</i> | 16 | 81•19•0* | 94•6•0 | 24.09 ±0.094 | 2.396 ±0.176** |

Appendix A:

| | | | | | | |
|--------------|------------------------------|----|---------------|-------------|--------------|------------------|
| | <i>GMR78G02-Gal4 Control</i> | 10 | 50•50•0 | 90•10•0 | 23.2 ±0.804 | 1.682 ±0.205 |
| | <i>GMR78G02 > ds-jet</i> | 13 | 62•31•8 | 92•0•8 | 24 ±0 | 2.078 ±0.224 |
| | <i>ChAT > ds-jet</i> | 10 | 70•30•0 | 100•0•0 | 24 ±0 | 2.335 ±0.297 |
| | <i>Control (Pooled)</i> | 55 | 36•47•17 | 84•0•16 | 33.67 ±0.047 | 1.515 ±0.069 |
| | <i>TUG Control</i> | 15 | 33•40•27 | 73•0•27 | 33.64 ±0.07 | 1.36 ±0.109 |
| | <i>TUG > ds-jet</i> | 59 | 41•32•27++++‡ | 70•3•27+++‡ | 33.58 ±0.107 | 1.529 ±0.077++++ |
| | <i>cry-Gal4 Control</i> | 14 | 29•64•7 | 93•0•7 | 33.69 ±0.121 | 1.455 ±0.12 |
| 5c/wk | <i>cry > ds-jet</i> | 15 | 47•40•13 | 87•0•13‡ | 33.62 ±0.061 | 1.592 ±0.099 |
| (††) | <i>Pdf-Gal4 Control</i> | 14 | 64•29•7 | 93•0•7 | 33.65 ±0.067 | 1.901 ±0.167 |
| | <i>Pdf > ds-jet</i> | 15 | 80•20•0** | 93•7•0 | 33.83 ±0.167 | 1.765 ±0.098† |
| | <i>GMR78G02-Gal4 Control</i> | 12 | 17•58•25 | 75•0•25 | 33.72 ±0.121 | 1.328 ±0.086 |
| | <i>GMR78G02 > ds-jet</i> | 16 | 56•38•6 | 88•6•6 | 33.5 ±0.162 | 1.623 ±0.089 |
| | <i>ChAT > ds-jet</i> | 13 | 77•15•8*‡‡ | 92•0•8 | 33.63 ±0.065 | 2.055 ±0.198‡ |

S.Table 12 Locomotor activity of male and female flies with *ds-jet* RNA (JF01506) in different clock cell subsets in 10, 7 and 5c/wk LD cycles.

Male (top) and female (bottom) flies of **genotype; Control (Pooled)** (Data for all isogenic controls combined), *UAS-Dcr-2 w*;tim(UAS)-Gal4/+;(Sb¹ or TM6B-Tb¹)/TM3-Ser¹ (TUG Control)*, *UAS-Dcr-2 w*;tim(UAS)-Gal4/+;UAS-ds-jet^{JF01506}/TM6BTb¹ (TUG > ds-jet)*, *UAS-Dcr-2 w*;;(UAS-ds-jet^{JF01506} or cry-Gal4-13)/TM3-Ser¹ (cry-Gal4 Control)*, *UAS-Dcr-2 w*;;UAS-ds-jet^{JF01506}/cry-Gal4-13 (cry > ds-jet)*, *UAS-Dcr-2 w*;Pdf-Gal4/+;+/TM3-Ser¹ (Pdf-Gal4 Control)*, *UAS-Dcr-2 w*;Pdf-Gal4/+;UAS-ds-jet^{JF01506}/+ (Pdf > ds-jet)*, *UAS-Dcr-2 w*;;(UAS-ds-jet^{JF01506} or GMR78G02-Gal4)/TM3-Ser¹ (GMR78G02-Gal4 Control)*, *UAS-Dcr-2 w*;;UAS-ds-jet^{JF01506}/GMR78G02-Gal4 (GMR78G02 > ds-jet)* and *UAS-Dcr-2 w*;ChAT-Gal4/+;UAS-ds-jet^{JF01506}/+ (ChAT > ds-jet)* with result of *Kruskal-Wallis* test comparing Period length (*) and RRP (†) between genotypes within each condition. **n**, number of flies. **%R•%WR•%AR**, percentage of flies classified and rhythmic (R), weakly rhythmic (WR) and arrhythmic (AR). **%ExT•%Other•%AR**, percentage of flies classified and entrained (ExT), “other” and arrhythmic (AR). *Fisher’s exact test* for each genotype vs. *Control (All)* (*) and for knockdown (Gal4 > dsRNA) vs. isogenic control (Gal4 Control) (#) in each condition for **%R•%WR•%AR** and **%ExT•%Other•%AR**. *Fisher’s exact test* between all conditions within each genotype for **%R•%WR•%AR**; 5/10 vs. 7c/wk (†) and 5 vs. 10c/wk (‡). **Tau (h) ±SEM**, mean period length. **RRP ±SEM**, mean relative rhythmic power. AR flies were assigned RRP=1 and omitted from period length analysis. *Pairwise Mann-Whitney test* for all genotype vs. *Control (All)* (*) and for knockdown (Gal4 > dsRNA) vs. isogenic control (Gal4 Control) (#) for Tau (h) ±SEM and RRP ±SEM. *Dunn’s Multiple Comparison test* between all conditions within each genotype for RRP ±SEM; 5/10 vs. 7c/wk (†) and 5 vs. 10c/wk (‡). In all cases (*, #, † and ‡): p ****<0.0001; 0.0001< p ***<0.001; 0.001< p **<0.01; 0.01< p *<0.05.

Appendix A:

| LD Condition | | Genotype | n | %R•%WR•%AR | %ExT•%Other•%AR | Tau (h) ±SEM | RRP ±SEM |
|--------------|----------------------|----------------------|----|------------------|------------------|-------------------|-----------------------|
| (K-W test) | | | | | | | |
| ♂ | 10c/wk (****††††) | Control | 34 | 35•55•10†††† | 64•26•10##††† | 18.44 ±0.513# | 1.611 ±0.089†††† |
| | | TUG > ds-cry | 58 | 59•34•7†††† | 34•59•7**†††† | 21.47 ±0.537* | 1.703 ±0.071†††† |
| | | TUG (-cry) > ds-cry | 16 | 94•0•6****## | 94•0•6*#### | 16.97 ±0.033## | 2.405 ±0.234**† |
| | | TUG (-Pdf) > ds-cry | 31 | 84•16•0***# | 77•23•0###† | 19.06 ±0.639 | 2.604 ±0.219****##††† |
| | | TUG (-ChAT) > ds-cry | 30 | 53•37•10†††† | 13•77•10****†††† | 23.83 ±0.582**** | 1.697 ±0.101†††† |
| ♂ | 7c/wk (†††) | Control | 32 | 90•10•0 | 100•0•0 | 24 ±0 | 3.104 ±0.192 |
| | | TUG > ds-cry | 67 | 94•6•0 | 100•0•0 | 24.01 ±0.007 | 2.98 ±0.091 |
| | | TUG (-cry) > ds-cry | 32 | 94•6•0 | 100•0•0 | 24.02 ±0.016 | 3.286 ±0.178 |
| | | TUG (-Pdf) > ds-cry | 31 | 100•0•0 | 100•0•0 | 24 ±0 | 3.676 ±0.105## |
| | | TUG (-ChAT) > ds-cry | 29 | 100•0•0 | 100•0•0 | 24.02 ±0.017 | 3.519 ±0.119# |
| ♂ | 5c/wk (****††††) | Control | 47 | 89•11•0#####†††† | 100•0•0#####†††† | 33.56 ±0.025##### | 2.163 ±0.083#####†††† |
| | | TUG > ds-cry | 63 | 40•54•6****†††† | 45•49•6****†††† | 29.18 ±0.559**** | 1.67 ±0.086****†††† |
| | | TUG (-cry) > ds-cry | 15 | 80•20•0# | 93•7•0## | 33.07 ±0.543## | 2.404 ±0.241##† |
| | | TUG (-Pdf) > ds-cry | 48 | 58•42•0**††††† | 90•10•0#### | 33.02 ±0.294##### | 2.079 ±0.136†††† |
| | | TUG (-ChAT) > ds-cry | 30 | 27•70•3****††††† | 37•60•3****†††† | 29.6 ±0.625**** | 1.447 ±0.069****†††† |

Appendix A:

| | LD Condition (K-W test) | Genotype | n | %R•%WR•%AR | %ExT•%Other•%AR | Tau (h) ±SEM | RRP ±SEM |
|---|----------------------------|----------------------|----|--------------------|------------------|---------------|---------------------|
| | | | | | | | |
| ♀ | 10c/wk (*) | Control | 34 | 43•30•27+++ | 56•17•27++++ | 18.27 ±0.551 | 1.713 ±0.14++ |
| | | TUG > ds-cry | 63 | 40•29•32++++ | 59•9•32++++ | 17.56 ±0.313 | 1.626 ±0.098++ |
| | | TUG (-cry) > ds-cry | 20 | 60•35•5#++ | 90•5•5*# | 17.42 ±0.421 | 1.812 ±0.159+++ |
| | | TUG (-Pdf) > ds-cry | 32 | 50•41•9#+++ | 91•0•9***## | 16.804 ±0.05* | 1.539 ±0.087++++ |
| | | TUG (-ChAT) > ds-cry | 29 | 38•38•24+++ | 66•10•24 | 17.98 ±0.611 | 1.5 ±0.111++++ |
| | 7c/wk (++++) | Control | 32 | 89•11•0# | 100•0•0 | 24 ±0 | 2.498 ±0.191 |
| | | TUG > ds-cry | 52 | 63•35•2* | 98•0•2 | 24 ±0.024 | 1.998 ±0.107 |
| | | TUG (-cry) > ds-cry | 30 | 97•3•0## | 100•0•0 | 24 ±0 | 3.039 ±0.158#### |
| | | TUG (-Pdf) > ds-cry | 30 | 93•7•0## | 100•0•0 | 24 ±0 | 2.97 ±0.164#### |
| | | TUG (-ChAT) > ds-cry | 19 | 95•0•5## | 95•0•5 | 24.06 ±0.038 | 2.785 ±0.19# |
| | 5c/wk (++++) | Control | 47 | 88•12•0#####+++ | 100•0•0#####+++ | 33.7 ±0.043 | 2.244 ±0.116#####+ |
| | | TUG > ds-cry | 57 | 25•35•40*****+++ | 49•11•40*****+++ | 33.44 ±0.247 | 1.353 ±0.07*****+++ |
| | | TUG (-cry) > ds-cry | 16 | 50•19•31*****+ | 69•0•31*****+ | 33.73 ±0.156 | 1.923 ±0.254++ |
| | | TUG (-Pdf) > ds-cry | 46 | 48•41•11****##++++ | 89•0•11#### | 33.54 ±0.044 | 1.598 ±0.072**++++ |
| | | TUG (-ChAT) > ds-cry | 29 | 62•28•10*##+ | 83•7•10*#### | 33.13 ±0.337 | 1.715 ±0.1#++ |

S.Table 13 Locomotor activity of male and female flies with *ds-cry* RNA (3772R2) in all clock cell subset with added spatial regulation using Gal80 constructs in 10, 7 and 5c/wk LD cycles.

Male (top) and female (bottom) flies of **genotype; Control** (Data for flies that do not express *ds-cry* RNA was pooled – average data was comparable across different control lines); *UAS-Dcr-2 w*;UAS-ds-cry^{3772R2}/tim(UAS)-Gal4;+/TM6B-Tb¹ (TUG>ds-cry)*, *UAS-Dcr-2 w*;UAS-ds-cry^{3772R2}/tim(UAS)-Gal4;cry-Gal80/+ (TUG(-cry)>ds-cry)*, *UAS-Dcr-2 w*;UAS-ds-cry^{3772R2}/tim(UAS)-Gal4;Pdf-Gal80/+ (TUG(-Pdf)>ds-cry)* and *UAS-Dcr-2 w*;UAS-ds-cry^{3772R2}/tim(UAS)-Gal4;ChAT-Gal80/+ (TUG(-ChAT)>ds-cry)* with result of *Kruskal-Wallis* test comparing Period length (*) and RRP (†) between genotypes within each condition. **n**, number of flies. **%R•%WR•%AR**, percentage of flies classified and rhythmic (R), weakly rhythmic (WR) and arrhythmic (AR). **%ExT•%Other•%AR**, percentage of flies classified and entrained (ExT), “other” and arrhythmic (AR). *Fisher’s exact test* for each genotype vs. *Control* (*) and for *TUG > ds-cry* (#) in each condition for %R•%WR•%AR and %ExT•%Other•%AR. *Fisher’s exact test* between all conditions within each genotype for %R•%WR•%AR; 5/10 vs.7c/wk (†) and 5 vs. 10c/wk (‡). **Tau (h) ±SEM**, mean period length. **RRP ±SEM**, mean relative rhythmic power. AR flies were assigned RRP=1 and omitted from period length analysis. Pairwise *Mann-Whitney test* for all genotype vs. *Control* (*) and for *TUG > ds-cry* (#) for Tau (h) ±SEM and RRP ±SEM. *Dunn’s Multiple Comparison test* between all conditions within each genotype for RRP ±SEM; 5/10 vs.7c/wk (†) and 5 vs. 10c/wk (‡). In all cases (*, #, † and ‡): p ****<0.0001; 0.0001< p ***<0.001; 0.001< p **<0.01; 0.01< p *<0.05. Selective knockdown data was collected and analysed with the help of Mr Mike Price.

Appendix A:

| LD Condition (K-W test) | Genotype | n | %R•%WR•%AR | %ExT•%Other•%AR | Tau (h) ±SEM | RRP ±SEM |
|----------------------------|-----------------------|----|-------------------|----------------------|-----------------------|-----------------------|
| 10c/wk (****††††) | Control | 46 | 63•20•17###†† | 76•7•17#####††† | 17.45 ±0.282# | 2.117 ±0.157† |
| | TUG > ds-jet | 55 | 38•55•7****†††† | 33•60•7*****†††† | 21.49 ±0.518* | 1.576 ±0.071†††† |
| | TUG (-cry) > ds-jet | 27 | 44•41•15†††† | 74•11•15##### | 19.24 ±0.743 | 1.548 ±0.085†††† |
| | TUG (-Pdf) > ds-jet | 16 | 56•44•0†† | 56•44•0***†† | 20.5 ±1.025 | 2.219 ±0.248†††† |
| | TUG (-ChAT) > ds-jet | 21 | 67•19•14#† | 0•86•14****#####†††† | 24.64 ±0.097****### | 1.874 ±0.154† |
| | TUG (-VGlut) > ds-jet | 13 | 15•70•15****†††† | 46•39•15*† | 20.5 ±1.124 | 1.278 ±0.092*†††† |
| 7c/wk (†††) | Control | 49 | 88•12•0 | 100•0•0 | 24 ±0 | 2.554 ±0.122## |
| | TUG > ds-jet | 33 | 100•0•0 | 100•0•0 | 24 ±0 | 3.427 ±0.078*** |
| | TUG (-cry) > ds-jet | 15 | 100•0•0 | 100•0•0 | 24 ±0 | 3.423 ±0.189* |
| | TUG (-Pdf) > ds-jet | 15 | 100•0•0 | 100•0•0 | 24 ±0 | 3.802 ±0.133**** |
| | TUG (-ChAT) > ds-jet | 18 | 100•0•0 | 100•0•0 | 24.17 ±0.057****##### | 2.59 ±0.219# |
| | TUG (-VGlut) > ds-jet | 10 | 100•0•0 | 100•0•0 | 24 ±0 | 3.286 ±0.095 |
| 5c/wk (****††††) | Control | 44 | 64•32•5####† | 95•0•5#####† | 33.6 ±0.043## | 1.878 ±0.1##†† |
| | TUG > ds-jet | 56 | 27•57•16****††††† | 57•27•16****††††††† | 31.03 ±0.557** | 1.501 ±0.081*††††† |
| | TUG (-cry) > ds-jet | 6 | 83•17•0# | 100•0•0 | 33.67 ±0.105 | 2.08 ±0.223 |
| | TUG (-Pdf) > ds-jet | 31 | 77•23•0##### | 97•3•0###†† | 33.27 ±0.346# | 2.344 ±0.167#####†††† |

♂

| | | | | | |
|---------------------------------|----|--------------|--------------|---------------|------------------|
| <i>TUG (-ChAT) > ds-jet</i> | 22 | 41•55•5†††† | 82•14•4†††† | 32.76 ±0.422 | 1.514 ±0.099†††† |
| <i>TUG (-VGlut) > ds-jet</i> | 14 | 21•79•0**††† | 57•43•0****† | 30.25 ±1.079* | 1.487 ±0.144†† |

| LD Condition (K-W test) | Genotype | n | %R•%WR•%AR | %ExT•%Other•%AR | Tau (h) ±SEM | RRP ±SEM | |
|---------------------------------|---------------------------------|-------------------------------|--------------|-------------------|---------------|------------------|---------------|
| ♀ | <i>Control</i> | 31 | 39•32•29 | 71•0•29# | 16.98 ±0.04 | 1.553 ±0.124 | |
| | <i>TUG > ds-jet</i> | 62 | 19•37•44†††† | 43•13•44*†††† | 18.47 ±0.563 | 1.273 ±0.051†††† | |
| | 10c/wk (****††††) | <i>TUG (-cry) > ds-jet</i> | 4 | 25•75•0† | 75•25•0 | 16.63 ±0.239 | 1.353 ±0.081† |
| | <i>TUG (-Pdf) > ds-jet</i> | 16 | 44•44•13#†† | 100•0•0*### | 16.93 ±0.049 | 1.666 ±0.21†† | |
| | <i>TUG (-ChAT) > ds-jet</i> | 27 | 19•48•33†††† | 22•45•33***##†††† | 21.56 ±1.012 | 1.23 ±0.051 | |
| | <i>TUG (-VGlut) > ds-jet</i> | 16 | 6•50•44†††† | 50•6•44†† | 16.61 ±0.398 | 1.121 ±0.045††† | |
| | <i>Control</i> | 37 | 46•35•19### | 81•0•9 | 23.97 ±0.058 | 1.689 ±0.122## | |
| | <i>TUG > ds-jet</i> | 38 | 90•5•5*** | 95•0•5 | 23.99 ±0.014 | 2.257 ±0.110** | |
| | 7c/wk (†††) | <i>TUG (-cry) > ds-jet</i> | 15 | 87•13•0* | 100•0•0 | 24 ±0 | 2.336 ±0.201 |
| | <i>TUG (-Pdf) > ds-jet</i> | 15 | 93•7•0** | 100•0•0 | 24 ±0 | 2.374 ±0.204* | |
| <i>TUG (-ChAT) > ds-jet</i> | 24 | 75•25•0*# | 96•4•0* | 24.19 ±0.079*## | 2.12 ±0.167 | | |
| <i>TUG (-VGlut) > ds-jet</i> | 13 | 85•15•0* | 100•0•0 | 23.96 ±0.038 | 2.401 ±0.222* | | |

Appendix A:

| | | | | | | |
|-------------------|---------------------------------|----|---------------|--------------|--------------|------------------|
| | <i>Control</i> | 30 | 57•37•7 | 90•3•7#‡ | 33.59 ±0.096 | 1.824 ±0.152 |
| | <i>TUG > ds-jet</i> | 59 | 41•32•27++++‡ | 70•3•27*++‡‡ | 33.58 ±0.107 | 1.529 ±0.077++++ |
| 5c/wk | <i>TUG (-cry) > ds-jet</i> | 9 | 56•44•0 | 100•0•0 | 33.78 ±0.169 | 1.596 ±0.106† |
| (****††††) | <i>TUG (-Pdf) > ds-jet</i> | 31 | 35•58•6#+++ | 90•3•6# | 33.52 ±0.088 | 1.644 ±0.129++ |
| | <i>TUG (-ChAT) > ds-jet</i> | 23 | 52•35•13‡ | 87•0•13‡‡‡‡ | 33.58 ±0.055 | 1.578 ±0.087 |
| | <i>TUG (-VGlut) > ds-jet</i> | 13 | 15•54•31*++ | 61•8•31† | 33.5 ±0.204 | 1.246 ±0.097+++ |

S.Table 14 Locomotor activity of male and female flies with *ds-jet* RNA (JF01506) in all clock cell subset with added spatial regulation using Gal80 constructs in 10, 7 and 5c/wk LD cycles.

Male (top) and female (bottom) flies of **genotype; Control** (Data for flies that do not express *ds-jet* RNA was pooled – average data was comparable across different control lines); *UAS-Dcr-2 w**; *tim(UAS)-Gal4/+;UAS-ds-jet^{JF01506}/+* (**TUG>ds-jet**), *UAS-Dcr-2 w**; *tim(UAS)-Gal4/+;UAS-ds-jet^{JF01506}/cry-Gal80* (**TUG(-cry)>ds-jet**), *UAS-Dcr-2 w**; *tim(UAS)-Gal4/+;UAS-ds-jet^{JF01506}/Pdf-Gal80* (**TUG(-Pdf)>ds-Jet**), *UAS-Dcr-2 w**; *tim(UAS)-Gal4/+;UAS-ds-jet^{JF01506}/ChAT-Gal80* (**TUG(-ChAT)>ds-Jet**) and *UAS-Dcr-2 w**; *tim(UAS)-Gal4/Vglut-Gal80;UAS-ds-jet^{JF01506}/+* (**TUG(-VGlut)>ds-jet**) with result of *Kruskal-Wallis test* comparing Period length (*) and RRP (+) between genotypes within each condition. **n**, number of flies. **%R•%WR•%AR**, percentage of flies classified and rhythmic (R), weakly rhythmic (WR) and arrhythmic (AR). **%ExT•%Other•%AR**, percentage of flies classified and entrained (ExT), “other” and arrhythmic (AR). *Fisher’s exact test* for each genotype vs. *Control* (*) and for *TUG > ds-jet* (#) in each condition for %R•%WR•%AR and %ExT•%Other•%AR. *Fisher’s exact test* between all conditions within each genotype for %R•%WR•%AR; 5/10 vs.7c/wk (+) and 5 vs. 10c/wk (‡). **Tau (h) ±SEM**, mean period length. **RRP ±SEM**, mean relative rhythmic power. AR flies were assigned RRP=1 and omitted from period length analysis. *Pairwise Mann-Whitney test* for all genotype vs. *Control* (*) and for *TUG > ds-jet* (#) for Tau (h) ±SEM and RRP ±SEM. *Dunn’s Multiple Comparison test* between all conditions within each genotype for RRP ±SEM; 5/10 vs.7c/wk (+) and 5 vs. 10c/wk (‡). In all cases (*, #, † and ‡): $p^{****}<0.0001$; $0.0001<p^{***}<0.001$; $0.001<p^{**}<0.01$; $0.01<p^*<0.05$. Selective knockdown data was collected and analysed with the help of Mr Mike Price.

| LD Condition (K-W test) | Genotype (in <i>cry⁰¹</i> background) | n | %R•%WR•%AR | %ExT•%Other•%AR | Tau (h) ±SEM | RRP ±SEM |
|----------------------------|--|----|---------------|-----------------|------------------|--------------------|
| | | | | | | |
| 10c/wk (*+) | <i>UAS-cry</i> | 28 | 32•61•7++++ | 25•68•7++++ | 21.23 ±0.648 | 1.367 ±0.066++++ |
| | <i>TUG > UAS-cry</i> | 30 | 42•42•16++++ | 60•23•17***** | 18.44 ±0.651* | 1.455 ±0.078++++ |
| | <i>Pdf > UAS-cry</i> | 37 | 21•31•48***** | 21•30•49***** | 20.45 ±0.92 | 1.267 ±0.072++++ |
| | <i>ChAT > UAS-cry</i> | 15 | 53•47•0++ | 80•20•0*** | 17.77 ±0.433* | 1.59 ±0.104++++ |
| ♂ 7c/wk (+++) | <i>UAS-cry</i> | 30 | 100•0•0 | 100•0•0 | 24 ±0 | 3.206 ±0.12 |
| | <i>TUG > UAS-cry</i> | 44 | 91•9•0 | 100•0•0 | 24 ±0 | 2.637 ±0.12** |
| | <i>Pdf > UAS-cry</i> | 41 | 80•20•0** | 100•0•0 | 24.05 ±0.03 | 2.282 ±0.13**** |
| | <i>ChAT > UAS-cry</i> | 15 | 100•0•0 | 100•0•0 | 24 ±0 | 3.207 ±0.114 |
| 5c/wk (*****+) | <i>UAS-cry</i> | 28 | 11•75•14++++ | 32•54•14++++ | 25.4 ±1.664 | 1.25 ±0.04++++ |
| | <i>TUG > UAS-cry</i> | 25 | 28•56•16++++ | 68•12•20***** | 33.35 ±0.825**** | 1.366 ±0.132++++ |
| | <i>Pdf > UAS-cry</i> | 25 | 4•72•24++++# | 60•16•24*****# | 31.89 ±0.849 | 1.175 ±0.032++++ |
| | <i>ChAT > UAS-cry</i> | 14 | 86•14•0**** | 100•0•0**** | 33.64 ±0.063** | 1.845 ±0.101++++** |
| LD Condition (K-W test) | Genotype (in <i>cry⁰¹</i> background) | n | %R•%WR•%AR | %ExT•%Other•%AR | Tau (h) ±SEM | RRP ±SEM |
| 10c/wk (+++) | <i>UAS-cry</i> | 24 | 21•50•29++++ | 54•14•32++++ | 17.59 0.313 | 1.342 0.102++++ |
| | <i>TUG > UAS-cry</i> | 30 | 50•33•17++ | 73•10•17++++ | 17.92 0.509 | 1.68 0.136+ |
| | <i>Pdf > UAS-cry</i> | 40 | 12•58•30++++ | 32•35•33++++ | 20.28 0.7 | 1.173 0.048++++ |
| | <i>ChAT > UAS-cry</i> | 16 | 12•44•44+ | 37•19•44+ | 18.17 0.651 | 1.207 0.091++ |
| ♀ 7c/wk (*+) | <i>UAS-cry</i> | 28 | 86•14•0 | 96•4•0 | 23.89 0.09 | 2.746 0.186 |
| | <i>TUG > UAS-cry</i> | 43 | 85•10•4 | 95•0•5 | 24 0 | 2.083 0.105* |
| | <i>Pdf > UAS-cry</i> | 41 | 73•25•2 | 98•0•2 | 24.05 0.03* | 2.017 0.111** |
| | <i>ChAT > UAS-cry</i> | 14 | 64•36•0 | 100•0•0 | 23.82 0.145 | 2.095 0.231 |
| 5c/wk (**) | <i>UAS-cry</i> | 24 | 29•54•17++++ | 29•46•25++++ | 23.2 2.116 | 1.408 0.082++++ |
| | <i>TUG > UAS-cry</i> | 29 | 30•43•27++++ | 55•17•28++++ | 33 0.568 | 1.647 0.16++ |
| | <i>Pdf > UAS-cry</i> | 23 | 47•40•13## | 87•0•13*****## | 33.65 0.097 | 1.605 0.123## |
| | <i>ChAT > UAS-cry</i> | 15 | 53•27•20 | 80•0•20**** | 33.71 0.074 | 1.685 0.166 |

Appendix A:

S. Table 15 Locomotor activity of male and female flies with rescue of CRY expression in different clock cell subsets, in a *cry*⁰¹ background, in 10, 7 and 5c/wk LD cycles.

Male (top) and female (bottom) flies of **genotype**; *w*^{*}; *UAS-cry*₂₄/*CyO*; *cry*⁰¹ (**UAS-cry**), *w*^{*}; *UAS-cry*₂₄/*TUG*; *cry*⁰¹ (**TUG>UAS-cry**), *w*^{*}; *UAS-cry*₂₄/*Pdf-Gal4*; *cry*⁰¹ (**Pdf>UAS-cry**) and *w*^{*}; *UAS-cry*₂₄/*CHAT-Gal4*; *cry*⁰¹ (**CHAT>UAS-cry**); with result of *Kruskal-Wallis test* comparing Period length (*) and RRP (†) between genotypes within each condition. **n**, number of flies. **%R•%WR•%AR**, percentage of flies classified and rhythmic (R), weakly rhythmic (WR) and arrhythmic (AR). **%ExT•%Other•%AR**, percentage of flies classified and entrained (ExT), “other” and arrhythmic (AR). *Fisher’s exact test* for each genotype vs. *UAS-cry* in each condition for %R•%WR•%AR and %ExT•%Other•%AR (*). *Fisher’s exact test* between all conditions within each genotype for %R•%WR•%AR; 5/10 vs. 7c/wk (†) and 5 vs. 10c/wk (‡). **Tau (h) ±SEM**, mean period length. **RRP ±SEM**, mean relative rhythmic power. AR flies were assigned RRP=1 and omitted from period length analysis. *Pairwise Mann-Whitney test* for all genotypes vs. *UAS-cry* in each condition for Tau (h) ±SEM and RRP ±SEM (*). *Dunn’s Multiple Comparison test* between all conditions within each genotype for RRP ±SEM; 5/10 vs. 7c/wk (†) and 5 vs. 10c/wk (‡). In all cases (*, † and ‡): $p^{****}<0.0001$; $0.0001<p^{***}<0.001$; $0.001<p^{**}<0.01$; $0.01<p^*<0.05$.

| Red LD Condition (K-W test) | Genotype | n | %R•%WR•%AR | %ExT•%Other•%AR | Tau (h) ±SEM | RRP ±SEM |
|--------------------------------|-----------------------------|----|----------------|-----------------|---------------------|---------------------|
| 10c/wk (*****+) | <i>cry</i> ⁰¹ /+ | 10 | 20•40•40++++ | 50•10•40† | 17.22 ±0.492 | 1.24 ±0.091++++ |
| | <i>cry</i> ⁰¹ | 13 | 92•8•0*** | 100•0•0** | 16.96 ±0.038† | 2.878 ±0.183**** |
| | <i>eya</i> ² | 16 | 63•38•0* | 0•100•0*****+† | 23.28 ±0.079+++ | 1.784 ±0.135 |
| | <i>GMR-hid</i> | 15 | 47•47•7 | 0•93•7*****+† | 24 ±0.367*** | 1.6 ±0.116 |
| | <i>norpA</i> ⁷ | 16 | 81•13•6** | 0•94•6*****+† | 24.43 ±0.083**** | 1.987 ±0.111* |
| | <i>Hdc</i> ^{JK910} | 16 | 56•44•0†† | 0•100•0*****+† | 24.14 ±0.077***** | 1.661 ±0.1†††† |
| | <i>ort</i> ¹ | 12 | 67•33•0* | 100•0•0** | 16.88 ±0.065+++ | 1.989 ±0.183 |
| | <i>HisCl</i> ^{T2} | 16 | 13•44•44†† | 31•25•44† | 19.72 ±1.236 | 1.224 ±0.084†† |
| 7c/wk (*****+) | <i>cry</i> ⁰¹ /+ | 14 | 100•0•0 | 100•0•0 | 24 ±0 | 3.492 ±0.156 |
| | <i>cry</i> ⁰¹ | 16 | 94•6•0 | 94•6•0 | 24 ±0 | 2.571 ±0.168 |
| | <i>eya</i> ² | 15 | 67•20•13* | 87•0•13 | 23.85 ±0.087 | 1.58 ±0.101**** |
| | <i>GMR-hid</i> | 16 | 44•31•25*** | 50•25•25** | 24.71 ±0.323* | 1.475 ±0.123**** |
| | <i>norpA</i> ⁷ | 12 | 100•0•0 | 100•0•0 | 24.71 ±0.323* | 1.633 ±0.135**** |
| | <i>Hdc</i> ^{JK910} | 15 | 100•0•0 | 100•0•0 | 24.47 ±0.033** | 2.69 ±0.146 |
| | <i>ort</i> ¹ | 11 | 100•0•0 | 100•0•0 | 24.45 ±0.045* | 2.716 ±0.076 |
| | <i>HisCl</i> ^{T2} | 14 | 64•36•0* | 100•0•0 | 24.18 ±0.145 | 1.844 ±0.164**** |
| 5c/wk (*****+) | <i>cry</i> ⁰¹ /+ | 14 | 21•79•0††††† | 79•21•0‡ | 32.35 ±0.714††††††† | 1.393 ±0.089†† |
| | <i>cry</i> ⁰¹ | 27 | 54•46•0††‡ | 93•7•0 | 33.11 ±0.372††††††† | 1.553 ±0.068††††††† |
| | <i>eya</i> ² | 16 | 88•13•0*** | 0•100•0*****+† | 23.31 ±0.077*****+† | 2.093 ±0.117***† |
| | <i>GMR-hid</i> | 16 | 25•44•31 | 0•69•31*****+† | 23.77 ±0.474**** | 1.274 ±0.074 |
| | <i>norpA</i> ⁷ | 16 | 63•31•6*† | 0•94•6*****+† | 24.17 ±0.105**** | 1.631 ±0.087‡ |
| | <i>Hdc</i> ^{JK910} | 16 | 81•13•6*** | 0•94•6*****+† | 24.4 ±0.072***‡† | 1.846 ±0.115†† |
| | <i>ort</i> ¹ | 11 | 36•64•0†† | 64•36•0‡ | 29.95 ±1.426†††† | 1.382 ±0.089†††† |
| | <i>HisCl</i> ^{T2} | 13 | 0•23•77*****+† | 8•15•77*****+† | 27.67 ±2.949‡ | 1.028 ±0.022†††† |

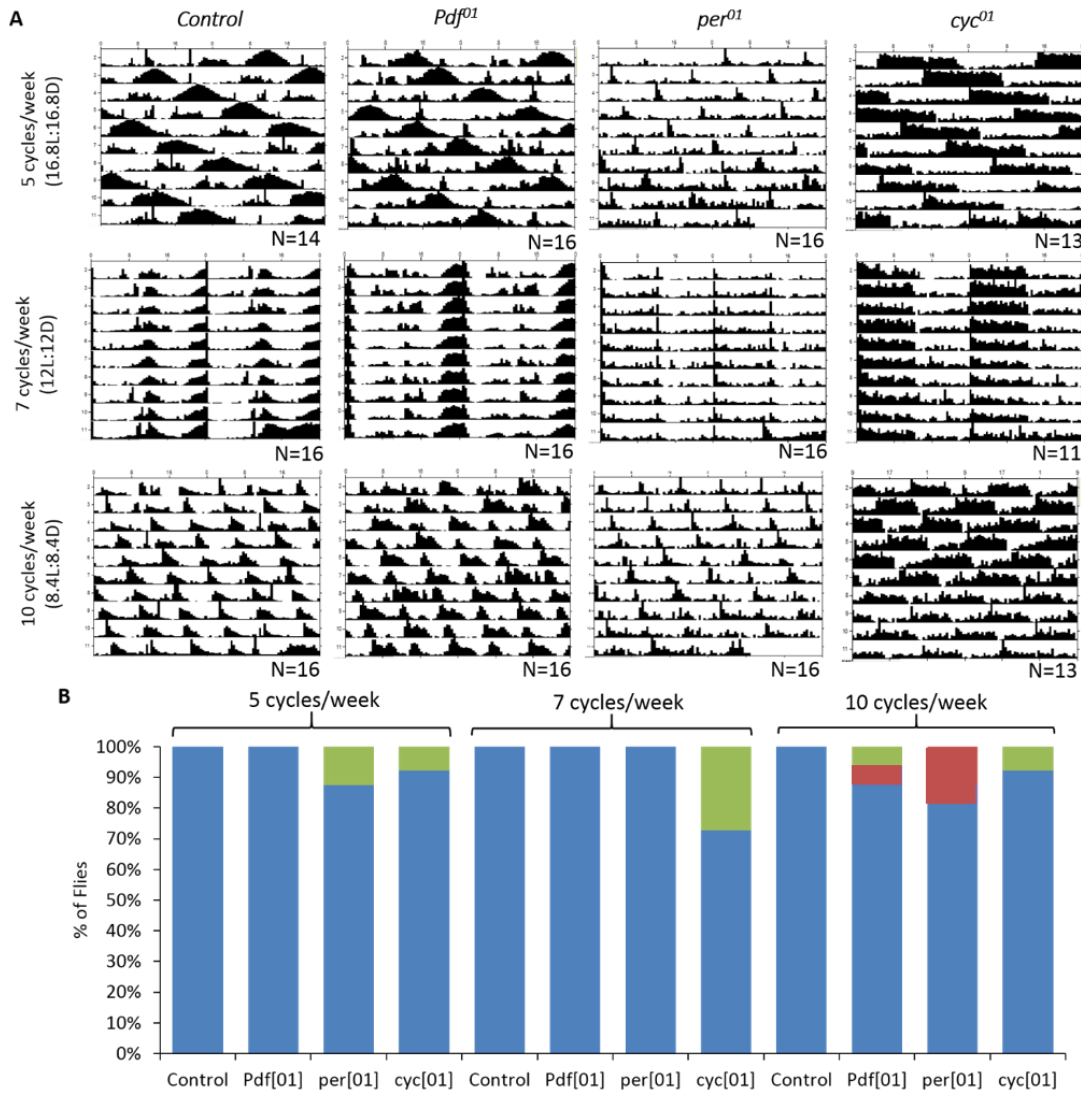
Appendix A:

| Red LD Condition | | Genotype | n | %R•%WR•%AR | %ExT•%Other•%AR | Tau (h) ±SEM | RRP ±SEM |
|-----------------------------|----------------|-----------------------------|-------------|-----------------|------------------|-------------------|------------------|
| 10c/wk (****+) | ♀ | <i>cry</i> ⁰¹ /+ | 11 | 45•55•0 | 91•9•0 | 16.97 ±0.271† | 1.565 ±0.117 |
| | | <i>cry</i> ⁰¹ | 15 | 80•20•0 | 100•0•0† | 16.93 ±0.049† | 2.015 ±0.151 |
| | | <i>eya</i> ² | 16 | 81•19•0 †† | 0•100•0****+††† | 23.63 ±0.056** | 2.062 ±0.14†† |
| | | <i>GMR-hid</i> | 13 | 31•38•31 | 0•69•31****+††† | 23.89 ±0.415** | 1.388 ±0.129 |
| | | <i>norpA</i> ⁷ | 15 | 87•13•0* | 0•100•0****+††† | 24.5 ±0.049**** | 2.156 ±0.172†† |
| | | <i>Hdc</i> ^{JK910} | 15 | 0•73•27**†† | 0•73•27****+††† | 24.02 ±0.372**** | 1.088 ±0.028††† |
| | | <i>ort</i> ¹ | 13 | 77•8•15* | 85•0•15 | 16.95 ±0.045†† | 2.092 ±0.235 |
| | | <i>HisCl</i> ^{T2} | 16 | 0•19•81**** | 13•6•81**** | 19.17 ±2.667 | 1.014 ±0.01* |
| | | <i>cry</i> ⁰¹ /+ | 16 | 56•38•6 | 94•0•6 | 24.03 ±0.033 | 1.527 ±0.083 |
| | | <i>cry</i> ⁰¹ | 12 | 42•42•16 | 75•8•17 | 24.4 ±0.163 | 1.753 ±0.222 |
| <i>eya</i> ² | 12 | 25•75•0 | 100•0•0 | 23.79 ±0.115 | 1.368 ±0.086 | | |
| 7c/wk (**+) | <i>GMR-hid</i> | 16 | 13•37•50** | 50•0•50* | 24.13 ±0.227 | 1.122 ±0.05* | |
| <i>norpA</i> ⁷ | 8 | 100•0•0* | 100•0•0 | 24.13 ±0.227 | 1.244 ±0.08 | | |
| <i>Hdc</i> ^{JK910} | 14 | 57•36•7 | 93•0•7 | 24.42 ±0.077 | 1.828 ±0.193 | | |
| <i>ort</i> ¹ | 15 | 87•13•0 | 100•0•0 | 24.13 ±0.124 | 2.656 ±0.185 | | |
| <i>HisCl</i> ^{T2} | 14 | 7•43•50** | 36•14•50 ** | 24.79 ±0.286 | 1.098 ±0.039* | | |
| 5c/wk (****+) | ♀ | <i>cry</i> ⁰¹ /+ | 16 | 0•100•0††††† | 62•38•0† | 30.74 ±0.975††††† | 1.112 ±0.03††††† |
| | | <i>cry</i> ⁰¹ | 23 | 9•65•26*†††† | 52•22•26†† | 31.15 ±1.041†††† | 1.147 ±0.055†††† |
| | | <i>eya</i> ² | 10 | 60•30•10*** | 0•90•10**†††† | 23.44 ±0.176**** | 1.535 ±0.089‡ |
| | | <i>GMR-hid</i> | 16 | 0•50•50**‡ | 0•50•50****+††† | 22.81 ±0.422****† | 1.085 ±0.033 |
| | | <i>norpA</i> ⁷ | 14 | 43•21•36****+†‡ | 0•64•36****+†††† | 24.33 ±0.144* | 1.442 ±0.127†† |
| | | <i>Hdc</i> ^{JK910} | 16 | 50•44•6***†† | 0•94•6****+††† | 24.53 ±0.133* | 1.521 ±0.078†† |
| | | <i>ort</i> ¹ | 14 | 36•50•14**†† | 72•14•14† | 31.79 ±1.093†††† | 1.406 ±0.08††† |
| | | <i>HisCl</i> ^{T2} | 15 | 0•33•67**** | 27•7•66**** | 32.9 ±0.621††† | 1.032 ±0.16 |

S.Table 16 Male and Female locomotor activity of mutant genotypes in 10, 7 and 5c/wk equinox red light LD cycles.

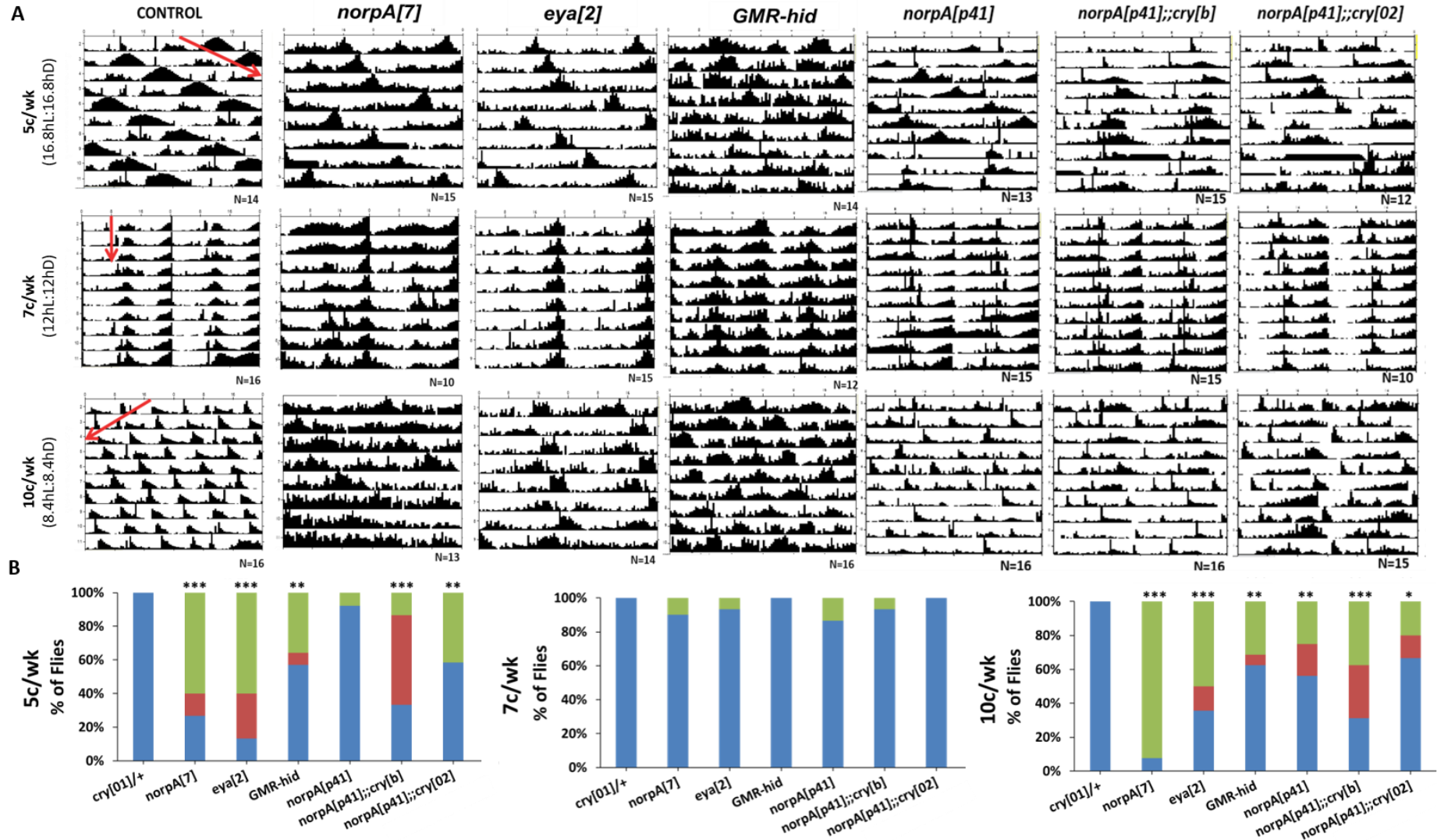
Male (top) and female (bottom) flies of **genotype**; $w^{1118};cry^{01}/+$, $w^{1118};cry^{01}$, eya^2 , $GMR-hid$, $norpA^7$, Hdc^{JK910} , ort^1 and st^1HisCl^{T2} with result of *Kruskal-Wallis test* comparing period length (*) and RRP (†) between all genotypes within each condition. **n**, number of flies. **%R•%WR•%AR**, percentage of flies classified and rhythmic (R), weakly rhythmic (WR) and arrhythmic (AR). **%ExT•%Other•%AR**, percentage of flies classified and entrained (ExT), other and arrhythmic (AR). *Fisher's exact test* vs. $cry^{01}/+$ in each condition for %R•%WR•%AR and %ExT•%Other•%AR (*). *Fisher's exact test* between all conditions within each genotype for %R•%WR•%AR and %ExT•%Other•%AR; 5/10 vs. 7c/wk (†) and 5 vs. 10c/wk (‡). **Tau (h) ±SEM**, mean period length – Ext period lengths; 10c/wk = 16.8 h, 7c/wk = 24 h and 5c/wk = 33.6 h. **RRP ±SEM**, mean relative rhythmic power. AR flies were assigned RRP=1 and omitted from period length analysis. *Pairwise Mann-Whitney test* vs. $cry^{01}/+$ in each condition for Tau (h) ±SEM and RRP ±SEM (*). *Dunn's Multiple Comparison test* between all conditions within each genotype for Tau (h) ±SEM and RRP ±SEM; 5/10 vs. 7c/wk (†) and 5 vs. 10c/wk (‡). In all cases (*, † and ‡): $p^{****}<0.0001$; $0.0001<p^{***}<0.001$; $0.001<p^{**}<0.01$; $0.01<p^*<0.05$. RLD behavioural data for visual and histamine signalling mutants was collected and analysed by Miss Nanthilde Malandain.

A.5 Supplementary Figures: Chapter 3



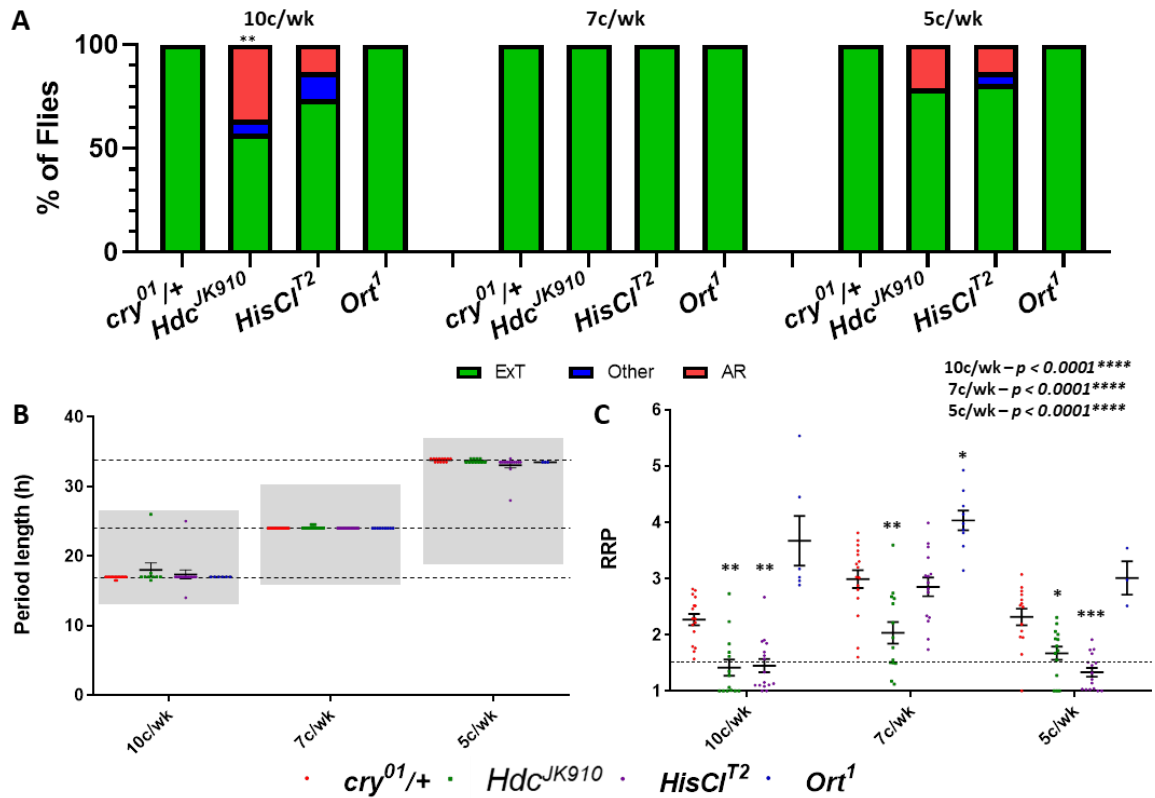
S.Figure 7 Other mutations to circadian genes affect aspects of locomotor behaviour but show no impact on entrainment to extreme photocycles

A) Double-plotted actograms showing average locomotor behaviour of male flies of the genotype $w^{1118};cry^{01}/+$ (**Control**), y^1w^* ; ***Pdf⁰¹***, y^1 ***per⁰¹*** w^* and ***cyc⁰¹*** ry^{506} (right to left) in 5, 7 and 10 cycles/week LD cycles (top to bottom) over 10 days, plotted on a 24 h time-scale. N defines number of flies used in each assay. **B)** Composite bar charts of percentage of flies showing entrained (blue), other (red) or arrhythmic (green) locomotor behaviour in 5, 7 and 10 c/wk LD (annotated in figure).



S.Figure 8 A functional visual system is required for behavioural plasticity in extreme photocycles.

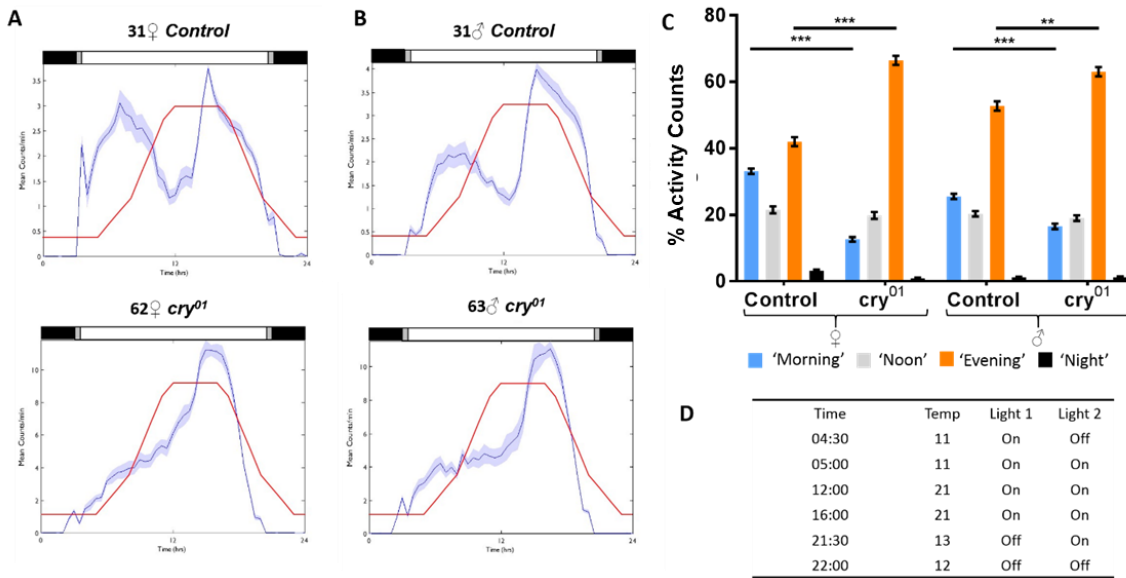
A) Average locomotor activity presented in double plotted actograms over a 24 h scale, for adult male flies of genotype; $w^{1118};cry^{01}/+$ (**Control**), $norpA^7$, eya^2 , $GMR-hid$, $norpA^{p41}$, $norpA^{p41};cry^b$ and $norpA^{p41};cry^{02}$ (left to right); in 5 (top), 7 (middle) and 10c/wk (bottom) equinox LD cycles. 'n' denotes number of flies and red arrows on $cry^{01}/+$ actograms indicate the direction of rhythmic behaviour. **B)** Composite bar charts showing percentage of flies showing entrained (blue), other (red) or arrhythmic (green) locomotor behaviour over 10 days in 5 (left), 7 (middle) and 10c/wk (right). *Fisher's exact test* to compare distribution of entrained, other and arrhythmic individuals for each genotype vs. $cry^{01}/+$; $p^{***}<0.0001$; $0.0001<p^{***}<0.001$; $0.001<p^{**}<0.01$; $0.01<p^*<0.05$.



S. Figure 9 Histamine signalling mutants do not greatly reduce behavioural entrainment in white LD cycles.

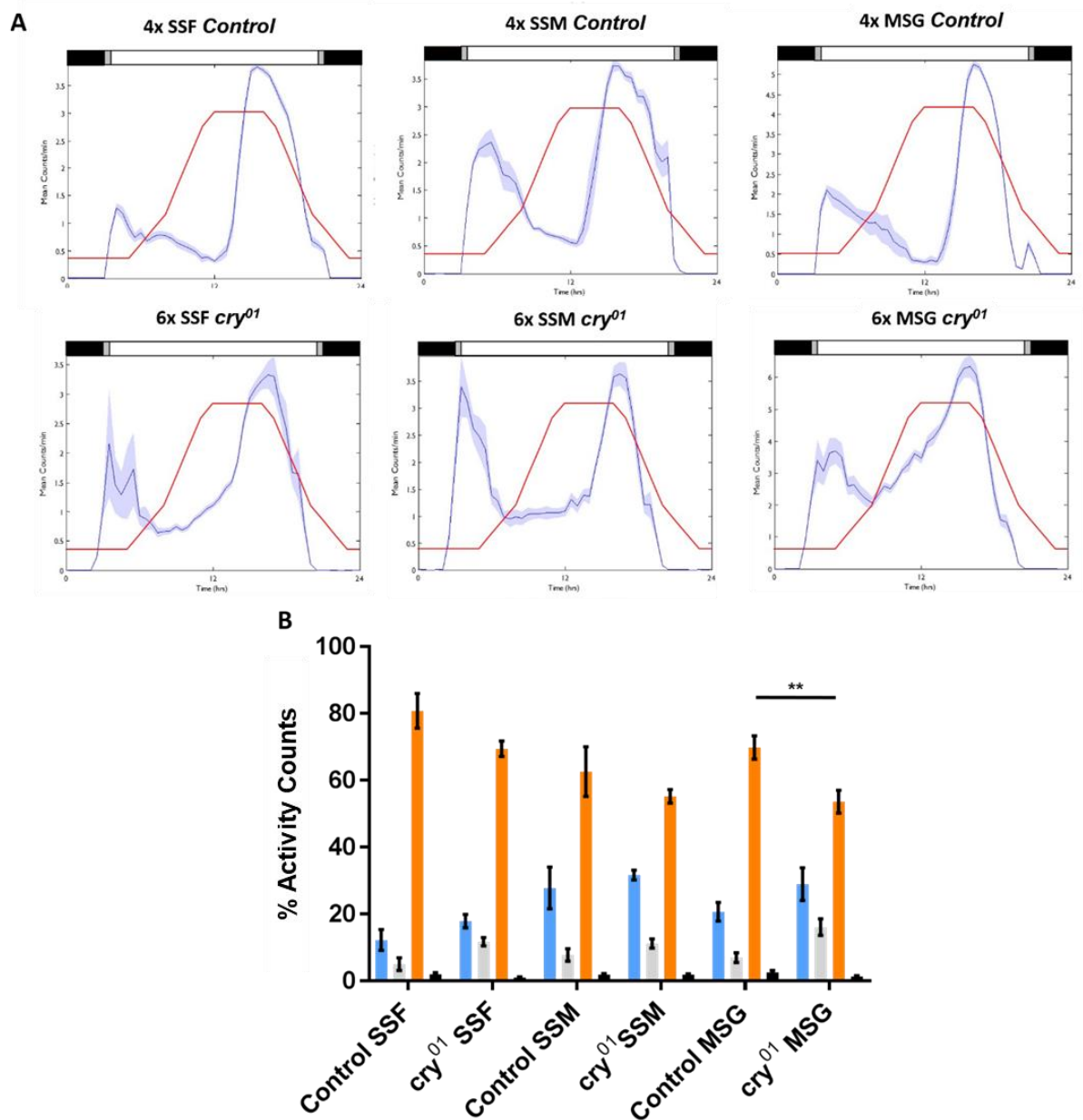
A) Composite bar charts showing percentage of flies showing entrained (green), other (blue) or arrhythmic (red) locomotor behaviour (see methods) for adult male flies of genotype; $w^{1118}; cry^{01/+}, Hdc^{JK910}, Ort^1$ and $st^1 HisCl^{T2}$ over 10 days in 10 (top), 7 (middle) and 5c/wk (bottom) LD. Fisher's exact test to compare distribution of entrained, other and arrhythmic individuals for each genotype vs. $cry^{01/+}$. For 10c/wk primary and secondary periodicities were compared for each individual and the dominant period length was used to categorise flies using only the 'Ext' range. **B, C)** Individual male period lengths (**B**) and RRP (**C**) for in 10, 7, and 5c/wk (left to right) LD for $cry^{01/+}$ (red), Hdc^{JK910} (green), $HisCl^{T2}$ (purple) and Ort^1 (blue). Error bars show mean period length (**B**) or RRP (**C**) \pm SEM. **B)** Dashed lines represent entrained period length for 10 (bottom), 7 (middle) and 5c/wk (top). Grey shading indicates analysis parameters used for individual fly analysis in each LD cycle. **C)** Dashed line indicated an RRP value of 1.5. Arrhythmic flies are assigned an RRP of 1. Results of Kruskal-Wallis test comparing RRP between genotypes within each condition are reported in the top right. Pairwise comparisons of RRP for each genotype vs. $cry^{01/+}$ with Mann-Whitney test. $p^{****} < 0.0001$; $0.0001 < p^{***} < 0.001$; $0.001 < p^{**} < 0.01$; $0.01 < p^* < 0.05$.

Appendix A:



S.Figure 10 *cry⁰¹* mutants show a preference for temperature cycling compared to light.

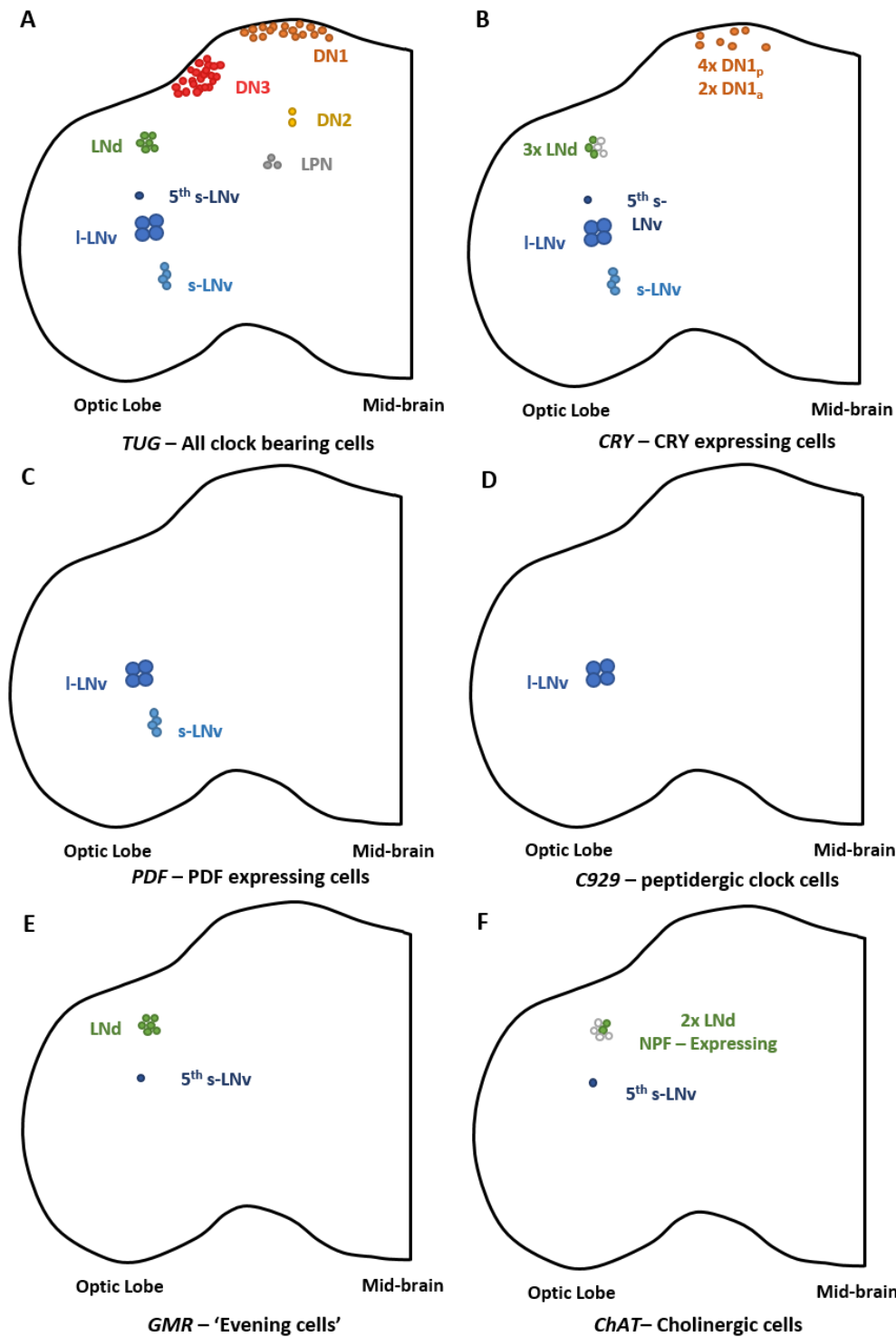
Average activity profiles of female (**A**) and male (**B**) flies of genotype $w^{1118};;cry^{01}/+$ (**Control**) (top) and $w^{1118};;cry^{01}$ (**cry⁰¹**) (bottom). Light condition is depicted by LD bar (black=dark; grey=1x light ; white=2x light) and red trace represents temperature fluctuation across 24 h. Profiles are shifted to incorporate entire light-phase flanked by half the dark phase, plotted over 24 h time-scale. Blue shading is \pm SEM. **C**) Percentage activity counts during 'Morning' (blue), 'Noon' (grey), 'Evening' (orange) and 'Night' (black) for female (left) and male (right) flies exposed to overlapping light and temperature cycling. *Tukey's multiple comparison test* to compare activity counts at each defined interval between genotypes; $p^{***}<0.001$, $0.001<p^{**}<0.01$ and $0.01<p^*<0.05$. **D**) Table showing light and temperature cycle protocol (24 h cycle).



S.Figure 11 Social interaction effects locomotion of group housed flies irrespective of light and temperature cycles.

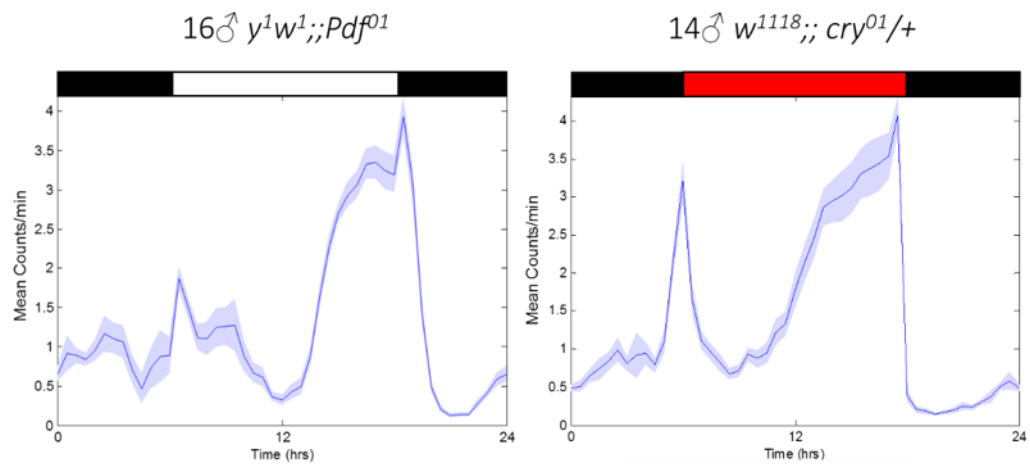
A) Average activity profiles of Single Sex Female (SSF), Single Sex Males (SSM) and Mixed Sex Groups (MSG) (left to right) group housed flies of genotype $w^{1118};cry^{01}/+$ (Control) (top) and $w^{1118};cry^{01}$ (*cry⁰¹*) (bottom). Light condition is depicted by LD bar (black=dark; grey=1x light; white=2x light) and red trace represents temperature fluctuation across 24 h. Profiles are shifted to incorporate entire light-phase flanked by half the dark phase, plotted over 24 h time-scale. Blue shading is \pm SEM. **B)** Percentage activity counts during ‘Morning’ (blue), ‘Noon’ (grey), ‘Evening’ (orange) and ‘Night’ (black) for female (left) and male (right) flies exposed to overlapping light and temperature cycling. Tukey’s multiple comparison test to compare activity counts at each defined interval between genotypes in each group; $p^{***}<0.001$, $0.001<p^{**}<0.01$ and $0.01<p^*<0.05$.

Appendix A:



S.Figure 12 Approximate location of neuronal clock cell subsets and specific cells targeted via different Gal4 driver lines.

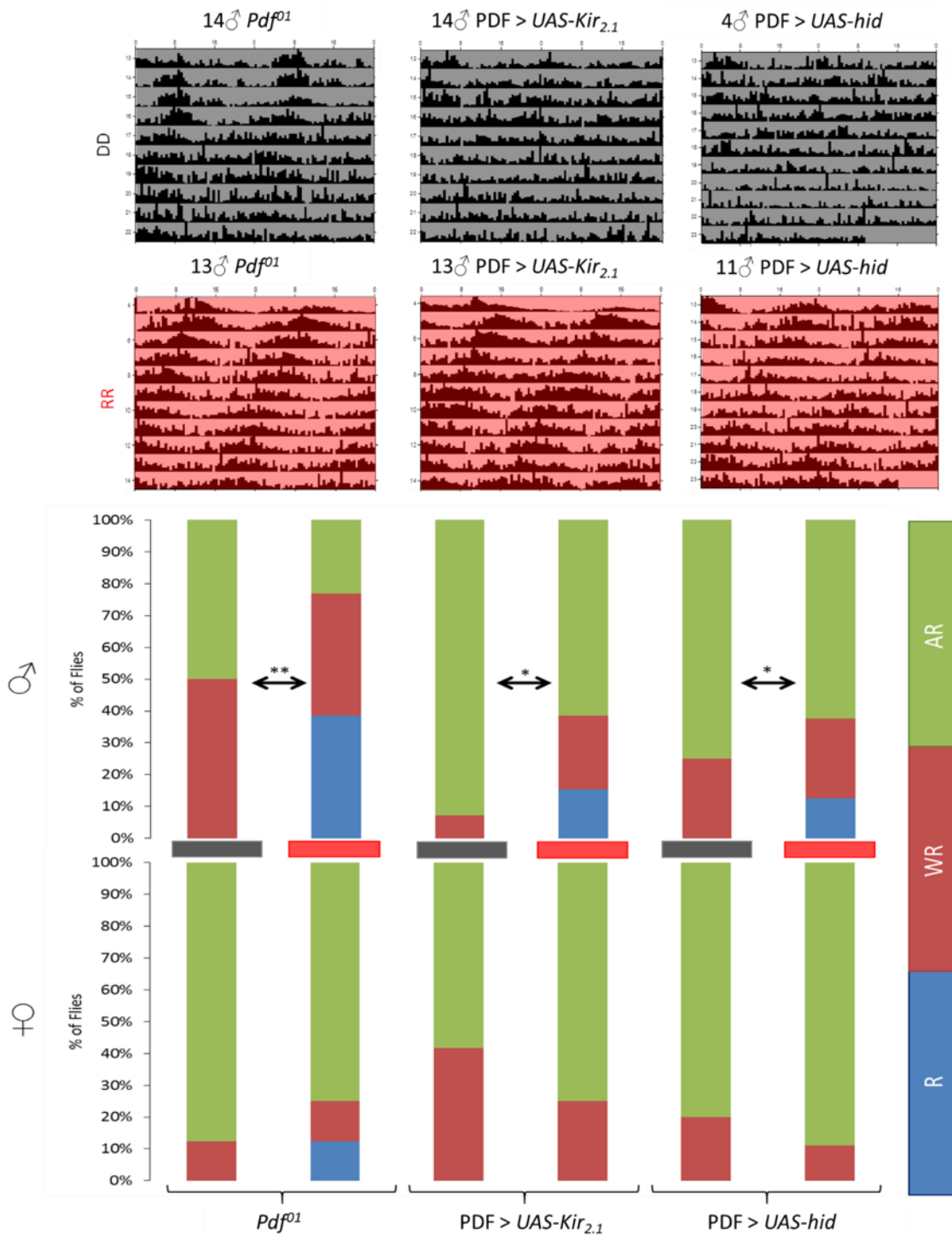
Schematic of approximate location of clock neuron cell bodies in one hemisphere of the *Drosophila* brain (spatial organisation is symmetrical) as well as clock cell clusters known to be targeted by driver lines of genotypes; **(A)** $w^*;tim(UAS)\text{-}Gal4;Sb^1/TM6B\text{-}Tb^1$ (Blau and Young, 1999), **(B)** $Cry\text{-}Gal4\text{-}13$ (Emery *et al.*, 2000b; Stoleru *et al.*, 2004), **(C)** $y^1w^*;Pdf\text{-}Gal4$ (Renn *et al.*, 1999), **(D)** $C929\text{-}Gal4$ (Taghert *et al.* 2001), **(E)** $GMR78G02\text{-}Gal4$ (Schlichting *et al.*, 2016). **(F)** $w^*;ChAT\text{-}Gal4.7.4$ (Lima and Miesenböck, 2005).



S. Figure 13 WT flies show advanced evening activity in RD, similar to that of Pdf^{01} flies in white LD.

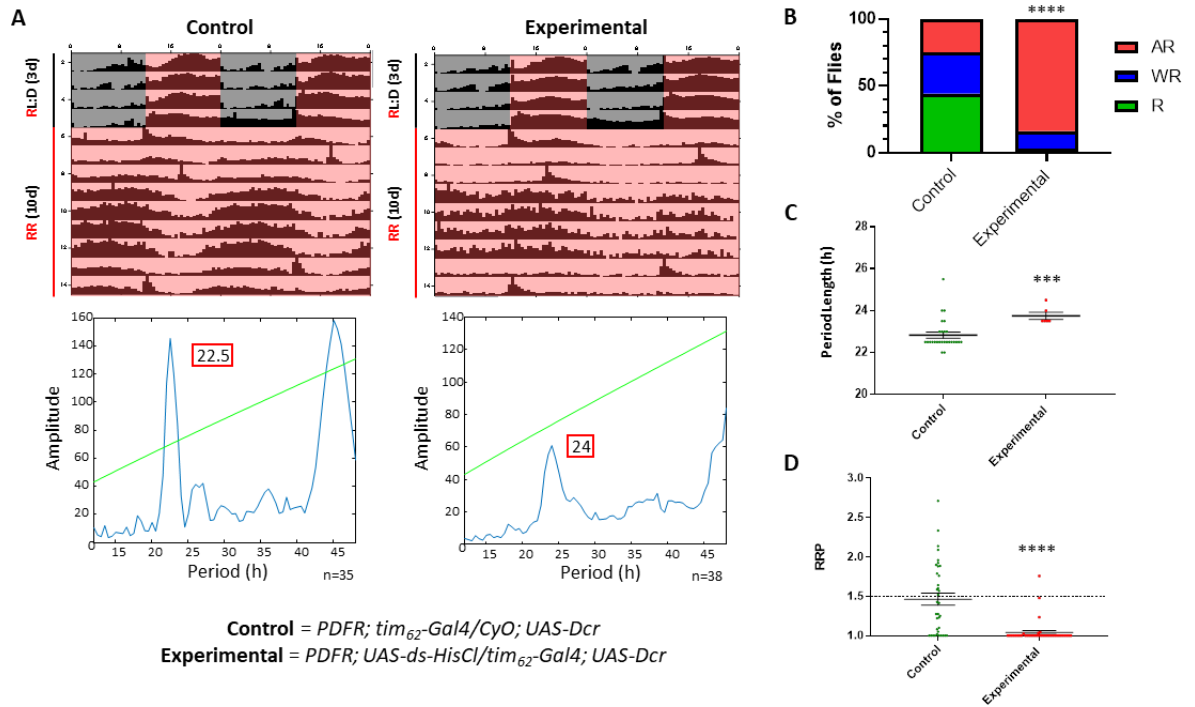
Activity profiles during a 7c/wk (24h) LD cycle in white light and red light (indicated by LD bar). Blue shading is \pm SEM.

Appendix A:



S.Figure 14 RR rescues DD arrhythmicity in PDF signalling mutants.

A) Average double plotted actograms (10 days) of 3 Pdf signalling pathway mutations; *Pdf* null (left), hyperpolarised Pdf neurones (middle) and ablated Pdf neurones (right) in DD (top) and RR (bottom) following LD entrainment. All flies are male and n is noted in figure B) Percentage rhythmic (R), weakly rhythmic (WR) and arrhythmic (AR) for all three genotypes in both DD and RR are shown in a composite bar chart for male (top) and female (bottom) flies. Fisher's exact test - $p^{***}<0.001$, $0.001<p^{**}<0.01$ and $0.01<p^*<0.05$.



S.Figure 15 Knockdown of the HISCL1 receptor reduces the rhythmicity of PDFR mutants in RR.

A) Average double plotted actograms (top) showing 3 days in 7c/wk RED LD followed by 10 days in constant red light (RR), for control (left) and experimental (right) genotypes (annotated in figure). χ^2 periodograms (bottom) plotted from 12-48 h indicate the dominant period peak (annotated). All flies used are male and 'n' denotes the number of flies. **B)** Composite bar chart showing percentage rhythmic (R), weakly rhythmic (WR) and arrhythmic (AR) in RR. Fisher's exact test - $p^{****}<0.0001$, $0.0001<p^{***}<0.001$, $0.001<p^{**}<0.01$ and $p^*<0.05$. **C)** Individual period lengths in RR. Mann-Whitney test; $p=0.0008$. Error bars indicate mean period length \pm SEM. **D)** Individual RRP in RR, dashed line at 1.5. Arrhythmic flies are assigned an RRP of 1. Mann-Whitney test; $p<0.0001$. Error bars indicate mean RRP \pm SEM.

Appendix A:

A.6 Supplementary Tables: Chapter 4

| LD Condition (K-W test) | Genotype | n | %R•%WR•%AR | %ExT•%Other•%AR | Tau (h) ±SEM | RAE ±SEM |
|-------------------------------|---|----------|------------------|------------------|-----------------|--------------------|
| 10c/wk (****) | <i>y¹w*;;tim-luc:10</i> | 88 | 31•15•54++++### | 33•12•54++++### | 18 ±0.291 | 0.5782 ±0.033 |
| | <i>y¹w*tim-luc;;cry⁰¹/TM3-Ser^s</i> | 16 | 31•25•44### | 44•12•44### | 17.79 ±0.877 | 0.6529 ±0.064 |
| | <i>y¹w*tim-luc;;cry⁰¹</i> | 47 | 13•34•53* | 13•34•53**#† | 21.99 ±0.791# | 0.7717 ±0.024** |
| | <i>y¹w*tim-luc;jet^{set}/CyO</i> | 17 | 76•12•12*** | 88•0•12*** | 17.09 ±0.048 | 0.5313 ±0.034 |
| | <i>y¹w*tim-luc;jet^{set}</i> | 9 | 11•44•45## | 22•33•45## | 21.35 ±2.007 | 0.7712 ±0.068 |
| ♂ 9c/wk (*****††) | <i>y¹w*;;tim-luc:10</i> | 51 | 57•37•6† | 80•14•6 | 19.01 ±0.104 | 0.5934 ±0.031 |
| | <i>y¹w*tim-luc;tim⁰¹/CyO</i> | 23 | 48•22•30*† | 70•0•30****††† | 18.7 ±0.093 | 0.5946 ±0.053 |
| | <i>y¹w*tim-luc;tim⁰¹</i> | 21 | 5•38•57****###† | 14•29•57****###† | 20.25 ±0.816 | 0.8479 ±0.048 |
| | <i>y¹w*tim-luc;;cry⁰¹/TM3-Ser¹</i> | 22 | 86•9•5 | 86•9•5 | 19.07 ±0.157 | 0.5187 ±0.04 |
| | <i>y¹w*tim-luc;;cry⁰¹</i> | 87 | 11•29•60****#### | 19•21•60****#### | 20.68 ±0.367*** | 0.7822 ±0.025**### |
| | <i>y¹w*tim-luc;jet^{set}/CyO</i> | 20 | 95•0•5***† | 95•0•5 | 18.83 ±0.028 | 0.4637 ±0.027† |
| | <i>y¹w*tim-luc;jet^{set}</i> | 63 | 41•16•43****###† | 44•13•43****### | 19.83 ±0.341* | 0.6312 ±0.031 |
| <i>GMR-hid/CyO;tim-luc:10</i> | 6 | 66•17•17 | 66•17•17 | 19.38 ±0.186 | 0.529 ±0.085 | |

Appendix A:

| | | | | | | |
|--------------------|---|----|-------------------|-----------------------|-----------------|------------------------|
| | <i>GMR-hid;tim-luc:10</i> | 16 | 94•6•0* | 94•6•0† | 18.94 ±0.063 | 0.4451 ±0.045††† |
| | <i>norpA⁷;tim-luc:10</i> | 25 | 100•0•0*****† | 96•4•0† | 18.97 ±0.037 | 0.3398 ±0.019*****†††† |
| | <i>y¹w*;tim-luc:10</i> | 77 | 74•14•12 | 79•9•12 | 24.34 ±0.099 | 0.5239 ±0.021 |
| | <i>y¹w*tim-luc;tim⁰¹/CyO</i> | - | - | - | - | - |
| | <i>y¹w⁺tim-luc;tim⁰¹</i> | 41 | 5•10•85*****# | 7•7•85**** | 24.68 ±0.895 | 0.8387 ±0.064** |
| | <i>y¹w*tim-luc;;cry⁰¹/TM3-Ser¹</i> | 23 | 52•31•17 | 83•0•17 | 24.01 ±0.088 | 0.6418 ±0.038 |
| 7c/wk | <i>y¹w*tim-luc;;cry⁰¹</i> | 45 | 11•13•76****##### | 13•11•76****##### | 23.99 ±0.332 | 0.7437 ±0.042** |
| (**†††††) | <i>y¹w*tim-luc;jet^{set}/CyO</i> | 23 | 52•26•22 | 74•4•22 | 24.03 ±0.128 | 0.6333 ±0.046 |
| | <i>y¹w*tim-luc;jet^{set}</i> | 40 | 20•25•55****# | 23•22•55****### | 24.5 ±0.346 | 0.7279 ±0.04** |
| | <i>GMR-hid/CyO;tim-luc:10</i> | 44 | 43•36•21**# | 50•30•21** | 24.39 ±0.28 | 0.6936 ±0.025*** |
| | <i>GMR-hid;tim-luc:10</i> | 45 | 74•13•13 | 58•29•13* | 24.39 ±0.16 | 0.592 ±0.02 |
| | <i>norpA⁷;tim-luc:10</i> | 59 | 78•17•5 | 68•27•5* | 24.84 ±0.094* | 0.5131 ±0.023 |
| | <i>y¹w*;tim-luc:10</i> | 43 | 77•7•16†††††††† | 68•16•16†††† | 33.94 ±0.172 | 0.4265 ±0.028††††† |
| | <i>y¹w*tim-luc;tim⁰¹/CyO</i> | 23 | 52•17•31† | 35•35•31*††† | 32.4 ±0.726 | 0.611 ±0.034** |
| 5c/wk | <i>y¹w*tim-luc;tim⁰¹</i> | 35 | 3•9•88****#####† | 3•9•88****#####† | 26.18 ±2.998 | 0.7878 ±0.066* |
| (****†††††) | <i>y¹w*tim-luc;;cry⁰¹/TM3-Ser¹</i> | 9 | 78•11•11 | 89•0•11 | 32.88 ±0.171 | 0.5373 ±0.067 |
| | <i>y¹w*tim-luc;;cry⁰¹</i> | 41 | 15•24•61****### | 0•39•61****#####††††† | 24.15 ±0.176*** | 0.7131 ±0.043**** |

| | | | | | | |
|--------------|---|----|-------------------|----------------------|--------------|------------------|
| | <i>y¹w*tim-luc;jet^{set}/CyO</i> | 3 | 100•0•0 | 100•0•0 | 33.05 ±0.096 | 0.592 ±0.066 |
| | <i>y¹w*tim-luc;jet^{set}</i> | 8 | 38•25•37 | 0•62•37***## | 27.24 ±2.174 | 0.584 ±0.091 |
| | <i>GMR-hid/CyO;tim-luc:10</i> | 4 | 50•25•25 | 75•0•25 | 32.48 ±0.316 | 0.5273 ±0.153 |
| | <i>GMR-hid;tim-luc:10</i> | 22 | 82•9•9 | 86•5•9† | 33.42 ±0.214 | 0.4832 ±0.032† |
| | <i>norpA⁷;tim-luc:10</i> | 45 | 87•11•2 | 91•7•2*† | 33.54 ±0.141 | 0.5075 ±0.024### |
| 4c/wk | <i>y¹w*;tim-luc:10</i> | 32 | 59•0•41++++###††† | 16•44•40++++###††††† | 39.75 ±0.386 | 0.4472 ±0.021 |

| LD Condition (K-W test) | Genotype | n | %R•%WR•%AR | %ExT•%Other•%AR | Tau (h) ±SEM | RAE ±SEM |
|----------------------------|---|----|----------------|--------------------|---------------|-----------------|
| ♀ | <i>y¹w*;tim-luc:10</i> | 93 | 17•21•62++++† | 25•13•62++++### | 17.42 ±0.267 | 0.6988 ±0.039†† |
| | <i>y¹w*tim-luc;;cry⁰¹/TM3-Ser¹</i> | 21 | 5•28•67++++† | 19•14•67+++ | 16.13 ±0.567 | 0.8044 ±0.042 |
| | <i>y¹w*tim-luc;;cry⁰¹</i> | 46 | 22•35•43* | 33•24•43 | 19.55 ±0.692# | 0.719 ±0.027 |
| | <i>y¹w*tim-luc;jet^{set}/CyO</i> | 15 | 0•13•87++++### | 13•0•87++++### | 17.53 ±0.035 | 0.848 ±0.008 |
| | <i>y¹w*tim-luc;jet^{set}</i> | 8 | 38•50•12#### | 13•75•12***####††† | 22.3 ±1.115* | 0.6919 ±0.056 |
| 9c/wk (*****†) | <i>y¹w*;tim-luc:10</i> | 35 | 34•29•37+++ | 60•3•37†† | 18.73 ±0.075 | 0.6359 ±0.037 |
| | <i>y¹w*tim-luc;tim⁰¹/CyO</i> | 18 | 28•39•33† | 61•6•33†† | 18.47 ±0.139 | 0.7042 ±0.043 |
| | <i>y¹w*tim-luc;tim⁰¹</i> | 21 | 0•29•71**# | 10•19•71***## | 19.85 ±1.459 | 0.8607 ±0.031 |

Appendix A:

| | | | | | | |
|-----------------|-------------------------------------|----|-----------------|------------------|---------------|-------------------------|
| | $y^1w^*tim-luc;;cry^{01}/TM3-Ser^1$ | 28 | 39•25•36 | 44•19•36 | 19.67 ±0.387 | 0.6287 ±0.048 |
| | $y^1w^*tim-luc;;cry^{01}$ | 80 | 24•34•42 | 28•30•42*** | 21.37 ±0.382* | 0.7297 ±0.021 |
| | $y^1w^*tim-luc;jet^{set}/CyO$ | 20 | 45•35•20 | 80•0•20 | 18.65 ±0.059 | 0.6462 ±0.052 |
| | $y^1w^*tim-luc;jet^{set}$ | 55 | 27•37•36 | 37•27•36***##++ | 20.17 ±0.498 | 0.7085 ±0.023 |
| | $GMR-hid/CyO;tim-luc:10$ | 3 | 67•33•0 | 33•67•0* | 18.91 ±1.807 | 0.67 ±0.065 |
| | $GMR-hid;tim-luc:10$ | 17 | 82•18•0***++++ | 100•0•0***#++++ | 18.69 ±0.071 | 0.5688 ±0.037 |
| | $y^1w^*;;tim-luc:10$ | 79 | 71•16•13 | 74•13•13 | 24.19 ±0.149 | 0.5158 ±0.02 |
| | $y^1w^*tim-luc;tim^{01}/CyO$ | - | - | - | - | - |
| | $y^1w^*tim-luc;tim^{01}$ | 35 | 3•11•86**** | 9•6•86**** | 23.1 ±1.456 | 0.7946 ±0.046* |
| | $y^1w^*im-luc;;cry^{01}/TM3-Ser^1$ | 20 | 60•30•10 | 70•20•10 | 24.06 ±0.297 | 0.6153 ±0.035 |
| 7c/wk | $y^1w^*tim-luc;;cry^{01}$ | 45 | 25•33•42****## | 33•25•42****## | 23.61 ±0.265 | 0.7316 ±0.028**** |
| (++++) | $y^1w^*tim-luc;jet^{set}/CyO$ | 22 | 59•23•18 | 65•17•18 | 24.17 ±0.372 | 0.5748 ±0.034 |
| | $y^1w^*tim-luc;jet^{set}$ | 41 | 49•32•19* | 68•12•19 | 24.14 ±0.193 | 0.6314 ±0.036 |
| | $GMR-hid/CyO;tim-luc:10$ | 42 | 32•27•41**** | 33•27•41**** | 23.71 ±0.254 | 0.697 ±0.036*** |
| | $GMR-hid;tim-luc:10$ | 42 | 22•14•64**** | 31•5•64****# | 24.43 ±0.179 | 0.6804 ±0.044 |
| 5c/wk | $y^1w^*;;tim-luc:10$ | 65 | 89•6•5†++++†††† | 81•14•5†++++†††† | 33.17 ±0.215 | 0.3499 ±0.022†††††††††† |
| (**††††) | $y^1w^*tim-luc;tim^{01}/CyO$ | 20 | 20•15•65****† | 16•16•65****† | 32.44 ±1.324 | 0.631 ±0.079* |

| | | | | | | |
|--------------|-------------------------------------|----|--------------------|----------------------------|-----------------|--------------------------|
| | $y^1w^*tim-luc;tim^{01}$ | 16 | 0•38•62**** | 19•19•62**** | 30.86 ±1.911 | 0.8218 ±0.036**** |
| | $y^1w^*tim-luc;;cry^{01}/TM3-Ser^1$ | 10 | 100•0•0‡‡‡‡‡‡ | 70•30•0‡‡ | 32.51 ±0.44 | 0.4667 ±0.041‡‡ |
| | $y^1w^*tim-luc;;cry^{01}$ | 33 | 64•21•15**†‡‡‡‡‡‡ | 33•52•15****†‡‡ | 28.52 ±0.919*** | 0.5724 ±0.029****†‡‡‡‡‡‡ |
| | $y^1w^*tim-luc;jet^{set}/CyO$ | - | - | - | - | - |
| | $y^1w^*tim-luc;jet^{set}$ | 5 | 40•60•0** | 60•40•0 | 30.38 ±2.084 | 0.6372 ±0.072* |
| | $GMR-hid/CyO;tim-luc:10$ | 4 | 75•0•25 | 25•50•25* | 30.2 ±3.214 | 0.4647 ±0.107 |
| | $GMR-hid;tim-luc:10$ | 23 | 44•17•39****‡‡ | 50•13•39****‡‡‡ | 32.54 ±0.722 | 0.6341 ±0.041**** |
| 4c/wk | $y^1w^*;;tim-luc:10$ | 30 | 67•3•30†‡‡‡‡‡‡‡‡‡‡ | 23•47•30††††††††††††‡‡‡‡‡‡ | 38.48 ±1.368 | 0.4279 ±0.038‡‡‡‡ |

S.Table 17 Male and Female *in vivo* luciferase activity of wild-type ($y^1w^*;;tim-luc:10$) and mutant genotypes in a wide range (4-10c/wk) equinox LD cycles.

Male (top) and female (bottom) flies in 10, 9, 7, 5 and 4c/wk (top to bottom) LD cycles with result of *Kruskal-Wallis test* comparing Period length (*) and RAE (†) between genotypes within each condition. Where possible, an isogenic control for each mutant genotype is included. **n**, number of flies. **%R•%WR•%AR**, percentage of flies classified and rhythmic (R), weakly rhythmic (WR) and arrhythmic (AR). **%ExT•%Other•%AR**, percentage of flies classified and entrained (ExT), other and arrhythmic (AR). *Fisher's exact test* vs. $y^1w^*;;tim-luc:10$ (*) and vs. isogenic control (#) in each condition for %R•%WR•%AR and %ExT•%Other•%AR. *Fisher's exact test* between all conditions within each genotype for %R•%WR•%AR and %ExT•%Other•%AR; 4/5/9/10 vs.7c/wk (†), 4/5/10 vs. 9c/wk (‡), 4/5 vs. 10c/wk (‡) and 4 vs. 5c/wk (‡). **Tau (h) ±SEM**, mean period length – Ext period lengths; 10c/wk = 16.8 h, 9c/wk = 18.66 h, 7c/wk = 24 h, 5c/wk = 33.6 h and 4c/wk = 42 h. **RAE ±SEM**, mean relative amplitude error. *Pairwise Mann-Whitney test* vs. $y^1w^*;;tim-luc:10$ (*) and vs. isogenic control (#) in each condition for Tau (h) ±SEM and RAE ±SEM. *Dunn's Multiple Comparison test* between all conditions within each genotype for RAE ±SEM; 4/5/9/10 vs.7c/wk (†), 4/5/10 vs. 9c/wk (‡), 4/5 vs. 10c/wk (‡) and 4 vs. 5c/wk (‡). In all cases (*, †, ‡, ‡ and ‡): $p^{****}<0.0001$; $0.0001<p^{***}<0.001$; $0.001<p^{**}<0.01$; $0.01<p^*<0.05$.

Appendix A:

| | | ♂ | | |
|----------|---------------------------------|------------------|-----------------|---------------|
| | | Fold change ±SEM | | |
| LD Cycle | ZT - [h post L _{off}] | <i>per</i> | <i>Clk</i> | <i>luc</i> |
| 9c/wk | ZT12 - [0] | 1.103 ±0.2089* | 0.8935 ±0.05339 | 1 ±0.1716 |
| | ZT0 - [9.33] | 1.518 ±0.3822 | 1.319 ±0.1635 | 3.352 ±0.1185 |
| | ZT12 _[2] - [18.66] | 1 ±0.2005 | 1 ±0.06786 | 1.726 ±0.3363 |
| | ZT0 _[2] - [27.99] | 1.315 ±0.1173 | 1.098 ±0.2223 | 2.14 ±0.3606 |
| 7c/wk | ZT12 - [0]*† | 8.478 ±2.063 | 1.238 ±0.5916 | - |
| | ZT20.4 - [8.4] | 1.082 ±0.2004 | 12.85 ±2.403 | - |
| | ZT4.8 - [16.8]† | 1 ±0.02876 | 20.38 ±3.578 | - |
| | ZT13.2 _[2] - [25.2]* | 9.356 ±3.253 | 1 ±0.1083 | - |
| 5c/wk | ZT12 - [0] | 3.957 ±0.5635 | 3.327 ±0.3972 | - |
| | ZT18 - [8.4] | 6.981 ±5.069 | 12.21 ±4.58 | - |
| | ZT0 - [16.8] | 1 ±0.06372 | 13.78 ±2.895 | - |
| | ZT6 - [25.2] | 6.524 ±1.464 | 1 ±0.3737 | - |
| | | ♀ | | |
| | | Fold change ±SEM | | |
| LD Cycle | ZT - [h post L _{off}] | <i>per</i> | <i>Clk</i> | <i>luc</i> |
| 9c/wk | ZT12 - [0] | 1.165 ±0.06595* | 1 ±0.1732 | 1.423 ±0.286 |
| | ZT0 - [9.33] | 1.39 ±0.09596 | 1.246 ±0.1821 | 2.655 ±1.131 |
| | ZT12 _[2] - [18.66] | 1 ±0.06418 | 1.175 ±0.1445 | 1 ±0.2547 |
| | ZT0 _[2] - [27.99] | 1.532 ±0.3654 | 1.013 ±0.167 | 1.897 ±0.1448 |
| 7c/wk | ZT12 - [0]* | 5.764 ±1.414 | 1 ±0.376 | - |
| | ZT20.4 - [8.4]† | 1 ±0.5743 | 4.602 ±0.9561 | - |
| | ZT4.8 - [16.8]† | 1.046 ±0.1476 | 2.472 ±0.9364 | - |
| | ZT13.2 _[2] - [25.2]* | 6.813 ±2.692 | 1.165 ±0.7611 | - |
| 5c/wk | ZT12 - [0] | 1.962 ±0.09612 | 1.388 ±0.3709 | - |
| | ZT18 - [8.4] | 5.817 ±5.495† | 6.053 ±0.1581 | - |
| | ZT0 - [16.8] | 1 ±0.4397 | 2.76 ±0.5633 | - |
| | ZT6 - [25.2] | 2.472 ±0.2945 | 1 ±0.3381 | - |

S.Table 18 Quantification of fold change in *per*, *Clk* and *luc* transcript in 9, 7 and 5c/wk LD from wild-type adult heads.

Fold change \pm SEM in *per* and *Clk* transcript (calculated for ratios of test transcript against *RP49* control transcript) in **5, 7 and 9c/wk LD cycles** (with addition of *luc* transcript in 9c/wk) from whole heads of male (top) and female (bottom) flies of genotype ***y¹w^{*};tim-luc:10***. **ZT**, time-point scales to 24 h LD cycles (_[2] indicates time-points in the second LD cycle), **h post L_{off}** in real-time in presented in []. Results of *Kruskal-Wallis* test comparing fold change across all time-points in each condition for *per* (*), *Clk* (†) and *luc* (‡) are presented in LD cycle column. Results of *Kruskal-Wallis* test comparing fold change across 9, 7 and 5c/wk LD cycles for matching time-points (i.e. corresponding to same/similar h post L_{off}) for *per* (*) and *Clk* (†) are presented in ZT column. Pairwise comparisons of fold change for 9 and 5c/wk vs. 7c/wk (*) and 9c/wk vs. 5c/wk (†) LD cycles for matching time-points (i.e. corresponding to same h post L_{off}) for *per* and *Clk* using *Tukey's multiple comparisons test* (*per* and *Clk* column). Pairwise comparisons of fold change for *luc* vs. *per* (*) and *luc* vs. *Clk* (†) for 9c/wk for matching time-points (i.e. corresponding to same h post L_{off}) with *Tukey's multiple comparisons test* (*luc* column). In all cases (*, † and ‡): p ****<0.0001; 0.0001<p***<0.001; 0.001<p**<0.01; 0.01<p*<0.05.

| | | ♂ | | |
|----------|---------------------------------|------------------|---------------|---------------|
| | | Fold change ±SEM | | |
| LD Cycle | ZT - [h post L _{off}] | <i>per</i> | <i>Clk</i> | <i>luc</i> |
| 10c/wk | ZT12 - [0] | 1 ±0.1929 | 1.492 ±0.4678 | 1 ±0.1883 |
| | ZT0 - [8.4] | 6.471 ±5.308 | 1 ±0.2643 | 13.43 ±0 |
| ### | ZT12 _[2] - [16.8] | 1.137 ±0.091 | 5.224 ±2.648 | 2.226 ±0.269 |
| | ZT0 _[2] - [25.2] | 4.966 ±1.355 | 1.217 ±0.5298 | 10.53 ±0.391† |

| | | ♀ | | |
|----------|---------------------------------|------------------|---------------|---------------|
| | | Fold change ±SEM | | |
| LD Cycle | ZT - [h post L _{off}] | <i>per</i> | <i>Clk</i> | <i>luc</i> |
| 10c/wk | ZT12 - [0] | 3.35 ±1.23 | 2.806 ±0.3452 | 1 ±0.1078 |
| | ZT0 - [8.4] | 3.24 ±0.9367 | 2.163 ±0.5532 | 8.574 ±1.007 |
| ## | ZT12 _[2] - [16.8] | 1 ±0.1333 | 2.45 ±0.2559 | 3.537 ±0.9317 |
| | ZT0 _[2] - [25.2] | 2.593 ±0.5418 | 1 ±0.1322 | 10.1 ±1.771† |

S.Table 19 Quantification of fold change in *per*, *Clk* and *luc* transcript in 10c/wk LD from wild-type adult heads.

Fold change ±SEM in *per*, *Clk* and *luc* transcript (calculated for ratios of test transcript against *RP49* control transcript) in **10c/wk LD cycles** from whole heads of male (top) and female (bottom) flies of genotype ***y¹w*;;tim-luc:10***. **ZT**, time-point scales to 24 h LD cycles (_[2] indicates time-points in the second LD cycle), **h post L_{off}** in real-time in presented in []. Results of *Kruskal-Wallis* test comparing fold change across all time-points in each condition for *per* (*), *Clk* (†) and *luc* (‡) are presented in LD cycle column. Pairwise comparisons of fold change for *luc* vs. *per* (*) and *luc* vs. *Clk* (†) for 9c/wk for matching time-points (i.e. corresponding to same h post L_{off}) with *Tukey's multiple comparisons test* (*luc* column). In all cases (*, † and ‡): p ****<0.0001; 0.0001<p***<0.001; 0.001<p**<0.01; 0.01<p*<0.05.

| LD Condition | Time-points | ♂ | | | ♀ | | |
|--------------|--|------------|------------|------------|------------|------------|------------|
| | | <i>per</i> | <i>Clk</i> | <i>luc</i> | <i>per</i> | <i>Clk</i> | <i>luc</i> |
| 10c/wk | ZT12 vs. ZT0 | 1.262269* | 0.747687 | - | 0.058088 | 0.773288 | 6.103383* |
| | ZT12 vs. ZT12 _[2] | 0.912684* | 2.368908* | 3.048388* | 2.685824* | 1.232757* | 2.208221* |
| | ZT12 vs. ZT0 _[2] | 4.099573* | 0.586529 | 17.931075* | 0.796864 | 7.966361* | 4.186948* |
| | ZT0 vs. ZT12 _[2] | 1.230149* | 1.925531* | - | 1.933551* | 0.38447 | 2.996829* |
| | ZT0 vs. ZT0 _[2] | 0.388438 | 0.821501* | - | 0.845641* | 2.892152* | 0.611437 |
| | ZT12 _[2] vs. ZT0 _[2] | 2.303056* | 1.484126* | 14.285894* | 2.331194* | 4.110189* | 2.677369* |
| 9c/wk | ZT12 vs. ZT0 | 0.777992 | 2.019848* | 11.282749* | 1.577946* | 0.799097 | 0.862245* |
| | ZT12 vs. ZT12 _[2] | 0.50544 | 1.744905* | 1.464055* | 2.534568* | 1.096605* | 0.901849* |
| | ZT12 vs. ZT0 _[2] | 1.249965* | 1.262175* | 2.334937* | 1.398617* | 0.075882 | 1.207135* |
| | ZT0 vs. ZT12 _[2] | 0.980102* | 1.471371* | 3.349667* | 2.758134* | 0.249322 | 1.165572* |
| | ZT0 vs. ZT0 _[2] | 0.716418 | 1.136868* | 2.40606* | 0.533724 | 1.33581* | 0.542771 |
| | ZT12 _[2] vs. ZT0 _[2] | 1.107351* | 0.344304 | 0.68547 | 1.170818* | 0.598883 | 2.499781* |

S.Table 20 Effect size calculation for short cycle qPCR of *per*, *Clk* and *luc* transcripts.

Effect size is calculated for transcripts in 9 and 10c/wk LD in a pairwise fashion between all time-points using Cohen's *d* (same sample size) or Hedge's *g* (different sample sizes) where $d=0.2$ is considered a 'small' effect size, 0.5 represents a 'medium' effect size and 0.8 a 'large' effect size. Large effect sizes are indicated by *. Time-points are scaled to a 24 h LD cycle and _[2] indicates time-points in the second LD cycle.

| LD Cycle | ZT - [h post L _{off}] | PER/HSP70 ±SEM | |
|------------------|-----------------------------------|-------------------------|------------------------|
| | | ♂ | ♀ |
| 10c/wk ++++ | ZT12 - [0] | 0.001022 ±0.000243**** | 0.001780 ±0.000549+++ |
| | ZT0 - [8.4] | 0.002161 ±0.00036***‡ | 0.005612 ±0.000742‡‡ |
| | ZT12 _[2] - [16.8] | 0.00124 ±0.000359+++ | 0.001752 ±0.000175**** |
| | ZT0 _[2] - [25.2] | 0.00147 ±0.000156‡‡ | 0.005534 ±0.000462 |
| 9c/wk ****†† | ZT12 - [0] | 0.002728 ±0.000586 | 0.003465 ±0.000464 |
| | ZT0 - [9.33] | 0.01220 ±0.0002913†† | 0.01135 ±0.001269†† |
| | ZT12 _[2] - [18.66] | 0.002933 ±0.000739 | 0.003476 ±0.000623†† |
| | ZT0 _[2] - [27.99] | 0.011481 ±0.003581††† | 0.008583 ±0.001655 |
| 7c/wk ****†† | ZT12 - [0]****†† | 0.004974 ±0.001112 | 0.004307 ±0.001736 |
| | ZT20.4 - [8.4]****†† | 0.013463 ±0.00086 | 0.011633 ±0.001751 |
| | ZT4.8 - [16.8]****†††† | 0.001995 ±0.00037 | 0.007486 ±0.002895 |
| | ZT13.2 _[2] - [25.2]*** | 0.003846 ±0.001173 | 0.008102 ±0.001103 |
| 5c/wk ****††† | ZT12 - [0] | 0.002968 ±0.000254 | 0.0072 ±0.000981 |
| | ZT18 - [8.4] | 0.0013663 ±0.000299**** | 0.005217 ±0.000741 |
| | ZT0 - [16.8] | 0.0062724 ±0.000479** | 0.014447 ±0.00146 |
| | ZT6 - [25.2] | 0.0013264 ±0.000264 | 0.005932 ±0.000573 |

S.Table 21 Quantification of PER protein in 10, 9, 7 and 5c/wk LD from wild-type adult heads.

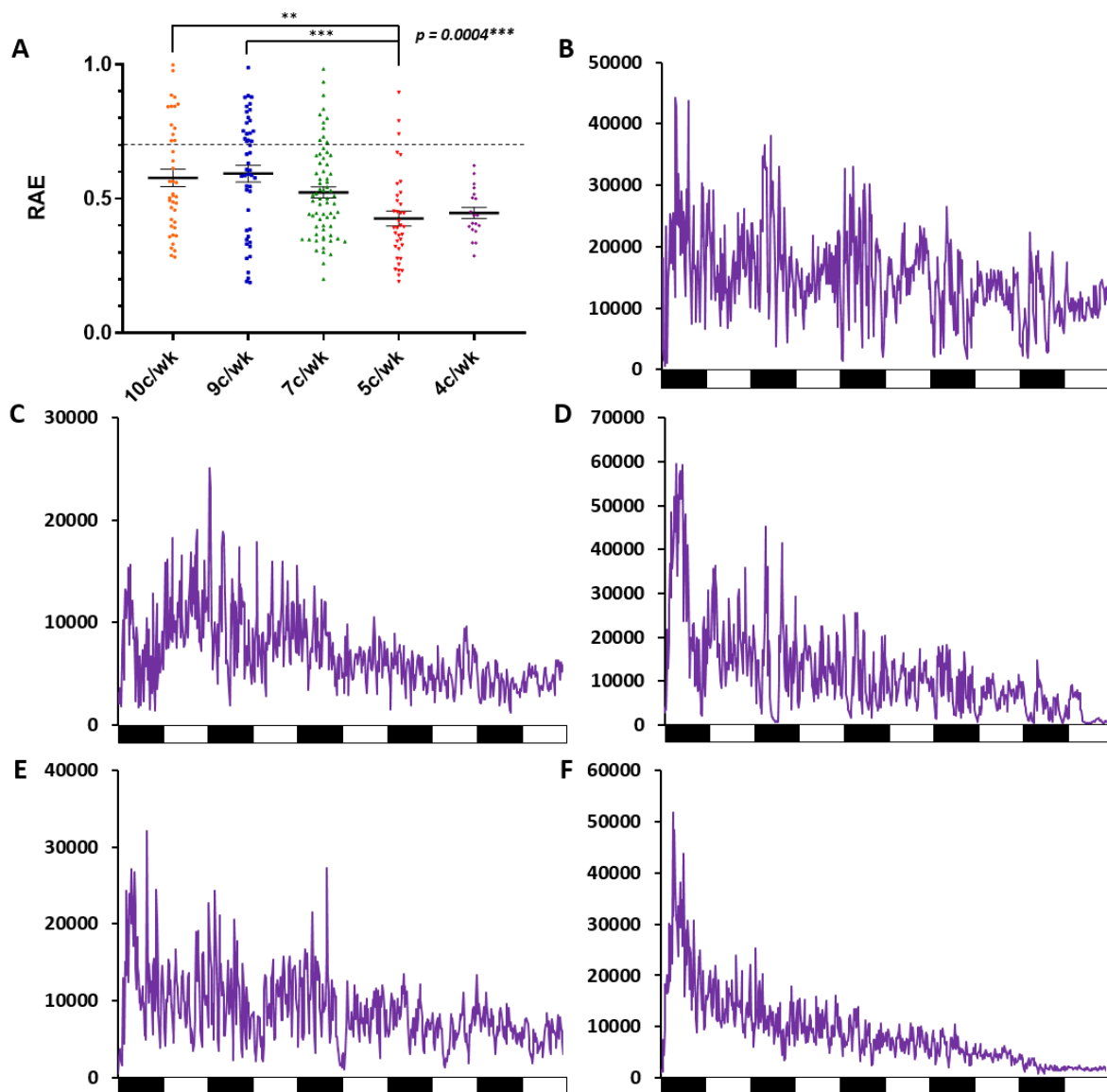
PER/HSP70 ±SEM (normalised to total protein loaded) in 10, 9, 7 and 5c/wk LD cycles from whole heads of male (♂) and female (♀) flies of genotype $y^1w^{*};tim-luc:10$. ZT, time-point scales to 24 h LD cycles (_[2] indicates time-points in the second LD cycle), h post L_{off} in real-time in presented in []. Results of *Kruskal-Wallis* test comparing PER/HSP70 across all time-points in each condition for males (*) and females (†) are presented in LD cycle column. Pariwise comparisons between all time-points within each condition are presented in **S.Table 22**). Results of *Kruskal-Wallis* test comparing PER/HSP70 across 10, 9, 7 and 5c/wk LD cycles for matching time-points (i.e. corresponding to same/similar h post L_{off}) for males (*) and female (†) are presented in ZT column. Pairwise comparisons of PER/HSP70 for 10, 9 and 5c/wk vs. 7c/wk (*), 10 and 9c/wk vs. 5c/wk (†) and 10c/wk vs. 9c/wk (‡) LD cycles for matching time-points (i.e. corresponding to same h post L_{off}) for males and females using *Tukey's multiple comparisons test* (♂ and ♀ column). In all cases (*, † and ‡): p ****<0.0001; 0.0001<p***<0.001; 0.001<p**<0.01; 0.01<p*<0.05.

| LD Cycle | Time-point | ♂ | ♀ | LD Cycle | Time-point | ♂ | ♀ |
|----------|--|-------------|----------|----------|--|-------------|-----------|
| | ZT12 vs. ZT0 | ns | 0.0034** | | ZT12 vs. ZT0 | 0.0047** | 0.0015** |
| | ZT12 vs. ZT12 _[2] | ns | ns | | ZT12 vs. ZT12 _[2] | ns | ns |
| 10c/wk | ZT12 vs. ZT0 _[2] | ns | 0.001** | 9c/wk | ZT12 vs. ZT0 _[2] | 0.0218* | ns |
| | ZT0 vs. ZT12 _[2] | ns | 0.0163* | | ZT0 vs. ZT12 _[2] | 0.0076** | 0.0009*** |
| | ZT0 vs. ZT0 _[2] | ns | ns | | ZT0 vs. ZT0 _[2] | ns | ns |
| | ZT12 _[2] vs. ZT0 _[2] | ns | 0.0056** | | ZT12 _[2] vs. ZT0 _[2] | 0.0332* | ns |
| LD Cycle | Time-point | ♂ | ♀ | LD Cycle | Time-point | ♂ | ♀ |
| | ZT12 vs. ZT20.4 | 0.0498* | 0.0017** | | ZT12 vs. ZT18 | ns | ns |
| | ZT12 vs. ZT4.8 | ns | ns | | ZT12 vs. ZT0 | ns | 0.0234* |
| 7c/wk | ZT12 vs. ZT13.2 _[2] | ns | ns | 5c/wk | ZT12 vs. ZT6 | ns | ns |
| | ZT20.4 vs. ZT4.8 | <0.0001**** | ns | | ZT18 vs. ZT0 | <0.0001**** | 0.0002*** |
| | ZT20.4 vs. ZT13.2 _[2] | 0.0038** | ns | | ZT18 vs. ZT6 | ns | ns |
| | ZT4.8 vs. ZT13.2 _[2] | ns | ns | | ZT0 vs. ZT6 | <0.0001**** | 0.001** |

S.Table 22 PER protein cycling statistics summary.

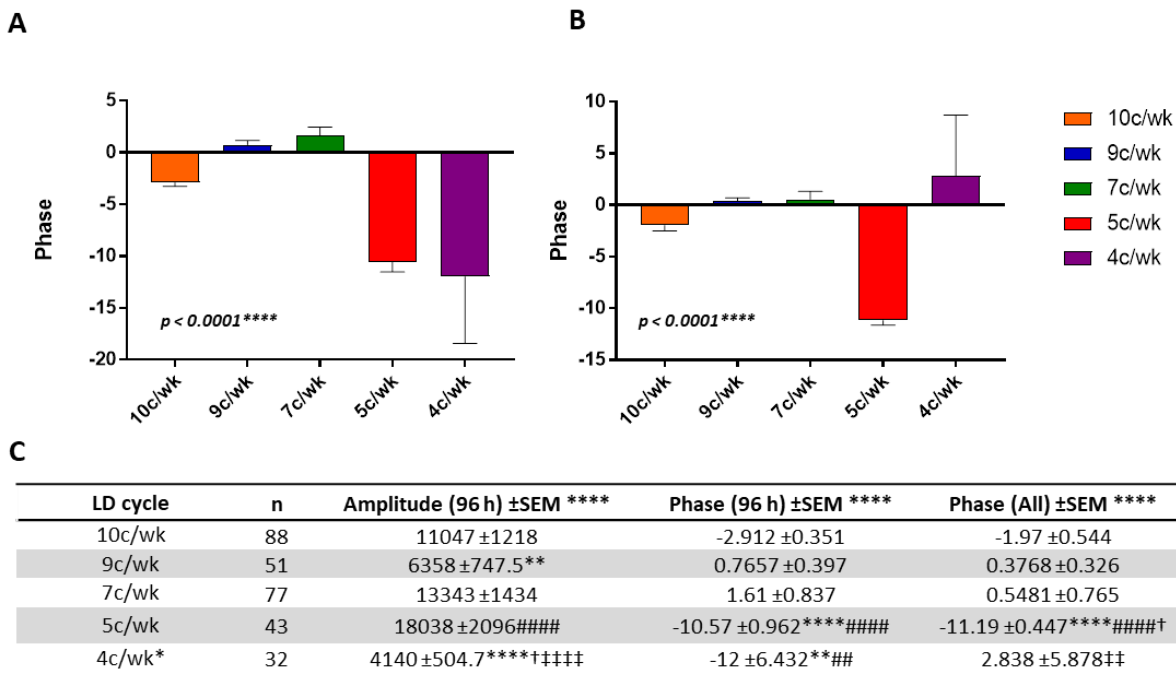
p values corresponding to the pairwise comparison of normalised PER protein levels between all time-points, within each condition, using *Dunn's multiple comparisons test* - $p^{****}<0.0001$, $0.0001<p^{***}<0.001$, $0.001<p^{**}<0.01$ and $p^{*}<0.05$. Time-points are scaled to a 24 h LD cycle and _[2] indicates time-points in the second LD cycle.

A.7 Supplementary Figures: Chapter 4



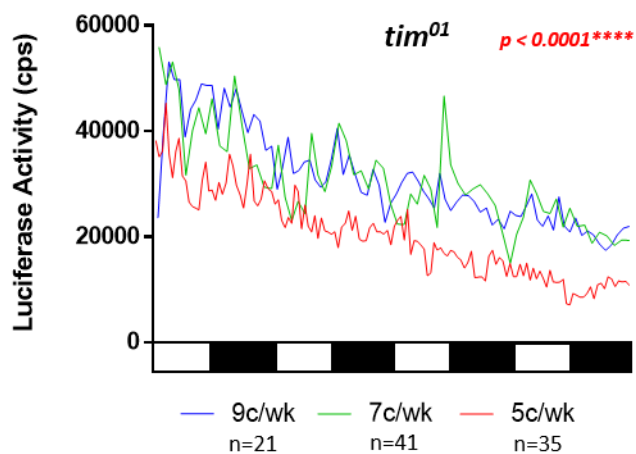
S.Figure 16 Strength of peripheral rhythms in 10-4c/wk LD cycles, quantification indicates strongest rhythms in 5 and 4c/wk.

A) Individual male RAE. Error bars show mean RAE \pm SEM. Dashed line indicates a RAE of 0.7. *p* value (top right) shows result of *Kruskal-Wallis* test across all conditions. Individual comparisons with *Dunn's multiple comparison test* (10 vs. 5c/wk; *p*=0.0079 and 9 vs. 5c/wk; *p*=0.0007. **B-F)** TopCount *in-vivo* luciferase activity traces for 5 individual males of the genotype $y^1w^{*};tim-luc:10$ in a 4c/wk LD condition. Flies **B-E** were rhythmic and thus a RAE value was calculated. Fly **F** was arrhythmic. RAE values calculated for 4c/wk individuals seemed to indicate stronger rhythms than expected based on the number of arrhythmic flies observed.



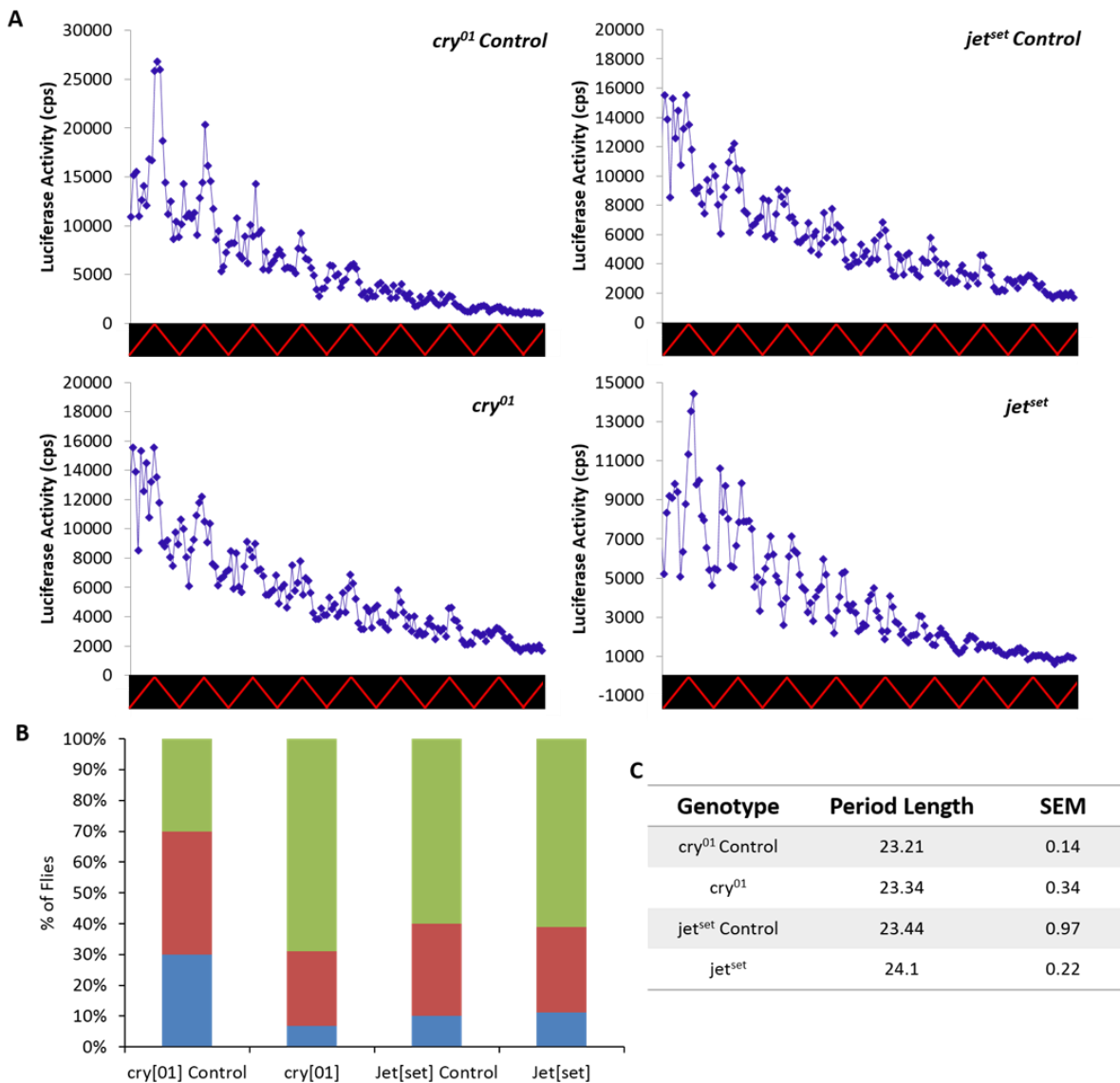
S.Figure 17 Phase of peripheral luciferase activity W.R.T photoperiod for $y^1w^{*};tim-luc:10$ males.

A, B Average phase (W.R.T photoperiod) (top) over the first 96 h (**A**) and all data (**B**) for each condition, error bars show mean \pm SEM. *p* values (bottom left) indicates results of *Kruskal-Wallis test* across all conditions. **C** Table shows mean (\pm SEM) amplitude and phase over first 96 hours of experiment, as well as phase over all data, for male flies of genotype $y^1w^{*};tim-luc:10$ in 10, 9, 7, 5 and 4c/wk (top to bottom). Results of *Kruskal-Wallis test* across all conditions is indicated in each heading (*). *Dunn's Multiple Comparison test* between all conditions for Amplitude (96 h), Phase (96 h) and Phase (All); 4/5/9/10 vs. 7c/wk (*), 4/5/10 vs. 9c/wk (#), 4/5 vs. 10c/wk (†) and 4 vs. 5c/wk (‡). Results of the comparison between phase over the first 96 h and all data within each condition with *Mann-Whitney test* annotated in LD cycle column (*). In all cases (*, #, † and ‡): $p^{****} < 0.0001$; $0.0001 < p^{***} < 0.001$; $0.001 < p^{**} < 0.01$; $0.01 < p^{*} < 0.05$. **Note:** Only flies with the correct entrained period length were included in phase analysis.



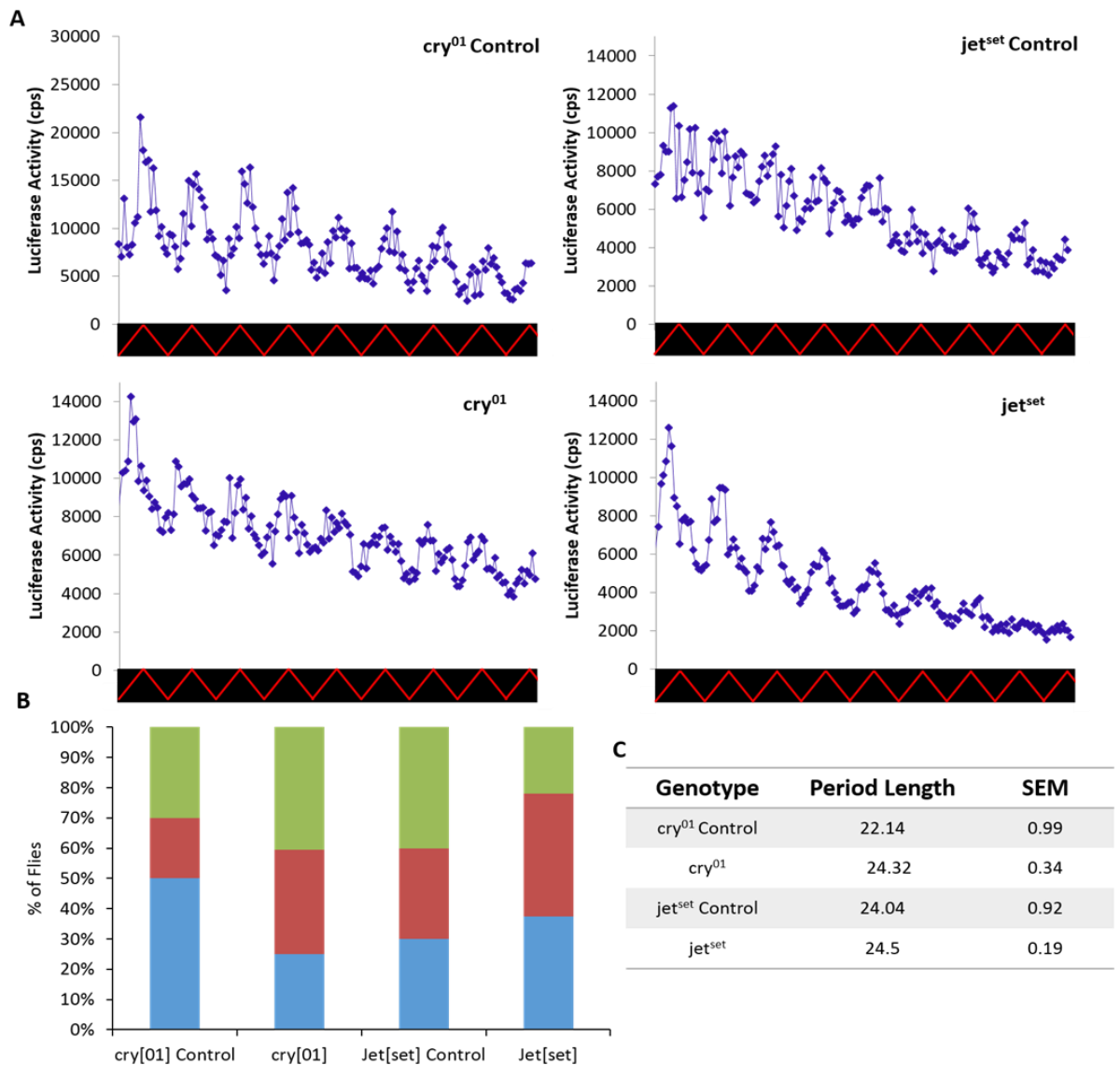
S.Figure 18 Luciferase activity traces for $y^1w*tim-luc;tim^{01}$ (tim^{01}) males.

Male flies of genotype $y^1w*tim-luc;tim^{01}$ (tim^{01}) in 9 (blue), 7 (green) and 5 (red) scaled to LD cycle. 'n' denotes number of flies for each condition. *Kruskal-Wallis test* across all conditions; $p < 0.0001$. *p* values (top right) indicate results of *Mann-Whitney test* vs. 7c/wk (5 vs. 7c/wk – red).



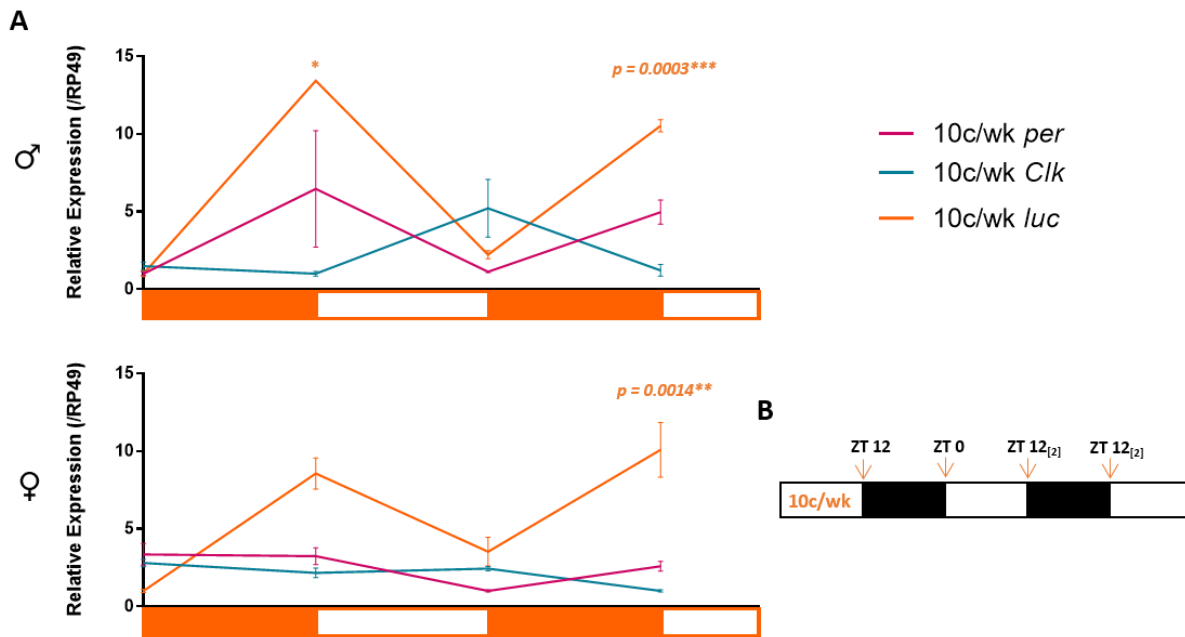
S.Figure 19 CRY and JET are not components of the peripheral oscillator.

A) Luciferase activity traces generated via TopCount for male flies of genotype; $y^1w*tim-luc;;cry^{01}/TM3-Ser^1$ (***cry⁰¹ Control***), $y^1w*tim-luc;;cry^{01}$ (***cry⁰¹***), $y^1w*tim-luc;jet^{set}/CyO$ (***jet^{set} Control***) and $y^1w*tim-luc;jet^{set}$ (***jet^{set}***) (annotated in figure). All traces represent 200 h in DD (black LD bar) with temperature cycling (min temp=17°C @06:30; max temp=23°C @18:30 – 0.5°C change/hour – red line). ‘n’ defines the number of flies. Traces generated using BRASS. (cps=counts per second). **B)** Composite bar chart displaying percentage of flies rhythmic (blue), weakly rhythmic (red) and arrhythmic (green) generated from RAE values calculated using FFT-NLLS analysis. **C)** Table of average period length and RAE for each genotype tested.



S.Figure 20 Female flies show better peripheral rhythms than males in a temperature cycle for both controls and *cry/jet* mutants.

A) Luciferase activity traces generated via TopCount for female flies of genotype; $y^1w^*tim-luc;;cry^{01}/TM3-Ser^1$ (***cry⁰¹* Control**), $y^1w^*tim-luc;;cry^{01}$ (***cry⁰¹***), $y^1w^*tim-luc;jet^{set}/CyO$ (***jet^{set}* Control**) and $y^1w^*tim-luc;jet^{set}$ (***jet^{set}***) (annotated in figure). All traces represent 200 h in DD (black LD bar) with temperature cycling (min temp=17°C @06:30; max temp=23°C @18:30 – 0.5°C change/hour – red line). ‘n’ defines the number of flies. Traces generated using BRASS. (cps=counts per second). **B)** Composite bar chart displaying percentage of flies rhythmic (blue), weakly rhythmic (red) and arrhythmic (green) generated from RAE values calculated using FFT-NLLS analysis. **C)** Table of average period length and RAE for each genotype tested.



S.Figure 21 mRNA expression cycling of *per*, *Clk* and *luc* in 10c/wk LD.

A) *per* (magenta), *Clk* (teal) and *luc* (orange) transcript cycling in 10c/wk LD only, from whole heads of male (top) and female (bottom) flies of genotype $y^1w^{*};tim-luc:10$ using qRT-PCR, plotted in real time (right – Dark=orange; white=light). Fold change is plotted for ratios of test transcript against *RP49* control transcript. *p* values (top right) indicate results of *Kruskal-Wallis test* across all time-points for each gene (*luc* = orange). *Dunn's multiple comparison test* to compare consecutive time-points (*luc*; ZT12 vs. 0 - $p=0.0294$). Error bars show mean \pm SEM. **B)** Sampling scheme for a 10c/wk LD cycle. Time-points are scaled to a 24 h LD cycle and _[2] indicates time-points in the second LD cycle. $p^{***}<0.0001$, $0.0001<p^{***}<0.001$, $0.001<p^{**}<0.01$ and $p^{*}<0.05$.

Appendix B: Supplementary Materials and Methods

B.1 *Drosophila* Husbandry

D. melanogaster were handled according to standard fly pushing practice, where anaesthetisation is achieved with CO₂ and flies manipulated using either a soft bristled paint brush or forceps.

B.1.1 Media

All *Drosophila* stocks and genetic crosses were maintained on 8-10ml of solidified standard cornmeal- agar diet with sucrose (**S.Table B.1**) - Bloomington Fly Food recipe. This medium facilitates all stages fly development with added Tegosept (Genesee Scientific, San Diego, CA) and Propionic acid (Fisher Scientific, UK) to inhibit fungal and microbial growth. All flies experimental flies used were raised on this standard medium and cultured at 23°C in an Environmentally Controlled Room (ECR) subject to a 12hL:12hD LD cycle, with a relative humidity of ~70%.

S.Table B. 1 Standard Cornmeal Medium

For 1000ml of Distilled Water

| | |
|---------------------------------|------|
| Agar (g) | 6 |
| Yeast (g) | 17.5 |
| Soya Flour (g) | 10 |
| Yellow Maize Meal (g) | 73.1 |
| Light Malt Extract (g) | 46 |
| Sucrose (60% in 80ml Water) (g) | 48 |
| Propionic Acid (ml) | 5 |
| Tegosept (ml) | 7 |

Note: Tegosept (A.K.A. Nipagen or Methyl-4-Hydroxybenzoate) – 10% w/v in 95% Ethanol

B.1.2 Stocks and Genetic Crosses

Fly stocks used in either experimentation or to create more complex lines were either obtained via *Drosophila* stock centres or generously donated by fellow fly researchers (**S.Table B.2** and **S.Table B.3**).

Flies have four pairs of chromosomes, the first (determines gender based on the ratio of X/autosomes; females = XX and males = X/Y), second and third pairs can all carry transgenic constructs however the fourth pair, as well as the Y chromosome, cannot due to their small size.

Appendix B:

Stable stocks are either homozygous for mutations of interest or maintained in a heterozygous state with a balancer chromosome. Balancer chromosomes possess a functional set of genes but are artificially altered so that genetic recombination cannot occur during meiosis, thus maintaining the chromosome of interest. Balancer chromosomes are themselves homozygous lethal and usually carry visible markers to allow for identification.

Common balancer chromosomes (Lindsley and Zimm, 1992);

- *CyO*¹ (II) - containing an allele of dual oxidase (*Duox*), *Duox_{Cy}*, identified by curly wings
- *TM3,ser*¹ (III) – identified by *serate*¹ (*ser*¹) wings
- *TM6B,Tb*¹ (III) - identified by *Tubby*¹ (*Tb*¹) in larvae/pupea and *Humeral* (Hu, neomorphicallele of *Antennapedia*, *Antp*) bristles in adults.

Crosses were set with virgin females to ensure genotype of offspring and males (virginity not required). Virgins were identified based either on the physical characteristics of newly eclosed flies (the presence of the meconium) or by time, as flies do not reach sexual maturity until ca. 8 h post eclosion. If the construct of interest is found on the X-chromosome, this must be the maternal parent, as males only have one copy of the X-chromosome. Crosses were left for 8-10 days before transferring to a new vial before F1 progeny eclose. F1 progeny were then harvested and assayed within 3-5 days, always before emergence of F2 progeny. Where possible, crosses were designed to generate isogenic controls alongside experimental genotypes and thus producing control offspring with a similar genetic composition.

S.Table B. 2 Mutants and Strains

| Genotype | Description | Source/Reference |
|--|---|---|
| <i>w</i> ¹¹¹⁸ | Wild-type control (w mutant background) | Bloomington #05905 (Hazelrigg, Levis and Rubin, 1984) |
| <i>w</i> ¹¹¹ ;; <i>cry</i> ⁰¹ | <i>cry</i> null mutation | Donated by J. Hall (Dolezelova, Dolezel and Hall, 2007) |
| <i>y</i> ¹ <i>per</i> ⁰¹ <i>w</i> [*] | <i>per</i> null mutation – nonsense point mutation (Q464) | Donated by M. Young (Konopka and Benzer, 1971) (Yu <i>et al.</i> , 1897) |
| <i>per</i> ⁵ | Short period phenotype - missense point mutation | Donated by M. Young (Konopka and Benzer, 1971) (Yu <i>et al.</i> , 1897) |
| <i>per</i> ¹ | Long period phenotypes – missense point mutation | Donated by M. Young (Konopka and Benzer, 1971) (Hamblen-Coyle <i>et al.</i> , 1992) |
| <i>y</i> ¹ <i>w</i> [*] ; <i>jet</i> ^{set} / <i>CyO</i> | <i>Jetlag</i> loss-of-function mutation | Donated by P. Emery (Lamba <i>et al.</i> , 2014) |
| <i>eya</i> ² | Eyes Absent – Protein null in the eye | Bloomington #2285 |

| | | |
|--|---|---|
| | but retains protein expression in the ocelli | (Bonini, Leiserson and Benzer, 1993) |
| <i>GMR-hid/CyO</i> | Expression of pro-apoptotic protein (hid) in the eyes | Bloomington #5771 (Grether <i>et al.</i> , 1995) |
| <i>norpA⁷</i> | Mutation in Phopsolipase C which removes visual transduction pathway | Bloomington #5685 and donated by G. Rubin (Bloomquist <i>et al.</i> , 1988) |
| <i>;;cyc⁰¹ ry⁵⁰⁶</i> | <i>cyc</i> null mutation | Donated by M. Young (Rutila <i>et al.</i> , 1998) |
| <i>yw;Pdf⁰¹</i> | Loss-of-function <i>Pdf</i> allele with nonsense point mutation (Y21) | Bloomington #26654 (Renn <i>et al.</i> , 1999) |
| <i>; Hdc^{JK910};</i> | Null mutation for <i>Hdc</i> – Histidine decarboxylase. Required in histamine synthesis | Bloomington #64203 (Burg <i>et al.</i> , 1993) (Melzig <i>et al.</i> , 1996) |
| <i>;; ort¹</i> | Null mutant for <i>ora transientless (ort)</i> – Histamine receptor | Bloomington #1133 (Iovchev <i>et al.</i> , 2009) |
| <i>;; st¹ HisCl^{T2}</i> | Nonsense mutation (G to A) in <i>Histamine-gated chloride channel subunit 1(HisCl1)</i> | Bloomington #29632 (Yusein <i>et al.</i> , 2008) (Yusein, Wolstenholme and Semenov, 2010) |
| <i>y¹w*;; tim-luc:10</i> | Luciferase reporter construct (Luciferase driven by <i>tim</i> promotor) | Donated by M. Rosbash and J. Hall (Stanewsky <i>et al.</i> , 1998) |
| <i>y¹w*; tim⁰¹</i> | <i>tim</i> null mutation | Donated by M. Young Sehgal <i>et al.</i> , (1994) |
| <i>w¹¹¹⁸;; cry⁰²</i> | <i>cry</i> null mutation | Donated by J. Hall (Dolezelova, Dolezel and Hall, 2007) |
| <i>;; cry^b rec^{#9}</i> | Point mutation if FAD binding domain of <i>cry</i> | Donated by M. Rosbash and J. Hall (Stanewsky <i>et al.</i> , 1998) |
| <i>Pdfr⁵³⁰⁴ w*</i> | PDF receptor loss-of-function allele with deletion of transmembrane domain | Bloomington #33068 (Hyun <i>et al.</i> , 2005) |
| <i>Hk¹</i> | Mutation in <i>Hyperkinetic</i> , the Beta subunit of Drosophila potassium channel Aldo/Keto reductase Domain | Bloomington #3562 (Fogle <i>et al.</i> , 2011) |
| <i>Hk²</i> | Mutation in <i>Hyperkinetic</i> , the Beta subunit of Drosophila potassium channel Aldo/Keto reductase Domain | Bloomington #55 (Fogle <i>et al.</i> , 2011) |
| <i>eag¹</i> | Hypomorphic allele of <i>Ether a-go-go</i> gene | Bloomington #3561 (Fogle <i>et al.</i> , 2011) |

S.Table B. 3 Gal4, Gal80 and UAS Constructs

| Genetic Element (Chromosome) | Description | Source/Reference |
|----------------------------------|---|---|
| <i>tim(UAS)-Gal4 (II)</i> | Expresses Gal4 in all clock-bearing cells | Donated by M. Young. Developed by S. Martinek (unpublished). (Blau and Young, 1999) |
| <i>UAS-mCD8:GFP (III)</i> | Expresses GFP fused with transmembrane murine CD8 | Donated by J Blau (Lee and Luo, 1999) |
| <i>UAS-Dcr-2w (I and</i> | UAS controlled Dicer2 enzyme | Bloomington #24648 (I) and #24651 |

Appendix B:

| | | |
|--|---|---|
| III) | expression in the presence of Gal4 – aids RNAi knockdown | (III) (Dietzl <i>et al.</i> , 2007) |
| <i>UAS-ds-cry</i>^{3772R2} (II) | Expresses double stranded <i>cry RNAi</i> | NIG-FLY stock collection #3772R-2 (<i>NM_169852.1</i>) |
| <i>UAS-ds-jet</i>^{JF01506} (III) | Expresses double stranded <i>jet RNAi</i> | Bloomington – TriP #31058 (Ni <i>et al.</i> , 2007) |
| <i>cry-gal4-13</i> (III) | Gal4 expression in the morning and evening cells | Donated by P. Emery (Emery <i>et al.</i> , 2000b) (Zhao <i>et al.</i> , 2003) |
| <i>Pdf-Gal4</i> (II) | Gal4 expression in all PDF-expressing neurones | Bloomington #6900 (Renn <i>et al.</i> , 1999) |
| <i>GMR78G02-Gal4</i> (III) | Gal4 expression driven in the evening cells – 3 <i>cry</i> ⁺ LN _d s and 5 th s-LN _v | Bloomington #40010 (Schlichting <i>et al.</i> , 2016) |
| <i>ChAT-Gal4.7.4</i> (II) | Expresses Gal4 specifically in cholinergic neurones | Bloomington #6798 (Salvaterra and Kitamoto, 2001) (Lima and Miesenböck, 2005) |
| <i>cry-Gal80</i> (III) | Expresses Gal80 in the CRY-expressing neurones | Donated by M. Rosbash (Stoleru <i>et al.</i> , 2004) |
| <i>Pdf-Gal80</i> (II) | Expresses Gal80 in the PDF-expressing neurones | Donated by M. Rosbash (Stoleru <i>et al.</i> , 2004) |
| <i>ChAT-Gal80</i> (III) | Expresses Gal80 under the control of ChAT regulatory sequences | Bloomington #60321 (Diao <i>et al.</i> , 2015) (Sonn <i>et al.</i> , 2018) |
| <i>UAS-cry₂₄</i> (II) | Expresses cryptochrome protein | Donated by P. Emery (Emery <i>et al.</i> , 1998) |
| <i>tim-luc</i> (I) | Luciferase reporter construct (Luciferase driven by <i>tim</i> promoter) | Wijnen Lab |
| <i>Vglut-Gal80</i> (II) | Expresses Gal80 in glutamatergic neurones | Bloomington #58448 |
| <i>UAS-hid</i> (II) | Expresses the pro-apoptotic protein Head involution defective (<i>Hid</i>) | Bloomington #65403 (Goyal <i>et al.</i> , 2000) |
| <i>UAS-kir2.1</i> (II) | Expresses the inward rectifier K ⁺ channel | Bloomington #6595 (Baines <i>et al.</i> , 2001) |
| <i>tim₆₂-Gal4</i> (II) | Expresses Gal4 in the circadian rhythm pattern of <i>tim</i> | Bloomington #7126 (Kaneko <i>et al.</i> , 2000) |
| <i>UAS-ds-HisC1</i>^{KK112578} (II) | Expresses double stranded <i>HisC1 RNAi</i> | VDRC #104966 |

Note: Flies lines are usually generated in the *w*¹¹¹⁸ mutant background (white-eyes compared to red in WT). Many transgenic constructs contain the WT allele (*w*⁺ or *miniwhite*) so eye colour indicates the presence of the construct. *w* is found on the X-chromosome and as such males are usually more sensitive to the presence of the *miniwhite* (possess only one copy).

B.2 Light:Dark Cycle Schedule for all photocycles assayed

| | 3 cycles/week | | 4 cycles/week | | 5 cycles/week | | 6 cycles/week | | 7 cycles/week | | 8 cycles/week | | 9 cycles/week | | 10 cycles/week | | 11 cycles/week | | |
|----|---------------|----------|---------------|----------|---------------|----------|---------------|----------|---------------|----------|---------------|----------|---------------|----------|----------------|----------|----------------|----------|----------|
| 1 | 28 | Tu 04:00 | 21 | Mo 21:00 | 16.8 | Mo 16:48 | 14 | Mo 14:00 | 12 | Mo 12:00 | 10.5 | Mo 10:30 | 9.33 | Mo 09:20 | 8.4 | Mo 08:24 | 7.64 | Mo 07:38 | |
| 2 | 56 | We 08:00 | 42 | Tu 18:00 | 33.6 | Tu 09:36 | 28 | Tu 04:00 | 24 | Tu 00:00 | 21 | Mo 21:00 | 18.67 | Mo 18:40 | 16.8 | Mo 16:48 | 15.27 | Mo 15:16 | |
| 3 | 84 | Th 12:00 | 63 | We 15:00 | 50.4 | We 02:24 | 42 | Tu 18:00 | 36 | Tu 12:00 | 31.5 | Tu 07:30 | 28.00 | Tu 04:00 | 25.2 | Tu 01:12 | 22.91 | Mo 22:54 | |
| 4 | 112 | Fr 16:00 | 84 | Th 12:00 | 67.2 | We 19:12 | 56 | We 08:00 | 48 | We 00:00 | 42 | Tu 18:00 | 37.33 | Tu 13:20 | 33.6 | Tu 09:36 | 30.55 | Tu 06:32 | |
| 5 | 140 | Sa 20:00 | 105 | Fr 09:00 | 84 | Th 12:00 | 70 | We 22:00 | 60 | We 12:00 | 52.5 | We 04:30 | 46.67 | Tu 22:40 | 42 | Tu 18:00 | 38.18 | Tu 14:32 | |
| 6 | 168 | Mo 00:00 | 126 | Sa 06:00 | 100.8 | Fr 04:48 | 84 | Th 12:00 | 72 | Th 00:00 | 63 | We 15:00 | 56.00 | We 08:00 | 50.4 | We 02:24 | 45.82 | Tu 21:49 | |
| 7 | | | 147 | Su 03:00 | 117.6 | Fr 21:36 | 98 | Fr 02:00 | 84 | Th 12:00 | 73.5 | Th 01:30 | 65.33 | We 17:20 | 58.8 | We 10:48 | 53.45 | We 05:27 | |
| 8 | | | 168 | Mo 00:00 | 134.4 | Sa 14:24 | 112 | Fr 16:00 | 96 | Fr 00:00 | 84 | Th 12:00 | 74.67 | Th 02:40 | 67.2 | We 19:12 | 61.09 | We 13:05 | |
| 9 | | | | | 151.2 | Su 07:12 | 126 | Sa 06:00 | 108 | Fr 12:00 | 94.5 | Th 22:30 | 84.00 | Th 12:00 | 75.6 | Th 03:36 | 68.73 | We 20:43 | |
| 10 | | | | | 168 | Mo 00:00 | 140 | Sa 20:00 | 120 | Sa 00:00 | 105 | Fr 09:00 | 93.33 | Th 21:20 | 84 | Th 12:00 | 76.36 | Th 04:21 | |
| 11 | | | | | | | 154 | Su 10:00 | 132 | Sa 12:00 | 115.5 | Fr 19:30 | 102.67 | Fr 06:40 | 92.4 | Th 20:24 | 84.00 | Th 12:00 | |
| 12 | | | | | | | 168 | Mo 00:00 | 144 | Su 00:00 | 126 | Sa 06:00 | 112.00 | Fr 16:00 | 100.8 | Fr 04:48 | 91.64 | Th 19:38 | |
| 13 | | | | | | | | | 156 | Su 12:00 | 136.5 | Sa 16:30 | 121.33 | Sa 01:20 | 109.2 | Fr 13:12 | 99.27 | Fr 03:16 | |
| 14 | | | | | | | | | 168 | Mo 00:00 | 147 | Su 03:00 | 130.67 | Sa 10:40 | 117.6 | Fr 21:36 | 106.91 | Fr 10:54 | |
| 15 | | | | | | | | | | | 157.5 | Su 13:30 | 140.00 | Sa 20:00 | 126 | Sa 06:00 | 114.55 | Fr 18:32 | |
| 16 | | | | | | | | | | | 168 | Mo 00:00 | 149.33 | Su 05:20 | 134.4 | Sa 14:24 | 122.18 | Sa 02:10 | |
| 17 | | | | | | | | | | | | | 158.67 | Su 14:40 | 142.8 | Sa 22:48 | 129.82 | Sa 09:49 | |
| 18 | | | | | | | | | | | | | 168.00 | Mo 00:00 | 151.2 | Su 07:12 | 137.45 | Sa 17:27 | |
| 19 | | | | | | | | | | | | | | | 159.6 | Su 15:36 | 145.09 | Su 01:05 | |
| 20 | | | | | | | | | | | | | | | 168 | Mo 00:00 | 152.73 | Su 08:53 | |
| 21 | | | | | | | | | | | | | | | | | 160.36 | Su 16:21 | |
| 22 | | | | | | | | | | | | | | | | | | 168.00 | Mo 00:00 |

B.3 Analysis of *Drosophila* Locomotor Behaviour

B.3.1 DAM Behavioural Assay

Experimental LD boxes were complete with blackout sheeting (Thorlab) and black tape (to ensure against light leakage) and a water tray to maintain around ~70% relative humidity. Water added to the water tray was treated with 0.01% A.S.A.B Biocide (Fisher Chemicals) and 4 drops of Polyclean algaecide (PolyScience) to prevent mould and bacterial growth over the course of the experiment.

Transitions between white light LD cycles and free-running conditions occurs during the dark phase to prevent the effect of light pulses and as to not interrupt a light cycle. Note: all monitors were moved under a red-light lamp as to impose minimal impact on the circadian oscillator as a result of brief light exposure.

Following red light LD cycles, monitors were moved to a constant red light condition (RR) instead of DD. In these instances, monitors were moved during the red-light phase.

S.Table B. 4 Sugar-agar Medium (5% sucrose, 1% agar and 0.07% Tegosept)

For 10ml of Distilled Water

| | |
|---------------------|-----|
| Agar (g) | 0.1 |
| Sucrose (g) | 0.5 |
| Tegosept (μ l) | 70 |

Individual activity records of each fly were first analysed in order to exclude those flies which did not survive the entire assay period using individual fly actograms (ClockLab). Individual fly data was exported to Microsoft Excel for processing and further analysis i.e. assessment of rhythmic strength, averaging and categorisation according to entrainment/rhythmicity.

B.3.2 DAM Behavioural Assay with a Combined LD and Temperature Cycle

The effect of a combined temperature cycle and LD cycle was investigated to test whether there is a differential effect between entrainment to different Zeitgebers (entrainment cues) e.g. temperature cycle: peak temp. 21°C @12:00; min temp. 11°C @04:30: Combined with 24 h light cycle; L_{ON} 04:30; L_{OFF} 22:00; 17.5hL:6.5hD. To achieve this, either LD cycles were programmed as previously described, with temperature cycling controlled using environmentally controlled rooms (FitoView system), or Percival DR-36VLI incubators (CLF Plant Climatics, Wertingen, Germany) were used to regulate both light and temperature conditions (set-up used is indicated within figures).

Appendix B:

Populations of flies were also tested with this assay, in either single sex (SS) groups (SSM – Male; SSF – Female) or mixed sex groups (MSG) and well and individual flies. When populations were being tested, larger 32 channel DAM monitors were used which house standard glass fly culture vials.

B.3.3 Analysis of Activity Counts

ClockLab was used to analyse the raw activity counts recorded from the DAM system during defined intervals throughout an LD cycle in the form of Light:Dark activity counts. In the analysis of experiments of combined temperature and light cycles, activity counts were analysed in four defined time frames; Morning (5-9.92 h), Noon (10-13.92 h), Evening (14-21.92 h) and Night (22-4.92 h). Individual fly data was pooled in 5 minute bins and intervals chosen to capture defined periods of activity and avoid overlapping.

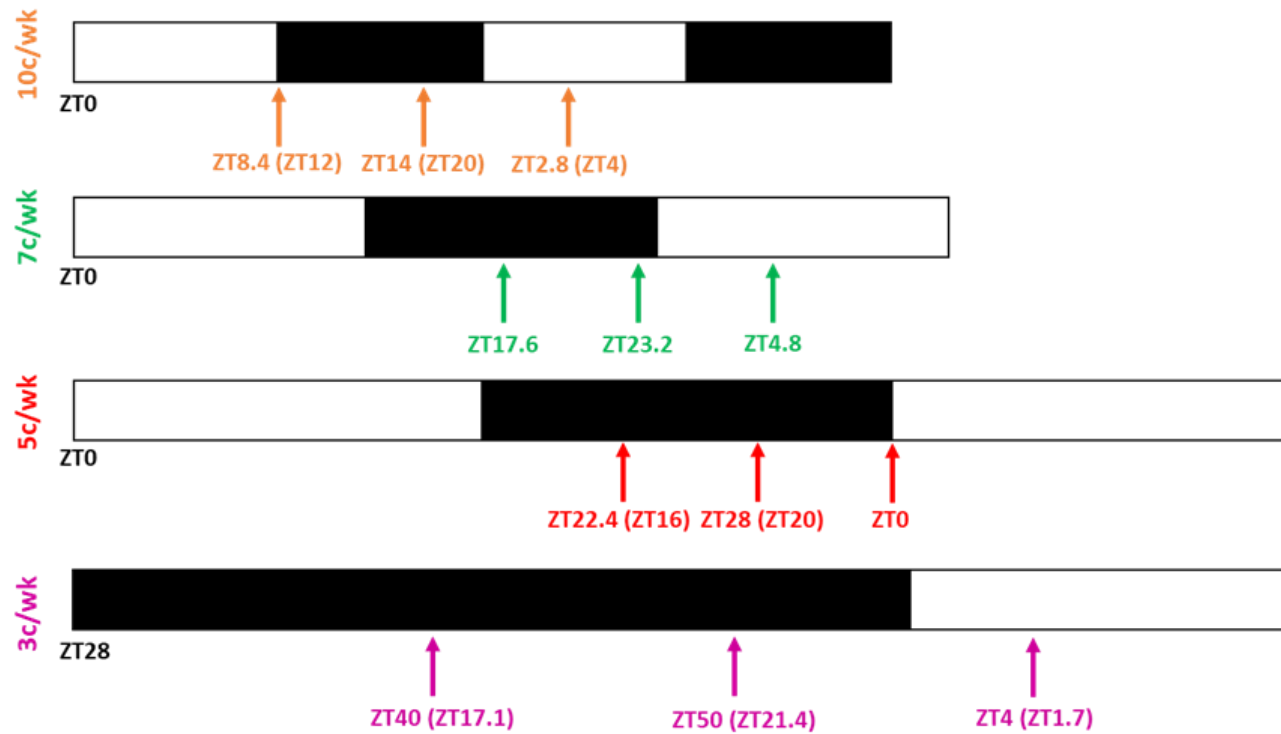
Percentage activity at each defined category was calculated and presented as a composite bar chart (Dawn – Blue; Day – Orange; Dusk – Grey; Night – Yellow). Data is qualitatively displayed as activity profiles, with the temperature cycle protocol superimposed. GraphPad Prism 7.05 was used to generate graphs and conduct analysis of variance (ANOVA) with the non-parametric *Kruskal-Wallis test* and *Tukey's multiple comparison test* for comparison between activity counts in each defined interval for each genotype/group.

| LD Cycle (c/wk) | ExT (h) | Standard Analysis Parameters (h) | Refined Analysis Parameters (h) | | | ExT Range | | Harmonic Range | |
|-----------------|------------|----------------------------------|---------------------------------|----------|---------|-----------------|-----------------|----------------|--------|
| | | | 0.5x | ExT | 1.5x | Min | Max | Min | Max |
| 11 | 15.27 | 13 - 26 | - | 14 - 16 | 22 - 24 | 14.583 | 15.957 | 21.870 | 23.931 |
| 10 | 16.8 | 13 - 26 | - | 16 - 18 | 24 - 26 | 16.044 | 17.556 | 24.066 | 26.334 |
| 9 | 18.7 | 14 - 28 | - | 18 - 20 | 27 - 29 | 17.827 | 19.507 | - | - |
| 8 | 21 | 14 - 28 | - | 20 - 22 | 30 - 33 | 20.055 | 21.945 | - | - |
| 7 | 24 | 15 - 30 | 11 - 13 | 23 - 25 | 35 - 37 | 22.920 | 25.080 | - | - |
| 6 | 28 | 16 - 32 | 13 - 15 | 27 - 29 | - | 26.740 | 29.260 | - | - |
| 5 | 33.6 | 18 - 36 | 16 - 18 | 32 - 35 | - | 32.088 | 35.112 | - | - |
| 4 | 42 | 22 - 44 | 20 - 22 | 40 - 44 | - | 40.110 | 43.890 | - | - |
| 3 | 56 (44.8*) | 23 - 50* | 21 - 23* | 43 - 46* | - | 53.48 (42.784*) | 58.52 (46.816*) | - | - |

S.Table B. 5 Analysis parameters used for Light:Dark DAM behavioural analysis.

Entrained period length is shown for all photocycles used in behavioural assays. Standard parameters for Chi² periodogram analysis, as well as refined parameters for better assessment of entrainment quality. Ranges used for categorising flies as entrained/harmonic, flies with period lengths outside of these ranges are categorised as 'other'. Entrained range was set after inspection of pilot data to allow a reasonable amount for variation around entrained period length to be still be considered as entrained. Entrained range is set at $\pm 4.5\%$ of entrained period length and calculated with the formula (similarly for harmonic); $Ext \pm (0.045 \times ExT)$

B.4 Analysis of the *Drosophila* central molecular clockwork



S.Figure B. 1 Dissection schedule for confocal immunofluorescence

White (light phase) and black (dark phase) bars for 10 (orange), 7 (green), 5 (red) and 3c/wk (magenta) photoperiods. Vertical arrows indicated time-points for dissection (colour coded). Time-points reported as; ZT'Real-time'(ZT'Scaled to 24h').

B.4.1 *D.melanogaster* Adult Brain Dissection and Immunostaining

See (Wu and Luo, 2006)

Dissection (Adult brains)

1. Anaesthetise and place adults on metal block on ice (can pre-chill in freezer)
2. Remove heads of all flies with forceps or a razor blade
3. Use forceps to apply gentle pressure to back of head – will make proboscis stick out, use second pair of forceps to remove **entire** proboscis leaving a large hole (If not all proboscis is removed, following steps will not work properly)
4. Use forceps to apply pressure either side of head (behind eyes) and brain will come out of hole made from removing proboscis
5. Gently remove any remaining cuticle

Fixing and Washes

6. Using a pipette (p200), transfer brains to 4% PFA in 0.2 ml PCR tubes – eject some fluid (PFA or PBT) onto the brain to aid aspiration
7. Fix brains in PFA for **20 mins** at RT on nutator (insectary)
8. Remove PFA and dispose into waste falcon
9. Add 200 μ l 0.3% PBT, invert a couple of times (quick wash), remove PBT and repeat (**total of 2 quick washes**)
10. Add 200 μ l and place on nutator at RT for **20 mins** (long wash) repeat twice (**total of 3 long washes**)

0.3% PBT Add 1.5 ml Triton-X 100 (US Biological, T8655) to 498.5 ml PB (100 mM

$\text{Na}_2\text{HPO}_4/\text{NaH}_2\text{PO}_4$, pH 7.2)

Blocking and Staining

11. Remove PBT, add 200 μ l of 5% PBT-NGS (Blocking Solution). Place on nutator at RT for **20 mins**
12. Add primary AB to block solution
13. Place on rocker/nutator in cold room (**4°C**) for **2 nights** (or up to 1 week)
14. Remove primary – Can be retained at 4°C and used 3+ times
15. Add PBT for 2 quick washes (step 9)
16. Add PBT for 3 long washes (step 10)
17. Remove PBT and add Secondary AB solutions
18. Place on rocker/nutator in cold room (**4°C**) for **2 nights** (or up to 1 week)

Mounting of Fixed and Stained Brains

19. Make barrier on microscope slide with nail polish (same size of cover slip) can do two coverslips per slide – allow to nail polish to dry at room temp
20. Remove secondary and discard
21. Add PBT for 2 quick washes (step 9)
22. Add PBT for 3 long washes (step 10)
23. Remove PBT and add **200 μ l** Vector Shield and allow brains to settle (in fridge)
24. Use cut off pipette tip to move brains to centre of microscope slide – remove excess vector shield and arrange brains (can use forceps)
25. Place cover slip over the brains – slowly pipette vector shield starting from one side of cover slip until sample completely covered
26. Carefully seal edges with nail polish – store at 4°C in a dark slide holder
27. Store slides at -20°C

Appendix B:

B.4.2 PERIOD antibody preparation

- To prepare 1:100 aliquots of α PER
 - Stock: 1.5 μ l aliquots of 1:1 α PER
1. Make 0.3% PBT (should be stock in main lab);
 - Add 0.75 ml of Triton-X to 249.25 ml of 0.1 M PB (pH 7.2)
 2. Make 5% PBT/NGS (make as required);
 - Add 50 μ l of NGS to 950 μ l of PBT
 3. Use 3x 1.5 μ l aliquots of 1:1 α PER
 4. Add 148.5 μ l of PBT/NGS to each aliquot – makes 1:100 dilution
 - Combine aliquots (to ensure conservation of all Ab) – total of 450 μ l of 1:100 α PER Ab
 5. **IF REQUIRED** (is for per) clean up Ab with embryo staining (see protocol **A.1.1**).
 6. Add Sodium Azide – 0.1% weight volume (0.1g per ml)
 7. Aliquot and store at -20°C

B.4.3 PERIOD antibody purification

Adapted from Wendy F Rothwell and William Sullivan (CSHL Press).

Materials:

- Fly collection cages (plastic beaker with base cut off + nylon lid)
 - Embryo baskets (sawn-off falcon tubes w/ hole in lid + nylon mesh)
 - Bleach (50% solution)
 - Squirt bottle containing H₂O
 - Sodium azide
1. **EXPAND STOCK - *y per*⁰¹ w** - Place 200-400 flies in a cage, The lid (small petri dish) contains juice agar + small amount of thick yeast paste;
 - 1 g agar; 1 g sugar; 10 ml apple juice
 - 1 g dried yeast in 1 ml water
 2. Keep the cages quiet during the egg laying period (ca. 24 h so embryos do not start to develop)
 3. **Embryo collection**; put H₂O on petri dish and use paintbrush to gently transfer embryos from the agar plates to the basket. Use water to rise embryos from paintbrush.
 4. **Dechoriation** (removing chorion layer); Place the baskets in a glass petri dish partially filled with 50% bleach. Rinse embryos continually using a Pasteur pipette for approx. 2 minutes. Check the status of the embryos on the microscope (more translucent).
 5. Wash the embryos water in a squirt bottle.
 6. Remove the mesh and blot gently with paper towel, taking care not to remove embryos.
 7. **Dehydration**; Place the mesh inside 5 ml glass/plastic vials; wash it with 1 ml of heptane using a Pasteur pipette (remove embryos from mesh).
 8. Remove the mesh and add 1 ml of methanol (MeOH). Cap the vial and shake vigorously for 15 seconds, let stand for 1 minute. The embryos should sink and MeOH/heptane should separate, with a layer of heptane above and a layer of MeOH below.
 9. Remove the heptane layer and most of the methanol leaving the embryos at the bottom. Add fresh methanol until two thirds full. Store at 4°C if required (up to 2 weeks).
 10. **Rehydration**; Transfer the embryos to an eppendorf tube and remove as much of the methanol as possible.
 11. When ready to stain, rehydrate embryos with decreasing MeOH gradations. (75, 50, 25% meOH in PBT for 5-10 mins each on nutator).
 12. Add 250 µl of methanol, and then 250 µl of PBTA (or PBT, or even PBS), taking care not to shake the tube (bubbles form and interfere)
 13. Add PBTA until 2/3 full and invert gently 3 times. Let the embryos sink.
 14. Remove solution and add 500 µl of PBTA.
 15. Keep the embryos rehydrating in PBTA solution for 15 minutes at room temperature on the rotator.
 16. Transfer embryos to a new eppendorf. Allow them to settle to the bottom and remove PBTA.
 17. **Staining**; Add primary antibody solution diluted in PBTA. (See Ab Prep Protocol).
 18. **Leave on nutator at 4°C for 2 days**
 19. Add 10% Na Azide to the solution in a 1:500 dilution, and store aliquots of diluted antibody at -20°C until needed. (preserves Ab)

B.5 Analysis of peripheral clock rhythms *in vivo* – TopCount

For all assays in this report, count time per well was 10 s with a 2 minute delay per plate. Assays were run for 10 days, due to technical errors some experiments did not complete 10 full days. As stated in 4.2.1.1, this assay is an automated process where plates are placed into a stacker and sequentially loaded into the scintillation counter. To ensure adequate light exposure, clear 96-well plates (OptiPlate; PerkinElmer) were placed between each assay plate in the stack. Note that all plates experience a brief period of constant darkness during luminescence recordings, even during the light phase. An identification barcode, read by the TopCount apparatus, was adhered to the plate and any excess film removed to prevent plates sticking together during the assay.

TopCount assays in DD in the presence of a temperature cycle, were conducted as stated in 4.2.1.1, however there was now no need for spacer plates. Temperature cycles are generated and controlled using ECRs (FitoView system), with a temperature change of 0.5°C per hour over a 12 h cycle (min temp=17°C @06:30; max temp=23°C @18:30). Prior to DD assays, flies were entrained to a 12hL:12hD cycle for 3 days at 23°C.

To ensure stability and accuracy of light and temperature cycling, environmental monitors are used.

S.Table B. 6 Sugar-agar Medium with D-Luciferin

| For 22 ml Distilled Water (4 assay plates) | |
|---|-----|
| Agar (g) | 0.2 |
| Sucrose (g) | 1 |
| Tegosept (µl) | 140 |
| 100mM Luciferin (µl) | 300 |

Note: Tegosept was added as an anti-fungal agent.

BRASS allows for the graphical representation of all bioluminescence recordings for each individual fly, and thus flies that did not survive the full assay can be omitted from all further analysis. Average graphs were generated using BRASS software however scaled graphs were made in GraphPad prism 7.05. Results of FFT-NLLS analysis conducted in BRASS was exported to Microsoft Excel for processing and further analysis i.e. assessment of rhythmic strength, averaging and categorisation according to entrainment/rhythmicity.

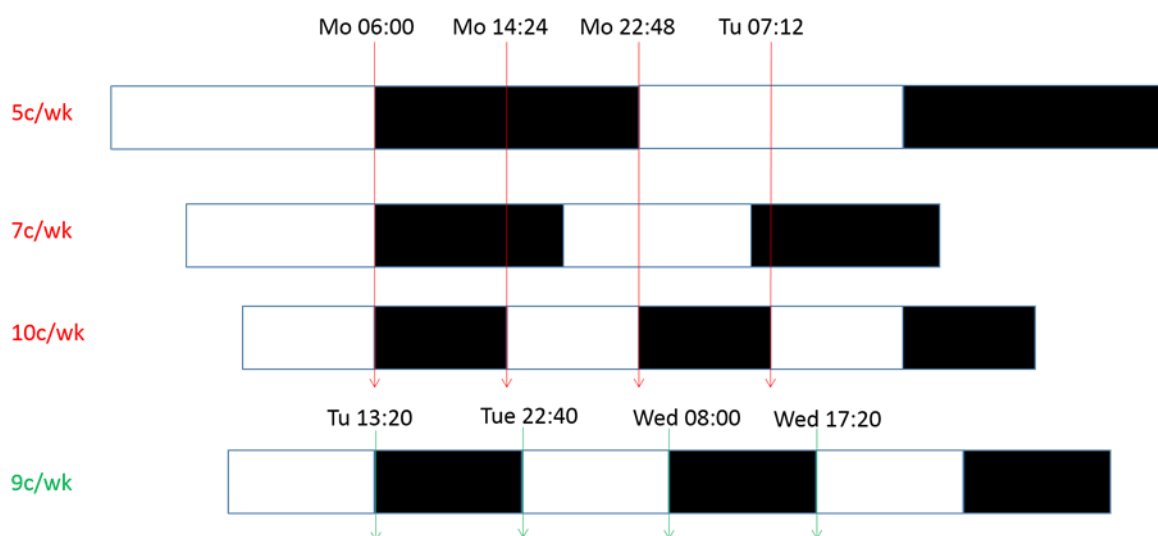
Data for amplitude of luciferase activity for each LD cycle was collected over the first 96 h only. This was to ensure uniformity across all conditions and because amplitude decreases over time due to luciferin depletion. Phase of luciferase activity is calculated with respect to photoperiod, therefore only flies with the correct entrained period length were used in phase analysis.

B.6 Analysis of the *Drosophila* peripheral molecular clockwork - qRT-PCR

B.6.1 Quantitative Reverse Transcriptase-PCR (qRT-PCR)

RNA extraction protocol includes RNase treatment and work area was cleaned with RNase Away (FisherScientific) to prevent RNA degradation and DNA contamination.

Flies were raised at 23°C in 12hL:12hD, and prior to incubation in different photocycles, they were separated into cohorts of 40 (for both males and female) and kept on standard cornmeal media. At each time-point, three biological replicates were collected for each gender, thus twelve cohorts of males and females were loaded into each condition, to account for biological variation. To account for PCR error, three technical replicates were conducted for each biological replicate, for each primer pair.



S.Figure B. 2 Sample collection schedule for qRT-PCR

White (light phase) and black (dark phase) bars represent at least 2 full LD cycles at each photoperiod (5, 7, 10 and 9c/wk). Vertical arrows indicated time-points for tissue collection. For 5, 7 and 10c/wk, time-points are dictated by LD transitions in the 10c/wk condition (red arrows), adapted in 9c/wk (green arrows) to the LD transitions for this condition.

B.6.2 Standard Curves and Primer efficiencies

For each primer pair, a standard curve was generated. A serial dilution of template RNA yielded five known concentrations; 100, 10, 1, 0.1 and 0.01 ng/μl. Template was amplified with each primer pair using the same protocol stated in B.6.4. Using Opticon Monitor 3 (BIORAD), plots of C(t) against Log(quantity) were generated with a straight line of best fit (higher template concentrations correlate to lower cycling thresholds). The equation of this line can then be used to calculate quantity of test RNA in samples with known C(t) values.

S.Table B. 7 Equations of standard curves for primers used for qRT-PCR.

Standard curves are straight lines with equation ' $y=mx+c$ ' where ' y ' is C(t), ' x ' is Log(quantity), ' m ' is the gradient and ' c ' is the y-intercept. ' r^2 ' is the result of linear regression analysis indicating how well the data fits the line of best fit (r^2 close to 1 denotes strong correlation).

| Target Gene | Standard Curve equation | r^2 |
|-------------|-------------------------|-------|
| <i>per</i> | $y = -3.226x + 26.37$ | 0.943 |
| <i>Clk</i> | $y = -2.704x + 25.62$ | 0.966 |
| <i>luc</i> | $y = -2.89x + 24.7$ | 0.995 |
| <i>rp49</i> | $y = -3.059x + 21.11$ | 0.973 |

Percentage primer efficiency was calculated using the following equation (as described by Bustin *et al.*, 2009);

$$\% \text{ Efficiency} = 100 \times (10^{(-1/\text{slope})} - 1)$$

An efficiency of 100% indicates the amount of product doubles with every cycle (Recommended efficiencies are between 80-120%)

B.6.3 RNA extraction protocol

Kit: RNAqueous®-4PCR Kit (Part Number AM1914)

NOTE: Clean with EtOH and RNASEfree/RNase zap during the protocol. Clean your gloves/get new ones periodically. Clean thoroughly if spill contents of any vial for to avoid contamination.

1. Add 500 µl of **Lysis buffer** per sample. Active homogenization for 2 minutes on ice.
2. Centrifuge 1 min at 10k.
3. Move supernatant to new collection tube (discard old tube with pellet)
4. Add 500 µl of EtOH 64%.
5. Centrifuge up to 500 µl (1 min at 13k) through a cartridge filter. Centrifuge then the remaining volume. **Discard filtered volume.** RNA (and others) remains at the cartridge.
6. Add 700 µl of **Wash Solution 1** to the cartridge and centrifuge (13k for 1 min). **Discard liquid.**
7. Add 500 µl of **Wash Solution 2/3** to the cartridge and centrifuge (13k for 1 min). **Discard liquid.**
8. Add 500 µl of **Wash Solution 2/3** to the cartridge and centrifuge (13k for 1 min). **Discard liquid.**
9. Move the cartridge to a new collection tube
10. Add 40 µl of **Elution Buffer** to the cartridge, centrifuge (30 seconds at 13k). **KEEP LIQUID**
11. Add 10 µl more of Elution buffer and centrifuge (30 seconds at 13k.)
12. Centrifuge 30 seconds at 13k one last time without adding EB. Discard filter – **KEEP LIQUID**
Note: this will give you a RNA solution of 50 µl. The more volume you add, the less concentrated the RNA will be. Up to you deciding if adding more EB if your numbers are high.
13. Add 5 µl (0.1 vol) of 10X **DNase buffer**.
14. Add 1 µl of DNase. Mix very gently by pipetting. Check the DNase solution is properly dissolved and does not look sticky inside the solution.
15. Incubate 30 minutes at 35°C
16. Add 5 µl of DNase inactivation buffer.
17. Mix for 1 minute by flicking the tubes with your finger. Avoid a precipitate forming.
18. Centrifuge (1 min at 10k)
19. Carefully, transfer supernatant to a new tube. **Do not touch the pellet**
20. Measure with NanoDrop and write down/print concentrations and Ratios of your sample

B.6.4 qRT-PCR and Cycling Protocol

- Plate out Mastermix, primers (see primer conc.) and sample. Keep plate on ice whilst plating.
- All RNA samples are diluted to a starting concentration of 12.5 ng/ μ l and 2 μ l of sample is added i.e. 25 ng of RNA per reaction.
- Total reaction volume = 20 μ l

Cycling protocol

1. Incubate @ 55°C for 10 mins
2. Incubate @ 95°C for 8mins
3. Incubate @ 95°C for 10s
4. Incubate @ 60°C for 1min
5. Plate Read
6. Go to line 3 for 39 more times
7. Melting curve from 50.0°C to 95.1°C – read every 0.2°C, hold 00:00:01
8. END

B.7 Analysis of the *Drosophila* peripheral molecular clockwork - Western Blot

B.7.1 Reagents

| Reagent | Source | Catalogue/Product No. |
|--|-------------------------|-----------------------|
| NaCl (Sodium Chloride) | ThermoFisher Scientific | 7647-14-5 |
| BSA (Bovine Serum Albumin) | ThermoFisher Scientific | BP9703-100 |
| HALT Protease and Phosphatase Inhibitor Cocktail (100x) | ThermoFisher Scientific | 78440 |
| PageRuler Plus (Pre-stained protein Ladder) | ThermoFisher Scientific | 26619 |
| Methanol | Fisher Chemical | M/4000/17 |
| MES (2-(N-Morpholinoethane-sulfonic acid sodium salt) | Sigma-Aldrich | M3671-50G |
| Sample Buffer, Laemmli 2x | Sigma-Aldrich | S3401-10VL |
| Ammonium Persulphate (APS) | Sigma-Aldrich | A-1433 |
| TEMED (N,N,N',N'-tetramethylethane-1,2-diamine) | Sigma-Aldrich | T9281-25ML |
| Acrylamide/Bis-acrylamide, 30% solution | Sigma-Aldrich | A3699-100ML |
| Immobilon – FL PVDF Transfer Membranes | Sigma-Aldrich | 05317-10EA |
| Triton X-100 | US Biological | T8655 |
| SDS (Sodium Dodecyl Sulphate) | US Biological | S5010 |
| Tris (HCl) | US Biological | T8600 |
| Tween20 (Polyoxyethylene sorbiton monooleate) | US Biological | P4379 |

B.7.2 Buffers

Running Buffer (RT): 10% Laemmli Buffer (10x), 90% dH₂O

Transfer Buffer (4°C): 10% Laemmli Buffer (10x), 70% dH₂O, 70% Methanol

Blocking Buffer (4°C): 3% BSA in 0.5% Tween-PBS

Appendix B:

B.7.3 Antibodies

| Antibody | Concentration | Initial Concentration | Source |
|--------------------------|----------------------|------------------------------|--------------------------------------|
| Rabbit anti-PER | 1:15000 | 1:100 | J.C. Hall (Liu <i>et al.</i> , 1992) |
| Mouse anti-HSP70 | 1:10000 | 1:1 | Sigma-Aldrich, H5147 |
| Goat anti-Rabbit (800cw) | 1:20000 | 1:1 | LiCor, 827-08365 |
| Goat anti-Mouse (680cw) | 1:20000 | 1:1 | LiCor, 827-08366 |

B.7.4 Protein extraction protocol

1. Make Homogenisation Buffer (HB);

| Homogenisation buffer (stock Conc.) | | |
|--|-------|--------|
| Reagent | 500µl | 1000µl |
| 150mM NaCl (1M) | 75 | 150 |
| 50mM MES (500mM) | 50 | 100 |
| 1% triton-X (10%) | 50 | 100 |
| HALT Protease/phosphatase inhibitor (100x) | 5 | 10 |
| EDTA - metalloprotease inhibitor (100x) | 5 | 10 |
| 1% SDS (20%) | 25 | 50 |
| Distilled Water | 295 | 590 |

2. Homogenise fly heads in HB using an Eppendorf pestle – in most cases use between 20-30 heads (100 µl of HB).
3. Centrifuge at 3,000 k for 2 mins (ensure balanced)
 1. Move supernatant to new tube (discard un-homogenised pellet).
 2. Protein assay – Take small volume-12.5 µl (dilute by half with dH₂O)
 3. Make up supernatant in 2 x SDS Sample Buffer (SB) (2-mecaptoethanol in SB).
NOTE: Add same volume of SB as HB.
4. Mix well (Vortex)
5. Boil at 95-100 °C for 5 mins
6. Load 12.5-20 µl of sample into gel (see Western Blot protocol)

B.7.5 Western Blot protocol

Bio-Rad Mini Protean 3 Cell and Bio-Rad PowerPac Basic used

Cast the gels;

1. Ensure plates are clean (avoid contamination and background) – clean with 70% ethanol and blue roll - Check have complementary plates (front and back).
2. Clip glass plates into the pouring stand – ensure plates are level and placed firmly on-top of the gaskets - to prevent leakage.



3. Make resolving gel (8%) – see other protocols for other % gels – NOTE: 6% is sufficient for PER protein BUT 8% working better, smaller proteins will need a higher % gel (see other protocol).

| 2(1)x 0.75ml gel (Resolving) | 6% | 8% |
|-------------------------------------|------------|-----------|
| dH ₂ O (ml) | 5.3 (2.65) | 4.6 (2.3) |
| 1.5M Tris(HCL) pH8.8 (ml) | 2.6 (1.3) | 2.6 (1.3) |
| 10% SDS (μl) | 100 (50) | 100 (50) |
| 30% Acrylamide Mix (ml) | 2 (1) | 2.6 (1.3) |
| 10% APS (μl) | 50 (25) | 50 (25) |
| TEMED (μl) (add last) | 10 (5) | 10 (5) |

Note: Ammonium persulphate (APS) and TEMED are polymerising agents – therefore add last and just prior to casting.

4. Mix well and cast the gel – bring up to just under green bar and overlay with dH₂O (get rid of bubbles and level top of gel). Casting can either be done by simply pouring gel or via pipet.
5. Leave to set for ca. **45mins**.
6. Whilst setting – make the stacking gel (5%) – wait to add APS and TEMED until Resolving gel has set. (may want to make excess in case of leakage).

| Stacking Gel (5%) | 2(1) x 0.75ml |
|---------------------------|----------------------|
| dH ₂ O (ml) | 2.4 (1.2) |
| 0.5M Tris(HCL) pH6.8 (ml) | 1 (0.5) |
| 30% Acrylamide Mix (ml) | 0.52 (0.26) |
| 10% SDS (μl) | 80 (40) |
| 10% APS (μl) | 40 (20) |
| TEMED (μl) (add last) | 10 (5) |

7. When set, remove water from resolving gel – cover pouring stand in blue roll and invert to blot away water.
8. Pipette stacking gel into casting apparatus – fill to the top of the plate.
9. Add comb immediately (and gently) to ensure there are no air bubbles.
10. Allow to set for ca. **15 mins**.
11. When set, gently and steadily remove the comb and fill wells with running buffer (pipet).

NOTE: Plates can be stored overnight if can't be used immediately – wrap in blue roll and soak with water to ensure gels don't dry out – Leave comb in. Wrap with foil and store in the fridge.

Loading the Gel;

1. Moisten seal on the gasket of loading tank.
2. Load gels into place – bigger plate facing outwards. Close clips to secure.
3. Place cassette in electrophoresis tank and add running buffer (1x) to the tank (can be retained and re-used past electrophoresis)
4. Load **20μl (10 well) or 12.5μl (15 well)** of sample in each well – note down order of samples, empty wells should be filled with sample buffer. Gel loading tips and bridges can be used to help.
5. Load **2μl (10 well) or 1μl (15 well)** of protein ladder (PageRuler Plus) to one well (edge will help with orientation).
6. Secure lid on – ensure correct orientation.
7. Run gel for **1.25 h** at **160 V** – 55 KDa band on ladder nearing bottom of the gel

Transfer (wet);

SET-UP: Transfer Buffer (1x) should be stored in the fridge (can be retained and re-used). Thick filter paper and transfer membranes should be cut to size (6.5x8.5 cm) and marked in bottom right corner (in pencil) for identification. Transfer tank insert should be filled with water and frozen prior to transfer.

NOTE: Transfer cassettes and foam pads can be borrowed from level 3

1. **SOAK transfer membrane in 100% methanol for 15 s then leave to equilibrate in TB for 5 mins**
2. Pour cold transfer buffer into a large Tupperware box.
3. Place one cassette into the transfer buffer (clear side down).

Appendix B:

4. Construct the Transfer “sandwich” – Foam Pad – Filter paper – Transfer membrane – Gel – Filter paper – Foam.

NOTE: Remove front glass plate and place gel face down onto membrane to ensure correct direction of transfer

5. Smooth out “sandwich” with pipette tip, close cassette and secure
6. Load cassette into transfer tank – black side facing black edge of transfer tank (can work with one or 2 cassettes).
7. Add ice tray insert, and fill tank to top with transfer buffer.
8. Secure lid in place - ensure correct orientation.
9. Blot for **1.5 h at 60 V**.
10. When finished transferring – unpack “sandwich”, gel can be discarded into SDS gel bins, membrane is retained for staining (can mark position of ladder in membrane at this stage if you wish).

Staining;

1. Incubate blots in blocking buffer (fridge - see protocols) on shaker for **30 mins – 1 h** (at RT).
2. Remove blocking buffer – can be retained and re-used.
3. Add appropriate **primary antibody** to blots– made up to correct concentration in blocking buffer (both primaries can be added to same BB).

| Antibody | Concentration | Final Volume (BB) (ml) | Volume of Ab (μl) |
|--------------------------|---------------|------------------------|-------------------|
| Rabbit anti-PER | 1:15000 | 10 | 66.6 |
| Mouse anti-HSP70 | 1:5000 | 10 | 2 |
| Goat anti-Rabbit (800cw) | 1:20000 | 10 | 0.5 |
| Goat anti-Mouse (680cw) | 1:20000 | 10 | 0.5 |

4. Incubate **OVERNIGHT** in **COLD ROOM (4°C)** on a shaker – **retain Ab and re-use (@ -20°C in BSA)**

- **NEXT DAY** – NOTE: all washes done on shaker at RT but warm PBS to 37°C -

5. Wash blots in **0.5% tween-PBS (37°C)** for **5 mins**.
6. **REPEAT 1 TIMES** (2 washes total) – changing solution and rinsing with water between each wash.
7. Incubate with appropriate **secondary antibody** – **wrap containers in foil** if using fluoro secondary Ab (which we are).
8. Stain for **1 h** at **RT** on shaker – **retain Ab and re-use**.
9. Wash blots in **0.5% tween-PBS (37°C)** for **5 mins**.
10. **REPEAT 2 TIMES** (3 washes total) – changing solution and rinsing with water between each wash.
11. After final wash add either BB or dH₂O to blots, wrap in foil and store in fridge until imaging.

Image blots with LiCor Odyssey Scanner with Image Studio 5.2 software

B.8 Genotyping

Genetic isoforms of *timeless* and *jetlag* have been shown to impact of circadian and light entrainment behaviour therefore flies genomic DNA was sequenced to identify the *tim* and *jet* isoforms present.

Genomic DNA was extracted (B.8.1) and amplified via PCR (B.8.2) using the primers listed in **S.Table B.8**. Following PCR, products were run on a gel to assess quality and fidelity of amplification (B.8.3), both primer pairs used for PCR show a single defined band of the correct size for the amplicon. PCR products were purified (B.8.4) and then sent for sequencing by Eurofin Genomics (TubeSeq Service) using the primers listed in **S.Table B. 9**.

Sequencing results were compared to the *Drosophila* genome using Standard Nucleotide BLAST (NIH) to identify isoform of *timeless* and *jetlag* present.

S.Table B. 8 Primers pairs used for PCR

| Target Gene Source | Direction | Sequence |
|--------------------------|-----------|-------------------------------|
| <i>tim</i> Invitrogen | f | 5'-TGGCTGGGGATTGAAAATAA-3' |
| | r | 5'- TTACAGATACCGCGCAAATG - 3' |
| <i>jet</i> Invitrogen | f | 5`-TGGGATAGAAGTCGTTCAAGT-3` |
| | r | 5'-TAGGCAGCTCCACAATCA-3' |

S.Table B. 9 Primer pairs used for sequencing

| Target Gene Source | Direction | Sequence |
|--------------------------|-----------|----------------------------|
| <i>tim</i> Invitrogen | f | 5'-TAGGTATCGCCCTCCAAG-3' |
| | r | 5'-TAGGCAGCTCCACAATCA-3' |
| <i>jet</i> Invitrogen | f | 5'-AGCCGATCATAGTGGAGTGC-3' |
| | r | 5'-AAGGCACGCACAGGTTTACT-3' |

Appendix B:

B.8.1 DNA Extraction Protocol

DNA Extract All Lysis Reagents – Applied Biosystems (4403319)

Lysis;

1. Thoroughly mix Lysis Solution (4°C) – Careful to avoid bubbles
2. Add 50 µl of Lysis Solution to **5 flies**
3. Homogenise with pestle for around 10s (just to break up slightly)
4. Add another 50 µl of Lysis Solution and vortex

Incubation;

1. Incubate **@98°C for 3 mins**
2. Spin for **30s @ 8k**
3. Remove Supernatant

Stabilisation;

1. Thoroughly mix Stabilisation Solution (4°C) – Careful to avoid bubbles
2. Add 100 µl of Stabilisation Solution and vortex

Quality Check;

1. Nanodrop extract – **260/280= ~1.8**
2. Aliquot Extracts and store **@-20°C**

(NB – Blank for Nanodrop = 5 µl Lysis Buffer + 5 µl Stabilisation Buffer)

Load **1 µl** of Extract in each PCR reaction (see **A.1.1**). **10-250 ng per 50 µl Reaction**

B.8.2 PCR protocol

Phusion Hot Start II High Fidelity PCR mastermix - ThermoFisher Scientific (F565S)

Sample Preparation;

1. Dilute samples 1:10 – 1 μ l sample to 9 μ l water
2. Make working solutions of primers (10 μ M) – 10 μ l of 100 μ M Stock in 90 μ l water

N.B. – New primers – warm @37°C for 5 mins and spin briefly before use

3. Make up MasterMix for reactions (all components except template) – all primers used at 0.5 μ M in all reactions.
4. Pipette 49 μ l of MasterMix to each well/tube to undergo a reaction– add 1 μ l of sample to corresponding well
5. Pipette 50 μ l of Black to corresponding well/tube
6. Seal with round caps, vortex and spin.

PCR Cycling Protocol – DNA Engine Tetrad 2 (Bio-RAD)

1. Initial Denaturation – 98°C 30s
2. Cycling steps – x34
 - a. Denaturation - 98°C 20s
 - b. Annealing - 60°C 15s
 - c. Extension - 72°C 30s
3. Final Extension - 72°C 60s
4. Hold/Incubate - 4°C 10min

B.8.3 Gel Electrophoresis Protocol

Make and Cast Gel (ca. 30min before needed);

1. Set up cast – secure edges with masking tape and place comb in desired place
2. Make 1.5% gel – Dissolve 2.25 g Agarose in 150 ml of 1X TAE (50X stock – 1X = 10 ml 50X in 450 ml water)
3. Boil in microwave to all agarose dissolved – don't let boil over (2-5 mins)
4. Let cool for 5 mins
5. Add 15 μ l of 6X gel red – allows visualisation of DNA
6. Cast gel and leave to set (20-30mins)

Sample Preparation;

1. Combine 10 μ l of each sample with 2 μ l of loading dye (total volume 12 μ l)
2. Combine 2 μ l of 100bp ladder with 2 μ l of loading dye and 8 μ l water (total volume 12 μ l)
3. Vortex and spin

Running gel;

1. When set – remove masking tape and place in electrophoresis tank
2. Fill tank with TAE (running buffer)
3. Remove comb
4. Load 12 μ l of sample in each well (as well as ladder)
5. Run @100 v for 1 h (check regularly)
6. Image gel

B.8.4 PCR Product Purification Protocol

QIAquick PCR Purification kit – Qiagen (28104)

Set up kit as per instructions – i.e. add ethanol to PE buffer and pH indicator to PB buffer

1. Add **5** volumes of Buffer PB to **1** volume of PCR product and mix (vortex), should be yellow (same as PB) – i.e. if use 50 µl of product add 250 of PB.
2. Place MinElute column in 2 ml collection tube (in kit) – **apply all of sample + PB buffer mix** to column and centrifuge **@13,000 RPM for 1min**
3. Discard flow-through and place column back in same tube
4. Add **750 µl** of Buffer PE to column and centrifuge **@13,000 RPM for 1 min**
5. Discard flow-through and place column back in same tube
6. Re-spin **@13,000 RPM for 1 min** to remove residual Buffer PE
7. Move Column to clean 1.5 ml microcentrifuge tube
8. Add **10 µl** of Buffer EB (10 mM Tris-Cl, pH8.5) to the **CENTRE** of the MinElute membrane
9. Let column stand for **1 min**
10. Centrifuge **@13,000 RPM for 1 min** to elute DNA
 - Nanodrop to obtain purified DNA conc – Dilute accordingly ready for sequencing

N.B. If the colour changes away from yellow in 1. (orange or violet) add 10µl of 1 M Sodium acetate (pH 5.2) and mix – should turn yellow.

Appendix C: Magnetoreception and other physiological functions of *Drosophila* CRYPTOCHROME

C.1 Introduction

An additional aim of this project was to further investigate CRYPTOCHROME (CRY)-mediated effects of electromagnetic fields (EMF) on *D.melanogaster* behaviour, of which there are several examples in the literature (Gegear *et al.*, 2008; Yoshii, Ahmad and Helfrich-Förster, 2009; Fedele *et al.*, 2014b). The data presented in this appendix represents the work conducted to date towards this aim, albeit preliminary in most cases.

C.1.1 Magnetoreception: A New Function of CRYPTOCHROME

C.1.1.1 Geomagnetic fields

The Earth's rotation and convective heat transfer from the inner core generates movement of the viscous molten metallic (iron) liquid that makes up the Earth's outer core (Gould, 2010). These convection currents result in a flow of electrons which generates a magnetic field felt at the Earth's surface (Gould, 2010).

Geomagnetic fields have long been understood to influence navigation, migration and homing behaviours in many organisms across a range of taxa (Painter *et al.*, 2013). The precise mechanism by which a magnetic field is detected and transduced to influence behaviour has been an area of extreme interest across many scientific disciplines (Gegear *et al.*, 2008). Since 2008, developments in structural biology, biophysics, spin chemistry and genetic studies in model organisms have allowed an in-depth analysis into the previously elusive molecular basis of magnetoreception (Dodson, Hore and Wallace, 2013).

C.1.1.2 Mechanisms for Biological Magnetoreception

Three main models exist for magnetoreception (Fedele *et al.*, 2014b):

1. **Magnetic Induction**; utilised by marine creatures i.e. migrating lobsters, and is only possible due to the high conductivity of salt water (Gould, 2010).
2. **The Magnetite Hypothesis**; sensing of the earth's magnetic field via the formation of superparamagnetic crystals i.e Magnetite ($\text{FeO} \bullet \text{Fe}_2\text{O}_3$) (Gould, 2010), which have been found some birds and salmonid fish (Fedele *et al.*, 2014a).

3. **The Radical Pair Mechanism (RPM)**; relies on quantum properties of specialised photoreceptors to create an iron-free chemical compass (Fedele *et al.*, 2014b; Ritz *et al.*, 2010; Ritz, Adem and Schulten, 2000; Rodgers and Hore, 2009).

The structural properties of cryptochromes identify the family as potential candidates for magnetoreception via the RPM mechanism. Photo-excitation of CRY's associated flavin cofactor (FAD) can result in the generation of a spin-correlated radical pair (SCRPs) between the excited FAD and the final tryptophan (Trp) residue in a conserved Trp-triad which act as 'stepping stones' in an electron transport chain between FAD and the protein surface (Henbest *et al.*, 2004; Maeda *et al.*, 2012; Byrdin *et al.*, 2010). Ordinarily, a SCRPs has a short lifetime and therefore cannot be influenced by a weak magnetic field e.g. the Earth's geomagnetic field (Ritz *et al.*, 2010). A combination of the distance between FAD and the distal Trp and the successive decrease in redox potentials created within the trp-triad establishes a SCRPs with an extended lifetime which is attributed to the increased difficulty for the reverse flow of electrons (Aubert *et al.*, 2000). The long-lived SCRPs potentially allows detection of geomagnetic fields thus generating of the biologically relevant signalling state.

C.1.1.3 Magnetic Field Effects on Circadian Rhythms

EMFs have been discussed as possible Zeitgebers since 1960 (Yoshii, Ahmad and Helfrich-Förster, 2009), however the means by which circadian clocks detect magnetic fields remained elusive, until CRY's potential to partake in the RPM was revealed (Rodgers, 2009; Rodgers and Hore, 2009). CRY-mediated magnetoreception is known to be blue-light dependent (Gegear *et al.*, 2008; Yoshii, Ahmad and Helfrich-Förster, 2009; Fedele *et al.*, 2014b), suggesting that CRY involvement centres on its action as a blue-light photoreceptor.

(Gegear *et al.*, 2008) used a simple choice paradigm to show that wild-type flies, which show naïve avoidance of an EMF, could associate an EMF with a sugar reward. Both this trained preference and naive avoidance was only present in full spectrum or short-wavelength light i.e. blue-light. Furthermore, *cry* null genotypes displayed decreased avoidance and trained preference, thus suggesting a role for CRY in magnetoreception (Gegear *et al.*, 2008). Locomotor activity of *Drosophila* assayed in the presence of light and an EMF showed that an EMF resulted in the lengthening of free-running rhythms in 40% wild-type flies (Yoshii, Ahmad and Helfrich-Förster, 2009). EMF effects on locomotion were similarly blue-light dependent and CRY-mediated as no period lengthening was seen in *cry* null or *cry^b* genotypes, and an overexpression of CRY lead to arrhythmic behaviour in an EMF (Yoshii, Ahmad and Helfrich-Förster, 2009).

A third assay to investigate the effect of magnetic fields on *Drosophila* behaviour involves the flies' innate negative geotactic behaviour, i.e. they climb away from gravity (Gegeer *et al.*, 2010). Fedele *et al.* (2014b) discuss how the EMF effect on behavioural conditioning are not robust enough to provide convincing evidence (Gegeer *et al.*, 2008), and some locomotor activity experiments yield highly variable results (Yoshii, Ahmad and Helfrich-Förster, 2009), thus indicating a need to a more robust and reliable assay. CRY has been shown to impact on climbing behaviour (Rakshit and Giebultowicz, 2013) and assaying negative geotaxis was shown to be a reliable method of investigating the effect of EMF on *Drosophila* behaviour (Fedele *et al.*, 2014b).

EMF disrupts negative geotaxis with reduced climbing of wild-type flies observed in the presence of an EMF (Fedele *et al.*, 2014b). Wild-type flies only showed a reduction in climbing in the presence of blue-light, corroborating previous observations. CRY mutants show reduced climbing in the absence of an EMF (Fedele *et al.*, 2014b), which is likely due to the aforementioned role of CRY in climbing behaviour (Rakshit and Giebultowicz, 2013); however climbing was not further reduced when an EMF was present (Fedele *et al.*, 2014b). CRY-mediated effects of EMFs on negative geotaxis was mapped to the three CRY positive LN_s and the 5th s-LN_v (Fedele *et al.*, 2014b), using *Mai179-Gal4* (Grima *et al.*, 2004), which is the same subset of cells where CRY expression is required for behavioural re-entrainment to a shifted Light:Dark (LD) cycle (1.2.5.1.3) (Yoshii *et al.*, 2015). This link to CRY's circadian function was supported by the deletion of CRY's CTT also reducing the EMF-dependent climbing phenotype (Fedele *et al.*, 2014b). Blue-light activation of CRY triggers a conformational change resulting in the rearrangement of the CTT allowing CRY to bind to TIMELESS (TIM) and target TIM for degradation (1.2.5.1.1) (Vaidya *et al.*, 2013; Ceriani *et al.*, 1999; Peschel *et al.*, 2009). Mutating the final Trp in the Trp-triad retained responsiveness to EMF suggesting the Trp-triad is not required for CRY-mediated magnetoreception; arguing against the notion that CRY magneto-sensitivity is mediated via the RPM.

C.1.1.4 Possible mechanisms for CRY-mediated Magnetoreception

Genetic analysis coupled with CRY biochemistry, suggest that downstream signalling following magnetoreception involves interaction with downstream targets, the identity of which remain elusive (Fedele *et al.*, 2014a). Therefore the exact mechanism of CRY signalling following the application of an EMF is unknown; however there are two main possibilities:

1. **Long-term interactions;** as seen in the CRY-mediated light entrainment of circadian clocks (Emery *et al.*, 1998; Stanewsky *et al.*, 1998; Dubruille and Emery, 2008), the result of which is protein ubiquitination and degradation (1.2.5.1).

Appendix C:

- 2. Protein-protein interactions or binding partner modulation;** it is conceivable that CRY forms part of a larger protein complex, and such CRY activation could modulate the activity of the complex with the downstream effect dependent on other constituent proteins. A theoretical putative magnetic receptor has been identified following genome-wide sequencing (Qin *et al.*, 2016). MagR (*Drosophila* CG8198) is predicted to partake in a multimeric magnetosensing rod-like protein complex, where CRY acts as an 'antenna' like molecule passing energy to MagR (Qin *et al.*, 2016). Although this complex has been validated using cellular, biochemical and biophysical techniques, it still remains theoretical and there is no current evidence for such a complex forming *in vivo*.

Many questions still need to be answered regarding the downstream signalling of CRY in response to an EMF e.g. is CRY the actual magnetoreceptor or an essential component of a larger receptor complex (Gegeer *et al.*, 2008; Qin *et al.*, 2016); to what extent does the nature of the biological environment influence the CRY-mediated magnetoreception (Evans *et al.*, 2013); does CRY bind its traditional circadian partners in response to an EMF or is there a new candidate for downstream signalling.

C.1.2 Wide-reaching Influences of CRY

CRY plays a crucial role as a circadian photoreceptor (Chapters 1, 3 and 4) and has been identified as a component in magnetoreception. In addition to these two functions, CRY has also been implicated in some other signalling pathways which share a common theme of light-activated CRY working at the membrane to modulate neuronal excitability.

Membrane excitability is a key contributor to the maintenance of a circadian rhythms and membrane properties are themselves circadian regulated (Fogle *et al.*, 2011; Fogle *et al.*, 2015). The Pigment Dispersing Factor (PDF) expressing ventrolateral neurones (LN_vs) can be subdivided into two clusters; the l-LN_vs are required for light-mediated arousal and increase their spontaneous firing frequency (SFF) in response to blue-light; and s-LN_vs are critical for circadian function (Renn *et al.*, 1999; Lear, Zhang and Allada, 2009; Fogle *et al.*, 2011). SFF peaks during the early day and then steadily decreases until dusk, with frequency recovering overnight (Sheeba *et al.*, 2008). A bright light pulse can induce a SFF increase of 20-200% in l-LN_vs, a response that is lost in *cry* null mutants and severely reduced in the presence of potassium channel blockers (Fogle *et al.*, 2011). Ectopic expression of CRY in clock-less olfactory neurones conferred light-evoked increases in SFF indicating that CRY's role in membrane excitability is independent of its clock function i.e. it doesn't require TIM (Fogle *et al.*, 2011). Furthermore, this membrane coupling is

readily reversible, whereas TIM binding and ubiquitination is not, therefore compounding the evidence for two distinct mechanisms (Fogle *et al.*, 2011).

Sequence and structural data suggests that the cytosolic voltage-gated potassium beta subunit (Kv β) is the site for light-activated CRY coupling to the membrane (Fogle *et al.*, 2015). Kv β channels act as redox sensors due to a conserved aldo-keto reductase domain (Barski, Tipparaju and Bhatnagar, 2008). In *Drosophila* there is one Kv β gene called HYPERKINETIC (Hk) which acts as a functional *in vivo* redox sensor translating redox biochemical signals into electrical potential changes at the membrane (Fogle *et al.*, 2015; Baik *et al.*, 2017; Baik *et al.*, 2018). Removal of Hk, either with a null mutation or via *RNAi* knockdown, attenuated light-evoked CRY mediated SFF responses with *Hk* null flies indistinguishable from *cry* null; however there is no evidence to suggest a direct interaction between CRY and Hk (Fogle *et al.*, 2015). Light is thought to alter the redox state of CRY which is then detected by Hk with the subsequent redox coupling likely mediated by intermediate species i.e. oxygen (Fogle *et al.*, 2015). Hk co-assembles with *Drosophila* Ether-a-Go-Go (EAG) family and EAG-Related-Gene (ERG) family potassium channels which trigger membrane depolarisation, underlying the CRY mediated light-evoked response at membrane via Hk (Fogle *et al.*, 2015). CRY is also capable of sensing UV-A light, which evokes acute night-time arousal, if administered in light flashes, or positive phototaxis, movement towards light, at low-intensities (Baik *et al.*, 2017; Baik *et al.*, 2018; Baik *et al.*, 2019). UV-mediated behavioural response are lost in the absence of CRY and Hk, suggesting CRY may transduce UV stimulation via the aforementioned mechanism of potassium channel modulation (Baik *et al.*, 2017; Baik *et al.*, 2018; Baik *et al.*, 2019).

Furthermore, it has been shown that this blue-light regulation of neuronal firing mediated by CRY can be modulated by EMF (Giachello *et al.*, 2016). A static 100 mT EMF coupled with blue-light resulted in a doubling in depolarisation compared to EMF with no CRY expression. This relatively high field strength thought to saturate typical radical pair interactions without resulting in heating of a biological system (Giachello *et al.*, 2016). This result required CRY's CTT, analogous to previous experiments involving magnetoreception (Fedele *et al.*, 2014b), and highlights a possible mechanism of action whereby EMFs potentiate CRY's effect at the cell membrane.

Clk^{irk} and *cyc⁰¹* flies, which lack the key transcription factors CLOCK (CLK) and CYCLE (CYC), which constitute the positive arm of the molecular clockwork (1.2.3), display a nocturnal phenotype in an LD cycle. *Clk^{irk}* flies have elevated CRY expression in the I-LN_vs as well as increased levels of tyrosine hydroxylase (TH), an enzyme involved in dopamine-synthesis, as both CRY and TH expression is CLK/CYC regulated (Kumar, Chen and Sehgal, 2012). This provides a possible mechanism for nocturnality whereby excess CRY in I-LN_vs leads to hyperexcitation, resulting in

Appendix C:

increased night-time l-LN_v firing rate and a switch to nocturnal behaviour (Sheeba *et al.*, 2008; Kumar, Chen and Sehgal, 2012). Furthermore, it has been proposed that CRY only promotes nocturnality in flies with elevated dopamine levels, with dopamine acting as a trigger for CRY activation (Kumar, Chen and Sehgal, 2012). There is an existing link between dopamine and nocturnality in humans with conditions such as Sundown Syndrome and Nocturnal Delirium being treated with risperidone, an antipsychotic which acts to reduce dopamine signalling (Falsetti, 2000). How CRY influences l-LN_v firing rate in the context of nocturnality is unknown; however there are clear similarities between CRY/HK mediated SFF changes, possibly indicating a conserved mechanism. A role for dopaminergic signalling in CRY-activation highlights a possible mechanism underlying CRY activity which is distinct from light.

It has been reported that CRY acts alongside potassium channels and Hk to maintain passive membrane properties in clock and non-clock tissues, independent of light (Agrawal *et al.*, 2017). As regulation in such cases is time- and light-independent, it was postulated that the redox state of the tissue is the likely driving force behind CRY activation (Agrawal *et al.*, 2017). A change in the redox environment in constant darkness is sufficient to drive CRY's FAD co-factor to its active signalling state (Vaidya *et al.*, 2013). Therefore, it is possible that CRY could function as a redox sensor within a cell, whereby a change in redox potential leads to CRY-activation as opposed to light.

It is clear that CRY is involved in many physiological and sensory processes with diverse underlying mechanisms. Differentiating these mechanisms and defining CRY's role in each is still ongoing, however it allows us to postulate that CRY activity could be tissue specific or that CRY could perform multiple roles within the same cell.

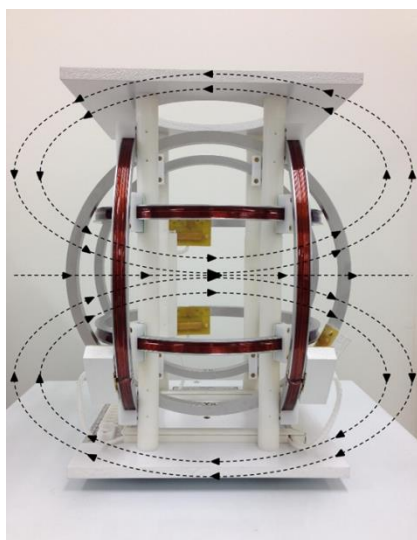
C.1.3 Aims

- **Recapitulate previously published results regarding the role of CRY in mediating EMF effects of *Drosophila* behaviour.**
- **Investigate the possible mechanisms for CRY-mediated magnetoreception i.e. via canonical circadian photoreception or action at the membrane.**

C.2 Methods

C.2.1 Negative Geotaxis

An adaptation of the experimental design described by (Fedele *et al.*, 2014b) was used to test the effect of EMFs on *Drosophila* behaviour. The apparatus consisted of six bifilar wound (50 windings each) Helmholtz coils (Kirschvink, 1992) (**S.Figure C. 1**). The six coils were aligned in pairs with the horizontal pair generating an electromagnetic field to disturb negative geotaxis i.e. perpendicular to the Earth's magnetic field (as shown in **S.Figure C. 1**), and the others acting to neutralise the Earth's geomagnetic field, as well as enabling complete uniform control of the EMF experienced within the coil (**S.Figure C. 1**). The bifilar winding i.e. windings in both directions around the coil, allowed us to produce both an EMF and a Sham exposure. Current passing through the coils in the same direction generated a constant static EMF. Current flowing in opposing directions generated no EMF but the coil still generated an equal amount heat, this was defined as the Sham condition. To minimise the external electromagnetic effect, all experiments took place in an environmentally controlled room with white-light illumination at constant 23 °C.



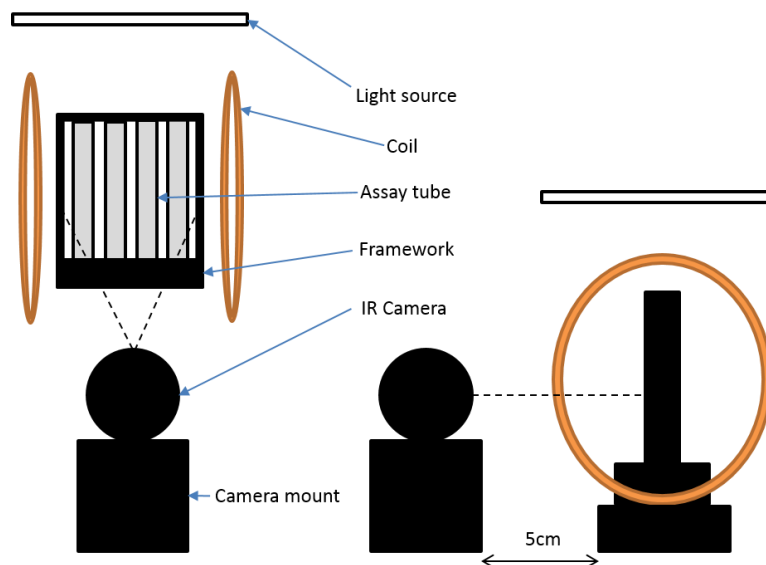
S.Figure C. 1 Apparatus for Negative Geotaxis Assay.

6 Helmholtz coils, arranged in three pairs generate an EMF in three directions. Field lines show EMF generated perpendicular to the Earth's magnetic field used for negative geotaxis assay.

Flies ~1 week old were anaesthetised and separated by genotype and gender into cohorts of 10 and placed into 15 cm long glass test tubes. Flies were tapped down to the bottom of the tube and left to climb. After 8 s those flies that climbed 12 cm were designated 'climbers' (Fedele *et al.*, 2014b). A custom made framework was used to ensure that the same force was applied over multiple repeats and allowed 4 cohorts to be assayed simultaneously (Fedele *et al.*, 2014b). Each cohort was tested 10 times, with a 30 s rest period between each trial and a 15 min rest following the first 5 trials (Fedele *et al.*, 2014b). Three biological replicates were conducted for each gender/genotype combination. Trials were filmed on an infrared security camera (Coomatec, 3.6mm DVRCam) so footage could be paused following 8 s to increase accuracy (**S.Figure C. 2**).

Appendix C:

Negative geotaxis was assayed under white-light illumination at 23°C with either a constant static 500 μT (Tesla) EMF or Sham field in all cases. Field strength was tested regularly with a Gauss meter.



S.Figure C. 2 Negative Geotaxis Assay Set-up.

Experimental set-up front view (left) and side view (right) showing 1 pair of Helmholtz coils. 4x 15 cm test tubes are encased within a custom built framework, which allows simultaneous tapping with equal force. Climbing is recorded with an infrared (IR) camera.

Videos were analysed using VLC media player, 8 s post flies being tapped down the video was paused and flies on or above 12 cm (denoted by a defined line on the apparatus) were counted. This was then repeated for all trials. Data for 10 trials were averaged for each cohort to account for technical variation. Further averages were taken across the three biological replicates to account for inherent biological variability. Percentage climbing was displayed using bar charts where error bars denote the SEM, generated using GraphPad Prism 7.05. SPSS was used to conduct analysis of variance (ANOVA) and post-hoc tests for pairwise comparisons. $p^{****} < 0.0001$; $0.0001 < p^{***} < 0.001$; $0.001 < p^{**} < 0.01$ and $0.01 < p^* < 0.05$.

C.2.2 DAM Behavioural Assay

Drosophila locomotor behaviour was assayed as described in 2.2.1.1. When assaying locomotor behaviour in the presence of an EMF, environmentally controlled rooms were used to generate a 12hL:12hD (7c/wk) white-light LD cycle with behavioural monitors (DAMSystem; TriKinetics, Waltham, MA) placed within the Helmholtz coil described in C.2.1. Flies were exposed to either a Sham or constant static EMF of 1,000 μT for 12 h each day (initial experiments using a 500 μT EMF yielded no effect). EMF/Sham was turned on half-way through the dark phase and persisted to

half-way through the light phase (relative midnight to midday) to coincide with high levels of CRY (Koh, Zheng and Sehgal, 2006; Peschel, Veleri and Stanewsky, 2006; Peschel *et al.*, 2009). During all assays a monitor was run alongside the EMF/Sham condition which experiences the same Light:Dark cycle but is not in the Helmholtz coil, termed Control.

C.2.2.1 Qualitative and Qualitative Analysis

Analysis of behavioural data was conducted as described in 2.2.1.2 and 2.2.1.3. In addition, average activity counts in the light and dark phases were collected for individual flies using ClockLab software (ActiMetrics; Wilmette, IL, USA). A ratio between light and dark activity counts, termed LD ratio, was calculated by dividing light counts by dark counts. An LD ratio > 1 indicated more activity happened in the light phase i.e. diurnal, and < 1 indicated more activity happened in the dark phase i.e. nocturnal. GraphPad Prism 7.05 was used to generate all graphs and conduct statistical analysis on LD ratio data. Analysis of variance (ANOVA) between genotypes or conditions were made with the non-parametric *Kruskal-Wallis test* with pairwise comparisons made using post hoc tests i.e. *Dunn's multiple comparison test* and *Mann-Whitney test* (test used is noted in figures). $p^{****} < 0.0001$; $0.0001 < p^{***} < 0.001$; $0.001 < p^{**} < 0.01$ and $0.01 < p^* < 0.05$.

C.3 Results

C.3.1 Effect of an electromagnetic field on negative geotaxis

Initial experiments aimed to optimise the right conditions and experimental set up to ensure our apparatus works effectively and yields results comparable to the published data (Fedele *et al.*, 2014b).

A difference between climbing behaviour was observed under a sham condition (no EMF) between flies of different genetic backgrounds and gender. Male flies climbed significantly better than females, and as such all the data presented in **S.Figure C. 3** represents male flies. The most evident difference in genetic background was present when comparing the climbing of red-eyed flies e.g. $w^{1118};cry^{01}/+$ (heterozygote controls described in 2.3.1) to white-eyed flies e.g. $y^1 per^{01} w^*$ (per^{01}) and $y^1 w^*;tim^{01}$ (tim^{01}). White-eyed flies did not climb as well as red-eyed flies under a sham condition (**S.Figure C.3, C**), which suggests there seems to be a real effect of eye pigmentation on climbing, even before other mutations are introduced. Flies carrying the *CyO* balancer chromosome have curly wings and did not climb as well as straight-winged flies, with increased variation amongst individuals (**S.Figure C. 3, A**). As *CyO* does not introduce any other abnormalities when tested in both DAM and TopCount assays (Chapters 3 and 4), it is possible that the lack of climbing seen could be as a result of curly wings reducing the space and thus physically hindering climbing ability. To confirm these observations an in-depth characterisation of genetic background on climbing behaviour would have to be conducted.

As a result of the observations discussed above, it is not possible to reliably compare the effect of sham and EMF treatments on climbing between the different genotypes tested. However the effect of an EMF can be compared to basal climbing ability i.e. under a sham condition, for each individual genotype tested. Wild-type flies ($cry^{01}/+$) displayed the published decrease in climbing when exposed to an EMF (Fedele *et al.*, 2014b). cry^{01} mutants show a decreased level of climbing under a sham condition compared to $cry^{01}/+$, which is further decreased on exposure to EMF (**S.Figure C. 3, A**), an observation not published in the current literature. This may indicate that CRY is not the only magnetoreceptor in *Drosophila* or a non-essential component of a complex that senses magnetic fields. *jet* loss-of-function mutants (jet^{set}) have white eyes, which may explain the very low percentage of flies climbing under sham conditions, but there was a significant increase in climbing when an EMF was applied (**S.Figure C. 3, A**). There was no effect of an EMF of flies heterozygous for jet^{set} (jet^{set}/CyO), but as previously discussed this may be as a result of the *CyO* (**S.Figure C. 3, A**); therefore showing the need to establish a robust control phenotype.

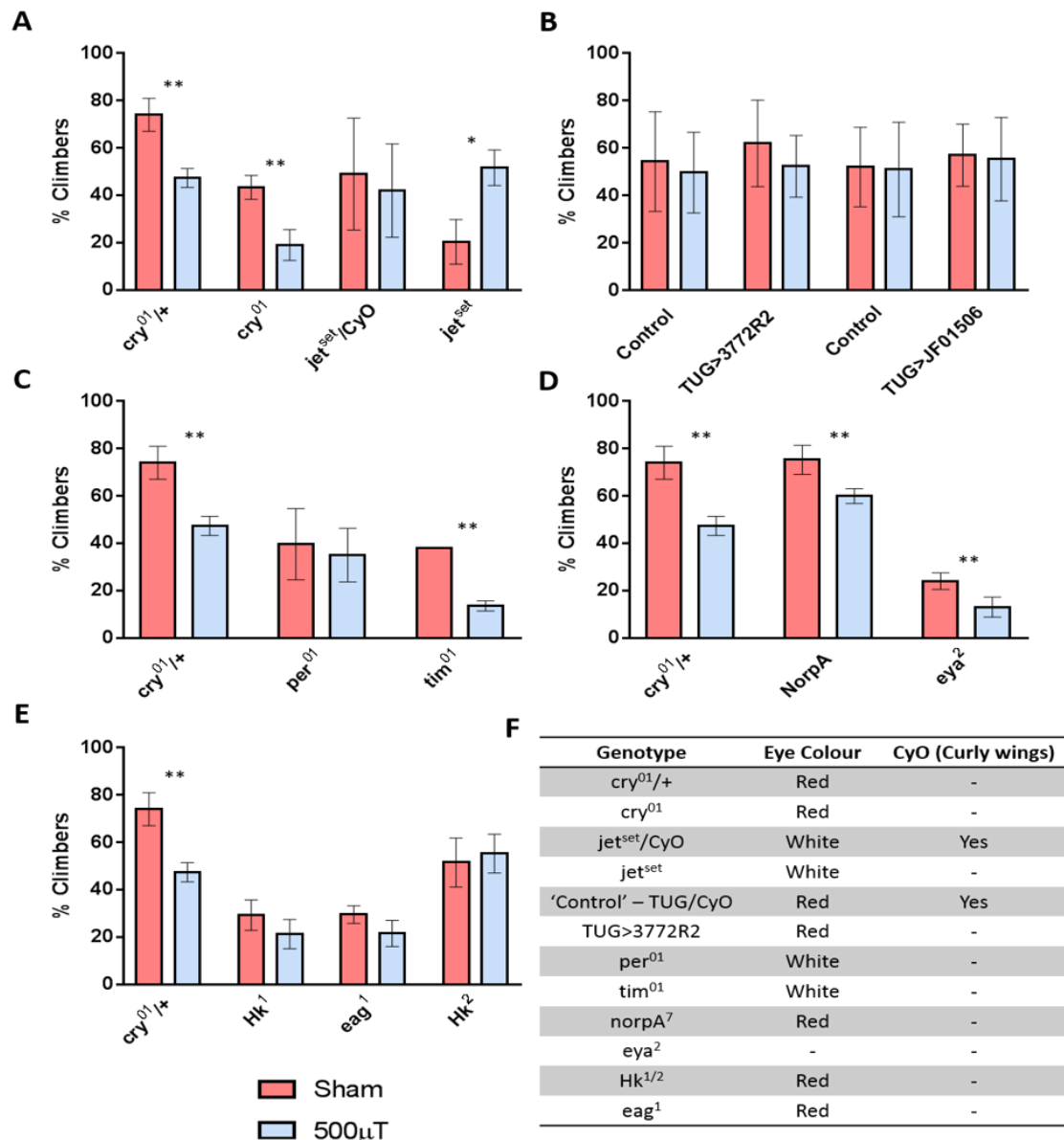
Pan-circadian knockdown of *cry* and *jet* using *tim(UAS)-Gal4 (TUG)* to drive expression of *ds-RNA* targeting *cry (TUG>3772R2)* and *jet (TUG>JF01506)* yielded results with no difference between sham and EMF conditions (**S.Figure C. 3, B**). There was also no difference between sham and EMF conditions for the isogenic control genotypes which does not agree with our wild-type/control data or published data. The large amount of variation calls into question the reliability of this data; as such, no conclusion can be drawn at present for the effect of *cry* and *jet* knockdown on magnetoreception.

In order to establish whether or not the EMF effect on negative geotaxis is via the circadian clockwork, two circadian mutants were assayed. Both *per⁰¹* and *tim⁰¹* mutants show decreased climbing under sham, but as discussed previously, this could be a result of white-eyed genetic background. When tested under an EMF *tim⁰¹* flies showed a significant decrease in climbing which was not seen with *per⁰¹* (**S.Figure C. 3, C**). No effect of an EMF could suggest that PER is involved in magnetoreception, thus removal of PER results in no effect of EMF. However, the high amount of variability suggests that this experiment needs to be repeated in order to confirm whether or not this effect is due to the lack of *per*. Decreased climbing in EMF compared to sham seen in *tim⁰¹* mutants mirrors what is seen with controls (*cry⁰¹/+*), suggesting TIM is not required for magnetoreception. In both cases a more appropriate controls for *per* and *tim* null mutants need to be assayed either in the same genetic background as the mutant or back-crossing these mutants onto a red-eyed wild-type background. This would hopefully eradicate the basal background variability.

Fedele *et al.* (2014b) reported that the absence of the compound eye decreased climbing under a sham condition with no further decrease seen upon exposure to an EMF. *eya²* (*eyes absent* - protein null in the eye but retain protein expression in the ocelli) decreased climbing under a sham condition compared to *cry⁰¹/+*, corroborating published data (**S.Figure C. 3, D**)(Fedele *et al.*, 2014b), suggesting the eyes themselves are necessary for climbing and orientation. Exposure to an EMF decreased climbing in *eya²* flies proportional to that seen in controls (**S.Figure C. 3, D**), suggesting the eyes do not play a role in magnetoreception. As this do did not agree with published data (Fedele *et al.*, 2014b), a second visual mutant was assayed that has no visual transduction pathway but retains an intact compound eyes (*no receptor potential A - norpA⁷*). *norpA⁷* mutants showed a high percentage of flies climbing in a sham field with a similar reduction in climbing in an EMF compared to *cry⁰¹/+* (**S.Figure C. 3, D**). This corroborates the findings with *eya²*, where the visual systems doesn't seem to be required for magnetoreception; however the presence of an intact compound eye (*norpA⁷*) allows wild-type levels of climbing under sham conditions.

Appendix C:

Changes in membrane excitability have been linked with CRY activity through a proposed interaction with the redox sensor Hk, a subunit of the voltage-gated Kv β potassium channel, whereby light-induced CRY activation increases spontaneous firing rate of LN_s (Fogle *et al.*, 2015; Fogle *et al.*, 2011). A recent study has shown that this CRY-dependent effect of neuronal excitability is potentiated under a 100 mT EMF (Giachello *et al.*, 2016), which could implicate hyperkinetic as a key modulator of CRY based magnetoreception. It is interesting to note that the strength of the EMF used is far higher than used in this project. Under 500 μ T EMF, two mutants for Hk (Hk^1 and Hk^2) as well as a mutant for Ether-a-go-go (eag^1) showed no reduction in climbing (**S.Figure C. 3, E**). This lack of an EMF-dependent effect on negative geotaxis indicates CRY/Hk regulation of membrane excitability as a possible pathway for magnetoreception.

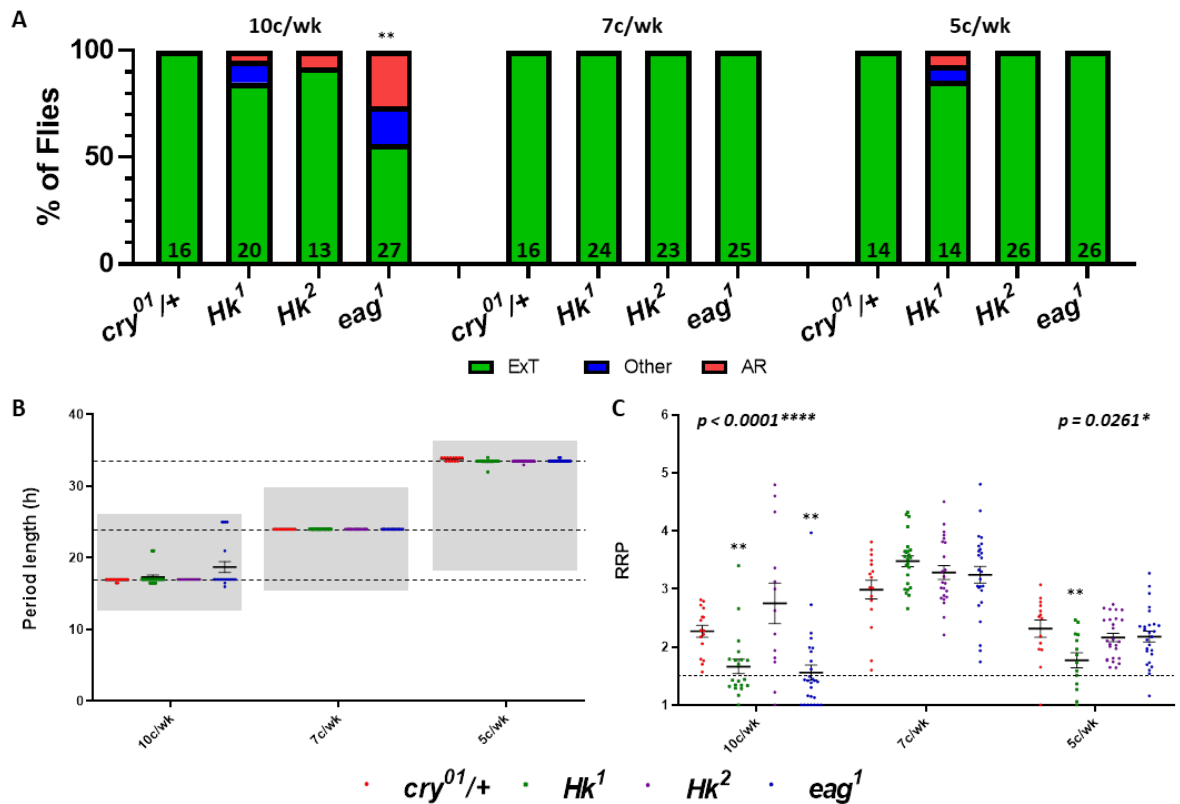


S. Figure C. 3 Negative geotaxis behaviour is affected both by genotype and magnetic fields.

A-E Percentage of male flies that climbed 12cm in 8 seconds during negative geotaxis assay averaged over 10 trails of climbing with 3 biological replicates under Sham (red) and 500µT (blue) EMF conditions. Error bars are SEM. *One-way ANOVA* comparing percentage climbers between sham and EMF conditions within each genotype. **A**) *cry* and *jet* mutants; *w¹¹¹⁸::cry⁰¹/+*, *w¹¹¹⁸::cry⁰¹*, *yw;jet^{set}/CyO* and *yw;jet^{set}*. **B**) Pan-circadian knockdown of *cry* and *jet*; *UAS-Dcr-2w*;tim(UAS)-Gal4/CyO* (**Control**), *UAS-Dcr-2w*;tim(UAS)-Gal4/UAS-ds-cry^{3772R2}* (**TUG>3772R2**), *UAS-Dcr-2w*;tim(UAS)-Gal4;+/TM3-Ser¹* (**Control**) and *UAS-Dcr-2w*;tim(UAS)-Gal4;UAS-ds-jet¹⁰¹⁵⁰⁶* (**TUG>JF01506**). **C**) Circadian Mutants; *y¹per⁰¹w** and *y¹w*;tim⁰¹*. **D**) Visual system mutants; *norpa⁷* and *eya²*. **E**) Membrane excitability mutants; *Hk¹*, *Hk²* and *eag¹*. **F**) Table showing eye colour and presence/absence of CyO in all genotypes assayed.

C.3.2 Mutations effecting possible CRY mediated membrane excitability have no effect on behavioural entrainment.

Hk¹, *Hk²* and *eag¹* flies showed no entrainment deficits when exposed to extreme equinox photocycles, except for *eag¹* flies in 10c/wk LD which showed an increase in arrhythmic and 'other' individuals compared to wild-type (*cry^{01/+}*) (**S.Figure C. 4, A**). The majority of 'other' *eag¹* individuals have a period length ~25 h, 1.5x the photocycles length in 10c/wk LD (see Chapter 2)(**S.Figure C. 4, B**), however even with this increase, no significant differences were seen when individual period lengths were compared across all genotypes or to control in 10c/wk. *Hk¹* and *Hk²* matched the expected entrained period length in 10c/wk, as do all three genotypes in 7 and 5c/wk (**S.Figure C. 4, B**). Average RRP values indicated all genotypes were strongly rhythmic in all conditions (RRP>1.5); however both *Hk¹* and *eag¹* flies had a relatively high proportion of weakly rhythmic individuals in 10c/wk (**S.Figure C. 4, C**). Although there were some impacts on rhythmicity under short LD cycles, the entrainment deficits were not comparable to that seen with *cry*, *jet* or visual mutants (Chapter 3); thus suggesting Hk and eag do not play a role in circadian behavioural entrainment.



S. Figure C. 4 Membrane Excitability mutants do not greatly reduce behavioural entrainment in white LD cycles.

A) Composite bar charts showing percentage of flies showing entrained (green), other (blue) or arrhythmic (red) locomotor behaviour (see methods) for adult male flies of genotype; *w¹¹¹⁸;;cry^{01/+}, HK¹, HK² and eag¹* over 10 days in 10 (top), 7 (middle) and 5c/wk (bottom) LD, with number of flies annotated in each bar. Fisher's exact test to compare distribution of entrained, 'other' and arrhythmic individuals for each genotype vs. *cry^{01/+}*. 'Other' includes flies that show a 1.5x harmonic period length with a greater RRP than the entrained period length. **B, C**) Individual male period lengths (**B**) and RRP (**C**) for in 10, 7, and 5c/wk (left to right) LD for *cry^{01/+}* (red), *HK¹* (green), *HK²* (purple) and *eag¹* (blue). **B**) Dashed lines represent entrained period length for 10 (bottom), 7 (middle) and 5c/wk (top). Error bars show mean period length \pm SEM. Grey shading indicates analysis parameters used for individual fly analysis in each LD cycle. Arrhythmic flies are not included in this analysis. **C**) Dashed line indicated an RRP value of 1.5. Arrhythmic flies are assigned an RRP of 1. Error bars show mean RRP \pm SEM. Results of Kruskal-Wallis test comparing RRP across all 4 genotypes in each conditions are presented in the figure. Pairwise comparisons of RRP for each genotype vs. *cry^{01/+}* were made using the Mann-Whitney test and annotated with asterisks.

C.3.3 An electromagnetic field increases nocturnality in *cyc*⁰¹ flies

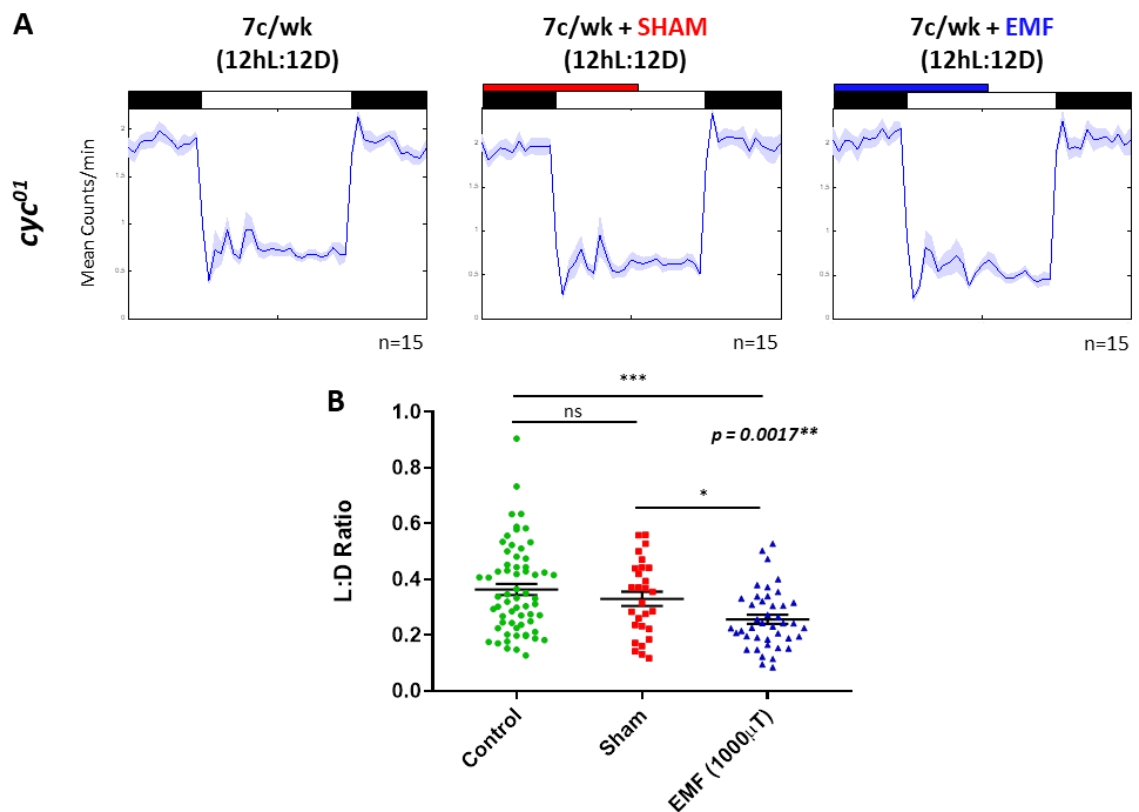
As negative geotaxis experiments yielded highly variable results, locomotor behaviour was assayed in the presence of overlapping 24 h cycles of Light:Dark (LD) and either a Sham field or a 1,000 μ T EMF advanced 6 h with respect to lights-on, as well as in a Control condition where flies experienced the same LD cycle but are not in the Helmholtz coil (2.2.1.1). *cyc*⁰¹ flies should have elevated CRY levels as CRY expression is regulated by CLK/CYC (C.1.2), therefore *cyc*⁰¹ flies were selected as a starting point for this approach to investigating electromagnetic fields as we hypothesise that we may see a greater impact on behaviour with increased CRY present (Kumar, Chen and Sehgal, 2012). Furthermore, *cyc*⁰¹ flies have a characteristic nocturnal phenotype where locomotor activity is elevated in the dark and suppressed in the light (**S.Figure C. 5, A**), providing a clear behavioural pattern for assaying the possible impacts of an EMF.

The waveform of *cyc*⁰¹ activity profiles did not change drastically between Control, Sham and EMF conditions (**S.Figure C. 5, A**). There did appear to be a difference, albeit subtle, between night-time activity day-time activity in the presence of an EMF compared to Control and Sham, suggestive of an increase in nocturnality (**S.Figure C. 5, A**). Calculation of LD ratio (C.2.2.1) confirmed that there was no difference in nocturnality between Control and Sham conditions (**S.Figure C. 5, B**), indicating that the heat, vibration etc. produced by the coil did not impact behaviour. There was a significant increase in night-time behaviour in the presence of an EMF compared to both Control and Sham conditions; with a greater difference seen compared to controls (**S.Figure C. 5, B**). The smaller difference seen between EMF and Sham may be due to the lower number of flies assayed in the Sham condition versus Control. The Sham experiment should therefore be repeated in order to increase the confidence in this EMF-mediated behavioural phenotype.

In *cyc* and *Clk* mutants CRY levels are elevated and it is thought that CRY acts to hyperexcite the l-LN_vs and shift the peak of neuronal firing from the light phase to the dark, resulting in a nocturnal phenotype (C.1.2) (Sheeba *et al.*, 2008; Kumar, Chen and Sehgal, 2012). In our assay, the presence of an EMF drives a more nocturnal phenotype suggesting that an EMF may exacerbate CRY activity, similar to what has been previously suggested (Fedele *et al.*, 2014a; Giachello *et al.*, 2016).

If this phenotype is reproducible it may provide means of assaying the possible mechanisms of behavioural modulation by EMF stimuli i.e. if mutations in possible pathways of CRY-mediated magnetoreception e.g. *Hk*, are combined with *cyc*⁰¹ and their behaviour assayed in the presence

and absence of an EMF. Such flies have been generated however their behaviour is yet to be fully characterised.



S.Figure C. 5 An EMF drives *cyc⁰¹* flies to become 'more nocturnal'.

A) Activity profiles (30 min bins) complete with LD bar (black=dark; white=light), showing the average daily activity (10 days) plotted over 24 h scale, for adult male *cyc⁰¹ry⁵⁰⁶* flies in a standard 7c/wk LD cycle (left). *y*-axis is uniform in all conditions. In addition, a 7c/wk sham field (red bar - middle) or 1,000 μ T EMF (blue bar - right), advanced 6 h W.R.T LD cycle, was applied. 'n' denotes number for flies. Blue shading is \pm SEM. **B)** L:D ratio for *cyc⁰¹* males in a standard 7c/wk LD cycle, plus the addition of a sham or EMF cycle. Error bars show mean \pm SEM. Control: n = 63. Sham: n = 28. EMF: n = 42. *p* value (top right) is the result of the *Kruskal-Wallis* test across all conditions. Multiple comparisons with the *Dunn's Multiple comparison test* (Control vs. EMF; $p=0.0004$ and Sham vs. EMF; $p=0.0239$).

C.4 Conclusions

The results presented in this Appendix have allowed us to draw the following conclusions regarding the impact of EMFs on *Drosophila* behaviour:

- 1. There is a large amount of inherent variation in climbing behaviour between flies of different genetic backgrounds.**
 - a. Eye colour appears to have the greatest impact, as well as more obstructive morphological mutations e.g. curly wings (**S.Figure C. 3**).

- 2. An EMF does not reduce negative geotaxis behaviour of flies with mutations that link CRY to membrane excitability.**
 - a. Climbing behaviour of *Hk*¹, *Hk*² and *eag*¹ was no different between sham and EMF conditions (**S.Figure C. 3**).
 - b. The same mutants had little effect on behavioural entrainment to extreme equinox photocycles (**S.Figure C. 4**)

- 3. Assaying the nocturnal behaviour of *cyc*⁰¹ flies in the presence of an EMF may provide possible means of investigating the pathways involved in CRY-mediated magnetoreception.**
 - a. *cyc*⁰¹ flies, which have elevated CRY levels, were 'more nocturnal' in the presence of an EMF (**S.Figure C. 5**). In *cyc* and *Clk* mutants, CRY acts to hyperexcite the l-LN_vs and shift the peak of neuronal firing from the light phase to the dark, driving a nocturnal phenotype. Therefore, it appears that an EMF exacerbates CRY activity.
 - b. *cyc*⁰¹ double mutants need to be assayed to hopefully elucidate the mechanism by which EMF impacts nocturnality behaviour.

Hyperkinetic has been shown to be involved in CRY-mediated modulation of neuronal excitability in the l-LN_vs in response to blue-light (Fogle *et al.*, 2011; Fogle *et al.*, 2015), and that this pathway can be modulated by EMFs (Giachello *et al.*, 2016). The results presented here support the hypothesis that blue-light activated CRY acts at the membrane via Hk and Kvβ channels and shows that this pathway is required to sense EMFs, which act to potentiate CRY activity.

Exacerbated CRY activity could result in a drastic change in membrane potential and bring about a behavioural change i.e. reduced climbing or increased nocturnality. With the current data on offer, this is a bold conclusion, but could represent a possible mechanism of CRY-mediated magnetoreception, however more work needs to be done in order to discount other options

Bibliography

- Agrawal, P., Houl, J. H., Gunawardhana, K. L., Liu, T., Zhou, J., Zoran, M. J. and Hardin, P. E. (2017) 'Drosophila CRY Entrain Clocks in Body Tissues to Light and Maintains Passive Membrane Properties in a Non-clock Body Tissue Independent of Light', *Curr Biol*.
- Ahmad, M. and Cashmore, R. (1993) 'HY4 gene of *A. thaliana* encodes a protein with the characteristics of a blue-light photoreceptor', *Letters to Nature*, 366, pp. 162-166.
- Akten, B., Jauch, E., Genova, G. K., Kim, E. Y., Edery, I., Raabe, T. and Jackson, F. R. (2003) 'A role for CK2 in the Drosophila circadian oscillator', *Nat Neurosci*, 6(3), pp. 251-7.
- Albrecht, U. (2012) 'Timing to perfection: the biology of central and peripheral circadian clocks', *Neuron*, 74(2), pp. 246-60.
- Alejevski, F., Saint-Charles, A., Michard-Vanhee, C., Martin, B., Galant, S., Vasiliauskas, D. and Rouyer, F. (2019) 'The HisCl1 histamine receptor acts in photoreceptors to synchronize Drosophila behavioral rhythms with light-dark cycles', *Nat Commun*, 10(1), pp. 252.
- Allada, R. and Chung, B. Y. (2010) 'Circadian organization of behavior and physiology in Drosophila', *Annu Rev Physiol*, 72, pp. 605-24.
- Allada, R., White, N. E., So, W. V., Hall, J. C. and Rosbash, M. (1998) 'A Mutant Drosophila Homolog of Mammalian Clock Disrupts Circadian Rhythms and Transcription of period and timeless', *Cell*, 93, pp. 791-804.
- Archer, S. N., Robilliard, D. L., Skene, D. J., Smits, M., Williams, A., Arendt, J. and von Schantz, M. (2003) 'A Length Polymorphism in the Circadian Clock Gene Per3 is Linked to Delayed Sleep Phase Syndrome and Extreme Diurnal Preference', *Sleep*, 26(4), pp. 413-415.
- Aschoff, J. (1960) 'Exogenous and Endogenous Components in Circadian Rhythms', *Cold Spring Harbor Symposia on Quantitative Biology*, 25, pp. 11-28.
- Ashburner, M. (1989) *Drosophila. A laboratory handbook*. Cold Spring Harbor, New York: Cold Spring Harbor Laboratory Press.
- Ashmore, L. J. and Sehgal, A. (2003) 'A Fly's Eye View of Circadian Entrainment', *Journal of Biological Rhythms*, 18(3), pp. 206-216.
- Aubert, C., Vos, M. H., Mathis, P., Eker, A. P. M. and Brettel, K. (2000) 'Intraprotein radical transfer during photoactivation of DNA photolyase', *Nature* 105, pp. 586-590.
- Bae, K., Lee, C., Hardin, P. E. and Edery, I. (2000) 'dCLOCK Is Present in Limiting Amounts and Likely Mediates Daily Interactions between the dCLOCK-CYC Transcription Factor and the PER-TIM Complex', *The Journal of Neuroscience*, 20(5), pp. 1746.
- Bae, K., Lee, C., Sidote, D., Chuang, K. Y. and Edery, I. (1998) 'Circadian regulation of a Drosophila homolog of the mammalian Clock gene: PER and TIM function as positive regulators', *Molecular and cellular biology*, 18(10), pp. 6142-6151.
- Baik, L. S., Fogle, K. J., Roberts, L., Galschiodt, A. M., Chevez, J. A., Recinos, Y., Nguy, V. and Holmes, T. C. (2017) 'CRYPTOCHROME mediates behavioral executive choice in response to UV light', *Proc Natl Acad Sci U S A*.

Bibliography

- Baik, L. S., Recinos, Y., Chevez, J. A., Au, D. D. and Holmes, T. C. (2019) 'Multiple Phototransduction Inputs Integrate to Mediate UV Light-evoked Avoidance/Attraction Behavior in *Drosophila*', *Journal of Biological Rhythms*, pp. 0748730419847339.
- Baik, L. S., Recinos, Y., Chevez, J. A. and Holmes, T. C. (2018) 'Circadian modulation of light-evoked avoidance/attraction behavior in *Drosophila*', *PLoS One*, 13(8), pp. e0201927.
- Baines, R. A., Uhler, J. P., Thompson, A., Sweeney, S. T. and Bate, M. (2001) 'Altered Electrical Properties in *Drosophila* Neurons Developing without Synaptic Transmission', *The Journal of Neuroscience*, 21(5), pp. 1523-1531.
- Baker, C. L., Loros, J. J. and Dunlap, J. C. (2012) 'The circadian clock of *Neurospora crassa*', *FEMS microbiology reviews*, 36(1), pp. 95-110.
- Bargiello, T. A., Jackson, F. R. and Young, M. W. (1984) 'Restoration of circadian behavioural rhythms by gene transfer in *Drosophila*', *Nature*, 312(5996), pp. 752-754.
- Bargiello, T. A. and Young, M. W. (1984) 'Molecular genetics of a biological clock in *Drosophila*', *Proceedings of the National Academy of Sciences of the United States of America*, 81(7), pp. 2142-2146.
- Barski, O. A., Tipparaju, S. M. and Bhatnagar, A. (2008) 'The aldo-keto reductase superfamily and its role in drug metabolism and detoxification', *Drug Metab Rev*, 40(4), pp. 553-624.
- Bass, J. and Takahashi, J. S. (2010) 'Circadian Integration of Metabolism and Energetics', *SCIENCE*, 330, pp. 1349-1354.
- Beaule, C. and Cheng, H. Y. (2011) 'The acetyltransferase Clock is dispensable for circadian aftereffects in mice', *J Biol Rhythms*, 26(6), pp. 561-4.
- Beaver, L. M., Gvakharia, B. O., Vollintine, T. S., Hege, D. M., Stanewsky, R. and Giebultowicz, J. M. (2002) 'Loss of circadian clock function decreases reproductive fitness in males of *Drosophila melanogaster*', *Proceedings of the National Academy of Sciences of the United States of America*, 99(4), pp. 2134-2139.
- Beckwith, E. J. and Ceriani, M. F. (2015) 'Communication between circadian clusters: The key to a plastic network', *FEBS Letters*, 589(22), pp. 3336-3342.
- Behnia, R. and Desplan, C. (2015) 'Visual circuits in flies: beginning to see the whole picture', *Current Opinion in Neurobiology*, 34, pp. 125-132.
- Bell-Pedersen, D., Cassone, V. M., Earnest, D. J., Golden, S. S., Hardin, P. E., Thomas, T. L. and Zoran, M. J. (2005) 'Circadian rhythms from multiple oscillators: lessons from diverse organisms', *Nature Reviews Genetics*, 6(7), pp. 544-556.
- Benedetti, F., Serretti, A., Colombo, C., Barbini, B., Lorenzi, C., Campori, E. and Smeraldi, E. (2003) 'Influence of CLOCK gene polymorphism on circadian mood fluctuation and illness recurrence in bipolar depression', *American Journal of Medical Genetics Part B-Neuropsychiatric Genetics*, 123B(1), pp. 23-26.
- Benito, J., Houl, J. H., Roman, G. W. and Hardin, P. E. (2008) 'The Blue-Light Photoreceptor CRYPTOCHROME Is Expressed in a Subset of Circadian Oscillator Neurons in the *Drosophila* CNS', *Journal of Biological Rhythms*, 23(4), pp. 296-307.
- Benito, J., Zheng, H. and Hardin, P. E. (2007) 'PDP1 Functions Downstream of the Circadian Oscillator to Mediate Behavioral Rhythms', *J Neurosci*, 27(10), pp. 2539-47.

- Bhadra, U., Thakkar, N., Das, P. and Pal Bhadra, M. (2017) 'Evolution of circadian rhythms: from bacteria to human', *Sleep Medicine*, 35, pp. 49-61.
- Blau, J. and Young, M. W. (1999) 'Cycling vrille Expression Is Required for a Functional Drosophila Clock', *Cell*, 99(6), pp. 661-671.
- Bloomquist, B. T., Shortridge, R. D., Schneuwly, S., Perdew, M., Montell, C., Steller, H., Rubin, G. and Pak, W. L. (1988) 'Isolation of a putative phospholipase c gene of drosophila, *norpA*, and its role in phototransduction', *Cell*, 54(5), pp. 723-733.
- Bolker, J. A. (1995) 'Model systems in developmental biology', *BioEssays*, 17(5), pp. 451-455.
- Bonini, N. M., Leiserson, W. M. and Benzer, S. (1993) 'The eyes absent gene: Genetic control of cell survival and differentiation in the developing Drosophila eye', *Cell*, 72(3), pp. 379-395.
- Brand, A. H. and Perrimon, N. (1993) 'Targeted gene expression as a means of altering cell fates and generating dominant phenotypes', *Development*, 118(2), pp. 401.
- Brandes, C., Plautz, J. D., Stanewsky, R., Jamison, C. F., Straume, M., Wood, K. V., Kay, S. A. and Hall, J. C. (1996) 'Novel Features of Drosophila period Transcription Revealed by Real-Time Luciferase Reporting', *Neuron*, 16, pp. 687-692.
- Brettel, K. and Byrdin, M. (2010) 'Reaction mechanisms of DNA photolyase', *Curr Opin Struct Biol*, 20(6), pp. 693-701.
- Bulthuis, N., Spontak, K. R., Kleeman, B. and Cavanaugh, D. J. (2019) 'Neuronal Activity in Non-LNV Clock Cells Is Required to Produce Free-Running Rest:Activity Rhythms in Drosophila', *Journal of Biological Rhythms*, pp. 0748730419841468.
- Bunning, E. 1935. Zur Kenntnis der erblichen Tagesperiodizitaet bei der Primaerblaettern von *Phaseolus multiflorus*. Jahrb Wissenschaftl Bot.
- Burg, M. G., Sarthy, P. V., Koliantz, G. and Pak, W. L. (1993) 'Genetic and molecular identification of a Drosophila histidine decarboxylase gene required in photoreceptor transmitter synthesis', *The EMBO Journal*, 12(3), pp. 911-919.
- Bustin, S. A., Benes, V., Garson, J. A., Hellems, J., Huggett, J., Kubista, M., Mueller, R., Nolan, T., Pfaffl, M. W., Shipley, G. L., Vandesompele, J. and Wittwer, C. T. (2009) 'The MIQE guidelines: minimum information for publication of quantitative real-time PCR experiments', *Clin Chem*, 55(4), pp. 611-22.
- Busza, A., Emery-Le, M., Rosbash, M. and Emery, P. (2004) 'Roles of the Two Drosophila CRYPTOCHROME Structural Domains in Circadian Photoreception', *SCIENCE*, 304, pp. 1503-1506.
- Busza, A., Murad, A. and Emery, P. (2007) 'Interactions between Circadian Neurons Control Temperature Synchronization of *Drosophila* Behavior', *The Journal of Neuroscience*, 27(40), pp. 10722.
- Byrdin, M., Lukacs, A., Thiagarajan, V., Eker, A. P. M., Brettel, K. and Vos, M. H. (2010) 'Quantum Yield Measurements of Short-Lived Photoactivation Intermediates in DNA Photolyase: Toward a Detailed Understanding of the Triple Tryptophan Electron Transfer Chain', *J Phys Chem A*, 114, pp. 3207-3214.
- C Hendricks, J., Lu, S., Kume, K., Yin, J., Yang, Z. and Sehgal, A. (2003) 'Gender Dimorphism in the Role of cycle (BMAL1) in Rest, Rest Regulation, and Longevity in *Drosophila melanogaster*', *J Biol Rhythms*, 18(1), pp. 12-25.

Bibliography

- Cao, G. and Nitabach, M. N. (2008) 'Circadian Control of Membrane Excitability in *Drosophila melanogaster* Lateral Ventral Clock Neurons', *The Journal of Neuroscience*, 28(25), pp. 6493.
- Cardozo, T. and Pagano, M. (2004) 'The SCF ubiquitin ligase: insights into a molecular machine', *Nat Rev Mol Cell Biol*, 5(9), pp. 739-751.
- Cavanaugh, D. J., Geratowski, J. D., Wooldorton, J. R. A., Spaethling, J. M., Hector, C. E., Zheng, X., Johnson, E. C., Eberwine, J. H. and Sehgal, A. (2014) 'Identification of a circadian output circuit for rest:activity rhythms in *Drosophila*', *Cell*, 157(3), pp. 689-701.
- Ceriani, M. F., Darlington, T. K., Staknis, D., Mas, P., Petti, A. A., Weitz, C. J. and Kay, S. A. (1999) 'Light-Dependent Sequestration of TIMELESS by CRYPTOCHROME', *SCIENCE*, 285, pp. 553-556.
- Chatterjee, A., Lamaze, A., De, J., Mena, W., Chelot, E., Martin, B., Hardin, P., Kadener, S., Emery, P. and Rouyer, F. (2018) 'Reconfiguration of a Multi-oscillator Network by Light in the *Drosophila* Circadian Clock', *Curr Biol*.
- Chen, C., Xu, M., Anantaprakorn, Y., Rosing, M. and Stanewsky, R. (2018) 'nocte Is Required for Integrating Light and Temperature Inputs in Circadian Clock Neurons of *Drosophila*', *Curr Biol*.
- Chen, D. M., Christianson, J. S., Sapp, R. J. and Stark, W. S. (1992) 'Visual receptor cycle in normal and period mutant *Drosophila*: microspectrophotometry, electrophysiology, and ultrastructural morphometry', *Vis Neurosci*, 9(2), pp. 125-35.
- Chen, W., Shi, W., Li, L., Zheng, Z., Li, T., Bai, W. and Zhao, Z. (2013) 'Regulation of sleep by the short neuropeptide F (sNPF) in *Drosophila melanogaster*', *Insect Biochem Mol Biol*, 43(9), pp. 809-19.
- Chiu, J. C., Ko, H. W. and Edery, I. (2011) 'NEMO/NLK phosphorylates PERIOD to initiate a time-delay phosphorylation circuit that sets circadian clock speed', *Cell*, 145(3), pp. 357-370.
- Chou, W.-H., Hall, K. J., Wilson, D. B., Wideman, C. L., Townson, S. M., Chadwell, L. V. and Britt, S. G. (1996) 'Identification of a Novel *Drosophila* Opsin Reveals Specific Patterning of the R7 and R8 Photoreceptor Cells', *Neuron*, 17(6), pp. 1101-1115.
- Chou, W. H., Huber, A., Bentrop, J., Schulz, S., Schwab, K., Chadwell, L. V., Paulsen, R. and Britt, S. G. (1999) 'Patterning of the R7 and R8 photoreceptor cells of *Drosophila*: evidence for induced and default cell-fate specification', *Development*, 126(4), pp. 607.
- Collins, B., Kane, E. A., Reeves, D. C., Akabas, M. H. and Blau, J. (2012) 'Balance of activity between LN(v)s and glutamatergic dorsal clock neurons promotes robust circadian rhythms in *Drosophila*', *Neuron*, 74(4), pp. 706-18.
- Collins, B., Kaplan, H. S., Cavey, M., Lelito, K. R., Bahle, A. H., Zhu, Z., Macara, A. M., Roman, G., Shafer, O. T. and Blau, J. (2014) 'Differentially timed extracellular signals synchronize pacemaker neuron clocks', *PLoS Biol*, 12(9), pp. e1001959.
- Collins, B., Mazzoni, E. O., Stanewsky, R. and Blau, J. (2006) '*Drosophila* CRYPTOCHROME is a circadian transcriptional repressor', *Curr Biol*, 16(5), pp. 441-9.
- Currie, J., Goda, T. and Wijnen, H. (2009) 'Selective entrainment of the *Drosophila* circadian clock to daily gradients in environmental temperature', *BMC Biol*, 7, pp. 49.
- Curtin, K. D., Huang, Z. J. and Rosbash, M. (1995) 'Temporally Regulated Nuclear Entry of the *Drosophila period* Protein Contributes to the Circadian Clock', *Neuron*, 14(365-372).

- Cusumano, P., Klarsfeld, A., Chelot, E., Picot, M., Richier, B. and Rouyer, F. (2009) 'PDF-modulated visual inputs and cryptochrome define diurnal behavior in *Drosophila*', *Nat Neurosci*, 12(11), pp. 1431-7.
- Cyran, S. A., Buchsbaum, A. M., Reddy, K. L., Lin, M., Glossop, N. R. J., Hardin, P. E., Young, M. W., Storti, R. V. and Blau, J. (2003) 'vrille, Pdp1, and dClock Form a Second Feedback Loop in the *Drosophila* Circadian Clock', *Cell*, 11, pp. 329-341.
- Czarna, A., Berndt, A., Singh, H. R., Grudziecki, A., Ladurner, A. G., Timinszky, G., Kramer, A. and Wolf, E. (2013) 'Structures of *Drosophila* cryptochrome and mouse cryptochrome1 provide insight into circadian function', *Cell*, 153(6), pp. 1394-405.
- Dahdal, D., Reeves, D. C., Ruben, M., Akabas, M. H. and Blau, J. (2010) '*Drosophila* pacemaker neurons require g protein signaling and GABAergic inputs to generate twenty-four hour behavioral rhythms', *Neuron*, 68(5), pp. 964-77.
- Damiola, F., Le Minh, N., Preitner, N., Kornmann, B., Fleury-Olela, F. and Schibler, U. (2000) 'Restricted feeding uncouples circadian oscillators in peripheral tissues from the central pacemaker in the suprachiasmatic nucleus', *Genes & development*, 14(23), pp. 2950-2961.
- Darlington, T. K., Wager-Smith, K., Ceriani, M. F., Staknis, D., Gekakis, N., Steeves, T. D. L., Weitz, C. J., Takahashi, J. S. and Kay, S. A. (1998) 'Closing the Circadian Loop: CLOCK-Induced Transcription of Its Own Inhibitors *per* and *tim*', *Science*, 280(5369), pp. 1599.
- Davidson, A. J., Sellix, M. T., Daniel, J., Yamazaki, S., Menaker, M. and Block, G. D. (2006) 'Chronic jet-lag increases mortality in aged mice', *Current biology : CB*, 16(21), pp. R914-R916.
- de Mairan, J. 1729. Observation botanique. Hist. Acad. Roy. Sci.
- DeBruyne, J. P., Weaver, D. R. and Reppert, S. M. (2007) 'CLOCK and NPAS2 have overlapping roles in the suprachiasmatic circadian clock', *Nat Neurosci*, 10(5), pp. 543-5.
- Diao, F., Ironfield, H., Luan, H., Diao, F., Shropshire, W. C., Ewer, J., Marr, E., Potter, C. J., Landgraf, M. and White, B. H. (2015) 'Plug-and-play genetic access to *Drosophila* cell types using exchangeable exon cassettes', *Cell Rep*, 10(8), pp. 1410-21.
- Dietzl, G., Chen, D., Schnorrer, F., Su, K. C., Barinova, Y., Fellner, M., Gasser, B., Kinsey, K., Oettel, S., Scheiblaue, S., Couto, A., Marra, V., Keleman, K. and Dickson, B. J. (2007) 'A genome-wide transgenic RNAi library for conditional gene inactivation in *Drosophila*', *Nature*, 448(7150), pp. 151-156.
- Dissel, S., Codd, V., Fedic, R., Garner, K. J., Costa, R., Kyriacou, C. P. and Rosato, E. (2004) 'A constitutively active cryptochrome in *Drosophila melanogaster*', *Nat Neurosci*, 7(8), pp. 834-40.
- Dissel, S., Hansen, C. N., Oezkaya, O., Hemsley, M., Kyriacou, C. P. and Rosato, E. (2014) 'The Logic of Circadian Organization in *Drosophila*', *Current Biology*, 24(19), pp. 2257-2266.
- Do, M. T. H. and Yau, K.-W. (2010) 'Intrinsically photosensitive retinal ganglion cells', *Physiological reviews*, 90(4), pp. 1547-1581.
- Dodd, A. N., Salathia, N., Hall, A., Kévei, E., Tóth, R., Nagy, F., Hibberd, J. M., Millar, A. J. and Webb, A. A. R. (2005) 'Plant Circadian Clocks Increase Photosynthesis, Growth, Survival, and Competitive Advantage', *Science*, 309(5734), pp. 630.
- Dodson, C. A., Hore, P. J. and Wallace, M. I. (2013) 'A radical sense of direction: signalling and mechanism in cryptochrome magnetoreception', *Trends Biochem Sci*, 38(9), pp. 435-46.

Bibliography

- Dolezelova, E., Dolezel, D. and Hall, J. C. (2007) 'Rhythm defects caused by newly engineered null mutations in *Drosophila*'s cryptochrome gene', *Genetics*, 177(1), pp. 329-45.
- Dominguez-Rodriguez, A., Abreu-Gonzalez, P., Sanchez-Sanchez, J. J., Kaski, J. C. and Reiter, R. J. (2010) 'Melatonin and circadian biology in human cardiovascular disease', *Journal of Pineal Research*, 49(1), pp. 14-22.
- Dubruille, R. and Emery, P. (2008) 'A plastic clock: how circadian rhythms respond to environmental cues in *Drosophila*', *Mol Neurobiol*, 38(2), pp. 129-45.
- Duffy, J. B. (2002) 'GAL4 system in *Drosophila*: a fly geneticist's Swiss army knife', *Genesis*, 34(1-2), pp. 1-15.
- Dunlap, J. C., Loros, J. J. and DeCoursey, P. J. (2004) *Chronobiology: Biological Timekeeping*. Sunderland, MA, US: Sinauer Associates.
- D'Costa, A., Reifegerste, R., Sierra, S. and Moses, K. (2006) 'The *Drosophila* ramshackle gene encodes a chromatin-associated protein required for cell morphology in the developing eye', *Mechanisms of Development*, 123(8), pp. 591-604.
- Emery, P., So, W. V., Kaneko, M., Hall, J. C. and Rosbash, M. (1998) 'CRY, a *Drosophila* Clock and Light-Regulated Cryptochrome, Is a Major Contributor to Circadian Rhythm Resetting and Photosensitivity', *Cell*, 95, pp. 669-679.
- Emery, P., Stanewsky, R., Hall, J. C. and Rosbash, M. (2000a) 'A unique circadian-rhythm photoreceptor', *Nature*, 404, pp. 456-7.
- Emery, P., Stanewsky, R., Helfrich-Foerster, C., Emery-Le, M., Hall, J. C. and Rosbash, M. (2000b) '*Drosophila* CRY Is a Deep Brain Circadian Photoreceptor', *Neuron*, 26, pp. 493-504.
- Evans, E. W., Dodson, C. A., Maeda, K., Biskup, T., Wedge, C. J. and Timmel, C. R. (2013) 'Magnetic field effects in flavoproteins and related systems', *Interface Focus*, 3(5), pp. 20130037.
- Evans, J. A. (2016) 'Collective timekeeping among cells of the master circadian clock', *The Journal of endocrinology*, 230(1), pp. R27-R49.
- Falsetti, A. (2000) 'Risperidone for control of agitation in dementia patients', *Am J Health Syst Pharm*, 57, pp. 862-870.
- Fang, Y., Sathyanarayanan, S. and Sehgal, A. (2007) 'Post-translational regulation of the *Drosophila* circadian clock requires protein phosphatase 1 (PP1)', *Genes Dev*, 21(12), pp. 1506-18.
- Fedele, G., Edwards, M. D., Bhutani, S., Hares, J. M., Murbach, M., Green, E. W., Dissel, S., Hastings, M. H., Rosato, E. and Kyriacou, C. P. (2014a) 'Genetic Analysis of Circadian Responses to Low Frequency Electromagnetic Fields in *Drosophila melanogaster*', *Plos Genetics*, 10(12).
- Fedele, G., Green, E. W., Rosato, E. and Kyriacou, C. P. (2014b) 'An electromagnetic field disrupts negative geotaxis in *Drosophila* via a CRY-dependent pathway', *Nat Commun*, 5, pp. 4391.
- Fernández, M. P., Berni, J. and Ceriani, M. F. (2008) 'Circadian Remodeling of Neuronal Circuits Involved in Rhythmic Behavior', *PLOS Biology*, 6(3), pp. e69.
- Fire, A., Xu, S., Montgomery, M. K., Kostas, S. A., Driver, S. E. and Mello, C. C. (1998) 'Potent and specific genetic interference by double-stranded RNA in *Caenorhabditis elegans*', *Nature*, 391(6669), pp. 806-811.
- Fischer, J. A., Giniger, E., Maniatis, T. and Ptashne, M. (1988) 'GAL4 activates transcription in *Drosophila*', *Nature* 332, pp. 853-856.

- Flourakis, M., Kula-Eversole, E., Hutchison, Alan L., Han, Tae H., Aranda, K., Moose, Devon L., White, Kevin P., Dinner, Aaron R., Lear, Bridget C., Ren, D., Diekman, Casey O., Raman, Indira M. and Allada, R. (2015) 'A Conserved Bicycle Model for Circadian Clock Control of Membrane Excitability', *Cell*, 162(4), pp. 836-848.
- Fogle, K. J., Baik, L. S., Houl, J. H., Tran, T. T., Roberts, L., Dahm, N. A., Cao, Y., Zhou, M. and Holmes, T. C. (2015) 'CRYPTOCHROME-mediated phototransduction by modulation of the potassium ion channel beta-subunit redox sensor', *Proc Natl Acad Sci U S A*, 112(7), pp. 2245-50.
- Fogle, K. J., Parson, K. G., Dahm, N. A. and Holmes, T. C. (2011) 'CRYPTOCHROME Is a Blue-Light Sensor That Regulates Neuronal Firing Rate', *SCIENCE*, 331, pp. 1409-13.
- Foster, R. G. and Wulff, K. (2005) 'The rhythm of rest and excess', *Nature Reviews Neuroscience*, 6(5), pp. 407-414.
- Fryxell, K. J. and Meyerowitz, E. M. (1987) 'An opsin gene that is expressed only in the R7 photoreceptor cell of *Drosophila*', *The EMBO journal*, 6(2), pp. 443-451.
- Fujii, S., Krishnan, P., Hardin, P. and Amrein, H. (2007) 'Nocturnal male sex drive in *Drosophila*', *Current biology : CB*, 17(3), pp. 244-251.
- Förster, C. 2010. The neuronal network of the endogenous clock. *e-Neuroforum*.
- Gao, S., Takemura, S. Y., Ting, C. Y., Huang, S., Lu, Z., Luan, H., Rister, J., Thum, A. S., Yang, M., Hong, S. T., Wang, J. W., Odenwald, W. F., White, B. H., Meinertzhagen, I. A. and Lee, C. H. (2008) 'The neural substrate of spectral preference in *Drosophila*', *Neuron*, 60(2), pp. 328-342.
- Gegear, R. J., Casselman, A., Waddell, S. and Reppert, S. M. (2008) 'Cryptochrome mediates light-dependent magnetosensitivity in *Drosophila*', *Nature*, 454(7207), pp. 1014-8.
- Gegear, R. J., Foley, L. E., Casselman, A. and Reppert, S. M. (2010) 'Animal cryptochromes mediate magnetoreception by an unconventional photochemical mechanism', *Nature*, 463(7282), pp. 804-7.
- Gekakis, N., Saez, L., Delahaye-Brown, A., Myers, M. P., Sehgal, A., Young, M. W. and Weitz, C. J. (1995) 'Isolation of timeless by PER Protein Interaction: Defective Interaction Between timeless Protein and Long-Period Mutant PERL', *SCIENCE*, 270, pp. 811-815.
- Gentile, C., Sehadova, H., Simoni, A., Chen, C. and Stanewsky, R. (2013) 'Cryptochrome Antagonizes Synchronization of *Drosophila*'s Circadian Clock to Temperature Cycles', *Current Biology*, 23(3), pp. 185-195.
- Giachello, C. N., Scrutton, N. S., Jones, A. R. and Baines, R. A. (2016) 'Magnetic Fields Modulate Blue-Light-Dependent Regulation of Neuronal Firing by Cryptochrome', *J Neurosci*, 36(42), pp. 10742-10749.
- Giebultowicz, J., Ivanchenko, M. and Vollintine, T. (2001) *Organization of the insect circadian system: Spatial and developmental expression of clock genes in peripheral tissues of *Drosophila melanogaster**.
- Giebultowicz, J. M. and Hege, D. M. (1997) 'Circadian clock in Malpighian tubules', *Nature*, 386(6626), pp. 664-664.
- Glaser, F. T. and Stanewsky, R. (2007) 'Synchronization of the *Drosophila* Circadian Clock by Temperature Cycles', *Cold Spring Harb Symp Quant Biol*.
- Glossop, N. R. J. and Hardin, P. E. (2002) 'Central and peripheral circadian oscillator mechanisms in flies and mammals', *Journal of Cell Science*, 115, pp. 3369-77.

Bibliography

- Glossop, N. R. J., Houl, J., Zheng, H., Ng, F. S., Dudek, S. M. and Hardin, P. E. (2003) 'VRILLE Feeds Back to Control Circadian Transcription of Clock in the *Drosophila* Circadian Oscillator', *Neuron*, 37, pp. 249-261.
- Glossop, N. R. J., Lyons, L. C. and Hardin, P. E. (1999) 'Interlocked Feedback Loops Within the *Drosophila* Circadian Oscillator', *Science*, 286(5440), pp. 766.
- Goda, T., Sharp, B. and Wijnen, H. (2014) 'Temperature-dependent resetting of the molecular circadian oscillator in *Drosophila*', *Proc Biol Sci*, 281(1793).
- Golden, S. S., Ishiura, M., Johnson, C. H. and Kondo, T. (1997) 'CYANOBACTERIAL CIRCADIAN RHYTHMS', *Annual Review of Plant Physiology and Plant Molecular Biology*, 48(1), pp. 327-354.
- Gorostiza, E. A., Depetris-Chauvin, A., Frenkel, L., Pérez, N. and Ceriani, M. F. (2014) 'Circadian pacemaker neurons change synaptic contacts across the day', *Current biology : CB*, 24(18), pp. 2161-2167.
- Gould, J. L. (2010) 'Magnetoreception', *Curr Biol*, 20(10), pp. R431-5.
- Goyal, L., McCall, K., Agapite, J., Hartweg, E. and Steller, H. (2000) 'Induction of apoptosis by *Drosophila* reaper, hid and grim through inhibition of IAP function', *The EMBO Journal*, 19(4), pp. 589-597.
- Grebler, R., Kistenpfennig, C., Rieger, D., Bentrop, J., Schneuwly, S., Senthilan, P. R. and Helfrich-Förster, C. (2017) '*Drosophila* Rhodopsin 7 can partially replace the structural role of Rhodopsin 1, but not its physiological function', *Journal of comparative physiology. A, Neuroethology, sensory, neural, and behavioral physiology*, 203(8), pp. 649-659.
- Grether, M. E., Abrams, J. M., Agapite, J., White, K. and Steller, H. (1995) 'The *head involution defective* gene of *Drosophila melanogaster* functions in programmed cell death', *Genes and Development*, 9, pp. 1694-1708
- Grima, B., Chelot, E., Xia, R. and Rouyer, F. (2004) 'Morning and evening peaks of activity rely on different clock neurons of the *Drosophila* brain', *Nature*, 431, pp. 869-873.
- Grima, B., Dognon, A., Lamouroux, A., Chelot, E. and Rouyer, F. (2012) 'CULLIN-3 controls TIMELESS oscillations in the *Drosophila* circadian clock', *PLoS Biol*, 10(8), pp. e1001367.
- Grima, B., Lamouroux, A., Chelot, E., Papin, C., Limbourg-Bouchon, B. and Rouyer, F. (2002) 'The F-box protein Slimb controls the levels of clock proteins Period and Timeless', *Nature*, 420(6912), pp. 178-182.
- Gunawardhana, K. L. and Hardin, P. E. (2017) 'VRILLE Controls PDF Neuropeptide Accumulation and Arborization Rhythms in Small Ventrolateral Neurons to Drive Rhythmic Behavior in *Drosophila*', *Curr Biol*, 27(22), pp. 3442-3453 e4.
- Guo, F., Cerullo, I., Chen, X. and Rosbash, M. (2014) 'PDF neuron firing phase-shifts key circadian activity neurons in *Drosophila*', *Elife*, 3.
- Guo, F., Holla, M., Díaz, M. M. and Rosbash, M. (2018) 'A Circadian Output Circuit Controls Sleep-Wake Arousal in *Drosophila*', *Neuron*, 100(3), pp. 624-635.e4.
- Guo, F., Yu, J., Jung, H. J., Abruzzi, K. C., Luo, W., Griffith, L. C. and Rosbash, M. (2016) 'Circadian neuron feedback controls the *Drosophila* sleep-activity profile', *Nature*.
- Halberg, F., Cornélissen, G., Katinas, G., Syutkina, E. V., Sothorn, R. B., Zaslavskaya, R., Halberg, F., Watanabe, Y., Schwartzkopff, O., Otsuka, K., Tarquini, R., Frederico, P. and Siggelova, J. (2003)

- 'Transdisciplinary unifying implications of circadian findings in the 1950s', *Journal of circadian rhythms*, 1(1), pp. 2-2.
- Hamasaka, Y. and Nassel, D. R. (2006) 'Mapping of serotonin, dopamine, and histamine in relation to different clock neurons in the brain of *Drosophila*', *J Comp Neurol*, 494(2), pp. 314-30.
- Hamasaka, Y., Rieger, D., Parmentier, M. L., Grau, Y., Helfrich-Förster, C. and Nassel, D. R. (2007) 'Glutamate and its metabotropic receptor in *Drosophila* clock neuron circuits', *J Comp Neurol*, 505(1), pp. 32-45.
- Hamasaka, Y., Wegener, C. and Nassel, D. R. (2005) 'GABA modulates *Drosophila* circadian clock neurons via GABAB receptors and decreases in calcium', *J Neurobiol*, 65(3), pp. 225-40.
- Hamblen-Coyle, M. J., Wheeler, D. A., Rutila, J. E., Rosbash, M. and Hall, J. C. (1992) 'Behavior of period-altered circadian rhythm mutants of *Drosophila* in light: Dark cycles (Diptera: Drosophilidae)', *Journal of Insect Behavior*, 5(4), pp. 417-446.
- Hanafusa, S., Kawaguchi, T., Umezaki, Y., Tomioka, K. and Yoshii, T. (2013) *Sexual Interactions Influence the Molecular Oscillations in DN1 Pacemaker Neurons in *Drosophila melanogaster**.
- Hanai, S., Hamasaka, Y. and Ishida, N. (2008) 'Circadian entrainment to red light in *Drosophila*: requirement of Rhodopsin 1 and Rhodopsin 6', *Neuroreport*, 19(14), pp. 1441-4.
- Hanai, S. and Ishida, N. (2009) 'Entrainment of *Drosophila* circadian clock to green and yellow light by Rh1, Rh5, Rh6 and CRY', *Neuroreport*, 20(8), pp. 755-8.
- Hao, H., Allen, D. L. and Hardin, P. E. (1997) 'A Circadian Enhancer Mediates PER-Dependent mRNA Cycling in *Drosophila melanogaster*', *Molecular and Cellular Biology* 17(7), pp. 3687-3693.
- Hardie, R. C. and Juusola, M. (2015) 'Phototransduction in *Drosophila*', *Current Opinion in Neurobiology*, 34, pp. 37-45.
- Hardin, P. E. (2004) 'Transcription Regulation within the Circadian Clock: The E-box and Beyond', *Journal of Biological Rhythms*, 19(5), pp. 348-360.
- Hardin, P. E. (2005) 'The circadian timekeeping system of *Drosophila*', *Curr Biol*, 15(17), pp. R714-22.
- Hardin, P. E. (2006) 'Essential and expendable features of the circadian timekeeping mechanism', *Curr Opin Neurobiol*, 16(6), pp. 686-92.
- Hardin, P. E. (2011) 'Molecular genetic analysis of circadian timekeeping in *Drosophila*', *Adv Genet*, 74, pp. 141-73.
- Hardin, P. E., Hall, J. C. and Rosbash, M. (1990) 'Feedback of the *Drosophila* period gene product on circadian cycling of its messenger RNA levels', *Nature*, 343(6258), pp. 536-540.
- Hardin, P. E., Hall, J. C. and Rosbash, M. (1992) 'Circadian oscillations in period gene mRNA levels are transcriptionally regulated', *PNAS*, 89, pp. 11711-11715.
- Hardin, P. E., Krishnan, B., Houl, J. H., Zheng, H., Ng, F. S., Dryer, S. E. and Glossop, N. R. J. (2003) 'Central and peripheral circadian oscillators in *Drosophila*', *Novartis Found Symp* 253, pp. 140-50.
- Harms, E., Kivimäe, S., Young, M. W. and Saez, L. (2004) 'Posttranscriptional and Posttranslational Regulation of Clock Genes', *Journal of Biological Rhythms*, 19(5), pp. 361-373.
- Harper, R. E., Dayan, P., Albert, J. T. and Stanewsky, R. (2016) 'Sensory Conflict Disrupts Activity of the *Drosophila* Circadian Network', *Cell Rep*, 17(7), pp. 1711-1718.

Bibliography

- Hastings, M. H., Brancaccio, M. and Maywood, E. S. (2014) 'Circadian pacemaking in cells and circuits of the suprachiasmatic nucleus', *J Neuroendocrinol*, 26(1), pp. 2-10.
- Hastings, M. H., Reddy, A. B. and Maywood, E. S. (2003) 'A clockwork web: circadian timing in brain and periphery, in health and disease', *Nature Reviews Neuroscience*, 4(8), pp. 649-661.
- Hattar, S., Liao, H. W., Takao, M., Berson, D. M. and Yau, K. W. (2002) 'Melanopsin-containing retinal ganglion cells: architecture, projections, and intrinsic photosensitivity', *Science (New York, N.Y.)*, 295(5557), pp. 1065-1070.
- Hazelrigg, T., Levis, R. and Rubin, G. M. (1984) 'Transformation of white locus DNA in *Drosophila*: Dosage compensation, zeste interaction, and position effects', *Cell*, 36(2), pp. 469-481.
- He, C., Cong, X., Zhang, R., Wu, D., An, C. and Zhao, Z. (2013) 'Regulation of circadian locomotor rhythm by neuropeptide Y-like system in *Drosophila melanogaster*', *Insect Mol Biol*, 22(4), pp. 376-88.
- He, Q., Wu, B., Price, J. L. and Zhao, Z. (2017) 'Circadian Rhythm Neuropeptides in *Drosophila*: Signals for Normal Circadian Function and Circadian Neurodegenerative Disease', *Int J Mol Sci*, 18(4).
- Helfrich-Förster, C. (1995) 'The period clock gene is expressed in central nervous system neurons which also produce a neuropeptide that reveals the projections of circadian pacemaker cells within the brain of *Drosophila melanogaster*', *PNAS*, 92, pp. 612-616.
- Helfrich-Förster, C. (1998) 'Robust circadian rhythmicity of *Drosophila melanogaster* requires the presence of lateral neurons: a brain-behavioral study of disconnected mutants', *Journal of Comparative Physiology A*, 182(4), pp. 435-453.
- Helfrich-Förster, C. (2000) 'Differential Control of Morning and Evening Components in the Activity Rhythm of *Drosophila melanogaster*—Sex-Specific Differences Suggest a Different Quality of Activity', *Journal of Biological Rhythms*, 15(2), pp. 135-154.
- Helfrich-Förster, C. (2004) 'The circadian clock in the brain: a structural and functional comparison between mammals and insects', *Journal of Comparative Physiology A*, 190(8), pp. 601-613.
- Helfrich-Förster, C. (2005) 'Neurobiology of the fruit fly's circadian clock', *Genes Brain Behav*, 4(2), pp. 65-76.
- Helfrich-Förster, C., Edwards, T., Yasuyama, K., Wisotzki, B., Schneuwly, S., Stanewsky, R., Meinertzhagen, I. A. and Hofbauer, A. (2002) 'The Extraretinal Eyelet of *Drosophila*: Development, Ultrastructure, and Putative Circadian Function', *The Journal of Neuroscience*, 22(21), pp. 9255.
- Helfrich-Förster, C., Shafer, O. T., Wulbeck, C., Grieshaber, E., Rieger, D. and Taghert, P. (2007) 'Development and morphology of the clock-gene-expressing lateral neurons of *Drosophila melanogaster*', *Journal of Comparative Neurology*, 500(1), pp. 47-70.
- Helfrich-Förster, C., Stengl, M. and Homberg, U. (1998) 'Organization of the Circadian System in Insects', *Chronobiology International*, 15(6), pp. 567-594.
- Helfrich-Förster, C., Winter, C., Hofbauer, A., Hall, J. C. and Stanewsky, R. (2001) 'The Circadian Clock of Fruit Flies Is Blind after Elimination of All Known Photoreceptors', *Neuron*, 30, pp. 249-261.
- Hemsley, M. J., Mazzotta, G. M., Mason, M., Dissel, S., Toppo, S., Pagano, M. A., Sandrelli, F., Meggio, F., Rosato, E., Costa, R. and Tosatto, S. C. (2007) 'Linear motifs in the C-terminus of *D. melanogaster* cryptochrome', *Biochem Biophys Res Commun*, 355(2), pp. 531-7.

- Henbest, K. B., Kukura, P., Rodgers, C. T., Hore, P. J. and Timmel, C. R. (2004) 'Radio Frequency Magnetic Field Effects on a Radical Recombination Reaction: A Diagnostic Test for the Radical Pair Mechanism', *JACS Comms*, 126, pp. 8102-8103.
- Hermann, C., Yoshii, T., Dusik, V. and Helfrich-Förster, C. (2012) 'Neuropeptide F immunoreactive clock neurons modify evening locomotor activity and free-running period in *Drosophila melanogaster*', *Journal of Comparative Neurology*, 520(5), pp. 970-987.
- Hermann-Luibl, C., Yoshii, T., Senthilan, P. R., Dirksen, H. and Helfrich-Förster, C. (2014) 'The ion transport peptide is a new functional clock neuropeptide in the fruit fly *Drosophila melanogaster*', *J Neurosci*, 34(29), pp. 9522-36.
- Hirota, T. and Fukada, Y. (2004) *Resetting Mechanism of Central and Peripheral Circadian Clocks in Mammals*. BIOONE.
- Ho, K. S. and Sehgal, A. (2005) 'Drosophila melanogaster: An Insect Model for Fundamental Studies of Sleep', in Young, M.W. (ed.) *Methods in Enzymology*: Academic Press, pp. 772-793.
- Hoang, N., Schleicher, E., Kacprzak, S., Bouly, J. P., Picot, M., Wu, W., Berndt, A., Wolf, E., Bittl, R. and Ahmad, M. (2008) 'Human and *Drosophila* cryptochromes are light activated by flavin photoreduction in living cells', *PLoS Biol*, 6(7), pp. e160.
- Hofbauer, A. and Buchner, E. (1989) 'Does *Drosophila* have seven eyes?', *Naturwissenschaften*, 76(7), pp. 335-336.
- Hong, S. T., Bang, S., Paik, D., Kang, J., Hwang, S., Jeon, K., Chun, B., Hyun, S., Lee, Y. and Kim, J. (2006) 'Histamine and its receptors modulate temperature-preference behaviors in *Drosophila*', *J Neurosci*, 26(27), pp. 7245-56.
- Hooven, L. A., Sherman, K. A., Butcher, S. and Giebultowicz, J. M. (2009) 'Does the clock make the poison? Circadian variation in response to pesticides', *PLoS One*, 4(7), pp. e6469.
- Horne, J. A. and Östberg, O. (1977) 'Individual differences in human circadian rhythms', *Biological Psychology*, 5(3), pp. 179-190.
- Horst, G. T. J. v. d., Muijtjens, M., Kobayashi, K., Takano, R., Kanno, S.-i., Takao, M., Wit, J. d., Verkerk, A., Eker, A. P. M., Leenen, D. v., Buijs, R., Bootsma, D., Hoeijmakers, J. H. J. and Yasui, A. (1999) 'Mammalian Cry1 and Cry2 are essential for maintenance of circadian rhythms', *Nature*, 398(6728), pp. 627-630.
- Huang, R. C. (2018) 'The discoveries of molecular mechanisms for the circadian rhythm: The 2017 Nobel Prize in Physiology or Medicine', *Biomed J*, 41(1), pp. 5-8.
- Huang, Z. J., Curtin, K. D. and Rosbash, M. (1995) 'PER Protein Interactions and Temperature Compensation of a Circadian Clock in *Drosophila*', *SCIENCE*, 267, pp. 1169-1172.
- Huber, A., Schulz, S., Bentrop, J., Groell, C., Wolfrum, U. and Paulsen, R. (1997) 'Molecular cloning of *Drosophila* Rh6 rhodopsin: the visual pigment of a subset of R8 photoreceptor cells 1', *FEBS Letters*, 406(1-2), pp. 6-10.
- Hunter-Ensor, M., Ousley, A. and Sehgal, A. (1996) 'Regulation of the *Drosophila* Protein Timeless Suggests a Mechanism for Resetting the Circadian Clock by Light', *Cell*, 84, pp. 677-685.
- Hyun, S., Lee, Y., Hong, S. T., Bang, S., Paik, D., Kang, J., Shin, J., Lee, J., Jeon, K., Hwang, S., Bae, E. and Kim, J. (2005) '*Drosophila* GPCR Han is a receptor for the circadian clock neuropeptide PDF', *Neuron*, 48(2), pp. 267-78.

Bibliography

- Im, S. H., Li, W. and Taghert, P. H. (2011) 'PDFR and CRY signaling converge in a subset of clock neurons to modulate the amplitude and phase of circadian behavior in *Drosophila*', *PLoS One*, 6(4), pp. e18974.
- Im, S. H. and Taghert, P. H. (2010) 'PDF receptor expression reveals direct interactions between circadian oscillators in *Drosophila*', *The Journal of comparative neurology*, 518(11), pp. 1925-1945.
- Iovchev, M., Kodrov, P., Wolstenholme, A. J., Pak, W. L. and Semenov, E. P. (2009) 'Altered Drug Resistance and Recovery from Paralysis in *Drosophila Melanogaster* with a Deficient Histamine-Gated Chloride Channel', *Journal of Neurogenetics*, 16(4), pp. 249-261.
- Isaac, R. E., Li, C., Leedale, A. E. and Shirras, A. D. (2010) 'Drosophila male sex peptide inhibits siesta sleep and promotes locomotor activity in the post-mated female', *Proceedings. Biological sciences*, 277(1678), pp. 65-70.
- Ito, C., Goto, S. G., Shiga, S., Tomioka, K. and Numata, H. (2008) 'Peripheral circadian clock for the cuticle deposition rhythm in *Drosophila melanogaster*', *Proceedings of the National Academy of Sciences*, 105(24), pp. 8446.
- Ito, C. and Tomioka, K. (2016) 'Heterogeneity of the Peripheral Circadian Systems in *Drosophila melanogaster*: A Review', *Frontiers in Physiology*, 7.
- Ivanchenko, M., Stanewsky, R. and Giebultowicz, J. M. (2001) 'Circadian Photoreception in *Drosophila*: Functions of Cryptochrome in Peripheral and Central Clocks', *Journal of Biological Rhythms*, 16(2), pp. 205-215.
- Iwata, T., Zhang, Y., Hitomi, K., Getzoff, E. D. and Kandori, H. (2010) 'Key dynamics of conserved asparagine in a cryptochrome/photolyase family protein by fourier transform infrared spectroscopy', *Biochemistry*, 49(41), pp. 8882-91.
- Jackson, F. R. (2011) 'Glial cell modulation of circadian rhythms', *Glia*, 59(9), pp. 1341-1350.
- Jackson, S. and Xiong, Y. (2009) 'CRL4s: the CUL4-RING E3 ubiquitin ligases', *Trends Biochem Sci*, 34(11), pp. 562-70.
- Jana, S., Chakraborty, C., Nandi, S. and Deb, J. K. (2004) 'RNA interference: potential therapeutic targets', *Applied Microbiology and Biotechnology*, 65(6), pp. 649-657.
- Johansson, C., Willeit, M., Smedh, C., Ekholm, J., Paunio, T., Kieseppa, T., Lichtermann, D., Praschak-Rieder, N., Neumeister, A., Nilsson, L. G., Kasper, S., Peltonen, L., Adolfsson, R., Schalling, M. and Partonen, T. (2003) 'Circadian clock-related polymorphisms in seasonal affective disorder and their relevance to diurnal preference', *Neuropsychopharmacology*, 28(4), pp. 734-9.
- Johard, H. A., Yoishii, T., Dirksen, H., Cusumano, P., Rouyer, F., Helfrich-Förster, C. and Nassel, D. R. (2009) 'Peptidergic clock neurons in *Drosophila*: ion transport peptide and short neuropeptide F in subsets of dorsal and ventral lateral neurons', *J Comp Neurol*, 516(1), pp. 59-73.
- Kadener, S., Menet, J. S., Schoer, R. and Rosbash, M. (2008) 'Circadian transcription contributes to core period determination in *Drosophila*', *PLoS Biol*, 6(5), pp. e119.
- Kadener, S., Stoleru, D., McDonald, M., Nawatheatan, P. and Rosbash, M. (2007) 'Clockwork Orange is a transcriptional repressor and a new *Drosophila* circadian pacemaker component', *Genes Dev*, 21(13), pp. 1675-86.
- Kaneko, M. (1998) 'Neural substrates of *Drosophila* rhythms revealed by mutants and molecular manipulations', *Curr Opin Neurobiol*, 8, pp. 652-658.

- Kaneko, M. and Hall, J. C. (2000) 'Neuroanatomy of cells expressing clock genes in *Drosophila*: Transgenic manipulation of the period and timeless genes to mark the perikarya of circadian pacemaker neurons and their projections', *Journal of Comparative Neurology*, 422(1), pp. 66-94.
- Kaneko, M., Helfrich-Förster, C. and Hall, J. C. (1997) 'Spatial and Temporal Expression of the period and timeless Genes in the Developing Nervous System of *Drosophila*: Newly Identified Pacemaker Candidates and Novel Features of Clock Gene Product Cycling', *The Journal of Neuroscience*, 17(17), pp. 6745-6760.
- Kaneko, M., Park, J. H., Cheng, Y., Hardin, P. E. and Hall, J. C. (2000) 'Disruption of Synaptic Transmission or Clock-GeneProduct Oscillations in Circadian Pacemaker Cells of *Drosophila* Cause Abnormal Behavioral Rhythms', *J Neurobiol*, 43, pp. 207-233.
- Khericha, M., Kolenchery, J. B. and Tauber, E. (2016) 'Neural and non-neural contributions to sexual dimorphism of mid-day sleep in *Drosophila melanogaster*: a pilot study', *Physiological entomology*, 41(4), pp. 327-334.
- Kim, E. Y., Bae, K., Ng, F. S., Glossop, N. R. J., Hardin, P. E. and Edery, I. (2002) 'Drosophila CLOCK Protein Is under Posttranscriptional Control and Influences Light-Induced Activity', *Neuron*, 34, pp. 69-81.
- Kim, E. Y. and Edery, I. (2006) 'Balance between DBT/CKIepsilon kinase and protein phosphatase activities regulate phosphorylation and stability of *Drosophila* CLOCK protein', *Proceedings of the National Academy of Sciences of the United States of America*, 103(16), pp. 6178-6183.
- King, A. N. and Sehgal, A. (2018) 'Molecular and circuit mechanisms mediating circadian clock output in the *Drosophila* brain', *Eur J Neurosci*.
- Kirschvink, J. L. (1992) 'Uniform Magnetic Fields and Double-Wrapped Coil Systems: Improved Techniques for the Design of Bioelectromagnetic Experiments', *Bioelectromagnetics*, 13, pp. 401-411.
- Kistenpfennig, C., Grebler, R., Ogueta, M., Hermann-Luibl, C., Schlichting, M., Stanewsky, R., Senthilan, P. R. and Helfrich-Förster, C. (2017a) 'A New Rhodopsin Influences Light-dependent Daily Activity Patterns of Fruit Flies', *Journal of Biological Rhythms*, 32(5), pp. 406-422.
- Kistenpfennig, C., Nakayama, M., Nihara, R., Tomioka, K., Helfrich-Förster, C. and Yoshii, T. (2017b) 'A Tug-of-War between Cryptochrome and the Visual System Allows the Adaptation of Evening Activity to Long Photoperiods in *Drosophila melanogaster*', *Journal of Biological Rhythms*, 33(1), pp. 24-34.
- Klarsfeld, A., Malpel, S., Michard-Vanhée, C., Picot, M., Chélot, E. and Rouyer, F. (2004) 'Novel Features of Cryptochrome-Mediated Photoreception in the Brain Circadian Clock of *Drosophila*', *The Journal of Neuroscience*, 24(6), pp. 1468.
- Kloss, B., Price, J. L., Saez, L., Blau, J., Rothenfluh, A., Wesley, C. S. and Young, M. W. (1998) 'The *Drosophila* Clock Gene double-time Encodes a Protein Closely Related to Human Casein Kinase I', *Cell*, 94, pp. 97-107.
- Kloss, B., Rothenfluh, A., Young, M. W. and Saez, L. (2001) 'Phosphorylation of PERIOD Is Influenced by Cycling Physical Associations of DOUBLE-TIME, PERIOD, and TIMELESS in the *Drosophila* Clock', *Neuron*, 30, pp. 699-706.
- Knowles, A., Koh, K., Wu, J. T., Chien, C. T., Chamovitz, D. A. and Blau, J. (2009) 'The COP9 signalosome is required for light-dependent timeless degradation and *Drosophila* clock resetting', *J Neurosci*, 29(4), pp. 1152-62.

Bibliography

- Ko, C. H. and Takahashi, J. S. (2006) 'Molecular components of the mammalian circadian clock', *Human Molecular Genetics*, 15(suppl_2), pp. R271-R277.
- Ko, H. W., Jiang, J. and Edery, I. (2002) 'Role for Slimb in the degradation of Drosophila Period protein phosphorylated by Doubletime', *Nature*, 420(6916), pp. 669-73.
- Koh, K., Zheng, X. and Sehgal, A. (2006) 'JETLAG Resets the Drosophila Circadian Clock by Promoting Light-Induced Degradation of TIMELESS', *SCIENCE*, 312, pp. 1809-1812.
- Kolosova, N., Gorenstein, N., Kish, C. M. and Dudareva, N. (2001) 'Regulation of circadian methyl benzoate emission in diurnally and nocturnally emitting plants', *Plant Cell*, 13(10), pp. 2333-2347.
- Kondo, T. (2007) 'A Cyanobacterial Circadian Clock Based on the Kai Oscillator', *Cold Spring Harb Symp Quant Biol*, 72, pp. 47-55.
- Konopka, R. J. and Benzer, S. (1971) 'Clock Mutants of Drosophila melanogaster', *PNAS*, 68(9), pp. 2112-2116.
- Konopka, R. J., Pittendrigh, C. and Orr, D. (1989) 'Reciprocal behaviour associated with altered homeostasis and photosensitivity of Drosophila clock mutants', *Journal of Neurogenetics*, 21(4), pp. 243-252.
- Kornmann, B., Schaad, O., Bujard, H., Takahashi, J. S. and Schibler, U. (2007) 'System-driven and oscillator-dependent circadian transcription in mice with a conditionally active liver clock', *PLoS Biol*, 5(2), pp. e34.
- Krishnan, B., Dryer, S. E. and Hardin, P. E. (1999) 'Circadian rhythms in olfactory responses of Drosophila melanogaster', *Nature*, 400(6742), pp. 375-378.
- Krishnan, B., Levine, J. D., Lynch, M. K. S., Dowse, H. B., Funes, P., Hall, J. C., Hardin, P. E. and Dryer, S. E. (2001) 'A new role for cryptochrome in a Drosophila circadian oscillator', *Letters to Nature*, 411, pp. 313-317.
- Krizo, J. A. and Mintz, E. M. (2015) 'Sex differences in behavioral circadian rhythms in laboratory rodents', *Frontiers in endocrinology*, 5, pp. 234-234.
- Krupp, J. J., Billeter, J.-C., Wong, A., Choi, C., Nitabach, M. N. and Levine, J. D. (2013) 'Pigment-dispersing factor modulates pheromone production in clock cells that influence mating in drosophila', *Neuron*, 79(1), pp. 54-68.
- Krupp, J. J., Kent, C., Billeter, J.-C., Azanchi, R., So, A. K. C., Schonfeld, J. A., Smith, B. P., Lucas, C. and Levine, J. D. (2008) 'Social Experience Modifies Pheromone Expression and Mating Behavior in Male Drosophila melanogaster', *Current Biology*, 18(18), pp. 1373-1383.
- Kumar, S., Chen, D. and Sehgal, A. (2012) 'Dopamine acts through Cryptochrome to promote acute arousal in Drosophila', *Genes Dev*, 26(11), pp. 1224-34.
- Lamaze, A., Kratschmer, P., Chen, K. F., Lowe, S. and Jepson, J. E. C. (2018) 'A Wake-Promoting Circadian Output Circuit in Drosophila', *Curr Biol*.
- Lamaze, A., Ozturk-Colak, A., Fischer, R., Peschel, N., Koh, K. and Jepson, J. E. (2017) 'Regulation of sleep plasticity by a thermo-sensitive circuit in Drosophila', *Sci Rep*, 7, pp. 40304.
- Lamba, P., Bilodeau-Wentworth, D., Emery, P. and Zhang, Y. (2014) 'Morning and evening oscillators cooperate to reset circadian behavior in response to light input', *Cell Rep*, 7(3), pp. 601-8.

- Lamba, P., Foley, L. E. and Emery, P. (2018) 'Neural network interactions modulate CRY-dependent photoresponses in *Drosophila*', *J Neurosci*.
- Lear, B. C., Merrill, C. E., Lin, J.-M., Schroeder, A., Zhang, L. and Allada, R. (2005) 'A G Protein-Coupled Receptor, groom-of-PDF, Is Required for PDF Neuron Action in Circadian Behavior', *Neuron*, 48(2), pp. 221-227.
- Lear, B. C., Zhang, L. and Allada, R. (2009) 'The neuropeptide PDF acts directly on evening pacemaker neurons to regulate multiple features of circadian behavior', *PLoS Biol*, 7(7), pp. e1000154.
- Lee, C., Bae, K. and Edery, I. (1999) 'PER and TIM inhibit the DNA binding activity of a *Drosophila* CLOCK-CYC/dbMAL1 heterodimer without disrupting formation of the heterodimer: a basis for circadian transcription', *Molecular and cellular biology*, 19(8), pp. 5316-5325.
- Lee, T. and Luo, L. (1999) 'Mosaic Analysis with a Repressible Cell Marker for Studies of Gene Function in Neuronal Morphogenesis', *Neuron*, 22(3), pp. 451-461.
- LeGates, T. A., Altimus, C. M., Wang, H., Lee, H.-K., Yang, S., Zhao, H., Kirkwood, A., Weber, E. T. and Hattar, S. (2012) 'Aberrant light directly impairs mood and learning through melanopsin-expressing neurons', *Nature*, 491, pp. 594.
- Lelito, K. R. and Shafer, O. T. (2012) 'Reciprocal cholinergic and GABAergic modulation of the small ventrolateral pacemaker neurons of *Drosophila*'s circadian clock neuron network', *Journal of Neurophysiology*, 107(8), pp. 2096-2108.
- Levi, F., Okyar, A., Dulong, S., Innominato, P. F. and Clairambault, J. (2010) 'Circadian Timing in Cancer Treatments', *Annual Review of Pharmacology and Toxicology*, 50(1), pp. 377-421.
- Levi, F. and Schibler, U. (2007) 'Circadian rhythms: mechanisms and therapeutic implications', *Annu Rev Pharmacol Toxicol*, 47, pp. 593-628.
- Levine, J. D., Funes, P., Dowse, H. B. and Hall, J. C. (2002a) 'Advanced analysis of a cryptochrome mutation's effects on the robustness and phase of molecular cycles in isolated peripheral tissues of *Drosophila*', *BMC Neuroscience*, 3(5).
- Levine, J. D., Funes, P., Dowse, H. B. and Hall, J. C. (2002b) 'Resetting the Circadian Clock by Social Experience in *Drosophila melanogaster*', *Science*, 298(5600), pp. 2010.
- Li, M. T., Cao, L. H., Xiao, N., Tang, M., Deng, B., Yang, T., Yoshii, T. and Luo, D. G. (2018) 'Hub-organized parallel circuits of central circadian pacemaker neurons for visual photoentrainment in *Drosophila*', *Nat Commun*, 9(1), pp. 4247.
- Li, Y., Guo, F., Shen, J. and Rosbash, M. (2014) 'PDF and cAMP enhance PER stability in *Drosophila* clock neurons', *PNAS*, 111, pp. 1284-1290.
- Liang, X., Ho, M. C. W., Zhang, Y., Li, Y., Wu, M. N., Holy, T. E. and Taghert, P. H. (2019) 'Morning and Evening Circadian Pacemakers Independently Drive Premotor Centers via a Specific Dopamine Relay', *Neuron*.
- Liang, X., Holy, T. E. and Taghert, P. H. (2016) 'Synchronous *Drosophila* circadian pacemakers display nonsynchronous Ca²⁺ rhythms in vivo', *SCIENCE*, 351(6276), pp. 976-981.
- Liang, X., Holy, T. E. and Taghert, P. H. (2017) 'A Series of Suppressive Signals within the *Drosophila* Circadian Neural Circuit Generates Sequential Daily Outputs', *Neuron*, 94(6), pp. 1173-1189.e4.

Bibliography

- Lim, C., Chung, B. Y., Pitman, J. L., McGill, J. J., Pradhan, S., Lee, J., Keegan, K. P., Choe, J. and Allada, R. (2007) 'clockwork orange encodes a transcriptional repressor important for circadian clock amplitude in *Drosophila*', *Curr Biol*, 17(12), pp. 1082-1089.
- Lima, S. Q. and Miesenböck, G. (2005) 'Remote Control of Behavior through Genetically Targeted Photostimulation of Neurons', *Cell*, 121(1), pp. 141-152.
- Lin, F. J., Song, W., Meyer-Bernstein, E., Naidoo, N. and Sehgal, A. (2001) 'Photic signaling by cryptochrome in the *Drosophila* circadian system', *Mol Cell Biol*, 21(21), pp. 7287-94.
- Lindsley, D. L. and Zimm, G. G. (1992) 'The Genome of *Drosophila melanogaster*.', *Academic Press, San Diego*, 1133.
- Linford, N. J., Bilgir, C., Ro, J. and Pletcher, S. D. (2013) 'Measurement of lifespan in *Drosophila melanogaster*', *J Vis Exp*, (71).
- Liu, X., Zwiebel, L. J., Hinton, D., Benzer, S., Hall, J. C. and Rosbash, M. (1992) 'The period Gene Encodes a Predominantly Nuclear Protein Adult *Drosophila*', *The Journal of Neuroscience*, 12(7), pp. 2735-2744.
- Liu, Y. and Lehmann, M. (2008) 'A Genomic Response to the Yeast Transcription Factor GAL4 in *Drosophila*', *Fly*, 2(2), pp. 92-98.
- Loesel, R. and Homberg, U. (2001) 'Anatomy and physiology of neurons with processes in the accessory medulla of the cockroach *Leucophaea maderae*', *Journal of Comparative Neurology*, 439(2), pp. 193-207.
- Maeda, K., Robinson, A. J., Henbest, K. B., Hogben, H. J., Biskup, T., Ahmad, M., Schleicher, E., Weber, S., Timmel, C. R. and Hore, P. J. (2012) 'Magnetically sensitive light-induced reactions in cryptochrome are consistent with its proposed role as a magnetoreceptor', *Proc Natl Acad Sci U S A*, 109(13), pp. 4774-9.
- Majercak, J., Sidote, D., Hardin, P. E. and Edery, I. (1999) 'How a Circadian Clock Adapts to Seasonal Decreases in Temperature and Day Length', *Neuron*, 24, pp. 219-230.
- Malpel, S., Klarsfeld, A. and Rouyer, F. (2002) *Larval optic nerve and adult extra-retinal photoreceptors sequentially associate with clock neurons during *Drosophila* brain development.*
- Mansour, H. A., Monk, T. H. and Nimgaonkar, V. L. (2005) 'Circadian genes and bipolar disorder', *Ann Med*, 37(3), pp. 196-205.
- Martinek, S., Inonog, S., Manoukian, A. S. and Young, M. W. (2001) 'A Role for the Segment Polarity Gene *shaggy/GSK-3* in the *Drosophila* Circadian Clock', *Cell*, 105, pp. 769-779.
- Matsumoto, A., Ukai-Tadenuma, M., Yamada, R. G., Houl, J., Uno, K. D., Kasukawa, T., Dauwalder, B., Itoh, T. Q., Takahashi, K., Ueda, R., Hardin, P. E., Tanimura, T. and Ueda, H. R. (2007) 'A functional genomics strategy reveals clockwork orange as a transcriptional regulator in the *Drosophila* circadian clock', *Genes Dev*, 21(13), pp. 1687-700.
- Matsuo, T. and Ishiura, M. (2010) 'New Insights into the Circadian Clock in *Chlamydomonas*', *International Review of Cell and Molecular Biology: Academic Press*, pp. 281-314.
- McClung, C. A. (2007) 'Circadian genes, rhythms and the biology of mood disorders', *Pharmacol Ther*, 114(2), pp. 222-32.
- McClung, C. R. (2006) 'Plant circadian rhythms', *The Plant cell*, 18(4), pp. 792-803.

- Mealey-Ferrara, M. L., Montalvo, A. G. and Hall, J. C. (2003) 'Effects of combining a cryptochrome mutation with other visual-system variants on entrainment of locomotor and adult-emergence rhythms in *Drosophila*', *Journal of Neurogenetics*, 17(2-3), pp. 171-221.
- Mei, Q. and Dvornyk, V. (2015) 'Evolutionary History of the Photolyase/Cryptochrome Superfamily in Eukaryotes', *PLoS One*, 10(9), pp. e0135940.
- Meireles-Filho, A. C. and Kyriacou, C. P. (2013) 'Circadian rhythms in insect disease vectors', *Mem Inst Oswaldo Cruz*, 108 Suppl 1, pp. 48-58.
- Melzig, J., Buchner, S., Wiebel, F., Wolf, R., Burg, M. G., Pak, W. L. and Buchner, E. (1996) 'Genetic depletion of histamine from the nervous system of *Drosophila* eliminates specific visual and mechanosensory behavior', *J Comp Physiol A*, 179, pp. 763-773.
- Menet, J. S., Abruzzi, K. C., Desrochers, J., Rodriguez, J. and Rosbash, M. (2010) 'Dynamic PER repression mechanisms in the *Drosophila* circadian clock: from on-DNA to off-DNA', *Genes Dev*, 24(4), pp. 358-67.
- Mertens, I., Vandingenen, A., Johnson, E. C., Shafer, O. T., Li, W., Trigg, J. S., De Loof, A., Schoofs, L. and Taghert, P. H. (2005) 'PDF receptor signaling in *Drosophila* contributes to both circadian and geotactic behaviors', *Neuron*, 48(2), pp. 213-9.
- Meyer-Bernstein, E. L. and Sehgal, A. (2001) 'Book Review: Molecular Regulation of Circadian Rhythms in *Drosophila* and Mammals', *The Neuroscientist*, 7(6), pp. 496-505.
- Mezan, S., Feuz, J. D., Deplancke, B. and Kadener, S. (2016) 'PDF Signaling Is an Integral Part of the *Drosophila* Circadian Molecular Oscillator', *Cell Rep*, 17(3), pp. 708-719.
- Mohawk, J. A., Green, C. B. and Takahashi, J. S. (2012) 'Central and peripheral circadian clocks in mammals', *Annual review of neuroscience*, 35, pp. 445-462.
- Montell, C., Jones, K., Zuker, C. and Rubin, G. (1987) 'A second opsin gene expressed in the ultraviolet-sensitive R7 photoreceptor cells of *Drosophila melanogaster*', *The Journal of Neuroscience*, 7(5), pp. 1558.
- Morioka, E., Matsumoto, A. and Ikeda, M. (2012) 'Neuronal influence on peripheral circadian oscillators in pupal *Drosophila* prothoracic glands', *Nature Communications*, 3, pp. 909.
- Mrosovsky, N. (1999) 'Masking: History, Definitions, and Measurement', *Chronobiology International*, 16(4), pp. 415-429.
- Muller, M. and Carell, T. (2009) 'Structural biology of DNA photolyases and cryptochromes', *Curr Opin Struct Biol*, 19(3), pp. 277-85.
- Muraro, N. I., Pérez, N. and Ceriani, M. F. (2013) 'The circadian system: Plasticity at many levels', *Neuroscience*, 247, pp. 280-293.
- Musiek, E. S. (2015) 'Circadian clock disruption in neurodegenerative diseases: cause and effect?', *Front Pharmacol*, 6, pp. 29.
- Myers, E. M., Yu, J. and Sehgal, A. (2003) 'Circadian Control of Eclosion: Interaction between a Central and Peripheral Clock in *Drosophila melanogaster*', *Current Biology*, 13(6), pp. 526-533.
- Myers, M. P., Wager-Smith, K., Rothenfluh, A. and Young, M. W. (1996) 'Light-Induced Degradation of TIMELESS and Entrainment of the *Drosophila* Circadian Clock', *SCIENCE*, 271, pp. 1736-1740.

Bibliography

- Naidoo, N., Song, W., Hunter-Ensor, M. and Sehgal, A. (1999) 'A Role for the Proteasome in the Light Response of the Timeless Clock Protein', *SCIENCE*, 285, pp. 1737-1741.
- Nassel, D. R. and Winther, A. M. (2010) 'Drosophila neuropeptides in regulation of physiology and behavior', *Prog Neurobiol*, 92(1), pp. 42-104.
- Ni, J.-Q., Markstein, M., Binari, R., Pfeiffer, B., Liu, L.-P., Villalta, C., Booker, M., Perkins, L. and Perrimon, N. (2007) 'Vector and parameters for targeted transgenic RNA interference in *Drosophila melanogaster*', *Nature Methods*, 5, pp. 49.
- Ni, J. D., Baik, L. S., Holmes, T. C. and Montell, C. (2017) 'A rhodopsin in the brain functions in circadian photoentrainment in *Drosophila*', *Nature*.
- Nitabach, M. N., Wu, Y., Sheeba, V., Lemon, W. C., Strumbos, J., Zelensky, P. K., White, B. H. and Holmes, T. C. (2006) 'Electrical hyperexcitation of lateral ventral pacemaker neurons desynchronizes downstream circadian oscillators in the fly circadian circuit and induces multiple behavioral periods', *The Journal of neuroscience : the official journal of the Society for Neuroscience*, 26(2), pp. 479-489.
- O'Tousa, J. E., Baehr, W., Martin, R. L., Hirsh, J., Pak, W. L. and Applebury, M. L. (1985) 'The *Drosophila ninaE* gene encodes an opsin', *Cell*, 40(4), pp. 839-850.
- Ogueta, M., Hardie, R. C. and Stanewsky, R. (2018) 'Non-canonical Phototransduction Mediates Synchronization of the *Drosophila melanogaster* Circadian Clock and Retinal Light Responses', *Curr Biol*.
- Oh, Y., Jang, D., Sonn, J. Y. and Choe, J. (2013) 'Histamine-HisCl1 receptor axis regulates wake-promoting signals in *Drosophila melanogaster*', *PLoS One*, 8(7), pp. e68269.
- Okamura, H., Miyake, S., Sumi, Y., Yamaguchi, S., Yasui, A., Muijtjens, M., Hoeijmakers, J. H. J. and van der Horst, G. T. J. (1999) 'Photic Induction of *mPer1* and *mPer2* in *Cry*-Deficient Mice Lacking a Biological Clock', *Science*, 286(5449), pp. 2531.
- Ozturk, N., Selby, C. P., Annayev, Y., Zhong, D. and Sancar, A. (2011) 'Reaction mechanism of *Drosophila* cryptochrome', *Proc Natl Acad Sci U S A*, 108(2), pp. 516-21.
- Ozturk, N., Selby, C. P., Zhong, D. and Sancar, A. (2014) 'Mechanism of photosignaling by *Drosophila* cryptochrome: role of the redox status of the flavin chromophore', *J Biol Chem*, 289(8), pp. 4634-42.
- Ozturk, N., Song, S. H., Selby, C. P. and Sancar, A. (2008) 'Animal type 1 cryptochromes. Analysis of the redox state of the flavin cofactor by site-directed mutagenesis', *J Biol Chem*, 283(6), pp. 3256-63.
- Ozturk, N., VanVickle-Chavez, S. J., Akileswaran, L., Van Gelder, R. N. and Sancar, A. (2013) 'Ramshackle (Brwd3) promotes light-induced ubiquitylation of *Drosophila* Cryptochrome by DB1-CUL4-ROC1 E3 ligase complex', *Proceedings of the National Academy of Sciences of the United States of America*, 110(13), pp. 4980-4985.
- Painter, M. S., Dommer, D. H., Altizer, W. W., Muheim, R. and Phillips, J. B. (2013) 'Spontaneous magnetic orientation in larval *Drosophila* shares properties with learned magnetic compass responses in adult flies and mice', *J Exp Biol*, 216(Pt 7), pp. 1307-16.
- Panda, S., Hogenesch, J. B. and Kay, S. A. (2002) 'Circadian rhythms from flies to human', *Nature*, 417(6886), pp. 329-335.

- Pandi-Perumal, S. R., Trakht, I., Spence, D. W., Srinivasan, V., Dagan, Y. and Cardinali, D. P. (2008) 'The roles of melatonin and light in the pathophysiology and treatment of circadian rhythm sleep disorders', *Nature Clinical Practice Neurology*, 4, pp. 436.
- Pantazis, A., Segaran, A., Liu, C. H., Nikolaev, A., Rister, J., Thum, A. S., Roeder, T., Semenov, E., Juusola, M. and Hardie, R. C. (2008) 'Distinct roles for two histamine receptors (hclA and hclB) at the *Drosophila* photoreceptor synapse', *J Neurosci*, 28(29), pp. 7250-9.
- Papatsenko, D., Sheng, G. and Desplan, C. (1997) 'A new rhodopsin in R8 photoreceptors of *Drosophila*: evidence for coordinate expression with Rh3 in R7 cells', *Development*, 124(9), pp. 1665.
- Parisky, K. M., Agosto, J., Pulver, S. R., Shang, Y., Kuklin, E., Hodge, J. J. L., Kang, K., Liu, X., Garrity, P. A., Rosbash, M. and Griffith, L. C. (2008) 'PDF Cells Are a GABA-Responsive Wake-Promoting Component of the *Drosophila* Sleep Circuit', *Neuron*, 60(4), pp. 672-682.
- Park, J. H., Helfrich-Förster, C., Lee, G., Liu, L., Rosbash, M. and Hall, J. C. (2000) 'Differential regulation of circadian pacemaker output by separate clock genes in *Drosophila*', *Proc Natl Acad Sci U S A*, 97(7), pp. 3608-13.
- Pegoraro, M., Bafna, A., Davies, N. J., Shuker, D. M. and Tauber, E. (2016) 'DNA methylation changes induced by long and short photoperiods in *Nasonia*', *Genome Res*, 26(2), pp. 203-10.
- Peschel, N., Chen, K. F., Szabo, G. and Stanewsky, R. (2009) 'Light-dependent interactions between the *Drosophila* circadian clock factors cryptochrome, jetlag, and timeless', *Curr Biol*, 19(3), pp. 241-7.
- Peschel, N. and Helfrich-Förster, C. (2011) 'Setting the clock-by nature: circadian rhythm in the fruitfly *Drosophila melanogaster*', *FEBS Lett*, 585(10), pp. 1435-42.
- Peschel, N., Veleri, S. and Stanewsky, R. (2006) 'Veela defines a molecular link between Cryptochrome and Timeless in the light-input pathway to *Drosophila*'s circadian clock', *Proc Natl Acad Sci U S A*, 103(46), pp. 17313-8.
- Pfeiffer, B. D., Ngo, T.-T. B., Hibbard, K. L., Murphy, C., Jenett, A., Truman, J. W. and Rubin, G. M. (2010) 'Refinement of Tools for Targeted Gene Expression in *Drosophila*', *Genetics*, 186(2), pp. 735.
- Picot, M., Cusumano, P., Klarsfeld, A., Ueda, R. and Rouyer, F. (2007) 'Light Activates Output from Evening Neurons and Inhibits Output from Morning Neurons in the *Drosophila* Circadian Clock', *PLoS Biology*, 5(11), pp. e315.
- Pittendrigh, C., Bruce, V. and Kaus, P. (1958) 'On the Significance of Transients in Daily Rhythms ', *PNAS*, 44, pp. 965-973.
- Pittendrigh, C. and Daan, S. (1975) 'A Functional Analysis of Circadian Pacemakers in Nocturnal Rodents', *Journal of Comparative Physiology*.
- Pittendrigh, C. S. (1954) 'ON TEMPERATURE INDEPENDENCE IN THE CLOCK SYSTEM CONTROLLING EMERGENCE TIME IN *DROSOPHILA*', *Proceedings of the National Academy of Sciences of the United States of America*, 40(10), pp. 1018-1029.
- Plautz, J. D., Kaneko, M., Hall, J. C. and Kay, S. A. (1997a) 'Independent Photoreceptive Circadian Clocks Throughout *Drosophila*', *SCIENCE*, 278, pp. 1632-1635.

Bibliography

- Plautz, J. D., Straume, M., Stanewsky, R., Jamison, C. F., Brandes, C., Dowse, H. B., Hall, J. C. and Kay, S. A. (1997b) 'Quantitative Analysis of *Drosophila* period Gene Transcription in Living Animals', *Journal of Biological Rhythms*, 12(3), pp. 204-217.
- Pollock, J. A. and Benzer, S. (1988) 'Transcript localization of four opsin genes in the three visual organs of *Drosophila*; RH2 is ocellus specific', *Nature*, 333(6175), pp. 779-782.
- Price, J. L., Blau, J., Rothenfluh, A., Abodeely, M., Kloss, B. and Young, M. W. (1998) 'double-time Is a Novel *Drosophila* Clock Gene that Regulates PERIOD Protein Accumulation', *Cell*, 94, pp. 83-95.
- Price, J. L., Dembinska, M. E., Young, M. W. and Rosbash, M. (1995) 'Suppression of PERIOD protein abundance and circadian cycling by the *Drosophila* clock mutation timeless', *The EMBO Journal*, 14(16), pp. 4044-4049.
- Qin, S., Yin, H., Yang, C., Dou, Y., Liu, Z., Zhang, P., Yu, H., Huang, Y., Feng, J., Hao, J., Hao, J., Deng, L., Yan, X., Dong, X., Zhao, Z., Jiang, T., Wang, H.-W., Luo, S.-J. and Xie, C. (2016) 'A magnetic protein biocompass', *Nature Materials*, 15(2), pp. 217-226.
- Qiu, J. and Hardin, P. E. (1996) 'per mRNA cycling is locked to lights-off under photoperiodic conditions that support circadian feedback loop function', *Molecular and Cellular Biology*, 16(8), pp. 4182.
- Rajashankar, K. P. and Singh, R. N. (1994) 'Neuroarchitecture of the tritocerebrum of *Drosophila melanogaster*', *The Journal of Comparative Neurology*, 349(4), pp. 633-645.
- Rakshit, K. and Giebultowicz, J. M. (2013) 'Cryptochrome restores dampened circadian rhythms and promotes healthspan in aging *Drosophila*', *Aging Cell*, 12(5), pp. 752-762.
- Rakshit, K., Krishnan, N., Guzik, E. M., Pyza, E. and Giebultowicz, J. M. (2012) 'Effects of Aging on the Molecular Circadian Oscillations in *Drosophila*', *Chronobiology International*, 29(1), pp. 5-14.
- Ramirez-Moreno, M. (2017) *The small GTPase Rho1 couples peptidergic control of circadian behaviour to molecular oscillator function in *Drosophila melanogaster**. Thesis for the degree of Doctor of Philosophy University of Southampton: UK.
- Reddy, P., Zehring, W. A., Wheeler, D. A., Pirrotta, V., Hadfield, C., Hall, J. C. and Rosbash, M. (1984) 'Molecular analysis of the *period* locus in *Drosophila melanogaster* and identification of a transcript involved in biological rhythms', *Cell*, 38(3), pp. 701-710.
- Renn, S. C. P., Park, J. H., Rosbash, M., Hall, J. C. and H., T. P. (1999) 'A pdf Neuropeptide Gene Mutation and Ablation of PDF Neurons Each Cause Severe Abnormalities of Behavioral Circadian Rhythms in *Drosophila*', *Cell*, 99, pp. 791-802.
- Rieger, D., Shafer, O. T., Tomioka, K. and Helfrich-Förster, C. (2006) 'Functional Analysis of Circadian Pacemaker Neurons in *Drosophila melanogaster*', *The Journal of Neuroscience*, 26(9), pp. 2531.
- Rieger, D., Stanewsky, R. and Helfrich-Förster, C. (2003) 'Cryptochrome, Compound Eyes, Hofbauer-Buchner Eyelets, and Ocelli Play Different Roles in the Entrainment and Masking Pathway of the Locomotor Activity Rhythm in the Fruit Fly *Drosophila Melanogaster*', *J Biol Rhythms*, 18(5), pp. 377-391.
- Ritz, T., Adem, S. and Schulten, K. (2000) 'A Model for Photoreceptor-Based Magnetoreception in Birds', *Biophysical Journal*, 78, pp. 707-718.

- Ritz, T., Ahmad, M., Mouritsen, H., Wiltschko, R. and Wiltschko, W. (2010) 'Photoreceptor-based magnetoreception: optimal design of receptor molecules, cells, and neuronal processing', *J R Soc Interface*, 7 Suppl 2, pp. S135-46.
- Roberts, L., Leise, T. L., Noguchi, T., Galschiodt, A. M., Houl, J. H., Welsh, D. K. and Holmes, T. C. (2015) 'Light Evokes Rapid Circadian Network Oscillator Desynchrony Followed by Gradual Phase Retuning of Synchrony', *Current Biology*, 25(7), pp. 858-867.
- Robie, A. A., Hirokawa, J., Edwards, A. W., Umayam, L. A., Lee, A., Phillips, M. L., Card, G. M., Korff, W., Rubin, G. M., Simpson, J. H., Reiser, M. B. and Branson, K. (2017) 'Mapping the Neural Substrates of Behavior', *Cell*, 170(2), pp. 393-406.e28.
- Roche, J. P., Tallyn, B. C. P. and Dowse, H. B. (1998) 'Courtship Bout Duration in per Circadian Period Mutants In *Drosophila melanogaster*', *Behavior Genetics*, 28(5), pp. 391-394.
- Rodgers, C. T. (2009) 'Magnetic field effects in chemical systems', *Pure and Applied Chemistry*, 81(1).
- Rodgers, C. T. and Hore, P. J. (2009) 'Chemical magnetoreception in birds: the radical pair mechanism', *Proc Natl Acad Sci U S A*, 106(2), pp. 353-60.
- Roenneberg, T., Allebrandt, Karla V., Mellow, M. and Vetter, C. (2012) 'Social Jetlag and Obesity', *Current Biology*, 22(10), pp. 939-943.
- Roenneberg, T. and Mellow, M. (2016) 'The Circadian Clock and Human Health', *Current Biology*, 26(10), pp. R432-R443.
- Rosato, E., Codd, V., Mozzotta, G., Piccin, A., Zordan, M., Costa, R. and Kyriacou, C. P. (2001) 'Light-dependent interaction between *Drosophila* CRY and the clock protein PER mediated by the carboxy terminus of CRY', *Curr Biol*, 11, pp. 909-917.
- Rosato, E., Trevisan, A., Sandrelli, F., Zordan, M., Kyriacou, C. P. and Costa, R. (1997) 'Conceptual translation of timeless reveals alternative initiating methionines in *Drosophila*', *Nucleic Acids Research*, 25(3), pp. 445-457.
- Ruby, N. F., Brennan, T. J., Xie, X., Cao, V., Franken, P., Heller, H. C. and O'Hara, B. F. (2002) 'Role of Melanopsin in Circadian Responses to Light', *SCIENCE*, 298, pp. 2211-2213.
- Rund, S. S. C., O'Donnell, A. J., Gentile, J. E. and Reece, S. E. (2016) 'Daily Rhythms in Mosquitoes and Their Consequences for Malaria Transmission', *Insects*, 7(2), pp. 14.
- Rush, B. L., Murad, A., Emery, P. and Giebultowicz, J. M. (2006) 'Ectopic CRYPTOCHROME Renders TIM Light Sensitive in the *Drosophila* Ovary', *Journal of Biological Rhythms*, 21(4), pp. 272-278.
- Rutila, J. E., Suri, V., Le, M., So, W. V., Rosbash, M. and Hall, J. C. (1998) 'CYCLE Is a Second bHLH-PAS Clock Protein Essential for Circadian Rhythmicity and Transcription of *Drosophila* period and timeless', *Cell*, 93, pp. 805-814.
- Saez, L., Derasmo, M., Meyer, P., Stieglitz, J. and Young, M. W. (2011) 'A key temporal delay in the circadian cycle of *Drosophila* is mediated by a nuclear localization signal in the timeless protein', *Genetics*, 188(3), pp. 591-600.
- Saez, L. and Young, M. W. (1996) 'Regulation of Nuclear Entry of the *Drosophila* Clock Proteins Period and Timeless', *Neuron*, 17(5), pp. 911-920.
- Saint-Charles, A., Michard-Vanhee, C., Alejevski, F., Chelot, E., Boivin, A. and Rouyer, F. (2016) 'Four of the six *Drosophila* rhodopsin-expressing photoreceptors can mediate circadian entrainment in low light', *J Comp Neurol*.

Bibliography

- Sakai, K., Tsutsui, K., Yamashita, T., Iwabe, N., Takahashi, K., Wada, A. and Shichida, Y. (2017) 'Drosophila melanogaster rhodopsin Rh7 is a UV-to-visible light sensor with an extraordinarily broad absorption spectrum', *Sci Rep*, 7(1), pp. 7349.
- Sakai, T. and Ishida, N. (2001) 'Circadian rhythms of female mating activity governed by clock genes in Drosophila', *Proceedings of the National Academy of Sciences of the United States of America*, 98(16), pp. 9221-9225.
- Salcedo, E., Huber, A., Henrich, S., V. Chadwell, L., Chou, W.-H., Paulsen, R. and Britt, S. (2000) *Blue- and Green-Absorbing Visual Pigments of Drosophila : Ectopic Expression and Physiological Characterization of the R8 Photoreceptor Cell-Specific Rh5 and Rh6 Rhodopsins*.
- Salvaterra, P. M. and Kitamoto, T. (2001) 'Drosophila cholinergic neurons and processes visualized with Gal4/UAS-GFP', *Gene Expression Patterns*, 1, pp. 73-82.
- Sancar, A. (2003) 'Structure and Function of DNA Photolyase and Cryptochrome Blue-Light Photoreceptors', *Chem Rev*, 103, pp. 2203-2237.
- Sandrelli, F., Tauber, E., Pegoraro, M., Mazzotta, G. M., Cisotto, P., Landskorn, J., Stanewsky, R., Piccin, A., Rosato, E., Zordan, M., Costa, R. and Kyriacou, C. P. (2007) 'A Molecular Basis for Natural Selection at the timeless Locus in Drosophila melanogaster', *SCIENCE*, 316, pp. 1898-1900.
- Sarfraz, M., Keddie, A. B. and Dossall, L. M. (2005) 'Biological control of the diamondback moth, *Plutella xylostella*: A review', *Biocontrol Science and Technology*, 15(8), pp. 763-789.
- Sathyanarayanan, S., Zheng, X., Xiao, R. and Sehgal, A. (2004) 'Posttranslational Regulation of Drosophila PERIOD Protein by Protein Phosphatase 2A', *Cell*, 116, pp. 603-615.
- Saunders, D. S., Gillanders, S. W. and Lewis, R. D. (1994) 'Light-pulse phase response curves for the locomotor activity rhythm in Period mutants of Drosophila melanogaster', *Journal of Insect Physiology*, 40(11), pp. 957-968.
- Schlichting, M., Grebler, R., Peschel, N., Yoshii, T. and Helfrich-Förster, C. (2014) 'Moonlight Detection by Drosophila's Endogenous Clock Depends on Multiple Photopigments in the Compound Eyes', *Journal of Biological Rhythms*, 29(2), pp. 75-86.
- Schlichting, M., Menegazzi, P., Lelito, K. R., Yao, Z., Buhl, E., Dalla Benetta, E., Bahle, A., Denike, J., Hodge, J. J., Helfrich-Förster, C. and Shafer, O. T. (2016) 'A Neural Network Underlying Circadian Entrainment and Photoperiodic Adjustment of Sleep and Activity in Drosophila', *J Neurosci*, 36(35), pp. 9084-96.
- Schlichting, M., Menegazzi, P., Rosbash, M. and Helfrich-Förster, C. (2019) 'A distinct visual pathway mediates high light intensity adaptation of the circadian clock in Drosophila', *J Neurosci*.
- Schnaitmann, C., Garbers, C., Wachtler, T. and Tanimoto, H. (2013) 'Color Discrimination with Broadband Photoreceptors', *Current Biology*, 23(23), pp. 2375-2382.
- Schubert, F. K., Hagedorn, N., Yoshii, T., Helfrich-Förster, C. and Rieger, D. (2018) 'Neuroanatomical details of the lateral neurons of Drosophila melanogaster support their functional role in the circadian system', *J Comp Neurol*.
- Sehadova, H., Glaser, F. T., Gentile, C., Simoni, A., Giesecke, A., Albert, J. T. and Stanewsky, R. (2009) 'Temperature Entrainment of Drosophila's Circadian Clock Involves the Gene nocte and Signaling from Peripheral Sensory Tissues to the Brain', *Neuron*, 64(2), pp. 251-266.
- Sehgal, A., Price, J. L., Man, B. and Young, M. W. (1994) 'Loss of Circadian Behavioral Rhythms and per RNA Oscillations in the Drosophila Mutant timeless', *SCIENCE*, 263, pp. 1603-1606.

- Senthilan, P. R., Grebler, R., Reinhard, N., Rieger, D. and Helfrich-Förster, C. (2019) 'Role of Rhodopsins as Circadian Photoreceptors in the *Drosophila melanogaster*', *Biology (Basel)*, 8(1).
- Shafer, O. T., Helfrich-Förster, C., Renn, S. C. P. and Taghert, P. H. (2006) 'Reevaluation of *Drosophila melanogaster*'s neuronal circadian pacemakers reveals new neuronal classes', *The Journal of comparative neurology*, 498(2), pp. 180-193.
- Shafer, O. T., Kim, D. J., Dunbar-Yaffe, R., Nikolaev, V. O., Lohse, M. J. and Taghert, P. H. (2008) 'Widespread Receptivity to Neuropeptide PDF throughout the Neuronal Circadian Clock Network of *Drosophila* Revealed by Real-Time Cyclic AMP Imaging', *Neuron*, 58(2), pp. 223-237.
- Shafer, O. T., Levine, J. D., Truman, J. W. and Hall, J. C. (2004) 'Flies by Night: Effects of Changing Day Length on *Drosophila*'s Circadian Clock', *Current Biology*, 14(5), pp. 424-432.
- Shafer, O. T., Rosbash, M. and Truman, J. W. (2002) 'Sequential Nuclear Accumulation of the Clock Proteins Period and Timeless in the Pacemaker Neurons of *Drosophila melanogaster*', *The Journal of Neuroscience*, 22(14), pp. 5946.
- Shafer, O. T. and Yao, Z. (2014) 'Pigment-Dispersing Factor Signaling and Circadian Rhythms in Insect Locomotor Activity', *Current opinion in insect science*, 1, pp. 73-80.
- Shang, Y., Donelson, N. C., Vecsey, C. G., Guo, F., Rosbash, M. and Griffith, L. C. (2013) 'Short neuropeptide F is a sleep-promoting inhibitory modulator', *Neuron*, 80(1), pp. 171-83.
- Shang, Y., Griffith, L. C. and Rosbash, M. (2008) 'Light-arousal and circadian photoreception circuits intersect at the large PDF cells of the *Drosophila* brain', *Proceedings of the National Academy of Sciences of the United States of America*, 105(50), pp. 19587-19594.
- Shaw, B., Brain, P., Wijnen, H. and Fountain, M. T. (2018) 'Reducing *Drosophila suzukii* emergence through inter-species competition', *Pest Management Science*, 74(6), pp. 1466-1471.
- Shaw, B., Fountain, M. T. and Wijnen, H. (2018) 'Recording and reproducing the diurnal oviposition rhythms of wild populations of the soft- and stone- fruit pest *Drosophila suzukii*', *PLoS One*, 13(10), pp. e0199406.
- Shearman, L. P., Zylka, M. J., Weaver, D. R., Kolakowski, L. F., Jr. and Reppert, S. M. (1997) 'Two period Homologs: Circadian Expression and Photic Regulation in the Suprachiasmatic Nuclei', *Neuron*, 19(6), pp. 1261-1269.
- Sheeba, V., Fogle, K. J., Kaneko, M., Rashid, S., Chou, Y.-T., Sharma, V. K. and Holmes, T. C. (2008) 'Large ventral lateral neurons modulate arousal and sleep in *Drosophila*', *Current biology : CB*, 18(20), pp. 1537-1545.
- Siwicki, K. K., Eastman, C., Petersen, G., Rosbash, M. and Hall, J. C. (1988) 'Antibodies to the period gene product of *drosophila* reveal diverse tissue distribution and rhythmic changes in the visual system', *Neuron*, 1(2), pp. 141-150.
- So, W. V. and Rosbash, M. (1997) 'Post-transcriptional regulation contributes to *Drosophila* clock gene mRNA cycling', *The EMBO journal*, 16(23), pp. 7146-7155.
- Sonn, J. Y., Lee, J., Sung, M. K., Ri, H., Choi, J. K., Lim, C. and Choe, J. (2018) 'Serine metabolism in the brain regulates starvation-induced sleep suppression in *Drosophila melanogaster*', *Proc Natl Acad Sci U S A*, 115(27), pp. 7129-7134.
- Srivastava, M., Varma, V., Abhilash, L., Sharma, V. K. and Sheeba, V. (2019) 'Circadian Clock Properties and Their Relationships as a Function of Free-Running Period in *Drosophila melanogaster*', *Journal of Biological Rhythms*, pp. 0748730419837767.

Bibliography

- Stanewsky, R., Jamison, C. F., Plautz, J. D., Kay, S. A. and Hall, J. C. (1997) 'Multiple circadian-regulated elements contribute to cycling period gene expression in *Drosophila*', *The EMBO Journal* 16, pp. 5006-5018.
- Stanewsky, R., Kaneko, M., Emery, P., Beretta, B., Wager-Smith, K., Kay, S. A., Rosbash, M. and Hall, J. C. (1998) 'The cryb Mutation Identifies Cryptochrome as a Circadian Photoreceptor in *Drosophila*', *Cell*, 95, pp. 681-692.
- Stanewsky, R., Lynch, K. S., Brandes, C. and Hall, J. C. (2002) 'Mapping of Elements Involved in Regulating Normal Temporal period and timeless RNA Expression Patterns in *Drosophila melanogaster*', *Journal of Biological Rhythms*, 17(4), pp. 293-306.
- Stevens, R. G., Blask, D. E., Brainard, G. C., Hansen, J., Lockley, S. W., Provencio, I., Rea, M. S. and Reinlib, L. (2007) 'Meeting report: the role of environmental lighting and circadian disruption in cancer and other diseases', *Environ Health Perspect*, 115(9), pp. 1357-62.
- Stoleru, D., Nawathean, P., Fernández, M. d. I. P., Menet, J. S., Ceriani, M. F. and Rosbash, M. (2007) 'The *Drosophila* Circadian Network Is a Seasonal Timer', *Cell*, 129(1), pp. 207-219.
- Stoleru, D., Peng, Y., Agosto, J. and Rosbash, M. (2004) 'Coupled oscillators control morning and evening locomotor behaviour of *Drosophila*', *Nature*, 431(7010), pp. 862-68.
- Stoleru, D., Peng, Y., Nawathean, P. and Rosbash, M. (2005) 'A resetting signal between *Drosophila* pacemakers synchronizes morning and evening activity', *Nature*, 438(7065), pp. 238-42.
- Strauss, R. and Heisenberg, M. (1993) 'A Higher Control Center of Locomotor Behavior in the *Drosophila* Brain', *J Neurosci*, 13(5), pp. 1852-1861.
- Suri, V., Qian, Z., Hall, J. C. and Rosbash, M. (1998) 'Evidence that the TIM Light Response Is Relevant to Light-Induced Phase Shifts in *Drosophila melanogaster*', *Neuron*, 21, pp. 225-234.
- Suster, M. L., Seugnet, L., Bate, M. and Sokolowski, M. B. (2004) 'Refining GAL4-driven transgene expression in *Drosophila* with a GAL80 enhancer-trap', *Genesis*, 39(4), pp. 240-5.
- Szular, J., Sehadova, H., Gentile, C., Szabo, G., Chou, W. H., Britt, S. G. and Stanewsky, R. (2012) 'Rhodopsin 5- and Rhodopsin 6-mediated clock synchronization in *Drosophila melanogaster* is independent of retinal phospholipase C-beta signaling', *J Biol Rhythms*, 27(1), pp. 25-36.
- Tang, C. H., Hinteregger, E., Shang, Y. and Rosbash, M. (2010) 'Light-mediated TIM degradation within *Drosophila* pacemaker neurons (s-LN_vs) is neither necessary nor sufficient for delay zone phase shifts', *Neuron*, 66(3), pp. 378-85.
- Taylor, G. K., Krapp, H. G. and Simpson, S. J. (2007) 'Sensory systems and flight stability: What do insects measure and why?', *ADVANCES IN INSECT PHYSIOLOGY: INSECT MECHANICS AND CONTROL*, 34, pp. 231-316.
- Tomioka, K., Miyasako, Y. and Umezaki, Y. (2008) 'PDF as a coupling mediator between the light-entrainable and temperature-entrainable clocks in *Drosophila melanogaster*', *Acta Biologica Hungarica*, 59(Supplement 2), pp. 149-155.
- Tomioka, K., Uwozumi, K. and Matsumoto, N. (1997) 'Light Cycles Given During Development Affect Freerunning Period of Circadian Locomotor Rhythm of period Mutants in *Drosophila melanogaster*', *Journal of Insect Physiology*, 43(3), pp. 297-305.
- Tähkämö, L., Partonen, T. and Pesonen, A.-K. (2019) 'Systematic review of light exposure impact on human circadian rhythm', *Chronobiology International*, 36(2), pp. 151-170.

- Vaidya, A. T., Top, D., Manahan, C. C., Tokuda, J. M., Zhang, S., Pollack, L., Young, M. W. and Crane, B. R. (2013) 'Flavin reduction activates Drosophila cryptochrome', *Proc Natl Acad Sci U S A*, 110(51), pp. 20455-60.
- VanVickle-Chavez, S. J. and Van Gelder, R. N. (2007) 'Action Spectrum of Drosophila Cryptochrome', *Journal of Biological Chemistry*, 282(14), pp. 10561-10566.
- Vecsey, C. G., Pérez, N. and Griffith, L. C. (2013) 'The Drosophila neuropeptides PDF and sNPF have opposing electrophysiological and molecular effects on central neurons', *Journal of Neurophysiology*, 111(5), pp. 1033-1045.
- Veleri, S., Brandes, C., Helfrich-Förster, C., Hall, J. C. and Stanewsky, R. (2003) 'A Self-Sustaining, Light-Entrainable Circadian Oscillator in the Drosophila Brain', *Current Biology*, 13(20), pp. 1758-1767.
- Veleri, S., Rieger, D., Helfrich-Förster, C. and Stanewsky, R. (2007) 'Hofbauer-Buchner eyelet affects circadian photosensitivity and coordinates TIM and PER expression in Drosophila clock neurons', *J Biol Rhythms*, 22(1), pp. 29-42.
- Vinayak, P., Coupar, J., Hughes, S. E., Fozdar, P., Kilby, J., Garren, E., Yoshii, T. and Hirsh, J. (2013) 'Exquisite Light Sensitivity of Drosophila melanogaster Cryptochrome', *Plos Genetics*, 9(7).
- Wheeler, D. A., Hamblen-Coyle, M. J., Dushay, M. S. and Hall, J. C. (1993) 'Behavior in Light-Dark Cycles of Drosophila Mutants That Are Arrhythmic, Blind, or Both', *Journal of Biological Rhythms*, 8(1), pp. 67-94.
- Wittmann, M., Dinich, J., Merrow, M. and Roenneberg, T. (2006) 'Social Jetlag: Misalignment of Biological and Social Time', *Chronobiology International*, 23(1-2), pp. 497-509.
- Wollnik, F. (1989) 'Physiology and regulation of biological rhythms in laboratory animals: an overview', *Laboratory Animals*, 23(2), pp. 107-125.
- Wu, J. S. and Luo, L. (2006) 'A protocol for dissecting Drosophila melanogaster brains for live imaging or immunostaining', *Nat Protoc*, 1(4), pp. 2110-5.
- Xu, K., Zheng, X. and Sehgal, A. (2008) 'Regulation of feeding and metabolism by neuronal and peripheral clocks in Drosophila', *Cell metabolism*, 8(4), pp. 289-300.
- Yang, Z., Emerson, M., Su, H. S. and Sehgal, A. (1998) 'Response of the Timeless Protein to Light Correlates with Behavioral Entrainment and Suggests a Nonvisual Pathway for Circadian Photoreception', *Neuron*, 21(1), pp. 215-223.
- Yang, Z. and Sehgal, A. (2001) 'Role of Molecular Oscillations in Generating Behavioral Rhythms in Drosophila', *Neuron*, 29(2), pp. 453-467.
- Yao, Z., Bennett, A. J., Clem, J. L. and Shafer, O. T. (2016) 'The Drosophila Clock Neuron Network Features Diverse Coupling Modes and Requires Network-wide Coherence for Robust Circadian Rhythms', *Cell Rep*, 17(11), pp. 2873-2881.
- Yao, Z. and Shafer, O. T. (2014) 'The Drosophila circadian clock is a variably coupled network of multiple peptidergic units', *Science (New York, N.Y.)*, 343(6178), pp. 1516-1520.
- Yasuyama, K. and Meinertzhagen, I. A. (1999) 'Extraretinal Photoreceptors at the Compound Eye's Posterior Margin in Drosophila melanogaster', *Journal of Comparative Neurology*, 412(2), pp. 193-202.
- Yoo, S.-H., Yamazaki, S., Lowrey, P. L., Shimomura, K., Ko, C. H., Buhr, E. D., Siepk, S. M., Hong, H.-K., Oh, W. J., Yoo, O. J., Menaker, M. and Takahashi, J. S. (2004) 'PERIOD2::LUCIFERASE real-time

Bibliography

- reporting of circadian dynamics reveals persistent circadian oscillations in mouse peripheral tissues', *Proceedings of the National Academy of Sciences of the United States of America*, 101(15), pp. 5339-5346.
- Yoshii, T., Ahmad, M. and Helfrich-Förster, C. (2009) 'Cryptochrome mediates light-dependent magnetosensitivity of *Drosophila*'s circadian clock', *PLoS Biol*, 7(4), pp. e1000086.
- Yoshii, T., Hermann, C. and Helfrich-Förster (2010) 'Cryptochrome-positive and -negative clock neurons in *Drosophila* entrain differentially to light and temperature', *J Biol Rhythms*, 25(6), pp. 387-98.
- Yoshii, T., Hermann-Luibl, C. and Helfrich-Förster, C. (2016) 'Circadian light-input pathways in *Drosophila*', *Commun Integr Biol*, 9(1), pp. e1102805.
- Yoshii, T., Hermann-Luibl, C., Kistenpennig, C., Schmid, B., Tomioka, K. and Helfrich-Förster, C. (2015) 'Cryptochrome-dependent and -independent circadian entrainment circuits in *Drosophila*', *J Neurosci*, 35(15), pp. 6131-41.
- Yoshii, T., Heshiki, Y., Ibuki-Ishibashi, T., Matsumoto, A., Tanimura, T. and Tomioka, K. (2005) 'Temperature cycles drive *Drosophila* circadian oscillation in constant light that otherwise induces behavioural arrhythmicity', *European Journal of Neuroscience*, 22(5), pp. 1176-1184.
- Yoshii, T., Todo, T., Wülbeck, C., Stanewsky, R. and Helfrich-Förster, C. (2008) 'Cryptochrome is present in the compound eyes and a subset of *Drosophila*'s clock neurons', *Journal of Comparative Neurology*, 508(6), pp. 952-966.
- Young, M. W. (2018) 'Time Travels: A 40-Year Journey from *Drosophila*'s Clock Mutants to Human Circadian Disorders (Nobel Lecture)', *Angewandte Chemie International Edition*, 57(36), pp. 11532-11539.
- Yu, Q., Jacquier, A. C., Citri, Y., Hamblen, M., Hall, J. C. and Rosbash, M. (1997) 'Molecular mapping of point mutations in the period gene that stop or speed up biological clocks in *Drosophila melanogaster*', *PNAS*, 84, pp. 784-788.
- Yu, W. and Hardin, P. E. (2006) 'Circadian oscillator of *Drosophila* and mammals', *Journal of Cell Science*, 119, pp. 4793-4795
- Yu, W., Houl, J. H. and Hardin, P. E. (2011) 'NEMO kinase contributes to core period determination by slowing the pace of the *Drosophila* circadian oscillator', *Current biology : CB*, 21(9), pp. 756-761.
- Yu, W., Zheng, H., Houl, J. H., Dauwalder, B. and Hardin, P. E. (2006) 'PER-dependent rhythms in CLK phosphorylation and E-box binding regulate circadian transcription', *Genes & development*, 20(6), pp. 723-733.
- Yu, W., Zheng, H., Price, J. L. and Hardin, P. E. (2009) 'DOUBLETIME plays a noncatalytic role to mediate CLOCK phosphorylation and repress CLOCK-dependent transcription within the *Drosophila* circadian clock', *Molecular and cellular biology*, 29(6), pp. 1452-1458.
- Yusein, S., Velikova, N., Kuppenova, P., Hardie, R., Wolstenholme, A. and Semenov, E. (2008) 'Altered ivermectin pharmacology and defective visual system in *Drosophila* mutants for histamine receptor HCLB', *Invert Neurosci*, 8(4), pp. 211-22.
- Yusein, S., Wolstenholme, A. and Semenov, E. (2010) 'Functional consequences of mutations in the *Drosophila* histamine receptor HCLB', *J Insect Physiol*, 56(1), pp. 21-7.

Zehring, W. A., Wheeler, D. A., Reddy, P., Konopka, R. J., Kyriacou, C. P., Rosbash, M. and Hall, J. C. (1984) 'P-element transformation with *period* locus DNA restores rhythmicity to mutant, arrhythmic *Drosophila melanogaster*', *Cell*, 39(2), pp. 369-376.

Zeng, H., Hardin, P. E. and Rosbash, M. (1994) 'Constitutive overexpression of the *Drosophila* period protein inhibits period mRNA cycling', *The EMBO Journal*, 13(15), pp. 3590-3598.

Zeng, H., Qian, Z., Myers, M. P. and Rosbash, M. (1996) 'A light-entrainment mechanism for the *Drosophila* circadian clock', *Nature* 380, pp. 129-135.

Zerr, D. M., Hall, J. C., Rosbash, M. and Siwicki, K. K. (1990) 'Circadian fluctuations of period protein immunoreactivity in the CNS and the visual system of *Drosophila*', *The Journal of Neuroscience*, 10(8), pp. 2749.

Zhang, L., Chung, B. Y., Lear, B. C., Kilman, V. L., Liu, Y., Mahesh, G., Meissner, R.-A., Hardin, P. E. and Allada, R. (2010a) 'DN1_p Circadian Neurons Coordinate Acute Light and PDF Inputs to Produce Robust Daily Behavior in *Drosophila*', *Current Biology*, 20(7), pp. 591-599.

Zhang, L., Lear, B. C., Seluzicki, A. and Allada, R. (2009) 'The CRYPTOCHROME Photoreceptor Gates PDF Neuropeptide Signaling to Set Circadian Network Hierarchy in *Drosophila*', *Current Biology*, 19(23), pp. 2050-2055.

Zhang, Y., Liu, Y., Bilodeau-Wentworth, D., Hardin, P. E. and Emery, P. (2010b) 'Light and temperature control the contribution of specific DN1 neurons to *Drosophila* circadian behavior', *Curr Biol*, 20(7), pp. 600-5.

Zhao, J., Kilman, V. L., Keegan, K. P., Peng, Y., Emery, P., Rosbash, M. and Allada, R. (2003) '*Drosophila* Clock Can Generate Ectopic Circadian Clocks', *Cell*, 113(6), pp. 755-766.

Zheng, X., Koh, K., Sowcik, M., Smith, C. J., Chen, D., Wu, M. N. and Sehgal, A. (2009) 'An isoform-specific mutant reveals a role of PDP1 epsilon in the circadian oscillator', *J Neurosci*, 29(35), pp. 10920-7.

Zheng, X. and Sehgal, A. (2008) 'Probing the Relative Importance of Molecular Oscillations in the Circadian Clock', *Genetics*, 178(3), pp. 1147.

Zheng, Y., Hirschberg, B., Yuan, J., Wang, A. P., Hunt, D. C., Ludmerer, S. W., Schmatz, D. M. and Cully, D. F. (2002) 'Identification of Two Novel *Drosophila melanogaster* Histamine-gated Chloride Channel Subunits Expressed in the Eye', *Journal of Biological Chemistry*, 277(3), pp. 2000-2005.

Zhu, H., Sauman, I., Yuan, Q., Casselman, A., Emery-Le, M., Emery, P. and Reppert, S. M. (2008) 'Cryptochromes define a novel circadian clock mechanism in monarch butterflies that may underlie sun compass navigation', *PLoS Biol*, 6(1), pp. e4.

Zhu, L., McKay, R. R. and Shortridge, R. D. (1993) 'Tissue-specific expression of phospholipase C encoded by the *norpA* gene of *Drosophila melanogaster*', *Journal of Biological Chemistry*, 268(21), pp. 15994-16001.

Zimmerman, J., Chan, M., Jackson, N., Maislin, G. and Pack, A. (2012) 'Genetic Background Has a Major Impact on Differences in Sleep Resulting from Environmental Influences in *Drosophila*', *Sleep*, 35(4), pp. 545-57.

Zoltowski, B. D. (2015) 'Resolving cryptic aspects of cryptochrome signaling', *Proc Natl Acad Sci U S A*, 112(29), pp. 8811-2.

Zoltowski, B. D., Vaidya, A. T., Top, D., Widom, J., Young, M. W. and Crane, B. R. (2013) 'Structure of full-length *Drosophila* cryptochrome (vol 480, pg 396, 2011)', *Nature*, 496(7444), pp. 252-252.

Bibliography

Zuker, C. S., Cowman, A. F. and Rubin, G. M. (1985) 'Isolation and structure of a rhodopsin gene from *D. melanogaster*', *Cell*, 40(4), pp. 851-858.

Zuker, C. S., Montell, C., Jones, K., Laverty, T. and Rubin, G. M. (1987) 'A rhodopsin gene expressed in photoreceptor cell R7 of the *Drosophila* eye: homologies with other signal-transducing molecules', *The Journal of Neuroscience*, 7(5), pp. 1550.